

# Journal of Polymer Science

## Part A-1: Polymer Chemistry

### Contents

I. O. SALYER and A. S. KENYON: Structure and Property Relationships in Ethylene-Vinyl Acetate Copolymers. . . . .	3083
A. W. P. JARVIE, C. G. MOORE, and D. SKELTON: Reactions of Some Organic Peroxides with Triphenylphosphine and Sodium Dialkyl Phosphites. . . . .	3105
H. SUMITOMO, M. OKADA, and H. ITO: Cationic Polymerization of 2-Vinyl-1,3-dioxane. . . . .	3115
V. A. ZAKHAROV and Y. I. ERMAKOV: Kinetic Study of Ethylene Polymerization with Chromium Oxide Catalysts by a Radiotracer Technique. . . . .	3129
A. NOSHAY, M. MATZNER, and C. N. MERRIAM: Polysulfone-Polydimethylsiloxane Block Copolymers. . . . .	3147
W. J. PRIEST and M. M. SIFAIN: Photochemical and Thermal Isomerization in Polymer Matrices: Azo Compounds in Polystyrene. . . . .	3161
L. T. C. LEE, E. M. PEARCE, and S. S. HIRSCH: Novel Aliphatic Polymers Containing Imide Ring. I. Polyspiroimide Based on Methanetetraacetic Acid. . . . .	3169
C. U. PITTMAN, JR. and P. L. GRUBE: Organometallic Polymers. XIV. Copolymerization of Vinylcyclopentadienyl Manganese Tricarbonyl and Vinylferrocene with <i>N</i> -Vinyl-2-Pyrrolidone. . . . .	3175
C. U. PITTMAN, JR., W. J. PATTERSON, and S. P. McMANUS: Organometallic Polymers. XV. Synthesis and Characterization of Some Ferrocene-Containing Oxysilane Polymers from Bis(dimethylamino)silanes. . . . .	3187
K. P. RAO, K. T. JOSEPH, and T. NAYUDAMMA: Characterization of the Collage-Vinyl Graft Copolymers Prepared by the Ceric Ion Method. I. Solution Properties. . . . .	3199
K. KOJIMA, S. IWABUCHI, K. KOJIMA, N. TARUMI, and E. MASUHARA: Grafting of Methyl Methacrylate and Its Derivatives onto Blood. . . . .	3213
S. K. CHATTERJEE and V. B. AGRAWAL: Titration Curves of <i>p</i> -Aminobenzoic Acid-Formaldehyde Polymer in Relation to Its Structure. . . . .	3225
C. G. OVERBERGER and I. SCHEINFELD: Synthesis and Characterization of Some Trithiols. . . . .	3233

(continued inside)

# Journal of Polymer Science      Part A-1: Polymer Chemistry

**Board of Editors:** H. Mark • C. G. Overberger • T. G. Fox

**Advisory Editors:**

R. M. Fuoss • J. J. Hermans • H. W. Melville • G. Smets

**Editor:** C. G. Overberger

**Associate Editor:** E. M. Pearce

**Advisory Board:**

T. Alfrey, Jr.	N. D. Field	R. W. Lenz	C. C. Price
W. J. Bailey	F. C. Foster	Eloisa Mano	B. Rånby
John Boor, Jr.	H. N. Friedlander	C. S. Marvel	J. H. Saunders
F. A. Bovey	K. C. Frisch	F. R. Mayo	C. Schuerch
J. W. Breitenbach	N. G. Gaylord	R. B. Mesrobian	W. H. Sharkey
W. J. Burlant	W. E. Gibbs	Donald Metz	V. T. Stannett
G. B. Butler	A. R. Gilbert	H. Morawetz	J. K. Stille
S. Bywater	M. Goodman	M. Morton	M. Szwarc
W. L. Carrick	J. E. Guillet	J. E. Mulvaney	A. V. Tobolsky
H. W. Coover, Jr.	George Hulse	S. Murahashi	E. J. Vandenberg
W. H. Daly	Otto Kauder	G. Natta	Herbert Vogel
F. Danusso	J. P. Kennedy	K. F. O'Driscoll	L. A. Wall
F. R. Eirich	W. Kern	S. Okamura	O. Wichterle
E. M. Fettes	J. Lal	P. Pino	F. H. Winslow

*Contents (continued)*

G. V. NIKONOVICH and KH. U. USMANOV: Crosslinking and Structural Changes of Cellulose Fibers.....	3245
S. M. COHEN, R. H. YOUNG, and A. H. MARKHART: Transparent Ultraviolet-Barrier Coatings.....	3263
B. M. MANDAL and S. R. PALIT: Quantitative Treatment of the Dye Partition Method of Analysis of Surfactants and of Ionic Groups in High Polymers.....	3301
N. V. ZOLOTOVA and E. T. DENISOV: Mechanism of Propagation and Degenerate Chain Branching in the Oxidation of Polypropylene and Polyethylene.....	3311
S. V. VINOGRADOVA, V. A. VASNYEV, T. I. MITAISHVILI, and A. V. VASIL'YEV: Low-Temperature Polyesterification in the Presence of Tertiary Amines.....	3321
SUSAN C. GROSS: Rotational Mobility of Nitroxyl Radicals in Polyesters.....	3327
ROY M. MORTIER, P. K. DUTT, J. HOEFNAGELS, and C. S. MARVEL: Polymers Containing Anthraquinone Units: Polymers from 1,5-Diaminoanthraquinone and Aralkyldiketones.....	3337

*(continued on inside back cover)*

The Journal of Polymer Science is published in four sections as follows: Part A-1, Polymer Chemistry, monthly; Part A-2, Polymer Physics, monthly; Part B, Polymer Letters, monthly; Part C, Polymer Symposia, irregular.

Published monthly by Interscience Publishers, a Division of John Wiley & Sons, Inc., covering one volume annually. Publication Executive, Editorial, and Circulation Offices at 605 Third Avenue, New York, N. Y. 10016. Second-class postage paid at New York, New York and additional mailing offices. Subscription price, \$325.00 per volume (including Parts A-2, B, and C). Foreign postage \$15.00 per volume (including Parts A-2, B, and C).

Copyright © 1971 by John Wiley & Sons, Inc. All rights reserved. No part of this publication may be reproduced by any means, nor transmitted, nor translated into a machine language without the written permission of the publisher.



## Structure and Property Relationships in Ethylene-Vinyl Acetate Copolymers

I. O. SALYER, *Monsanto Research Corporation, Dayton Laboratory,  
Dayton, Ohio 45407* and A. S. KENYON, *Monsanto Company, Central  
Research, St. Louis, Missouri 63166*

### Synopsis

The effects of vinyl acetate content on crystallinity of ethylene-vinyl acetate (E/VA) copolymers were investigated by x-ray diffraction and differential thermal analysis (DTA). The values of these parameters obtained from DTA were found to agree quantitatively with data calculated from x-ray, probability equations, and copolymer theory. The melting points of the crystalline copolymers, and the molar amounts of vinyl acetate to produce a completely amorphous rubber corresponds exactly to that predicted by the Flory theory. The random character expected in E/VA copolymers is thereby confirmed. The physical properties of E/VA copolymers of all ranges of compositions and crystallinity were determined. Depending directly upon vinyl acetate content, the copolymers changed progressively from highly crystalline polyethylene to semicrystalline polyethylene, a completely amorphous rubber, a soft plastic with a glass transition near room temperature. Properties which were correlated with copolymer composition include: crystallinity, melting point, density, modulus, tensile strength, glass transition, and solubility. Finally, the effect on crystallinity and physical properties of replacing the acetoxy group in E/VA with the smaller, highly polar hydroxyl group (ethylene-vinyl alcohol copolymer) was also investigated.

### INTRODUCTION

Ethylene can be readily copolymerized with vinyl acetate by the high-pressure process to yield a range of copolymers having a wide variety of physical properties. The incorporation of vinyl acetate comonomer units into a polyethylene backbone chain has three separate effects. Crystallinity of the polyethylene is reduced in proportion to the molar concentration of comonomer. Vinyl acetate is more polar than ethylene and causes a corresponding change in solubility. There is a gradual shift in the glass transition of the copolymers to higher  $T_g$  with increasing vinyl acetate content.

The reactivity ratios of ethylene and vinyl acetate monomers are both near 1 and equal. The equal reactivity has several important consequences. The chemical composition of the feed monomers and the product copolymer will always be equivalent (regardless of the monomer ratio, or the conversion). Uniformly random copolymers containing from 0 to 100% vinyl acetate comonomer can be produced. The sequence length of

each monomer unit in the copolymer chain will be determined on a probability basis, and by the concentration of the monomers in the feed. The most probable sequence length for each monomer, and the distribution of sequences, can be calculated from probability equations. The results predicted from such theoretical analysis can then be checked experimentally by various analytical determinations. From a structure and property relation standpoint, the most significant single phenomenon investigated was the variation in crystallinity with vinyl acetate content and the accompanying systematic changes in the physical properties of the product.

The second largest effect was the progressive change in solubility and glass transition that occur with incorporation of increasing amounts of vinyl acetate comonomer.

Even more pronounced changes in solubility and glass transition were observed in the replacement of vinyl acetate with vinyl alcohol by hydrolysis.

The wide variety of products which can be produced, and the theoretically predictable results which are obtained in ethylene-vinyl acetate and ethylene-vinyl alcohol copolymers makes this a near ideal system in which to determine the validity of various copolymer theories, and the relationship of chemical composition and structure to the crystallinity and physical properties of the products.

## EXPERIMENTAL AND DISCUSSION

### Analysis of E/VA Copolymer Composition

The basic parameters which determine the physical and chemical properties of a polymer or copolymer are the molecular weight, and distribution of molecular weights, which make up the polymer chains; and the chemical composition and steric disposition of the units.

The overall chemical composition of the E/VA copolymers was determined by elemental analysis (C, H, and O), saponification (alcoholic

TABLE I  
Relationship between Monomer Feed and Product Composition in  
E/VA Copolymers<sup>a</sup>

	E/VA copolymer composition	Vinyl acetate in feed, wt-%	Vinyl acetate in product, wt-%
1	96/4	4.0	4.3
2	85/15	15.0	15.4
3	69/31	31.0	29.6
4	60/40	40.0	41.8
5	56/44	44.0	43.7
6	50/50	50.0	51.7
7	40/60	60.0	62.2
8	25/75	75.0	75.9

<sup>a</sup> Product analysis by elemental determination of C, H, and O.

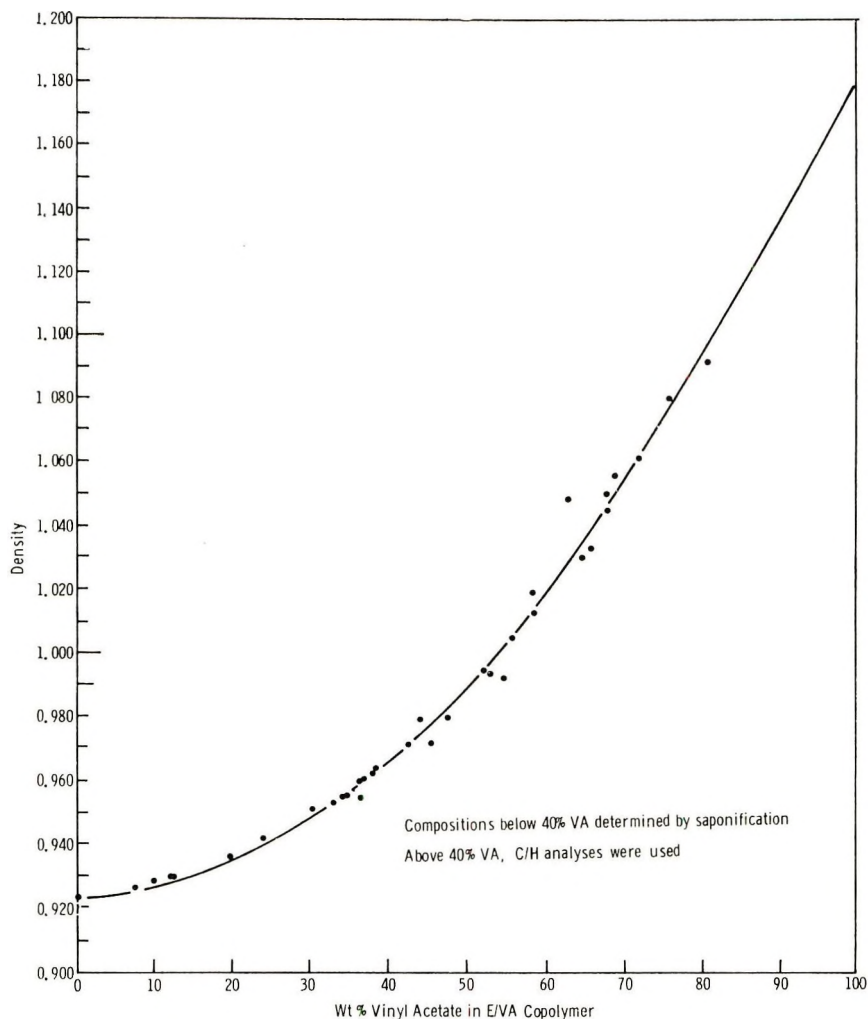


Fig. 1. Correlation between density and chemical composition in E/VA copolymers.

KOH), and infrared absorption. Of these three methods, the elemental analysis proved to be the most accurate and reliable.

The relationship of monomer feed to product composition was determined by elemental analysis for copolymers containing from 4 to 75% by weight vinyl acetate. The close agreement between monomer feed ratio and product composition (Table I) indicates that the E/VA copolymers are uniform as predicted by reaction kinetics.

Using elemental analysis and saponification for determining overall vinyl acetate content, correlations with product density were established. A graph of density versus product composition is shown in Figure 1 for copolymers containing from 0 to 100% vinyl acetate. Because of off-setting effects, a curved relationship of density to composition is found

in semicrystalline copolymers containing 0–40% vinyl acetate. Product density is a linear function of vinyl acetate content in the amorphous copolymers containing 40–100% acetate.

### Molecular Weight and Distribution of E/VA Copolymers

In concurrent research, the molecular weight and distribution of four E/VA copolymers were determined as part of a program of extensive characterization of the solution properties of these products. Detailed presentation and discussion of the solution properties of the E/VA copolymers is reserved for later publication. However, a summary of the results is appropriate to establish that the molecular weight of the E/VA copolymers were sufficiently high that physical properties would be relatively unaffected by further increases in this parameter. Molecular weight distributions were normal for high-pressure-polymerized ethylene polymer and copolymers.

The molecular weights of four E/VA copolymers were determined by solvent-nonsolvent fractionation of the whole copolymer in a mixed solution of xylene and cellosolve at 124°C. The whole polymers and the fractions obtained were characterized by elution fractionation, light scattering, osmometry, and intrinsic viscosity. Weight-average molecular weight  $\bar{M}_w$ , number-average molecular weight  $\bar{M}_n$ , and the calculated  $\bar{M}_w/\bar{M}_n$  ratio are shown in Table II.

TABLE II  
Molecular Weight and Distribution in E/VA Copolymers

	Copolymer composition	Vinyl acetate, wt-%	$\bar{M}_w$	$\bar{M}_n$	$\bar{M}_w/\bar{M}_n$
1	91/9	9	258,800	33,500	7.7
2	84.6/15.4	15.4	513,700	33,500	15.5
3	55/45	45.0	285,000	26,400	10.8
4	29.4/70.6	70.6	566,000	38,800	14.6

Although the solution properties of the E/VA copolymers exhibited some noteworthy differences from polyethylene, the molecular weights and distributions are similar to polyethylene in overall character. There is no indication that vinyl acetate comonomer causes any increase in the long chain branching of the polymer chains over that which is normally present in polyethylene. The  $\bar{M}_n$  of the samples investigated ranged from a low of 26,400 for the E/VA (55/45) copolymer to a high of 38,800 for the E/VA (29/71) copolymer. Thus, all of the copolymers have chains whose lengths are greater than 1000 vinyl monomer units.

### Short-Chain Branching in E/VA Copolymers

According to Mandelkern's definition of a copolymer,<sup>1</sup> the ethylene-vinyl acetate copolymers may be considered as terpolymers made up of



segments of linear polyethylene,  $\alpha$ -olefins other than ethylene, and vinyl acetate. When the copolymer theory is assumed and the  $\alpha$ -olefin and vinyl acetate considered as monomer B, the molar concentration of the linear polyethylene portion may be calculated. If we consider an E/VA copolymer having a melting point of 103°C and the  $\Delta H$  for the HDPE as 1600 cal, the calculated molar concentration of linear polyethylene will be 84 mole-%. Such a polymer contains a total of 16 mole-% of branched monomers (combined vinyl acetate and  $\alpha$ -olefins). This particular polymer contained 4.3 mole-% vinyl acetate and therefore the remaining comonomer or branched olefin must be present as 11.7 mole-%.

On the basis of the E/VA containing some alkyl side branches as well as the acetate, the  $\text{CH}_3/\text{CH}_2$  were calculated for alkyl groups ranging from methyl to butyl.

The results of the calculated methyl/methylene ratios are shown in Table III and compared with  $\text{CH}_3/\text{CH}_2$  ratios measured by infrared. This agreement between observed and calculated values indicate that in E/VA copolymers the short branches have an average length of  $\text{C}_4$  which correlates with previously reported data of Bryant and Voter<sup>2</sup> on high-pressure polyethylene. Considerations apply only to the short-chain branching which directly affects crystallinity.

TABLE III  
Length of Ethylene Side Chains in Ethylene-Vinyl Acetate Copolymers

	Mp, °C	$\Delta H$ , cal/mole	Assignment	$\text{CH}_3/100 \text{ CH}_2$ (cal)	$\text{CH}_3/100$ $\text{CH}_2$ (IR)
E/VA (88/12) (4.28 mole-% vinyl acetate)	103	1500	Methyl	5	—
			Ethyl	4.75	—
			Propyl	4.55	—
			Butyl	4.3	4.2

#### Sequence Length of Ethylene and Vinyl Acetate Units in E/VA Copolymer Chains Calculated from Polymerization Kinetics

The length of uninterrupted ethylene sequences, and uninterrupted vinyl acetate sequences in ethylene/vinyl acetate copolymers can be calculated from the reactivity ratios and probabilities by assuming Monte Carlo type statistics apply in the copolymerization. Since the monomer activity for ethylene and vinyl/acetate are both nearly one and equal (monomer A = monomer B = 1), the most probable and the maximum sequence length can be calculated as a function of monomer charge composition which, in this case, is also approximately identical with the product composition.

Several different values of a monomer activity,  $r_1$  for ethylene and  $r_2$  for vinyl acetate, have been reported in the literature. Although all of these reported values are near 1 and nearly equal, some dependence

TABLE IV  
Calculated Length of Monomer Sequences in E/VA Copolymers versus Monomer Activity Ratio and Per Cent Conversion

Initial feed composition, mole-%	Polymer composition, mole-%	Chain breaks/ 100 molecules	Number-average sequence length		Probabilities			
			A <sub>n</sub>	B <sub>n</sub>	A-A	A-B	B-B	B-A
Case A. Initial (1%) conversion, A = ethylene, r <sub>1</sub> = 0.79; B = vinyl acetate, r <sub>2</sub> = 0.85								
91/9	89.2/10.8	19.8	9.0	1.1	0.88	0.11	0.08	0.91
55/45	53.7/46.3	54.6	2.0	1.7	0.49	0.50	0.41	0.58
9/91	10.1/89.9	18.7	1.07	9.0	0.07	0.92	0.89	0.10
Case B. 25% Conversion; A = ethylene, r <sub>1</sub> = 0.79; B = vinyl acetate, r <sub>2</sub> = 0.85 <sup>a</sup>								
91/9	91.4/8.6	19.8	9.4	1.1	0.88	0.11	0.08	0.91
55/45	54/46	54.6	2.0	1.7	0.49	0.50	0.41	0.58
9/91	10/90	18.7	1.1	9.9	0.07	0.92	0.89	0.10
Case C. Initial (1%) conversion; A = ethylene, r <sub>1</sub> = 1.07; B = vinyl acetate, r <sub>2</sub> = 1.08								
91/9	91/9	15.5	11.76	1.16	0.91	0.08	0.14	0.86
55/45	55/45	47.7	2.3	1.9	0.56	0.43	0.47	0.53
9/91	8/92	15.3	1.0	12.0	0.04	0.96	0.92	0.08

<sup>a</sup> Sequence Length remains constant over range 0-65% conversion.

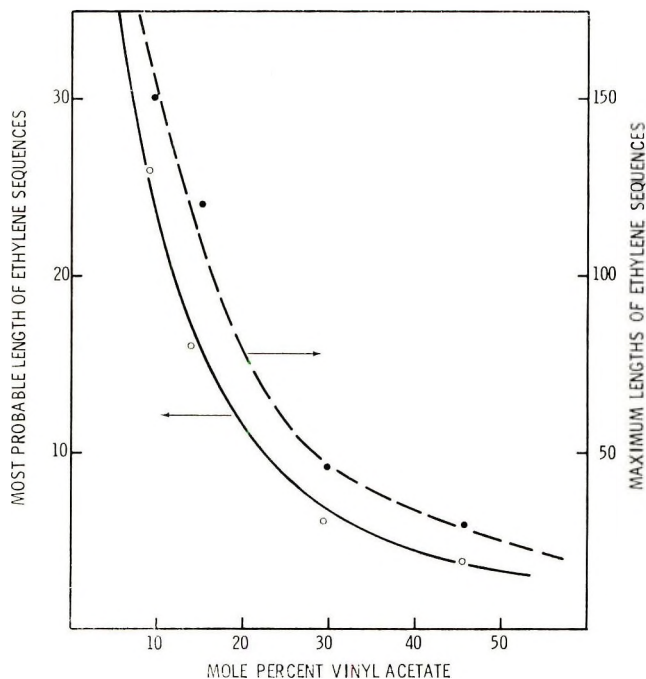


Fig. 2. Calculated ethylene sequence length in E/VA copolymers vs. product composition.

on polymerization pressure and temperature has been reported. For example, an  $r_1$  value 0.79 and an  $r_2$  value of 0.85 has been determined by us for polymerization of ethylene and vinyl acetate at a pressure of 30,000 psi and 120°C. Using these  $R_1$  and  $R_2$  values, the polymer product composition, number of breaks per 100 monomer units, the number-average sequence length for both monomer A (ethylene) and monomer B (vinyl acetate), and the probabilities for sequence composed of A-A, A-B, B-B, and B-A were computed by methods of Meyer and Lowry<sup>3</sup> and Harwood and Ritchey,<sup>4</sup> for three different feed compositions, as shown in Table IV; for initial conversion (case A) and 25% conversion (case B). The same data were then computed for  $r_1 = 1.07$  and  $r_2 = 1.08$  for polymerization<sup>5</sup> conducted at 25,000 psi at 90°C and are summarized in Table IV Case C.

These data collectively illustrate that the composition of the product, number average sequence length, etc., are not sensitive to small changes in activity ratios within the scope of those reported, or in the percent conversion of monomer to polymer. Second, the data also showed that the sequence length of ethylene and vinyl acetate units should be present in the polymer in a random manner.

The same type of data are shown in Figure 2, wherein the most probable ethylene sequence length is plotted as the ordinate against the mole percent of vinyl acetate as the abscissa. As expected from the above calculations,

the most probable ethylene sequence length is approximately equal to the ratio of the monomers charged and the sequence length becomes very short at equal molar compositions of ethylene and vinyl acetate. Longer sequences of vinyl acetate units then occur in the same manner at high molar ratios of vinyl/acetate.

### Ethylene Crystal Sequence Length in Ethylene-Vinyl Acetate Copolymers Calculated from DTA Melting Points

If it is assumed that the crystals within a polyethylene chain can be considered as a mixture of normal paraffin hydrocarbons, then an estimation of the crystal segment lengths may be determined from the DTA thermogram by using the Charlesby equation:<sup>6</sup>

$$1/T_m = (1/A_n) + (B/N)$$

where  $T_m$  is the melting point of the polymer,  $A_n$  denotes the melting point of an infinitely long segment of crystals,  $N$  is the number of monomeric units in a crystal, and  $B$  is the slope of the plot of reciprocal of melting point of copolymer versus reciprocal of number of monomer units in the hydrocarbon crystal.

If polyethylene is considered as a mixture of paraffin hydrocarbons, many reference materials are available to establish a melting curve for paraffins of different length. The estimated lengths of crystal segments of ethylene for the various vinyl acetate concentrations are shown in Table V.

TABLE V  
Ethylene Chain Sequence Length in Crystals  
of Ethylene-Vinyl Acetate Copolymers

Comonomer (VA), mole-%	Melting range, °C	Monomer lengths, Å
4.3	83-103	21-36
7.6	72-98	18-30
16.8	61-77	14-18
27.0	41-44	10

The longest crystal sequence in the 16.8 mole-% VA copolymer would have a segment corresponding in length to dotriacontane, 32 carbons (16 monomer units) and a melting point of 74°C. The 27% polymer would have sequences equivalent to eicosane (mp 38°C).

Ethylene sequences exist in the semicrystalline range; the length of these sequences depend upon the monomer concentrations. The above crystal sequences represent those segments which are not interrupted by a branch or by entanglement.



The total ethylene sequences in both the crystalline and noncrystalline phases, as determined from melting point data, can be compared with that calculated from the reactivity ratios and probabilities by assuming Monte Carlo type statistics in the copolymerization.

### **Melting Points of E/VA Copolymers Determined by Differential Thermal Analysis and Dilatometry Compared with that Predicted by Copolymer Theory**

Melting of crystalline polymers and copolymers has received a lot of attention by many workers. Flory,<sup>7</sup> Mandelkern,<sup>1</sup> and Nielsen,<sup>8</sup> have discussed the theory of melting in systems where the comonomer B is not capable of entering into crystallization. These theories lay the foundation of this work. Since the Flory and Mandelkern theories of melting require some measure of heat of fusion in order to be applied to a copolymer system, the application of this theory is limited to systems where data for heat of fusion are available.

Dole and Wunderlich<sup>9</sup> have measured the enthalpies ( $\Delta H$ ) and entropies ( $\Delta S$ ) in polymer systems by precise calorimetric methods. These methods required very high precision equipment and are applicable to all types of polymer systems.

In the ethylene polymer and copolymer systems, it is possible to measure enthalpy and entropies of fusion by means of differential thermal analysis. Ke<sup>10</sup> reported such a system of measuring  $\Delta H$  and  $\Delta S$  for several polyethylenes. The method of DTA lends itself to such measurements because suitable reference standards exist.

The melting points of E/VA copolymers, determined by DTA, versus vinyl acetate content is shown graphically in Figure 3. The linear relationship between copolymer composition and melting point is clearly apparent.

Mandelkern<sup>1</sup> has classed polymeric materials as copolymers where units are introduced into the chain which are either chemically, stereochemically, or structurally different from the predominant chain repeating element. The introduction of such groups produces certain limitations and restrictions on the crystallization process and also changes the fusion.

The predictions of the copolymer theory has been used for ethylene-vinyl acetate copolymer systems to determine the effects of the different monomer ratios and heterogeneity of the units within the chain. In the case where the  $r_1$  and  $r_2$ , (the reaction rates for the two comonomers) are nearly equal and close to unity, as is the case for E/VA, then the monomers are distributed in a purely random manner. In the case of a random copolymer where  $p$  is unity, then the melting is proportional to the molar concentration of the monomers present, as follows:

$$[(1/T_m) - (1/T_m^\circ)] = - (R/\Delta H) \ln X_a$$

where  $T_m$ ,  $T_m^\circ$  denote Melting Points of copolymer and homopolymer, respectively;  $R$  is the gas constant;  $\Delta H_\mu$  denotes the heat of fusion of

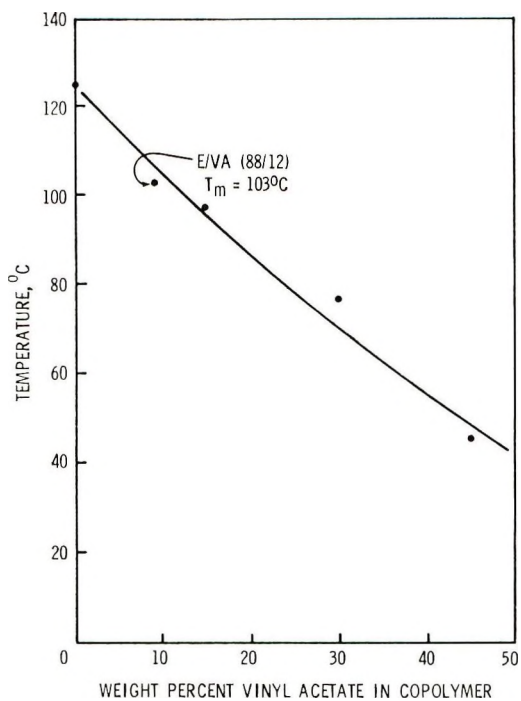


Fig. 3. Melting of E/VA copolymers by DTA vs. chemical composition

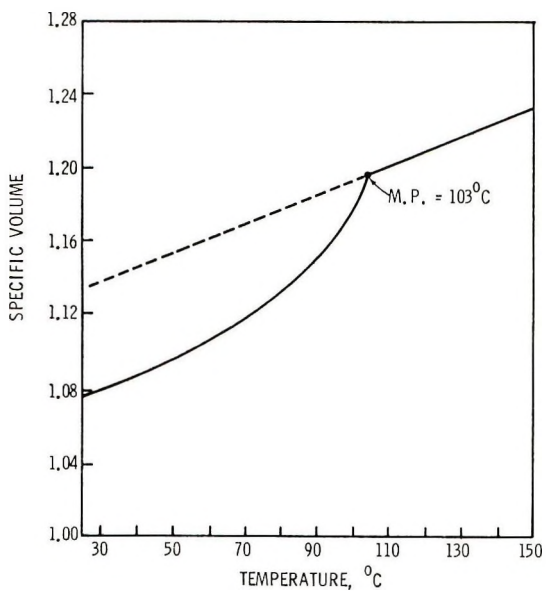


Fig. 4. Melting point of E/VA (82/12) copolymer by dilatometry.

homopolymer;  $p$  is a probability derived from monomer activity, and  $X_a$  is mole fraction of crystallizing monomer.

The melting points of four E/VA copolymers were determined by DTA. The melting points were also calculated by the copolymer theory, based upon the freezing point depression by a comonomer which cannot crystallize and the heat of fusion of highly branched polyethylene as 960 cal/mole of repeat unit when the crystallinity is in the order of 60%. Table VI shows the comparison of observed and calculated melting points. The calculated values agree with the observed, which is characteristic of a random copolymer.

TABLE VI  
Comparison of DTA Melting Point of E/VA Copolymers with Values Calculated from Copolymer Theory

Comonomer (VA), mole-%	Melting point, °C	
	Found by DTA	Calcd by theory
4.28	103	106.2
7.60	98	97.6
16.8	77	72.0
27.0	44	44.0

The melting point observed in the E/VA copolymers by DTA agreed with dilatometric data as shown in Figure 4. The melting point for a 4.28 mole-% VA copolymer (12 wt-% VA) was observed at 103°C by DTA and 104°C by dilatometry. Such small difference is due to the variations of heating rate and the fact that both methods represent approaches to equilibrium, but to different degrees.

#### Correlation of Crystallinity *via* X-Ray with E/VA and E/VOH Copolymers

The crystallinity of ethylene-vinyl acetate copolymers as measured by x-ray (Fig. 5) show a gradual decrease until zero crystallinity is observed at approximately 25 mole-% vinyl acetate. The hydrolyzed E/VA polymers show a decrease, but on a molar basis, the rate of decrease is much lower. The hydrolyzed E/VA polymers pass through a minimum at approximately 52 mole-%; however, some crystallinity exists. Crystallinity was present in all compositions of the hydrolyzed polymer.

Since XRD can detect crystallinity in the order of 1%, a check of the crystallinity was made by differential thermal analysis. The heat of fusion was observed as a function of composition and the heat of fusion plotted against the mole concentration of vinyl acetate (Fig. 6). The point where the heat of fusion is zero ( $\Delta H$ ) defines the point of zero crystallinity. This point occurs at 25 mole-%. A branch point in a polyethylene crystal interrupts crystallinity four carbon atoms on each side of the branch and prevents these atoms from entering the ethylene crystal. Thus, 25 mole-% of

randomly spaced, branched comonomer units would interrupt crystallinity four carbons on each side of the branch and leave no carbons for possible crystallization. The results here would confirm the prediction of the four carbon interruptions on each side of the branch.

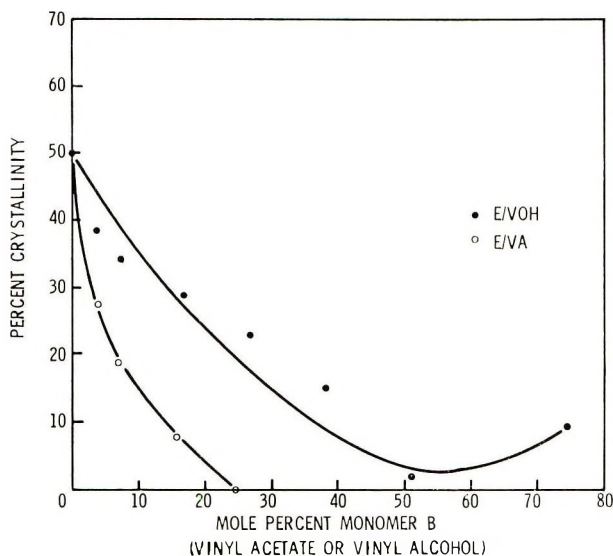


Fig. 5. Crystallinity in E/VA and E/VOH copolymers by x-ray diffraction.

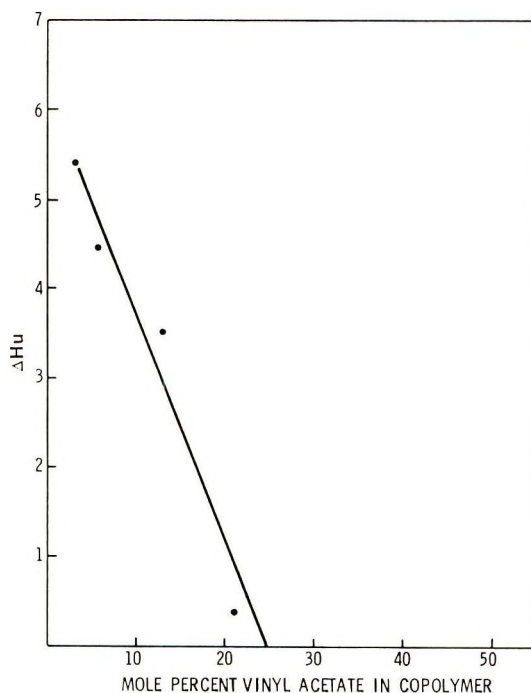


Fig. 6. Heats of fusion for E/VA copolymers.



When the acetate groups is hydrolyzed to replace the acetoxy group by a hydroxyl, very different melting points are also observed. Here the observed melting point is much higher than the calculated even though the molar concentration of the comonomers are the same as the ethylene vinyl acetates. It is also noticed that the spacing within the crystal gradually increases. The increased melting point and the spacing is evidence that the OH group enters into the ethylene crystal, but only causes the crystal to be strained. Bunn<sup>11</sup> has also indicated that OH groups can enter into the ethylene crystal lattice. Table VII shows the x-ray diffraction data for the ethylene-vinyl acetate and ethylene-vinyl alcohol copolymers. As the vinyl acetate concentration increases, the ethylene crystal lattice dimensions ( $D_{110}$ ) changes very little, with a typical distance of 4.1655 Å. On the other hand, increased hydroxyl branching instead of the acetoxy group causes the  $D_{110}$  plane to be distorted, resulting in a change from 4.181 to 4.2887 Å.

Differential thermal analyses show the melting points of E/VA copolymer to agree with calculated melting points of E/VA copolymer on the basis of copolymer depression of the freezing point.

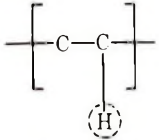
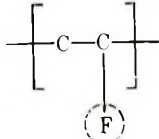
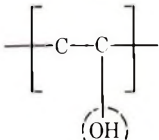
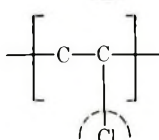
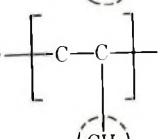
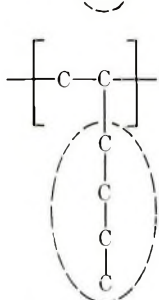
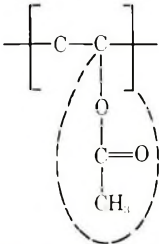
The calculated  $T_m$  for ethylene-vinyl alcohol copolymers do not agree with the experimental melting point. These data show evidence that the hydroxyl group enters into the ethylene crystal lattice and will not depress the freezing point proportional to its molar concentration. Size of the branch becomes very important in the crystallization process.

The importance of the size of the branch point in reducing crystallinity has been experimentally verified by us in other ethylene copolymers. Table VIII shows the atomic radius as estimated by the method of Pauling<sup>12</sup> for several ethylene copolymer systems including copolymers with vinyl fluoride, vinyl alcohol, vinyl chloride, propylene, hexane-1, and vinyl acetate. Good qualitative correlation between the observed crystallinity

TABLE VII  
X-Ray Diffraction Data for E/VA and E/VOH Copolymers

Comonomer, mole-%	Crystallinity XRD, %	Crystal size Å	$D_{110}$ , Å	Melting point, °C	
				Found by DTA	Calcd by theory
E/VA					
4.28	27.4	190	4.1655	103	106.2
7.60	19.9	160	4.1713	98	97.6
16.8	Amorphous	—	—	77	72.0
27.0	Amorphous	—	—	44	44.0
E/VOH					
4.28	38.1	275	4.1811	112	100.2
7.60	34.9	260	4.2025	113	97.6
16.8	28.2	95	4.2583	107	72.0
27.0	23.2	40	4.2887	110	44.0

TABLE VIII. Correlation of Crystallinity Reduction in Polyethylene with Atomic Radius of Interrupting Unit

Comonomer type	Interrupting group	Crystallinity interrupting distance <sup>a</sup>	Comonomer for zero crystallinity, mole-%	Atomic radius, Å <sup>b</sup>
Ethylene		—	—	1.29
Vinyl fluoride		<2	>50	1.35
Vinyl alcohol		2	~52	1.56
Vinyl chloride		2.5	34	1.80
Propylene		3.0	31	2.00
Hexene-1 <sup>c</sup>		4.0	25	3.67
Vinyl acetate		4.0	25	2.60

<sup>a</sup> Crystallinity interrupting distance is the number of carbon atoms on each side of the branch point that crystallinity is prevented by the interfering group.

<sup>b</sup> Atomic radius estimated from data by Pauling.<sup>12</sup>

<sup>c</sup> Hexene-1 describes the comonomer equivalent to produce *n*-butyl side chains which are generated by the "back-biting" mechanism in high-pressure, free-radical, ethylene

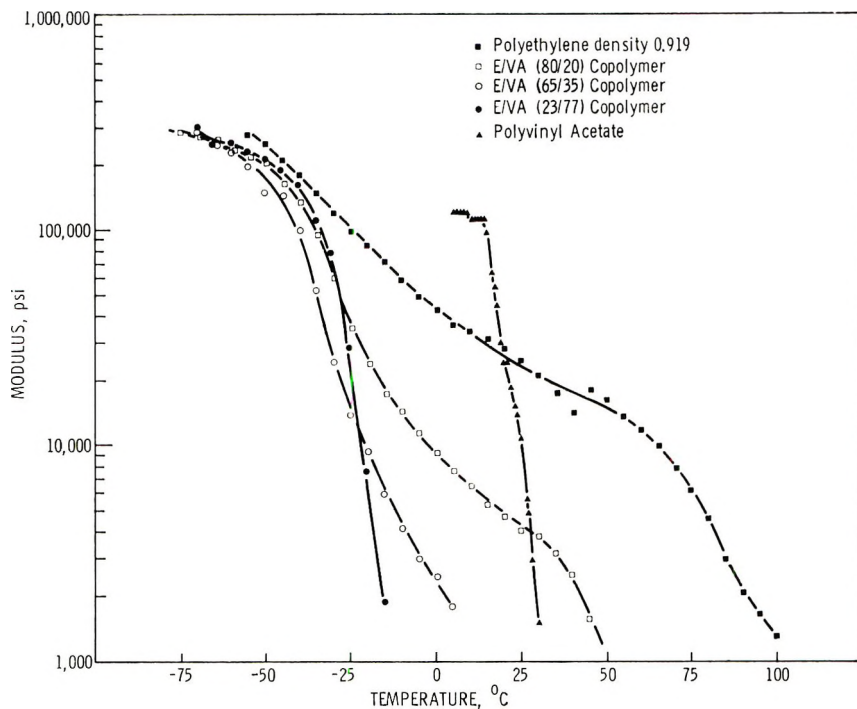


Fig. 7. Clash-Berg modulus curves of E/VA copolymers.

reduction in polyethylene with the calculated atomic radius of the interrupting unit was found for the ethylene copolymers listed.

### Physical Properties of E/VA Copolymers

The physical properties of E/VA copolymers were determined by standard ASTM tests. Physical tests applied were density, melting point, Clash-Berg modulus, and tensile strength and elongations. The tensile data were obtained at a straining rate of 5 in./min on a 1-in. test length (500%/min).

Densities were obtained by the displacement method in silicone fluid at 25°C.

The plot of density versus composition (Fig. 1) showed a straight-line relationship in the copolymers containing >50% vinyl acetate. However, it is not linear over the entire composition range because of combined crystallinity and composition. The plot departs from the straight line in copolymers containing less than 45 wt-% vinyl acetate.

Since the physical properties are dependent upon the crystalline state, a study of the crystallinity and the melting process will show clearly why the copolymer has the observed properties. Figure 3 showed how the melting point of the polymer changed as the vinyl acetate is varied.

The Clash-Berg moduli were obtained over a temperature range of -50 to 120°C.

The Clash-Berg  $T_f$ , the temperature where the modulus equals 135,000 psi, gives a measure of the low-temperature properties of the polymer and represents the practical low-temperature limits of application. Below this temperature, the polymer will tend to be brittle.

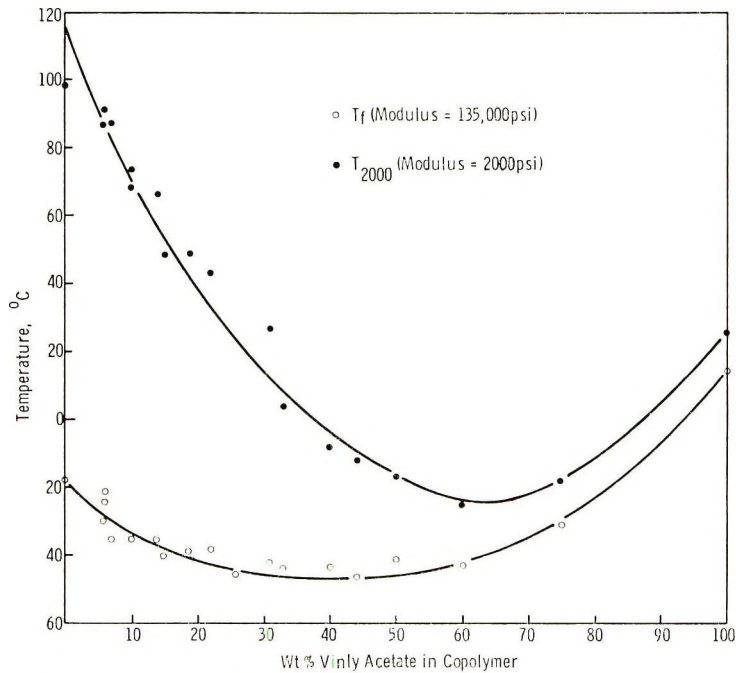


Fig. 8. Clash-Berg  $T_f$  and  $T_{2000}$  vs. E/VA copolymer composition.

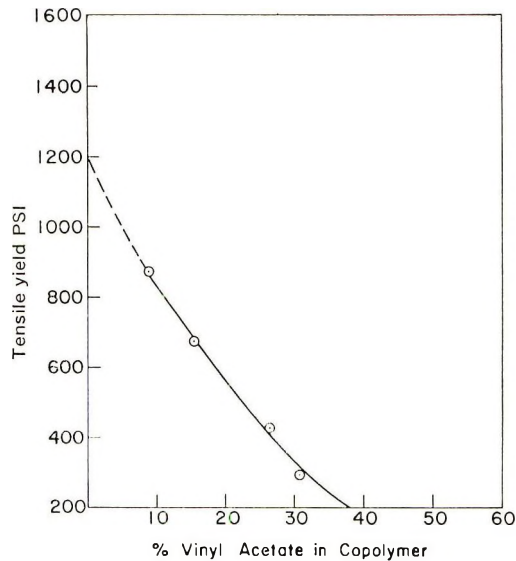


Fig. 9. Tensile yield strength vs. chemical composition is unvulcanized E/VA copolymers.



The glass transition  $T_g$  lies below  $T_f$  in all crystalline compositions where the ethylene concentration is high.  $T_g$  lies very close to  $T_f$  in amorphous compositions containing 50 wt-% vinyl acetate or more.

The Clash-Berg  $T_{2000}$  is the temperature where the modulus is 2000 psi. The accepted temperature of the melting point ( $T_m$ ) usually lies near the  $T_{2000}$  temperature. Complete Clash-Berg curves for high-pressure polyethylene, two E/VA copolymers, and for poly(vinyl acetate) are shown in Figure 7.

The Clash-Berg curve ( $T_f$  and  $T_{2000}$ ) of a polymer is a combined function of crystallinity and the chemical composition. As the vinyl acetate content in the composition increases, the modulus gradually decreases due to the reduction in crystallinity. The decrease in modulus due to loss of crystallinity is greater than the additive effect of composition change. The modulus continues to decrease until a composition is reached where the

TABLE IX  
Physical Properties of Crystalline and Semicrystalline E/VA Copolymers  
(without Vulcanization or Reinforcing Fillers)

Property	Copolymer				
	9 wt-% VA	15.4 wt-% VA	26.3 wt-% VA	30.9 wt-% VA	45 wt-% VA
Clash-Berg $T_f$ , °C	-38	-40	-41.0	-46.5	-42.5
Clash-Berg $T_{2000}$ , °C	73.5	58.5	40.0	13.5	-17.0
Stifflex range, °C	111.5	98.5	81.0	60.0	25.5
25°C modulus, psi	18,000	7,000	3200	1600	100
Density, g/cc	0.926	0.934	0.940	0.954	0.976
Tensile strength, psi <sup>a</sup>	870/2700	670/2980	420/2640	290/1900	.../667
Tensile elongation, <sup>a</sup> %	27/800	28/970	46/1200	37/1390	.../196

<sup>a</sup> Tensile strength and elongation of yield and break respectively.

crystallinity is zero. Beyond the point of zero crystallinity, the modulus increases until it reaches that of a 100% vinyl acetate composition. A plot of Clash-Berg  $T_f$  and  $T_{2000}$  temperatures for E/VA copolymers containing from 0 to 100% vinyl acetate is shown in Figure 8. The Clash-Berg data provide a good method of describing the practical temperature utility limits for the E/VA copolymer system.

Physical properties such as tensile strength and elongation follow the crystallinity. Tensile yield properties (Fig. 9) also change from a typical polyethylene through to rubber.

Table IX shows a summary of the physical properties as a function of vinyl acetate composition up to 45 wt-%. Unvulcanized polymers having VA contents of greater than 45% are very weak thermoplastic rubbers. However, vulcanized 45% and 65% vinyl acetate copolymers, unfilled and filled, have excellent tensile strength and other physical properties, as summarized in Table X.<sup>13</sup>

TABLE X  
Tensile Strength of Vulcanized E/VA Copolymers

Property	44% VA, gum unfilled	44% VA, silica-filled (Hi Sil 203, 30 parts)	44% VA (Carbon black, Ster- ling SRF, 50 parts)	65% VA (Carbon black, ster- ling SRF 60 parts)
1 200% Modulus, psi	305	1720	1445	1500
2 Tensile strength break, psi	1405	3360	2395	2175
3 Tensile elongation break, %	660	590	350	290
4 Shore hardness (Shore number)	59	62	69	67

### Physical Properties of E/VOH Copolymers

E/VA copolymers can be hydrolyzed by either alcoholic KOH or strong acids to produce the corresponding series of ethylene/vinyl alcohol derivatives. As already pointed out, the OH group can fit rather well into the polyethylene crystal lattice so that on a mole basis about twice as many branch points are required (as compared to vinyl acetate) to reduce crystallinity to zero. Additionally, hydrogen-bonding effects enter in to increase intermolecular attractive forces to higher levels. The net result is

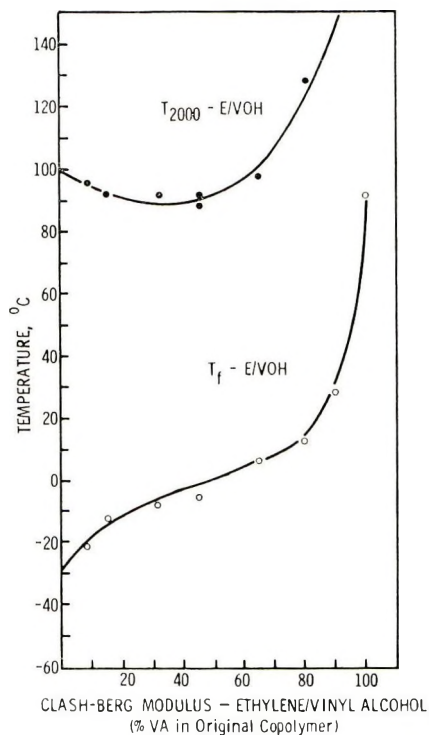


Fig. 10. Clash-Berg  $T_f$  and  $T_{2000}$  vs. E/VOH copolymer composition.

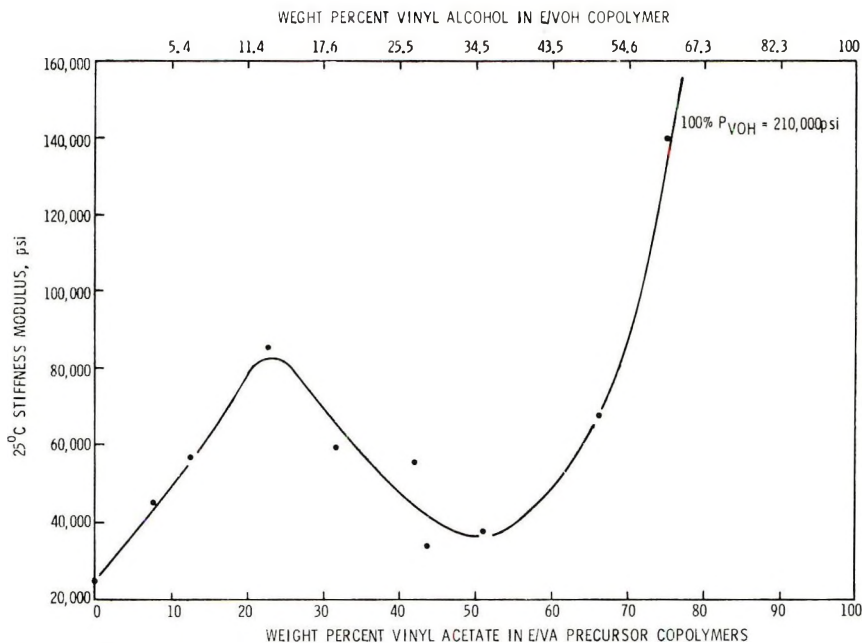


Fig. 11. Room temperature (25°C) modulus of E/VOH copolymers vs. chemical composition.

that in E/VOH copolymers, modulus, tensile, and other physical properties do not go through a pronounced minimum in the amorphous region as do the E/VA precursors. The E/VOH copolymers increase steadily in modulus properties from 0 to 100% VOH. The most rapid changes occur as the chemical composition of the copolymer approaches 100% VOH.

The unusual physical properties of the E/VOH copolymers are illustrated by plots of Clash-Berg modulus data in Figure 10. Numerical values of the room temperature modulus, as summarized in Table XI, show a maximum in stiffness in the composition derived from product initially containing 22.5 wt-% vinyl acetate. This product has higher modulus than most high-pressure polyethylene and much better clarity. A minimum in the room temperature modulus is found in hydrolyzed compositions derived from E/VA (50/50). The modulus then rises rapidly to very high values in the E/VOH copolymers derived from starting E/VA's containing initially ~70 wt-% or more vinyl acetate. The room temperature modulus of hydrolyzed E/VA copolymer compositions is shown graphically in Figure 11.

## CONCLUSIONS

The physical properties and the melting behavior of ethylene-vinyl acetate copolymers indicate clearly that the comonomers react to produce a random copolymer. The depression of the melting point has been shown to be directly proportional to the molar composition of the comonomer when

TABLE XI  
Physical Properties of E/VOH Copolymers from E/VA  
(without Vulcanization or Reinforcing Fillers)

	4.04% VOH (from 7.5% VA)	6.8% VOH (from 12.5% VA)	13.0% VOH (from 22.6% VA)	19.2% VOH (from 31.6% VA)	27.1% VOH (from 42.0% VA)	28.3% VOH (from 43.4% VA)	32.5% VOH (from 50.8% VA)	53.2% VOH (from 68.9% VA)	59.8% VOH (from 75% VA)	82.3% VOH (from 90% VA)	100% VOH (from 100% VA)
Clash-Berg $T_i$ , °C	-12	-7	5.0	12.0	5.0	-2.0	1.0	29.0	15.0	29.0	93.5
Clash-Berg, $T_{200g}$ , °C	98.0	97.0	101.0	95.0	100.0	88.0	91.0	110.0	128.0	155.0	224.0
Stifflex range, °C	110.0	104.0	96.0	83.0	95.0	90.0	90.0	101.0	113.0	126.0	130.5
25°C modulus, psi	45,000	57,000	86,000	60,000	56,000	34,000	39,000	66,000	140,000	210,000	750,000
Density, g/cc	0.9305	0.9328	0.9520	0.9622	0.9801	0.9904	1.0059	1.0567	—	—	—
Tensile strength, psi	1520	1300	2250	1810	2490	3980	3500	4730	—	—	—
Tensile elongation %	490	540	560	280	590	900	930	540	—	—	—



the comonomer cannot enter into crystallization. The replacement of the acetate group by equimolar concentrations of OH does not depress the freezing point proportionally and the VOH comonomer enters into the ethylene crystal with some distortion of the lattice.

The ethylene-vinyl acetate system has been shown to follow the ideal copolymer theory due to the very close reactivity ratios for ethylene and vinyl acetate.

### References

1. L. Mandelkern, *Rubber Chem. Technol.*, **32**, 1392 (1950).
2. W. M. D. Bryant and R. C. Voter, *J. Amer. Chem. Soc.*, **75**, 6113 (1953).
3. V. E. Meyer and C. G. Lowry, *J. Polym. Sci., A*, **3**, 2843 (1965).
4. H. J. Harwood and W. M. Ritchey, *J. Polym. Sci. B*, **2**, 601 (1964).
5. R. D. Burkhart and N. L. Zutty, *J. Polym. Sci. A*, **1**, 1137 (1963).
6. A. Charlesby and L. Callaghan, *J. Phys. Chem. Solids*, **4**, 227 (1958).
7. F. J. Flory, *J. Chem. Phys.*, **17**, 223 (1940).
8. L. E. Nielsen, *Mechanical Properties of Polymers*, Reinhold, New York, 1962.
9. M. Dole and B. Wunderlich, *Makromol. Chem.*, **34**, 29 (1959).
10. B. Ke, *J. Polym. Sci.*, **42**, 15 (1960).
11. C. W. Bunn, *Fibers from Synthetic Polymers*, R. Hill, Ed., Elsevier, New York-Amsterdam, 1953.
12. L. Pauling, *Nature of the Chemical Bond*, Cornell Univ. Press, Ithaca, N. Y., 1945.
13. I. O. Salyer and H. M. Leeper, *Rubber Age*, in press.

Received April 19, 1971

## Reactions of Some Organic Peroxides with Triphenylphosphine and Sodium Dialkyl phosphites

A. W. P. JARVIE, C. G. MOORE,\* and D. SKELTON, *Department of Chemistry, University of Aston in Birmingham, Gosta Green, Birmingham 4, Great Britain*

### Synopsis

The reactions of the allylic peroxides ascaridole, cyclohexadiene endoperoxide, and  $\alpha$ -phellandrene peroxide with triphenylphosphine follow an  $S_Ni'$ -type mechanism. In contrast, the acyclic allylic compounds, allyl *tert*-butyl peroxide,  $\alpha$ -cumyl cyclohexenyl peroxide, and *tert*-butyl cyclohexenyl peroxide apparently react with triphenylphosphine by a free-radical mechanism. The saturated cyclic peroxide dihydroascaridole, in which there is no possibility of an allylic rearrangement, gives with triphenylphosphine a mixture of olefinic alcohols. Di-*n*-butyl peroxide is readily cleaved by sodium dialkyl phosphites, but sterically hindered peroxides do not react under similar conditions. Reaction can, however, take place at the oxygen adjacent to a large group if a smaller substituent is present on the other oxygen atom.

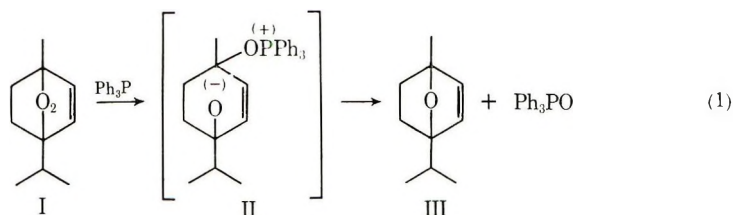
### INTRODUCTION

The reactions of triphenylphosphine and sodium dialkyl phosphites with allylic disulfides have been established,<sup>1,2</sup> and these reagents have been used extensively as chemical probes for the elucidation of the structures of sulfur-vulcanized rubbers.<sup>3</sup>

We now report the results of an investigation of the reactions of triphenylphosphine and sodium dialkyl phosphites with some organic peroxides. These studies were carried out with a view to developing chemical probes which could be used for deducing the structures of oxidized polymer networks. We examined initially the reactions of triphenylphosphine with some simple allylic peroxides, since the allylic peroxides may be considered as model systems for the oxidized polymer networks.

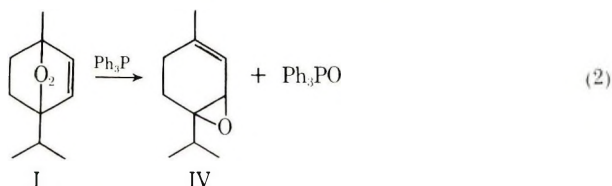
The reaction of the allylic peroxide ascaridole (I) with triphenylphosphine has previously been investigated by Horner and Jurgeleit,<sup>4</sup> who suggested that this reaction proceeds via the intermediate ion pair (II) to give the products 1,4-oxido-*p*-menth-2-ene (III) and triphenylphosphine oxide.

\* Deceased.



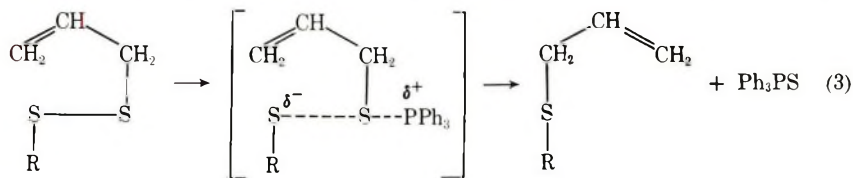
## RESULTS AND DISCUSSION

We found that triphenylphosphine reacts with ascaridole in the dark at 80°C to give triphenylphosphine oxide and 3,4-epoxy-*p*-menth-1-ene (IV) and not III as previously reported.

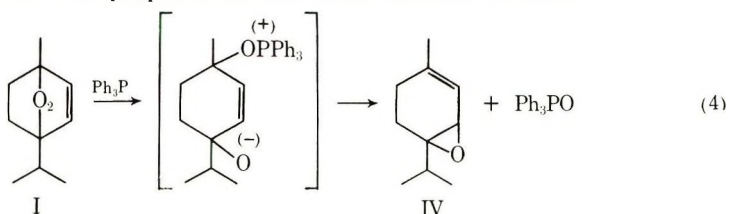


Since the experimental conditions were slightly different from those reported by Horner and Jurgeleit, the reaction was repeated under their original conditions. In this case difficulty was encountered in separating the volatile product from the solvent (petroleum ether); however NMR analysis of the reaction mixture indicated that the product IV was again formed. In order to overcome the difficulties associated with the removal of the petroleum ether, the reaction was carried out again at 100°C in toluene, and once again the product was shown to be IV.

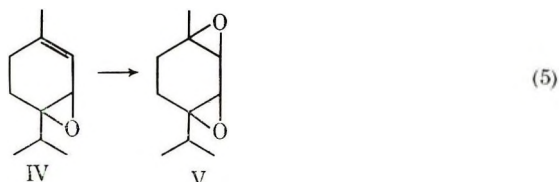
In the reaction of allylic disulfides with triphenylphosphine, Moore<sup>1,2</sup> proposed that desulfuration occurred by the  $S_N2'$  mechanism [eq. (3)].



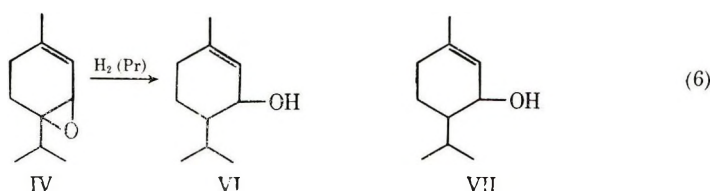
Apart from establishing that ascaridole does not undergo thermal homolysis or isomerization under the conditions used, we have not examined the mechanism of this reaction of ascaridole with triphenylphosphine, but the product composition suggests that the reaction follows an ionic pathway similar to that proposed for the desulfuration reaction:



The structure of the product (IV) was elucidated by using spectroscopic and chemical techniques. Oxidation of IV with perbenzoic acid indicated that the molecule contained only one double bond, and the oxidation product<sup>5,6</sup> was shown to be isoascaridole (V).



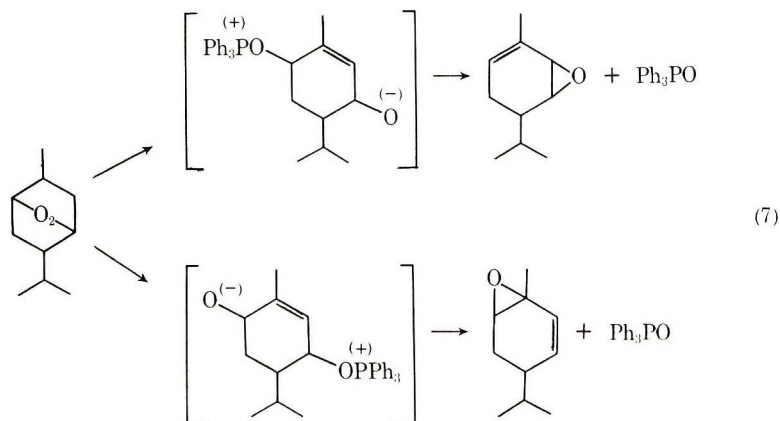
On hydrogenation, one mole of hydrogen per mole of IV was absorbed, apparently confirming that this molecule contained only one double bond. Gas-liquid chromatographic (GLC) analysis of the hydrogenation products indicated two major components, and the infrared spectrum of the reaction mixture showed an intense band at  $3400\text{ cm}^{-1}$  indicative of a hydroxyl group. The simplest interpretation of these data is that the  $\alpha$ -epoxide ring has been reduced in preference to the double bond to yield a mixture of the two alcohols, VI and VII.



The disappearance of the infrared band at  $870\text{ cm}^{-1}$ , attributed to the  $\alpha$ -epoxide, provides some further confirmation that this reaction follows eq. (6). The ease of the reduction of the epoxide ring in IV must be due to the effect of the allylic double bond, because the diepoxide, isoascaridole, is stable under the same conditions.

The allylic peroxides cyclohexadiene and  $\alpha$ -phellandrene endoperoxide react in the same way as ascaridole with triphenylphosphine. The products of the reaction of  $\alpha$ -phellandrene endoperoxide were not completely characterized, but information gained from the infrared and NMR spectra indicated that this reaction followed eq. (7). Unlike the ascaridole reaction, triphenylphosphine attack occurs at both oxygen atoms.

In contrast, the acyclic allylic peroxides, allyl-*tert*-butyl peroxide,  $\alpha$ -cumyl cyclohexenyl peroxide, and *tert*-butyl cyclohexenyl peroxide apparently react with triphenylphosphine by a free-radical mechanism. Because these peroxides are known to undergo radical decomposition<sup>7</sup> at relatively low temperatures, the reactions were initially carried out at  $40^\circ\text{C}$ . Under these conditions,  $\alpha$ -cumyl cyclohexenyl peroxide with triphenylphosphine gave less than 10% of triphenylphosphine oxide after 136 hr. These reactions were therefore repeated at  $80^\circ\text{C}$ , but even at this temperature, after 200 hr, less than 50% of triphenylphosphine oxide



was formed. Surprisingly the yield of triphenylphosphine oxide decreased with increasing concentration of reagents.

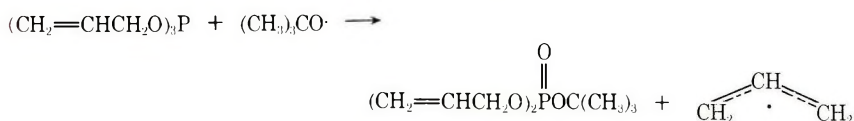
GLC analysis of the volatile mixture of products from the reaction of  $\alpha$ -cumyl cyclohexenyl peroxide indicated that cumyl alcohol was the major component and that the remaining components were numerous, none being more than 10% of the total. A large number of products were also formed in the reactions of the other two allylic peroxides with triphenyl phosphine and no attempt was made to identify these products. It seems probable from the nature and the diversity of products formed that these reactions of acyclic peroxides are homolytic processes, the first stage in the reaction being cleavage of the peroxidic linkage and the formation of the alkoxy radical. The reactions of alkoxy radicals with various organophosphorus compounds have been investigated by Kochi and Krusic,<sup>8</sup> who found that these reactions follow a variety of pathways, the particular route used depending upon the nature of the organophosphorus compound. Trialkylphosphines react with *tert*-butoxy radicals to produce alkyl radicals derived from the phosphine [eq. (8)],



whereas with trialkylphosphites only the *tert*-butyl radical was detected [eq. (9)]

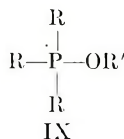
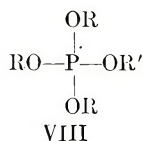


and in the reaction of triallyl phosphites only the spectrum of the allyl radical was observed [eq. (10)].

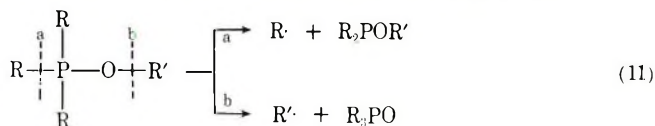


It has been suggested that the reactions of phosphites and phosphines with alkoxy radicals proceed via four coordinate phosphorus-centered radicals such as VIII and IX. These





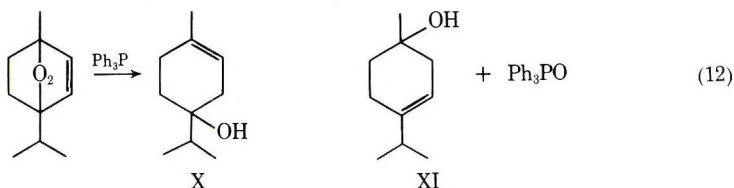
intermediates fragment to yield the most stable radical [eq. (11)]



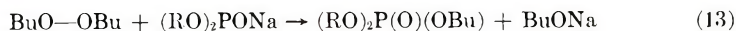
Since triphenylphosphine oxide is a product of the reaction of triphenylphosphine with  $\alpha$ -cumyl cyclohexenyl peroxide the fragmentation must proceed at least in part by pathway (11 b).

The dialkyldisulfides do not react with triphenylphosphine<sup>1,2</sup> under the conditions which are used for the allylic disulfide, which suggests that  $S_N2$  displacement by  $\text{RS}^-$  at saturated carbon is an unfavorable process. Consequently, a study of the reaction of triphenylphosphine with dihydroascaridole was of some interest, since in this 1,4-endoperoxide there is no possibility of an allylic rearrangement analogous to that observed in the reaction of triphenylphosphine with ascaridole.

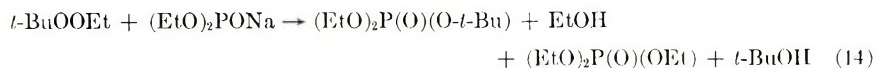
Dihydroascaridole reacts with triphenylphosphine in the dark at 80°C to give a mixture of the isomeric alcohols X and XI [eq. (12)].



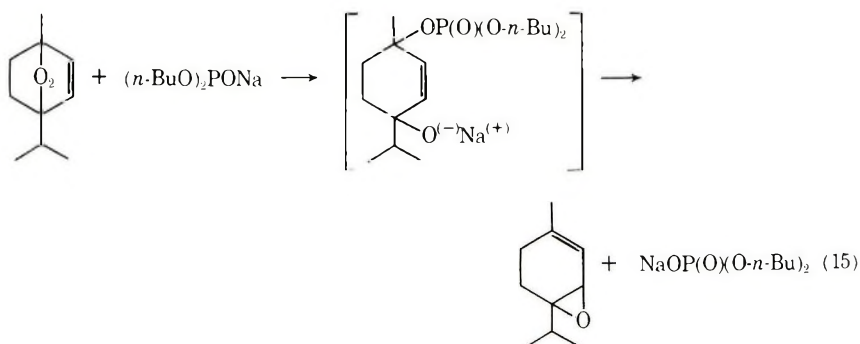
Since ascaridole and dihydroascaridole have similar stereochemistry, it is difficult to see why attack by triphenylphosphine should occur specifically at one oxygen atom in ascaridole but at both oxygen atoms in dihydroascaridole. One possible explanation is that ascaridole may react by an ionic mechanism and dihydroascaridole by a homolytic mechanism and that electronic effects are less important in this latter case. We have found that there is no reaction between cyclohexene and dihydroascaridole at 140°C. Therefore, if this is a radical reaction the initial radicals are not formed by thermal homolysis of the peroxidic linkage. It is possible however that homolysis of the  $-\text{O}-\text{O}-$  bond may be induced by the triphenylphosphine. We have also examined the reactions of some simple organic peroxides with sodium diethyl phosphite (XII) and sodium di-*n*-butyl phosphite (XIII) in benzene solution. Di-*n*-butyl peroxide is readily cleaved by both XII and XIII at 15°C. These reactions are highly exothermic, and the products are the corresponding phosphate and sodium alkoxide.



Di-*tert*-butyl peroxide and di- $\alpha$ -cumyl peroxide were both recovered unchanged after heating with XII at 40°C for 28 days. This stability is almost certainly due to the bulky *tert*-butyl and  $\alpha$ -cumyl groups hindering nucleophilic attack on oxygen. Reaction can, however, take place at oxygen adjacent to a *tert*-butyl group if a smaller alkyl constituent is present on the second oxygen atom. Reactions of XII and XIII with *tert*-butyl *n*-butyl peroxide and *tert*-butyl ethyl peroxide yield products corresponding to attack at both oxygen atoms [eq. (14)].

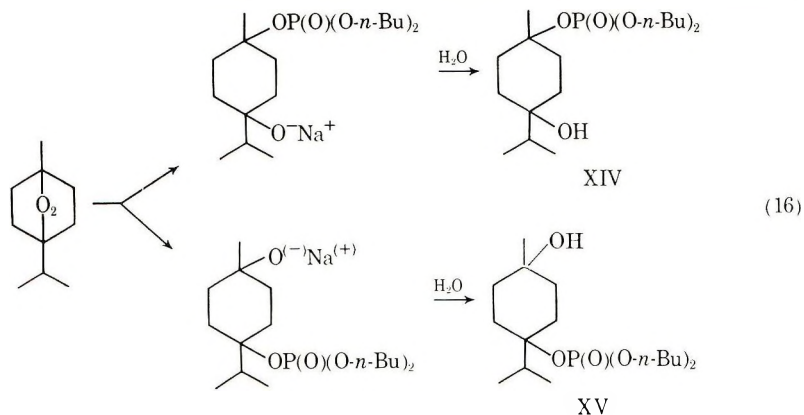


Ascaridole reacts in a mildly exothermic manner with XIII to give 3,4-oxido-*p*-menth-1-ene quantitatively.



This allylic rearrangement is similar to the one observed in the reaction of ascaridole with triphenylphosphine. Since the reduction of ascaridole proceeds more rapidly with XIII than with triphenylphosphine and since the former is a better nucleophile, it is probable that the rate-determining step is cleavage of the peroxidic bond. As in the cleavage by triphenylphosphine, attack occurs specifically at one oxygen atom.

Dihydroascaridole reacted with XIII to give products which could not be identified. The reaction mixture was hydrolyzed and ether-extracted,



and the residue obtained after removal of the ether was investigated by infrared and NMR spectroscopy. From these spectroscopic data and elemental analysis it appeared that the reaction product was XIV or XV or a mixture of these two isomers, but the spectra were too complex for a complete characterization of the product to be made.

## EXPERIMENTAL

### Materials

Triphenylphosphine, ascaridole and dibenzoyl peroxide were obtained commercially and purified before use. Di-*n*-butyl peroxide,<sup>9</sup> *tert*-butyl ethyl peroxide,<sup>10</sup> *tert*-butyl *n*-butyl peroxide,<sup>10</sup> allyl *tert*-butyl peroxide,<sup>7</sup> *tert*-butyl cyclohexenyl peroxide,<sup>11</sup> cyclohexenyl cumyl peroxide,<sup>11</sup>  $\alpha$ -phellandrene endoperoxide,<sup>12</sup> dihydroascaridole,<sup>13</sup> isoascaridole,<sup>14</sup> *tert*-butyl diethyl phosphate,<sup>15</sup> *n*-butyl diethylphosphate,<sup>15</sup> and di-*n*-butyl ethyl phosphate<sup>15</sup> were prepared as described in the literature.

**1,4-Cyclohexene Endoperoxide.** 1,3-Cyclohexadiene<sup>16</sup> (0.75 mole) was photolytically oxidized in isopropanol (1500 ml) containing 0.5 g of methylene blue. When the reaction was complete, the solvent was removed and the residue distilled. The fraction boiling at 38°C/0.1 mm solidified in the condenser. The solid was extracted with benzene; evaporation of the benzene gave the peroxide in 20% yield. Recrystallization from *n*-pentane gave a product, mp 70°C. The infrared and NMR spectra were consistent with this compound having the structure assigned. Elemental analysis was unsuccessful due to the explosive nature of this peroxide.

**Di-*n*-Butyl *tert*-Butyl Phosphate.** This compound was prepared from sodium *tert*-butoxide and diethylchlorophosphate by the method outlined by Allen.<sup>15</sup> The product was obtained in 50% yield; bp 95–96°C/0.05 mm.

ANAL. Calcd for  $C_{12}H_{27}O_4P$ : C, 54.30%; H, 10.24%; P, 11.60%. Found: C, 54.26%; H, 10.06%; P, 11.79%.

### Reactions

**Reaction of Peroxides with Triphenylphosphine.** Ascaridole (0.05 mole) and triphenylphosphine (0.11 mole) were dissolved in benzene (190 ml). The solution was maintained at 80°C under nitrogen in the dark for 160 hr. The benzene was removed and the product distilled under vacuum to give 3,4-epoxy-*p*-menth-1-ene, bp 63°C/0.3 mm; yield 56%. NMR of significant absorptions showed a quartet,  $\tau$  8.9 (intensity 6); singlet,  $\tau$  8.3 (intensity 3); doublet  $\tau$  7.1 (intensity 1), multiplet,  $\tau$  4.3 (intensity 1). The infrared showed  $\alpha$ -epoxide absorption, 860  $cm^{-1}$ .

ANAL. Calcd. for  $C_{10}H_{16}O$ : C, 79.0%; H, 10.50%. Found: C, 79.08%; H, 10.88%.

The residue was shaken with 150 ml diethyl ether to dissolve the triphenylphosphine. The insoluble triphenylphosphine oxide was filtered off (yield 95%). The ether was evaporated and excess triphenylphos-

phine was filtered off from the dark viscous oil which was shown by NMR to be a mixture of approximately 67% volatile product and 33% triphenylphosphine. Because of the difficulty in isolating the product, the total yield was determined by GLC; by this method it was found that the reaction gave a quantitative yield of volatile product.

Ascaridole was reacted with triphenylphosphine in toluene and petroleum ether at 100°C for 63 and 60 hr, respectively.

A number of reactions were carried out under conditions identical to those described above for the reaction of ascaridole with triphenylphosphine in benzene, the only difference being in the reaction time, which varied from system to system.

**Reaction of Dihydroascaridole with Triphenylphosphine (260 hr).** The products were isolated as in the ascaridole reaction. The yield of triphenylphosphine oxide was quantitative. The volatile fraction had bp 60–65°C/0.5 mm. The NMR showed a multiplet,  $\tau$  4.7; broad singlet,  $\tau$  7.2 moving to  $\tau$  7.6 on dilution; multiplet,  $\tau$  8.0; singlet  $\tau$  8.3. The infrared spectrum showed hydroxyl stretching, 3400  $\text{cm}^{-1}$ .

ANAL. Calcd. for  $\text{C}_{10}\text{H}_{18}\text{O}$ : C, 77.80; H, 11.77%. Found: C, 77.26%; H, 11.48%.

**Reaction of  $\alpha$ -Phellandrene Endoperoxide with Triphenylphosphine (1 hr).** The yield of triphenylphosphine oxide was 100%. The volatile product had bp 42°C/0.5 mm; yield 90%. The NMR spectrum showed a multiplet,  $\tau$  4.1; multiplet,  $\tau$  4.6; multiplet,  $\tau$  6.7–7.2; singlet,  $\tau$  8.2; multiplet,  $\tau$  8.9–9.2.

ANAL. Calcd. for  $\text{C}_{10}\text{H}_{16}\text{O}$ : C, 79.0%; H, 10.5%. Found: C, 78.04%; H, 10.18%.

**Reaction of Cyclohexadiene Peroxide with Triphenylphosphine (28 hr).** At the end of this time the benzene was removed under reduced pressure (66 mm). The remaining volatile material was removed at a temperature of 75°C and a pressure of 0.001 mm and collected in a cold trap. The volatile products were fractionated and the fraction boiling at 130–134°/760 mm was collected; yield 50%. Significant NMR absorptions were multiplet,  $\tau$  4.1 (intensity 2); multiplet,  $\tau$  6.5 (intensity 1); multiplet,  $\tau$  6.8 (intensity 1). The infrared showed absorptions attributed to C=C stretching at 1645  $\text{cm}^{-1}$ ,  $\alpha$ -epoxide ring vibrations at 1430, 1250, and 920  $\text{cm}^{-1}$ .

**Reaction of  $\alpha$ -Cumyl Cyclohexenyl Peroxide with Triphenylphosphine.** The peroxide (0.05 mole) was added to triphenylphosphine (0.1 mole) in benzene (50 ml). The solution was outgassed with nitrogen, sealed in a Carius tube, and heated at 80°C in the dark for 120 hr. The benzene was removed under reduced pressure (15 mm) and the products distilled at 0.01 mm. There was obtained 4.6 g of a material boiling at 42–44°C (fraction A). The residue was molecularly distilled 0.002 mm. The temperature was raised slowly to 100°C and liquid-distilled throughout



the range (fraction B). GLC analysis of fractions A and B indicated that both were complex mixtures. The residue contained triphenylphosphine, yield 25%, and triphenylphosphine oxide, yield 75%.

**Oxidation of 3,4-Oxido-*p*-menth-1-ene (IV).** IV (1.87 g) was reacted with excess perbenzoic acid in chloroform at 40°C for 24 hr. The resultant solution was washed first with aqueous bicarbonate and then with water, then dried. After removal of the chloroform there was obtained 1.56 g of a liquid whose NMR and infrared spectra were identical to those of isoascaridole.

**Reaction of Ascaridole with Sodium Di-*n*-butyl Phosphite.** Ascaridole (0.05 mole) was added dropwise to a stirred solution of sodium di-*n*-butyl phosphite (0.1 mole) in benzene (200 ml). After addition was complete the solution was kept at 40°C for 90 hr. During this time the yellow solution separated into a clear upper layer and a yellow viscous lower layer; 50 ml of water was added to dissolve the lower layer. After ether extraction the alcohol product was analyzed by GLC. The ether was then removed, giving 9.0 g of a pale yellow liquid. Distillation gave 8.4 g of a colorless liquid, bp 68°C/12 mm.

ANAL. Calcd for  $C_{10}H_{16}O$ : C, 79.0%; H, 10.5%. Found: C, 77.9%; H, 10.68%.

The NMR and infrared spectra of this product were identical with those of 3,4-oxido-*p*-menth-1,2-ene.

The following reactions were carried out by using the procedures described above for the reaction of ascaridole with sodium di-*n*-butyl phosphite, the only difference being in the reaction time, which varied from system to system.

**Reaction of Di-*n*-butyl Peroxide with Sodium Di-*n*-butyl Phosphite (0.5 hr).** The product had bp 94°C/0.04 mm; yield 8.6 g.

ANAL. Calcd. for  $C_{12}H_{22}O_4P$ : C, 54.20%; H, 10.25%; P, 12.80%. Found: C, 55.53%; H, 10.81%; P, 13.02%.

**Reaction of Di-*n*-butyl Peroxide with Sodium Diethyl Phosphite (0.5 hr).** The product had bp 80–82°C/1.0 mm; yield 6.8 g.

ANAL. Calcd. for  $C_8H_{18}O_4P$ : C, 44.1%; H, 12.4%; P, 14.2%. Found: C, 43.82%; H, 12.14%; P, 13.3%.

**Reaction of Di- $\alpha$ -Cumyl Peroxide with Sodium Di-*n*-butyl Phosphite (28 days).** The product had bp 80–100°C/0.01 mm; yield 11.2 g. The infrared spectrum of this liquid was identical to that of di- $\alpha$ -cumyl peroxide, and on standing for several days the liquid solidified. Recrystallization gave 10 g of di- $\alpha$ -cumyl peroxide, mp 33°C.

**Reactions of Di-*tert*-butyl Peroxide with Sodium Diethyl Phosphite and Sodium Di-*n*-butyl Phosphite.** GLC analyses showed that there was no reaction of the di-*tert*-butyl peroxide.

**Reaction of Dihydroascaridole with Sodium Di-*n*-butyl Phosphite (120 hr.).** The product had bp 35–50°C/0.001 mm; yield 7.5 g.



ANAL. Calcd for  $C_{18}H_{37}O_4P$ : C, 59.3%; H, 10.15%; P, 8.52%. Found: C, 58.94%; H, 10.01%; P, 7.96%.

**Reaction of *tert*-Butyl Ethyl Peroxide and Sodium Di-*n*-butyl Phosphite (5 days).** The product had bp 90–94°C/0.05 mm.

ANAL. Calcd. for  $(n\text{-BuO})_2P(O)O\text{-}t\text{-Bu}$ : P, 11.67%; calcd. for  $(n\text{-BuO})_2P(O)OEt$ : P, 13.0%. Found: P, 12.4%; *t*-BuOH: EtOH, 3:7.

**Reaction of *tert*-Butyl Ethyl Peroxide and Sodium Diethyl Phosphite. (5 days).** The product had bp 55–60°C/1.0 mm;  $n_D^{25}$  1.4070 [ $(EtO)_2P(O)\text{-}OBu'$ ,  $n_D^{25}$  1.4085;  $(EtO)_2P(O)OEt$ ,  $n_D^{25}$  1.4040].

ANAL. Calcd for  $(EtO)_2P(O)O\text{-}t\text{-Bu}$ : P, 14.75%; calcd for  $(EtO)_2P(O)OEt$ : P, 17.05%. Found: P, 15.61%. BuOH: EtOH, 4:6.

**Reactions of *n*-Butyl *tert*-Butyl Peroxide with Sodium Diethyl Phosphite (5 days).** The product had bp 70–72°C/1.0 mm;  $n_D^{25}$  1.4135 [ $(EtO)_2P(O)O\text{-}t\text{-Bu}$ ,  $n_D^{25}$  1.4085;  $(EtO)_2P(O)O\text{-}n\text{-Bu}$ ,  $n_D^{25}$  1.4110]; *t*-BuOH: *n*-BuOH, 3:7.

We thank Albright and Wilson Ltd. for the gift of chemicals and one of us (D.S.) thanks N.R.P.R.A. for a maintenance grant.

### References

1. C. G. Moore and B. R. Trego, *Tetrahedron*, **18**, 208 (1962).
2. C. G. Moore and B. R. Trego, *Tetrahedron*, **19**, 1251 (1963).
3. C. G. Moore and B. R. Trego, *J. Appl. Polym. Sci.*, **15**, 299 (1961).
4. L. Horner and W. Jurgeleit, *Ann.*, **591**, 138 (1955).
5. A. S. Danilova, *J. Org. Chem. (U.S.S.R.)*, **1**, 514 (1965).
6. A. S. Danilova and A. I. Koltsov, *J. Org. Chem. (U.S.S.R.)*, **1**, 972 (1965).
7. T. W. Campbell and G. M. Coppinger, *J. Amer. Chem. Soc.*, **73**, 1788 (1951).
8. J. K. Kochi and P. J. Krusic, *J. Amer. Chem. Soc.*, **91**, 3944 (1969).
9. H. R. Williams and H. S. Mosher, *J. Amer. Chem. Soc.*, **76**, 2984 (1954).
10. F. R. Rust, F. H. Seubold, and J. E. Vaughan, *J. Amer. Chem. Soc.*, **72**, 338 (1950).
11. M. S. Kharasch and A. Fino, *J. Org. Chem.*, **24**, 72 (1959).
12. G. O. Schenck, K. G. Kinkel, and H. J. Mertens, *Ann.*, **584**, 125 (1953).
13. H. Paget, *J. Chem. Soc.*, **1938**, 829.
14. M. Matie and D. A. Sutton, *J. Chem. Soc.*, **1953**, 349.
15. J. F. Allen, S. K. Reed, O. H. Johnson, and N. T. Brunswald, *J. Amer. Chem. Soc.*, **78**, 3715 (1956).
16. J. Hine, J. A. Brown, L. H. Zalkov, W. E. Gardner, and M. Hine, *J. Amer. Chem. Soc.*, **77**, 594 (1955).

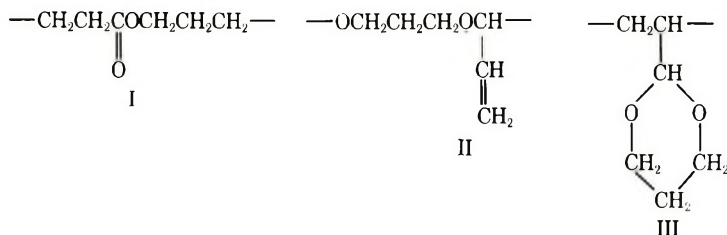
Received April 14, 1971

## Cationic Polymerization of 2-Vinyl-1,3-dioxane\*

HIROSHI SUMITOMO, MASAHIKO OKADA, and HIROSHI ITO,  
*Faculty of Agriculture, Nagoya University, Chikusa, Nagoya, Japan*

### Synopsis

The cationic polymerization of 2-vinyl-1,3-dioxane initiated with triethyloxonium tetrafluoroborate was studied with particular emphasis on elucidation of the structure of the polymer. The polymer was a light yellow powdery material with a molecular weight of several thousands which was soluble in most organic solvents. The infrared and NMR investigations on the polymer, together with chemical analyses, showed that the polymer consisted of the three structural units I, II, and III, the contents of which were estimated to be 5–10%, 20–25%, and 65–70%, respectively.



The formation of the structural units I and II was discussed in detail.

### INTRODUCTION

Acrolein cyclic acetals, such as 2-vinyl-1,3-dioxolane and 2-vinyl-1,3-dioxane, have two functional groups which can participate in cationic polymerization, that is, a carbon-carbon double bond and a cyclic acetal ring. Therefore, it would be indispensable to clarify the structures of the polymers obtained from these monomers for evaluation of the reactivities of the functional groups in their cationic polymerization. Recently, there have been published a few papers on the cationic polymerizations of these cyclic acetals. Tada et al.<sup>1</sup> first confirmed the presence of ester groups in the polymer chain of 2-vinyl-1,3-dioxolane prepared by Lewis acids and interpreted the formation in terms of the hydride shift of the acetal hydrogen to the carbonium ion produced by vinyl addition, followed by the ring-opening rearrangement of the resulting 1,3-dioxolenium ion. Nordstrom<sup>2</sup> reported that poly-2-vinyl-4-methyl-1,3-dioxolane prepared with boron trifluoride

\*Paper presented at the 23rd Annual Meeting of the Chemical Society of Japan, Tokyo, April 1970, and the 19th Symposium on Macromolecules of the Society of Polymer Science, Japan, Kyoto, October, 1970.

etherate as an initiator consisted of three kinds of structural units resulting from simple vinyl addition, ring-opening reaction, and vinyl addition with hydride shift and subsequent rearrangement, respectively. More recently, Madrid and Mateo<sup>3</sup> observed that the cationic polymer of 2-vinyl-2-methyl-1,3-dioxolane, which has no acetal hydrogen available for hydride shift, also contained ester units, suggesting the migration of the methyl group. As to the cationic polymerization of 1,3-dioxane derivatives, Jedlinski and Solich<sup>4</sup> described only briefly the polymerization of 2-vinyl-1,3-dioxane and 2-isopropenyl-1,3-dioxane.

The polymerization of these cyclic acetals initiated with conventional Lewis acids, in general, gives rise to oily or semi-solid polymers with a molecular weight in the range of several hundreds, or crosslinked materials insoluble in common organic solvents. Our preliminary experiments, however, showed that completely soluble polymers with a moderately high molecular weight could be obtained from 2-vinyl-1,3-dioxane by use of triethyloxonium tetrafluoroborate as an initiator. The purpose of the present study is to elucidate the structure of the polymer thus obtained.

## EXPERIMENTAL

### Materials

2-Vinyl-1,3-dioxane was prepared from the condensation of acrolein and trimethylene glycol according to the procedure described by Fischer et al.<sup>5</sup>, with a slight modification. It was purified by drying over calcium hydride, followed by repeated fractional distillation before use, bp 71.5–72.5°C/64 mm Hg.

Triethyloxonium tetrafluoroborate was synthesized by the reaction of epichlorohydrin and boron trifluoride etherate in anhydrous ethyl ether.<sup>6</sup> It was kept in anhydrous ether in a refrigerator.

Commercial methylene chloride of an analytical grade was purified by careful fractional distillation over phosphorus pentoxide.

2-Methyl-1,3-dioxenium tetrafluoroborate was prepared from 3-ethoxypropyl acetate and triethyloxonium tetrafluoroborate by a method similar to that described for 2-methyl-1,3-dioxolenium tetrafluoroborate.<sup>7</sup>

### Polymerization Procedure

**Cationic Polymerization.** A cold solution of triethyloxonium tetrafluoroborate dissolved in methylene chloride was added to a solution of 2-vinyl-1,3-dioxane in the same solvent. The ampoule was then cooled in a liquid nitrogen bath, evacuated, and sealed off. It was allowed to stand at a constant temperature. After the polymerization had been terminated by adding a few milliliters of pyridine-methanol solution, the reaction mixture was washed with water to remove the initiator residues and subsequently poured into a large volume of petroleum ether to precipitate a polymer. It was purified by repeated reprecipitation by using methylene

chloride-petroleum ether as a solvent-precipitant pair and dried under reduced pressure to a constant weight.

The consumption of the monomer during the polymerization was followed by determining the unreacted monomer in the reaction mixture by gas chromatography with the use of tetralin as an internal standard.

**Radical Polymerization.** Radical polymerization of 2-vinyl-1,3-dioxane was carried out in benzene at 60°C for 90 hr by using azobisisobutyronitrile as an initiator. The reaction mixture was poured into a large volume of petroleum ether to isolate a polymer, which was purified in the same way as described above.

### Characterization

**Determination of Ester Units by Saponification.** To a solution of 100–150 mg of a polymer sample dissolved in 5 ml of benzene was added 10 ml of 0.1*N* alcoholic potassium hydroxide solution, and the resulting mixture was refluxed in a water bath for several hours. The excess alkali was then titrated by 0.1*N* hydrochloric acid solution in ethylene glycol-isopropanol (1:1 volume ratio) by using phenolphthalein as an indicator.

**Determination of Carbon-Carbon Double Bonds by Hanus' Method.** To a solution of 50–100 mg of a polymer sample dissolved in 10 ml of chloroform was added 25 ml of freshly prepared Hanus' iodine monobromide solution, and after having been made homogeneous by thorough shaking, the mixture was allowed to stand at 0°C for 30 min in a dark place. A 100-ml portion of water and subsequently 10 ml of 15% aqueous potassium iodide were added to the reaction mixture. The iodine thus liberated was titrated by 0.1*N* aqueous sodium thiosulfate with a few drops of aqueous starch solution as an indicator.

**Determination of 1,3-Dioxane Rings by Acidic Ethanolysis.** Ethanol (5 ml) and concentrated sulfuric acid (100 mg) were added in this order to a solution of 300–400 mg of a polymer sample dissolved in 5 ml of dioxane, and the mixture was stirred mechanically at room temperature for one day. After the solution was neutralized by aqueous sodium hydroxide, trimethylene glycol thus produced was determined by gas chromatography with the use of *o*-cresol as an internal standard.

Acidic ethanolysis under more drastic reaction conditions, such as in a mixture of ethanol and 2*N* aqueous hydrochloric acid (1:1 volume ratio) at reflux temperature, yielded a considerable amount of by-products which prevented an accurate determination of the structural unit having the 1,3-dioxane ring.

Attempted acid-catalyzed hydrolysis of the 1,3-dioxane rings of the polymer in 1,4-dioxane-water (5:1 volume ratio) was unsuccessful both at room temperature and at elevated temperature.

**Infrared and NMR Measurements.** Infrared spectra were taken with a Hitachi grating infrared spectrophotometer, Model 215, on KBr disks. NMR spectra were recorded on a Japan Electronics Model JNM-4H-100



working at 100 MHz in ca. 10% carbon tetrachloride solution at 70°C by using tetramethylsilane as an internal standard.

**Determination of Molecular Weight.** The number-average molecular weight of the polymer was determined with a Hewlett Packard vapor pressure osmometer, Model 302, on solutions in benzene at 37°C.

## RESULTS

The polymerization of 2-vinyl-1,3-dioxane was carried out in methylene chloride by using triethyloxonium tetrafluoroborate as an initiator. The course of the polymerization was followed by determining the unreacted monomer in the reaction mixture by gas chromatography on one side, and by isolating and weighing the petroleum ether-insoluble polymer on the other side. Figure 1 shows typical time-monomer consumption and time-polymer yield curves thus obtained. After a prolonged reaction time, the monomer charged was completely consumed, but there was a significant difference between the consumption of the monomer and the yield of the petroleum ether-insoluble polymer. In this connection, Nordstrom<sup>2</sup> has reported that a large amount of a cyclic dimer is formed in the cationic polymerization of 2-vinyl-4-methyl-1,3-dioxolane. In the present case, however, only a trace of an unidentified compound could be detected by gas chromatography of a polymerization mixture. Therefore, the formation of

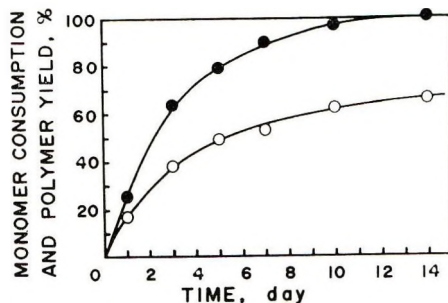


Fig. 1. Cationic polymerization of 2-vinyl-1,3-dioxane: (●) monomer consumption; (○) yield of petroleum ether-insoluble fraction. Monomer, 5 g; methylene chloride, 15 g; initiator (triethyloxonium tetrafluoroborate), 4.5 mole-%; temperature, 0°C.

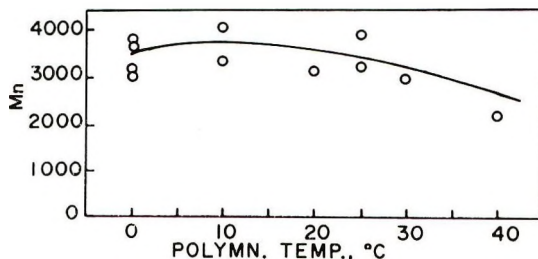


Fig. 2. Dependence of molecular weight of polymer on polymerization temperature. Initiator, 1 mole-%; conversion, 10–37%.



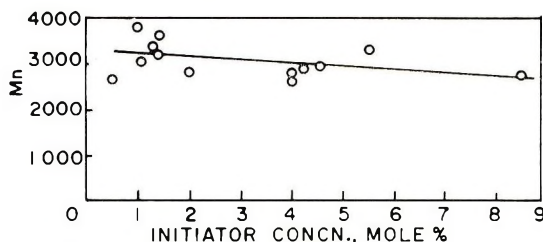


Fig. 3. Dependence of molecular weight of polymer on initiator concentration. Polymerization temperature, 0°C; conversion, 12–36%.

a cyclic dimer of 2-vinyl-1,3-dioxane in a similar manner seems to be negligible under the conditions used in the present study. This was substantiated by examining the petroleum ether-soluble part of the reaction products. A petroleum ether solution of a reaction mixture from which the precipitated polymer had been separated was evaporated at room temperature under reduced pressure. The resulting viscous residue was found to consist of polymeric materials with a molecular weight of several hundreds. The NMR and infrared spectra of this petroleum ether-soluble part were in accord with those of the insoluble part. In addition, the weight of the soluble part could account for the difference between the consumption of the monomer and the yield of the petroleum ether-insoluble part.

Some of the results on the polymerization of 2-vinyl-1,3-dioxane are summarized in Table I and Figures 2 and 3. Poly-2-vinyl-1,3-dioxane thus obtained was a yellow powder with a softening point of about 60°C, soluble in most organic solvents and somewhat hygroscopic. The number-average molecular weight of the polymer was found to be in the range from 2500 to 5400, independent of the conversion, the polymerization temperature, and the initiator concentration. The elementary analysis on the polymer, as shown in Table I, seems to indicate that the polymerization of 2-vinyl-1,3-dioxane proceeds without destruction of the monomeric unit, namely, without liberation of an acrolein molecule from the growing chain end. However, even when such a destruction of the monomeric unit occurs, the carbon and hydrogen contents of the resulting polymer do not differ so much (calcd for  $C_3H_6O$ : C, 62.04%; H, 10.42%) from those of a 2-vinyl-1,3-dioxane unit. Accordingly, the excellent accordance of the analytical data with the theoretical values can not completely rule out the possibility of the occurrence of the detachment of an acrolein molecule from the active chain end. This matter will be discussed in the later section.

It is expected that 2-vinyl-1,3-dioxane undergoes radical polymerization to yield a straightforward vinyl polymer, because the ring-opening polymerization of cyclic acetals can not be induced with any radical initiator, and that the examination of the NMR and infrared spectra of the radical polymer, together with those of the cationic polymer, may provide useful information on the structure of the latter. Table II shows the results on the radical polymerization of 2-vinyl-1,3-dioxane in benzene at 60°C with

TABLE I  
 Cationic Polymerization of 2-Vinyl-1,3-dioxane<sup>a</sup>

No.	Initiator, mole-%	Temp, °C	Time, day	Conversion, %	$\bar{M}_n^b$
117	1.1	0	8	18.1	3780
121	4.1	"	12	62.0	3890
160	5.0	"	4	44.0	3390
161	"	"	7	61.6	5420
124 <sup>c</sup>	5.5	"	4	33.2	3280
130	1.4	10	1	9.4	4090
126	5.5	"	"	19.7	3980
122	4.1	15	"	40.2	3110
135	1.3	30	1/8	11.1	2870
141	4.7	40	"	58.8	3420

<sup>a</sup> Monomer, 5 g; methylene chloride, 15 g; initiator,  $(C_2H_5)_3O^+BF_4^-$ .

<sup>b</sup> By vapor-pressure osmometry, benzene, 37°C.

<sup>c</sup> Elementary analytical data for the resulting polymer are as follows. Calcd for  $C_6H_{10}O_2$ : C, 63.13%; H, 8.76%. Found: C, 63.24%; H, 8.94%.

azobisisobutyronitrile as an initiator. The polymerization proceeded very slowly to give a polymer of a low molecular weight, as expected from its allylic structure. The polymer thus obtained was very similar to the cationic polymer in its appearance and solubility.

 TABLE II  
 Radical Polymerization of 2-Vinyl-1,3-dioxane<sup>a</sup>

No.	Initiator, mole-%	Conversion, %	$\bar{M}_n^b$
149 <sup>c</sup>	2.55	12.7	1670
150	2.45	14.0	1550
151	0.83	4.4	2220

<sup>a</sup> Monomer, 10 g; benzene, 10 g; initiator, azobisisobutyronitrile; 60°C; 90 hr.

<sup>b</sup> Vapor pressure osmometry; benzene; 37°C.

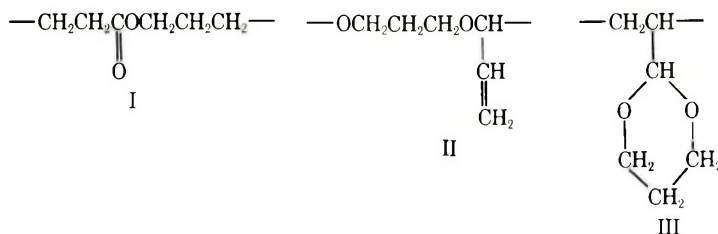
<sup>c</sup> Elementary analytical data for the resulting polymer are as follows. Calcd for  $C_6H_{10}O_2$ : C, 63.13%; H, 8.76%. Found: C, 62.48%; H, 8.78%.

The infrared spectra of the cationic and radical polymers are given in Figure 4. Both of the spectra show a C=O stretching absorption at 1735  $cm^{-1}$  and C—O—C stretching absorptions in the region from 1000 to 1150  $cm^{-1}$ . With respect to the latter absorption band, the relative intensity of the absorption at 1100  $cm^{-1}$  for the cationic polymer is obviously stronger than that for the radical polymer. This is an indication for the presence of open-chain ether linkages in the former polymer. Furthermore, only the spectrum of the cationic polymer exhibits a clear C=C absorption at 1640  $cm^{-1}$ .

Figure 5 shows the NMR spectra of the cationic and radical polymers. The complex signals appearing at 5.8–6.5  $\tau$  are ascribable to the methylene protons adjacent to oxygen atoms of the 1,3-dioxane ring, and signals at

around  $8.8 \tau$  to one of the  $\beta$ -methylene protons of the ring, from the comparison with the spectrum of 2-vinyl-1,3-dioxane monomer. The weak signals at  $7.5 \tau$  should be due to the methylene protons adjacent to carbonyl group, the presence of which is confirmed by infrared spectroscopy. The spectrum of the cationic polymer differs remarkably from that of the radical polymer in that it exhibits signals due to vinyl protons in the region from 4 to  $5 \tau$  and those due to the methylene protons adjacent to the oxygen atoms of linear ether linkages at  $6.5$ – $6.9 \tau$ . Furthermore, the former spectrum is somewhat complex in the region from  $5.3$  to  $5.8 \tau$ , compared with the latter spectrum which shows simple signals due to methine proton of the 1,3-dioxane ring.

On the basis of the infrared and NMR spectra, it is inferred that the radical polymer consists of the structural units I and III, while the cationic polymer consists of the structural units I, II, and III.



The determination of these structural units in the polymer was attempted by NMR and chemical analyses. The content of the structural unit I can be estimated from the relative peak area of the signals at  $7.5 \tau$  due to the methylene protons adjacent to the carbonyl group of the ester unit. Saponification of a sample by potassium hydroxide in benzene-ethanol mixture

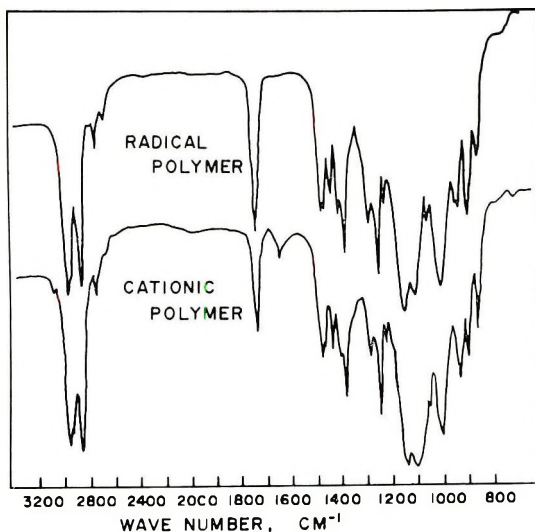


Fig. 4. Infrared spectra of radical and cationic polymers of 2-vinyl-1,3-dioxane.

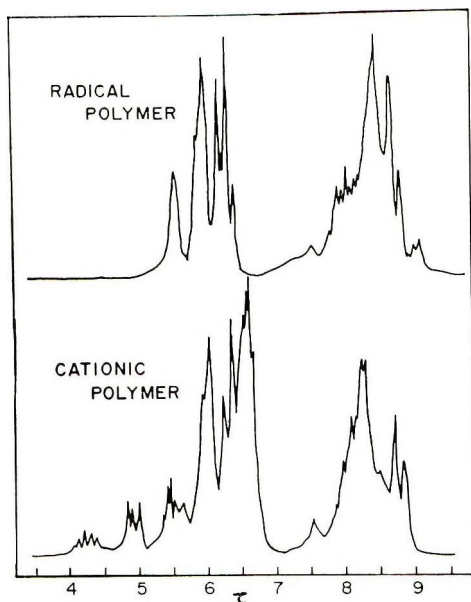


Fig. 5. NMR spectra of radical and cationic polymers of 2-vinyl-1,3-dioxane. Solvent, carbon tetrachloride; concentration, 12%; temperature, 70°C.

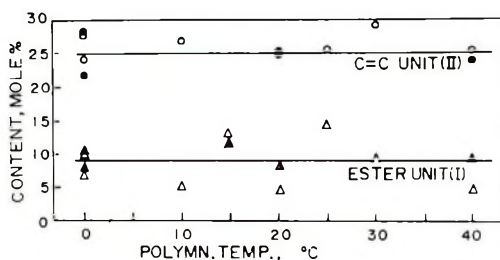


Fig. 6. Dependence of contents of structural units I and II on polymerization temperature: (●, ▲) from NMR analysis; (○, △) from chemical analysis. Initiator concentration, 1–5 mole-%; conversion, 33–58%; molecular weight, 2800–3400.

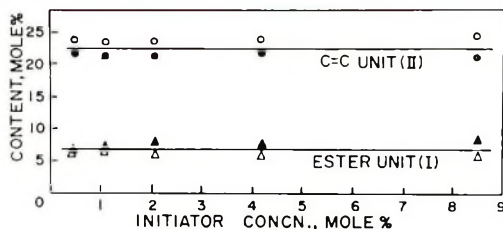


Fig. 7. Dependence of contents of structural units I and II on initiator concentration: (●, ▲) from NMR analysis; (○, △) from chemical analysis. Polymerization temperature, 0°C; conversion, 12–36%; molecular weight, 2600–3000.

also gives the content of the structural unit I. Carbon-carbon double bonds in a sample, which are relevant to the structural units II, can be determined from the relative peak area of the total vinyl protons from 4 to 5 $\tau$  in its NMR spectrum, and also chemically by Hanus' procedure. On the contrary, direct determination of the structural unit III by NMR and chemical analyses was unsuccessful, except for the radical polymer. The content of the structural unit III in the radical polymer was estimated from the relative peak area of the methine proton of the acetal ring appearing at 5.5 $\tau$  in its NMR spectrum, and also by determining trimethylene glycol liberated by the acid catalyzed ethanolysis of the polymer by means of a gas chromatograph. However, the NMR spectrum of the cationic polymer shows complex signals in this region, and it is, therefore, difficult to determine accurately the relative peak area of the acetal proton signals of the structural unit III. Neither the signals of the  $\alpha$ -methylene protons nor those of the  $\beta$ -methylene protons of the 1,3-dioxane ring can be used for the determination of the structural unit III because of the overlapping by the neighbouring signals. On the other hand, quantitative ethanolysis or hydrolysis of the 1,3-dioxane ring in the cationic polymer in the presence of mineral acids could not be achieved without being accompanied by the cleavage of the main chain.

The results on the NMR and chemical analyses of the structural units I and II are illustrated in Figure 6 and 7. The contents of the structural units I and II in the cationic polymers remain nearly constant, irrespective of the polymerization temperature, the catalyst concentration, and the molecular weight of the polymer.

## DISCUSSION

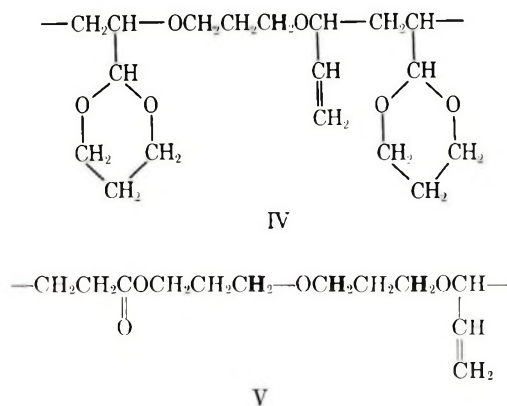
The relatively high content of the structural unit II in the cationic polymer, as shown in Figures 6 and 7, strongly suggests that some of the monomer polymerized was incorporated into the polymer chain by ring-opening mechanism, although a part of the carbon-carbon double bonds in the polymer might arise from chain transfer reaction. Five- or six-membered cyclic acetals, in general, do not homopolymerize,<sup>8</sup> but under certain conditions, some of these cyclic acetals polymerize to give not polyacetals but rather polyethers.<sup>9</sup> The latter are supposed to form by the preferential elimination of the corresponding aldehyde from the growing chain end before the addition of the next monomer occurs.

In the present system, therefore, it seems important to reveal whether acrolein is liberated during the ring-opening reaction of 2-vinyl-1,3-dioxane, and if this is not the case, whether the structural units II form sequences in the polymer chain. In fact, no acrolein was detected in the polymerization mixture, but this does not provide confirmative evidence against the destruction of the monomer unit during the polymerization process, because acrolein, a very reactive compound, even if it is liberated from an active chain end, may not remain as such under acidic conditions. However, it is



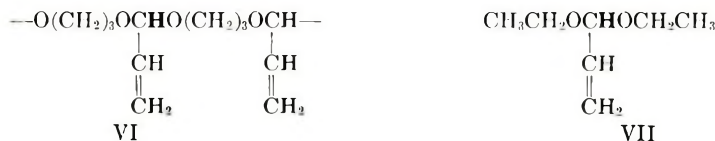
unlikely that acrolein, once liberated from a growing chain end, is incorporated again into a polymer chain through vinyl polymerization, because no aldehyde proton could be detected by NMR spectroscopy in both the petroleum ether soluble and insoluble polymers.

The presence of the structural unit II in the polymer gives rise to methylene protons adjacent to the ether oxygen atoms as indicated in a bold face in structure IV, which is a composite of structures II and III, and V, which is a composite of I and II.



These protons should give NMR signals in the region of 6.4–6.9  $\tau$ , the relative peak area of which was found roughly 1.5 times than that of the total vinyl protons. As the estimation of the former peak area is accompanied by an appreciable error on account of the overlapping of the neighbouring signals, the observed ratio of the peak areas may be taken as a proof for the expected structures of the polymer. From the foregoing discussion, together with the data of the elementary analysis, it can not be conclusive, but may be reasonable, to say that the ring-opening reaction of 2-vinyl-1,3-dioxane is not accompanied by the elimination of an acrolein molecule.

If the structural units II form sequences of two or longer units in a polymer chain, there appears the acrolein acetal structure VI.

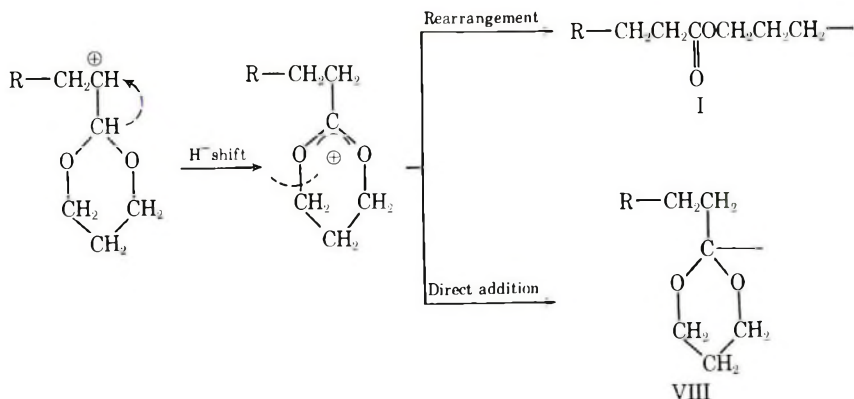


It is expected, therefore, that the acetal proton of this structure should give NMR signals at nearly the same magnetic field as the acetal proton of acrolein diethyl acetal VII. However, no signals can be seen in this region of the NMR spectrum of the polymer. On the assumption that the distribu-

tion of the structural unit II in a polymer chain is statistically random, the ratio of the consecutive structural units II to the total structural units II is calculated to be approximately 0.2. This means that the acetal protons resulting from such consecutive structural units II should give rise to NMR signals, the intensity of which is about one fifth of the methine protons of the total vinyl groups. As the signals of such an intensity can be detected, the absence of the signals in the NMR spectrum of the polymer indicates that there are, if any, very few consecutive structural units II in the polymer chain. If there are sequences of the structural units II in the polymer chain, catalytic hydrogenation of the polymer followed by acidic ethanolysis would produce propionaldehyde diethyl acetal. However, attempts were made without success to hydrogenate quantitatively all the vinyl groups in the polymer with the use of Adams' platinum catalyst, presumably because the adsorption of the vinyl groups to the active sites on the surface of the catalyst was hindered sterically by the bulky 1,3-dioxane rings.

The finding that the structural units II amounting to more than 20 mol-% are incorporated into the polymer chain in the cationic polymerization of 2-vinyl-1,3-dioxane is noteworthy in view of the fact that 1,3-dioxane and its derivatives do not homopolymerize at all, possibly due to the great stability of the 1,3-dioxane ring. In the present system, it is very probable that the vinyl group attached to the 1,3-dioxane ring plays an important role in the ring-opening reaction; it facilitates the cleavage of the oxonium ion formed by the attack of a growing chain end to one of the oxygen atoms of the monomer by delocalizing the incipient positive charge on the acetal carbon atom.

As to the structural unit I, it seems reasonable to assume, as Tada et al.<sup>1</sup> proposed for the polymerization of 2-vinyl-1,3-dioxolane, that it is formed by the hydride transfer reaction of the carbonium ion produced by vinyl addition, followed by the ring-opening rearrangement of the resulting carboxonium ion by nucleophilic attack of the monomer. The direct



addition of the monomer to the electron deficient central carbon atom of the carboxonium ion would lead to the structural unit VIII which retains 1,3-dioxane ring. However, the positive charge on this carbon atom is, to a great extent, delocalized by the adjacent two oxygen atoms, and in view of the fact that only strong bases attack the electron-deficient central carbon atom of 2-methyl-1,3-dioxolenium ion,<sup>5</sup> such a direct addition of 2-vinyl-1,3-dioxane, a weak nucleophile, to the central carbon atom of the carboxonium ion is less likely to take place. 2-Methyl-1,3-dioxonium tetrafluoroborate, a model compound for the intermediate carboxonium ion, was prepared from 3-ethoxypropyl acetate and triethyl-oxonium tetrafluoroborate.<sup>7</sup> Its NMR spectrum measured in nitromethane solution showed the triplet signals of the  $\alpha$ -methylene protons at 4.92 $\tau$ , the shift being more than 1.0 ppm to the lower magnetic field from the signals of the corresponding methylene protons of 2-ethyl-1,3-dioxane. Such a marked chemical shift implies that a considerable positive charge lies on these methylene carbon atoms. Furthermore, it has been reported by Yamashita and his co-workers<sup>10</sup> that the polymerization of tetrahydrofuran initiated with 2-methyl-1,3-dioxolenium perchlorate produces a polymer, each molecule of which contains an acetoxy end group. Therefore, it is probable that, once the carboxonium ion is formed by the hydride shift, it leads to the structural unit I by the subsequent ring-opening rearrangement as illustrated above.

In conclusion, 2-vinyl-1,3-dioxane undergoes cationic polymerization in three different ways, that is, vinyl addition with hydride shift followed by ring-opening rearrangement, ring-opening reaction, and simple vinyl addition, to give the structural units I, II, and III, respectively. The contents of these units in the polymer were found to be 5–10, 20–25, and 65–70% in the order above, irrespective of the polymerization conditions employed in the present study. The content of the structural unit II is a little lower than that of the corresponding structural unit for poly-2-vinyl-1,3-dioxolane.<sup>3</sup> This difference is probably ascribed to the higher stability of the 1,3-dioxane ring compared with that of the 1,3-dioxolane ring.

## References

1. K. Tada, T. Saegusa, and J. Furukawa, *Makromol. Chem.*, **95**, 168 (1966).
2. J. D. Nordstrom, *J. Polym. Sci. A-1*, **7**, 1349 (1969).
3. J. M. Madrid and J. L. Mateo, *Makromol. Chem.*, **136**, 113 (1970).
4. Z. Jedlinski and J. M. Solich, *J. Polym. Sci. A-1*, **6**, 3182 (1968).
5. R. F. Fisher and C. W. Smith, *J. Org. Chem.*, **25**, 319 (1960).
6. H. Meerwein et al., *J. Prakt. Chem.*, **154**, 83 (1939).
7. H. Meerwein et al., *Ann.*, **632**, 38 (1960).
8. J. Furukawa and K. Tada, in *Ring-Opening Polymerization*, K. C. Frisch and S. L. Reegen, Eds., Dekker, New York, 1969, p. 160.

9. T. Saegusa, private communication.
10. Y. Yamashita et al., paper presented at the 23rd Annual Meeting of the Chemical Society of Japan, Tokyo, April, 1970.

Received April 7, 1971

Revised June 7, 1971

## Kinetic Study of Ethylene Polymerization with Chromium Oxide Catalysts by a Radiotracer Technique\*

V. A. ZAKHAROV and YU. I. ERMAKOV, *Institute of Catalysis, Siberian Branch of the Academy of Sciences of the USSR, Novosibirsk, USSR*

### Synopsis

The quenching of polymerization with a chromium oxide catalyst by radioactive methanol  $^{14}\text{CH}_3\text{OH}$  enables one to determine the concentration of propagation centers and then to calculate the rate constant of the propagation. The dependence of the concentration of propagation centers and the polymerization rate on reaction time, ethylene concentration, and temperature was investigated. The change of the concentration of propagation centers with the duration of polymerization was found to be responsible for the time dependence of the overall polymerization rate. The propagation reaction is of first order on ethylene concentration in the pressure range 2–25 kg/cm<sup>2</sup>. For catalysts of different composition, the temperature dependence of the overall polymerization rate and the propagation rate constant were determined, and the overall activation energy  $E_{ov}$  and activation energy of the propagation state  $E_p$  were calculated. The difference between  $E_{ov}$  and  $E_p$  is due to the change of the number of propagation centers with temperature. The variation of catalyst composition and preliminary reduction of the catalyst influence the shape of the temperature dependence of the propagation center concentration and change  $E_{ov}$ .

### INTRODUCTION

The dependence of the polymerization rate and molecular weight of a polymer on reaction conditions is often used to draw conclusions about the polymerization mechanism. However, the polymerization rate and the molecular weight depend on various parameters of the polymerization system. For heterogeneous catalytic polymerization, the rate of polymer formation  $V$  is equal to the propagation rate  $V_p$ , which is proportional to the propagation rate constant  $K_p$ , the surface concentration of active centers  $n_s$ , and the effective surface of the catalyst  $S_{ef}$ :

$$V = K_p n_s S_{ef}$$

In general  $K_p$ ,  $n_s$ , and  $S_{ef}$  are variables and depend on the catalyst composition, the method of catalyst preparation, and conditions of the poly-

\* Paper presented to the Symposium on Macromolecular Chemistry, Budapest, August 1969.



merization process as well. Therefore the use of methods which provide a separate determination of the active center concentration and the propagation rate constant on the overall polymerization rate is very important for an understanding of the kinetic behavior of the polymerization system.

In this paper the kinetics of ethylene polymerization by means of chromium oxide catalysts was followed by the determination of the propagation center concentration. To determine this value we used the method of quenching of polymerization by alcohol labeled with  $^{14}\text{O}$  in the alkoxy group.<sup>1-3</sup> The results obtained give valuable information about the mechanism of initiation and propagation stages in the ethylene polymerization with chromium oxide catalysts.

### EXPERIMENTAL

The composition of the chromium oxide catalyst used is given in Table I.

The catalyst preparation procedure and the conditions of the vacuum activation were described earlier.<sup>2</sup> In some cases catalyst III after vacuum treatment was reduced with carbon monoxide at 300°C.

The ethylene polymerization was carried out at 40–90°C and ethylene pressure 2–25 kg/cm<sup>2</sup> in benzene or cyclohexane in a stainless steel autoclave with stirring. The apparatus used, the polymerization and quenching technique, the specification of reagents, the polymer treatment and recovery, and the measurement of polymer radioactivity were described in a previous paper.<sup>2</sup>

The concentration of propagation centers  $n$ , (in mole/g of catalyst) was calculated from the radioactivity  $A$  (in  $\mu\text{C/g}$ ) of polymers obtained. This concentration is related to the quantity  $b$  of polymer produced up to the moment of stopping, the reaction weight  $a$  of the catalyst and specific radioactivity  $Q$  of methanol used (in  $\mu\text{C/mole}$ ):

$$n = Ab/aQ \quad (2)$$

From the concentration of the active centers, the value of the polymerization rate  $V$  (mole/g catalyst-hr) at the moment of inhibitor injection and the monomer concentration  $C$  (mole/l.) the propagation rate constant  $K_p$  (l./mole-hr) was calculated in accordance with eq. (3).

$$V = K_p n C_m \quad (3)$$

TABLE I  
Chromium Oxide Catalysts

Catalyst	Support	Chromium content in catalyst, %	Specific surface area, m <sup>2</sup> /g	Pore volume, cm <sup>3</sup> /g
I	Silica	2.5	400	1.0
II	Silica + alumina (3.5% Al <sub>2</sub> O <sub>3</sub> )	2.5	300	1.1
III	Alumina	1.4	170	0.42

## RESULTS

The polymerization of ethylene with chromium oxide catalysts in general is a nonsteady-state process: the overall rate varies with the reaction duration. We have found the number of propagation centers and calculated the propagation rate constants corresponding to different reaction moments. For this purpose the polymerization was stopped in the course of each run by injecting radioactive methanol. For each catalyst the polymerization rates thus obtained in different runs are on the same kinetic curve within some error (curves A, Figs. 1 and 2). These kinetic curves were compared with the time dependence of concentration of propagation centers which was obtained in the same runs (curves B, Figs. 1 and 2). An increase of the reaction rate in time was in good agreement with

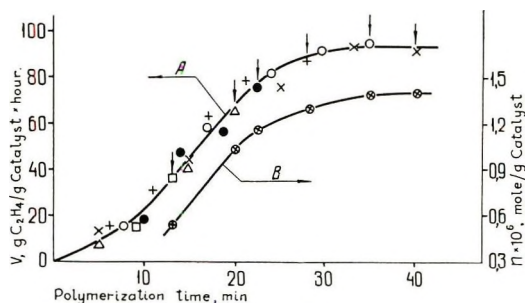


Fig. 1. Change of (A) polymerization rate and (B) number of propagation centers with reaction time (catalyst I, 75°C, 15 kg/cm<sup>2</sup>). Various symbols are used for different runs. Arrows indicate the moment of inhibitor injection in every run.

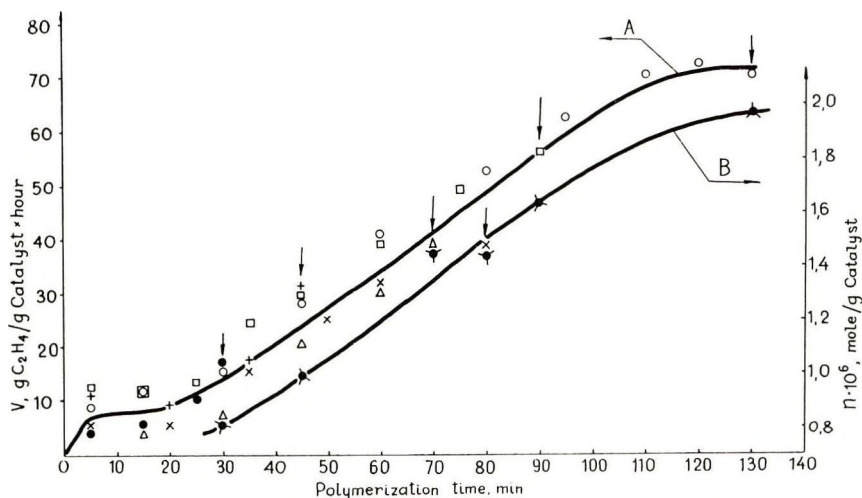


Fig. 2. Change of (A) polymerization rate and (B) number of propagation centers with reaction time (catalyst II, 75°C, 15 kg/cm<sup>2</sup>). Various symbols are used for different runs.

TABLE II  
 $n$  and  $K_p$  for Different Reaction Times<sup>a</sup>

Run	Reaction time, min	Reaction rate at injection of inhibitor, g C <sub>2</sub> H <sub>4</sub> /g catalyst-hr	Polymer yield, g	$n \times 10^6$ , mole/g	$K_p \times 10^{-6}$ , l./mole-hr
9-VI	13.0	36.0	0.46	0.55	2.32
3-II	20.0	65.5	1.60	1.05	2.20
10-V	22.5	75.0	1.80	1.15	2.34
5-V	28.0	86.0	2.73	1.27	2.42
20-II	35.0	95.0	4.05	1.37	2.48
2-II	40.0	90.0	5.00	1.40	2.27

<sup>a</sup> Conditions: 0.1 g catalyst I; 75°C; 15 kg/cm<sup>2</sup>.

the increase of the number of propagation centers. In our experiments, after a period of an acceleration of the reaction of a duration dependent on the catalyst composition and the reaction parameters, a constant polymerization rate was achieved. The propagation rate constants calculated on the basis of  $n$  values for different polymerization moments were independent of the reaction time and polymer yield within experimental error and were characteristic of the catalyst composition (Tables II and III).

The influence of the ethylene concentration in the pressure range 2–25 kg/cm<sup>2</sup> on the polymerization rate, the propagation rate constant, and the number of active centers was studied for the chromium oxide catalyst on

 TABLE III  
 $n$  and  $K_p$  for Different Reaction Time<sup>a</sup>

Run	Weight of catalyst, g	Reaction time, min	Reaction rate at the injection of inhibitor, g C <sub>2</sub> H <sub>4</sub> /g catalyst-hr	Polymer yield, g	$n \times 10^6$ , mole/g	$K_p \times 10^{-6}$ , l./mole-hr
3	0.109	30	17	0.95	0.81	0.75
11	0.183	45	31	2.70	0.99	1.12
6	0.103	70	39	3.05	1.45	0.96
8	0.103	80	38	3.20	1.45	0.92
4	0.113	90	56	5.91	1.63	1.23
9	0.104	130	71	10.43	1.97	1.29
14	0.10	25	24	0.29	0.73	1.19
16	0.10	35	32	1.35	1.40	0.81
13	0.10	37	33.5	1.38	1.28	0.94
17	0.10	50	46	2.86	1.80	0.91
18	0.10	70	67	4.75	2.00	1.21

<sup>a</sup> Conditions: catalyst II; 75°C; 15 kg/cm<sup>2</sup>; 1st series; runs 3–4; 2nd series; runs 13–18.

silica. Figure 3 shows the kinetic curves for one of the experimental series. Figure 4 shows the dependence of the steady polymerization rate on monomer concentration. These data were obtained both for different experiments at various ethylene pressure and for a single experiment in which the pressure was decreased stepwise after the achievement of a steady-stage rate period. The steady-stage polymerization rate was found to be directly proportional to the pressure of ethylene. The number of

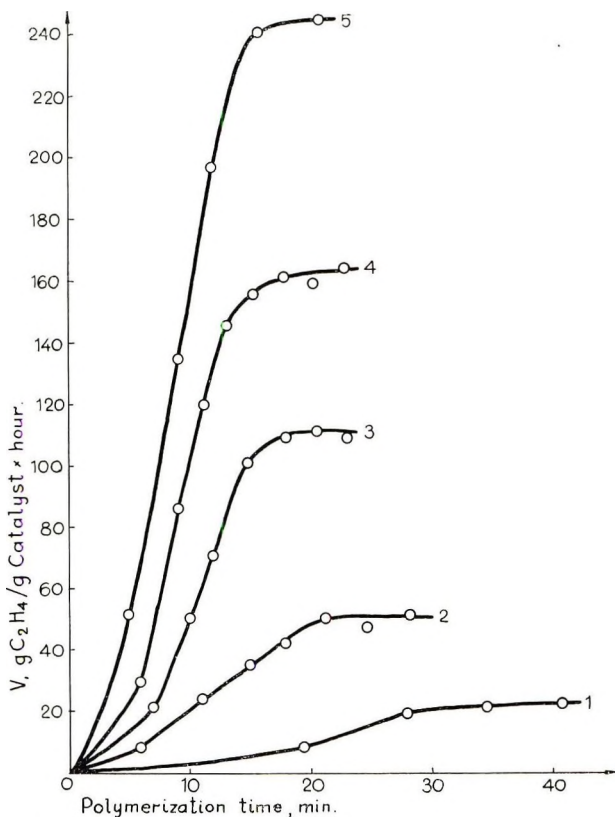


Fig. 3. Kinetic curves for runs at different ethylene pressures (catalyst I, 75°C): (1) 2 kg/cm²; (2) 5 kg/cm²; (3) 10 kg/cm²; (4) 15 kg/cm²; (5) 25 kg/cm².

active centers was measured, and the propagation rate constants were calculated for various monomer concentrations (Table IV);  $K_p$  values calculated according to eq. (3) were constant and not dependent on ethylene pressure. The stationary concentrations of active centers corresponding to the steady-stage polymerization rate were calculated on the basis of  $K_p$  values. These concentrations proved to be independent of the pressure in the considered range (see Fig. 5).

The influence of reaction temperature on the polymerization rate, concentration of active centers, and propagation rate constant was investi-

gated at 40–90°C. During these experiments the monomer concentration in benzene was maintained constant by changing pressure according to ethylene solubility in benzene.<sup>4</sup> Figures 6–8 show kinetic curves for some

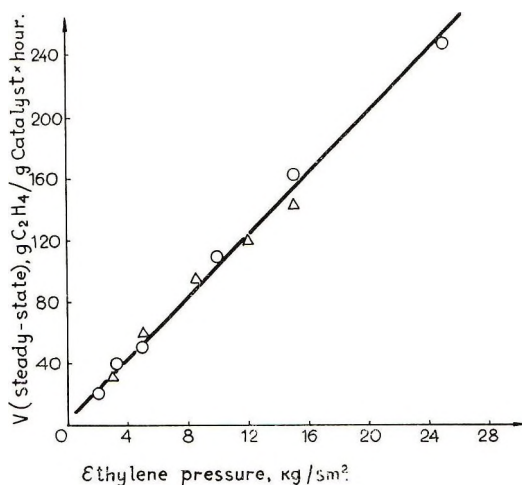


Fig. 4. Steady-state polymerization rate at different monomer concentrations (catalyst I, 75°C): (—O—) runs carried out at different monomer pressures; (— $\Delta$ —) experiment with stepwise pressure decrease.

experimental series performed at various temperatures with different chromium oxide catalysts. At 40–75°C the polymerization rate increases with temperature, but above 75°C the polymerization rate becomes slower.

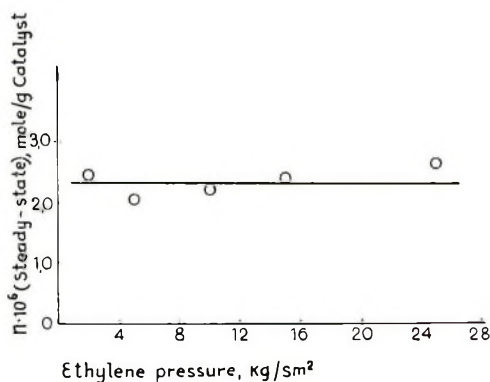


Fig. 5. Stationary concentration of propagation centers at different ethylene pressures (catalyst I, 75°C).

The overall activation energy of polymerization ( $E_{ov}$ ) was calculated from Arrhenius plots for the steady-state polymerization rate at 40–75°C (Figs. 9–11). For various polymerization temperatures,  $K_p$  values were determined (Tables V–VII). The activation energies of propagation reaction



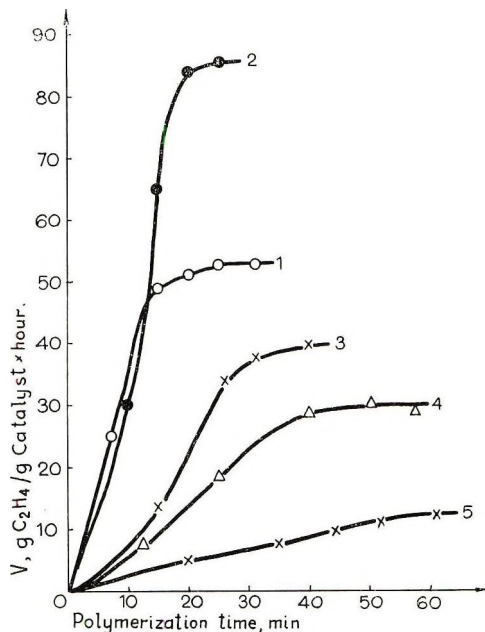


Fig. 6. Kinetic curves for runs at different polymerization temperatures (catalyst I,  $C_m = 0.95$  mole/l.) (1) = 90°; (2) = 75°; (3) = 60°; (4) = 50°; (5) = 40°.

( $E_p$ ) were calculated from Arrhenius plots for the propagation rate constants (Figs. 9–11).  $E_{ov}$  and  $E_p$  thus obtained are given in Table VIII.

Figure 12 shows the dependence of stationary concentration of the propagation centers on the reaction temperature for the catalysts of different composition. One can see that at 40–90°C the steady-state number of

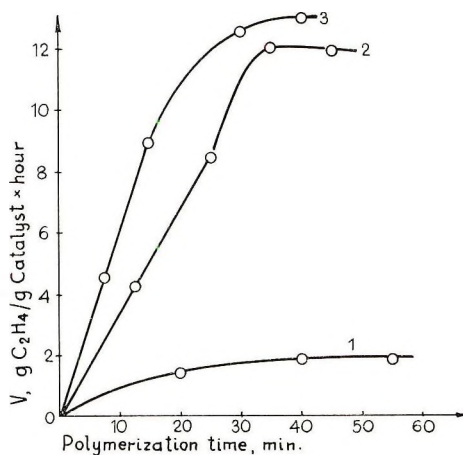


Fig. 7. Kinetic curves for runs at different polymerization temperatures (catalyst III,  $C_m = 0.95$  mole/l.): (1) 50°C; (2) 75°C; (3) 90°C.

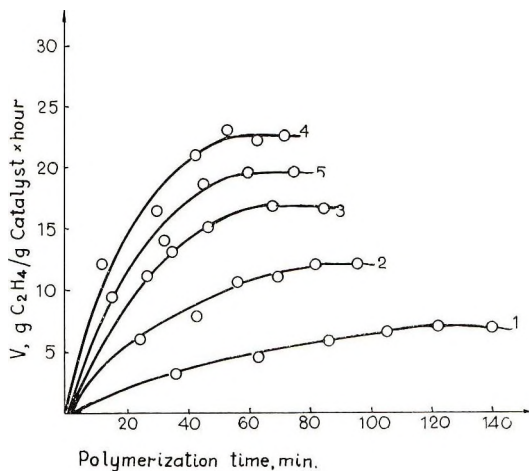


Fig. 8. Kinetic curves for runs at different polymerization temperatures (catalyst III, reduced by carbon monoxide;  $C_m = 0.95$  mole/l.): (1) 40°C; (2) 50°C; (3) 60°C; (4) 75°C; (5) 90°C.

active centers becomes higher with temperature. The temperature dependence of the polymerization rate was also determined in a single run by decreasing the temperature stepwise after the achievement of a steady-

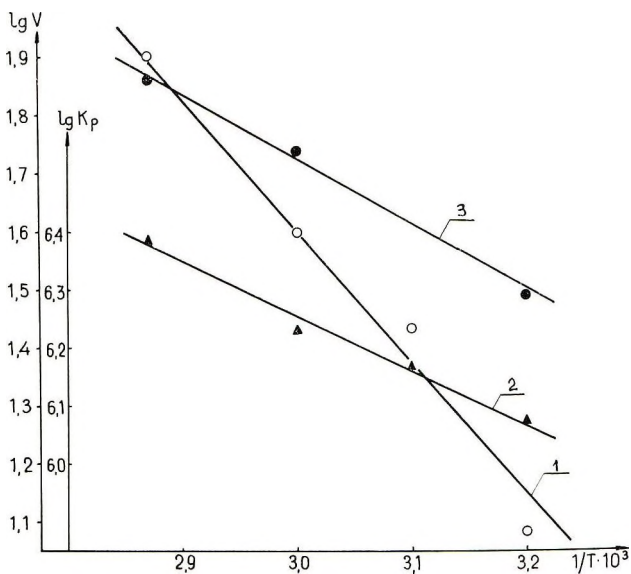


Fig. 9. Arrhenius plots for steady-state polymerization rates and propagation rate constant (catalyst I,  $C_m = 0.95$  mole/l.): (1) dependence of polymerization rate on temperature, changed from run to run,  $E_{ov} = 10$  kcal/mole; (2)  $K_p$  dependence on temperature,  $E_p = 4.2$  kcal/mole; (3) dependence of polymerization rate when temperature change in single run,  $E = 4.6$  kcal/mole.

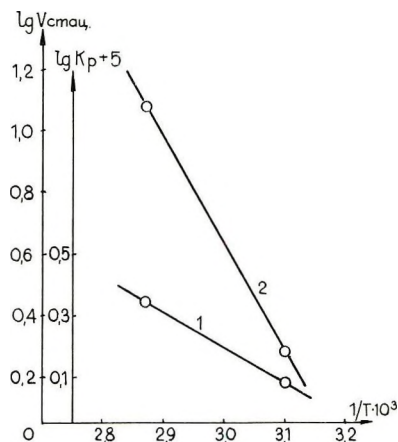


Fig. 10. Arrhenius plots for (1) propagation rate constant and (2) steady-state polymerization rate (catalyst III,  $C_m = 0.95$  mole/l.);  $E_p = 5.4$  kcal/mole;  $E_{ov} = 1.6$  kcal/mole.

state polymerization rate. The dependence thus obtained differs from that found for the case when the reaction temperature was changed from run to run (Figs. 13 and 9, curves 1 and 3). The activation energy calculated on the basis of the data obtained in a single polymerization run was  $4.6 \pm 1$  kcal/mole.

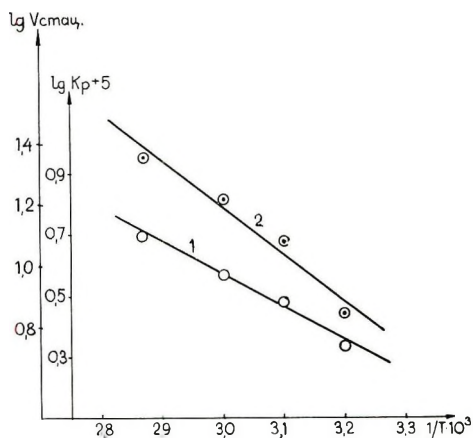


Fig. 11. Arrhenius plots for (1) propagation rate constant and (2) stationary polymerization rate (catalyst III, reduced by carbon monoxide;  $C_m = 0.95$  mole/l.);  $E_p = 4.7$  kcal/mole  $E_{ov} = 6.5$  kcal/mole.

TABLE IV  
 $n$  and  $K_p$  for Various Ethylene Pressures<sup>a</sup>

Run	Ethylene pressure, kg/cm <sup>2</sup>	Catalyst concentration, g/l	Reaction rate at injection of inhibitor, g C <sub>2</sub> H <sub>4</sub> /g catalyst-hr	$n \times 10^6$ , mole/g	$K_p \times 10^{-6}$ , l./mole-hr	$K_p \times 10^{-6}$ , l./hr
14-VI	2	2.6	21.5	2.48	2.31	0.29
11-VI	5	1.3	50	2.04	2.63	0.88
10-VI	10	1.3	102	2.03	2.68	1.78
16-VI	15	1.3	160	2.38	2.40	2.53
13-VI	25	0.7	242	2.65	2.01	3.31

<sup>a</sup> Conditions: catalyst I; 75°C.
 TABLE V  
 $n$  and  $K_p$  for Different Temperatures of Polymerization<sup>a</sup>

Run	Temperature, °C	Reaction rate at injection of inhibitor, g C <sub>2</sub> H <sub>4</sub> /g catalyst-hr	$n \times 10^6$ , mole/g	$K_p \times 10^{-6}$ , l./mole-hr	$K_p \times 10^{-6}$ , (average value), l./mole-hr
6-V	90	53.3	1.30	1.53	—
28-V	90	55.0	1.95	1.02	
31-V	75	121.0	1.82	2.48	2.40
5-V	75	86.0	1.27	2.42	
10-V	75	75.0	1.15	2.34	
9-V	75	36.0	0.54	2.39	
12-V	60	38.0	0.83	1.63	1.68
25-V	60	22.0	0.46	1.72	
8-V	50	24.0	0.64	1.35	1.48
14-V	50	30.0	0.65	1.65	
16-V	50	9.5	0.24	1.45	
13-V	40	11.3	0.30	1.38	1.20
27-V	40	8.5	0.30	1.02	

<sup>a</sup> Conditions: Catalyst I;  $C_m = 0.95$  mole/l.

TABLE VI  
 $n$  and  $K_p$  for Different Temperatures of Polymerization<sup>a</sup>

Run	Temperature of polymerization, °C	Reaction rate at injection of inhibitor, g C <sub>2</sub> H <sub>4</sub> /g catalyst-hr	$n \times 10^6$ , mole/g	$K_p \times 10^{-6}$ , l./mole-hr	$K_p \times 10^{-6}$ , (average value), l./mole-hr
3-V	90	13.0	2.42	0.21	—
29-V	90	15.5 <sup>b</sup>	2.36	0.24	
1-V	75	10.0	1.88	0.19	0.22
2-V	75	12.0	1.72	0.25	
9-V	75	12.0	1.86	0.23	
4-V	50	7.0 <sup>b</sup>	1.90	0.13	0.12
18-V	50	2.0	0.46	0.15	
11-V	50	1.6	0.67	0.09	

<sup>a</sup> Conditions: catalyst III;  $C_m = 0.95$  mole/l.<sup>b</sup> Experiments from other series.
 TABLE VII  
 $n$  and  $K_p$  for Different Temperatures of Polymerization<sup>a</sup>

Run	Temperature of polymerization, °C	Reaction rate at injection of inhibitor, g C <sub>2</sub> H <sub>4</sub> /g catalyst-hr	$n \times 10^6$ , mole/g	$K_p \times 10^{-6}$ , mole/hr	$K_p \times 10^{-6}$ , (average value), l./mole-hr
20-V	90	19.0	1.59	0.44	—
22-V	75	27.0 <sup>b</sup>	1.76	0.54	0.50
24-V	75	16.0 <sup>b</sup>	1.20	0.48	
19-V	75	22.0	1.65	0.48	
23-V	60	18.0	1.74	0.37	0.37
25-V	50	11.2	1.25	0.32	0.30
26-V	50	4.5 <sup>b</sup>	0.58	0.28	
21-V	40	6.9	1.18	0.21	0.21

<sup>a</sup> Conditions: Catalyst III; reduced monoxide;  $C_m = 0.95$  mole/l.<sup>b</sup> Experiments from other series.
 TABLE VIII  
 Activation Energies for Chromium Oxide Catalysts of Different Compositions

	Catalyst I	Catalyst II	Catalyst III (reduced by carbon monoxide)
$E_{00}$ , kcal/mole	$10 \pm 1$	16	6.5
$E_p$ , kcal/mole	$4.2 \pm 0.5$	$5.4 \pm 1$	$4.7 \pm 1$



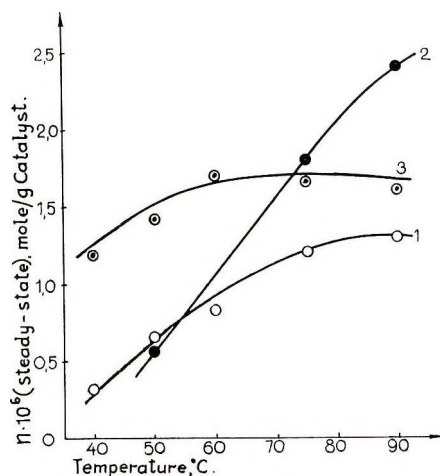


Fig. 12. Dependence of steady-state concentration of propagation centers on polymerization temperature for different chromium-oxide catalysts ( $C_m = 0.95$  mole/l.): (1) catalyst I, (2) catalyst III; (3) catalyst III, reduced by carbon monoxide.

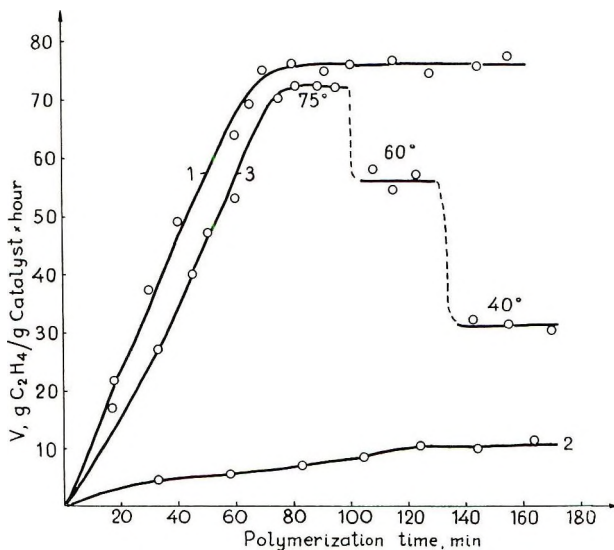


Fig. 13. Kinetic curves for runs at different polymerization temperatures (catalyst I,  $C_m = 0.95$  mole/l.): (1) 75°C; (2) 40°C; (3) experiment with stepwise temperature decrease.

## DISCUSSION

### Possibility of Quantitative Determination of $n$ and $K_p$

The determination of the number of propagation centers by the quenching technique with the use of a radioactive inhibitor is possible when the interaction between an inhibitor and propagation centers is of a quantita-

tive character. The occurrence of a reaction in the kinetic region provides a possibility of  $K_p$  calculation from the polymerization rate and the number of propagation centers. Dissolving ethylene was not a rate-controlling step. In our case the steady-stage polymerization rate per gram of catalyst did not depend on the catalyst concentration in a solvent.

For the catalysts of the same chemical composition the following factors did not influence the propagation rate constant (within possible experimental errors): (1) quantity of inhibitor injected (provided there is complete stopping of the polymerization; the quantity of methanol- $^{14}\text{C}$  used for quenching varied from  $1 \times 10^{-4}$  to  $1 \times 10^{-3}$  mole/g of catalyst); (2) catalyst concentration in a solvent (from 0.6 to 4.0 g/l. in our experiments); (3) polymerization duration up to quenching (from 13 to 130 min); (4) polymerization rate (and the number of propagation centers) at the moment of inhibitor injection (the polymerization rate varied from 17 to 150 g  $\text{C}_2\text{H}_4$ /g catalyst-hr and the number of propagation centers for catalyst I varied from 0.5 to  $2.5 \times 10^{-6}$  mole/g); (5) pore structure of a support (as proved by using two types of silica with surface areas of 400 and 200  $\text{m}^2/\text{g}$  and two types of silica-alumina with surface areas of 300 and 400  $\text{m}^2/\text{g}$ ); (6) initial dimensions of catalyst particles (fractions of silica-alumina less than 0.1 mm and 0.25–0.5 mm were studied); (7) physical state of the reaction medium;  $K_p$  did not depend on whether polymerization took place in a liquid (benzene) or in a gas phase (without solvent).

At 75°C the average value of the propagation rate constant was  $1 \times 10^6$  l./mole-hr (catalyst II) and  $2.5 \times 10^6$  l./mole-hr (catalyst I) when silica-alumina and silica were used as supports, respectively. The constancy of the  $K_p$  value should be taken as a reason in favor of the quantitative character of the measurement of the number of propagation centers for investigated catalytic systems.

Within the temperature range up to 75°C the polymerization process is not limited by diffusion of monomer from the volume to the propagation centers on the surface of a catalyst; it follows from the fact that the polymerization rate per propagation center (that is,  $K_p$  value) does not depend on concentration of propagation centers or catalyst particle size.

When diffusion influences the polymerization rate, the change of calculated  $K_p$  with variation of time, with the number of propagation centers, and with an overall polymerization rate should be expected.<sup>5-7</sup> The consideration of the role of mass and heat transfer in ethylene catalytic polymerization<sup>8</sup> also illustrates that the diffusion of monomer to propagation centers on the catalyst surface does not control the overall polymerization rate while porous grains of insoluble polymer are being formed.

The data obtained at 90°C when a low molecular part of polyethylene is likely to be soluble indicate the diffusional restrictions at this temperature. The polymerization rate at 90°C is less than at 75°C, while the number of propagation centers either increases or remains constant. As a consequence the calculated  $K_p$  value at 90°C is lower than at 75°C. We assume this phenomenon to be caused by a decrease of the monomer con-

centration below equilibrium in the environment of an active center. Therefore for the calculation of activation energies only the data obtained at 40–75°C were used; these data were not effected by diffusion of ethylene.

### Proportion of "Working" Chromium

The number of propagation centers on chromium oxide catalysts measured in our experiments under different conditions was  $0.3 \times 10^{-6}$ – $2.5 \times 10^{-6}$  mole/g of catalyst. It is easy to calculate from these data that only a small part of chromium was active. In the experiments described this part approached 0.5% of the total content of chromium in a catalyst (a propagation center is assumed to involve one chromium atom).

Possible reasons of the low concentration of propagation centers of chromium oxide catalysts may be the following: (a) a low content of initial surface compound (active component) whose interaction with reaction medium produces propagation centers; (b) a low yield of propagation centers in the initiation process; (c) effective surface of catalyst is only a small part of the total surface area of the support; (d) inhibition by the impurities in reaction medium.

It is difficult to evaluate the relative importance of the reasons just mentioned, but it should be pointed out that the catalytic activity and therefore the proportion of "working" chromium depends to a great extent on the presence of poisons. A significant increase of polymerization rate and a polymer yield were observed when pure raw materials were used. Naturally, a catalyst will have maximum activity when all the chromium atoms deposited on a catalyst are involved in propagation centers. The value of maximum catalytic activity can be calculated by using the values of propagation rate constant found. For the chromium oxide catalyst on silica at 75°C and monomer concentration of 1 mole/l. (15 kg/cm<sup>2</sup> in cyclohexane) this value is  $1.4 \times 10^6$  g of polyethylene/g of chromium per hour or  $33.5 \times 10^3$  g of polyethylene/g catalyst per hour for catalyst with 2.5% chromium content.

The polymerization of ethylene with chromium oxide catalyst is as usual a nonsteady-state process. An acceleration period of the reaction is followed by a constant polymerization rate after which the latter decreases. In some cases a steady-state period was not observed: the kinetic curves showed a maximum.<sup>4,9</sup> Our data on the measurements of the number of propagation centers at different polymerization times (Figs. 1 and 2) showed that an increase of polymerization rate with time is determined by an increase in the number of propagation centers and the steady-state period on kinetic curve is due to establishing a stationary concentration of propagation centers. To explain the increase in the number of propagation centers with polymerization time the following reasons should be mentioned: (a) a low rate of the initiation process; (b) an increase of the effective surface area of a catalyst due to its disintegration.

Besides, there is a possibility of a decrease in catalyst activity and in the proportion of "working" chromium due to the inhibiting effect of impurities.

In the case of supported oxide catalysts the polymerization rate and its time dependence seem to be determined by simultaneous interference of all the three processes. Depending on the conditions of polymerization process, the method of catalyst preparation, chemical composition of catalyst, and structure of the support, the relative importance of these processes can vary so governing different forms of kinetic curves for various cases of polymerization.

### Dependence of Propagation Rate on Monomer Concentration

Our measurements of the number of propagation centers at different ethylene pressures show that for the propagation stage an equation of first order on monomer concentration (and of overall second order) is valid. The  $K_p$  values calculated for different runs on the basis of eq. (3) are constant ( $2.4 \times 10^6 \pm 15\%$  l./mole-hr, see Table IV). As calculated from the equation

$$V = K_p' C_p \quad (4)$$

i.e., on the assumption of a zero order equation on monomer,  $K_p$  values vary from  $0.28 \times 10^6$  to  $3.3 \times 10^6$  l./hr.

The stationary concentration of propagation centers experimentally determined does not depend on monomer concentration in the pressure range from 2 to 25 kg/cm<sup>2</sup> (Fig. 4), and the overall polymerization rate is proportional to monomer concentration. The reaction is of the same order on monomer both when ethylene pressure is changed from one run to another and when monomer pressure is changed in the course of a single run after approaching a steady-state polymerization rate. These results show that at a constant temperature an initiation process proceeds up to establishing a definite stationary state of catalyst, regardless of the monomer concentration. According to the data of Clark and Bailey<sup>10</sup> at the higher ethylene concentration a polymerization rate does not depend on ethylene pressure; propagation reaction in this case is likely to be of a zero order on monomer concentration and is governed by eq. (4).

### Influence of Polymerization Temperature on Kinetic Parameters of Propagation Reaction

From the temperature dependence of the overall polymerization rate the overall activation energy ( $E_{ov}$ ) can be calculated. As usual, this value differs from the activation energy of the propagation stage ( $E_p$ ). The coincidence between  $E_{ov}$  and  $E_p$  is possible only in the case when a temperature dependence of polymerization rate is determined only by variation of  $K_p$  and the concentration of propagation centers remains unchanged



with temperature. For catalytic polymerization processes the temperature as a rule influences the number of active centers, and  $E_p$  may be found only from a temperature dependence of the propagation rate constant. For chromium oxide catalyst activated *in vacuo*  $E_p$  differs from  $E_{ov}$  (Table VIII). This difference is caused by the dependence of the concentration of propagation centers on polymerization temperature (Fig. 12, curves 1 and 2). The character of this dependence changes with variation of catalyst composition. The value of effective activation energy for chromium oxide catalysts changes when different supports are used (silica or alumina). The dependence of  $n$  on the reaction temperature may be explained on the assumption that the formation of propagation centers occurs as a result of reduction of chromium in an active component with ethylene. The difference between temperature dependencies on  $\text{SiO}_2$  and  $\text{Al}_2\text{O}_3$  is caused by the difference in stability of  $\text{Cr}^{+6}$  compounds on the surface of these supports. It was shown<sup>11</sup> that one expects an increase in the ability of surface chromate-type compounds to undergo reduction when electronegativity of the carrier cation increases. So in the case of  $\text{SiO}_2$  a deeper reduction degree of  $\text{Cr}^{+6}$  is possible than in the case of  $\text{Al}_2\text{O}_3$ . This was observed elsewhere.<sup>12</sup>

The role of reduction in the formation of propagation centers is proved by a comparison of catalyst prepared on the same support and activated in vacuum (system II) with one reduced with carbon monoxide (system III). A preliminary reduction of catalyst with carbon monoxide nearly excludes the influence of polymerization temperature on the number of propagation centers (Fig. 12, curves 2 and 3); the overall activation energy becomes 6.5 kcal/mole instead of 16 kcal/mole.

The oxidation number of chromium in the catalyst reduced by CO at 300°C is not more than 3. In the case of catalyst reduced with ethylene at polymerization temperatures the oxidation number is more than 3 and increases when the reduction temperature decreases; for example, in catalyst I reduced with ethylene at 75°C for 90 min the oxidation number of chromium is 3.37; for the reduction 40°C the oxidation number is 3.70. So the preliminary reduction of chromium oxide catalyst may result in an increase in the active center concentration in comparison with the vacuum-treated catalyst when the polymerization temperature is not high enough for the deep reduction of initial chromium compounds with ethylene. For catalyst II, the increase of the number of the active centers as a result of the preliminary reduction occurs at polymerization temperatures less than 70°C (see Fig. 12, curves 2 and 3).

If the formation of the propagation centers is an irreversible reaction, it is possible to avoid the influence of temperature on the number of propagation centers by determining the dependence of the steady-state polymerization rate on temperature in a single run. In this case, the value of the activation energy should correspond to the  $E_p$  value. The results of



the determination of activation energy with variation of temperature in the same run show (Figs. 13 and 9) that the value thus obtained ( $\sim 4.6$  kcal/mole) differs considerably from the overall activation energy and coincides fairly well with the activation energy of the propagation stage.

It is known<sup>4,10,13</sup> that the chromium oxide catalyst is very active at 110–140°C. As is seen from our data, the overall rate decrease at 90°C is not due to a decrease in the number of active centers but is caused by diffusion restrictions. At higher temperatures (above 110°C) polyethylene is soluble in a hydrocarbon solvent; in this case, diffusion seems to vanish.

## CONCLUSIONS

The method of quenching the polymerization by methanol labeled in the alkoxy group seems to have a successful application in the study of oxide catalysts. This technique gave valuable information on the reasons for the change of the polymerization rate with reaction conditions.

For the typical Ziegler-Natta catalysts the applicability of an alcohol quenching technique is restricted<sup>5,6,14,15</sup> as the total number of metal-polymer bonds is determined when polymerization is stopped by alcohol labeled with tritium in the hydroxyl group. Some of these metal-polymer bonds are inactive, so the quantitative determination of the propagation centers becomes ambiguous.

The typical Phillips polymerization catalysts are one-component systems, and all the catalyst-polymer bonds are active. The determination of the number of these bonds makes it possible to give important characteristics of the propagation center—the rate constant of the propagation stage—and thus to obtain real kinetic parameters for one of the elementary stages of the catalytic polymerization.

## References

1. V. A. Zakharov, Yu. I. Ermakov, E. G. Kushnareva, and V. A. Balashov, *Vysokomol. Soedin.*, **9B**, 173 (1967).
2. Yu. I. Ermakov, V. A. Zakharov, paper presented at the IVth International Congress on Catalysis, Moscow, 1968; preprint 16.
3. V. A. Zakharov, Yu. I. Ermakov, and E. G. Kushnareva, *Kinetikai Kataliz.*, **8**, 1391 (1967).
4. V. R. Gurevich, M. A. Dalin, and K. M. Arutyunova, *Azerbaizhan Khim. Zh.*, **1964**, No. 4, 69.
5. C. F. Feldman and E. Perry, *J. Polym. Sci.*, **46**, 217 (1967).
6. G. Bier, W. Hoffman, G. Lehman and G. Seydel, *Makromol. Chem.*, **58**, 1 (1962).
7. E. A. Youngman and J. Boor, *J. Polym. Sci. B*, **4**, 913 (1966).
8. Yu. I. Ermakov, et al., *Plasticheskie massy*, **1970**, No. 9, 7.
9. Yu. I. Ermakov and L. P. Ivanov, *Kinetikai Kataliz*, **8**, 357 (1967).
10. A. Clark and G. Bailey, *J. Catal.*, **2**, 241, (1963).
11. G. D. Kolovertnov, Thesis, Novosibirsk, 1966.
12. K. G. Miessero, *Neftekhim.*, **2**, 681 (1962).
13. A. Clark, *Ind. Eng. Chem.*, **59**, 29 (1967).

14. E. Kohn, H. Schuurmas, I. V. Cavender, and R. A. Mendelson, *J. Polym. Sci.*, **52**, 681 (1962).

15. H. W. Coover, in *Macromolecular Chemistry, Paris 1963* (*J. Polym. Sci. C*, **4**), M. Magat, Ed., Interscience, New York, 1964, p. 1511.

Received October 2, 1969

Revised June 18, 1971

## Polysulfone-Polydimethylsiloxane Block Copolymers

A. NOSHAY, M. MATZNER, AND C. N. MERRIAM, *Chemicals and Plastics, Union Carbide Corporation, Bound Brook, New Jersey 08805*

### Synopsis

Alternating block copolymers have been synthesized from dihydroxyl-terminated polysulfone and bis(dimethylamine)-terminated polydimethylsiloxane oligomers. The products are soluble, amorphous, and transparent, and display excellent thermal and hydrolytic stability. Elastomeric and rigid compositions can be prepared by varying oligomer molecular weight. Copolymers made with oligomers of  $>5000$  molecular weight are two-microphase systems which display glass transition temperatures at  $-120^{\circ}\text{C}$  and at  $+160^{\circ}\text{C}$ , and therefore have a wide useful temperature range.

### INTRODUCTION

The interesting and useful properties of two-phase block copolymers such as the styrene-diene block copolymers are well documented.<sup>1</sup> However, from a practical standpoint, the utility of these materials is limited by the relatively low glass transition temperature of the polystyrene segments and by the poor stability of the unsaturated polydiene blocks. Polysulfone-polydimethylsiloxane block copolymers have now been synthesized which overcome both of these drawbacks. Polysulfone has a high glass transition temperature<sup>2-5</sup> and both polysulfone and polydimethylsiloxane are very stable.<sup>2-6</sup>

The synthesis and properties of bisphenol A polycarbonate-polydimethylsiloxane block copolymers have been reported.<sup>7-11</sup> The polysulfone-polydimethylsiloxane block copolymers are superior to these materials in elevated temperature properties due to the higher glass transition temperature of polysulfone ( $190^{\circ}\text{C}$ )<sup>2-5</sup> as compared to that of bisphenol A polycarbonate ( $150^{\circ}\text{C}$ ).<sup>7-11</sup>

The polycarbonate-siloxane copolymers are synthesized by the phosgenation of a mixture of bisphenol A and a bisphenol A-capped siloxane oligomer. Three different types of carbonate-forming condensation reactions take place simultaneously: (1) bisphenol A-bisphenol A, which builds up the polycarbonate blocks; (2) polycarbonate-siloxane, which forms the bridge between blocks; and (3) siloxane-siloxane, which in effect increases the siloxane oligomer molecular weight. The net result is that the block structure of the copolymer product is uncertain. In contrast to this, the polysulfone-polydimethylsiloxane block copolymers are synthesized from preformed, characterized oligomers bearing different, mutually reactive endgroups. Therefore, the block structure of these materials is

well defined and strictly controlled. The average molecular weight and the polydispersity of the segments of the block copolymer are the same as those of the parent oligomeric starting materials.

The following is a discussion of the synthesis, stability, morphology, and wide-ranging mechanical properties of polysulfone-polydimethylsiloxane block copolymers.

## EXPERIMENTAL

### Oligomers

Polysulfone is synthesized from the disodium salt of bisphenol A and dichlorodiphenylsulfone in chlorobenzene-dimethyl sulfoxide solution.<sup>2-5</sup> The dihydroxyl-terminated oligomers used in this work were prepared by this procedure, by using excess bisphenol A disodium salt, followed by neutralization with oxalic acid. Oligomers of varying  $\bar{M}_n$ , as measured by potentiometric end group titration, were prepared by using different ratios of the two monomers. A typical synthesis follows.

Bisphenol A (113 g, 0.495 mole), 450 ml of chlorobenzene, and 450 ml of dimethylsulfoxide were heated to 100°C. A solution of 39.6 g (0.99 mole) of NaOH in 45.0 ml of H<sub>2</sub>O was added, and water was removed by azeotropic distillation. When the pot temperature reached 178°C, 73 ml of H<sub>2</sub>O and 458 ml of solvent had distilled out. The temperature was reduced to 145°C, and a solution of 129.2 g (0.45 m.) of dichlorodiphenylsulfone in 240 ml. of chlorobenzene (kept at 75°C) was added. The pot temperature was raised to 165°C to remove the last traces of H<sub>2</sub>O (160 ml of moist solvent distilled off). The temperature was then again reduced to 145°C and maintained at that level for 3 hr. It was then raised to 174°C, during which time most of the remaining chlorobenzene (57 ml) was removed. After cooling the reaction solution to room temperature and diluting with 120 ml of dimethylsulfoxide, the product was neutralized and coagulated with a solution of 60 g of oxalic acid in 3000 ml of H<sub>2</sub>O. The filtered product was slurried for 8 hr with a solution of 1.5 g of oxalic acid in 400 ml of H<sub>2</sub>O, and then was water-washed four times. The product (206.8 g; 98.8% yield) was an off-white powder which had an  $\bar{M}_n$  of 4700.  $\bar{M}_n$  was determined by the potentiometric titration of 0.5–1.0 g of sample in 50 ml of pyridine with a 0.025*N* solution of tetrabutylammonium hydroxide in 90/10 benzene-methanol by use of a Metrohm Potentiograph E336.\*

The bisdimethylamine-terminated polydimethylsiloxane oligomers used in this work were kindly supplied by Mr. T. C. Williams of the Silicones Department of Union Carbide Corporation.

### Polysulfone-Polydimethylsiloxane Block Copolymers

The block copolymers are synthesized by reacting the above oligomers in chlorobenzene (preferably) or in tetrahydrofuran solution at tempera-

\* This analytical procedure was developed by Mr. R. C. Hazelton of these laboratories.

tures ranging from ambient to 120°C. Both of these solvents form azeotropes with water, which allows the system to be dehydrated before addition of the siloxane oligomer. Dehydration is important, since water can react with the amine end groups of the siloxane oligomers. The following is an example of a typical block copolymer synthesis from a 4700  $\bar{M}_n$  polysulfone oligomer and a 5100  $\bar{M}_n$  polydimethylsiloxane oligomer, as determined by endgroup titration.

A four-necked, 1-liter Morton flask was fitted with a mechanical stirrer, a reflux condenser with a Drierite drying tube, an addition funnel, a thermometer, a short-path distillation take-off, and a dry nitrogen inlet. The apparatus was dried with a heat gun, and a blanket of dry nitrogen was maintained throughout the reaction. Chlorobenzene (700 ml) and 25.0 g (0.00532 mole) of a 4700  $\bar{M}_n$  polysulfone oligomer were charged to the reactor. After the oligomer dissolved, 300 ml of chlorobenzene was distilled out, after which the temperature was adjusted to and maintained at 70°C. A small excess of a 5100  $\bar{M}_n$  polydimethylsiloxane oligomer fluid (29.0 ml; 27.9 g; 0.00547 mole) was then added to the reaction solution in the following increments, at 30-min intervals: 10 ml, 5 ml, 5 ml, 3 ml, 2 ml, 2 ml, 1 ml, 1 ml. Shorter interval times may also be used. This incremental addition procedure allows the true stoichiometric endpoint to be approached gradually, thus assuring high molecular weight product.

The evolution of dimethylamine throughout the reaction was detected with moist litmus paper and by a change in the color of the Drierite (light to dark blue). There was little change in the viscosity of the reaction solution until the first 2-ml increment of siloxane was added. The viscosity then increased dramatically with each additional increment, the final viscosity being very high. One hour after addition of the final increment of siloxane, the reaction solution was cooled to room temperature and coagulated with 3 liters of methanol. The product (48.0 g, after drying overnight *in vacuo* at 80°C) was a white, fluffy material with a reduced viscosity of 0.80 (0.2 g/dl in  $\text{CH}_2\text{Cl}_2$  at 25°C). Films cast from the reaction solution, or from a 10% methylene chloride solution of the coagulated product, were colorless, transparent, flexible, and tough.

A slightly modified procedure was used to obtain the stoichiometry and reaction rate data shown in Figures 1 and 2. All of the siloxane was added in one portion in these runs. In the case of the rate experiments, aliquot samples were periodically withdrawn from the reaction solution and cast into films for reduced viscosity measurement.

## RESULTS AND DISCUSSION

### Synthesis

The polysulfone-polydimethylsiloxane block copolymers were prepared by the interaction of preformed dihydroxyl-terminated polysulfone and bisdimethylamine-terminated polydimethylsiloxane oligomers as shown in eq. (1).





The reaction was carried out in chlorobenzene or tetrahydrofuran solution at 25–120°C. The evolution of gaseous dimethylamine by-product leaves an essentially pure solution of block copolymer product. Product isolation was achieved either by solvent evaporation or by coagulation with methanol.

This reaction scheme was developed after a model study indicated that bisphenol A and 1,9-bis(dimethylamino)decamethylpentasiloxane reacted very smoothly in refluxing tetrahydrofuran to give polymers of high molecular weight. The reaction is very facile due to the high reactivity of the Si-N bonds<sup>12</sup> in the siloxane oligomer toward phenolic compounds. A somewhat similar reaction has been reported<sup>13</sup> to give polymers from dianilino silanes and bisphenols. This latter reaction, however, is carried out via a melt

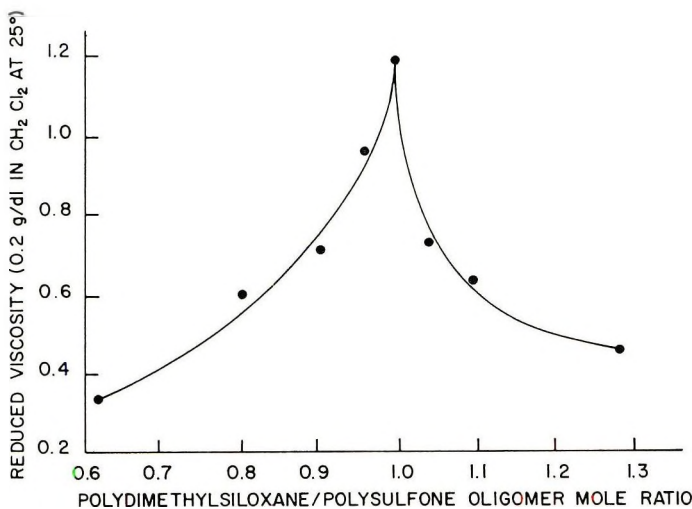


Fig. 1. Effect of stoichiometry on block copolymer molecular weight based on 4700  $\bar{M}_n$  polysulfone and 5100  $\bar{M}_n$  polydimethylsiloxane oligomers.

process at  $\sim 300^\circ\text{C}$  and is not amenable to the synthesis of block copolymers, due to oligomer incompatibility. The reaction of bisphenol A with chlorine-terminated siloxanes in the presence of pyridine was also investigated. In comparison to our preferred procedure, this technique was more sluggish, gave lower molecular weight polymer, and was not as "clean" due to the formation of pyridine hydrochloride by-product.

As can be seen from eq. (1), the block copolymers have an alternating  $\text{-(A-B)-}_n$  block sequence structure. These structures are well defined and strictly controlled, since the two oligomers can interact with each other but not with themselves. As a result, the structure of the blocks in the copolymers is identical to that of the oligomers. The structure shown in the equation is idealized. In practice, the end blocks are both polysulfone or both polydimethylsiloxane, depending on the actual final stoichiometry of the reaction.

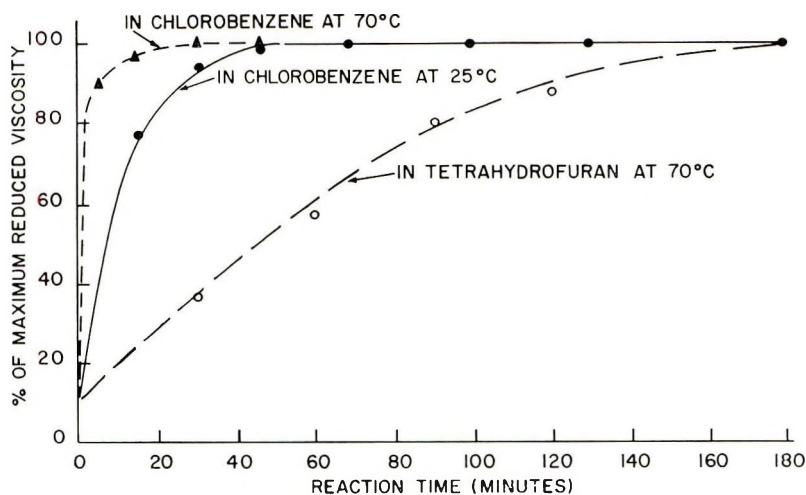


Fig. 2. Rate of block copolymer formation.

While the molecular weight and composition of the block copolymers can be varied by using stoichiometric excess amounts of either of the oligomers, maximum molecular weight is, of course, achieved at the equivalent stoichiometric point. The effect of stoichiometry on product molecular weight is illustrated in Figure 1. Since there is some degree of uncertainty in determining the exact molecular weights of the oligomers, it is more difficult to predict the stoichiometric point, *a priori*, in this system than in traditional condensation polymerizations which use low molecular weight monomeric starting materials. This problem has been circumvented by adding the siloxane oligomer to the polysulfone oligomer reaction solution slowly, in progressively smaller increments, in order to approach the stoichiometric end point gradually and thus achieve high molecular weight. Block copolymers with reduced viscosities (0.2 g/dl in methylene chloride at 25°C) as high as 1.60 dl/g have been obtained by this technique. This corresponds to a weight-average molecular weight of about 238,000, as determined by ultracentrifugation in tetrahydrofuran solution.<sup>14</sup>

The facile nature of the block copolymerization reaction is illustrated by the extremely rapid rate of reaction in chlorobenzene solution. As can be seen from the rate data in Figure 2, the maximum molecular weight level is reached almost instantaneously at a reaction temperature of 70°C. Even at 25°C, the maximum molecular weight level is achieved in only 45 min. The success of the incremental addition technique, described above, is due to this rapid rate of reaction.

The rate of copolymerization is affected by the type of reaction solvent used. Figure 2 illustrates that reaction at 70°C was much slower in tetrahydrofuran than in chlorobenzene. The reason for this effect is not entirely clear. It does not appear to be due to a difference in the degree of chain extension, and therefore endgroup availability, since the reduced

viscosities of polysulfone oligomers and block copolymers are essentially the same in both solvents, (e.g., 0.14 and 1.24, respectively in chlorobenzene vs. 0.16 and 1.31, respectively, in tetrahydrofuran). The effect may be due to hydrogen bonding of the polysulfone oligomer hydroxyl with tetrahydrofuran. This would reduce the availability of the phenolic hydrogen for hydrogen bonding with the nitrogen of the silylamine endgroups. This  $\text{—N—H}$  bonding in a solvent such as chlorobenzene would be expected to weaken the  $\text{Si—N}$  bond and make the Si more susceptible to attack by the O of the polysulfone endgroups.

### Stability

As expected from the known properties of the parent homopolymers,<sup>2-6</sup> the thermal and thermal-oxidative stability of the polysulfone-polydimethylsiloxane block copolymers were found to be very good. Thermogravimetric analysis of a block copolymer prepared from  $\sim 5000$  molecular weight polysulfone and polydimethylsiloxane oligomers gave results intermediate to those obtained with polysulfone and polydimethylsiloxane homopolymers (Fig. 3).

This block copolymer (10-mil cast film) was also aged in a circulating air oven at  $170^\circ\text{C}$  along with a commercial elastomeric polyurethane (Estane X-7) block copolymer for comparison. The polyurethane became badly discolored and crosslinked after one day. After 14 days, the polysulfone-polydimethylsiloxane block copolymer was unchanged in appearance, soluble, and had retained 90% of its initial reduced viscosity (see Fig. 4).

The polysulfone-polydimethylsiloxane block copolymers also display good hydrolytic stability, even though the segments are linked by  $\text{Si—O—C}$  bonds, which are reportedly unstable hydrolytically.<sup>15</sup> This is illustrated by Fig-

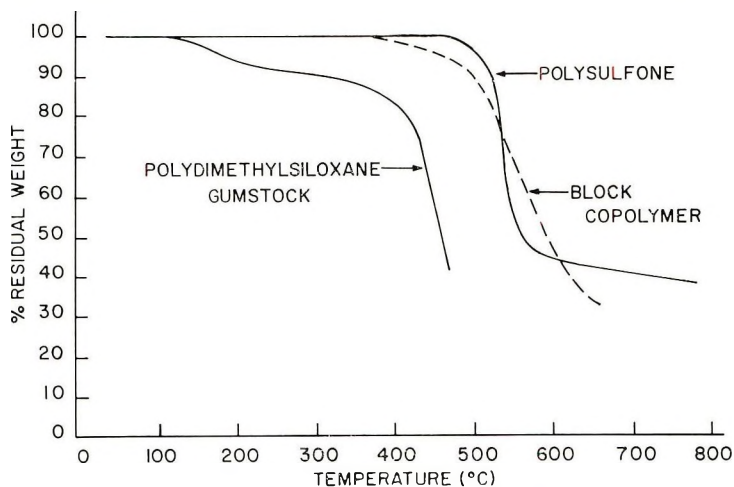


Fig. 3. TGA of polysulfone-polydimethylsiloxane block copolymer and homopolymers (in nitrogen at  $10^\circ\text{C}/\text{min}$ ).

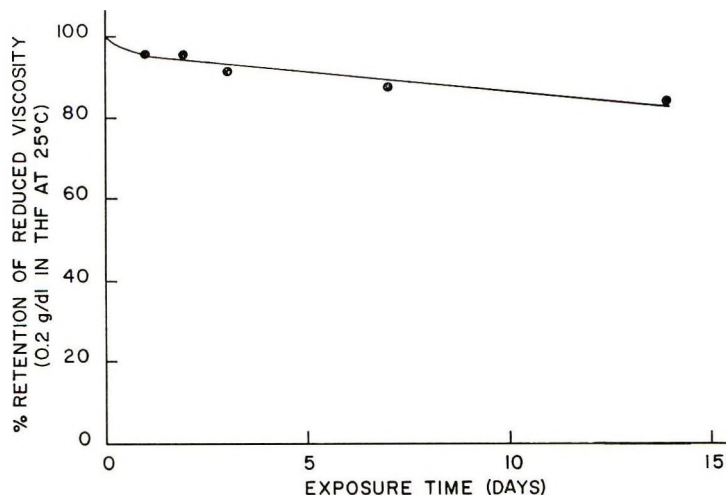


Fig. 4. Polysulfone-polydimethylsiloxane air oven aging stability at 170°C (10 mil film; initial reduced viscosity = 0.84).

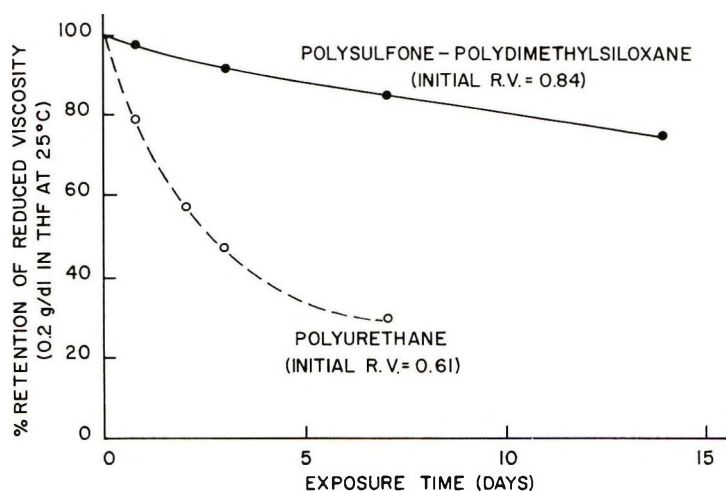


Fig. 5. Boiling water stability of 10-mil films of polyurethane and polysulfone-polydimethylsiloxane.

ure 5, which shows the superior boiling water stability of a 10-mil film of the polysulfone-polydimethylsiloxane block copolymer in comparison to that of the polyurethane control sample. This hydrolytic stability may be due, in part, to the hydrophobic nature of the block copolymer film. However, solutions of the block copolymer also exhibited good hydrolytic stability. Little or no loss in reduced viscosity was observed when wet tetrahydrofuran or chlorobenzene solutions (containing 5% water) were refluxed for 3 days. This suggests that the stability may be due to steric hindrance of the Si—O—C linkage.



TABLE I  
Environmental Stability of  
Polysulfone-Polydimethylsiloxane Block Copolymer<sup>a</sup>

Days exposed	Reduced viscosity, $\eta_{sp}/c$ retained after exposure to <sup>b</sup>			
	Water	10% NaOH	10% HCl	ASTM Oil #1
30	99	100	82	98
60	96	100	46	96

<sup>a</sup> 10-mil cast films exposed at room temperature.

<sup>b</sup> Reduced viscosity determined at 0.2 g/dl in  $\text{CH}_2\text{Cl}_2$  at 25°C. Initial reduced viscosity = 0.82.

Other environmental stability tests (see Table I) showed the block copolymer to be essentially unaffected by two months' exposure, at room temperature, to water, 10% NaOH, and ASTM oil #1. However, significant degradation did occur during exposure to 10% HCl for the same period of time.

### Properties

Block copolymers were synthesized from polysulfone oligomers of 4700 to 9300  $\bar{M}_n$  (number-average molecular weight) and polydimethylsiloxane oligomers of  $\bar{M}_n$  ranging from 350 to 25,000. The temperature-modulus curves shown in Figure 6 for the products obtained with 4700  $\bar{M}_n$  polysulfone oligomer and three of the polydimethylsiloxane oligomers illustrate the effect of siloxane block molecular weight on the morphology of the block copolymer. The 350  $\bar{M}_n$  siloxane oligomer gave a single-phase system, which had one glass transition temperature ( $T_g$ ) at 125°C, as determined from modulus and resilience measurements. A 1700  $\bar{M}_n$  siloxane oligomer produced a copolymer which showed a very small degree of phase separation, as indicated by the slight shoulder at -100°C and the major transition at +140°C. The block copolymer synthesized from the 5100  $\bar{M}_n$  siloxane oligomer displayed a high degree of phase separation (domain formation) and exhibited two very definite  $T_g$ 's, one at -120°C due to the polydimethylsiloxane phase and another at +160°C due to the polysulfone phase.

The very broad, flat modulus plateau between the two transition temperatures displayed by these two-phase block copolymers indicates that these materials have a very broad useful temperature range.

It is interesting to note that two-phase systems are obtained at such low block molecular weight levels in these amorphous copolymers (i.e., both blocks =  $\sim 5000 \bar{M}_n$ ). Much higher block molecular weights are required for domain formation in styrene-butadiene copolymers (e.g., 5,000–10,000  $\bar{M}_n$  for polystyrene and  $\sim 50,000 \bar{M}_n$  for polybutadiene).<sup>16</sup> We interpret this as being due to an inherently greater degree of polysulfone-polydimethyl siloxane incompatibility than is the case with polystyrene and polybutadiene.

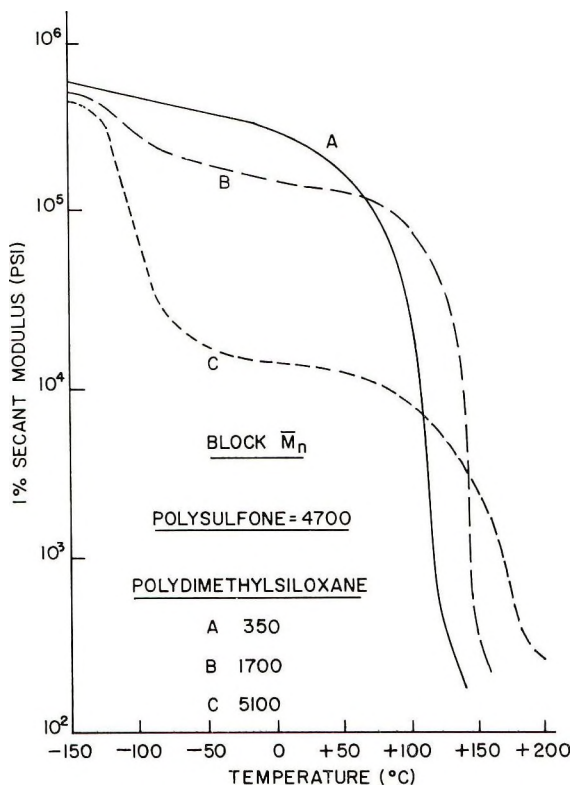


Fig. 6. Temperature-modulus curves for block copolymers of polysulfone ( $\bar{M}_n = 4700$ ) with polydimethylsiloxane: (A) polydimethylsiloxane  $\bar{M}_n = 350$ ; (B) polydimethylsiloxane  $\bar{M}_n = 1700$ ; (C) polydimethylsiloxane  $\bar{M}_n = 5100$ .

The mechanical properties of the polysulfone-polydimethylsiloxane block copolymers vary widely depending upon their composition, which in turn depends primarily on the molecular weight of the oligomers used in their synthesis. The data shown in Table II demonstrate that copolymers have been prepared which range in properties from rigid, low elongation materials to very flexible, high elongation compositions. All of the solution cast films on which these properties were measured are transparent and colorless.

The compositions of high siloxane content display substantial recovery properties and behave like crosslinked silicone rubbers, even though they are not crosslinked. This is the result of their two-phase morphology, the polysulfone domains acting as "anchor" sites to produce a pseudo physically crosslinked system. The strength of these compositions is greater than that of unfilled, crosslinked silicone rubbers, and about equivalent to that of filled silicones. This is presumably the result of the reinforcement effect of the polysulfone domains, which act as "filler" particles. The excellent clarity of the block copolymers is due to the small size of these domains, about 150 Å as determined by electron microscopy.<sup>17</sup>

TABLE II  
Effect of Block  $\bar{M}_n$  on Block Copolymer Properties

Block $\bar{M}_n$		Siloxane wt-%	Reduced viscosity <sup>a</sup>	Tensile modulus, psi	Tensile strength, psi	Elongation, %	$T_g$ , °C <sup>b</sup>
Polysulfone	Polydimethyl- siloxane						
4700	350	10	0.4	240,000	6000	5	+125
4700	1700	28	1.1	170,000	4700	12	+140
9300	4900	41	0.4	29,000	2700	150	-110; +170
4700	5100	55	0.8	20,000	2400	350	-120; +160
4700	9200	67	1.5	2,000	1300	500	-120; +160
6500	25,000	79	1.3	300	900	550	-120; +160

<sup>a</sup> 0.2 g/dl in  $\text{CH}_2\text{Cl}_2$  at 25°C.

<sup>b</sup> Determined from temperature-modulus and resilience measurements.

## SUMMARY AND CONCLUSIONS

Block copolymers of polysulfone-polydimethylsiloxane have been prepared. The synthesis is carried out by the interaction of oligomers bearing mutually reactive endgroups, i.e., dihydroxyl-terminated polysulfone and bis(dimethylamine)-terminated polydimethylsiloxane. The reaction is very rapid (minutes at 70°C), and product isolation is facile, since the only by-product is gaseous dimethylamine. The block copolymers are soluble, amorphous, and transparent, and display good thermal and hydrolytic stability.

The alternating  $-(A-B)_n$  block structure of the copolymers is strictly controlled since the starting materials are pairs of preformed, well-characterized oligomers which can react only with their opposite kinds. Properties ranging from rigid to flexible are obtained by varying the molecular weights of the oligomers, and therefore the composition of the products.

The morphology of the copolymers can also be controlled by varying oligomer molecular weight. Very low molecular weight oligomers produce single-phase copolymers, while higher molecular weight oligomers ( $\geq 5000 \bar{M}_n$ ) give two-phase systems. The latter display dual glass transition temperatures, e.g.,  $-120^\circ\text{C}$  and  $+160^\circ\text{C}$ , indicating a broad useful temperature range for these materials. Compositions of high siloxane content and low modulus exhibit good elastomeric properties resulting from the reinforcing and physical crosslinking effects of the polysulfone domains.

The authors wish to thank Mr. T. C. Williams for supplying the polydimethylsiloxane oligomers used in this work. We are also indebted to Mr. W. D. Niegisch for the electron microscope results, to Dr. J. V. Koleske for the ultracentrifugation data, and to Mr. R. C. Hazelton for the polysulfone oligomer end-group analyses.

## References

1. J. Moacanin, G. Holden, and N. W. Tschoegl, Eds., *Block Copolymer Symposium* (*J. Polym. Sci. C*, **26**), Interscience, New York, 1969.
2. R. N. Johnson, in *Encyclopedia of Polymer Science and Technology*, Vol. 11, J. Brandrup and E. H. Immergut, Eds., Interscience, New York, 1969, pp. 447-463.
3. R. N. Johnson, A. G. Farnham, R. A. Clendinning, W. F. Hale, and C. N. Merriam, *J. Polym. Sci. A-1*, **5**, 2375 (1967).
4. R. N. Johnson, and A. G. Farnham, *J. Polym. Sci. A-1*, **5**, 2415 (1967).
5. W. F. Hale, A. G. Farnham, R. N. Johnson, and R. A. Clendinning, *J. Polym. Sci. A-1*, **5**, 2399 (1967).
6. R. N. Meals and F. M. Lewis, *Silicones*, Reinhold, New York, 1959.
7. H. A. Vaughn; paper presented to Division of Organic Coatings and Plastics Chemistry, American Chemical Society Meeting, Minneapolis, April 1969; *Abstracts*, **29**, No. 1, 133 (1969).
8. H. A. Vaughn; *J. Polym. Sci. B*, **7**, 569 (1969).
9. R. P. Kambour; *J. Polym. Sci. B*, **7**, 573 (1969).
10. D. G. Legrand; *J. Polym. Sci. B*, **7**, 579 (1969).
11. R. P. Kambour, paper presented at American Chemical Society Meeting, New York, September 1969; *Polym. Preprints*, **10**, No. 2, 885 (1969).
12. S. H. Langer, S. Connell, and J. Wender, *J. Org. Chem.*, **23**, 50 (1958).

13. W. R. Dunnivant, R. A. Markle, P. B. Stickney, J. E. Curry, and J. D. Byrd, *J. Polym. Sci. A-1*, **5** 707 (1967).
14. J. V. Koleske, private communication; to be discussed in detail in a forthcoming paper.
15. M. M. Sprung and F. O. Guenther; *J. Amer. Chem. Soc.*, **77**, 3990 (1955).
16. D. J. Meier in *Block Copolymer Symposium (J. Polym. Sci. C, 26)*, J. Moacanin, G. Holden, and N. W. Tschoegl, Eds., Interscience, New York, 1969, p. 81.
17. W. D. Niegisch, private communication; to be discussed in detail in a forthcoming paper.

Received May 27, 1971

Revised July 6, 1971



## Photochemical and Thermal Isomerization in Polymer Matrices: Azo Compounds in Polystyrene

W. J. PRIEST and M. M. SIFAIN, *Research Laboratories, Eastman Kodak Company Rochester, New York 14650*

### Synopsis

Photochemical and thermal geometrical isomerizations of monoazo compounds have been studied in polystyrene-*n*-butylbenzene compositions. *Cis-trans* isomer ratios established by light absorption were found to depend on matrix viscosity. Where the compositions were above their respective glass temperatures, all thermal isomerizations conformed to first-order kinetics. Where compositions were below their respective glass temperatures, the initial isomerization rates were abnormally fast, decaying to normal first-order processes after substantial amounts of reaction had taken place. These effects have been interpreted in terms of the vitreous properties of polystyrene.

### INTRODUCTION

Two recent publications deal with the influence of polymer matrices on thermal bleaching of photoproducts obtained by illumination of indolinyI spiropyrans.<sup>1,2</sup> These isomerizations are combinations of valence bond and configurational changes wherein transformations among the several labile (ground-state) species formed by absorption of light in the spiropyran may occur as sequential processes. In fluid solutions, according to these reports, fading of colored photoproducts follows first-order kinetics. In compositions in which polymers below their respective glass transition temperatures are "solvent," the bleaching does not conform to first-order kinetics. First-order plots show maximum nonlinear portions at the start, gradually reverting to slower, constant values in the terminal portions. Garlund<sup>3</sup> proposes that these kinetics could be resolved into two first-order sequential processes, which are differentiated in polymer (below glass transition temperature) but not in fluid solutions.

We have examined a number of thermal isomerization processes, including *cis*  $\rightarrow$  *trans* configurational changes in monoazo compounds under similar conditions. The first-order plots obtained for all of these show the same form as those reported for the indolinyI merocyanine thermal bleaching. In isomerizations such as these, which involve only one labile form, Garlund's mechanism is inapplicable; hence it is necessary to account for the observations in some other manner. The work reported here embodies a detailed study of isomerizations of monoazo compounds in polystyrene.

## EXPERIMENTAL

### Materials

*n*-Butylbenzene (Eastman Reagent Grade) was used as received. A commercial grade polystyrene, Koppers 8X, was purified by precipitation of the polymer from a benzene solution to acetone.

Commercial 2,2'-azonaphthalene (I) was recrystallized from benzene;  $\epsilon_{380 \text{ nm}} = 2.16 \times 10^4$ ,  $\epsilon_{345 \text{ nm}} = 2.54 \times 10^4$  (*n*-butylbenzene).

4-Ethoxyazobenzene (II) was prepared from *p*-phenylazophenol by the ethylation procedure of Jacobson and Fischer.<sup>4</sup>

### Sample Preparation

Solutions of dye, polymer, and small quantities of a stabilizer, 1,4-diazabicyclo[2.2.2]octane (to prevent the acid catalysis), were dissolved in the solvent which was normally benzene. A portion of the solution was coated on a film of polyester support with a coating tool. The volatile solvents were completely removed by heat treatment of the film for about 20 min in a vacuum oven. The film thicknesses were about 10  $\mu$  and dye concentrations were about  $2.5 \times 10^{-2} M$ . Where films containing residual solvent were required, evaporation of the solvent was interrupted at stages following coating by covering with a sheet of polyester. The laminate was thereafter bonded by passing through a set of warm pressure rollers. Samples which contained no solvent were normally cooled rapidly in air following heating to the vicinity of polymer glass temperature. Except where specified otherwise, these "quenched" samples were standard. Annealed samples were heated for three weeks at 80°C, a temperature which is about 30°C below the glass temperature.

### Measurements

Film samples were placed in 1-cm, Nujol-filled spectrophotometer cells and held vertical by 9-mm silica spacers. For photoisomerization, solution of film samples were illuminated with G. E. Black Light fluorescent lamps arrayed in a flat bank. Corning glass band-pass filters were usually used to modulate the lamp radiation. Absorbance measurements were made in a Beckman DB spectrophotometer. Thermal rates of return following illumination were measured in thermostatted samples. The samples were removed at selected times for absorbance measurements in the spectrophotometer, whose sample compartment was maintained near the temperature of the thermostat by circulating water. Temperatures were maintained to 0.15°C.

The rate data throughout are displayed in first-order format according to the relation:

$$\log [(D_{\infty} - D_0)/(D_{\infty} - D_t)] = Kt/2.3$$

where  $D_0$ ,  $D_t$  and  $D_\infty$  are observed absorbances in the peak of the long-wavelength bands of the respective *trans* isomers at subscript times. These absorbances are substantially proportional to concentrations of *trans* isomers in view of the low extinctions of corresponding *cis* forms at the wavelengths monitored.

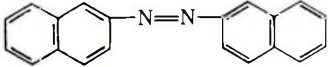
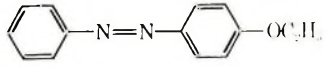
Measurements of glass transition temperatures of polystyrene and *n*-butylbenzene were made by Mrs. A. S. Marshall by differential thermal analysis.

## RESULTS

### Photoisomerization

Both of the azo compounds were wholly *trans* after dark equilibration. Absorption spectra of *trans* and *cis* isomers are shown in Figure 1. Steady-state conversions were obtained by illumination for a few minutes by use of a Corning 7-39 band-pass filter. Initial absorbances of all samples were adjusted to give an absorbance of about 1.0 in the long-wave-band maximum. The amount of conversion to respective *cis* isomers was monitored in terms of decreases in absorbance of these absorption bands. Steady-state isomer ratios were achieved somewhat more rapidly with fluid solutions than with polymer samples. At the temperature of illumination, the respective thermal return reactions were not rapid enough to influence the steady-state isomer ratios appreciably. The amounts of conversion in the steady state under the conditions described are given in Table I.

TABLE I  
Photochemical Conversion of Azo Compounds

Species	Solvent (butylbenzene- polystyrene), wt-% butylbenzene	Concentration, mole/l.	$T_g$ , °C	% <i>cis</i> in steady state
2,2'-Azonaphthalene  (I)	0 <sup>a</sup>	$2.2 \times 10^{-2}$	+109	37
	0	"	+109	45
	14	"	+ 75	52
	33	"	+ 28	58
	44	"	+ 1	58
	75	$2.6 \times 10^{-5}$	- 75	73
	100	"	-136	78
4-Ethoxyazobenzene  (II)	0 <sup>a</sup>	$2.6 \times 10^{-2}$	+109	93
	0	"	+109	96
	100	$3.0 \times 10^{-5}$	-136	96

<sup>a</sup> Annealed.

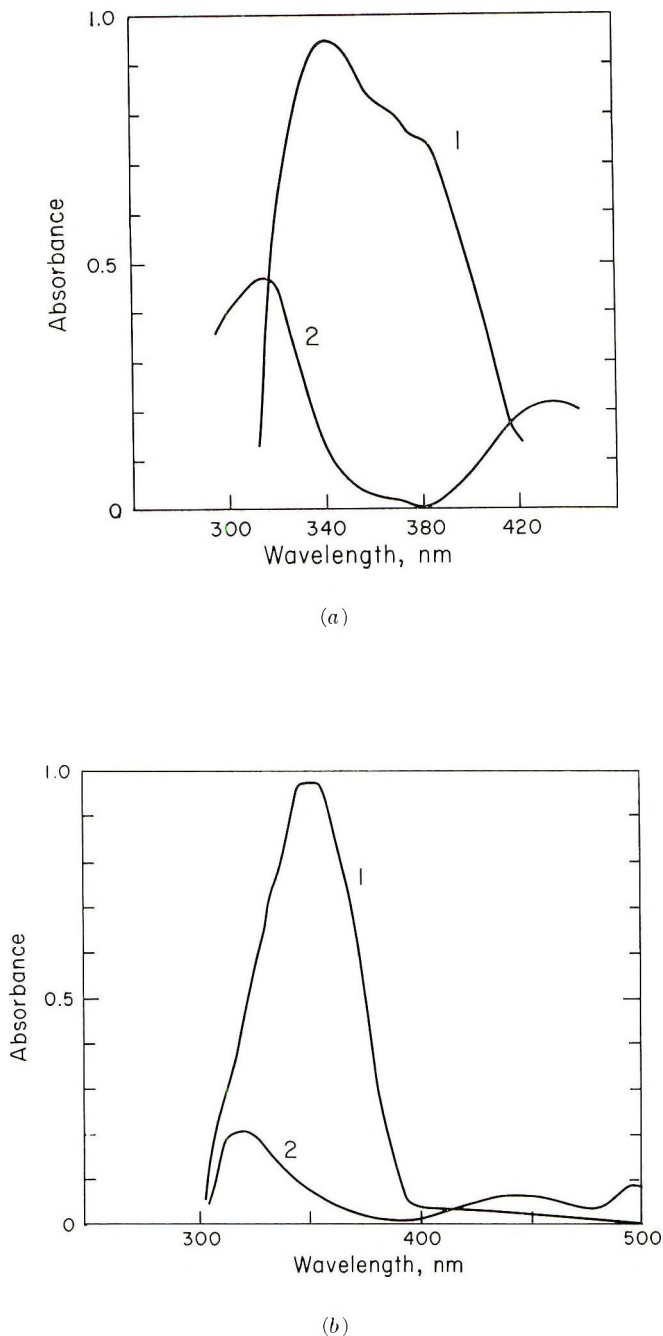


Fig. 1. Absorption spectra of azo species: (a) 2,2'-azobiphenyl I, [(1) data for *trans* isomer in *n*-butylbenzene at room temperature and (2) a construct of the *cis* isomer in isopropanol at  $-40^{\circ}\text{C}$ .<sup>5</sup> (b) 4-ethoxyazobenzene [(1) data for the *trans* isomer in *n*-butylbenzene at room temperature and (2) *cis* construct in *n*-butylbenzene at room temperature, method of Fischer<sup>5</sup>].

### Thermal Isomerization

Thermal *cis*  $\rightarrow$  *trans* isomerizations were measured following photochemical population of the *cis* form to the greatest practicable extent. Exposures longer than those necessary to achieve the steady state did not lead to observable changes in kinetics of the thermal return reactions. Rate measurements made with a series of compositions of azo species I

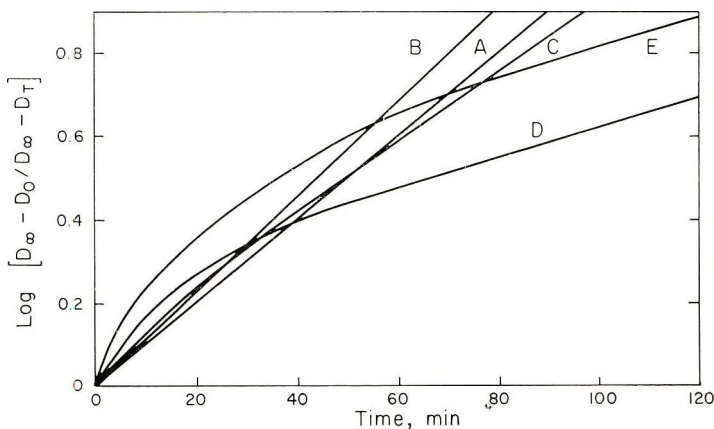


Fig. 2. Thermal *cis*  $\rightarrow$  *trans* isomerizations of I in polystyrene-*n*-butylbenzene compositions at 45°C: (A) *n*-butylbenzene; (B) 56% polystyrene; (C) 86% polystyrene; (D) 100% polystyrene (quenched); (E) 100% polystyrene (annealed).

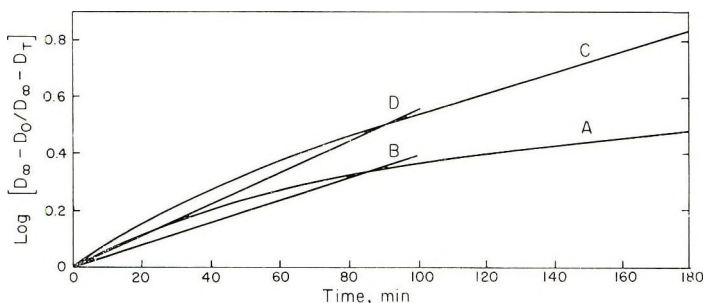


Fig. 3. Thermal isomerizations of azo compounds I and II in polystyrene and *n*-butylbenzene: (A) I, 35°C, polystyrene; (B) I, 35°C, *n*-butylbenzene; (C) II, 55°C, polystyrene; (D) II, 55°C, *n*-butylbenzene.

in polystyrene-*n*-butylbenzene compositions gave the data summarized in Figure 2 and Table II.

Similar rate measurements were made for azos I and II in butylbenzene and in polystyrene at each of two temperatures. Curves obtained for the lower temperature in each case are shown in Figure 3. Temperatures chosen for rate measurements of polymer samples were such that there were well-defined linear portions in the first-order plots in Figure 3. Rate



TABLE II  
Isomerization of *cis*-2,2'-Azonaphthalene  
in Butylbenzene-Polystyrene Mixtures at 45°C

<i>n</i> -Butylbenzene in composition, %	<i>T</i> <sub>g</sub> , °C	Isomerization rate × 10 <sup>2</sup> , min <sup>-1</sup>
0 <sup>a</sup>	+109	0.82
0	+109	0.80
14	+ 75	1.97
33	+ 28	2.26
44	+ 1	2.60
75	- 75	2.67
100	-136	2.33

<sup>a</sup> Annealed.

TABLE III  
Comparative Rate Constants for Azo Compounds  
in Styrene and Butylbenzene

Species	Solvent	<i>T</i> , °C	10 <sup>2</sup> × <i>K</i> , min <sup>-1</sup>	<i>E</i> , kcal/mole
2,2'-Azonaphthalene	Butylbenzene	45	2.326	22.6
		35	0.899	
	Polystyrene	45	0.797	21.4
		35	0.302	
4-Ethoxyazobenzene	Butylbenzene	65	3.570	18.70
		55	1.278	
	Polystyrene	65	2.222	19.92
		55	0.848	

constants corresponding to these and also for the butylbenzene solutions at the same temperatures are summarized in Table III.

## DISCUSSION

With equivalent light intensities, *cis*-isomer contents in the steady state diminish with increases in viscosity of the medium (Table I). These effects with polystyrene and mixtures of polystyrene-*n*-butylbenzene are similar to those reported for similar species in glasses at low temperatures, and may be understood in terms of competitive reactions among excited species, as proposed by Malkin and Fischer.<sup>6</sup> Photochemical conversions in annealed polymers were smaller than those obtained for similar but quenched samples. Annealed samples subsequently reheated briefly to the vicinity of the glass transition temperature of the matrix, then quenched, have the same properties as unannealed samples. These effects suggest that a fraction of the overall reduction in free volume which occurs in annealing is partitioned among the dye molecule sites.

Thermal isomerization of I in a series of *n*-butylbenzene-polystyrene compositions (Fig. 2) shows that curvature in the initial portions of the

respective first-order plots is obtained only when the temperature of measurement is lower than the glass transition temperature.\* With increasing amounts of *n*-butylbenzene "plasticizer," the curvature diminishes and the onset of the linear terminal portion of the rate curve occurs earlier in the course of reaction. When sufficient *n*-butylbenzene is present to depress  $T_g$  below the temperature at which the isomerization is run, the entire course of the reaction can be represented by a linear plot. Numerical values for rates of isomerization calculated from the terminal linear portions of the plots for I show that the isomerizations were slowest in unplasticized polystyrene. An estimate of the specific solvent influence of hypothetical "mobile" polystyrene on the rate of reaction was obtained by extrapolation of the rate values obtained with compositions of polystyrene-*n*-butylbenzene below  $T_g$  to a composition representing 100% polymer. For I at 45°C, the extrapolated value is  $2.9 \times 10^{-2}$  ( $\pm 0.1$ )  $\text{min}^{-1}$ , about four times the observed value for unplasticized polystyrene run under the same conditions ( $8.0 \times 10^{-3}$  ( $\pm 0.3$ )  $\text{min}^{-1}$ ).

In solvents of low to medium polarity, rates of isomerization of the simple azo prototype have been found to be comparatively insensitive to solvent, showing only a twofold rate increase in hydrocarbons relative to acetone.<sup>8</sup> The low rate of reaction in the terminal phase of isomerization in unplasticized polystyrene may be attributed to decreases in probability for formation of configurations corresponding to activated complex within the free volume associated with many dye sites. An alternative possibility, that significant fractions of dye molecules have envelopes which exert larger polar solvent influences, is less attractive. In either case, little readjustment of polymer enveloping individual dye sites appears to occur under the conditions in which *cis* isomer is produced, since return thermal kinetics were not measurably affected by increasing times of illumination or by holding photo-isomerized samples in the dark prior to rate measurement.

Values for activation energy characterizing thermal bleaching of merocyanines obtained from illumination of indolinyl spiropyrans for a series of xylene-polystyrene compositions were recently reported.<sup>1</sup> These values ranged from 17.3 to 31.7 kcal/mole for 100% to 5% solutions. In view of these findings, it was of interest to determine whether there were similar differences in rate parameters for isomerizations of the azo species in chemically similar solvents and polymers. The values for activation energy obtained for each of the two azo compounds studied do not show any systematic differences between fluid vitreous situations. If differences exist, they are within the limits of accuracy of the data (Table III).

In the data reported for 1,3,3-trimethylindolinyl-6'-nitrospiropyran,<sup>1</sup> it is noteworthy that the largest increase in activation energy (19.7 to 25.0 kcal/mole) occurs with changes of composition from 16 to 25% polystyrene. Both of these compositions have glass transition tempera-

\* The referee has called attention to a similar observation.<sup>7</sup>

tures well below room temperature. Values for activation energy of the same compound have recently been measured in a number of solvents.<sup>9</sup> For benzene, the value given compares favorably with the value for xylene.<sup>1</sup> However, even in the solvent of highest polarity (ethanol), the activation energy is only 25 kcal/mole. From these considerations, it appears that the high values reported for activation energy in xylene-polystyrene compositions containing appreciable amounts of polystyrene<sup>1</sup> are questionable.

### References

1. I. Shimizu, K. Yoshida, H. Kobayashi, M. Nakzawa, H. Kokado, and E. Inoue, *Kogyo Kagaku Zasshi*, **72**, 166 (1969).
2. Z. Garlund and J. Lavery, *J. Polym. Sci. B*, **7**, 719 (1969).
3. Z. Garlund, *J. Polym. Sci. B*, **6**, 57 (1968).
4. P. Jacobson and W. Fischer, *Ber.*, **25**, 994 (1892).
5. E. Fischer, *J. Amer. Chem. Soc.*, **82**, 3249 (1960).
6. S. Malkin and E. Fischer, *J. Phys. Chem.*, **66**, 2482 (1962).
7. H. Morowetz, *Accs. Chem. Res.*, **3**, 354 (1970).
8. J. Halpern, G. Brady, and C. Winkler, *Can. J. Res.*, **28B**, 140 (1955).
9. J. Flannery, *J. Amer. Chem. Soc.*, **90**, 5660 (1968).

Received June 11, 1971

Revised July 15, 1971

## Novel Aliphatic Polymers Containing Imide Ring. I. Polyspiroimide Based on Methanetetraacetic Acid

LESTER T. C. LEE, ELI M. PEARCE, and STEPHEN S. HIRSCH,\*  
*Corporate Chemical Research Laboratory, Allied Chemical Corporation,  
Morristown, New Jersey 07960*

### Synopsis

High molecular weight polyspiroimides have been prepared by reacting diamines with the dianhydride of carboxymethanetetraacetic acid in polar organic solvents. Alternatively, thermal condensation of the preformed salt made from equimolar amounts of diamine and methanetetraacetic acid (MTA) can be used. These all-aliphatic polyimides are soluble in certain organic solvents, and possess good thermal-oxidative stability.

### Introduction

Imide-ring formation has occupied an important position in the preparation of high-temperature performance polymers. Outstanding examples are the aromatic polyimides derived from the pyromellitic dianhydride and various aromatic diamines.<sup>1-6</sup> These rigid aromatic polyimides are usually nonmelting, resistant to organic solvents, and their glass transition temperatures are often very high.<sup>7</sup> Therefore, the synthesis and application of the wholly aromatic polyimides are usually processed as the polyamic acid intermediate<sup>4-6,8</sup> and then converted into the imide form.

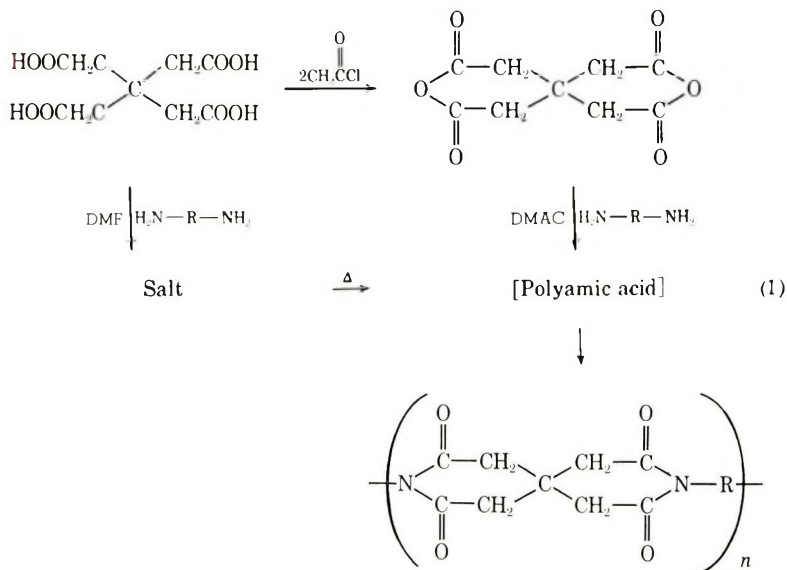
The investigation of aliphatic polyimides is far less extensive than their aromatic counterparts. Some earlier work showed that the aliphatic polyimides are inferior in thermal properties and low in melting point.<sup>9-11</sup> However, polyimides having good high-temperature physical properties derived from 1,2,3,4-butanetetracarboxylic acid and aromatic diamines have recently been reported by Lonerini<sup>12</sup> and Kudryavtsev.<sup>13</sup> This paper describes the preparation and properties of novel aliphatic polyimides derived from methanetetraacetic acid (MTA) and various diamines.

### Results and Discussion

High molecular weight polyspiroimides were obtained via solution polymerization by reacting the dianhydride of methanetetraacetic acid with diamines in dimethylacetamide at low temperature. The polymerization was completed by removing the solvent under vacuum, and

\*Present address: Geigy Chemical Corporation, Ardsley, New York.

heating the residue at a higher temperature for a short period of time. The dianhydride was prepared by heating the methanetetraacetic acid (MTA) with acetyl chloride according to the method described by Ingold.<sup>14</sup> The same polyspiroimide was also obtained by a one-step process where the preformed equimolar salt of MTA and diamine were thermally polymerized in a sealed vacuum tube. The general scheme for the preparation of the polyspiroimide can be shown in eqs. (1).



The polyspiroimide structure was confirmed spectroscopically by observing the infrared imide bands at 1725 and 725  $\text{cm}^{-1}$ . When sampling was carried out during the polymerization period via the salt process, the gradual disappearance of the amide band at 1645  $\text{cm}^{-1}$  was detected, thus suggesting the presence of the polyamic acid as the precursor. The conversion of the polyamic acid to the cyclic polyimide was also apparent in the low-temperature solution polymerization of the dianhydride of MTA with diamines. The complete transformation of the amide band to the imide bands upon heating of the initially formed high molecular weight polyamic acid as shown by infrared was consistent with the above interpretation.

A number of polyspiroimides were prepared and are listed in Table I. In most cases, the MTA was reacted with aliphatic diamines. These high molecular weight aliphatic polyimides, unlike the aromatic polyimides, were soluble in organic solvents such as trifluoroethanol and hot *m*-cresol, and their glass transition temperatures were clearly detected by differential thermal analysis (DTA). Compression-molded films formed from these polymers were tough and flexible. By comparison, when 4,4'-diaminodiphenyl ether was reacted with MTA, the polyimide obtained was colored and only partially soluble in the hot *m*-cresol and trifluoroethanol.



TABLE I  
Properties of Polyimides Based on Methanetetraacetic Acid

Diamines	Inherent viscosity, dl/g	$T_g$ , °C	Properties of film <sup>a</sup>	Weight loss at 400°C, %	
				Air	N <sub>2</sub>
Ethylenediamine	0.31	205	Flexible	—	—
1,6-Hexanediamine	1.03	125	Flexible	2.0	0.40
1,10-Decanediamine	0.70	78	Flexible	—	3
4,4'-Diamino-diphenyl ether	—	Not definite	Brittle	—	9

<sup>a</sup>The film was judged to be flexible if it would taken two full 180° bends against a sharp rod without wrinkling and cracking.

### Thermal-Oxidative Stability

Excellent thermal-oxidative stability up to 400°C is shown by these aliphatic polyimides. Thermogravimetric analysis (TGA) data for the polyimide from MTA and 1,6-hexanediamine are shown in Figure 1. In the absence of oxygen, a weight retention of 99.6% and 98.3% of the polymer was measured at 400 and 450°C, respectively. The polymer was comparatively less stable when heated in air, with a 2.0% weight loss occurring at 400°C.

The thermal-oxidative stability of the aliphatic polyimide was also studied under isothermal conditions. Thin films prepared from MTA and 1,6-hexanediamine were placed in an air circulating oven at 200 or 230°C for 100 hr. Their weight-loss was 1.7 and 7.0%, respectively

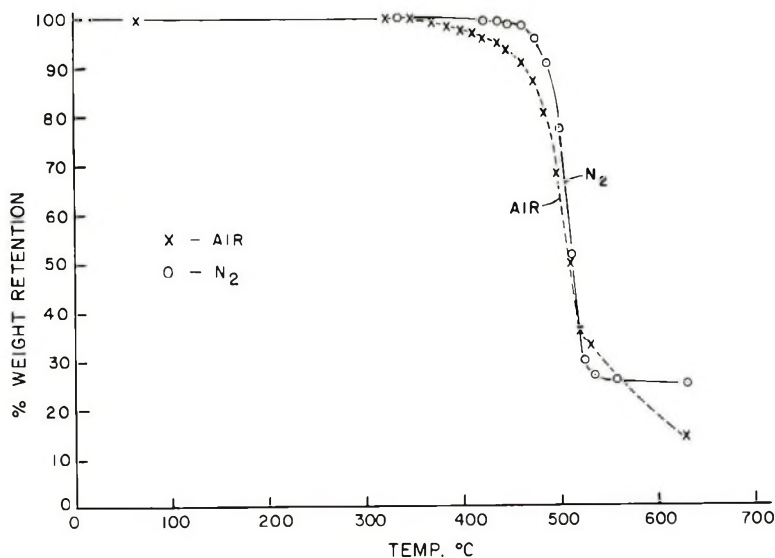


Fig. 1. TGA thermograms of polyimide from MTA and 1,6-hexanediamine in nitrogen and air.

(Table II). The TGA curves (Figure 2) of this polyspiroimide [poly(hexamethylene)methane tetraacetodiimide] are compared with several other classes of polymers including poly(ethylene terephthalate), poly(*m*-

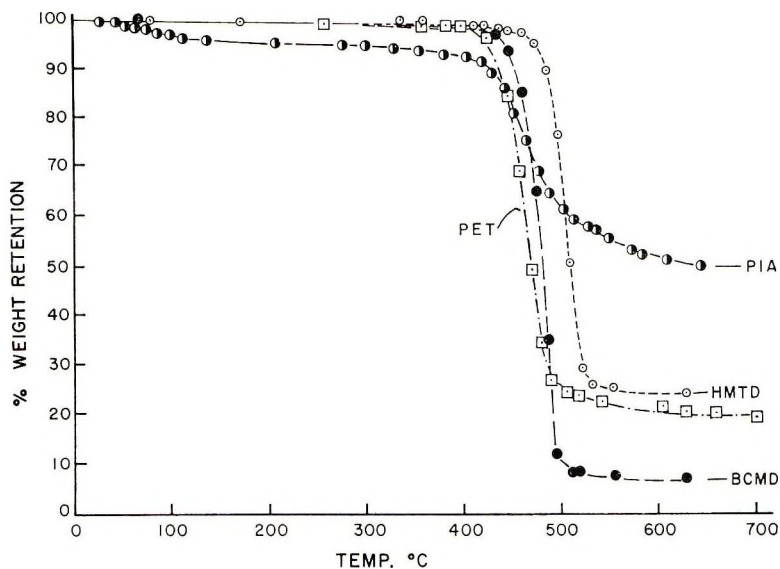


Fig. 2. Comparisons of TGA thermograms in nitrogen of (○) spiro polyimide, poly-[(hexamethylene)methanetetraacetodiimide] with other polymers: (□) poly(ethylene terephthalate) (PET); (●) poly-*m*-phenyleneisophthalamide (PIA); (●) poly[bis(4-cyclohexylene)methylenedodecamide] (BCMD).

phenylene isophthalamide) and poly [bis(4-cyclohexylene)methylene dodecamide] which is prepared from bis(4-aminocyclohexyl)methane in isomer ratio of 75% *trans-trans*, 20% *cis-trans*, and 5% *cis-cis*.

### Physical

Some typical physical properties of the polyimide from MTA and 1,6-hexanediamine were determined from a 5-mil thick film (Table II).

TABLE II  
Physical Properties of Polyimide from MTA and 1,6-Hexanediamine

Tensiles				
Ultimate Tensile Strength psi $\times 10^3$	Ultimate Elongation, %	1% secant modulus, psi $\times 10^5$	Weight loss in 100 hr, %	
			At 200°C	At 230°C
7.84	3.6	3.4	1.76	7.00

## Experimental

### Preparation of Polyimides

Methanetetraacetic acid and its dianhydride were prepared according to the method described by Ingold.<sup>14</sup> A typical procedure for preparation of the polyspiroimide is detailed for the reaction of MTA and 1,6-hexanediamine.

**Low-Temperature Polymerization.** A solution of 4.64 g (4.0 mmoles) of 1,6-hexanediamine in 40 ml *N,N*-dimethylacetamide was added to a stirred solution of 8.48 g (4.0 mmole) of the dianhydride of carboxymethanetetraacetic acid in 80 ml of *N,N*-dimethylacetamide maintained at 10–15°C under a nitrogen atmosphere, and stirred at room temperature for 2 hr. The initial cloudy solution became clear. The temperature of the reaction was raised gradually until it reached 165°C, and remained at that temperature for 3 hr. The solvent was then removed under high vacuum and the solid residue heated at 250°C and 1.0 mm Hg for 1 hr and 300°C/0.3 mm for 25 min. After cooling to room temperature, the solid mass was separated from the glass by cooling in liquid nitrogen. The polymer was ground to small particles and washed with acetone and water, then dried to constant weight. The yield is 10.5 g (85%). The reduced viscosity (0.5 concentrated *m*-cresol) is 0.98. The infrared spectrum showed major bands at 725 and 1725 cm<sup>-1</sup> for an imide group. The glass transition temperature, as measured by DTA, is 125°C.

**Salt Polymerization.** A solution of 1,6-hexanediamine (1.41 g or 1.21 mmole) in 15 ml absolute ethanol is added quantitatively to the methanetetraacetic acid (3.00 g or 1.21 mmole) in 100 ml absolute ethanol and crystallization occurred. After standing overnight, the salt was filtered; the yield was 4.38 g (99%). The salt melts at 225°C and had a pH of 7.3, determined on a 1% solution of salt in distilled water.

The salt was charged into glass ampoules which are then sealed under vacuum. The ampoule was heated at 245°C for 3½ hr, then heated at 260°C for 30 min. The reduced viscosity (0.5% concentration, *m*-cresol) was 1.03, and the glass transition temperature was 125°C.

### Physical Measurements

Infrared measurements were obtained on the Perkin-Elmer Model 21 infrared spectrometer. Reduced viscosities were determined in *m*-cresol or trifluoroethanol. Glass transition-temperature data was obtained on the DuPont 900 differential thermal analyzer or the Perkin-Elmer DSC 12 differential scanning calorimeter at a heating rate of 20°C/min in nitrogen. Thermogravimetric analysis (TGA) data were obtained by using the Ainsworth TGA balance (RZA with AU recorder), 25 mg of sample being heated at a 10°C/min rate.

We wish to acknowledge the contributions of Mrs. E. Turi for obtaining and interpreting the TGA and DTA data; Dr. John Sibilia and Mrs. L. Komarowski for obtaining the IR spectra; Mr. H. D. Fardon for determining the physical properties of the polymers; and Mr. George Brunner for obtaining the viscosity data.

## References

1. W. M. Edwards and I. M. Robinson (to DuPont), U.S. Pat. 2,710,853 (1955).
2. G. M. Bower and L. W. Frost, *J. Polym. Sci. A-1*, **3**, 3135 (1965).
3. J. Jones, J. Ochnyski and F. Rackley, *Chem Ind.* (London), **1955**, 1686.
4. W. M. Edwards (to DuPont), U. S. Pat. 3,179,630 (1965).
5. C. E. Sroog, A. L. Endrey, S. V. Abramo, C. E. Berr, W. M. Edwards, and K. L. Oliver, *J. Polym. Sci. A* **3**, 1373 (1965).
6. J. Preston and W. B. Black, *J. Polym. Sci. B*, **3**, 84 (1965).
7. S. L. Copper, A. D. Mair, and A. V. Tobolsky, *Text Res. J.*, **35**, 1110 (1965).
8. J. H. Freeman, L. W. Frost, G. M. Bower, and E. J. Traynor, *SPE Trans.* **5**, (2), 75 (1965).
9. British Pat. 470,858 (1945).
10. C. J. Frosch, U.S. Pat. 2,421,024 (1947).
11. J. Lincoln and J. G. Frewitt U.S. Pat. 2,502,576 (1949).
12. D. G. Lonerini and J. M. Witzel, *J. Polym. Sci. A-1*, **7**, 2185 (1969).
13. V. V. Kudryavtsev, A. P. Rudakov, and M. M. Koton, *Vysokomol. Soedin.*, **A 9**, 1985 (1967).
14. C. K. Ingold and L. C. Nickolls, *J. Chem. Soc.*, **1922**, 1638.

Received June 11, 1971

Revised July 15, 1971

## Organometallic Polymers. XIV. Copolymerization of Vinylcyclopentadienyl Manganese Tricarbonyl and Vinylferrocene with *N*-Vinyl-2-Pyrrolidone

CHARLES U. PITTMAN, JR.\* and PAUL L. GRUBE,  
*Department of Chemistry, University of Alabama,  
University, Alabama 35486*

### Synopsis

*N*-Vinyl-2-pyrrolidone(I) has been copolymerized with vinylferrocene(II) and vinylcyclopentadienyl manganese tricarbonyl(III) in degassed benzene solutions with the use of azobisisobutyronitrile (AIBN) as the initiator. The polymerizations proceed smoothly, and the relative reactivity ratios were determined as  $r_1 = 0.66$ ,  $r_2 = 0.40$  (for copolymerization of I with II,  $M_1$  defined as II) and  $r_1 = 0.14$  and  $r_2 = 0.09$  (for copolymerization of I with III,  $M_1$  defined as III). These copolymers were soluble in benzene, THF, chloroform,  $\text{CCl}_4$ , and DMF. Molecular weights were determined by viscosity and gel-permeation chromatography studies (universal calibration technique.) The copolymers exhibited values of  $\bar{M}_n$  between  $5 \times 10^3$  and  $10 \times 10^3$  and  $\bar{M}_w$  between  $7 \times 10^3$  and  $17 \times 10^3$  with  $\bar{M}_w/\bar{M}_n < 2$ . Upon heating to  $260^\circ\text{C}$  under  $\text{N}_2$ , copolymers of III underwent gas evolution and weight loss. The weight loss was enhanced at  $300^\circ\text{C}$ , and the polymers became increasingly insoluble. Copolymers of vinylferrocene were oxidized to polyferricinium salts upon treatment with dichlorodicyanoquinone (DDQ) or *o*-chloranil (*o*-CA) in benzene. Each unit of quinone incorporated into the polysalts had been reduced to its radical anion. The ratio of ferrocene to ferricinium units in the polysalts was determined. The polysalts did not melt at  $360^\circ\text{C}$  and were readily soluble only in DMF.

### INTRODUCTION

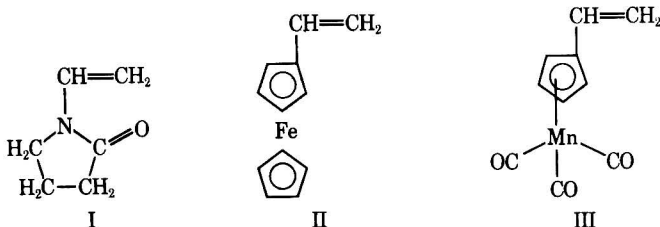
*N*-Vinyl-2-pyrrolidone (I) is a versatile vinyl monomer which is readily copolymerized with other vinyl monomers in virtually any proportions. Its homopolymer is soluble in water, and it forms hard, transparent films which are strongly adhesive to smooth surfaces, and it is largely inert toxicologically.

Monomer I is of special interest for paints based on poly-(vinyl acetate) or acrylates. For example, vinyl acetate-*N*-vinyl-2-pyrrolidone copolymers exhibit unusually strong bonding to glass, Mylar, nylon, and cellophane, and in plastisols improved bonding to aluminum is exhibited.<sup>1,2</sup> Copolymers of I with acrylic acid or its esters show excellent adhesion to glass, form clear hard films or films which are very tacky, flexible, and resistant

\* To whom inquiries should be addressed.



to water spotting.<sup>3-5</sup> The patent literature teaches the use of acrylate-*N*-vinyl-2-pyrrolidone copolymers in silver halide emulsion vehicles and backing layers for photographic films, as antifoggant in films emulsion or developing baths.<sup>6-9</sup> The adhesive properties of I have been capitalized upon in acrylamide copolymers<sup>10</sup> used as binding agents and in vinyl chloride copolymers used as glass fiber finishes, precoating agents for polyester laminates, safety glass laminating agents, and as protective coatings for aerosol bottles.<sup>11</sup> Copolymers of I and acrylonitrile have been reported in compounding adhesives and in coating formulations.<sup>12,13</sup> *N*-Vinyl-2-pyrrolidone is an effective dispersant and wetting agent for pigments, and it increases dye affinity in copolymers.<sup>7,14-16</sup> These properties make I an ideal potential comonomer to use in organometallic coatings and plastics containing



vinylferrocene (II) or vinylcyclopentadienyl manganese tricarbonyl (III) (common name is vinylcymantrene).

The homo- and copolymerization of vinylferrocene has recently been described in detail by one of us<sup>17-19</sup> as part of a general study of transition metal-containing organic polymers.<sup>20</sup> The relative reactivity ratios, which were obtained in the AIBN-initiated solution copolymerizations of vinylferrocene with styrene, methyl acrylate, methyl methacrylate, acrylonitrile, and maleic anhydride, illustrated that vinylferrocene was much less reactive vinyl monomer than styrene.<sup>18,19</sup> Ferrocene-containing acrylates have also been polymerized.<sup>21,22</sup> The ease of incorporation of vinylferrocene into organic polymers coupled with the fact that ferrocene can serve as both an efficient quencher and sensitizer of photochemically generated triplet states<sup>23,24</sup> make II an interesting candidate for coatings which would serve as UV stabilizers or as a photochemically active material. Ferrocene's low toxicity and high absorption of ultraviolet<sup>25</sup> and  $\gamma$ -radiation<sup>26</sup> further encourage its use.

Vinylcyclopentadienyl manganese tricarbonyl (III) has only been briefly reported as a polymer precursor. At 170°C in the absence of an inhibitor, III homopolymerizes to give an orange, glasslike polymer softening at 80°C.<sup>27</sup> Pittman et al. have copolymerized III with styrene, acrylonitrile, vinyl acetate, methyl acrylate, and vinylferrocene in solution and obtained the relative reactivity ratios in these AIBN-initiated processes.<sup>28</sup> The presence of manganese and its polar carbonyl groups might lead to useful adhesive properties, especially in *N*-vinyl-2-pyrrolidone copolymers.

## RESULTS

### Copolymerizations

*N*-Vinyl-2-pyrrolidone was copolymerized with both vinylferrocene and vinylcyclopentadienyl manganese tricarbonyl (III) in degassed benzene solutions at 70°C with AIBN initiation. The polymerizations took place smoothly to give benzene-soluble polymers which were purified by repeated precipitation from 30–60°C petroleum ether. For each monomer pair, two sets of copolymerizations were carried out at starting mole ratios ( $M_1^0/M_2^0$ ) of 70/30 and 30/70 ( $M_1$  always refers to the organometallic monomer, II or III). In each of these sets a wide range of conversions was obtained, so that for each monomer pair, two polymer composition-conversion curves could be constructed at each of the initial  $M_1^0/M_2^0$  ratios. The copolymer composition ( $M_1/M_2$  ratio in copolymer), in each case, was determined by elemental analysis.\* From these data the relative reactivity ratios were determined by employing the integrated form of the copolymer equation.<sup>29</sup> The computer programs of Montgomery and Fry<sup>30</sup> were employed in these calculations, and our use of these techniques has already been described in detail.<sup>21,22</sup> In addition, the programs of Mortimer and Tidwell,<sup>31</sup> involving use of a nonlinear least-squares statistical approach to fitting the best relative reactivity ratios to experimental data, was employed. Tables I and II summarize representative experimental runs. The values of the relative reactivity ratios are summarized in Table III. The poor correlation between time and yield in each set is attributed to traces of oxygen which were present, in spite of the degassing procedure used in these runs. This is emphasized by the higher yields of runs 10 and 19 performed under  $N_2$  pressure. However, for the purposes of  $r_1, r_2$  studies, this variation is not important.

### Copolymer Characterization

Molecular weight studies were performed by viscosity and gel permeation chromatography studies in THF. A Waters, Model 301 GPC was calibrated by using narrow distribution polystyrene standards whose viscosities had been measured in THF. This permitted the use of a universal calibration<sup>32,33</sup> to which the copolymers could be compared once their intrinsic viscosities had also been obtained in THF. Several representative copolymers were examined and shown to be true polymers of a relatively narrow molecular weight distribution ( $\bar{M}_w/\bar{M}_n > 2$ ) in each case (see Table IV).

\* Elemental analyses were performed by Galbraith Laboratories, Knoxville, Tenn. and Atlantic Microlabs, Atlanta, Ga. The metal analyses were performed both colorimetrically and by atomic absorption spectroscopy and agreed quite well with each other and with the analyses for percent carbon. Also, a known manganese or iron compound of known structure was included in each set sent for analyses, and results were only accepted when the metal analysis for this standard was correct.

TABLE I  
Copolymerization of *N*-Vinyl-2-pyrrolidone with Vinylferrocene  
at 70°C in Benzene Solution<sup>a</sup>

Run number	Vinylferrocene in feed, g	Mole ratio in feed $M_1^0/M_2^0$ <sup>b</sup>	Reaction time, hr	Conversion, %	Fe in copolymer, %	Mole fraction of $M_1$ in copolymer
1	3.9202	70/30	24	16.00	22.30	0.704
2	"	"	48	8.42	21.43	0.696
3	"	"	72	6.98	21.45	0.697
4	"	"	96	10.40	21.53	0.701
5	"	"	120	9.02	21.36	0.692
6	"	"	86	18.90	21.25	0.686
7	"	"	182	19.50	21.31	0.689
8	"	"	350	18.88	21.87	0.719
9	"	"	288	28.60	21.40	0.694
10 <sup>c</sup>	"	"	192	54.50	22.30	0.743
11	2.1379	30/70	24	16.00	15.10	0.413
12	"	"	72	28.70	14.87	0.404
13	"	"	144	22.37	15.00	0.409
14	"	"	264	20.80	14.48	0.390
15	"	"	432	20.20	14.91	0.406
16	"	"	600	12.33	14.65	0.396
17	"	"	288	21.00	15.08	0.412
18	"	"	7	10.70	15.29	0.420
19 <sup>d</sup>	"	"	192	46.00	16.46	0.466

<sup>a</sup> Each polymerization was run in 19 ml of degassed benzene unless otherwise specified. In runs 1–10, 0.9215 g of *N*-vinyl-2-pyrrolidone used; 2.6120 g used in runs 11–19.

<sup>b</sup>  $M_1$  is vinylferrocene.

<sup>c</sup> Under  $N_2$  pressure.

<sup>d</sup> In 8.5 cc benzene.

TABLE II  
Copolymerization of *N*-Vinyl-2-pyrrolidone with Vincyclopentadienyl  
Manganese Tricarbonyl at 70°C in Benzene Solution<sup>a</sup>

Run number	Monomer III in feed, g	Mole ratio in feed $M_1^0/M_2^0$ <sup>b</sup>	Reaction time, hr	Conversion, %	Mn in copolymer, %	Mole fraction of $M_1$ in copolymer
1	0.7771	70/30	24	18.59	17.18	0.553
2	"	"	5.0	7.06	13.14	0.371
3	"	"	10.0	11.05	16.87	0.537
4	"	"	72.0	23.80	18.22	0.608
5	"	"	144.0	33.50	18.48	0.623
6	0.5126	30/70	24	64.13	13.54	0.387
7	"	"	2.5	12.08	15.82	0.487
8	"	"	5	26.88	15.91	0.491
9	"	"	10.0	43.87	15.37	0.466
10	"	"	14.5	55.33	14.67	0.435
11	"	"	192.0	72.30	14.60	0.432

<sup>a</sup> Each polymerization was run in 19 ml. of degassed benzene unless otherwise specified. In runs 1–5, 0.1282 g of *N*-vinyl-2-pyrrolidone used; 0.3919 g used in runs 6–11.

<sup>b</sup>  $M_1$  is vincyclopentadienyl manganese tricarbonyl.

TABLE III  
Relative Reactivity Ratios in *N*-Vinyl-2-pyrrolidone Copolymerizations  
with Vinylferrocene and Vinylcymantrene

Monomer 1	Technique <sup>a</sup>	$r_1$	$r_2$
Vinylferrocene	MF	0.66	0.40
	MT <sup>b</sup>	0.67	0.33
Vinylcymantrene	MF	0.140	0.094
	MT <sup>b</sup>	0.053	0.085

<sup>a</sup> MF = Montgomery and Fry method;<sup>30</sup> MT = Mortimer and Tidwell method.

<sup>b</sup> The 95% confidence limits computed as previously reported<sup>30</sup> for the values of  $r_1$  and  $r_2$  in vinylferrocene copolymerizations was  $r_1 = 0.72$ – $0.59$  and  $r_2 = 0.334$ – $0.290$ . For vinylcymantrene these limits were  $r_1 = 0.05$ – $0.10$  and  $r_2 = 0.05$ – $0.09$ . Considering other possible errors these limits are probably optimistic.

TABLE IV  
Representative Viscosity and Molecular Weight Studies of *N*-Vinyl-2-pyrrolidone  
Copolymers with Vinylferrocene and Vinylcymantrene at 70°C

Polymer	Comonomer	$[\eta]$ , ml/g <sup>a</sup>	$\bar{M}_n$	$\bar{M}_w$	$\bar{M}_w/\bar{M}_n$
2	Vinylferrocene	3.28	6,500	10,200	1.57
10	"	4.25	7,300	11,500	1.57
9	"	3.25	5,800	8,000	1.20
12	"	2.85	5,760	9,400	1.63
19	"	3.15	6,400	10,454	1.64
1	Vinylcymantrene	3.62	6,400	7,720	1.20
5	"	3.08	5,300	7,500	1.40
8	"	3.42	6,700	7,700	1.27
10	"	3.30	5,540	7,800	1.40

<sup>a</sup> Intrinsic viscosities were obtained in THF at 30°C at the same temperature at which GPC studies were performed. Viscosity and molecular weight values cannot be directly compared through this series, since the  $M_1/M_2$  ratio varies in these polymers.

The molecular weight data in Table IV is based on the assumption that a universal calibration is adequate for the determination of the absolute molecular weights of these copolymers. This assumption was checked by employing a normal calibration method and calculating the molecular weights employing *Q* factors of 88 for vinylferrocene,\* 85 for vinylcymantrene, and 45 for vinylpyrrolidone. By use of the mole ratio of  $M_1$  to  $M_2$  in each polymer, an effective *Q* for each polymer was calculated and used in the molecular weight calculations. A close correspondence between the two methods suggests the universal calibration is adequate.

In addition to elemental analyses (Table I and II), infrared spectroscopy confirmed the presence of both monomers in the polymers. In the vinylferrocene copolymers the  $sp^2$  C—H stretching frequency of the cyclopentadienyl ring was found at 3100  $\text{cm}^{-1}$ . In addition, absorptions at 997 and 1100  $\text{cm}^{-1}$ , confirming the presence of unsubstituted cyclopentadienyl ring of ferrocene, (9–10  $\mu$  rule) were present, as was the strong 815  $\text{cm}^{-1}$  band

\* *Q* factors were determined in the usual way by employing vapor pressure osmometry.

TABLE V  
Solubilities of *N*-Vinyl-2-pyrrolidone Copolymers with Vinylferrocene and Vinylcyclopentadienyl Manganese Tricarbonyl

Polymer type <sup>a</sup>	Metal-containing monomer, mole-%	Solubility <sup>b</sup>											
		Water	Methanol	Acetone	THF	Diethyl ether	Pet. ether (30-60°C)	Chloroform	Carbon tetrachloride	DMF	Ethyl acetate	Ethanol	Benzene
VP-VF	70	i	i	s	s	i	i	s	s	s	s	i	s
VP-VF	40	i	i	s	s	i	i	s	s	s	s	i	s
VP-VCMT	55	i	i	s	s	i	i	s	s	s	s	i	s
VP-VCMT	45	i	i	s	s	i	i	s	s	s	s	i	s

<sup>a</sup> VP-VF = vinylferrocene copolymers; VP-VCMT = vinylcyclopentadienyl manganese tricarbonyl copolymers.

<sup>b</sup> s = soluble; sls = slightly soluble, enough to give color to the solution; i = insoluble.



assigned to the out-of-plane bending of the ring hydrogens. A strong carbonyl band at  $1690\text{ cm}^{-1}$  confirmed the presence of the pyrrolidone ring, but the vinyl stretch at  $1620\text{ cm}^{-1}$ , present in the monomer was absent. An intense band at  $1280\text{ cm}^{-1}$  (N-C) in *N*-vinyl-2-pyrrolidone was present in all the copolymers. The vinylcymantrene copolymers exhibited bands at  $3100$  ( $sp^2\text{ C-H}$  stretch),  $2005$ , and  $1905\text{ cm}^{-1}$  ( $\text{C}\equiv\text{O}$  stretch of metal bound carbonyls) characteristic of that monomer.

All the copolymers were readily soluble in THF, DMF, chloroform, carbon tetrachloride, and benzene. Table V summarizes the solubilities of these copolymers over a range of compositions for each copolymer.

The thermal decomposition of the copolymers of vinylcyclopentadienyl manganese tricarbonyl was studied briefly by observing several samples during heating in test tubes under nitrogen. At  $180^\circ\text{C}$  the appearance changed from that of a rather crystalline looking solid to that of an amorphous solid. At about  $195^\circ\text{C}$  a shiny plastic look appeared. At  $210^\circ\text{C}$  bubbles appeared in the plastic mass. It appeared that gas evolution was taking place, presumably CO evolution. Heating to  $270^\circ\text{C}$  produced no further visual change. Two samples were heated at  $260^\circ\text{C}$  for 30 min. During this period darkening occurred, and weight losses of 10.3 and 8.6% were recorded, respectively. Upon cooling, these polymers now exhibited a reduced solubility in benzene and acetone (only about 50% was soluble). Their infrared spectra were not as clear and well defined, but no new absorptions were readily apparent. A sample heated to  $280^\circ\text{C}$  for 30 min showed a weight loss of about 10%, turned a deep brown color, had a glassy appearance, and was only about 20% soluble in benzene. The infrared spectrum of the soluble material had no new easily detectable bands, but the insoluble portion exhibited an absorption at  $1850\text{ cm}^{-1}$  not present before heating. This band is at much lower frequency than the metal-bound carbonyl groups present before heating.

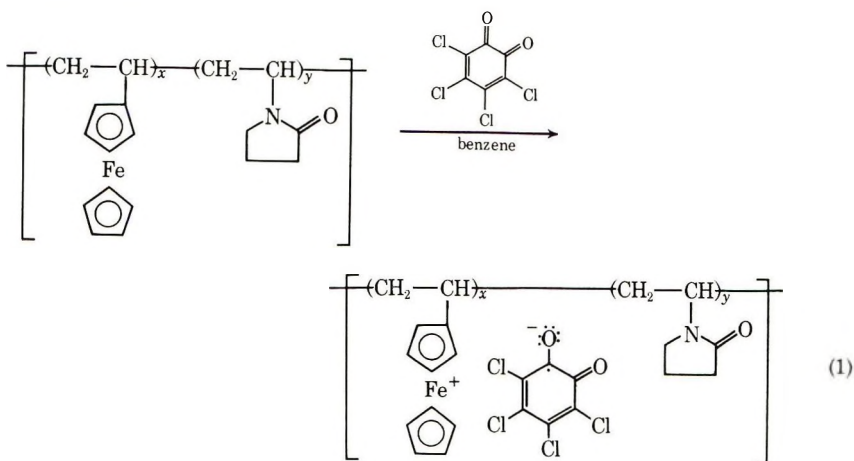
Heating at  $300^\circ\text{C}$  for 30 min caused a 14% weight loss, and the resulting polymer was totally insoluble in benzene. The ir exhibited the  $1850\text{ cm}^{-1}$  band. After 2 hr at  $300^\circ\text{C}$  a 30.3% weight loss was recorded, and the infrared spectrum showed little detail.

The processes occurring during polymer decomposition process are still undefined. The  $\pi\text{-C}_5\text{H}_5\text{Mn}(\text{CO})_3$  moiety is relatively inert, and substitution of carbonyl groups may usually only be achieved under ultraviolet irradiation. However, Nesmayanov et al.<sup>34</sup> demonstrated the thermal decomposition of  $\pi\text{-C}_5\text{H}_5\text{Mn}(\text{CO})_3$  at temperatures greater than  $200^\circ\text{C}$  gave carbon monoxide, manganese metal, and cyclopentadiene polymers. This mode can be invoked to explain the gas evolution we observed and the decrease in copolymer solubility. The decrease in solubility could result from crosslinking between neighboring chains by cyclopentadienyl dimerization. Also free manganese distributed throughout the polymer would result in decrease solubility and darkening. However, the decompositions are undoubtedly more complex, and the origin of the  $1850\text{ cm}^{-1}$  infrared absorption remains unexplained.

The polymers could be cast into rather brittle films which showed only weak adherence to Teflon and a tendency to undergo a transition into a more crystalline material.

### Preparation of Polyferricinium Salts

Upon treatment with strongly oxidizing quinones, such as *o*-chloranil (*o*-CA) and dichlorodicyanoquinone (DDQ), ferrocene groups in polymers are oxidized to ferricinium units.<sup>17</sup> Treatment of vinylferrocene-*N*-vinyl-2-pyrrolidone copolymers with each of these quinones in benzene resulted in electron transfer from iron to quinone. The resulting polysalts [see eq. (1)] precipitated from solution. Reactions with DDQ were conducted at room temperature while those with *o*-CA were run for 4 min at 70°C. The salts were black solids which were soluble in dimethylformamide but only very slightly soluble in acetone. Their solubility behavior is summarized in Table VI. The polysalts were purified by repeated washings with benzene and acetone. Heating to 360°C did not cause melting or any other visible change in the polysalts.



Infrared spectroscopy demonstrated that each mole of quinone, which was incorporated into the polysalts, had been reduced to its radical anion. The powerful carbonyl stretching frequencies of DDQ (1680  $\text{cm}^{-1}$ ) and *o*-CA (1640  $\text{cm}^{-1}$ ) were always shifted to lower frequencies. For example, in the DDQ polysalts the carbonyl band was shifted to 1570  $\text{cm}^{-1}$ . This shift is just what is expected for the DDQ radical anion.<sup>35,36</sup> The original 1680  $\text{cm}^{-1}$  band was absent in the spectra of the polysalts. In addition to the cyclopentadienyl C—H out-of-plane bending frequency at 820  $\text{cm}^{-1}$ , normally exhibited by ferrocene derivatives,<sup>37</sup> an additional band was found at 850–860  $\text{cm}^{-1}$  in all the polysalts. This is due to the ring C—H out-of-plane bending frequency of the ferricinium nucleus.<sup>38</sup> The presence of both

TABLE VI  
Stoichiometry and Solubility Behavior of Poly(ferricinium Salts) Prepared from Vinylferrocene-*N*-Vinyl-2-pyrrolidone  
Copolymers and Oxidizing Quinones

Number of copolymer used	Mole fraction of M <sub>1</sub> in copolymer	Quinone	Quinone, mole/mole vinylferrocene in polysalt	Solubility <sup>a</sup>							
				Water	DMF	Methanol	Acetone	Ethyl acetate	Chloroform	Carbon tetrachloride	Benzene
10	0.743	DDQ	0.767	sls	s	sls	sls	i	sls	i	i
19	0.420	DDQ	0.850	sls	s	sls	sls	i	sls	i	i
10	0.743	o-CA	0.381	i	s	sls	sls	sls	i	i	i
19	0.420	o-CA	0.520	i	s	sls	sls	sls	i	i	i
9 <sup>b</sup>	0.694	DDQ	0.300	sls	s	sls	sls	sls	sls	i	i

<sup>a</sup> s = soluble; sls = slightly soluble, enough to give a trace of color in solution; i = insoluble.

<sup>b</sup> Prepared in DMF.

bands illustrates that not all the ferrocene units have been oxidized. Apparently precipitation from solution occurs before complete oxidation takes place. Thus, the infrared spectra of these polysalts are completely consistent with the detailed discussion infrared spectra of poly(ferricinium quinone) salts (which was further substantiated by Mössbauer spectroscopy) published earlier.<sup>17</sup> The reader is referred to this study for a more complete discussion.

Elemental analyses confirmed the infrared results. The mole ratios of quinone to ferrocene calculated from these analyses in the polysalts were less than one (see Table VI). This result was confirmed both by iron and chlorine analyses.

## EXPERIMENTAL

*N*-Vinyl-2-pyrrolidone (trade name V-PYROL) was obtained from General Aniline and Film Corporation and vacuum-distilled before use (bp 46°C/0.1 mm) with center cuts used. Vinylferrocene<sup>18,19,39</sup> and vinylcyclopentadienyl manganese tricarbonyl<sup>39</sup> were prepared as described previously starting from ferrocene (Arapahoe Chemical Co.) and cyclopentadienyl manganese tricarbonyl (Ethyl Corporation), respectively. Vinylferrocene was sublimed and recrystallized from hexane before use (mp 51°C, lit.<sup>39</sup> mp 51°C). Vinylcyclopentadienyl manganese tricarbonyl was purified by vacuum distillation (bp 60–65°C/0.05 mm Hg, lit.<sup>40</sup> bp 29–30°C/0.005 mm Hg).

The copolymerizations were carried out in degassed (three freeze-thaw cycles) benzene in Fischer-Porter aerosol compatibility tubes, with triply recrystallized (from methanol) AIBN as the initiator. This technique has previously been described in detail.<sup>17–29</sup> Following the polymerization, the copolymers were precipitated by dropwise addition of the benzene solutions to rapidly stirring 30–60° petroleum ether and collected by filtration. This was repeated three times to insure purity and the polymers were dried by rotary evaporation and overnight drying of powdered samples in a vacuum drying oven at 60°C. The viscosity and GPC measurements were performed by standard methods which are described elsewhere.<sup>17–22</sup>

Copolymers of I and II were treated with commercial DDQ and *o*-CA (Aldrich Chemical Co.) used without further purification. Benzene solutions of the copolymers were added to benzene solutions of the quinones (room temperature for DDQ and 70°C for 5 min for *o*-CA). The polysalts were recovered as black precipitates from the benzene solutions. They were purified by repeated washings of finely powdered material with benzene and acetone. This removes any unreacted polymer and quinone.

Infrared spectra of the copolymers are summarized: copolymers of I and II, 3100, 2970, 2930, 2860, 1690, 1450, 1430, 1280, 1130, 1110, 1075, 998, 815, 500, 475 cm<sup>-1</sup>; copolymers of I and III, 3100, 2980, 2935, 2865, 2005, 1905, 1670, 1460, 1420, 1360, 1280, 1036, 900, 834, 660, 630, 535 cm<sup>-1</sup>.



The authors would like to thank the Paint Research Institute for a Research Fellowship (to P. L. G.) and the Research Corporation for a research grant for the purchase of gel permeation chromatography equipment. The research reported in this paper was also sponsored in part by the Air Force Cambridge Research Laboratories under contract number F19628-71-C-0107, but this report does not necessarily reflect endorsement by the sponsor. Mr. Gary Marlin is thanked for the preparation of quantities of vinylcyclopentadienyl manganese tricarbonyl, and Mr. Thane Rounsefell is thanked for help in programming and running the computer programs used in relative reactivity ratio calculations.

## References

1. *Chem. Week*, **81**, 62, (Oct. 26, 1957).
2. J. Werner, R. Steckler, and F. A. Hessel, U. S. Pat. 2,809,953.
3. J. F. Bork and L. E. Coleman, *J. Polym. Sci.*, **43**, 413 (1960).
4. F. Cech, Ph.D. Thesis, University of Vienna, Austria (1957).
5. *Vinylpyrrolidone*, Technical Bulletin 7543-037, General Aniline and Film Corporation, New York.
6. H. Loleit, German Pat. 881,445.
7. J. R. Caldwell and R. Gilkey, U. S. Pat. 2,882,255.
8. D. A. Smith and C. C. Unruh, U. S. Pat. 2,882,262.
9. Gavaert Photo & Producten N. V., Brit. Pat. 805,386.
10. H. Fikentscher and H. Wilhelm, U. S. Pat. 2,808,383.
11. W. M. Perry, U. S. Pat. 2,958,614.
12. C. Schildknecht, U. S. Pat. 2,776,947.
13. H. Fikentscher, German Pat. 743,945.
14. W. W. Chaney, U. S. Pat. 2,688,010.
15. H. Fikentscher, H. Wilhelm, H. Wirth, and K. Dachs, German Pat. 1,014,957.
16. A. Henglein, W. Schnabel, and K. Heine, *Angew. Chem.*, **70**, 461 (1958).
17. C. U. Pittman, Jr., J. C. Lai, D. P. Vanderpool, M. Good, and R. Prados, *Macromolecules*, **3**, 746 (1970).
18. J. C. Lai, T. D. Rounsefell, and C. U. Pittman, Jr., *J. Polym. Sci. A-1*, **9**, 591 (1971).
19. C. U. Pittman, Jr., R. L. Voges, and J. Elder, *J. Polym. Sci. B*, **9**, 194 (1971).
20. C. U. Pittman, Jr., *Chem. Technol.*, **1**, 416 (1971).
21. J. C. Lai, T. D. Rounsefell, and C. U. Pittman, Jr., *Macromolecules*, **4**, 155 (1971).
22. C. U. Pittman, R. L. Voges, and W. Jones, *Macromolecules*, **4**, 291, 298 (1971).
23. J. H. Richards, *J. Paint Technol.*, **39**, 569 (1967).
24. A. J. Fry, R. S. H. Lui, and G. S. Hammond, *J. Amer. Chem. Soc.*, **88**, 4781 (1966).
25. R. G. Schmitt and R. C. Hirt, American Cyanamid Co., Air Force WADC Tech. Reports, 59-354; 60-704; and 61-298 (available from the Defense Documentation Center, Alexandria, Va.).
26. R. C. McIlhenny and S. A. Honigstein, July 1965, Air Force Report No. AF MLTR-65-294, AD 476623, Contract No. AF-33-(615)-1694.
27. J. Kozikowski and M. Cais, U. S. Pat., 3,290,337 (1966); U. S. Pat. 3,308,141 (1967).
28. C. U. Pittman, Jr., J. Saad, J. Chapman, J. C. Lai, and T. D. Rounsefell, paper presented at Joint Southeast-Southwest Regional Meeting of the American Chemical Society, New Orleans, La., Dec. 2-4, 1970, papers 627, 664, and 666; *Abstracts*, pp. 187, 199-200.
29. F. R. Mayo and F. M. Lewis, *J. Amer. Chem. Soc.*, **66**, 1594 (1944).
30. D. R. Montgomery and C. E. Fry, in *The Computer in Polymer Science* (*J. Polym. Sci. C*, **25**), J. B. Kinsinger, Ed., Interscience, New York, 1968, p. 59.
31. P. W. Tidwell and G. A. Mortimer, *J. Polym. Sci. A*, **3**, 369 (1965).



32. Z. Grubisic, P. Rempp, and H. Beniot, *J. Polym. Sci. B*, **5**, 753 (1967).
33. H. Coll and D. K. Gilding, *J. Polym. Sci. A-2*, **8**, 89 (1970).
34. O. D. Krichevskaya, N. A. Belozerskii, L. D. Segal, N. E. Kolobova, K. N. Anisimov, and A. N. Nesmeyanov, *Zh. Neorgan. Khim.*, **8**, 1806 (1963); *Chem. Abstr.*, **59**, 10975.
35. R. L. Brandon, J. H. Osiecki, and A. Ottenberg, *J. Org. Chem.*, **31**, 1214 (1966).
36. Y. Iida, *Bull. Chem. Soc. Japan*, **43**, 345 (1970).
37. I. Pavlik and V. Plechacek, *Collect. Czech. Chem. Commun.*, **31**, 2083 (1966).
38. I. J. Spilners, *J. Organometal. Chem.*, **11**, 381 (1968).
39. J. C. Lai, Ph.D. Thesis, University of Alabama (1970).
40. A. N. Nesmeyanov, *Dokl. Akad. Nauk SSSR*, **154**, 39 (1964); *Chem. Abstr.*, **60**, 10705.

Received May 11, 1971

Revised July 12, 1971

## Organometallic Polymers. XV. Synthesis and Characterization of Some Ferrocene-Containing Oxysilane Polymers from Bis(dimethylamino)silanes

CHARLES U. PITTMAN, JR.,\* and WILLIAM J. PATTERSON,† *Department of Chemistry, University of Alabama, University, Alabama 35486* and SAMUEL P. McMANUS, *Department of Chemistry, University of Alabama at Huntsville, Huntsville, Alabama 35807*

### Synopsis

Three bis(dimethylamino)silane monomers have been polymerized with 1,1'-bis(hydroxymethyl)ferrocene to give ferrocene-containing polyoxysilanes I and II. They were bis(dimethylamino)dimethylsilane (III), bis(dimethylamino)diphenylsilane (IV), and 1,4-bis(*N,N*-dimethylaminodimethylsilyl)benzene (V). Mixing of the diol and III or IV at 0°C followed by heating resulted in polymerization to higher molecular weights than when the monomers were initially mixed at higher temperatures. At higher temperatures the formation of monomeric cyclic products seriously competed with polymerization, and the five atom bridged derivative, 3-sila-2,4-dioxa-3,3-diphenyl[5]ferrocenophane (VI) was isolated in good yield. The use of silane V, where cyclization is not expected to compete, led to higher polymer yields and molecular weights. The polymers were low melting and I ( $R = C_6H_5$ ) could be cast into films and weak fibers were drawn from its melt. The polymers were sensitive to hydrolytic decomposition; those containing Si-CH<sub>3</sub> linkages were completely hydrolyzed in refluxing THF-H<sub>2</sub>O (10:1) in 1 hr. The polymers were characterized by viscosity studies, gel-permeation chromatography, and infrared and NMR spectroscopy.

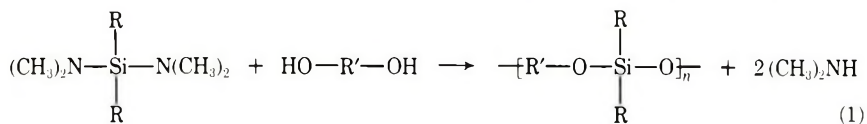
### INTRODUCTION

Organosilicon polymers are currently of immense industrial importance. One class of silicon polymers, organosilicon heteropolymers, have been the subject of intense interest in recent years.<sup>1</sup> One subgroup of this class incorporates organometallic structures into the silicon polymer. The availability of ferrocene, which is thermally stable, has stimulated much research on ferrocene-containing silicon polymers. This work has recently been reviewed by Neuse and Rosenberg.<sup>2</sup> However, close examination of published research reveals that existing ferrocene-silicon polymers have relatively low molecular weights. This is true for polymers with silicon bonded to the cyclopentadienyl rings<sup>3-7</sup> or isolated from the rings.<sup>8,9</sup>

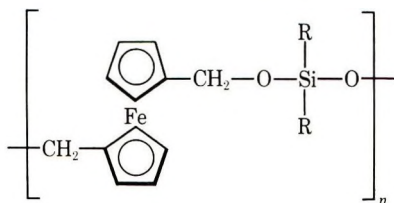
\* To whom inquiries should be addressed.

† Present address: Marshall Space Flight Center, Astronautics Laboratory Materials Division, Huntsville, Alabama 35812.

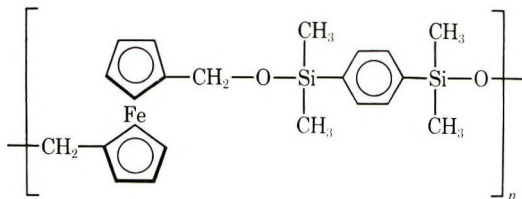
As part of an extensive investigation of transition metal-containing organic polymers,<sup>10</sup> we decided to investigate the propensity of 1,1'-bis-(hydroxymethyl)ferrocene to undergo polycondensation with a series of bis(dimethylamino)silanes. The general reaction of diols with bis(dimethylamino)silanes [eq. (1)] was first employed by Curry and Byrd<sup>11</sup> to



prepare high molecular weight aryloxysilane polymers. One of us has further explored the utility of this reaction in a variety of polysiloxane preparations<sup>12,13</sup> where dimethylamine was rapidly evolved under mild conditions. This reaction should be of singular advantage when using ferrocene diols because dimethylamine will not degrade ferrocene under the reaction conditions. The use of dichlorosilanes as comonomers would result in HCl generation during heating, and the cleavage of ferrocene's cyclopentadienyl rings from iron under such conditions is a well known reaction.<sup>14-16</sup> Ferrocene-silicon polymers of structures I or II have not yet been reported, and this reaction appeared to offer a facile route for their preparation.



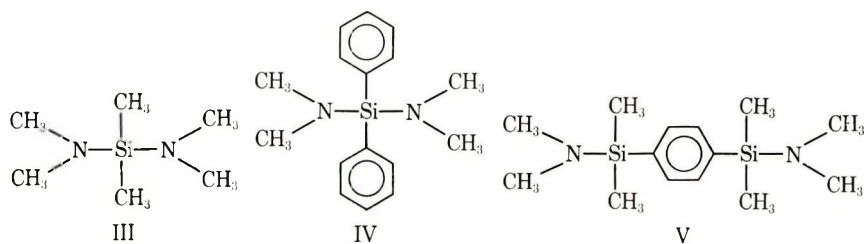
I



II

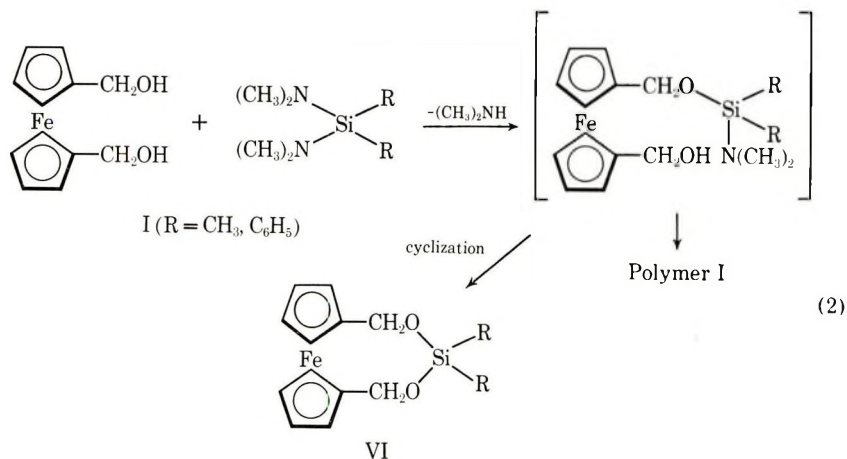
## RESULTS

Three bis(dimethylamino)silanes were prepared and condensed with 1,1'-bis(hydroxymethyl)ferrocene to give a series of three new ferrocene-containing polysiloxanes I ( $\text{R} = \text{CH}_3$ ,  $\text{C}_6\text{H}_5$ ) and II. The silanes used were bis(dimethylamino)dimethylsilane (III), bis(dimethylamino)diphenylsilane (IV), and 1,4-bis(*N,N*-dimethylaminodimethylsilyl)benzene (V). These polymers were most efficiently prepared by condensing stoichiometric amounts of each monomer in a small amount of dried toluene at



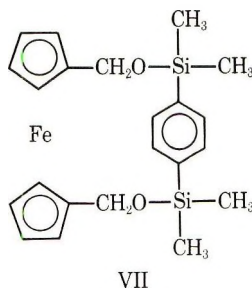
about 0°C under nitrogen (method one). After stirring at 0°C for 1–2 hr, the reaction was warmed to room temperature and heated under an aspirator vacuum to about 100°C to drive off remaining dimethylamine efficiently and complete the polymerization.

The expected propensity of this reaction to form cyclic products [eq. (2)] was realized in reactions which were started at room temperature. Reactions begun at room temperature or above gave lower molecular weight products, and in the case of monomer IV, reasonable yields of cyclic VI ( $R = C_6H_5$ ) were isolated.



The rapid rate of dimethylamine displacement at low temperatures appears to be one advantage of using bis(dimethylamino)silanes instead of dichlorosilanes. Since the cyclization reaction is only favored at elevated temperatures, successful polymerizations were carried out at 0°C where the polymerization rate was still conveniently rapid. Thus, reasonably high molecular weight polysiloxanes were obtained in spite of this cyclization reaction. The use of monomer V should reduce the rate of such a cyclization reaction.\* The cyclic ferrocenophane derivative, VII, was never isolated. Thus, it was not surprising to find the highest polymer

\* It should be noted that the cyclic molecule VII could be constructed using molecular models, and it did not appear to be strained. However, the frequency factor for this cyclization should be markedly lower than that for the cyclization in eq. (2).



yields and molecular weights were obtained when bis(dimethylamino)-silane V was used.

When 1,1'-bis(hydroxymethyl)ferrocene was condensed with monomer IV in refluxing toluene for 4 hr, a 80.6% yield of the cyclic product 3-sila-2,4-dioxa-3,3-diphenyl[5]ferrocenophane(VI),  $R = C_6H_5$ , was obtained which after two recrystallizations from hot *n*-hexane gave an analytically pure sample; mp 134–134.5°C; mass spectrum, 426 parent ion: infrared and NMR spectra and elemental analysis in agreement with this structure. A similar reaction with monomer III gave low molecular weight polymers and presumably cyclic VI ( $R = CH_3$ ). However, this cyclic product has eluded all attempts at isolation to date. The polymer and cyclic product mixture was repeatedly precipitated from THF into 30–60°C petroleum ether, followed by column chromatography of these fractions on  $Al_2O_3$  with several solvents. However, analytical gel-permeation chromatography indicated cyclic VI remained mixed with polymeric products.

### Polymer Characterization

The yields, molecular weights, approximate melting temperature, and intrinsic viscosities of representative polysiloxanes prepared in this work are presented in Table I. Polymers 1 and 3 (from Table I) were amorphous, waxy solids, and polymer 2 was a glossy solid. All were soluble in THF, benzene, and DMF but were easily precipitated from either petroleum ether or methanol. Polymer 2 was cast as a continuous film from THF and benzene, and weak fibers could be drawn from its melt.

The effect of the initial monomer mixing temperature on molecular weight is clearly illustrated in Table I. Equimolar mixing of monomers at 50°C (method 3) resulted in a significantly lower product molecular weight compared to initial mixing at 0°C. An attempt was made to obtain high molecular weights by first generating VIII upon the addition of 1,1'-bis(hydroxymethyl)ferrocene to a tenfold excess of silane IV at ~50°C over a period of 1 hr. (method 2). After heating at 60–70°C for an additional hour, toluene was removed at 100 mm Hg to 0.05 mm Hg. Then the excess IV was completely removed (100°C/0.05 mm Hg), and a molar equivalent of 1,1'-bis(hydroxymethyl)ferrocene in dry toluene was added to VIII at room temperature followed by heating to 50–60°C. Then toluene was stripped off, and the polymer further heated to 100° at 0.05 mm for 1



TABLE I  
 Ferrocene-Containing Polyoxysilanes

Polymer	Polymer structure	Silane used	Polymerization method <sup>a</sup>	Polymer yield, %	[ $\eta$ ], ml/g <sup>b</sup>	Molecular weight <sup>c</sup>		$\bar{M}_w/\bar{M}_n$	$T_m$ , °C <sup>d</sup>
						$\bar{M}_n$	$\bar{M}_w$		
1	I, R = CH <sub>3</sub>	III	1 <sup>a</sup>	51	7.56	4,800	10,600	2.20	50-55
2	I, R = C <sub>6</sub> H <sub>5</sub>	IV	1	62	5.73	8,900	19,000	2.14	40-45
	I, R = C <sub>6</sub> H <sub>5</sub>	IV	2	45	4.67	4,250	8,500	2.00	
	I, R = C <sub>6</sub> H <sub>5</sub>	IV	3	42	3.20	3,450	7,850	2.28	
3	II	V	1	93	22.0	9,900	26,900	2.72	60-65

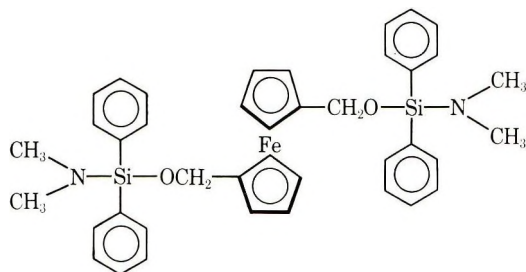
<sup>a</sup> Method 1: equimolar addition of monomers at 0°C, retain at 0°C for 1-2 hr followed by warming to 30°C and finally to 100°C with aspiration. Method 2: initial addition of diol to a large excess of silane at 50°C followed by heating and simultaneous aspiration. Method 3: equimolar addition of the monomers at 50°C followed by further heating under aspiration to 100-110°C.

<sup>b</sup> Intrinsic viscosities were measured at 30°C in THF.

<sup>c</sup> Calculated from gel-permeation chromatograms by using a universal type of calibration. Chromatograms were run at 30°C in THF. A bank of four Styragel columns with ratings of  $5-1.5 \times 10^4$ , two of  $1.5 \times 10^4$  to  $3 \times 10^4$  Å, and 700 to 350 Å was used.

<sup>d</sup> Approximated by using the temperature at which the polymer would spread out between two glass plates of a Fisher Johns melting point apparatus when gentle pressure was applied. These results were essentially identical to determinations performed by using a Kofler Heizbank hot bar technique at which the lowest temperature of melting is considered the PMT.

<sup>e</sup> When polymer I, R = CH<sub>3</sub>, was prepared by methods 2 and 3, lower molecular weights were obtained as evidenced by  $[\eta] = 4.0-4.5$  ml/g.



VIII

hr. The molecular weight of the resulting material was significantly lower than that observed by using method 1, where initial mixing at 0°C was employed.

Each of these polymers contain the  $-\text{CH}_2-\text{O}-\text{Si}-\text{O}-$  linkage which normally exhibits hydrolytic instability. In these polymers carbon-oxygen heterolytic cleavage would be promoted by the exceptional stability of the resulting  $\alpha$ -ferrocenyl carbonium ion.<sup>17-19</sup> This might be a sufficient condition to promote an  $S_N1$  hydrolysis mechanism in polar solvents. Alternatively, water might preferentially attack silicon to give a penta-coordinated transition state<sup>21</sup> which decomposes via  $\text{Si}-\text{O}$  cleavage. This hydrolytic instability was confirmed by refluxing 10:1 (by volume)  $\text{THF}-\text{H}_2\text{O}$  solutions of each of the polymers for 1 hr at 60–65°C. The residues were analyzed by GPC. Under these conditions polymer types I ( $\text{R} = \text{CH}_3$ ) and II were entirely degraded and absolutely no polymer peak could be detected by GPC. Conversely, the hydrolysis of polymer I ( $\text{R} = \text{C}_6\text{H}_5$ ) was markedly slower. A GPC of this residue showed the polymer was largely intact, but some degradation was evident from a lowering of the molecular weight from  $\bar{M}_n = 8,900$ ,  $\bar{M}_w = 19,000$  and  $[\eta] = 5.73$  ml/g to  $\bar{M}_n = 2100$ ,  $\bar{M}_w = 4340$  and  $[\eta] = 3.10$  ml/g. Thus, it is clear these polymers are not suitable for use under hydrolyzing conditions.

The far slower rate of hydrolysis of polymer I ( $\text{R} = \text{C}_6\text{H}_5$ ) is evidence that hydrolysis occurs by nucleophilic attack of water on silicon. The phenyl rings can provide steric hinderance to nucleophilic attack at Si especially in a structure such as I. However, if the decomposition proceeded by a rate-determining unimolecular  $-\text{CH}_2-\text{O}-$  bond cleavage ( $S_N1$ ) there is no obvious reason why the diphenylsiloxane polymer should hydrolyze more slowly than its dimethyl analog. In fact, hydrolysis might be faster if the phenyl inductive effect was significantly felt or if the phenyls cause any measurable increase in strain (compared to methyls) which might be relieved during  $-\text{CH}_2-\text{Si}$  bond cleavage.

## EXPERIMENTAL

### Preparation of Bis(dimethylamino)dimethylsilane (III)

Dimethyldichlorosilane (Pierce Chemical Co.), which was distilled prior to use, was added (146.3 g, 1.0 mole) to a 5 mole excess of dimethylamine

in anhydrous diethylether (300 ml) at  $-5$  to  $0^{\circ}\text{C}$  under nitrogen. Particular care was taken to thoroughly dry all glassware prior to its use. Following this addition the mixture was warmed slowly and stirred at ether reflux for 1 hr. The hydrochloride salts were then filtered under nitrogen and the salts were washed twice with excess ether. Ether was removed from the combined filtrates and the residue was carefully fractionated through a vacuum-jacketed, silvered, 15-in. Oldersaw column under a 5:1 reflux ratio. A center cut was collected at  $125^{\circ}\text{C}/760$  mm Hg (lit.<sup>22</sup> bp  $124\text{--}127^{\circ}\text{C}/760$  mm). The infrared and NMR spectra agreed with the literature and were in accord with the structure. GLPC analysis on a 4-ft SE 30-Chromasorb W column at  $100^{\circ}\text{C}$  demonstrated the purity was greater than 99%. The yields of purified silane ranged from 55 to 60%.

#### Preparation of Bis(dimethylamino)diphenylsilane (IV)

Diphenyldichlorosilane (Pierce Chemical Co.) was distilled prior to use and then treated with dimethylamine in exactly the manner previously described for monomer III. The crude fraction was purified by distillation (as with III): bp  $125\text{--}126^{\circ}\text{C}/1.0$  mm Hg (lit.<sup>22</sup> bp  $138\text{--}140^{\circ}\text{C}/1.9$  mm Hg). GLPC analysis at  $275^{\circ}\text{C}$  (same column as used for III) showed the purity exceeded 99%. The infrared and NMR spectra agreed with the structure. Yields of purified product ranged from 50 to 60%.

#### Preparation of 1,4-bis(dimethylaminodimethylsilyl)benzene (V)

The preparation of 1,4-bis(chlorodimethylsilyl)benzene was carried out as described by Sveda<sup>23</sup> and fractionated to give a material with bp  $100\text{--}101^{\circ}\text{C}/1.0$  mm (lit.<sup>23</sup> bp  $108\text{--}110^{\circ}\text{C}/1.5$  mm). The dichloride was converted to V by treatment with excess dimethylamine by the same procedure used in the preparation of III and IV. Crude V was fractionated twice and the material obtained had bp  $73\text{--}74^{\circ}\text{C}/0.06$  mm (lit.<sup>24</sup> bp  $100\text{--}101^{\circ}\text{C}/0.5$  mm). The NMR spectrum exhibited three sharp singlets at,  $\sigma$ , 0.31, area 12 ( $\text{Si}-\text{CH}_3$ ), 2.51, area 12 ( $\text{N}-\text{CH}_3$ ), and 7.30, area 4 (phenyl protons). The infrared was in accord with structures with characteristic bands at 3070 ( $sp^2\text{C}-\text{H}$ ), 2980, 2910, 2875, 2860, 2810, 1480, 1450, 1375, 1255 ( $\text{Si}-\text{CH}_3$ <sup>25</sup>), 1040 ( $\text{Si}-\text{C}_6\text{H}_5$ ),<sup>26</sup> 995, 815 (out-of-plane C—H deformation of ferrocene), 775, 690, and  $620\text{ cm}^{-1}$ . GLPC analysis indicated the purity in excess of 99%. Yields of pure monomer were about 40–60%.

#### 1,1'-Bis(hydroxymethyl)ferrocene

This was obtained from Strem Chemical Co. and was purified by repeated recrystallization from hexane/methanol to a constant melting point of  $107\text{--}108^{\circ}\text{C}$  (lit.<sup>27</sup> mp  $107\text{--}108^{\circ}\text{C}$ ).

#### Preparation of 3-Sila-2,4-dioxa-3,3-diphenyl[5]ferroceneophane (VI)

Both 1,1'-bis(hydroxymethyl)ferrocene, (4.0 g, 0.0162 mole), and aminosilane IV (4.40 g, 0.0162 mole) were combined with dried toluene (20 ml)

under nitrogen in rigorously dried glassware. This mixture was refluxed for 4 hr, cooled, and added to 2500 ml of dried 30–60° petroleum ether. The polymeric portion of the reaction product precipitated and was filtered off. The petroleum ether layer was concentrated to dryness, and a yellow crystalline solid which remained was washed repeatedly with methanol until the washings were colorless to remove residual diol. The crude product was recrystallized from hot hexane twice and 5.6 g (80.6% yield) of VI was obtained. This compound, not previously reported in the literature, was thoroughly characterized: mp 134–134.5°C; mass spectrum, 426 parent ion (theory 426 for  $C_{24}H_{22}FeO_2Si$ ). The NMR spectrum showed  $\sigma$ , 7.37, *m*, area 6 (*ortho* and *para* phenyl protons); 7.74, *m*, area 4 (*meta* phenyl protons); 4.65, *s*, area 4 ( $—CH_2—O—$ ); 4.16 and 4.26, *t*,  $J = 1.8$  Hz, area of each was 4 (cyclopentadienyl ring protons). Infrared absorptions (KBr) were at 3100, 3015 ( $sp^2$  C—H stretch), 2945, 2870, 1430, and 1120–1130 ( $C_6H_5—Si$ ),<sup>26</sup> 1000 ( $C_6H_5—Si$ ),<sup>26</sup> 1070–1090 ( $Si—O—C$ ),<sup>28</sup> 922, 809, 782, 740, 713, and 700  $cm^{-1}$ .

ANAL. Calcd for ( $C_{24}H_{22}FeO_2Si$ ): C, 67.60%; H, 5.21%; Si, 6.59; Fe, 13.09%. Found: C, 67.70%; H, 5.15%; Si, 6.65%; Fe, 12.58%.

### Preparation and Analysis of Polymers

#### *Polymer I* ( $R = CH_3$ )

Silane III (1.2754 g, 0.0090 mole), and 1,1'-bis(hydroxymethyl)ferrocene (2.215 g, 0.0090 mole) were added together under nitrogen in predried glassware at 0°C. Dry toluene (20 ml) was injected by syringe, and the mixture was stirred for 1 hr at 0°C. The pressure in the flask was then reduced to 100 mm by using an aspirator-drying train sequence, and the temperature was gradually raised to room temperature and held at this point under vacuum for another hour. Toluene was added as necessary to keep the reaction fluid. Next, the temperature was raised to 100°C and the toluene stripped off. Then the pressure was lowered to ~0.1 mm and the temperature maintained at 100°C for 1 hr. At this point the very viscous polymeric residue was dissolved into the minimum amount of THF (under  $N_2$ ) and added to 2500 ml of dried 30–60°C petroleum ether. The polymeric fraction precipitated as a brown gum and was filtered. This residue was twice again reprecipitated from THF. A portion was eluted from an alumina column by using the solvent sequence, hexane, THF, methanol. Most of the polymer eluted in the THF fraction. Intrinsic viscosities of both the chromatographed and unchromatographed product were essentially the same ( $[\eta] = 7.56$  ml/g). Molecular weights were determined by gel-permeation chromatography in THF and are summarized in Table I together with yield and  $T_m$  determinations.

Spectral data were in accord with structure I. The NMR showed  $\sigma$ , 0.35, *s*, area 6 ( $Si—CH_3$ ); 4.26, broad unresolved, area 8 (cyclopentadienyl ring protons); 4.59, *s*, area 4 ( $—CH_2—O—$ ). Infrared absorption (KBr) showed key bands at 3300–3400 (traces of terminating  $Si—OH$  groups),



3100 ( $sp^2$  C—H), 2960–2830, 1240 (Si—CH<sub>3</sub>), 1070–1090 (Si—O—C), and 815  $\text{cm}^{-1}$  (ring out-of-plane hydrogen deformations).

ANAL. Calcd for (C<sub>14</sub>H<sub>18</sub>O<sub>2</sub>FeSi): C, 55.63%; H, 6.01%; Si, 9.29%. Found: C, 55.20%; H, 5.85%; Si, 9.05%.

*Polymer I* ( $R = C_6H_5$ )

**Method 1.** Silane IV (2.4344 g, 0.0090 mole), and 1,1'-bis(hydroxymethyl)ferrocene, (2.2148 g, 0.0090 mole), were polymerized by the procedure outlined above, and the polymer was worked up in the same manner. Obtained in 62% yield, the polymer was analyzed by GPC (molecular weights and  $T_m$  see Table I) and its intrinsic viscosity in THF was 5.73 ml/g. Spectral data were in accord with structure. The NMR showed  $\sigma$ , 7.59, *m*, area 4 (*meta* phenyl protons); 7.24, *m*, area 3 (*ortho* and *para* phenyl protons); 4.3–4.5, broad, area 4 (—CH<sub>2</sub>O—); 4.03, broad, area 8 (cyclopentadienyl ring protons). Infrared bands (KBr) were at 3090 and 3055 ( $sp^2$  C—H stretch of phenyl and ferrocene), 2935, 2870, 2860, a combination 1425, 1120–1130, and 1000 (Si—C<sub>6</sub>H<sub>5</sub>), 1080–1020 (Si—O—C), 740, and 700  $\text{cm}^{-1}$  (monosubstituted phenyl).

ANAL. Calcd for (C<sub>24</sub>H<sub>22</sub>O<sub>2</sub>FeSi): C, 67.60%; H, 5.21%; Si, 6.59%. Found: C, 67.40%; H, 5.65%; Si, 6.35%.

**Method 2.** This method utilized the prior preparation of diadduct VIII and has been adequately described in the text (also see Table I).

**Method 3.** Silane IV (2.4344 g, 0.0090 mole) was added by syringe to a dry toluene solution of the diol (2.2148 g, 0.0090 mole) in carefully dried glassware under nitrogen at 50°C. The temperature was then increased to 100–110°C for 4 hr. The toluene-polymer solution was then added dropwise to 2500 ml of 30–60°C petroleum ether. The precipitated polymer was reprecipitated from a minimum amount of THF in more petroleum ether, recovered and dried. Its properties are described in Table I.

*Polymer II*

Silane V (2.7827 g, 0.0099 mole) and 1,1'-bis(hydroxymethyl)ferrocene (2.4412 g, 0.0099 mole) were added together under nitrogen in predried glassware at 0°C. Dry toluene (25 ml) was added by syringe, and the mixture was stirred for 1 hr at 0°C. The flask pressure was then reduced to ~100 mm by using an aspirator-drying tube sequence, and the temperature was gradually raised to 30°C where it was held under vacuum for 1 hr. The temperature was then raised to 90–100°C and toluene was stripped off. The pressure was then lowered to 0.1 mm and the temperature was held constant at 100°C for 1 hr. Then the viscous polymeric residue was dissolved in the minimum amount of tetrahydrofuran and added dropwise to 500 ml of dried 30–60°C petroleum ether. The polymer, which precipitated as a brown gum, was subsequently reprecipitated twice more from petroleum ether to give a 93% yield of product. Intrinsic viscosity and molecular weight were determined for the polymer (summarized in Table



I) together with yield and  $T_m$  determinations. Spectral data were in accord with structure. NMR showed  $\sigma$ , 7.67, s, area 4 (phenyl protons); 4.50, s, area 4 ( $-\text{CH}_2\text{O}-$ ); 4.12, unresolved  $m$ , area 8.3 (cyclopentadienyl ring protons); 0.48, s, area 12 ( $\text{Si}-\text{CH}_3$ ). The infrared spectrum (KBr) had bands at 3400–3450 (trace of terminal  $\text{Si}-\text{OH}$ ), 3100 ( $sp^2 \text{CH}$ ), 2950–2850 ( $sp^3 \text{C}-\text{H}$ ), 1255 and 1264 ( $\text{Si}-\text{CH}_3$ ), 1140 ( $\text{Si}$ -phenyl), 1050–1080 ( $\text{Si}-\text{O}-\text{C}$ ), 815 ( $\text{C}-\text{H}$  out-of-plane ring deformation), and 775  $\text{cm}^{-1}$ .

ANAL. Calcd for  $\text{C}_{22}\text{H}_{28}\text{O}_2\text{FeSi}_2$ : C, 60.53%; H, 6.48%; Si, 12.8%. Found: C, 60.30%; H, 6.60%; Si, 12.45%.

This paper is taken from work submitted by W. J. Patterson in his Ph.D. thesis.

The National Aeronautics and Space Administration, Marshall Space Flight Center, Astronautics Laboratory is thanked for support of W. J. Patterson during a two-semester residence at the University of Alabama. The partial support of this work by the U. S. Air Force Cambridge Laboratories, Contract No. F19628-71-C-0107, is acknowledged, although the views expressed here do not necessarily reflect endorsement by the Air Force. Additional support of this work was provided in part by Petroleum Research Fund Grant No. 4479AC1,3, by a Research Corporation Grant to purchase the GPC instrumentation, and by the Paint Research Institute. The authors thank Mr. P. L. Grube for assistance in running the chromatograms cited in this work.

## References

1. S. N. Borisov, M. G. Voronkov, and E. Ya. Lukevits, *Organo-silicon Heteropolymers and Heterocompounds*, Plenum Press, New York, 1970.
2. E. W. Neuse and H. Rosenberg, *J. Macromol. Sci.-Rev. Macromol. Chem.*, **C4**, 1 (1970).
3. R. L. Schaaf, P. T. Kan, and C. T. Lenk, *J. Org. Chem.*, **26**, 1790 (1961).
4. R. L. Schaaf, U. S. Pat. 3,036,105 (1962).
5. H. Rosenberg, U. S. Pat. 3,426,053 (1969).
6. H. Rosenberg, J. M. Barton, and M. M. Hollander, paper presented at 2nd International Symposium on Organometallic Chemistry, Madison, Wisconsin, 1965; *Abstr. Proc.*, p. 42.
7. G. Greber and M. L. Hallensleben, *Makromol. Chem.*, **83**, 148 (1965); *ibid.*, **104**, 90 (1967).
8. G. Greber and M. L. Hallensleben, *Makromol. Chem.*, **104**, 77 (1967).
9. E. V. Wilkus and W. H. Rauscher, *J. Org. Chem.*, **30**, 2889 (1965).
10. C. U. Pittman, Jr., *Chem. Technol.*, **1**, 416 (1971) and references therein.
11. J. E. Curry and J. D. Byrd, *J. Appl. Polym. Sci.*, **9**, 295 (1965).
12. N. Bilow, R. F. Murphy, and W. J. Patterson, *J. Appl. Polym. Sci.*, **11**, 2109 (1967).
13. W. J. Patterson and N. Bilow, *J. Polymer Sci.*, **7**, 1089 (1969).
14. V. Weinmayr, *J. Amer. Chem. Soc.*, **77**, 3009 (1955).
15. E. W. Neuse, R. K. Crossland, and K. Koda, *J. Org. Chem.*, **31**, 2409 (1966).
16. C. U. Pittman, Jr., *J. Polym. Sci. A-1*, **5**, 2927 (1967).
17. J. H. Richards and E. A. Hill, *J. Amer. Chem. Soc.*, **81**, 3484 (1959); *ibid.*, **83**, 3840 (1961); *ibid.*, **85**, 4216 (1963).
18. T. G. Traylor and J. C. Ware, *J. Amer. Chem. Soc.*, **89**, 2304 (1967).
19. C. U. Pittman, Jr., *Tetrahedron Letters*, **1967**, 3619.
20. M. Cais, *Organometal. Chem. Rev.*, **1**, 435 (1966).
21. L. H. Sommer, *Stereochemistry, Mechanism, and Silicon*, McGraw-Hill, New York, 1965.

22. S. S. Washburne and W. P. Peterson, Jr., *J. Organometal. Chem.*, **21**, 59 (1970).
23. M. Sveda, U. S. Pat. 2,562,000 (1951).
24. A. C. Tanquary, R. E. Burks, Jr., and M. V. Jackson, Naval Air Systems Command TR, Contract N00019-68-C-0138, June 1969, p. 11.
25. C. W. Young, J. S. Koehler, and D. S. McKinney, *J. Amer. Chem. Soc.*, **69**, 1410 (1947).
26. C. W. Young, P. C. Servais, C. C. Currie, and J. M. Hunter, *J. Amer. Chem. Soc.*, **70**, 3758 (1948).
27. P. L. Pauson, M. A. Sandhu, and W. E. Watts, *J. Chem. Soc.*, **1966**, 251.
28. R. E. Richards and H. W. Thompson, *J. Chem. Soc.*, **1949**, 124.

Received May 11, 1971

Revised July 12, 1971

## Characterization of the Collagen-Vinyl Graft Copolymers Prepared by the Ceric Ion Method. I. Solution Properties

K. PANDURANGA RAO, K. THOMAS JOSEPH, and  
Y. NAYUDAMMA, *Department of Biopolymers, Central  
Leather Research Institute, Madras 20, India*

### Synopsis

Graft copolymerization of vinyl monomers on to collagen was carried out by the ceric ion method. The grafted vinyl polymer chains were isolated by both acid and enzymatic hydrolysis of the collagen backbone in order to characterize the graft copolymers. Proof of grafting was obtained through the detection of amino acid endgroups in the grafts isolated by both the methods. The grafts isolated gave the characteristic blue color normally associated with the presence of amino acids. The presence of amino acid endgroups was further confirmed by dinitrophenylation of the isolated grafts. The absorption spectra of the dinitrophenylated (DNP) grafts showed absorption maximum in the ultraviolet region of 340–360 m $\mu$ , characteristic of DNP-amino acids. Soluble collagen grafted with polyacrylamide (PAA) formed fibrils on heating to 37°C at neutral pH but, unlike the native collagen, these fibrils did not redissolve on cooling at 2°C. These results show that the redispersion property of soluble collagen was impaired, probably by attachment of the PAA side chains to the collagen molecule. The turbidimetric titration behavior of the grafts, their general behavior of swelling in different solvents, and the intrinsic viscosity of the copolymers in mixed solvents also provided additional proof of grafting.

### INTRODUCTION

Modification of natural and synthetic polymers by graft copolymerization has been the subject of numerous investigations. However, relatively little effort has been directed toward a systematic investigation of their structure and properties. Quite recently investigations on the structure and properties of the graft copolymers have been taken up by a number of workers.<sup>1-7</sup>

Graft copolymers of collagen and poly(methyl methacrylate) (PMMA) formed through ceric ammonium nitrate (CAN) initiator, have been studied<sup>8-10</sup> in detail to determine what factors govern the percent grafting and the number of grafting sites and the molecular weight of the grafted PMMA. It is common that the graft copolymers are inevitably contaminated with at least one of the homopolymers of the species which make up the copolymer segments. For an unambiguous characterization of these

copolymers, it is necessary to isolate them from the homopolymers present in the polymerization products. The separation poses a major problem when the solubility differences between the graft copolymers and the homopolymers are not large enough to allow adequate separation. Collagen graft copolymers, just as in the case of wool, cellulose, and starch graft copolymers, have the following two advantages from the point of view of composition studies: (1) the solubility difference between the collagen backbone and the grafted side chain polymers is usually sufficiently great to enable adequate separation to be made; (2) the collagen backbone can be hydrolyzed away, thus enabling the molecular weight and the grafting frequency of the grafted side chains to be measured.

This paper is concerned with the physicochemical characterization of collagen-vinyl graft copolymers. The grafted vinyl polymer chains were isolated by both acid and enzymatic hydrolysis of the collagen backbone to characterize the graft copolymers. Several lines of evidence were sought to distinguish between a true graft copolymer and a physical mixture of collagen and vinyl polymers.

## EXPERIMENTAL

### Materials

**Collagen.** Collagen prepared from the middle corium of buffalo hide was used as the source of insoluble collagen. Since a uniform stock of material which would be sufficient for the whole investigation was required, a large amount was initially prepared and all the experiments were carried out with the same sample.

Soluble collagen was prepared from calf dermis following a procedure similar to that of Hörmann and Hafter.<sup>11</sup>

**Monomers.** Methyl methacrylate(MMA) and methyl acrylate(MA) were obtained from Rohm & Hass, U.S.A. and acrylamide was obtained from American Cyanamid Co.

**Chemicals.** Ceric ammonium nitrate  $[\text{Ce}(\text{NH}_4)_2(\text{NO}_3)_6]$  and ceric ammonium sulfate  $[\text{Ce}(\text{NH}_4)_4(\text{SO}_4)_4]$  (Puriss, Fluka) were used without further purification. Pronase (B grade, Cal Biochem, U.S.A.) was used without further purification. Other chemicals used were reagent grade.

### Purification of Monomers

MMA and MA were purified by washing with a 6–8% sodium hydroxide solution to remove the inhibitor. After this treatment, the monomers were washed with distilled water to remove the alkali completely and dried over anhydrous calcium chloride overnight. The monomers were then distilled under vacuum and stored in a refrigerator. Acrylamide was recrystallized twice with benzene-acetone.

### Preparation of Initiator Solution

The required quantity of CAN dissolved in 1*N* nitric acid was used. Fresh solutions were prepared for each experiment.

### Grafting Procedure

The graft copolymerization reactions were carried out in a round bottomed three-necked flask of one liter capacity fitted with a water-sealed glass stirrer, a gas outlet, and a thermometer. All the grafting experiments were carried out at a stirring speed of 100–150 rpm at room temperature. In a typical experiment, 10 g of hide powder was dispersed in 400 ml distilled water. After oxygen-free nitrogen was bubbled through the solution for 30 min, the required amount of monomer was added followed by ceric ammonium nitrate solution (0.1*M*) in 1*N* nitric acid. The final concentration of monomer was 0.5 mole/l. and that of CAN was  $2.5 \times 10^{-5}$  mole/l. The reaction was allowed to proceed for 3 hr, at the end of which the resulting products were separated by filtration, washed with distilled water, and extracted with the appropriate solvents to remove the loosely bound homopolymer.

### Homopolymer Extraction

Preliminary studies with the use of the tumbled bottle method and the Soxhlet extraction method to compare the extraction efficiencies showed that the tumbled bottle method is more efficient for the extraction of the homopolymer. Hence in all subsequent studies this method was followed for extraction of homopolymers from the graft copolymers. The graft copolymers were extracted for 72 hr with two changes of fresh solvents at room temperature. In general, extraction of the crude collagen graft copolymers with solvent for the homopolymer removed only traces of the polymer, and hence no systematic investigations were carried out on the estimation of the amounts of these ungrafted homopolymers.

For grafting on skins, an emulsion polymerization technique was followed.<sup>12</sup> The per cent grafting in the final products were determined from the total nitrogen values as reported previously.<sup>10</sup>

### Hydrolysis of the Collagen Backbone with Hydrochloric Acid

Acid hydrolysis was carried out by heating the graft copolymer with 6*N* HCl for 18 hr according to the procedure outlined in a previous paper.<sup>10</sup>

### Digestion of the Collagen Backbone with Pronase

Samples of collagen-PMMA graft copolymer (samples GC<sub>1</sub> and GC<sub>3</sub>, 0.1–0.3 g) were heat-denatured in water and made 0.02*M* in CaCl<sub>2</sub>, and the pH was adjusted to 8 with 0.1*N* NaOH. A 10-mg portion of pronase dissolved in 0.5 ml of water was then added, together with a drop of toluene to prevent bacterial growth. The mixture was then incubated at 37°C for



18 hr, while the pH was kept constant by addition of 0.01*N* NaOH. The insoluble graft was removed by centrifugation, washed, and dried. A physical mixture of collagen and PMMA was also digested under identical conditions. The physical mixture (1:1 w/w) was prepared by grinding the mixture well in a mortar. The residues left after enzyme digestion were thoroughly washed with hot water, centrifuged, and dried.

### **Treatment of the Isolated Grafts with Ninhydrin**

Approximately 100 mg of the isolated grafts obtained by the above procedures were weighed and placed into test tubes containing 2 ml of distilled water. A 2-ml portion of the ninhydrin reagent of Moore and Stein<sup>13</sup> was added, and the solutions thoroughly mixed by gently shaking the tubes. The tubes were capped and placed in a rigorously boiling water bath for 20 min. The solution was cooled and 5 ml of the diluent (ethanol-water, 1:1 v/v) solution was added and the whole mixed and centrifuged. The absorbence of the supernatant was measured in a Beckman DU spectrophotometer at 570 m $\mu$ .

### **Grafting on Soluble Collagen**

For grafting on soluble collagen it was desirable to use a monomer, the homopolymer of which will also remain in solution after grafting. Acrylamide(AA) was thought to be suitable for this purpose, and hence attempts were made to graft AA on soluble collagen.

A 0.1% solution of soluble collagen in 0.1*N* acetic acid was used for this purpose. The grafting conditions were exactly same as in the case of insoluble collagen. After grafting, the viscous solution was exhaustively dialysed against 0.1*N* acetic acid. The fibril-forming property of the grafted collagen was then studied in comparison with an ungrafted soluble collagen solution and also with a physical mixture of collagen and poly(AA).

### **Fibril Formation**

Soluble collagen in cold neutral salt solutions has the interesting property of precipitating on warming to 37°C as a rigid gel composed of fibrils. If the gel is cooled immediately to 2°C, it will redissolve and will form again upon reheating. Conditions which enhance hydrogen bonding favor the formation of fibrils, while those which rupture hydrogen bonds reverse the equilibrium. It was, therefore, of interest to examine the fiber-forming and resolution properties of the grafted collagen solution. Fiber formation was carried out and measured mainly as described by Gross and Kirk.<sup>14</sup>

Redispersion was studied by placing the opaque gelled system in an ice-water bath and measuring the clearing as fall in turbidity at various times. Changes were measured at 0.5-hr intervals for 2.5–3.5 hr and again after 18 hr.

### Dinitrophenylation of the Isolated Grafts

Dinitrophenylation of the amino acid endgroups of the isolated grafts was used by us<sup>9</sup> as a technique for obtaining proof of grafting in the case of collagen-vinyl graft copolymers. This technique has been subsequently followed by Arai et al.<sup>15</sup> for the endgroup analysis of isolated PMMA from the graft copolymers of wool. Hence in the present paper, in continuation of the work reported earlier,<sup>9</sup> the absorption spectra of the dinitrophenylated grafts isolated by both acid and pronase digestion were studied.

The dinitrophenylation was carried out by two different methods. In the first method, the isolated polymer was suspended in aqueous sodium bicarbonate and treated with an alcoholic solution of 2,4-dinitrofluorobenzene (DNFB) according to the procedure adopted by Sanger.<sup>16</sup> In the second procedure, the isolated polymer was dissolved in benzene and treated with DNFB in the presence of triethylamine by the method of Whalley<sup>17</sup> as followed by Arai et al.<sup>15</sup> The dinitrophenylated polymer (DNP-polymer) was precipitated by adding excess cold methanol. The DNP-polymers obtained by the two procedures were washed thoroughly with distilled water and soxhlet extracted with methanol for 12 hr. The purified samples, when subjected to thin-layer chromatography on silica gel plates as reported earlier,<sup>9</sup> showed only one spot which remained at the origin. No other spots corresponding to dinitrophenol or any other artifacts were observed on the plate.

The purified DNP-polymers were dissolved in ethyl acetate (4 g/l.), and the absorption spectra were measured in a Beckman DU-model spectrophotometer with the use of 1-cm quartz cells. The absorption spectra of the isolated polymers without dinitrophenylation were also measured under identical conditions. In the case of polymer isolated by pronase digestion the DNP-polymer was not readily soluble in ethyl acetate, and hence in this case it was dissolved in dichloroacetic acid (DCA).

### Precipitation Turbidimetric Titrations

Collagen grafted with PMMA (sample GC<sub>1</sub>) was dissolved in dichloroacetic acid by keeping the suspension for a few days at room temperature. The solution was then centrifuged, and the clear solution was suitably diluted with DCA to give a 0.1% solution. Turbidity measurements were made in a Klett-Summerson photoelectric colorimeter with a green filter. Different precipitants were tried, and diisopropyl ether was finally selected. A 5-ml portion of the polymer solution was taken, and the precipitant was added rapidly from a microburet with gentle hand stirring. The precipitant was added in 1-ml aliquots until within 1 ml of the commencement of precipitation. Then 0.1 ml aliquots were added until 50% precipitation, and 0.5–1.0 ml aliquots were then used until precipitation was complete. All the titration experiments were performed in a room kept at 21°C but were not otherwise thermostated.

The turbidity of the solution after addition of each increment of the precipitant was measured in the colorimeter and the observed readings were corrected for the dilution effect by the formula<sup>18</sup>

$$D(V + v)/V = D(\text{corr.})$$

where  $D$  is the optical density,  $V$  the original volume of solution and  $v$  the volume of precipitant added. The results of the experiments were plotted as graphs of per cent turbidity against volume (milliliters) of nonsolvent added. Ungrafted collagen and PMMA homopolymer and the physical mixture of collagen and PMMA were also dissolved in DCA and the titration performed under identical conditions.

### Equilibrium Swelling Measurements in Different Solvents

Goat skins grafted with PMMA and PMA (samples GP<sub>1</sub> and GP<sub>2</sub>) were used in these experiments. About 0.2 g of the grafted samples were accurately weighed and immersed in 10–15 ml of the liquids in weighing bottles and allowed to swell. The samples were then taken out at intervals of 12 hours, surface cleaned with filter paper, placed in a previously weighed bottle, and quickly weighed in an analytical balance. The equilibrium swellings which were reached after 48 hr were calculated as volume (milliliters) of liquid absorbed per gram of sample. All measurements were carried out in a room maintained at  $23 \pm 2^\circ\text{C}$ . The equilibrium swelling values were plotted against the solubility parameters (solvent power functions) of the solvents used.

### Determination of Intrinsic Viscosity of Collagen Graft Copolymers in Mixed Solvents

The intrinsic viscosities of the graft copolymers were measured in DCA–benzene by using an Ubbelohde dilution viscometer at a temperature of  $30^\circ\text{C}$ . For this, the collagen graft copolymers (samples GC<sub>1</sub> and GC<sub>2</sub>) were dissolved in DCA as mentioned earlier, and the intrinsic viscosities were plotted as a function of the percentage of the nonsolvent (benzene) added. The composition of the mixed solvents were 10, 20, 30, 40, 50, and 60 vol.-% benzene. Higher benzene content gave turbidity, leading to precipitation.

## RESULTS AND DISCUSSION

One of the most important problems in the characterization of collagen–vinyl graft copolymers in common with other graft copolymers is the fundamental question whether true grafting has really occurred or not. Although it is relatively simple to determine that the monomer to be grafted has been converted to polymer and also the degree of conversion, it is much more difficult to establish the proof of grafting unequivocally as opposed to an intimate mixture where no primary chemical bonds exist between collagen and the vinyl polymers. The apparent per cent grafting in the

TABLE I  
Composition of Collagen-Vinyl Graft Copolymers

Nature of modified collagen	Apparent grafting, %
PMMA-collagen graft(GC <sub>1</sub> )	159.60
PMA-collagen graft(GC <sub>2</sub> )	121.80
Goat skin-PMMA graft(GP <sub>1</sub> )	26.89
Goat skin-PMA graft(GP <sub>2</sub> )	27.56

various products used in these studies is given in Table I. Results obtained with the various methods used to characterize the collagen graft copolymers were as follows.

### Solvent Extraction

The simplest method of obtaining evidence of formation of graft copolymer is based on differences in solubilities between the graft copolymer and nongrafted loosely bound homopolymer. Extraction experiments were carried out to obtain evidence of grafting of the vinyl polymers to the collagen substrate. One would expect ungrafted polymer to be readily extracted; grafted polymer, being chemically bound, would not be extracted. Extraction of the collagen graft copolymer with the solvent for the homopolymer removed only traces of the polymer from the products. Extractions with solvents for the homopolymer yield some information, but still not complete proof of grafting. When collagen was grafted with vinyl monomers by ceric ion, the resulting products may contain some amount of the ungrafted homopolymer even after extraction of the product with the appropriate solvents for the homopolymers. Grafting could not, however, be proved simply by extraction, because crosslinked or intertangled (intertwined) high molecular weight homopolymer may still remain in the fibrillar mesh.

### Treatment of the Isolated PMMA Grafts with Ninhydrin Reagent

Better proof of grafting can be obtained through the detection of amino acid endgroups in the grafts isolated by acid and enzymatic hydrolysis of the graft copolymers. The grafts isolated by both acid and enzymatic methods from collagen grafted with PMMA were treated with ninhydrin reagent which gave the characteristic blue color normally associated with the presence of amino acids.

In the case of physical mixture of PMMA and collagen, the residue obtained after enzymatic digestion of collagen did not give any color with ninhydrin. These results indicated that actual grafting of the polymer to the amino acid residues in collagen has occurred.

### Dinitrophenylation of the Isolated Grafts

The presence of amino acids could be further confirmed through the detection of dinitrophenylated amino endgroups with isolated grafts. The



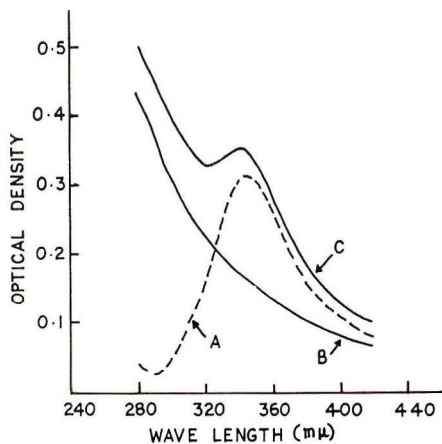


Fig. 1. Absorption spectra of (A) DNP-serine; (B) isolated polymer, (C) DNP-polymer in ethyl acetate (isolated by acid hydrolysis).

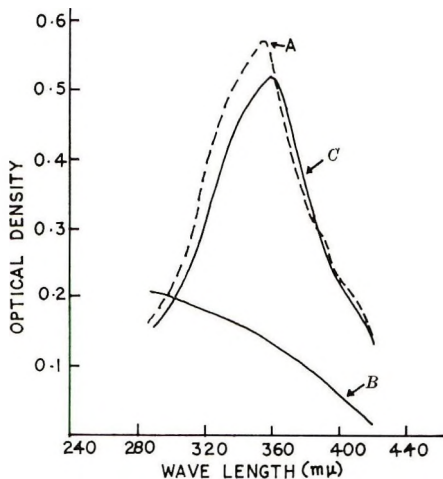


Fig. 2. Absorption spectra of (A) DNP-serine; (B) DNP-polymer in dichloroacetic acid (isolated by pronase digestion); (C) isolated polymer.

spectral absorption curves from 280 to 420  $m\mu$  for isolated DNP-MMA polymers are shown in Figures 1 and 2. The dinitrophenylated grafts isolated by both the acid and enzyme methods showed an absorption maximum at 343  $m\mu$  in ethyl acetate and at 360  $m\mu$  in dichloroacetic acid. DNP-serine also showed identical spectra in these two solvents. The isolated polymer without dinitrophenylation did not show any maximum in these regions. The DNP grafts isolated by the enzyme method showed more pronounced absorption maxima in the 340–360  $m\mu$  region, which indicates that the number of DNP-amino acid endgroups in these polymer chains is greater than in the case of grafts isolated by the acid hydrolysis method. This is to be expected because in the enzyme digestion method



TABLE II  
Average Molecular Weight of Isolated PMMA and Number of DNP-Amino Acid Endgroups per Polymer Chain Determined by the DNP Method

Sample	Average mw of isolated grafts (by viscosity)	Number of DNP-amino acid endgroups per polymer chain	
		By sodium bicarbonate method	By triethylamine method
Collagen-PMMA graft copolymer (GC <sub>3</sub> ) <sup>a</sup>	$0.82 \times 10^5$	0.41	0.45
Collagen-PMMA graft copolymer (GC <sub>1</sub> )	$2.075 \times 10^6$	Trace	Trace

<sup>a</sup>In the preparation of this sample, the ceric ion concentration used was  $1 \times 10^{-2}$  mole/l.

bigger peptide fragments will be attached to the polymer chain which may contain more amino groups. Table II shows the DNP-amino acid values obtained for the grafts isolated by the acid hydrolysis method. The number of amino acid endgroups calculated per polymer chain is less than unity in both the methods. The lower values obtained may be due to the inaccessibility of the amino groups to the bulky reagent. When the molecular weight of the grafted product was extremely high, the number of amino acid endgroups was so insignificant as barely to be detected by di-nitrophenylation. Only trace of DNP-amino acid could be detected in these isolated grafts. In the case of grafts isolated by pronase, no attempt was made to calculate the DNP-amino groups, since in this case the polymer chains are attached to large peptide fragments.

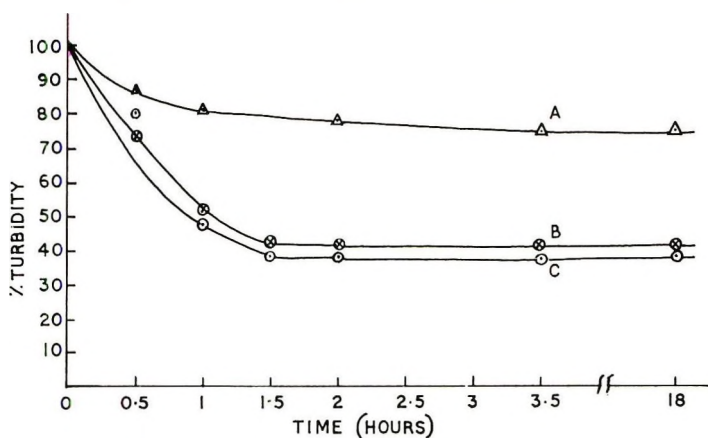


Fig. 3. Redispersion of acrylamide-grafted soluble collagen: (A) grafted collagen; (B) physical mixture of soluble collagen and polyacrylamide; (C) control untreated collagen.

### Fibril Formation

The redispersion property of soluble collagen grafted with PAA is shown in Figure 3. In the case of the control, the reconstituted fibrils redissolved to the extent of about 60% at the end of 4 hr, whereas in the case of PAA grafted collagen the redispersion was only about 20%. These results show that the redispersion property of soluble collagen was impaired probably by attachment of the polyacrylamide(PAA) side chain to the soluble collagen molecule. Analysis of the heat-precipitated collagen after grafting also showed the presence of AA polymer in the precipitate. The physical mixture of soluble collagen and PAA, on the other hand, redissolved on cooling and behaved as untreated soluble collagen.

### Precipitation Turbidimetric Titrations

The turbidimetric titration method is closely related to the method of fractional precipitation. The time-consuming operation, work-up and analysis of the fractions is here, in the words of Morey and Tamblyn,<sup>19</sup> replaced by "optical weighing." Even though the turbidimetric titration method is only a relative method for the determination of the molecular weight distribution, it is a simple, rapid, and reproducible method for the characterization of graft copolymers.

Curve *A* in Figure 4 represents the turbidimetric titration of a solution of collagen in DCA against diisopropyl ether. Per cent turbidity, that is, the ratio of optical density to optical density at complete precipitation, is plotted against the volume of precipitant added. Curve *B* represents the titration of a solution of PMMA, curve *C* of a physical mixture of collagen and PMMA, and curve *D* that of collagen-PMMA graft copolymer, under identical conditions. It can be seen that in curve *C* of the physical mixture, the turbidity increases rapidly on addition of 6–10 ml of diisopropyl ether and again on addition of 18–25 ml. These steps may be attributed to

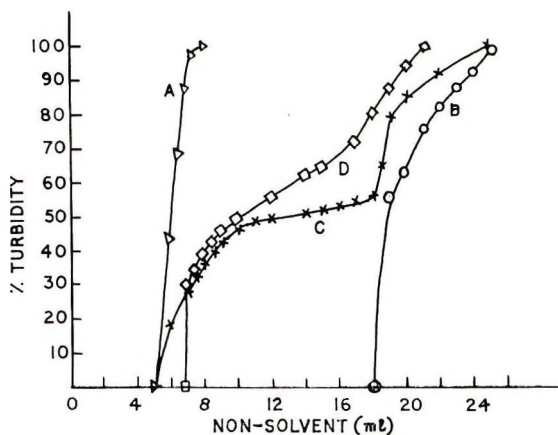


Fig. 4. Variation in turbidity with added nonsolvent: (A) collagen; (B) PMMA; (C) physical mixture of collagen and PMMA; (D) collagen-PMMA graft copolymer.

the precipitation of collagen and PMMA fractions, respectively. However, in the case of graft copolymers, the curve *D* is more or less continuous, and no well marked inflection was observed. This indicates that actual grafting has occurred. Generally, the chemical nature of the polymer has a much greater influence on its solubility than its molecular weight. The meager data available in the literature indicate that a graft copolymer will normally display solubility characteristics intermediate between those of the homopolymers. The solubility of collagen graft copolymer is intermediate between those of the corresponding polymers.

### Viscosity in Mixed Solvents

Benoit and his co-workers<sup>20-22</sup> have established that the solution properties of graft copolymers are very much affected by interactions between chemically unlike sequences. If viscosity measurements are made in solvent-nonsolvent medium in which one solvent is a good solvent for both the backbone and branches, and the nonsolvent is a solvent for the branches only, repulsive interactions between the backbone and nonsolvent can be large enough to cause the formation of so-called molecular micellae.<sup>23-25</sup> The molecular micellae are maintained in solution by the surrounding solvated branches even though the backbone remains unsolvated.

In Figure 5 plots of percentage of benzene against the intrinsic viscosity of collagen-PMMA and collagen-PMA graft copolymers are shown. There is a slight increase in the intrinsic viscosity initially, followed by a significant decrease as the amount of benzene is increased. Protection of the backbone by solvated grafts often prevents precipitation. This may be due to the formation of the so-called polymolecular micellae. When the protection effect is not sufficient to keep the solution in molecular dispersion (as the benzene content increases) the macromolecule shrinks,

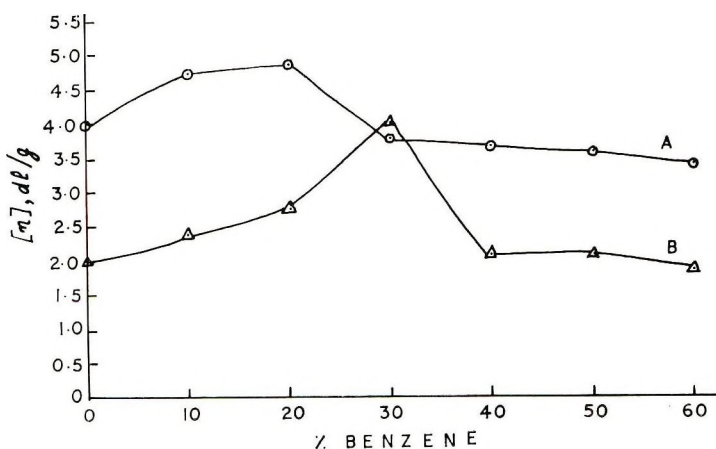


Fig. 5. Variation of intrinsic viscosities for graft copolymers of collagen as a function of solvent composition: (A) collagen-PMMA graft copolymer; (B) collagen-PMA graft copolymer.

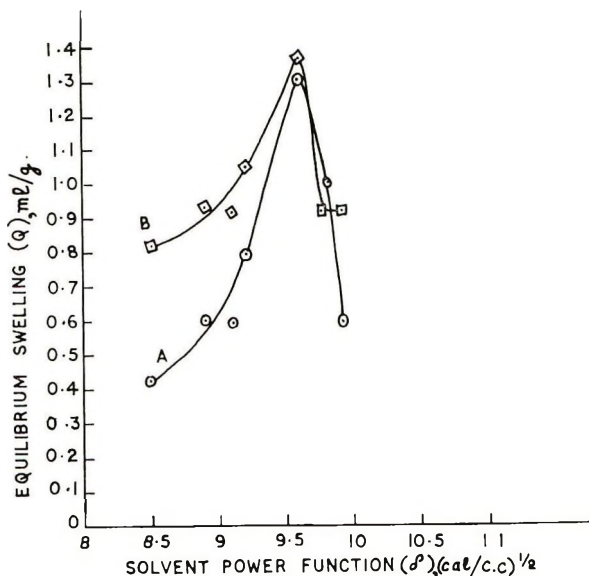


Fig. 6. Dependence of swelling of copolymers on solvent power function: (A) collagen-PMMA graft copolymer; (B) Collagen-PMA graft copolymer.

with the result that the intrinsic viscosity decreases very rapidly. The slight increase in the intrinsic viscosity observed initially may be due to an increase of the molecular dimensions of the polymer caused by changes in conformation or due to the expansions of the graft polymer chains as benzene (which is a good solvent for the side chains) is added to the solvent. Such initial expansion followed by contraction of graft copolymers in other solvents has already been reported. The shape of the curves obtained in the present study were, however, in general agreement with those of other graft copolymers obtained by other investigators.<sup>26-28</sup>

### Equilibrium Swelling Measurements in Different Solvents

Figure 6 illustrates the equilibrium swelling of the collagen-PMMA and collagen-PMA graft copolymers in a series of solvents comprising esters, ketones, and chlorinated hydrocarbons. The equilibrium swelling values were plotted against the solubility parameters (solvent power function) of the different solvents used; the general shape of the curves is similar to that of curves obtained with other types of graft copolymers.<sup>29,30</sup>

### CONCLUSIONS

The different lines of evidence obtained in this study indicate that the copolymers obtained by ceric ion-initiated free-radical polymerization of vinyl monomers on collagen are not physical mixtures of collagen and the homopolymer. Indications that our products are true grafts are provided by the turbidimetric titration behavior of the grafts, their general behavior



with respect to swelling in different solvents, the intrinsic viscosity of the copolymers in mixed solvents and by the detection of the DNP-amino acid endgroups in the isolated grafts. The ceric ion method of grafting vinyl monomers onto various substrates is known to have the advantage that little or no homopolymer is formed. In the present study, an attempt was also made to remove all occluded and loosely bound homopolymers by exhaustive and prolonged extraction with the appropriate solvents for the homopolymers. Hence the apparent per cent grafting shown in Table I can be taken for all practical purposes as the true per cent grafting.

The infrared spectra of the isolated grafts by acid and enzymatic hydrolysis of the grafted products and the electron microscopic studies of grafted collagen fibrils and ultrathin sections of fibrils are reported in another paper under publication.

This research has been financed in part by a grant made by the U.S. Department of Agriculture, Agricultural Research Service, under PL-480. Grateful acknowledgements are made to Prof. Dr. M. Santappa for his valuable suggestions and encouragement.

This paper is taken in part from the doctoral thesis of K.P.R. submitted to the University of Madras, 1970.

### References

1. H. Yasuda, J. A. Wray, and V. Stannett, in *Fourth Cellulose Conference (J. Polym. Sci., C 2)*, R. H. Marchessault, Ed., Interscience, New York, 1963, p. 387.
2. R. Y. M. Huang, B. Immergut, E. H. Immergut, and W. H. Rapson, *J. Polym. Sci. A*, **1**, 1257 (1963).
3. C. E. Brockway, *J. Polym. Sci. A*, **2**, 3721 (1964).
4. N. J. Morris, F. A. Blouin, and J. C. Arthur, Jr., *J. Appl. Polym. Sci.*, **12**, 373 (1968).
5. Y. Iwakura, Y. Imai, and K. Yagi, *J. Polym. Sci. A-1*, **6**, 801 (1968).
6. S. P. Rao and M. Santappa, *J. Polym. Sci. A-1*, **5**, 2681 (1967).
7. J. J. O'Malley and R. H. Marchessault, *J. Phys. Chem.*, **70**, 3235 (1966).
8. K. P. Rao, K. T. Joseph, and Y. Nayudamma, *Leath. Sci.*, **14**, 73 (1967).
9. K. P. Rao, K. T. Joseph, and Y. Nayudamma, *Leder*, **19**, 77 (1968).
10. K. P. Rao, K. T. Joseph, and Y. Nayudamma, *Leath. Sci.*, **16**, 401 (1969).
11. H. Hörmann and R. Hafter, *Leder*, **14**, 293 (1963).
12. K. P. Rao, Ph.D. Thesis, University of Madras, Madras, July 1970.
13. S. Moore and W. H. Stein, *J. Biol. Chem.*, **176**, 367 (1948).
14. J. Gross and D. S. Kirk, *J. Biol. Chem.*, **233**, 355 (1958).
15. K. Arai, S. Komine, and M. Negishi, *J. Polym. Sci. A-1*, **8**, 917 (1970).
16. F. Sanger, *Biochem. J.*, **39**, 507 (1945).
17. W. B. Whally, *J. Chem. Soc.*, **1950**, 2241.
18. H. W. Melville and B. D. Stead, *J. Polym. Sci.*, **16**, 505 (1955).
19. D. R. Morey and J. W. Tamblyn, *J. Appl. Phys.*, **16**, 419 (1945).
20. Y. Gallot, E. Franta, P. Rempp, and H. Benoit, in *Macromolecular Chemistry, Paris 1963 (J. Polym. Sci. C, 4)*, M. Magat, Ed., Interscience, New York, 1964, p. 473.
21. A. Dondos, P. Rempp, and H. Benoit, *J. Chem. Phys.*, **62**, 821 (1965).
22. A. Dondos, P. Rempp, and H. Benoit, *J. Polym. Sci. A-2*, **5**, 230 (1967).
23. J. J. O'Malley and R. H. Marchessault, in *Polymer Reactions (J. Polym. Sci. C, 24)* E. M. Fettes, Ed., Interscience, New York, 1968, p. 179.
24. G. E. Molau and W. M. Wittbrodt, *Macromolecules*, **1**, 260 (1968).



25. R. J. Ceresa, in *Block Copolymers* (*J. Polym. Sci. C*, **26**), J. Moacanin, G. Holden, and N. W. Tschoegl, Eds., Interscience, New York, 1969, p. 201.
26. J. D. Wellons, J. L. Williams, and V. Stannett, *J. Polym. Sci. A-1*, **5**, 1341 (1967).
27. A. B. Gosnell, D. K. Woods, J. A. Gervasi, J. L., Williams, and V. Stannett, *Polymer*, **9**, 561 (1968).
28. H. C. Beachell, R. Blumstein, and J. C. Peterson, in *Macromolecular Chemistry, Brussels-Louvain 1967* (*J. Polym. Sci. C*, **22**) G. Smets, Ed., Interscience, New York, 1969, p. 569.
29. S. K. Patra, S. Ghosh, B. K. Patnaik, and R. T. Thampy, *Symposium on Solution Properties of Natural Polymers*, Chemical Society Special Publication, No. 23, Edinburg, 1967, p. 90.
30. S. R. Rafikov and G. K. Serganova, *Soviet Plastics*, **2**, 6 (1966).

Received April 7, 1971

Revised July 1, 1971

## Grafting of Methyl Methacrylate and Its Derivatives onto Blood

KUNIHARU KOJIMA, SUSUMU IWABUCHI, KOICHI KOJIMA,  
*Department of Applied Chemistry, Faculty of Engineering, Chiba University,  
Yayoi-cho, Chiba, Japan, and NIRO TARUMI and EIICHI MASUHARA,  
Institute for Medical and Dental Engineering, Tokyo Medical and Dental  
University, Kanda-Surugadai, Chiyoda-ku, Tokyo, Japan*

### Synopsis

The grafting of vinyl monomers by tri-*n*-butylborane to blood has been investigated. The infrared spectra indicated that the monomers were grafted onto blood components. The grafting seems to occur onto blood proteins, mainly onto hemoglobin. The presence of water was essential to the grafting. The hydrolysis of the graft suggests that basic amino acids in the blood proteins, such as lysine and histidine, play an important role in the grafting.

### INTRODUCTION

Since the use of alkylboranes as the initiators for the polymerization of ordinary vinyl monomers was first reported by Furukawa et al.<sup>1</sup> and independently by Kolesnikov et al.,<sup>2</sup> many publications on the alkylborane initiators have appeared.<sup>3</sup> Fujii et al.<sup>4</sup> indicated that oxygen accelerated the polymerization of vinyl acetate by triethylborane and that small amounts of alcohol and water were effective as cocatalysts. Furukawa et al.<sup>5</sup> found that oxygen and oxygen-containing compounds promoted the action of organoborane compounds in the polymerization of vinyl acetate. Recently, we reported that pyridine and its derivatives gave cocatalytic effects on the polymerization of methyl methacrylate (MMA) by tri-*n*-butylborane (Bu<sub>3</sub>B).<sup>6</sup> We also described the graft copolymerization of MMA by Bu<sub>3</sub>B onto natural and synthetic polymers.<sup>7,8</sup>

On the other hand, many authors have published their studies on the preservation of blood by chemical treatments. Suzuki et al.<sup>9</sup> tried to protect blood by the reaction of aldehyde with hemoglobin. Kondo<sup>10</sup> disclosed that blood can be stabilized by enclosing or "wrapping" it with colloidal gelatin.

We have tried to develop a new method for the preservation of blood by means of the grafting of vinyl monomers onto blood.<sup>11</sup> A study of the infrared spectra of the acetone-insoluble product indicated that the monomers were grafted onto blood components. The grafting seems to occur onto blood proteins, mainly onto hemoglobin. It is interesting to note that the

hydrogen peroxide-decomposing and oxidation-reduction properties of hemoglobin remained unchanged. The present paper describes some results of our recent work.

## EXPERIMENTAL

### Materials

**Methyl Methacrylate (MMA).** One liter of commercial MMA was washed with three 100-ml portions of saturated sodium hydrosulfite solution in a separatory funnel, then with three 100-ml portions of 5% NaOH solution, and finally with three 100-ml portions of 20% NaCl solution. The MMA so washed was allowed to stand over silica gel over night, filtered, and distilled in a nitrogen atmosphere under reduced pressure; bp 46°C/100 mm Hg.<sup>12</sup>

**Tri-*n*-butylborane (Bu<sub>3</sub>B).** Commercial Bu<sub>3</sub>B (Callery Chemical Co., U.S.) was purified by vacuum distillation under nitrogen atmosphere; bp 90–92°C/10 mm Hg. The purity was determined by gas chromatography (column: SE 30).

**Blood and its Components.** Healthy and fresh rat blood (*Rattus norvegicus albinus*) was drawn just before use in a glass tube, the wall of which was kept wet with 1% heparin solution to prevent coagulation. Dried blood was prepared from the blood of a Holstein cow by freeze-drying. Commercial hemoglobin (cattle), hemin, and hematoporphyrin were used without further treatment.

### Grafting Procedure

A mixture of 10 ml of isotonic NaCl solution and 2 ml of 1% heparin solution was placed in a tapered glass tube with a capacity of about 60 ml; to this was added 5 ml of the blood, and a mixture of MMA and Bu<sub>3</sub>B was poured in it. Then, the glass tube was shaken in a thermostatted shaking apparatus at 37°C. The reaction was stopped by pouring the mixture into 200 ml of methanol. The precipitate was filtered, washed with methanol, and dried at 37°C *in vacuo* to constant weight. The dry precipitate was extracted with acetone in a Soxhlet extractor for 48 hr. The acetone-soluble extract was reprecipitated with methanol to yield the homopolymer. Both the acetone-insoluble residue (the graft) and the homopolymer were dried at 37°C *in vacuo* to constant weights.

### Calculations

The total conversion, the percentage of grafting and the efficiency of grafting were calculated according to:

$$\begin{aligned}
 \text{Total conversion} &= \frac{\text{Weights of PMMA grafted and homopolymer}}{\text{Weight of MMA charged}} = \frac{\text{II} + \text{III}}{\text{I}} \\
 \text{Percentage of grafting} &= \frac{\text{Weight of PMMA grafted}}{\text{Weight of MMA charged}} = \frac{\text{II}}{\text{I}} \\
 \text{Efficiency of grafting} &= \frac{\text{Weight of PMMA grafted}}{\text{Weights of PMMA grafted and homopolymer}} = \frac{\text{II}}{\text{II} + \text{III}}
 \end{aligned}$$

where I denotes weight of MMA charged, II denotes weight of acetone-insoluble component minus weight of solid blood components; III denotes weight of acetone-soluble component (homopolymer).

### Spectral Measurements

The infrared spectra were recorded on a Hitachi Model EPI-G2 spectrophotometer.

## RESULTS AND DISCUSSION

### Grafting of MMA onto Blood

In order to investigate whether MMA could be grafted onto blood, the polymerization of MMA in blood was carried out with various initiators. The results are given in Table I.

When the polymerization was initiated by the benzoyl peroxide–dimethyl-*p*-toluidine system (BPO/DMT), the total conversion and the efficiency of grafting were 21.4% and 0.22%, respectively, while those for the

TABLE I  
Grafting of Methyl Methacrylate onto Blood<sup>a</sup>

Expt.	Initiator (Bu <sub>3</sub> B), ml	Re- ac- tion time, hr	Total yield, g	Conver- sion, %	Weight of homo- poly- mer, g	Weight of graft poly- mer, g	Percent- age of graft- ing, %	Effi- ciency of graft- ing, %
2	0.2	1	1.74	10.8	0.48	1.08	0.5	4.8
3	0.2	2	1.99	16.9	0.74	1.11	1.2	7.0
4	0.2	4	2.50	28.2	1.22	1.15	2.1	7.5
5	0.2	8	3.24	37.7	1.61	1.21	3.2	8.6
7	0.1	2	1.96	15.5	0.71	1.07	0.4	2.8
10	0.4	2	2.16	19.4	0.82	1.15	1.9	10.1
47	BPO/DMT <sup>b</sup>	5	2.37	21.7	1.02	1.06	0.05	0.2

<sup>a</sup> Grafting conditions: MMA, 5 ml; blood, 5 ml; isotonic NaCl solution, 5 ml; 37°C.

<sup>b</sup> For comparison: with BPO/DMT, 0.05 g each of benzoyl peroxide and dimethyl-*p*-toluidine.

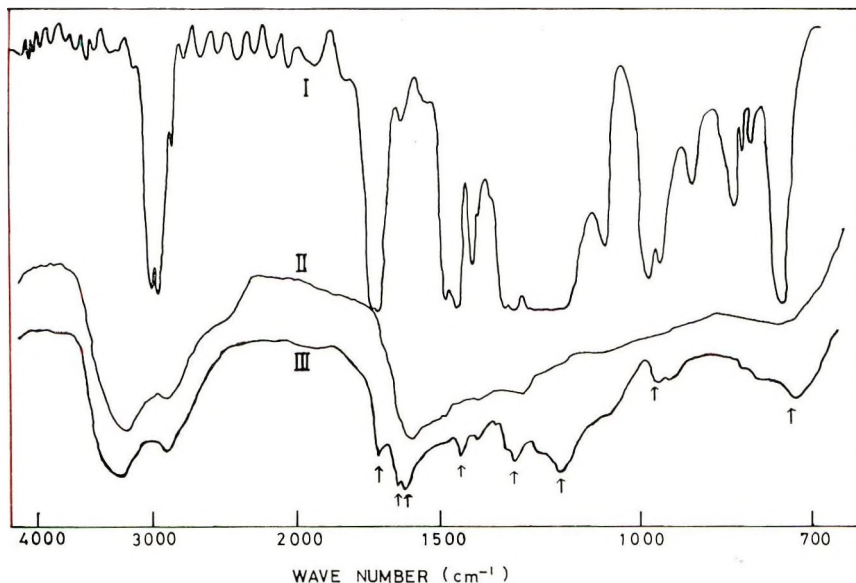


Fig. 1. Infrared spectra of (I) PMMA; (II) blood protein; (III) graft polymer.

polymerization by  $\text{Bu}_3\text{B}$  were 10.8% and 4.76%, respectively. This indicates that  $\text{Bu}_3\text{B}$  was more effective on the grafting than BPO/DMT.

The infrared spectra of the acetone-insoluble component of the copolymerization product showed characteristic absorptions at 1730, 1440, and 1240 and 1140  $\text{cm}^{-1}$ , which may be assignable to  $\text{C}=\text{O}$  stretching,  $\text{CH}_3-\text{C}$  bending, and ester-CO stretching, respectively. Since the spectra of PMMA showed the same bands and they were not found in those of the methanol-insoluble component of blood, the acetone-insoluble component so obtained is believed to be the graft polymer (Fig. 1).

The work-up procedure could be denaturing and it is possible that the blood proteins on being denatured encapsulate the PMMA homopolymer, so that extraction of polymer with acetone is not possible. In order to clarify this, the homopolymer was dissolved in MMA monomer, mixed with blood and worked up without  $\text{Bu}_3\text{B}$  as usual. No increase in the weight of the acetone-insoluble component was observed within the limits of experimental error. This experiment would indicate that no physical entrapment of homopolymer occurred.

In the polymerization by  $\text{Bu}_3\text{B}$ , the higher the total conversion, the greater was the percentage of grafting and efficiency of grafting, as Table I also shows; i.e., an increase in the former results in an increase in the latter. In order to raise the total conversion, the following are assumed to be effective: longer reaction time, higher initiator concentration, higher backbone-polymer concentration, higher MMA concentration, and higher reaction temperature. Increased reaction temperature could, however, exert unfavorable influences on blood, such as denaturation of protein, and



this seems to be not suitable for the purpose. The effects of the first four items on the grafting of MMA by  $\text{Bu}_3\text{B}$  onto blood were studied.

In order to determine if grafting could occur on heparin, control experiments were carried out with and without heparin under otherwise identical conditions. Since there was no difference in the total yield within the limits of experimental error, heparin was assumed to have no effect on the grafting under these conditions.

**Reaction Time.** Figure 2 illustrates the dependence of the total conversion, the percentage of grafting, and the efficiency of grafting on the reaction time. These all increased gradually as the reaction time became

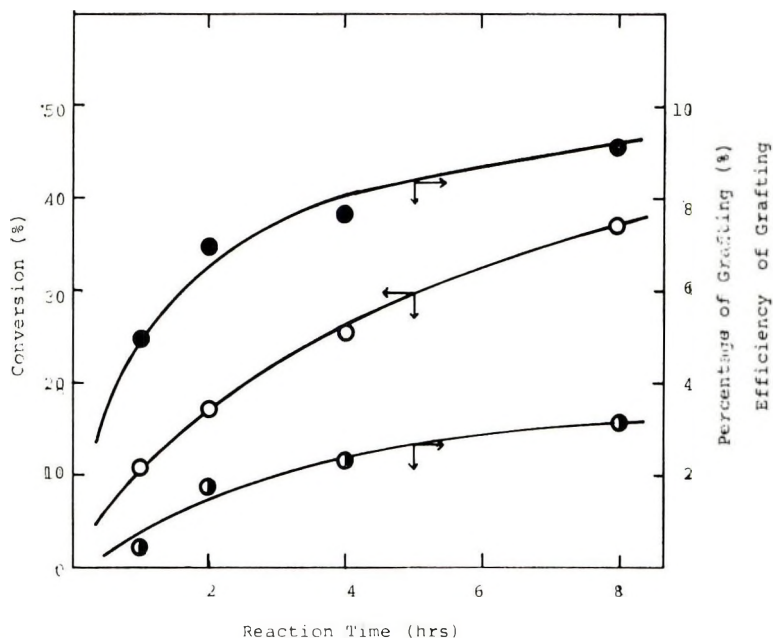


Fig. 2. Effects of reaction time on (O) total conversion; (◐) percentage of grafting; (●) efficiency of grafting.

longer. This suggests that a considerable number of the active centers were formed as expected (Fig. 2).

**Initiator Concentration.** The effects of the initiator concentration on the grafting are shown in Figure 3. The concentration ranged from 0.1 ml of  $\text{Bu}_3\text{B}$  per 20 ml of the blood solution to 0.4 ml of  $\text{Bu}_3\text{B}$  per 20 ml of the solution. The total conversion reached a maximum at a concentration of 0.2 ml/20 ml or more, while the percentage of grafting and the efficiency of grafting increased gradually as the concentration became higher. This fact could be interpreted by assuming that the addition of more initiator yields more grafting sites, which result in the consumption of MMA more for the grafting and in a balance between the rate of homopolymerization and that of grafting, i.e., no increase in the total conversion.

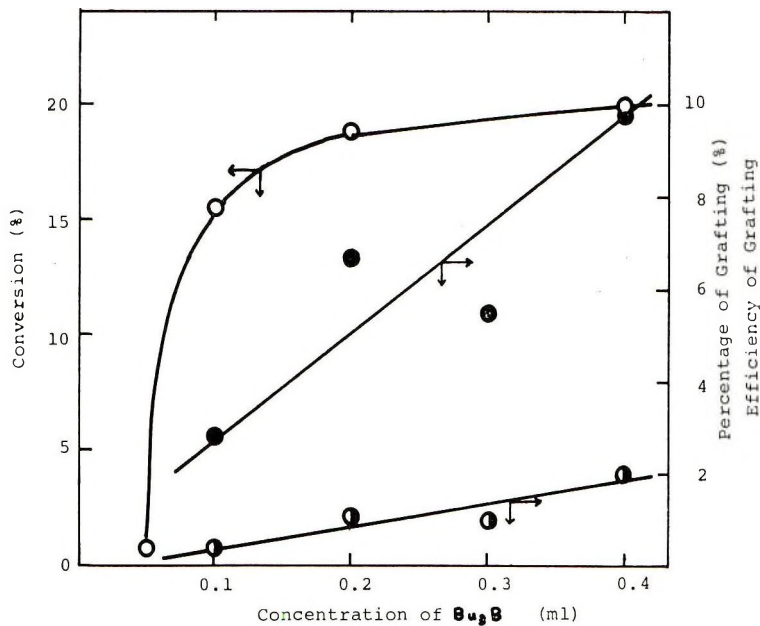


Fig. 3. Effects of initiator concentration on (○) total conversion; (◐) percentage of grafting; (●) efficiency of grafting.

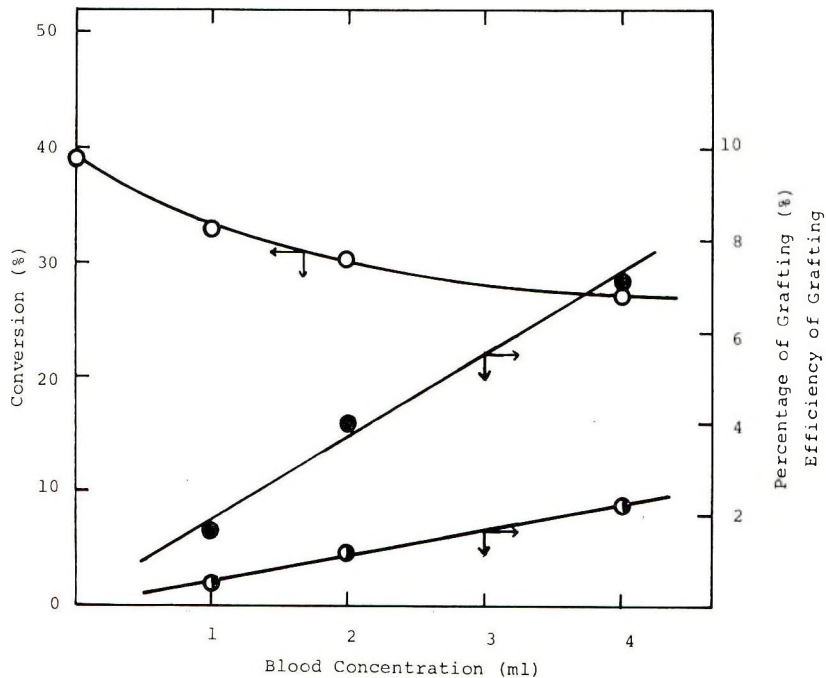


Fig. 4. Effects of blood concentration on (○) total conversion; (◐) percentage of grafting; (●) efficiency of grafting.

**Blood Concentration.** The dependences of the grafting on the blood concentration were studied in the range of 1–4 ml of blood per 20 ml of the blood solution containing heparin and isotonic NaCl solution. The results are illustrated in Figure 4. With an increase in the blood concentration, the percentage of grafting and the efficiency of grafting were observed to increase remarkably, although the total conversion decreased (Fig. 4). This would mean that the higher the blood concentration, the more grafting sites were formed. Thus, higher blood concentration and probably lower MMA are also expected to give higher efficiencies of grafting.

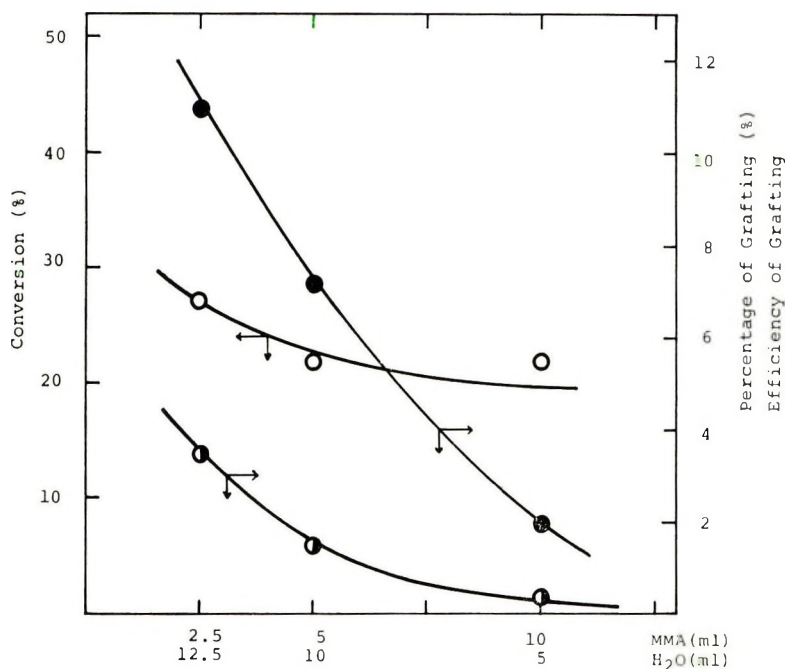


Fig. 5. Effects of monomer concentration on (○) total conversion; (◐) percentage of grafting; (●) efficiency of grafting.

**MMA Concentration.** Figure 5 presents the effects of the monomer concentration on the grafting. When the MMA concentration was raised, the total conversion was observed rather to decrease than to increase. This seems to deviate from the fact that the rate of polymerization is proportional to the monomer concentration in the usual polymerization of vinyl monomers by trialkylborane initiators, when the initiator concentration is constant. However, the deviation can be explained by the idea that the rate of grafting depends practically not on the monomer concentration but mainly on the initiator concentration and the blood concentration; since the mole concentration of the MMA charged far exceeds those of Bu<sub>3</sub>B and blood, an increase in the MMA concentration causes a decrease in the total conversion.

It is obvious from the above assumption that the numerator becomes almost constant and that, when the monomer concentration is raised, the denominator becomes larger and the total conversion will reduce accordingly.

It is interesting to note that water exerts a marked influence on the polymerization. If the percentage of grafting and the efficiency of grafting are extrapolated to zero water content (Fig. 5), they approach zero; i.e. no grafting would occur in the absence of water, so that MMA does not graft onto dried blood. This will be discussed below.

### Solvent Effects

The same procedure was repeated in the usual organic solvents, such as chloroform, cyclohexanone, tetrahydrofuran (THF), and toluene. The results are listed in Table II. The percentage of grafting and the efficiency of grafting were observed to decrease in the presence of cyclohexanone and THF (expts. 107 and 108). The addition of pyridine (Py) and

TABLE II  
Grafting of Methyl Methacrylate onto Blood in the Presence of Various Organic Solvents and Additives<sup>a</sup>

Expt.	Solvents or additives	Total yield, g	Conversion, %	Weight of homo-polymer, g	Weight of graft polymer, g	Percentage of grafting, %	Efficiency of grafting, %
107	Tetrahydrofuran <sup>b</sup>	1.72	15.4	0.50	1.02	0.4	2.8
108	Cyclohexanone <sup>b</sup>	1.55	11.8	0.37	1.06	1.3	10.9
109	Toluene <sup>b</sup>	1.60	12.8	0.30	1.19	4.1	31.7
110	Chloroform <sup>b</sup>	1.78	16.7	0.39	1.25	5.3	32.5
104	Pyridine <sup>c</sup>	5.02	85.9	2.12	2.57	33.6	39.1
105	<i>t</i> -BuOOH <sup>c</sup>	4.82	81.6	2.22	2.16	24.8	30.4
103	None <sup>d</sup>	2.52	32.5	0.89	1.29	6.2	19.1

<sup>a</sup> Grafting conditions: MMA, 5 ml; blood, 5 ml; isotonic NaCl solution, 10 ml; Bu<sub>3</sub>B, 0.10 ml.

<sup>b</sup> 5 ml; solvents were mixed with MMA.

<sup>c</sup> 0.1 ml.

<sup>d</sup> Isotonic NaCl solution, 15 ml.

*tert*-butyl peroxide (*t*-BuOOH) raised the percentage of grafting and the efficiency of grafting (expts. 104 and 105). Since Py<sup>6</sup> and peroxides<sup>13</sup> are known to promote the polymerization of vinyl compounds initiated by trialkylboranes, the cocatalytic effects of Py and *t*-BuOOH may be interpreted analogously. However, it is not clear why the percentage of grafting and the efficiency increased when solvents such as chloroform and cyclohexanone were added (expts. 109 and 110).

### Other Vinyl Monomers

The results with other vinyl monomers than MMA are summarized in Table III. The reactivity of the monomers were in the order: (2-hydroxy)ethyl methacrylate > glycidyl methacrylate > acrylamide > acrylic acid >>> acrylonitrile  $\sim$  vinyl acetate  $\sim$  vinylpyridine. Neither styrene nor isoprene was grafted onto blood. This fact indicates that the polarity and solubility of the monomers play important roles in the grafting. The presence of a hydrophilic group in the monomers seems to be necessary for the reaction to occur. These would suggest that the grafting of the vinyl compounds could proceed via a complex involving water, solid blood components, and monomer.

TABLE III  
Grafting of Vinyl Monomers onto Blood<sup>a</sup>

Expt.	Vinyl monomers <sup>b</sup>	Total yield, g	Conversion, %	Weight of homopolymer, g	Weight of graft polymer, g	Percentage of grafting, %	Efficiency of grafting, %
21	HEMA	5.61	84.9	0.14	5.46	82.3	96.9
29	GMA	4.26	56.6	0.66	3.40	43.7	78.0
27	Acrylamide	3.58	43.6	0.50	2.71	33.1	76.9
28	Acrylic acid	1.60	7.5	0.15	1.29	4.6	61.7
22	VAc	1.06	1.3	0.01	0.91	—	—
24	AN	1.14	2.4	0.01	0.12	—	—
26	VP	1.09	1.9	0.02	1.01	—	—

<sup>a</sup> Grafting conditions: blood, 5 ml; isotonic NaCl solution, 5 ml; Bu<sub>3</sub>B, 0.2 ml; 37°C; 2 hr; monomer, 0.1 mole.

<sup>b</sup> HEMA: (2-hydroxy)ethyl methacrylate; GMA: glycidyl methacrylate; VAc: vinyl acetate; AN: acrylonitrile; VP: 4-vinylpyridine.

### Grafting of MMA onto Blood Cells and Blood Plasma

In order to investigate onto what component of blood MMA was grafted, the same polymerization procedure was applied to blood cells and blood plasma. After blood was mixed with the same volume of an isotonic solution containing 0.01% heparin, the mixture was separated into the above two components. As shown in Table IV, the percentage of grafting for the cells and the plasma were 13.5 and 1.50%, respectively (expts. 31 and 32); MMA was obviously grafted better onto the cells.

The grafting was continued onto dried blood, hematoporphyrin, hemin, and hemoglobin. Hemoglobin was found to be the best backbone polymer (expt. 203). Hemin, which was obtained from hemoglobin by the removal of proteins, showed a larger percentage of grafting but a smaller efficiency of grafting (expt. 204). No grafting occurred onto hematoporphyrin in which Fe<sup>++</sup> and CH<sub>2</sub>=CH— group were removed from hemoglobin (expt. 205).



TABLE IV  
Grafting of Methyl Methacrylate onto Blood Components<sup>a</sup>

Exp. no.	Blood components	ISC		Total yield, g	Conversion, %	Weight of homopolymer, g	Weight of graft polymer, g	Percentage of grafting, %	Efficiency of grafting, %
		g	ml						
31	Blood plasma	2.0	10	0.69	14.7	0.42	0.07	1.5	10.1
32	Blood cells	2.5	10	1.41	30.1	0.57	0.63	13.5	44.7
201	—	—	20	1.05	22.4	1.05	—	—	—
202	Dry blood	0.5	20	2.27	48.5	1.29	0.66	14.1	29.1
203	Hemoglobin	0.5	20	2.83	60.5	1.48	0.84	17.9	29.7
204	Hemin	0.5	20	4.51	96.4	3.23	0.33	7.1	7.3
205	Hematoporphyrin	0.5	20	1.02	21.8	0.63	0.02	0.4	2.0

<sup>a</sup> MMA: 5 ml; Bu<sub>3</sub>B: 0.1 ml; 37°C; 2 hr. ISC: Isotonic NaCl solution.

The inherent viscosities ( $\eta_{inh}$ ) of the homopolymers which were obtained by the reaction in the presence of hemoglobin, dried blood, hemin, and hematoporphyrin, a blank were 0.96, 0.64, 0.43, 0.51, and 0.51, respectively. Pittman reported that chain transfer to the vinyl group of vinylferrocene occurred in the copolymerization of vinylferrocene.<sup>14</sup> Similarly, chain transfer should be taken into consideration. However, these high viscosity values could be explained better by assuming that, in addition to chain transfer, both hemoglobin and  $Bu_3B$  participated in the formation of grafting sites.

### Hydrolysis of the Graft Polymer

The next problem was to determine onto what parts of the methanol-insoluble component of blood the MMA was grafted. In order to clarify this, the graft polymer was hydrolyzed to its simple amino acids. Since some amino acids containing the grafting sites are probably surrounded with grafted PMMA the amounts of amino acids in the hydrolysis products are assumed to be quite less than those obtained from the methanol-insoluble component of blood. Table V shows the hydrolysis products. For purposes of comparison, the methanol-insoluble component of blood was also hydrolyzed. The amounts of both histidine and lysine were found to decrease markedly. This fact suggests that these basic amino acids play an important role in the grafting of MMA by  $Bu_3B$  onto blood.

TABLE V  
Amino acid analysis of hydrolysis products

Amino acid	Amino acid content, mole-% <sup>a</sup>	
	Blood protein	Graft polymer
Lysine	5.8	3.6
Histidine	5.8	3.6
Arginine	9.7	8.6
Aspartic acid	8.4	9.3
Serine	7.1	7.8
Glutamic acid	7.1	7.8
Proline	3.2	4.3
Glycine	7.7	7.8
Alanine	11.0	10.7
Valine	9.0	10.0
Isoleucine	8.4	8.6
Leucine	12.3	12.9
Phenylalanine	4.5	5.0

<sup>a</sup> Recorded on a Japan Electron Optics Laboratory Co. Model JLC-5AH amino acid analyser.

### Oxidation-Reduction Properties

Hemoglobin is known to be capable of promoting the decomposition of hydrogen peroxide, ceric ammonium sulfate, benzoquinone, etc.<sup>11</sup> The

TABLE VI  
Hydrogen Peroxide-Decomposing and Oxidation-Reduction Properties<sup>a</sup>

	Reactivity <sup>b</sup>			
	Hydrogen peroxide	Ceric ammonium sulfate	Nitric acid	Benzoquinone
Blood protein	+	+	—	+
Homopolymer	—	—	—	—
Graft polymer	+	+	—	+

<sup>a</sup> Data of Kojima et al.<sup>11</sup>

<sup>b</sup> + denotes oxidizable or reducible.

effects of the graft on the decomposition were investigated. The graft was found to be effective. (Table VI). However, the graft had less influence on the decomposition than hemoglobin. This can be explained by a decrease in the affinity to water; it would be improved by grafting a hydrophilic monomer.

We are indebted to Dr. Yoshitaka OGAWA, Japan Electron Optics Laboratory Co., for the amino acid analyses.

### References

1. J. Furukawa, T. Tsuruta, and S. Inoue, *J. Polym. Sci.*, **26**, 234 (1957).
2. G. S. Kolesnikov and L. S. Fedorova, *Izv. Akad. Nauk SSSR*, **1957**, 236; *Chem. Abstr.*, **51**, 11291 (1957).
3. L. Reich and A. Schindler, *Polymerization by Organometallic Compounds*, Interscience, New York, 1966, pp. 431, 472.
4. K. Fujii, T. Eguchi, J. Ukeda, and M. Matsumoto, *Kobunshi Kagaku*, **16**, 519 (1959).
5. J. Furukawa, T. Tsuruta, T. Imada, and H. Fukutani, *Makromol. Chem.*, **31**, 122 (1959).
6. K. Kojima, Y. Iwata, M. Nagayama, and S. Iwabuchi, *J. Polym. Sci. B*, **8**, 541 (1970).
7. E. Masuhara, K. Kojima, N. Tarumi and Y. Higuchi, *Repts. Res. Inst. Dental Materials*, **2**, No. 9, 788 (1966).
8. K. Kojima, S. Iwabuchi, K. Kojima, and N. Tarumi, *J. Polym. Sci. B*, **9**, 25 (1971).
9. S. Suzuki and Y. Hachimori, *Nippon Kagaku Zasshi*, **89**, 614 (1968).
10. A. Kondo, Japan. Pat. 521,609.
11. K. Kojima, S. Iwabuchi, K. Kojima and N. Tarumi, *J. Polym. Sci. B*, **9**, 453 (1971).
12. S. Kambara et al., *Monomer Synthesis*, Kyoritu Shuppan, Tokyo, 1957, p. 140.
13. J. Furukawa, T. Tsuruta, and S. Shimatani, *J. Polym. Sci.*, **46**, 238 (1959).
14. C. U. Pittman, Jr., *J. Polym. Sci. A-1*, **6**, 1687 (1968).

## Titration Curves of *p*-Aminobenzoic Acid-Formaldehyde Polymer in Relation to Its Structure

S. K. CHATTERJEE, *Department of Chemistry, University of Delhi*, and V. B. AGRAWAL, *Hans Raj College, University of Delhi, Delhi 7, India*

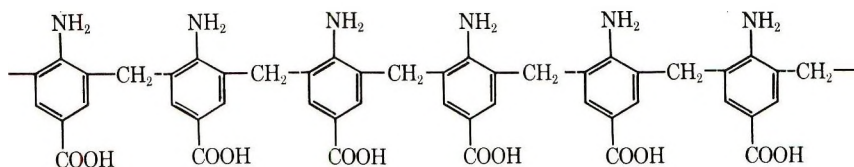
### Synopsis

*p*-Aminobenzoic acid and formaldehyde were condensed in the presence of acid catalyst. The linear condensation polymer thus obtained was then separated into four fractions by a fractional precipitation method. Conductometric titrations were carried out on these four polymer fractions and the conglomerate in nonaqueous solvents with acid as well as base. The titration curves indicated a large number of additional breaks before the complete neutralization of COOH or NH<sub>2</sub> groups. These observations have been interpreted in terms of degree of polymerization and the structure of the polymer.

Synthetic polymers, which are heterogeneous systems, can be separated into various fractions having a narrower distribution of chain lengths. It may be of interest to find out a convenient method for differentiating the degree of polymerization (DP) of such fractions. Some preliminary studies on nonaqueous titration of *p*-(OH) benzoic acid-formaldehyde polymer revealed that it may be possible to assess the DP of the various fractions separated from the linear polymer.<sup>1</sup> Thus it was considered worthwhile to study the titrimetric behavior of a linear polymer having acidic as well as basic functional groups in its repeat unit; the *p*-aminobenzoic acid-formaldehyde condensation product is a typical example of such a polymer. One would normally expect that non-aqueous titration of this polymeric system should indicate only the total quantity of acidic or basic groups in a given weight of the polymer. But the conductometric titration curves of some fractions separated from *p*-aminobenzoic acid-formaldehyde polymer showed some very interesting features. A large number of additional breaks were observed in the titration curves before all the COOH or NH<sub>2</sub> groups were neutralized. An attempt has been made in this paper to correlate these features of the titration curves with the degree of polymerization and structure of the polymer.

### Experimental

*p*-Aminobenzoic acid-formaldehyde condensation product (I) was prepared by



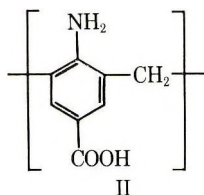
I

refluxing 13.7 g (0.1 mole) of *p*-aminobenzoic acid and 8 g (0.1 mole) of 40% formaldehyde in the presence of 2 cc of 10*N* HCl as catalyst for 3 h at 120°C. The reaction mixture was then poured into ice-cold water and the product washed several times with distilled water. The polymer yield was about 70%. Since the condensate was not readily soluble in the usual organic solvents, therefore it was refluxed with methyl alcohol for about 1/2 hr. The soluble portion of the condensate was then separated from the insoluble residue. The soluble portion, which is by and large linear product, was then precipitated with water, filtered, and dried. It was then fractionated by dissolving about 2.1 g of this product in methyl alcohol, the higher molecular weight fraction being separated on addition of water as nonsolvent. Approximately, 0.68, 0.29, 0.38, and 0.73 g of condensate separated at four consecutive stages of precipitation.

A Pt-Ir bridge was used in conjunction with a Muirhead audio-frequency oscillator as the source of alternating EMF for conductometric titrations. The titrations were carried out at room temperature and about 2 min time was allowed to obtain equilibrium readings.

### Results and Discussion

In Figure 1, are presented the conductometric titration curves of the conglomerate and of the four fractions separated from *p*-aminobenzoic acid-formaldehyde polymer. The titrations were carried out in pyridine with tetramethylammonium hydroxide (TMAH) as the titrant base. This solvent and base were highly recommended by the earlier workers for titrating carboxyl groups.<sup>2,3</sup> The chain molecules of *p*-aminobenzoic acid-formaldehyde polymer are compared of the repeating unit II,



II



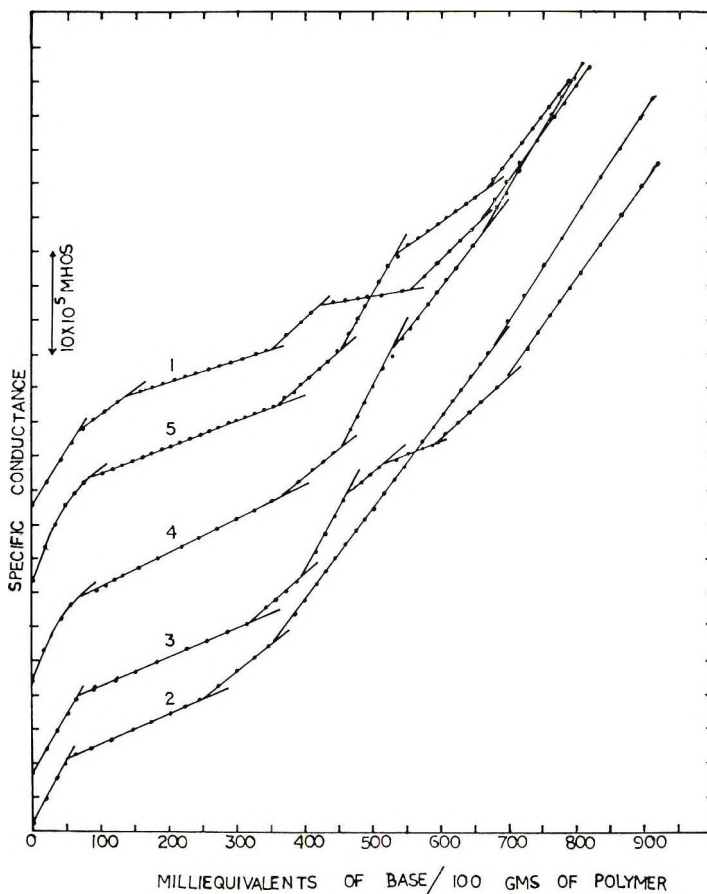


Fig. 1. Conductometric titration curves of *p*-aminobenzoic acid-formaldehyde condensates in pyridine with tetramethylammonium hydroxide: (1) conglomerate; (2) fraction I; (3) fraction 2; (4) fraction 3; (5) fraction 4.

From the molecular weight (149) of this repeat unit, 100 g of condensate should contain 671 meq each of COOH and NH<sub>2</sub> groups.

A noteworthy feature of the titration curves of all the fractions is that each shows a final break at which the calculated amount of base is used up. Apart from this final break, a number of additional breaks were also observed in each of the titration curves. Another important feature of the titration curves is the fact that they showed breaks at more or less regular intervals. For instance in the case of fraction I, the smallest interval between successive breaks is about 50 meq of base/100 g of polymer. All other intervals between successive breaks are simple multiples of this smallest interval. The smallest interval between successive breaks was found to be different for the various fractions of the polymer.

In Figure 2 are presented conductometric titration curves of the same four fractions and the conglomerate of *p*-aminobenzoic acid-formaldehyde

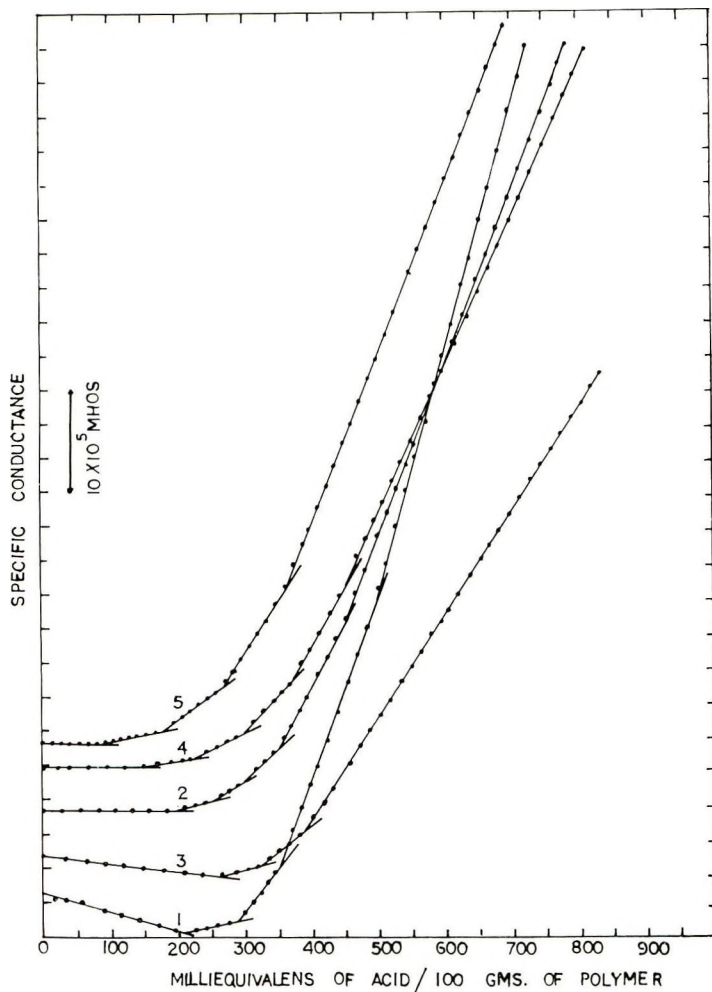


Fig. 2. Conductometric titration curves of *p*-aminobenzoic acid-formaldehyde condensates in acetic acid-formic acid mixture with perchloric acid: (1) conglomerate; (2) fraction 1; (3) fraction 2; (4) fraction 3; (5) fraction 4.

polymer in acidic medium. A mixture of glacial acetic acid and formic acid was used as the medium and perchloric acid as the titrant. This combination was found to be quite effective for titrating amino groups. An important feature of these titration curves is the absence of a break where the calculated amount of acid is added for complete neutralization of  $\text{NH}_2$  groups. However, as already stated, the complete neutralization of  $\text{COOH}$  groups was indicated in the titration curves. Apart from this difference, the main features of the titration curves with acid are more or less identical to those with base. An important point which is worth consideration is that the amount of acid added for a particular fraction at the smallest interval between any two successive breaks coincides with the correspond-

TABLE I  
Observed Amounts of Acidic and Basic Groups in *p*-Amino-benzoic Acid-Formaldehyde Condensate and the Four  
Fractions Separated from It

Break	Conglomerate, meq/100 g		Fraction 1, meq/100 g		Fraction 2, meq/100 g		Fraction 3, meq/100 g		Fraction 4, meq/100 g	
	Acidic	Basic	Acidic	Basic	Acidic	Basic	Acidic	Basic	Acidic	Basic
1st	70	210	50	200	65	265	75	145	90	90
2nd	135	285	250	250	325	325	375	225	360	180
3rd	350	355	350	300	395	390	455	300	450	270
4th	420	400	670	355	460	—	530	375	535	365
5th	555	—	—	450	520	—	660	455	665	—
6th	660	—	—	—	585	—	—	—	—	—
7th	—	—	—	—	690	—	—	—	—	—
Smallest interval	70	—	50	—	65	—	75	—	90	—
Avg. DP	9.5	—	13.4	—	10.3	—	8.9	—	7.4	—
Avg. MW	1413	—	1996	—	1534	—	1326	—	1102	—

ing amount of base added at the smallest interval for the same fraction. This coincidence has been observed in the titration curves of all four fractions of the polymer. This result is to be expected, since each repeat unit of the polymer contains a  $\text{NH}_2$  and a  $\text{COOH}$  group. It is evident that the coincidence does not refer to the amount of acid or base added at the first, second, or third break in the titration curve for a particular fraction. Non-coincidence of values at the various breaks is expected, in view of the fact that medium of titration was different in the two cases. The resolution of a polybasic acid depends on a number of factors, e.g., dielectric constant of the solvent, its solvating power, its acidic or basic character, the chain conformation of the polymer molecule in the solvent, extent of ion-pair formation, etc. Thus it is obvious some functional groups may merge in one medium, whereas the same functional groups may neutralize independently in another medium. This was actually observed in the titration curves. The point of interest is that the smallest interval for a particular fraction is constant irrespective of whether it is titrated with acid or with a base. All other breaks in the titration curve for a given fraction are simple multiples of this smallest interval. These observations are summarized in Table I.

The fact that some of the  $\text{COOH}$  and  $\text{NH}_2$  groups are neutralized earlier than others in the same polymer molecule indicates that they have a stronger acid or basic character. In the case of the *o,o'*-dihydroxydiphenylmethane type of polynuclear compounds, the hyperacid character of some of the  $\text{OH}$  groups in the molecule has been attributed to intramolecular hydrogen bond formation between neighboring  $\text{OH}$  groups.<sup>4-6</sup>

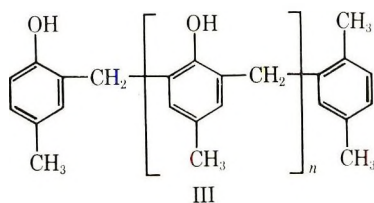
It is likely that a similar type of intramolecular hydrogen bond formation may also take place between neighboring  $\text{COOH}$  groups as well as between adjacent  $\text{NH}_2$  groups. As a result of intramolecular hydrogen bond formation, some of the  $\text{COOH}$  and  $\text{NH}_2$  groups in the chain may acquire enhanced acid or basic character. The number of carboxyl (or amino) groups likely to be involved in a particular hydrogen bond bridge in the polymer molecule depends to a large extent on the orientation of that particular molecule in solution. Since in case of polynuclear phenolic compounds, it was observed that enhancement of acidity of  $\text{OH}$  group is proportional to the length of the hydrogen bond bridge,<sup>4</sup> therefore, it is likely that acidity and basicity of  $\text{COOH}$  and  $\text{NH}_2$  groups should also depend on the length of the intramolecular hydrogen bond bridges in the polymer molecules. As a result of such hydrogen bond formation, various types of anions or cations are expected to conjugate with the corresponding undissociated acid or base and give rise to a series of acid-anion or base-cation complexes. Perhaps, the degrees of dissociation of such complexes are different, and hence they are likely to be neutralized in distinct steps. Kolthoff<sup>7-9</sup> and his co-workers have shown recently that such homoconjugation does take place in a medium of low dielectric constant.

An important aspect of these studies is that it provides an apparently simple method of calculating the degree of polymerization (DP) of the

various fractions separated from a linear polymer. Assuming that the smallest interval in the titration curve would be one in which each chain contributes only one COOH group, the average degree of polymerization can be calculated by dividing the total quantity of base (in milliequivalents/100 g of polymer) to the final break in the titration curve by the amount added during the shortest interval. The average DP of fraction I, for instance, should be equal to  $671/50 = 13.4$ . The product of average DP and the formula weight (149) of the repeat unit, should give the average molecular weight of the condensate. The average molecular weight referred to is likely to be a number-average value, because the number of polymer chains will matter in such calculations and not their weight.

Table I shows the amounts of base or acid which correspond to the various breaks in the titration curves, smallest interval between successive breaks for the various fractions, and their average molecular weights.

The assumption on which DP is calculated would be invalid, firstly, if some of the chains did not contribute any COOH group during the shortest interval, and secondly if some chains were to contribute more than one COOH group during this interval. Since this particular polymeric system could be titrated with a base as well as with an acid, it provides additional evidence about the authenticity of the various breaks, and also of the amounts of acid or base added at the various steps. Apart from this, the validity of the titrimetric method has been checked from the study of polynuclear compounds of known molecular weights. Some oligomeric compounds of the type III



$$n = 4, 5, 6, 7$$

have been prepared by stepwise synthesis, which gives a homogeneous system of known molecular weight. These molecular weights have been compared by titrimetric methods and found to be in excellent agreement.<sup>6,10</sup>

Thus nonaqueous titrations may provide a rapid and convenient method for determining the average degree of polymerization of condensation polymers having acidic or basic functional groups.

### References

1. S. K. Chatterjee, *J. Polym. Sci.*, **8**, 1299 (1970).
2. N. Van Meurs and E. A. M. F. Dahmen, *Anal. Chim. Acta*, **21**, 443 (1959).
3. N. Van Meurs and E. A. M. F. Dahmen, *Anal. Chim. Acta*, **19**, 64 (1958).
4. G. R. Sprengling, *J. Amer. Chem. Soc.*, **76**, 1190 (1954).
5. R. P. Mitra and S. K. Chatterjee, *Indian J. Chem.*, **1**, 62 (1963).



6. S. K. Chatterjee, *Can. J. Chem.*, **47**, 2323 (1969).
7. I. M. Kolthoff, S. Bruckenstein, and M. K. Chantooni, *J. Amer. Chem. Soc.*, **83**, 3927 (1961).
8. I. M. Kolthoff and M. K. Chantooni, *J. Amer. Chem. Soc.*, **85**, 2195 (1963).
9. I. M. Kolthoff and M. K. Chantooni, *J. Amer. Chem. Soc.*, **87**, 1004 (1965).
10. S. K. Chatterjee, *Indian J. Chem.*, **6**, 605 (1969).

Received October 7, 1970

Revised March 2, 1971

## Synthesis and Characterization of Some Trithiols

C. G. OVERBERGER\* and I. SCHEINFELD,† *Department of Chemistry, Polytechnic Institute of Brooklyn, Brooklyn, New York 11201*

### Synopsis

The preparation of 1,3,5-pentane-trithiol is described to provide model systems for poly(vinyl mercaptan). In addition, the preparation and identification of the three stereoisomers of 2,4,6-heptane-trithiol are reported as models for isotactic, syndiotactic, and heterotactic poly(vinyl mercaptan).

The discoveries by Patt et al.<sup>1</sup> and by Ephrat<sup>2</sup> that cysteine and glutathione, respectively, provided protection against the biologically deleterious effects of x-rays, have provided stimuli for the study of the synthesis and oxidation of mercaptans. Earlier publications<sup>3-9</sup> described the syntheses of a variety of mono- and polyfunctional mercaptans prepared for the investigation of the effects of structural variations on the rate of mercaptan oxidation. As part of this work, the stereoisomers of vicinal dithiols were synthesized,<sup>8</sup> and *meso* and racemic 2,4-pentane-dithiol were also separated and identified<sup>9</sup> to study the effects of configuration on oxidation rates. As a continuation of this study, this paper describes the preparation of 1,3,5-pentane-trithiol and the synthesis, separation, and identification of the three stereoisomers of 2,4,6-heptane-trithiol.

The fact that the rate of oxidation of dithiols was found to be greater than the rate of oxidation of monothiols has been attributed to a proximity effect.<sup>4</sup> This suggested that the ease of formation of cyclic disulfide (stable or unstable) might be correlated with oxidation rate. It was further reported that poly(vinyl mercaptan) was oxidized much faster than its model, 2,4-pentane-dithiol. The relatively fast rate for the polymer was attributed partly to the fact that a single thiol group of the polymer has two nearest neighbors, although this may not be the complete explanation. In part, to test this hypothesis, the synthesis of trithiols was undertaken. In addition, 2,4,6-tri-substituted heptanes have been used as model compounds for the investigation of physical and chemical properties of vinyl polymers.<sup>10-12</sup> Isotactic, syndiotactic, and heterotactic 2,4,6-heptane-trithiol can be used as models for the oxidation of isotactic, syndiotactic and heterotactic poly(vinyl mercaptan), and their high

\* Present address: Department of Chemistry and the Macromolecular Research Center, The University of Michigan, Ann Arbor, Michigan 48104.

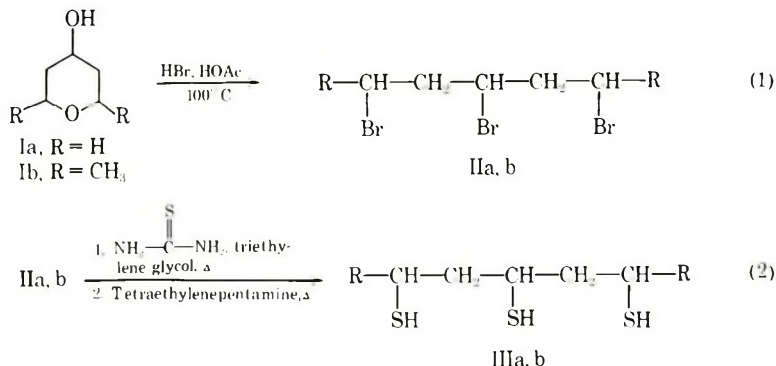
† Present address: Sloan Kettering Institute, Rye, New York, 10580.

resolution nuclear magnetic resonance (NMR) spectra may enable a determination of the polymer tacticity.

## RESULTS AND DISCUSSION

### Preparation of Trithiols

The scheme adopted for the preparation of the trithiols is outlined in eqs. (1) and (2).



The precursor of 1,3,5-pentanetrithiol, tetrahydropyranol-4 (Ia), was prepared via the Prins reaction by using 3-buten-1-ol and formaldehyde. It was found that less charring resulted when an ion-exchange resin was used as the catalyst instead of sulfuric acid, as in earlier syntheses.<sup>13,14</sup> Proof of the pyranol structure was established by independent synthesis.

2,6-Dimethylpyrone-4 was catalytically hydrogenated to provide the precursor of the heptanetrithiol, 2,6-dimethyltetrahydropyranol-4 (Ib).

### Separation and Characterization of the Stereoisomers of 2,4,6-Heptanetrithiol

Complete separation of 2,4,6-heptanetrithiol isomers was achieved via vapor-phase chromatography (VPC) of the product mixture.

### Nuclear Magnetic Resonance Spectra

The 60 Mc/sec NMR spectra of the thiols in Silanor-C (deuterated chloroform containing 1% tetramethylsilane v/v) are given in Figures 1-3.

**Isomer I (Syndiotactic 2,4,6-Heptanetrithiol).** The NMR spectrum of the first pure isomer eluted by VPC showed the central thiol proton as a doublet  $\delta$  1.30 (one peak obscured,  $J = 8$  cps), the methyl protons as a doublet  $\delta$  1.39 ( $J = 6.6$  cps) and a third doublet, assignable to the end thiol protons, at  $\delta$  1.47 ( $J = 7$  cps). The methylene protons showed a triplet with the central peak split at  $\delta$  1.69. The methinyl protons appeared as a complex multiplet at  $\delta$  3.27 (see Fig. 1).

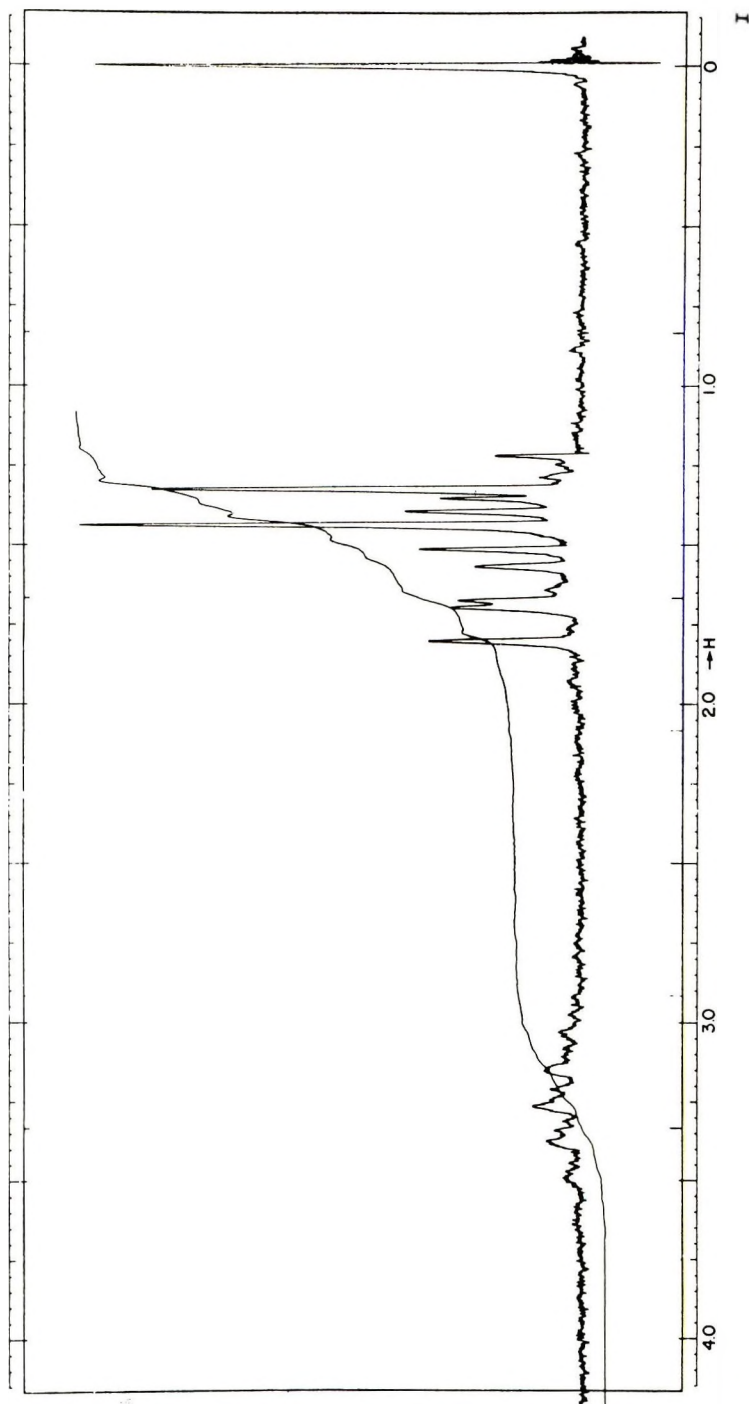


Fig. 1. Proton resonance spectrum at 60 Mc/sec of syndiotactic 2,4,6-heptanetrithiol in Silanor-C (10% solution) (tetramethylsilane = 0 ppm).

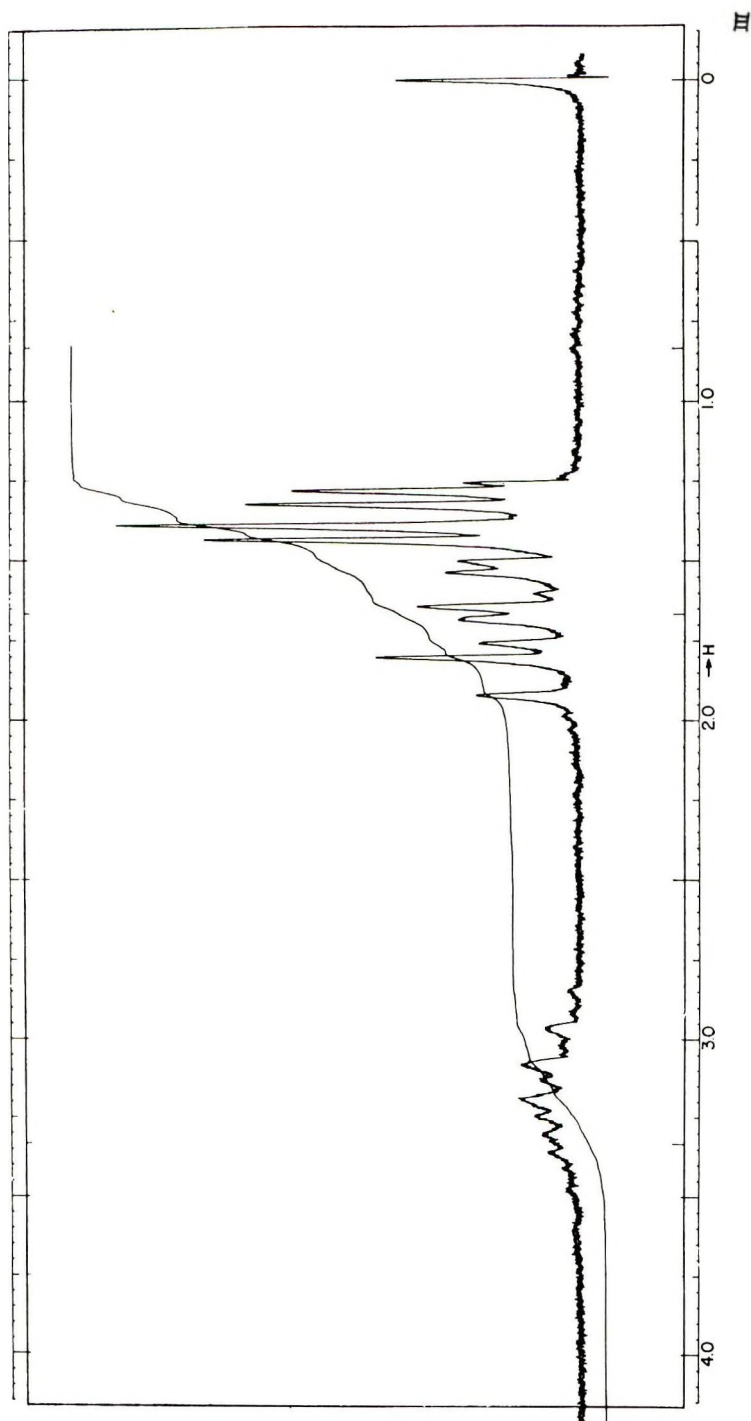


Fig. 2. Proton resonance spectrum at 60 Mc/sec of heterotactic 2,4,6-heptanethiol in Silanor C (10% solution) (tetramethylsilane = 0 ppm).



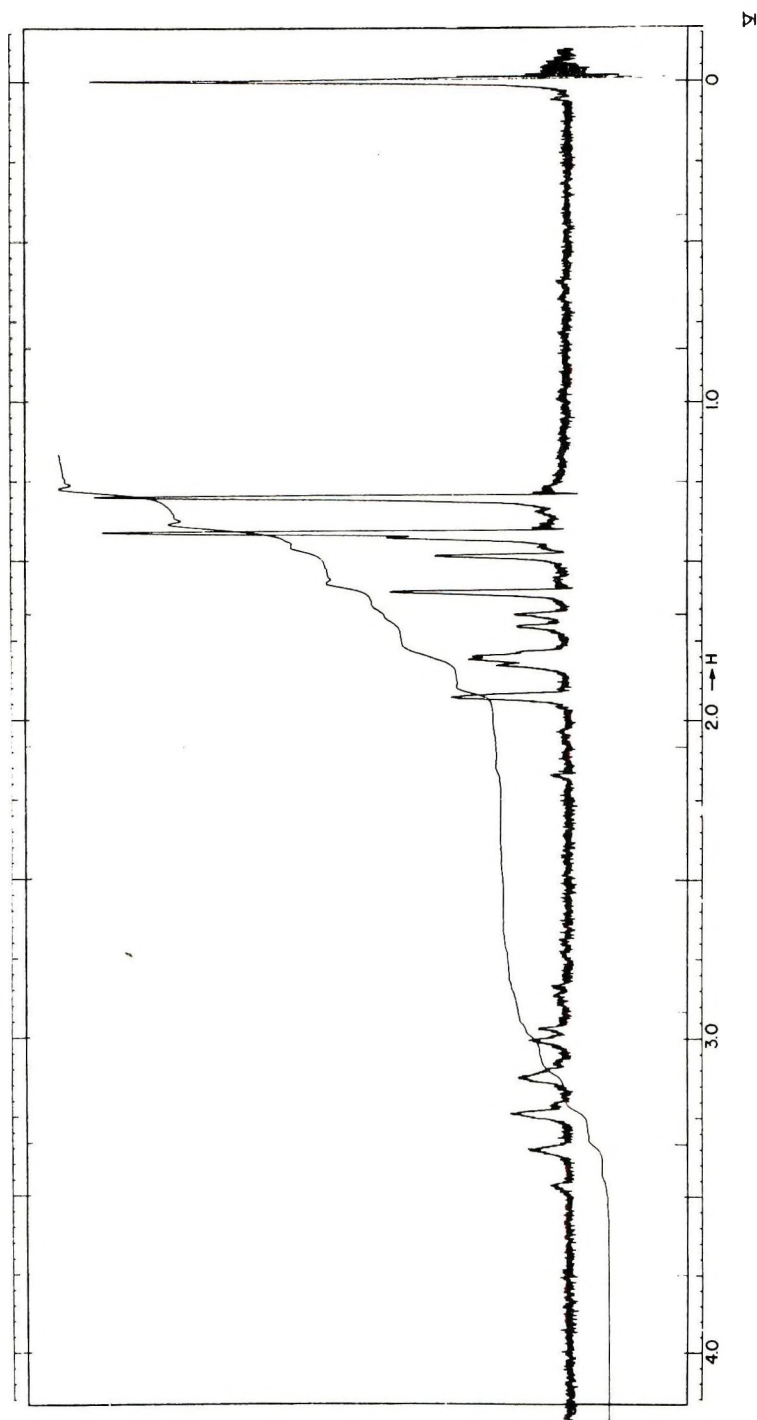


Fig. 3. Proton resonance spectrum at 60 Mc/sec of isotactic 2,4,6-heptanetriol in Silanor-C (10% solution) (tetramethylsilane = 0 ppm).

This isomer was identified as the syndiotactic 2,4,6-heptane-trithiol because it was found to have the simplest spin-spin interaction profile in the methylene region of the three isomers. This was to be expected for the most symmetrical structure. In addition, this profile (triplet with center peak split) is similar to that obtained by Overberger and Kurtz<sup>9</sup> for racemic 2,4-pentanedithiol. Also, Bovey et al.<sup>15</sup> state, “. . . one expects that, in syndiotactic polymers (and in syndiotactic sequences in random polymers), the methylene protons will appear as a ‘triplet’ having a split center peak . . .” Finally, the relative chemical shift of the methyl protons is consistent with the generalization proposed by Ritchey and Knoll,<sup>16</sup> that the relatively low field resonance lines of methyl protons (as compared with the isotactic isomer), are attributable to the syndiotactic isomer, where the functional group causes a deshielding effect. This effect was explained on the basis of anisotropy of a functional group in the polymer affecting protons on the neighboring carbons.

**Isomer II (Heterotactic 2,4,6-Heptanetrithiol).** The NMR spectrum of isomer II was the most complicated of the spectra that were obtained. It showed three different types of thiol protons which appeared as doublets  $\delta$  1.33 (central,  $J = 7.7$  cps), 1.45 (end,  $J = 7.0$  cps), and 1.49 (end,  $J = 6.5$  cps). One peak of each of these doublets was obscured. The methyl protons showed two doublets, one at  $\delta$  1.34 ( $J = 6.5$  cps) and the other at  $\delta$  1.39 ( $J = 6.5$  cps). The remainder of the spectrum consisted of two complex envelopes, one at  $\delta$  1.78, due to the methylene protons, and the other  $\delta$  3.18 due to the methine protons (see Fig. 2).

This isomer was identified as the heterotactic 2,4,6-heptane-trithiol. The heterotactic isomer may be considered to be a combination of the syndiotactic and the isotactic isomers. This would explain the complexity of the spectrum in the methylene region, the appearance of three doublets for the thiol protons (whereas only two doublets appear for each of the other isomers), and two doublets for the methyl protons (as compared to one doublet for the other two isomers). The chemical shift for the low field doublet coincides with the methyl proton doublet of the syndiotactic isomer,  $\delta$  1.39, and the higher field pair with that of the isotactic isomer,  $\delta$  1.34. In addition, in all cases reported in the literature where vapor phase chromatography was used to separate trisubstituted heptane isomers, the heterotactic isomers always appeared second.<sup>17-19</sup> Finally, this isomer was found to be the largest component of the isomer mixture as determined by vpc analysis. If the configuration of each potentially asymmetric center is determined in a random way, then the heterotactic component would be expected to predominate.<sup>18,19</sup>

**Isomer III (Isotactic 2,4,6-Heptanetrithiol).** The NMR spectrum of isomer III shows the methyl group as a doublet at  $\delta$  1.34 ( $J = 6.5$  cps). The thiol protons show two doublets, one at  $\delta$  1.35 (central, one peak obscured,  $J = 7.5$  cps), and the other at  $\delta$  1.54 (end,  $J = 6.5$  cps). The rest of the spectrum was composed of two complex multiplets, one at  $\delta$  1.82, assignable to the methylene protons, the other at  $\delta$  3.11 due to the methine protons (see Fig. 3).

This was based on the relatively high chemical shift of the methyl protons (as this isomer was assigned as the isotactic 2,4,6-heptanetrithiol). Also, Overberger and Kurtz,<sup>9</sup> using the same VPC column, found that the *meso*-2,4-pentanedithiol had a longer retention time than the racemic isomer. The syndiotactic trimer is analogous to the racemic dimer, and the isotactic trimer is comparable to the *meso* dimer.<sup>18</sup>

## EXPERIMENTAL

### Tetrahydropyranol-4(Ia)

3-Buten-1-ol was prepared by the selective dehydration of 1,3-butanediol with *p*-toluenesulfonic acid according to the method of Birch and McAllan.<sup>20</sup>

Earlier procedures<sup>13,14</sup> were modified. 3-Buten-1-ol, 36 g (0.5 mole), aqueous formaldehyde (40% by volume), 37 ml (0.5 mole) and Rexyn AG 50 (H) resin, 40 g, were combined and heated at reflux for 15 hr. The resulting mixture was filtered, neutralized with saturated aqueous sodium carbonate, and extracted with ether. The ether extracts were dried over sodium sulfate. The oil obtained after removal of the drying agent and solvent, was distilled to yield 20 g (39%) of a liquid; bp 97°C, 25 mm;  $n_D^{20}$  1.4595 (lit.<sup>13,14</sup> bp 97°C/25 mm;  $n_D^{20}$  1.4606).

To make certain that the structure of the condensation product was correct, an alternative synthesis was undertaken.

Chelidonic acid (4-pyrone-2,6-dicarboxylic acid) was decarboxylated to  $\gamma$ -pyrone according to the method of Heuberger and Owen,<sup>21</sup> by heating at 250–260°C in 10-g batches in the presence of copper powder and pumice.  $\gamma$ -Pyrone, 2 g, dissolved in 200 ml of ethanol, was catalytically hydrogenated in a Parr apparatus in the presence of 5 g of 5% platinum on carbon for 24 hr at 55°C. The mixture was then filtered and dried over potassium carbonate. The oil obtained after removal of the drying agent and solvent, was distilled, bp 98°C/25 mm. The NMR and infrared spectra of the compound obtained in this manner were identical to those obtained from the condensation of 3-buten-1-ol and formaldehyde.

### 1,3,5-Pentanetribromide(IIa)

The method of Paul and Tchelitcheff<sup>22</sup> was modified. Tetrahydropyranol-4, 51 g (0.2 mole), dissolved in 100 ml of glacial acetic acid, was placed in a 250-ml round-bottomed three-necked flask fitted with a gas-inlet tube, a thermometer, a reflux condenser, and a magnetic stirring bar. Hydrogen bromide gas was allowed to pass through the solution while the temperature was maintained at 100°C, initially with cooling, then with heating. After 20 hr, ice was added, the solution was neutralized with a saturated, aqueous solution of potassium bicarbonate and extracted with ether. The ether extracts were dried over calcium chloride. The oil obtained after filtering the solution and evaporating the solvent was distilled, bp 139°C/16 mm. The distillate was colored and was therefore eluted with cyclohexane from a column packed with acid alumina. The

eluent was evaporated and the residual oil was distilled from hydroquinone, yielding 90.4 g (59%) of a colorless liquid; bp 135–137°C/15 mm;  $n_D^{19}$  1.5580 (lit.<sup>22</sup> bp 134–136°C/14 mm;  $n_D^{19}$  1.5581). The compound showed only one peak upon VPC analysis performed on a Perkin-Elmer Model 154D Vapor Fractometer.

### 1,3,5-Pentanetrithiol(IIIa)

The method of Cossar et al.<sup>23</sup> for the preparation of mono- and dithiols was applied to the preparation of trithiols. A mixture of 100 ml of triethylene glycol and 63 g (0.825 mole) of thiourea was stirred in a 250-ml three-necked round-bottomed flask equipped with a thermometer, a vented dropping funnel (by means of which nitrogen gas was passed through the system), a Vigreux distilling column having a variable take-off head affixed to it, and a magnetic stirring bar. The pot temperature was raised to 75°C, and 77.3 g (0.25 mole) of 1,3,5-pentanetribromide was added dropwise. The temperature was kept below 130°C. After the solution became homogeneous, the reaction was allowed to proceed for an additional 15 min. Tetraethylene-pentamine, 142 g (0.75 mole), was then added dropwise. The reaction was exothermic. After the addition of amine was completed, the product was vacuum-distilled at 1 mm Hg. The distillate was eluted with ether from a column of acid alumina. The eluent was evaporated, and the residual viscous oil was distilled to give 24.9 g (59%) of a yellow liquid; bp 101–103°C/0.6 mm.

A solution of the yellow-colored trithiol, 16.8 g (0.1 mole), dissolved in 50 ml of ether was added dropwise to 5.7 g (0.2 mole) of lithium aluminum hydride suspended in 100 ml of ether. After heating at reflux for 2.5 hr, ice water was cautiously added. The solution was then carefully neutralized with 6*N* hydrochloric acid and extracted with ether. The ether extracts were dried over sodium sulfate. The oil obtained after filtering the solution and evaporating the solvent was distilled to give 10.6 g (63.5% recovery) of a liquid; bp 110–111°C/1.8 mm;  $n_D^{25}$  1.5732;  $d_4^{25}$  1.1415 g/cc. Infrared analysis showed mercaptan absorption at 3.93  $\mu$ .

ANAL. Calcd for  $C_5H_{12}S_3$ : C, 35.70%; H, 7.20%; S, 57.10%. Found: C, 35.85%; H, 7.06%; S, 57.08%.

A derivative was prepared by the reaction of the product with phenyl isocyanate in the presence of pyridine. To a solution of 0.503 g (3 mmole) of trithiol in 1.422 g (11.9 mmole) phenylisocyanate was added 3 drops of dry pyridine. The mixture was heated on a steam bath for 30 min. The product, 1,3,5-pentane trithiocarbanilate, was filtered, washed with methanol and recrystallized from ethyl acetate.

ANAL. Calcd for  $C_{26}H_{27}N_3O_3S_3$ : C, 59.40%; H, 5.18%; N, 7.99%; S, 18.30%. Found: C, 59.42, 59.27%; H, 5.30, 5.26%; N, 7.90, 7.87%; S, 18.40, 18.34%.

It is to be noted that although the product was treated with lithium aluminum hydride to reduce any disulfide present, in this work, such



measures may be unnecessary because of the effectiveness of the gas chromatographic separation.

### 2,6-Dimethyltetrahydropyranol-4(Ib)

2,6-Dimethylpyrone-4 was prepared according to the method of King, et al.<sup>24</sup> by the acid-catalyzed hydrolysis of dehydroacetic acid.

2,6-Dimethylpyrone-4, 24.8 g (0.2 mole), dissolved in 200 ml of absolute ethanol, was hydrogenated in the presence of 6 g of 5% platinum on carbon in a Parr apparatus at 55°C for 24 hr. The work-up was similar to that described by Borsche and Frank,<sup>25</sup> i.e., 60 g of ammonium sulfate was added and the resulting solution was filtered through Celite. The filtrate was extracted with ether and dried over potassium carbonate. After removal of the drying agent and solvent, the remaining liquid was distilled to give 23.6 g (91%) of a colorless liquid; bp 101°C/30 mm (lit.<sup>26</sup> bp 102°C/30 mm).

### 2,4,6-Heptanetribromide(IIb)

2,6-Dimethyltetrahydropyranol-4, 40 g (0.3 mole), was dissolved in 80 ml of glacial acetic acid and treated as described for 1,3,5-pentane-tribromide. A brown oil with a boiling point range of 103°C/14 mm (113°C/0.8 mm) was obtained which was eluted with cyclohexane from a column of acid alumina. The eluent was evaporated and distilled from hydroquinone to give 22.5 g (22%) of a colorless liquid; bp 117°C/4 mm;  $n_D^{25}$  1.5272.

ANAL. Calcd for  $C_7H_{13}Br_3$ : C, 24.95%; H, 3.89%; Br, 71.15%. Found: C, 25.15%; H, 3.97%; Br, 71.12%.

### 2,4,6-Heptanetrithiol(IIIb)

Tetraethylene glycol (25 ml) and 16.75 g (0.22 mole) of thiourea was stirred in the apparatus described in the synthesis of IIIa. The pot temperature was raised to 75°C and 22.5 g (0.067 mole) of 2,4,6-heptane-tribromide was added dropwise. The temperature was maintained at 75–80°C during the course of the addition. After the addition of the tribromide was completed, external heat was applied until the temperature reached 125°C, when an exotherm caused the temperature to reach 150°C. The resulting solution was homogeneous. The reaction was allowed to proceed for an additional 15 min. Tetraethylenepentamine, 18.2 g, was then added dropwise. The work-up was performed as described for IIa. The product mixture was distilled at 0.5 mm Hg. The distillate was eluted with ether from a column of acid alumina. The eluent was evaporated and distilled to give 6.1 g of a yellow-colored liquid; bp 96–98°C/0.6 mm.

A solution of the yellow-colored trithiol, 2.5 g (0.013 mole), dissolved in 10 ml of ether was added dropwise to a 0.58 g (0.02 mole) of lithium aluminum hydride suspended in 15 ml of ether. The resulting mixture was heated at reflux for 2 hr, and then ice water was cautiously added.



After careful neutralization with 6*N* hydrochloric acid, the solution was extracted with ether and the extracts were dried over sodium sulfate. After filtering the solution and evaporating the solvent, the residue was distilled to give 0.93 g (37% recovery) of a colorless liquid; bp 82°C/0.3 mm;  $n_D^{25}$  1.5378. Infrared analysis showed mercaptan absorption at 3.92  $\mu$ .

ANAL. Calcd for  $C_7H_{16}S_3$ : C, 42.80%; H, 8.21%; S, 49.08%. Found: C, 43.05%; H, 8.25%; S, 48.90%.

2,4,6-Hepanetriethiol was separated into its stereoisomers by means of preparative vapor-phase chromatography. The apparatus used to achieve the separation was an Aerograph Model A-700 (Wilkens Instrument and Research). The column used was a 20 ft  $\times$   $\frac{3}{8}$  in. od aluminum column packed with 20% by weight of ethylene glycol succinate on 60–80 mesh Chromosorb W.

Operational details of the separation were: carrier gas (helium) inlet pressure, 60 psig; approximate flow rate, 60 cc/min; injection port temperature, 259°C; column temperature, 183°C; detector block temperature, 245°C; and filament current, 150 mA. Portions of the mixture (50  $\mu$ l) were injected directly onto the column at 52 min intervals and collected in receivers cooled by a Dry Ice–acetone mixture. Retention times for the isomers were: syndiotactic, 121 min; heterotactic, 135 min; and isotactic, 148 min. Five fractions were obtained, the second and the fourth, being mixtures, were discarded.

Each isomer was shown to be isomerically pure by analytical VPC on an aluminum column 2 m  $\times$  6 mm od, containing diethylene glycol succinate on Firebrick G. C. 22, 60–80 mesh. Operational details were: carrier gas (helium) inlet pressure, 15 psig; flow rate, 4.4 cc/min; and column temperature, 154°C. Retention times for the isomers were: syndiotactic, 25 min; heterotactic, 27.5 min; and isotactic, 29.5 min.

Final purification of the first two isomers was achieved on the Aerograph by using a 20 ft  $\times$   $\frac{3}{8}$  in. od aluminum column, packed with 20% Carbowax 20-M on 60–80 mesh DMCS-AW Chromosorb W. Operational details were: carrier gas (helium) inlet pressure, 50 psig; approximate flow rate, 135 cc/min; injection port temperature, 225°C; and detector block temperature, 220°C. Column temperatures and retention times are shown in Table I.

TABLE I  
Separation of Isomers

Isomer	Column temperature, °C	Retention time, min
Syndiotactic	200	71
Heterotactic	210	71
Isotactic	190	102

Slight decomposition of the isotactic isomer was found to have occurred as a result of injection onto the Carbowax column. The decomposition products were removed by reinjection onto the ethylene glycol succinate column under the conditions cited above.

### Nuclear Magnetic Resonance Spectra

For the measurement of the NMR spectra, ca. 15% (w/v) solutions of each of the stereoisomers of 2,4,6-heptanetrithiol in Silanor-C [deuterated chloroform containing 1% tetramethylsilane (v/w)] were placed in 7-in. micro NMR tubes; tube od, 0.195/0.196 in.; bore diameter, 1.5 mm; cavity height, 10 mm, cavity id, 0.166 in.; and base height 10 mm (supplied by Wilmad Glass Co., Buena, N. J.). The spectra were run on a Varian Model A-60 analytical NMR spectrometer at 40°C.

Financial support by the U. S. Public Health Service, National Institutes of Health, under Grants Nos. DE-01769-03, DE-01769-04 and DE-01769-05, is gratefully acknowledged. Grateful acknowledgement is also made to Mr. H. Talts for the NMR determinations and to Dr. F. Bovey for his aid in interpreting the NMR spectra.

This paper is taken from the dissertation of I. Scheinfeld submitted to the faculty of the Polytechnic Institute of Brooklyn in partial fulfillment of the requirements for the degree of Doctor of Philosophy (Chemistry), 1967.

### References

1. H. M. Patt, E. P. Tyree, R. L. Straube, and D. F. Smith, *Science*, **110**, 213 (1949).
2. E. Ephrat, *Biochem. J.*, **42**, 383 (1948).
3. C. G. Overberger and J. J. Ferraro, *J. Org. Chem.*, **27**, 3539 (1962).
4. C. G. Overberger, J. J. Ferraro, and F. W. Orttung, *J. Org. Chem.*, **26**, 3458 (1961).
5. C. G. Overberger and H. Aschkenasy, *J. Org. Chem.*, **25**, 1648 (1960); *J. Amer. Chem. Soc.*, **82**, 4357 (1960).
6. C. G. Overberger and P. V. Bonsignore, *J. Amer. Chem. Soc.*, **80**, 5427, 5431 (1958).
7. C. G. Overberger and A. Levovits, *J. Amer. Chem. Soc.*, **78**, 4792 (1956).
8. C. G. Overberger and A. Drucker, *J. Org. Chem.*, **29**, 360 (1964).
9. C. G. Overberger and T. Kurtz, *J. Org. Chem.*, **31**, 288 (1966).
10. Y. Fujiwara, S. Fujiwara, and K. Fujii, *J. Polym. Sci. A-1*, **4**, 257 (1966).
11. T. Shimanouchi, M. Tasumi, and Y. Abe, *Makromol. Chem.*, **86**, 48 (1965).
12. D. Doskocilova, J. Stokr, E. Votavova, B. Schneider, and D. Lim, *J. Polym. Sci. C*, **16**, 2225 (1965).
13. E. Hanschke, *Chem. Ber.*, **88**, 1053 (1955).
14. M. I. Farberov, E. P. Tepenitsyna, and N. K. Shemyakin, *Dokl. Akad. Nauk SSSR*, **99**, 793 (1954).
15. F. A. Bovey, F. P. Hood, III, E. W. Anderson, and L. C. Snyder, *J. Chem. Phys.*, **43**, 3900 (1965).
16. W. M. Ritchey and F. J. Knoll, *J. Polym. Sci. B*, **4**, 853 (1966).
17. J. Petranek, M. Kolinsky, and D. Lim, *Nature*, **207**, 1290 (1966).
18. H. G. Clark, *Makromol. Chem.*, **86**, 107 (1965).
19. D. Lim, M. Kolinsky, E. Votavova, M. Ryska, and J. Lukas, *J. Polym. Sci. B*, **4**, 573 (1966).
20. S. F. Birch and D. T. McAllan, *J. Chem. Soc.*, **1951**, 2556.
21. O. Heuberger and L. N. Owen, *J. Chem. Soc.*, **1952**, 910.
22. R. Paul and S. Tchelitcheff, *Bull. Soc. Chim. France* **1951**, 550.

23. B. C. Cossar, J. O. Fournier, D. L. Fields, and D. D. Reynolds, *J. Org. Chem.*, **27**, 93 (1962).
24. L. C. King, F. J. Ozog, and J. Moffat, *J. Amer. Chem. Soc.*, **73**, 301 (1951).
25. W. Borsche and R. Frank, *Ber.*, **59**, 237 (1926).
26. J. J. DeVrieze, *Rec. Trav. Chim.*, **78**, 91 (1959).

Received June 10, 1971

Revised July 21, 1971

## Crosslinking and Structural Changes of Cellulose Fibers

G. V. NIKONOVICH and KH. U. USMANOV, *Research Institute for Cotton Cellulose Chemistry and Technology, Tashkent, U.S.S.R.*

### Synopsis

The supermolecular structure of various cellulose fibers modified with crosslinking reagents has been investigated by electron microscopy methods. The density, degree of crystallinity (DC), and length changes in alkaline solutions were measured for the modified celluloses. The samples treated with monofunctional analogs of the crosslinking reagents as well as the fiber preparations containing linear and network polymer were also investigated. Three main problems are suggested for the discussion: (1) the general regularities of the structural changes in cellulose in the process of crosslinking; (2) the specific features of the structural changes, as observed in different cellulose samples; (3) the relation between the degree of modification, the type of modifying reagent, and the structure of the crosslinked cellulose. The characteristic structural changes, i.e., the increase in the thickness of fragments, the specific coggled edges, the increase in the lateral dimensions of structural elements all seem to be most representative in native cellulose fibers and are perfectly well distinguished. Similar changes are found in viscose fibers but are less clearly defined. Crosslinking proceeds rather uniformly through the whole of the fiber cross section. It appeared to be most evident when the cross sections are treated with solvents, or when etched in gaseous discharge. Only in cases when the modification is performed in nonaqueous solutions does the reaction proceed mainly in the peripheral regions of the fiber. In fibers subjected to strong swelling, crosslinking results in a real increase in the lateral dimensions of the microfibrils, with the layer thicknesses remaining the same. As a rule, the modification does not imply significant changes in the fiber surface. The crystallite size decreases in the process of crosslinking. This appears to be peculiar to viscose fibers, especially to those subjected to crosslinking in the swollen state. The degree of crystallinity and density of the fibers decrease sharply, which seems to be especially evident in epichlorohydrin-modified samples. Cellulose structure remains unchanged when linear or network polymer forms in the fiber or when the samples are treated with monofunctional reagents. Changes in properties and structure of cellulose caused by crosslinking are most apparent if elongation of the fibers in alkaline solution before and after the modification is compared.

### INTRODUCTION

The supermolecular structure of cellulose modified with crosslinking reagents has been studied by many authors.<sup>1-7</sup> Results achieved in our laboratory led us to certain conclusions on the mechanism of cellulose crosslinking on the supermolecular level. Experimental data and the results of the investigations of the crosslinked cellulose and particularly of a variety of viscose fibers are reported here.



Three main problems suggested for the discussion: (1) general regularities characteristic of the structural changes in cellulose fibers in the process of crosslinking; (2) specific peculiarities of the structural changes as detected in different cellulose samples; (3) relation between the degrees of modification, the nature of the modifying reagent, and the structure of the crosslinked cellulose.

### Materials and Methods

Cellulose fibers modified with formaldehyde, dimethylolurea (DMU), dimethylolthiourea (DMTU), dimethylolethylenurea (DMEM), acrolein, diepoxy resin, epichlorohydrin (ECH), cyanuric chloride, and some other bifunctional reagents (all of them shown<sup>8-12</sup> to crosslink with cellulose) were used in the investigations. In addition, samples treated with analogs of these compounds but possessing only one functional group, i.e., monomethylolthiourea (MMTU), monomethylolurea (MMU), propylene oxide, etc., and fibers containing linear and network polymers were studied.

Cotton cellulose, polynosic fibers, tire cords of different strength, viscose and cuprammonium rayons were used. The supermolecular structure of the modified samples was studied by means of various methods of electron microscopy.

The fiber fragments, ultrathin sections, surface replica as well as crystallites isolated by hydrolysis were investigated. In all cases, additional information on the supermolecular structure of the samples was obtained by treatment with some solvents, both before and after sample preparation, or by etching in gaseous discharge. The degree of crystallinity (DC) was estimated by method of x-ray diffraction; the density of the modified fibers was measured by a gradient column method. The elongation of the modified and untreated fibers at a constant load in alkaline solution was also evaluated. More details of the methods used have been reported earlier.<sup>1,2</sup>

### Results and Discussion

Cellulosic materials subjected to treatment with bifunctional reagents are characterized by a significant increase in the fragment thickness and by the absence of fibrillation in ultrasonic disintegration. In addition, on the fragments there appear certain cogged edges transverse to the long axis of the structural elements which are accompanied by formation of large amounts of small chippy particles (Figs. 2a,b) (These features on the electron micrographs are indicated by arrows.) For comparison see Figure 1a, where a thin layer of untreated cotton cellulose with smooth and even edges is shown.

These changes are obviously the result of crosslinking produced by treatment with bifunctional reagents. The process of crosslinking must have evidently begun in the most accessible regions. For native cellulose preparations, which possess distinct microfibrils and lamellar structure, the regions of accessibility appeared to decrease in the following order: inter-



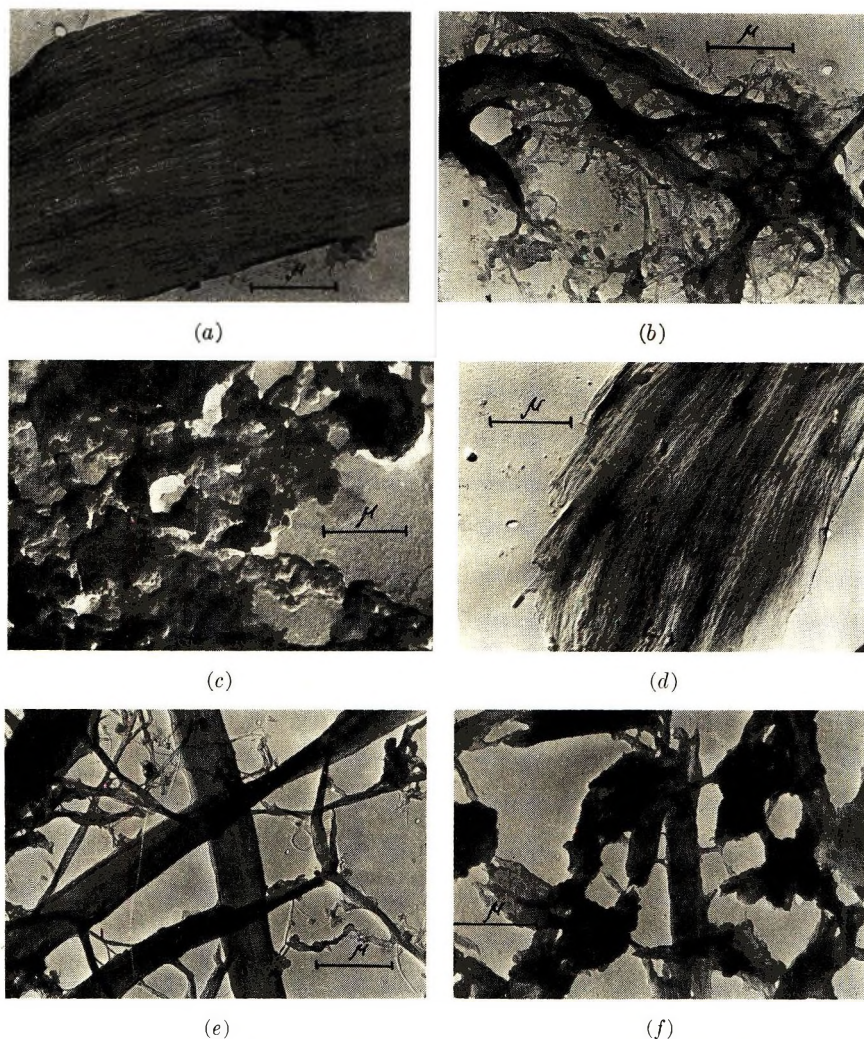


Fig. 1. Fragmentation patterns of untreated fibers: (a) cotton; (b) tire cord; (c) viscose rayon; (d) Polycot; (e) BX fiber; (f) tire cord subjected to 7 min hydrolysis.

layer, interlamellar, interfibrillar, and intrafibrillar areas. Crosslinking is enhanced due to possible penetration of macromolecules and microfibrils into the space between the structural elements (a kind of fringe).

This is why the fragments are the thickest in native cellulose preparations in which the newly formed crosslinks between the layers and lamellae make them interlock with each other. In viscose fibers, which are not characterized by a so well developed fibrillar and layered structure, the features of the supermolecular structure seem to be less clearly distinguished. To a certain degree this inhibits objective interpretation of the obtained experimental data.

The most accessible in this case are the areas between the various types



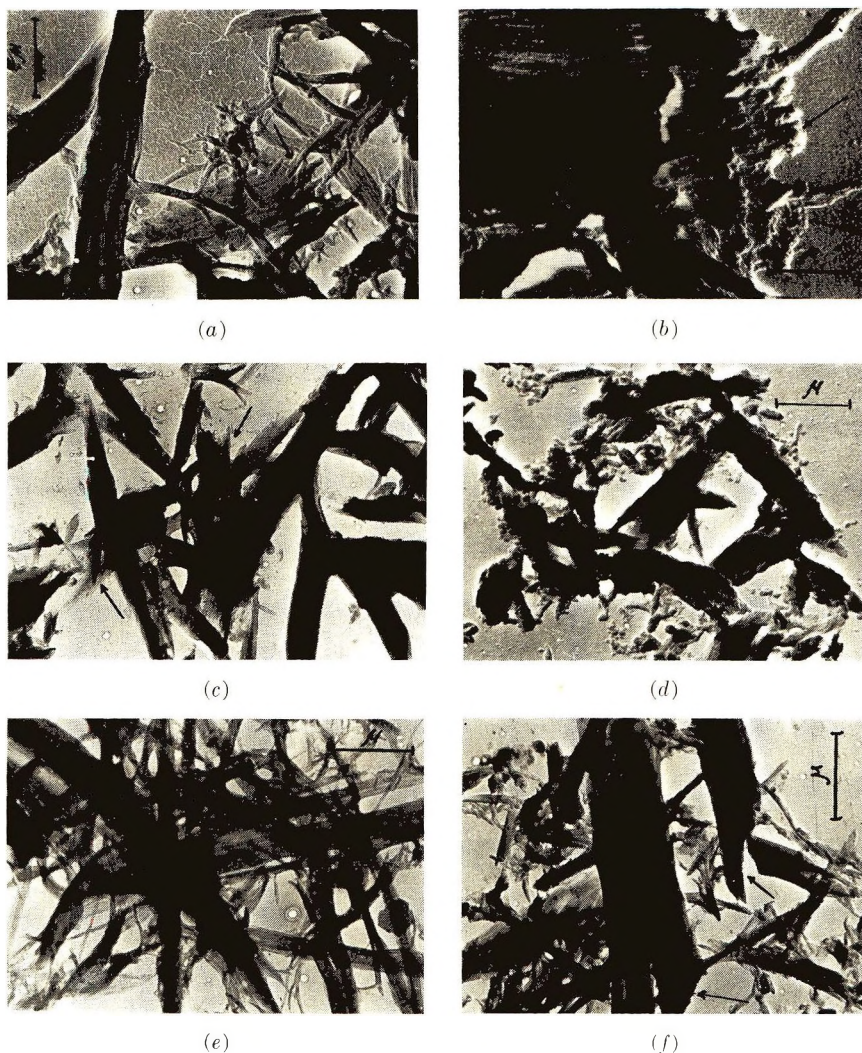


Fig. 2. Fragmentation patterns of the modified fibers: (the most characteristic features of the structure are indicated by arrows): (a) cotton modified with  $\text{CH}_2\text{O}$ ; (b) cotton modified with acrolin; (c) tire cord modified with DMM (This is on the same scale as the other parts of Fig. 2.); (d) viscose rayon modified with  $\text{CH}_2\text{O}$ ; (e) BX fiber modified with  $\text{CH}_2\text{O}$ ; (f) Polycot modified with  $\text{CH}_2\text{O}$ .

of molecular arrangement, i.e., the region between the tapelike bands and fibrils. It must be noted, that there exists a wide range of types of molecular order within this or other fiber species.

As has already been shown,<sup>13</sup> in the disintegration of tire cords layers are formed which are characterized by a poorly organized inner structure and a considerable amount of structureless matter (Fig. 1b). After the modification, the thickness of the fragments increases and the amount of the structureless matter becomes even less (Fig. 2c). It is evident, that in the modification of tire cord, in which clearly observed boundaries separating

the structural elements and structureless matter are absent, crosslinking proceeds in the most loose areas as well as in the transitional zones between them, and the structureless matter seems to be crosslinked with the ordered areas and the structural elements.

Actually, microphotographs of the disintegrated preparations show almost no structureless matter. Even in the viscose and cuprammonium rayon samples, which contain the largest amounts of structurally unorganized cellulose, one can detect some small amounts of crosslinked material, as compared to the initial samples (Figs. 1c and 2d). Polynosic fibers are characterized by a somehow better defined fibrillar and layered structure (Fig. 1d),<sup>14</sup> while the structure of the BX-type fibers might be considered as a system of layers, composed of tightly packed microfibrils with numerous small pores in them (Fig. 1e). Since after the crosslinking there can be observed no distinct increase in the thickness of the fiber fragments, one can suggest that the modification process proceeds mainly on the submicroscopic pores walls and to a less degree in the interlayer zones (Fig. 2e). In the polynosic rayons such as Polycot, Hypolan, and Z-54 fibers, the interlayer crosslinking seems to be much better defined. This results in a significant increase in the thickness of the fragments, accompanied by the formation of a large amount of "chippy" particles (Fig. 2f) as compared to the original samples (Fig. 1d). The structural changes become especially evident when  $\text{CH}_2\text{O}$ , DMM, DMEM, and DMTM are used for the modification.

Thus, an increase in the lateral dimensions of the structural elements becomes one of the most characteristic features of the process of crosslinking in cellulose. It is evident that layers, lamellae, and microfibrils, as they are, retain their initial dimensions as observed in cellulose preparations prior to the treatment. However, the formation of crosslinks between the structural elements results in the fact, that in many processes in which cellulose participates, especially in physico-mechanical processes, the largest structural units take part. Cellulose fibers lose those properties characteristic of the fibrillar structure when crosslinks are too numerous and behave like a three-dimensional network. This brings about an abrupt increase in the fiber brittleness, which causes them to break into small particles.

As a rule, the increased brittleness of the crosslinked viscose fibers is attributable to the immobility of the accessible regions in the space between structural elements. In this sense, crosslinking affects the fibers structure and properties as partial hydrolysis does when the most accessible regions become depolymerized and destroyed. This is why identical pictures are observed in preparations of disintegrated crosslinked cellulose and of hydrolyzed fibers (Fig. 1f).

The "cogged" edges, which characterize the modified fiber fragments, are the result of increased brittleness and unequal force distribution in the disintegration of the crosslinked fibers. Generally, this is related to the crosslinking in the lateral directions of the microfibrils and other layer-forming structural elements, which leads to the fact that the fibers show brittle fractures as the natural weak points.

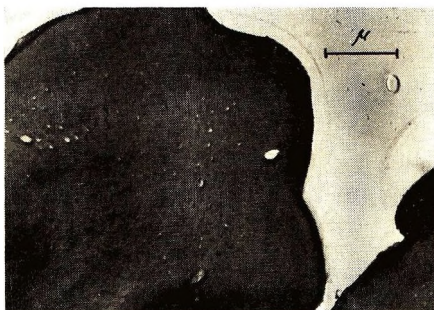


The enlargement of the effective dimensions of the structural elements is found in ultrathin cross and longitudinal sections. The "buttends" dimensions of the structural elements increase (they are indicated by arrows), and their number per unit cross-sectional area decreases markedly compared to the untreated fibers (see Figs. 3 and 4). As might be expected, this is seen most clearly in fibers which are characterized by well-defined structural elements (native cellulose fibers, for example, Fig. 4a), and becomes less in the case of cross sections of viscose fibers (Fig. 4b).

It must be noted, however, that the ultrathin longitudinal cross sections



(a)



(b)



(c)

Fig. 3. Ultrathin sections of unmodified fibers: (a) cotton; (b) viscose rayon; (c) BX fiber (longitudinal section).

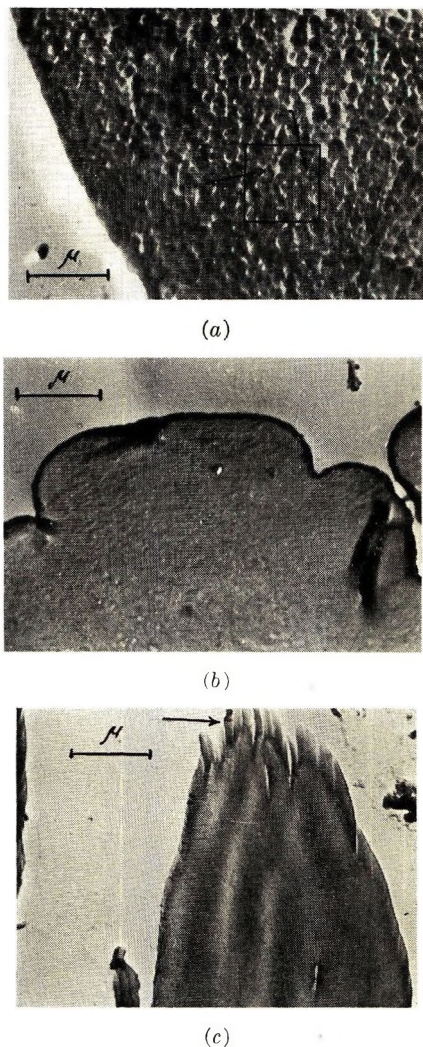


Fig. 4. Ultrathin sections of modified fibers: (a) cotton modified with acrolein; (b) viscose rayon modified with DMM; (c) BX fiber (longitudinal section).

reveal some clearly distinct coggled edges similar to those of the crosslinked fiber fragments (Fig. 4c, see for comparison also Fig. 3c). On the cross sections tangentially arranged cracks can be observed. These changes can be considered as the result of the increased brittleness of the fibers. There was found no polymerization products in the pores.

Up to now we discussed the apparent increase in the transverse dimensions of the structural elements. Under certain conditions there appears a real possibility of detecting an increase in the dimensions of the structural elements and even of some changes in their mutual arrangement. This is observed when crosslinking proceeds at low temperatures and when cellu-



lose preparations have been subjected to strong swelling. The fibers pre-swollen in alkaline solutions and modified with ECH or cyanuric chloride are examples of such a process.<sup>15,16</sup> The specific peculiarities of ECH modification will be discussed later.

Let us now consider the reagent distribution in the crosslinked samples. Examination of the cross sections of the fibers pretreated with some solvents and the investigation of how the solvent affects the fiber cross sections indicate that crosslinking proceeds rather uniformly through the whole fiber volume; its structural heterogeneity is certainly taken into consideration. This is expressed in equal cross-section etching on treatment with solvents and in homogenous reduction of the degree of swelling across the cross-sectional area of the fiber (Fig. 6a-e). A comparison is given in the microphotographs of cross sections unmodified fibers treated with solvents and those of preswollen fibers (Fig. 5a-d). It is clear that the unmodified fibers swell markedly and the cross-sections dissolve almost completely when treated with quaternary base. Homogenous etching of the cross sections in gaseous discharge also proves that the modification is uniform in character (Fig. 7a, b). It must be noted that the areas which remain undestroyed become significantly larger than those of the untreated fibers.

Localization of reagents in peripheral areas of the fiber seem to be real

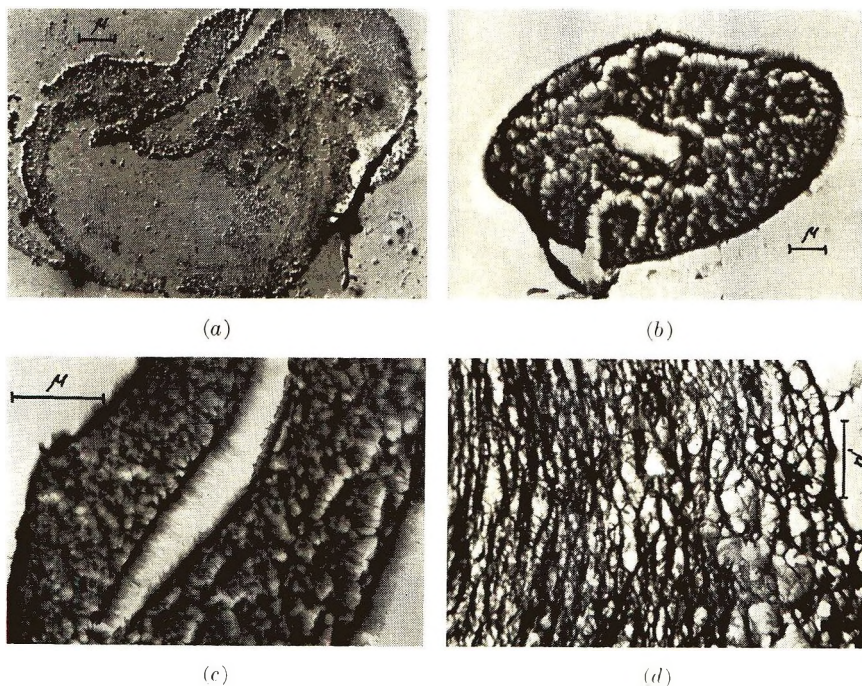


Fig. 5. Ultrathin sections of unmodified fibers, subjected to some treatment: (a) cotton, cross section treated with a quaternary ammonia base (QAB), low magnification; (b) cotton, cross section of the fiber preswollen in  $H_3PO_4$ , low magnification; (c) same as (b), high magnification; (d) cotton crosssection of the fiber preswollen in QAB.



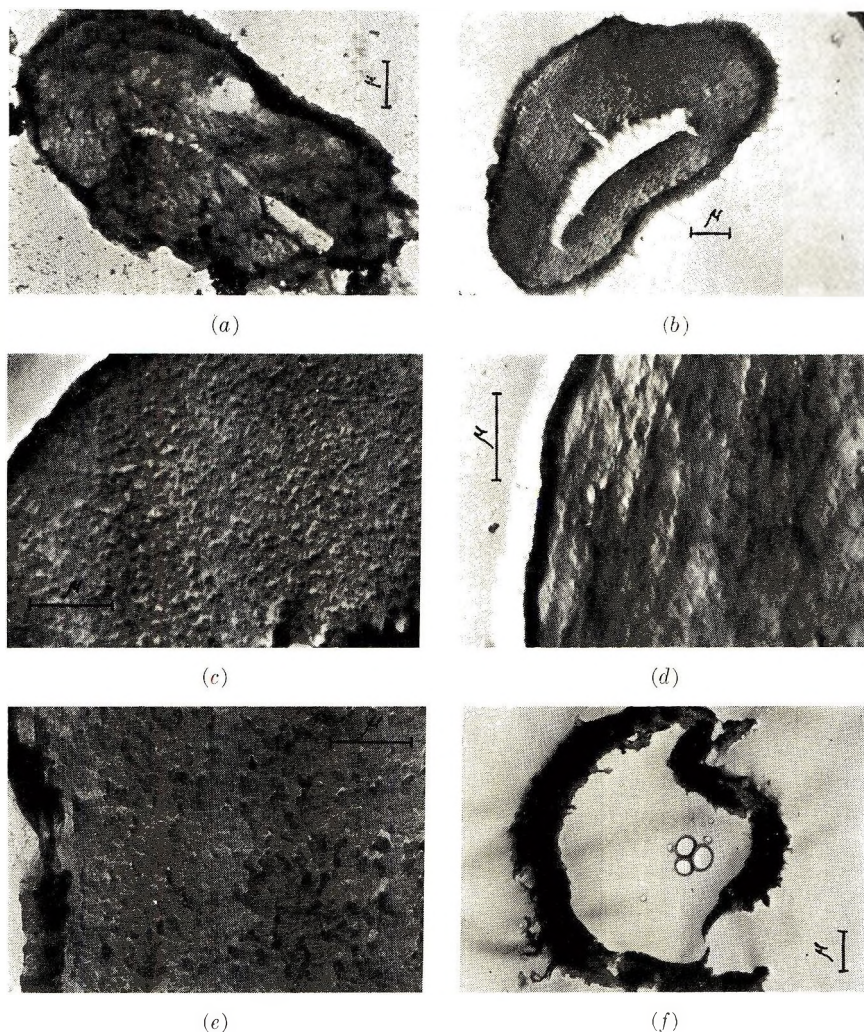


Fig. 6. Ultrathin cross-section of the modified fibers subjected to some treatment: (a) cotton modified with acrolein, cross section treated with QAB; (b) cotton modified with DMM, cross section of the fiber preswollen in  $\text{H}_3\text{PO}_4$ , low magnification; (c) same as (b), high magnification; (d) cotton modified with DMM, cross section of fiber preswollen in QAB; (e) cotton modified by DMM, cross section treated with QAB; (f) cotton modified with acrolein, cross section treated with QAB.

only at low degrees of substitution under special nonaqueous conditions; modification by acrolein in organic solvent (ethyl ether) is an example. Treatment of such a fiber with quaternary ammonia base leads to dissolution of the internal part, while there remains a narrow ring of undissolved crosslinked cellulose (Fig. 6f).

Structural changes of cellulose depend on the nature of the crosslinking reagent used and on the conditions under which crosslinking proceeds. Reagents possessing symmetric molecules and equal functional groups

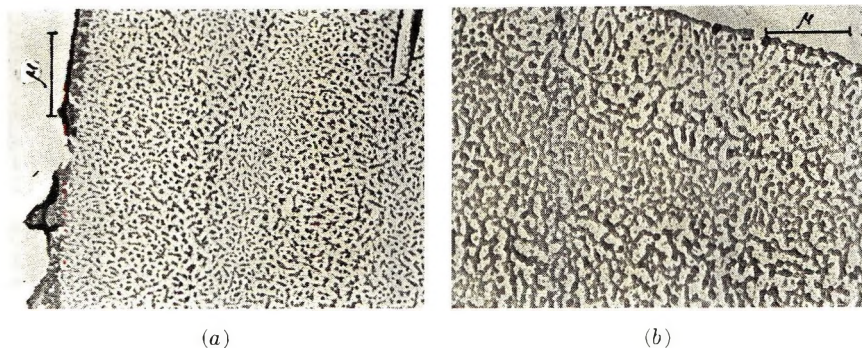


Fig. 7. Ultrathin cross section of viscose rayons subjected to gaseous discharge etching: (a) unmodified; (b) DMM-modified sample.

which under certain conditions do not form large amounts of polymerization products appear to be most effective in changing cellulose structure and properties. Formaldehyde, in the form of monohydrate  $\text{CH}_2(\text{OH})_2$ , is one of them. The above-mentioned structural changes are observed with formaldehyde crosslinking when weight gains are below 1%. On the other hand, acrolein, which has different functional groups and easily forms homopolymers appears to be less effective. A weight gain of 10% or more is necessary for significant changes in the structure and properties of the acrolein-modified-fibers.

As was already stated, ECH and cyanuric chloride modification performed on strongly swollen fibers reveals some specific features. Investigations of the cross sections subjected to treatment with solvents show that the process uniformly covers the whole of the fiber cross sections (Fig. 8a). However, the increase in the thickness of the fragments can be compared to that of the unmodified fibers. Fragments which were isolated by disintegration of native as well as of viscose fibers are rather thin (Fig. 8b), though broad and defined by certain coggled uneven edges (Fig. 8c, d). It follows that generally crosslinking proceeds in the direction perpendicular to the long axis of the structural elements, while in the radial direction those are separated by a considerable space, ascribed to strong swelling.

Infrared spectroscopy data and the results of chemical analysis prove that the fact of intramolecular addition of ECH occurring bifunctionally cannot be excluded.<sup>15</sup>

When there is intensive modification within microfibrils, their width multiplies many times (up to 400–500 Å); in addition, periodicity with intervals of about 650 Å can be observed in cyanuric chloride-modified cellulose preparations (Fig. 8e).

The results of investigations of epoxide-treated fibers appeared to be quite unexpected: in the disintegrated products there are found numerous particles of noncellulosic origin; also the fragments differ hardly at all from those of the untreated cellulose (Fig. 9a). Cross sections show a dense and wide polymer layer clearly visible surrounding the fiber (Fig. 9b). It



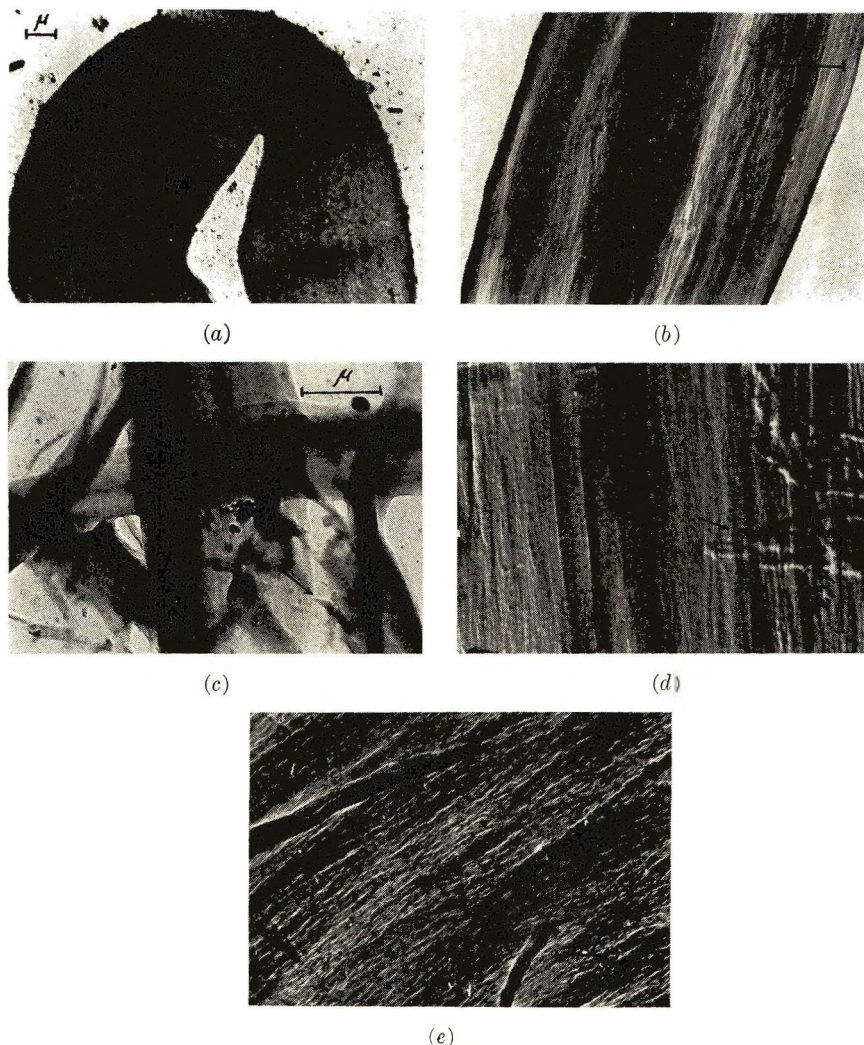


Fig. 8. Structure of fibers subjected to crosslinking in the swollen state: (a) cotton treated with ECH, cross section treated with QAB; (b) cotton treated with ECH, fragmentation pattern; (c) polycot treated with ECH, fragmentation pattern; (d) cotton treated with ECH, fragmentation pattern at high magnification.

is probable, that the resin does not penetrate the fiber due to its high molecular weight, though, on its surface a homopolymer layer is formed.

Modification by DMM, DMEM, and  $\text{CH}_2\text{O}$  virtually does not affect the cellulose fiber surface (Fig. 11a). The surface structure elements of ECH-modified samples look smooth, which appears to be the result of marked swelling (Fig. 11b).

The surface of epoxide-treated fibers seems to be damaged. This is caused by peeling off of the polymer layer, revealing strong adhesion to the fiber in the course of replication (Fig. 11c). The changes in structural

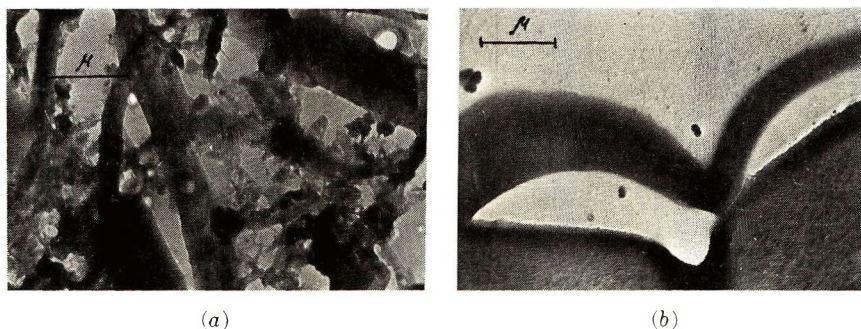


Fig. 9. Epoxide-treated fibers: (a) tire cord, fragmentation pattern; (b) tire cord cross section.

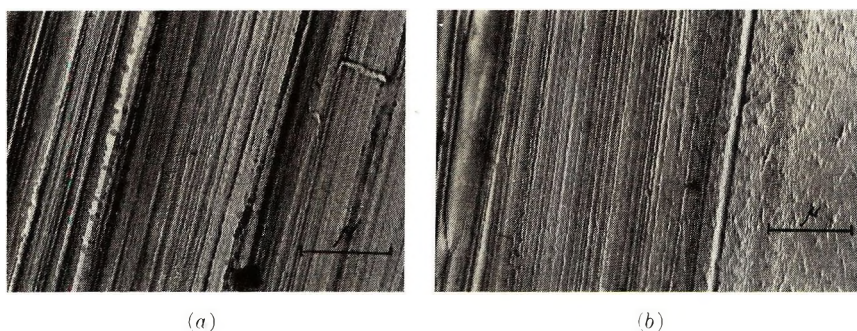


Fig. 10. Surface of unmodified fibers: (a) BX fiber; (b) tire cord.

elements in the fiber surface become most evident when the modified fiber preparations are compared to the untreated fibers (Fig. 10a).

The possibility of crosslink formation in the most densely packed regions of cellulose, i.e., crystallites, presents a very important problem. Investigations of crystallites isolated by hydrolysis from the crosslinked cellulose fibers show that their average length appears to be a bit smaller than that of the untreated fibers, differing only by some 150–300 Å in the case of native cellulose preparations (Figs. 11a and b, and 12c). The most obvious changes in crystallites are found in cellulose preparations modified with ECH or treated with cyanuric chloride. The length of the crystallites is reduced two- to threefold in the case of native cellulose and five- to six-fold in viscose fiber preparations (Fig. 12d, e). This proves that the modifying reagents possibly penetrate into the crystallites. As a result, the dimensions of the viscose fiber crystallites are reduced so much, that the very term "crystallites" loses its meaning.

Experiments involving treatment of crystallites isolated from native cellulose with  $\text{CH}_2\text{O}$ , followed by estimation of their swelling capacity prove the objectiveness of the possibility of modification.<sup>16</sup>

The degree of crystallinity of crosslinked cellulose fibers was estimated by x-ray diffraction methods according to Segal et al.<sup>17</sup> It was found that in



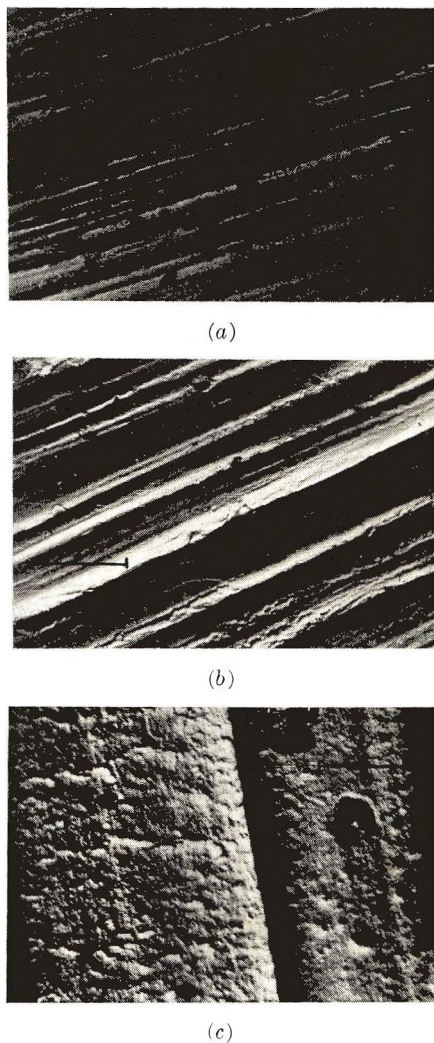


Fig. 11. Surface of modified fibers: (a) BX fiber modified with DMM; (b) BX fiber modified with ECH; (c) tire cord treated with epoxide resin.

all cases the degree of crystallinity (DC) is decreased after crosslinking. This is especially evident for samples with high weight gains (Table I). The DC of ECH-modified samples was the least, which agrees with an abrupt decrease in their crystallite dimensions.

The x-ray patterns of crosslinked preparations and mechanical mixtures of cellulose with the corresponding homopolymers were investigated in order to estimate the ratio of the intensities of crystalline and amorphous scattering at  $2\theta = 22.4$  and  $18^\circ$ , and their effect on the evaluated DC.<sup>18</sup> It is found that in some cases the decrease in DC is mainly connected with the reduction of the intensity of the (002) reflection ( $2\theta = 22.4^\circ$ ), while in other

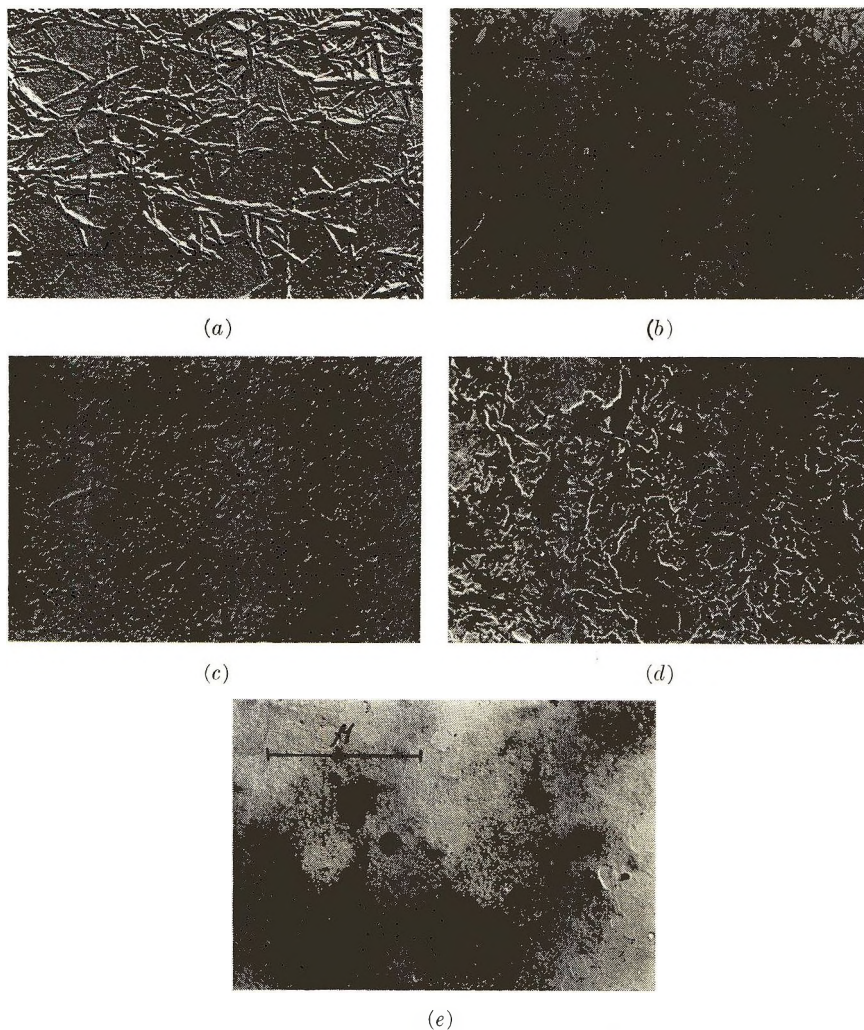


Fig. 12. Fiber crystallites: (a) cotton, untreated; (b) BX fiber, untreated; (c) cotton modified with acrolein; (d) cotton modified with cyanuric chloride; (e) BX fiber modified with ECH.

cases it is caused by the increase in amorphous scattering at  $2\theta = 18^\circ$ . The former is characteristic of the ECH-modified derivatives, while on the other hand amorphous scattering greatly increases in the epoxide-treated samples.

Electron microscopic investigations show that diepoxide generally precipitates on the surface of the fibers. Thus, the x-ray diffraction method makes it possible to differentiate between a real DC decrease, caused by the cellulose structure modification, and an apparent decrease attributable to screening of the scattering centers by polymerization products. Moreover, x-ray data confirm the results of electron microscopic

TABLE I  
DC of the Modified Fibers

Cellulose sample	DC, %			
	Unmodified	CH <sub>2</sub> O-treated	DMM-treated	ECH-treated
Cotton	78.5	63.0	75.0	52.0
Polynosic fiber A	53.0	50.0	49.0	32.5
Polynosic fiber B	62.0	61.0	61.0	38.0
Tire cord A	44.0	—	43.0	—
Tire cord B	60.0	39.0	42.0	—
Viscose rayon	41.0	—	—	28.5

TABLE II  
Density of the Modified Fibers

Cellulose sample	Density, g/cc			
	Unmodified	CH <sub>2</sub> O-treated	DMM-treated	ECH-treated
Cotton	1.5420	1.5380	1.5440	1.4195
Polynosic fiber A	1.5120	1.5100	1.5230	1.4885
Polynosic fiber B	1.5039	1.4995	1.5090	1.4620
Tire cord A	1.5175	1.5110	1.5240	1.4715
Tire cord B	1.5015	1.4955	1.5130	1.4655

investigations indicating the possibility of cellulose crystallite modification.

Changes in the density of fibers on modification with CH<sub>2</sub>O and DMM are negligible (Table II). There is a certain rise in the density of the DMM-treated samples ascribed to homopolymer formation in the fiber, while there is an abrupt decrease in density after ECH modification. This is a sign of a considerable loosening of the fiber structure.

Changes in the properties of the modified fibers caused by their structural transformations can be clearly seen on relaxation and elongation curves in alkaline solutions at constant loads (Fig. 13). The untreated fibers are characterized by curves with an evident elongation. In all cases the elongation drops sharply after crosslinking. Even viscose rayon, which prior to the modification elongates rapidly, almost completely loses its ability to elongate after crosslinking. The changes in the properties evidently result from the immobility of structural elements after the crosslinking. It is interesting, that ECH-modified fibers retain considerable elongation, which, though, is less than that of the untreated samples. The comparison of the structural changes caused when cellulose is treated with bifunctional reagents and their monofunctional analogs is also of interest. If in the first case the structural changes are most evident, it is difficult to detect any in the modified samples structure after cellulose has reacted with MMM, MMTM, or propylene oxide. The samples swell and dissolve almost completely in the usual solvents for cellulose and after dis-



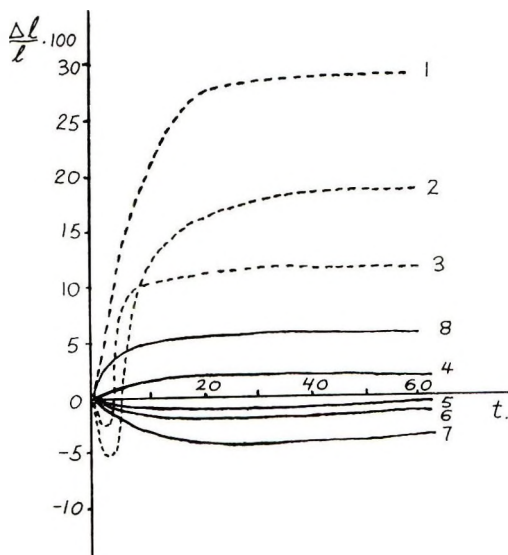


Fig. 13. Changes in length of fibers (2% alkali): (1) viscose rayon; (2) tire cord A; (3) tire cord B; (4) viscose rayon modified with  $\text{CH}_2\text{O}$ ; (5) tire cord A modified with  $\text{CH}_2\text{O}$ ; (6) tire cord A, modified with DMM; (7) tire cord B modified with DMM; (8) tire cord B treated with ECH.

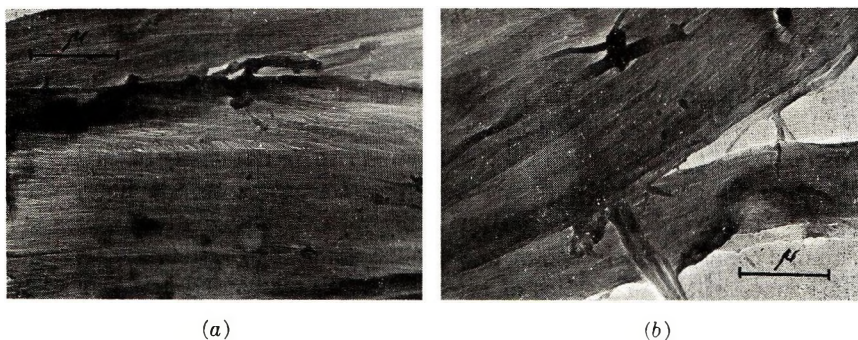


Fig. 14. Fragmentation patterns of fibers (a) modified with monofunctional reagent and (b) containing the network polymer: (a) cotton modified with MMTM; (b) cotton containing hexamethylenediamine-glycerine.

integration show fragmentation similar to that of the untreated fibers (Fig. 14a). Preparations containing linear and network polymers to a great extent more closely resemble the untreated samples rather than the crosslinked fibers (Fig. 14b).

Thus, the structural changes produced as a result of treatment of cellulose with bifunctional reagents are caused mainly by the formation of crosslinks and not by accumulation of polymerization products or by monofunctional substitution.

## References

1. G. V. Nikonovich, S. A. Leontyeva, and Kh. U. Usmanov, *Khim. Volokna*, **No. 6**, 55 (1963).
2. G. V. Nikonovich, S. A. Leontyeva, and Kh. U. Usmanov, in *Macromolecular Chemistry, Prague 1965* (*J. Polym. Sci. C*, **16**), O. Wichterle and B. Sedláček, Eds., Interscience, New York, 1967, p. 877.
3. G. V. Nikonovich, S. A. Leontyeva, and Kh. U. Usmanov, *Vysokomol. Soedin.*, **10**, 2682 (1968).
4. M. L. Rollins, A. T. Moore, W. R. Goynes, J. H. Carra, and I. V. DeGruy, *Am. Dyestuff Rpt.*, **54**, 35 (1965).
5. M. L. Rollins, A. T. Moore, and V. W. Tripp, *Text. Res. J.*, **33**, 117 (1963).
6. J. B. McKelvey, R. R. Benerito, R. J. Berni, and B. G. Burgis, *J. Appl. Polym. Sci.*, **7**, 1372 (1963).
7. H. Dohuetsch and D. Brederick, *Melliand Textilber.*, **48**, 561 (1967).
8. R. Steele, *Text. Res. J.*, **25**, 545 (1955).
9. P. C. Mehta and R. D. Mehta, *Text. Res. J.*, **32**, 77 (1962).
10. H. Tovey, *Text. Res. J.*, **31**, 185 (1961).
11. J. T. Marsh, *Text. Mfr.*, **93**, 25 (1967).
12. A. Smith, *J. Soc. Dyers Colourists*, **77**, 416 (1961).
13. G. V. Nikonovich, N. D. Burkhanova, S. A. Leontyeva, and Kh. U. Usmanov, *Cellulose Chem. Technol.*, **2**, 231 (1968).
14. G. V. Nikonovich, S. A. Leontyeva, and Kh. U. Usmanov, *Khim. Volokna*, **No. 3**, 40 (1965).
15. G. V. Nikonovich, S. A. Leontyeva, V. P. Shatkina, Kh. U. Usmanov, A. A. Adylov, and Yu. Tashpulatov, *Vysokomol. Soedin.*, **7**, 2132 (1965).
16. G. V. Nikonovich, S. A. Leontyeva, and Kh. U. Usmanov, *Struktura i Modifikatsiya Khlopkovoy Tsellosy*, Vol. 3, Izdatelstvo FAN, Tashkent, U.S.S.R., 1967.
17. L. Segal, J. J. Creely, A. E. Martin, and C. M. Conrad, *Text. Res. J.*, **29**, 781 (1959).
18. G. V. Nikonovich, T. Saidaliyev, Yu. T. Tashpulatov, and Kh. U. Usmanov, *Vysokomol. Soedin.*, **10**, 960 (1968).

Received June 22, 1970

Revised March 19, 1971



## Transparent Ultraviolet-Barrier Coatings

S. M. COHEN, R. H. YOUNG\*, and A. H. MARKHART,  
*Monsanto Company, Research Department, Plastic Products & Resins  
Division, Springfield, Massachusetts 01101*

### Synopsis

A number of phenyl polyesters have been synthesized to furnish molecules whose backbones rearrange under ultraviolet irradiation to an *o*-hydroxybenzophenone structure. This photochemical Fries rearrangement produces ultraviolet opacity in the irradiated film while maintaining visual transparency. Thin coatings of these polyesters completely protect substrates ordinarily sensitive to ultraviolet light. Spectroscopic analysis of various rearranged films and coatings clearly shows that the *o*-hydroxybenzophenone polymer formed is concentrated at the irradiated surface of the original polyester coating as a "skin". Such a skin, formed *in situ* during the irradiation, functions to protect both the original polyester coating as well as the coated substrate from degradation by ultraviolet irradiation. Furthermore, a significant "healing" mechanism appears inherent in these coatings, for as the exposed skin ultimately degrades under extended ultraviolet irradiation, more of the underlying polyester layer apparently rearranges to compensate for the loss. Thus the clear coating functions both as a protective skin and a rearrangeable reservoir. Modified structures of the polyesters have been prepared which possess, in addition to their protective film properties, a useful solubility spectrum and a good solution shelf life.

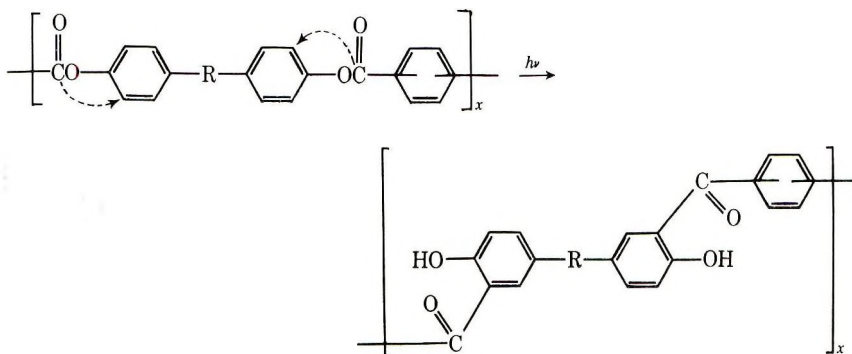
### INTRODUCTION

At present, the major method of obtaining clear exterior coatings which are relatively stable to ultraviolet radiation and which simultaneously protect substrates against ultraviolet degradation consists in incorporating certain monomeric ultraviolet screening compounds into clear polymer films.<sup>1-3</sup> These additives usually absorb strongly in the ultraviolet region but negligibly in the visible region, producing the desired ultraviolet opacity in otherwise transparent coatings. However, the use of monomeric additives has some critical limitations: a low level of protection for extremely thin polymer films; possible nonuniform distribution in the polymer; potential migration; excessive extractability; and occasional volatility.<sup>4</sup>

One possible means of improving many of these flaws is by using polymeric ultraviolet screeners. To this end, some new polymer systems containing chemically combined ultraviolet screeners of the *o*-hydroxyaroyl ketone and ester types have been reported recently.<sup>5-7</sup>

\* Present address: Freeport Kaolin Company, Gordon, Ga. 31031.

Another approach to such coatings has become accessible recently via the photochemical Fries rearrangement of aromatic polyesters to polymeric *o*-hydroxybenzophenones:



Essentially this technique permits formation of the ultraviolet screening polymer *as needed* during exterior exposure to sunlight. Significant clarification of the reaction limits and mechanism has been achieved by studies of the monomeric rearrangement.<sup>8-12</sup> In addition, some work has been done with polymeric systems.<sup>8,13-15</sup> The objective of the present work was to incorporate both ultraviolet stability and ultraviolet-barrier behavior via the photochemical Fries rearrangement into clear coatings which possessed otherwise excellent protective properties.

## EXPERIMENTAL

### Monomers

Most of the dihydric phenol monomers used were obtained from Distillation Products Industries or Aldrich Chemical Co. An exception, however, was Nopco 1750A, which was furnished by Nopco Chemical Co. Although the majority of phenolic monomers could be used without further purification, technical grade 4,4'-sulfonyldiphenol, obtained as a brown powder (mp 135–200°C), required treatment with activated charcoal and recrystallization from boiling water. Even so, the resulting solid (mp 157–215°C.) was believed to be a mixture of the 2,4'- and 4,4'-isomers.

4,4-Bis(4'-hydroxyphenyl) pentanoic acid (Diphenolic Acid, S. C. Johnson and Son, Inc.) and its esters, i.e., the methyl (mp 132–134°C), ethyl (mp 125–128°C), butyl (mp 102–103°C) and lauryl (mp 53–56°C) were obtained from S. C. Johnson and Son, Inc. Although the acid (mp 170–173°C) was received pure, the esters yielded workable polymers only if their solutions were extracted with aqueous saturated sodium bicarbonate to remove residual acid and the residues then recrystallized.

Both the butyl Cellosolve ester (Union Carbide Corp.) and the piperidide of Diphenolic Acid were synthesized by standard procedures. The former was a tan, extremely viscous liquid which could not be crystallized or distilled and so was used in this form after extractive purification. In contrast, the piperidide was a tan solid (mp 205–208°C).

Isophthaloyl and terephthaloyl chlorides were obtained from Hooker Chemical Company; the *o*-phthaloyl chloride (reagent grade material), from Fisher Chemical Company; and the aliphatic diacid chlorides, from Distillation Products Industries. All were used without further purification.

### Polyester Preparations

For the preparation of these polyesters, both interfacial and solution polymerization techniques were used.

Most of the polymers were prepared by the general interfacial polycondensation process described in the literature.<sup>16</sup> However, depending on the particular monomers, various modifications were required. Thus, when resorcinol or similar dihydric phenols were used as monomers, oxidation had to be minimized by bubbling nitrogen in the stirred emulsion both prior to and during polymerization. Also, when Diphenolic Acid was present as a monomer, only two equivalents of sodium hydroxide out of a theoretical maximum of three were used. Further, to prevent hydrolysis of the ethyl ester side chains of that Diphenolic Acid ester during polymerizations, anisole was substituted in the organic phase in place of the ordinarily used chloroform or methylene chloride solvent. Finally, the polymerizations were run at 0–5°C; and an antifoam agent was added periodically during polymerization.

Solution polymerizations also were performed by modification of the procedure described in the literature.<sup>16</sup> In such reactions, the phenol and acid chloride monomers first were dissolved in anhydrous tetrahydrofuran, and polymerization was initiated by dropwise addition of a stoichiometric amount of triethylamine. The reaction then was maintained for 3 hr at 15°C, and the final polymer was precipitated in excess water.

### Coating Technique

Polymer solutions were coated onto the various substrates with a draw-down blade and allowed to dry at room temperature. As soon as the solvent evaporated, the coatings could be exposed to radiation since no cure was involved.

### Accelerated Ultraviolet Irradiation

For accelerated irradiation studies, two ultraviolet intensity levels were used. A lower level was produced with a Hanovia 100-W high-pressure quartz mercury-vapor lamp (model 608A) placed 25 cm above the irradiated film samples. The approximate intensity of radiation between 200 and 400 m $\mu$  reaching the films was  $7.1 \times 10^2 \mu\text{W}/\text{cm}^2$ . For a higher intensity level, a 450-W Hanovia ultraviolet lamp (model 679-A) was used, also at a height of 25 cm above the film samples. In this case, the approximate intensity of radiation between 200 and 400 m $\mu$  reaching the films was  $1.3 \times 10^4 \mu\text{W}/\text{cm}^2$ . Both values were obtained by extrapolating from the manufacturer's data at a distance of 50 cm by using the relationship of the inverse square of the distance.

All accelerated studies were carried out in a hood sealed against the escape of any stray ultraviolet radiation and in which a slight air current was drawn continuously over the film samples to remove those ozone traces formed by simultaneous irradiation of atmospheric oxygen.

### Spectra

Infrared spectra were obtained by film transmission with a Beckman IR-5A spectrophotometer; and film surface spectra, by attenuated total reflectance by use of Model 9 Wilks Scientific attachment with a  $45^\circ$  angle of entrance and with air as the reference standard. Film ultraviolet curves were obtained on a Beckman DK-2 spectrophotometer, also with air as the reference standard.

### Viscosity

Inherent viscosities were measured at  $30^\circ\text{C}$  on  $\sim 0.5\%$  polymer solutions (0.1250 g polymer in 25 ml of an analytical grade solvent prepared from 70 ml phenol and 30 ml of 1,1,2,2-tetrachloroethane).

### Film Weathering

Preliminary coated samples were exposed in a Weather-O-Meter. Subsequently, exterior exposures were carried out in Massachusetts, Arizona, and Florida.

## RESULTS AND DISCUSSION

### Polyester Structure and Solubility Properties

Most of the polyesters prepared in this work were based on monomers which were structural modifications of the phenols I and II and acid chlorides III and IV.

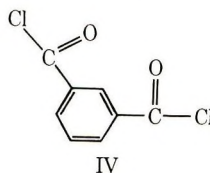
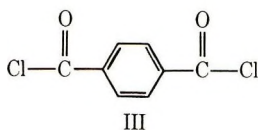
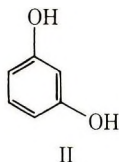
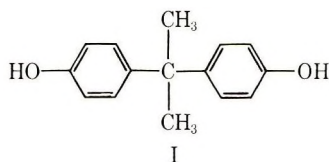
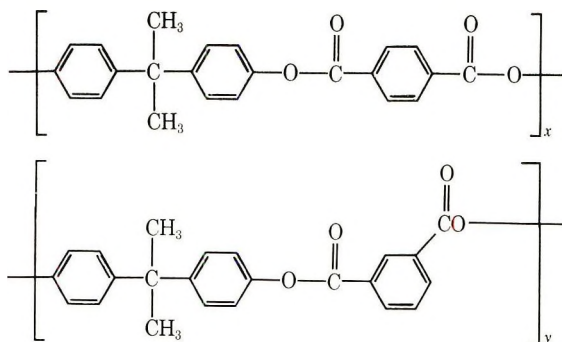


Table I lists the specific phenol and acid monomer structures.

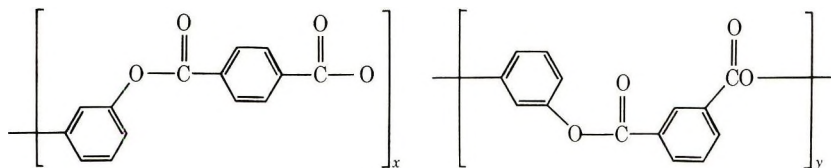
With these monomers, the polyesters of Tables IIA-IID were prepared for evaluation as exterior ultraviolet-barrier coatings.



Of the polyesters prepared (Table II), two that showed promising ultraviolet-barrier properties early were polymers 5 and 17.



Polyester 5 ( $x:y = 1:1$ )



Polyester 17 ( $x:y = 1:1$ )

However, both of them also possess grave solubility deficiencies when considered as potential surface coatings. They dissolve in only a relatively small number of solvents, usually of higher price and frequently somewhat toxic. Also they dissolve only at unacceptably low concentrations; and the resulting solutions gel rapidly—sometimes within minutes after complete solution. Because critical requirements for any polymer which is to perform as a commercially acceptable coating are both solubility in relatively nontoxic solvents and formation of stable solutions which can be applied easily, these polymers in their present form were unacceptable coating candidates despite their promising ultraviolet protective behavior. Practical utility required that their structures be modified to overcome these solubility limitations.

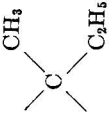


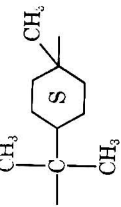
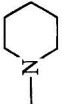
Since the critical ultraviolet-barrier properties are derived from rearranged aromatic polyester backbone, any structural changes introduced to improve the solubility behavior of the polymers had to be chosen so as to avoid interfering with the desired subsequent photochemical rearrangement. A large factor influencing the polyester solubility problem was believed to be crystallinity. If so, one possible way to improve the solubility performance was to produce increased structural irregularity, either by introducing long or bulky substituents or by copolymerizing with appropriate comonomers.

On Bisphenol-A in polymer 5 (Table II), substitutions were made at the central carbon atom. Thus, longer side chains (Table II; polymers



TABLE I  
Monomer Structures Used in Polyester Preparations

Structure	No.	Substituents			Name
		R <sub>1</sub>	R <sub>2</sub>	R <sub>3</sub>	
	A1	H	H	None	4,4'-Dihydroxybiphenyl
	A2	H	H		4,4'-Isopropylidenediphenol (Bisphenol-A)
	A3	H	H		2,2-Bis(4'-hydroxyphenyl)butane
	A4	H	H		2,2-Bis(4'-hydroxyphenyl)-3-methylbutane
	A5	H	H		4,4'-Sulfonyldiphenol
	A6	H	H		4,4'-Dihydroxybenzophenone
	A7	H	H		Phenolphthalein

A8	H	CH <sub>3</sub>		2,2-Bis(3'-methyl-4'-hydroxy-phenyl)butane
				2,2-Bis(3',5'-dimethyl-4'-hydroxy-phenyl)propane
				2,2-Bis(3',5'-dichloro-4'-hydroxy-phenyl)propane
				Dipentene Bisphenol
A9	CH <sub>3</sub>	CH <sub>3</sub>		
A10	Cl	Cl		
A11	H	H		
B1	H			4,4-Bis(4'-hydroxyphenyl)pentanoic acid (Diphenolic Acid)
B2	CH <sub>3</sub>	CH <sub>3</sub>		Diphenolic Acid, methyl ester
B3	C <sub>2</sub> H <sub>5</sub>			Diphenolic Acid, ethyl ester
B4	C <sub>4</sub> H <sub>9</sub>			Diphenolic Acid, butyl ester
B5	—CH <sub>2</sub> CH <sub>2</sub> —O—C <sub>4</sub> H <sub>9</sub>			Diphenolic Aid, butyl Cellosolve ester
B6	C <sub>12</sub> H <sub>25</sub>			Diphenolic Acid, lauryl ester
B7				Diphenolic Acid, piperidine

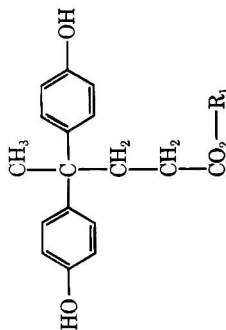
*continued*

TABLE I (continued)  
Substituents

Structure	No.	R <sub>1</sub>	R <sub>2</sub>	R <sub>3</sub>	Name
	C1	H	H	H	Resorcinol
	C2	CH <sub>3</sub>	H	H	2-Methylresorcinol
	C3	H	H	CH <sub>3</sub>	5-Methylresorcinol
	C4	H	H	H	4-Benzylresorcinol
	C5	H	H	H	2,4-Dihydroxyacetophenone
	D1	—	—	—	2-Methylhydroquinone
	E1	—	—	—	Nopeo 1750A
	F1	—	—	—	o-Phthaloyl chloride
					Isophthaloyl chloride
					Terephthaloyl chloride
	G1	—	—	—	Fumaryl chloride
	H1	—	—	—	Sebacyl chloride

TABLE IIA  
Polyesters Containing 4,4'-Isopropylidenediphenol (Bisphenol-A)

Run	Phenolic monomer, mole-% <sup>a</sup>				4,4'- Sul- fonyl- di- phenol	Acid chloride monomer, mole-% <sup>c</sup>				Method of pre- para- tion <sup>b</sup>	Polyester		Polyester appearance <sup>d</sup>  Film    Resin
	Bis- phenol- A	DPA ethyl ester	DPA butyl ester	DPA Cello- solve ester		Iso- phthal- oyl chloride	Tereph- thal- oyl chloride	Phthal- oyl chloride	Fu- maryl chloride		Yield, ent vis- cosity <sup>e</sup> %	Inher-	
1	100				100				I	100	1.49	F	C
2	100					100			I	96	1.91	F	C
3	100						100		I	28	0.17	B	C
4	100								I	91	0.27	B	Sl.Y
5	100				50	50			I	96	0.71	F	C
6	100				33	33	34		I	87	0.61	F	C
7	100					50	50		I	69	0.28	B	C
8	85	15			50	50			I	90	1.63	—	C
9	50	50			50	50			I	80	0.21	—	C
10	75		25		50	50			I	84	1.15	F	Sl.T
11	75			25	50	50			I	87	0.59	F	C
12	75		25		50	50			I	42	0.69	F	C
13	50			50	50	50			I	74	0.64	F	Sl.Y
14	85			50	50	50			I	73	1.09	F	C
15	20				50	50			I	74	0.30	F	Sl.T

<sup>a</sup> DPA denotes 4,4-bis(4'-hydroxyphenyl)pentanoic acid (Diphenolic Acid, S. C. Johnson).

<sup>b</sup> Polyesters prepared either by an interfacial technique (I) or a low-temperature solution technique (S).

<sup>c</sup> Measured in 70/30 (v/v) phenol-tetrachloroethane at 0.5 wt-% concentration at 30°C.

<sup>d</sup> C = colorless; Y = yellow; T = tan; Sl. = slightly; S = soft; F = flexible; B = brittle.

TABLE IIB  
Polyesters Containing Resorcinol or Its Derivatives

Run	Phenolic monomer, mole-% <sup>a</sup>										Acid chloride monomer, mole-%		Method of preparation <sup>b</sup>	Polyester		Polyester appearance <sup>d</sup>	
	Re- sor- cinol	DPA methyl ester	DPA butyl ester	DPA lauryl ester	Phe- nol- phtha- lein	2,4-Dihy- droxy- aceto- phenone				Iso- phthal- oyl- chlo- ride	Tereph- thal- oyl- chlo- ride	Yield, %		Inherent vis- cosity <sup>c</sup>	Film	Resin	
						2- Meth- yl- resor- cinol	4- Ben- zyl- resor- cinol	5- Meth- yl- resor- cinol	2,4- Dihy- droxy- aceto- phenone								
16	100									100		I	91	0.81	—	C	
17	100									50	50	I	97	0.91	F	C	
18	100									25	25	S	87	0.66	F	C	
19	50	50								50	50	S	92	0.45	F	C	
20	75	25								100		S	100	0.36	F	C	
21	75		25							50	50	S	98	0.86	F	C	
22	75		25							50	50	I	100	0.96	F	C	
23	17	83								50	50	S	79	0.21	F	C	
24	75									50	50	S	85	0.48	F	C	
25	50			50						100		S	93	0.28	F	C	
26	75			25						50	50	S	100	0.64	F	C	
27	50			50						50	50	I	96	0.47	F	C	
28	75			25						50	50	I	88	0.70	F	C	
29			100							50	50	I	97	0.57	F	Sl.Y	
30	75									50	50	S	94	0.52	F	C	
31									25	50	50	I	91	0.47	F	Sl.Y	
32								100		50	50	I	61	0.18	B	C	
33	50									50	50	S	76	0.11	B	Sl.Y	

<sup>a</sup> DPA denotes 4,4-bis(4'-hydroxyphenyl) pentanoic acid (Diphenolic Acid, S. C. Johnson). Nopco 1750 A is a technical grade of 2,2'-methylenebis(4'-octylphenol) from Nopco Chemical Co.

<sup>b</sup> Polyesters prepared either by an interfacial technique (I) or a low-temperature solution technique (S).

<sup>c</sup> Measured in 70/30 (v/v) phenol-tetrachloroethane at 0.5 wt-% concentration at 30°C.

<sup>d</sup> C = colorless; Y = yellow; T = tan; Sl. = slightly; S = soft; F = flexible; B = brittle.



TABLE IIC  
Homopolymers of DPA Derivatives and Related Copolymers Not Listed in Tables IIA or IIB

Run	Phenolic monomer, mole-% <sup>a</sup>				DPA butyl ester	DPA lauryl ester	DPA butyl ester	DPA ethyl ester	DPA methyl ester	2,2-Bis-(4'-hydroxyphenyl)-butane	Acid chloride monomer, mole-%			Method of preparation <sup>b</sup>	Polyester		Polyester appearance <sup>d</sup>	
	DPA butyl ester	DPA lauryl ester	DPA butyl ester	DPA ethyl ester							DPA methyl ester	2,2-Bis-(4'-hydroxyphenyl)-butane	Terephthaloyl chloride		Iso-phthaloyl chloride	Sebacoyl chloride		
34	100										50	50		S	92	0.45	F	C
35	100										30	30	40	S	82	0.35	F	C
36	100										25	25	50	S	88	0.31	F,S	C
37	100										20	20	60	S	79	0.30	F,S	Sl,Y
38		100									50	50		I	92	0.77	F	C
39			100								50	50		I	87	1.10	F	C
40			25			75					50	50		I	94	0.83	F	C
41				100							50	50		I	90	1.11	F,S	Y
42				25		75					50	50		I	94	0.82	C	C
43					100						50	50		I	87	0.68	F	T
44											50	50		I	72	0.56	F	Sl,T

<sup>a</sup> DPA denotes 4,4-bis(4'-hydroxyphenyl)pentanoic acid (Diphenolic Acid, S. C. Johnson).

<sup>b</sup> Polyesters prepared either by an interfacial technique (I) or a low-temperature solution technique (S).

<sup>c</sup> Measured in 70/30 (v/v) phenol-tetrachloroethane at 0.5 wt-% concentration at 30°C.

<sup>d</sup> C = colorless; Y = yellow; T = tan; Sl. = slightly; S = soft; F = flexible; B = brittle.



34-39, 41, 43, 54, and 55) as well as bulky groups (Table II; polymers 44, 46, 47, and 53) were introduced into the homopolymer. In a related approach, the resorcinol in polymer 17 (Table II) was substituted by various groups at one of the three indicated ring positions (Table I; monomers C2-C5) (Table II; polymers 29, 31, and 32). Finally, copolymers were prepared with a variety of comonomer structures (Table II; polymers 8-15, 19-29, and 33). The effect of such modifications was measured via changes in the solubility parameter range and solution stability of the new polyesters. These changes can be observed in Tables III and IV.

From Table IV, certain tentative relationships between structure and solubility are evident.

(1) Homopolymers derived from one bisphenol and one diacid show poorer solubility characteristics than corresponding copolymers (compare polymers C1 and C2 with A5, C6, and C7; and C16 with A17).

TABLE III  
Solvents Used in Determining Polyester Solubility Parameter Range

A. Low hydrogen-bonding solvents			B. Medium hydrogen-bonding solvents			C. High hydrogen-bonding solvents		
No.	Solvent	$\delta$	No.	Solvent	$\delta$	No.	Solvent	$\delta$
1	Xylene	8.8	9	Diethyl Carbitol	8.1 <sup>a</sup>	27	Methyl isobutyl carbinol	10.0
2	Toluene	8.9	10	Methyl isobutyl ketone	8.4	28	Pyridine	10.7
3	Benzene	9.2	11	Cellosolve acetate	8.7	29	Ethanol (95%)	12.7
4	Styrene	9.3	12	Ethyl acetate	9.1			
5	Chloroform	9.3	13	Tetrahydrofuran	9.1			
6	Methylene chloride	9.7	14	Methyl Cellosolve acetate	9.2			
7	Ethylene chloride	9.8	15	Diacetone alcohol	9.2			
8	2-Nitropropane	9.9	16	Methyl ethyl ketone	9.3			
			17	Butyl Carbitol	9.5			
			18	Acetone	9.9			
			19	Cyclohexanone	9.9			
			20	Dioxane	10.0			
			21	Acetophenone	10.5 <sup>a</sup>			
			22	Cellosolve	10.5			
			23	Dimethylacetamide	10.8			
			24	Methyl Cellosolve	11.4			
			25	Dimethyl sulfoxide	12.0			
			26	Dimethylformamide	12.1			

<sup>a</sup> Value calculated from group constants of Small.<sup>18</sup>

TABLE IVA  
Solubility Parameter Range and Solution Stabilities for Polyesters of (1:1) Isophthalate/Terephthalate Having 1 Phenolic Monomer

Poly- ester run no. from Table II	Phenolic monomer	Estimated solubility parameter range according to H-bonding type			Solution stability		
		Low	Medium	High	Solvent (wt-% polyester)	1 month	3 months
5	Bisphenol-A	9.2-9.7	9.1; 9.9-12.1	10.7	{Cyclohexanone(10%) {CH <sub>2</sub> Cl <sub>2</sub> (5%)	No	—
17	Resorcinol	9.3-9.8	9.9-10.8	10.7	{Dioxane(10%) {1,2-Dichloroethane(5%)	No	Yes
29	2-Methylresorcinol	9.3-9.8	9.1; 9.9- 10.8	10.7	{1,2-Dichloroethane(15%) {CH <sub>2</sub> Cl <sub>2</sub> (15%)	No	—
31	5-Methylresorcinol	9.3-9.8	9.1; 9.9- 12.1	10.7	—	No	—
34	DPA methyl ester	9.2-9.8	9.1; 9.9- 12.1	10.7	—	—	—
38	DPA ethyl ester	8.9-9.8	9.1; 9.9- 12.1	10.7	{Styrene(10%) {Styrene(20%)	Yes	Yes
39	DPA butyl ester	8.8-9.8	9.1; 9.9- 12.1	10.7	Toluene(10%)	Yes	Yes

41	DPA lauryl ester	8.8-9.8	9.1; 9.9- 12.1	10.7	Xylene (10%)	Yes	Yes
43	DPA butyl Cellosolve ester	8.8-9.3	8.7-9.1; 9.9-12.1	10.7	{ Cellosolve Ac.(20%) Styrene(20%)	Yes Yes	Yes Yes
44	DPA piperidine	0	10.8-12.1	0	—	—	—
45	2-Methylhydroquinone	0	10.8	0	—	—	—
46	Phenolphthalein	9.3-9.7	9.9-12.1	10.7	CHCl <sub>3</sub> (10%)	Yes	Yes
50	4,4'-Sulfonyldiphenol	0	10.8	0	—	—	—
51	4,4'-Dihydroxybiphenyl	0	0	0	—	—	—
52	4,4'-Dihydroxybenzophenone	0	0	0	—	—	—
53	Dipentene Bisphenol	8.8-9.8	8.7-12.1	10.7	Toluene(10%)	Yes	Yes
54	2,2-Bis(4'-hydroxyphenyl) butane	9.2-9.8	9.1; 9.9- 12.1	10.7	Toluene(10%)	No	—
55	2,2-Bis(4'-hydroxyphenyl)-3-methyl- butane	8.8-9.8	9.1-12.1	10.7	Toluene(10%)	Yes	Yes
56	2,2-Bis(3'-methyl-4'-hydroxyphenyl) butane	9.3-9.8	9.1; 9.9- 12.1	10.7	—	—	—
57	2,2-Bis(3',5'-dimethyl-4'-hydroxyphenyl) propane	8.9-9.8	9.1; 9.9- 12.1	10.7	—	—	—
58	2,2-Bis(3',5'-dichloro-4'-hydroxyphenyl) propane	9.2-9.8	9.1; 9.9- 12.1	10.7	—	—	—



TABLE IVB  
Solubility Parameter Range and Solution Stabilities for Polyesters of (1:1) Isophthalate/Terephthalate Having 2 Phenolic Monomers

Polyester run no. from Table II	Phenolic monomer I (mole-%)	Phenolic monomer II (mole-%)	Estimated solubility parameter range according to H-bonding type			Solution stability		
			Low	Medium	High	Solvent (wt-% polyester)	1 month	3 months
8	Bisphenol-A(85)	DPA(15)	0	9.9-12.1	0	—	—	—
9	Bisphenol-A(50)	DPA(50)	0	0	0	—	—	—
10	Bisphenol-A(75)	DPA ethyl ester(25)	9.2-9.8	9.1; 9.9-12.1	10.7	{Cyclohexanone(10%) Styrene(10%) CH <sub>2</sub> Cl <sub>2</sub> (10%) CH <sub>3</sub> Cl <sub>2</sub> (10%)	Yes No Yes Yes	No — Yes Yes
11	Bisphenol-A(75)	DPA butyl ester(25)	9.2-9.8	9.1; 9.9-12.1	10.7	—	—	—
12	Bisphenol-A(75)	DPA lauryl ester(25)	9.2-9.8	9.1; 9.9-12.1	10.7	—	—	—
13	Bisphenol-A(50)	DPA butyl Cellosolve ester(50)	9.3-9.8	9.1; 9.9-12.1	10.7	—	—	—
14	Bisphenol-A(85)	DPA piperidine(15)	9.3-9.8	9.1; 9.9-12.1	0	—	—	—
19	Resorcinol(50)	DPA methyl ester(50)	9.3-9.8	9.1; 9.9-12.1	10.7	CH <sub>2</sub> Cl <sub>2</sub> (10%)	Yes	Yes
21	Resorcinol(75)	DPA butyl ester(25)	9.3-9.8	9.1; 9.9-12.1	10.7	{CH <sub>2</sub> Cl <sub>2</sub> (15%) 1,2-Dichloroethane(15%)	Yes Yes	Yes Yes
24	Resorcinol(75)	DPA lauryl ester(25)	9.3-9.8	9.1; 9.9-12.1	10.7	—	—	—
26	Resorcinol(75)	Phenolphthalein(25)	9.3-9.8	9.1; 9.9-12.1	10.7	—	—	—
27	Resorcinol(50)	2-Methylresorcinol(50)	9.3-9.8	9.1; 9.9-10.8	0	—	—	—
28	Resorcinol(75)	2-Methylresorcinol(25)	9.3-9.8	9.1; 9.9-10.8	0	{CH <sub>2</sub> Cl <sub>2</sub> (15%) 1,2-Dichloroethane(15%)	Yes No	Yes —
30	Resorcinol(75)	4-Benzyl resorcinol(25)	9.3-9.8	9.9-10.8	10.7	—	—	—
40	2,2-Bis(4'-hydroxy- phenyl) butane(75)	DPA butyl ester(25)	8.9-9.8	9.1; 9.9-12.1	10.7	—	—	—
42	2,2-Bis(4'-hydroxy- phenyl) butane(75)	DPA lauryl ester(25)	8.8-9.8	9.1; 9.9-12.1	10.7	Xylene(10%)	Yes	Yes

TABLE IVC  
Solubility Parameters Range and Solution Stabilities for Polyesters Having 1 Phenolic  
Monomer and Acids Other Than (1:1) Isophthalate/Terephthalate

Poly- ester run no. from Table II	Phenolic monomer	Acid composition (mole-%)	Estimated solubility parameter range according to H-bonding type		
			Low	Medium	High
1	Bisphenol-A	Isophthalic(100)	0	0	0
2	Bisphenol-A	Terephthalic(100)	0	0	0
6	Bisphenol-A	{ o-Phthalic(33), Iso- phthalic(33), Terephthalic(33)	9.2-9.8	9.1; 9.9- 12.1	10.7
7	Bisphenol-A	{ o-Phthalic(50), Terephthalic(50)	9.3-9.8	9.1; 9.9- 12.1	10.7
16	Resorcinol	Isophthalic(100)	9.3-9.7	9.9-10.8	0
47	Phenolphthalein	Isophthalic(100)	9.3-9.7	9.9-12.1	10.7

(2) Polymers with relatively rigid main chains are practically insoluble in all solvents tried (note polymers A50-52).

(3) Increasing the aliphatic side chain length attached to the central carbon of bisphenol-A appears to widen slightly the solubility range of the resulting polymers in low hydrogen-bonding solvents. Some hint also exists that branching of the aliphatic chain lowers the minimum solubility parameter value even further in the desired direction (compare polymers A5, A54, and A55; and A34, A38, A39, and A41). On the other hand, methyl substituents on the resorcinol ring do not greatly change the resulting polymer solubility pattern (compare polymers A17, A29, and A31). Whether longer or bulkier substituents would show a significant effect here was not examined.

(4) Polymers based on Diphenolic Acid carboxylic acid derivatives as monomers demonstrate the following solubility relationship:



(compare polymers A34, A38, A39, and A41 with A44 and with B8 and B9).

(5) The additional presence of an ether oxygen in the Diphenolic Acid ester side chain produces a second separate solubility parameter range in medium hydrogen-bonding solvents. The original medium solubility parameter range apparently illustrates polymer solution via main chain solubilization. In contrast, the additional solubility range suggests an alternative route to polymer solution via side chain contributions (compare polymers A43 and A41).

(6) Finally, in the spectrum of solvent structures examined, alcohol hydroxyl groups appeared to inhibit polymer solution. However, chlorine atoms on aliphatic hydrocarbons produced solution as long as a hydrogen atom also was present on the solvent halogenated carbon. The most use-

ful film-forming solvents were cyclic aliphatic ethers, such as tetrahydrofuran and dioxane; cyclic ketones, such as cyclohexanone; aromatic ketones, such as acetophenone; and halogenated hydrocarbons, such as methylene chloride and chloroform. In this area, antagonistic solvent combinations producing polymer precipitation like that reported by Morgan<sup>17</sup> were encountered when halogenated hydrocarbon solutions of a given polyester were mixed with cyclic aliphatic ether solutions of the same polymer.

As a result of the modifications introduced, a significant improvement in polymer solubility performance was obtained. Long or bulky groups substituted on the bisphenol-A central carbon atom widened the choice of useful solvents and/or lengthened solution nongelation lifetime to at least 3 months (compare original polymer A5 with modified polymers A38, A39, A41, A43, A46, A53, and A55, Table IV). Alternatively, copolymers incorporating at least 25 mole-% of such substituted monomers also showed similar improved solubility behavior (compare original polymer A5 with copolymers B11, B12, and B42; and original polymer A17 with copolymers B19 and B21, Table IV). Solution performance no longer was an obstacle to the useful application of these ultraviolet protective coatings.

### Photochemical Rearrangement of Films and Analysis of Rearranged Structure

The photochemical rearrangement of these aromatic polyesters to their corresponding *o*-hydroxybenzophenone structures is demonstrated clearly by comparing infrared spectra of the top and bottom surfaces, as measured by attenuated total reflectance, of thin films which have been irradiated on one side only. Figures 1 and 2 illustrate the rearrangement by examining infrared spectra of parent polyesters 5 and 17 (Table II). For both polyesters, 5 and 17, the surface infrared spectra initially showed no absorption peak at 6.1  $\mu$ , which is about where the *o*-hydroxy benzophenone carbonyl group is found. After 50 hr of ultraviolet irradiation, however, the top (irradiated) film surfaces in Figures 1 and 2 show the appearance of significant new carbonyl peaks at 6.1  $\mu$ . In contrast, the bottom (unirradiated) film surfaces remain unchanged and continue to show no such ketone absorption.

Curves similar to those of Figure 1, but obtained by transmission instead, have been reported previously.<sup>19</sup> Those earlier curves confirm the spectral changes of polymer 5 as a function of ultraviolet irradiation. Figures 1 and 2, however, show in addition that the rearranged "skin" is quite thin and yet sufficiently opaque to those wavelengths producing the photochemical reaction to prevent rearrangement by the bottom film surface.

Similarly, ultraviolet absorption spectra of the same films, irradiated on one side only, are presented in Figures 3 and 4. Because of the inherently greater sensitivity of ultraviolet measurements compared to infrared, however, changes in these spectra as a function of irradiation time also are presented.

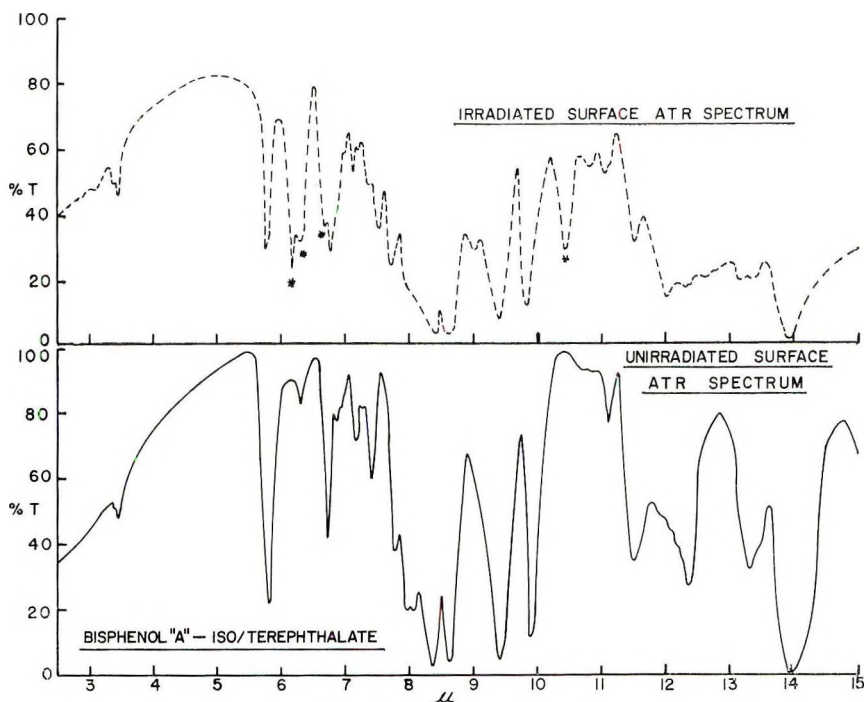


Fig. 1. (ATR) Infrared spectra of polymer 5 film surfaces after 50 hr of ultraviolet exposure to 450-W Hanovia lamp (film thickness, 0.5 mil): (—) bottom surface (unirradiated); (-----) top surface (irradiated).

Consistent with an earlier study of the photochemical Fries rearrangement,<sup>20</sup> the broadening of the two ultraviolet absorption spectra from an initial cutoff at 310–320  $m\mu$  to an ultimate 355–385  $m\mu$  correlates with the appearance of *o*-hydroxybenzophenone units. Significantly, moreover, total absorption between 200 and 355–385  $m\mu$  by the newly rearranged polymer skins effectively makes both sample films opaque to wavelengths within that range while retaining visual transparency. Thus, the rearranged films are able to function as ultraviolet barrier coatings for any substrates. This principle also is illustrated by the comparative spectra in Figures 1 and 2. Unlike alternative films containing monomeric ultraviolet stabilizers, however, the *rearranged skins* of polymers 5 and 17 are *concentrated at the exposed surfaces of the polyester films where they can protect both the original coatings and the substrates from ultraviolet irradiation*.

One pertinent observation is that irradiated films of polymer 5 turn yellow, whereas comparable films of polymer 17 remain almost colorless. A comparison of the rearranged absorption spectra in Figures 3 and 4 explains why. The slope of the final curve in Figure 3 is sufficient to produce 46% absorption at 410  $m\mu$ . Visually, 410  $m\mu$  is the approximate borderline of color perception, and a yellow color thus is observed for rearranged polymer 5. In contrast, although the slope of the final curve in Figure 4

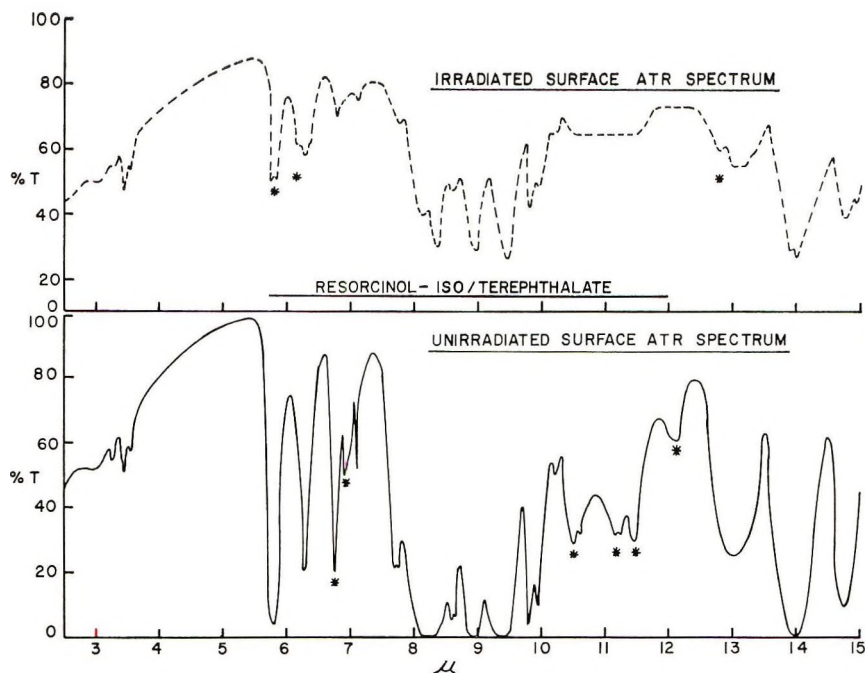


Fig. 2. (ATR) Infrared spectra of polymer 17 film surfaces after 50 hr of ultraviolet exposure to 450-W Hanovia lamp (film thickness, 0.5 mil): (—) bottom surface (unirradiated); (---) top surface (irradiated).

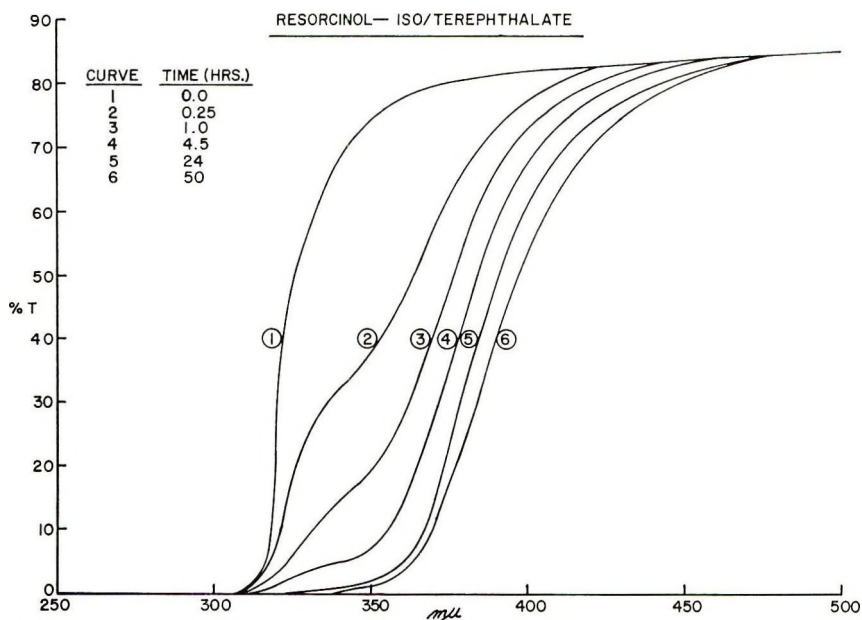


Fig. 3. Shift of ultraviolet absorption spectrum by polymer 5 film during 50 hr of ultraviolet irradiation by 450-W Hanovia lamp (film thickness, 0.4 mil).



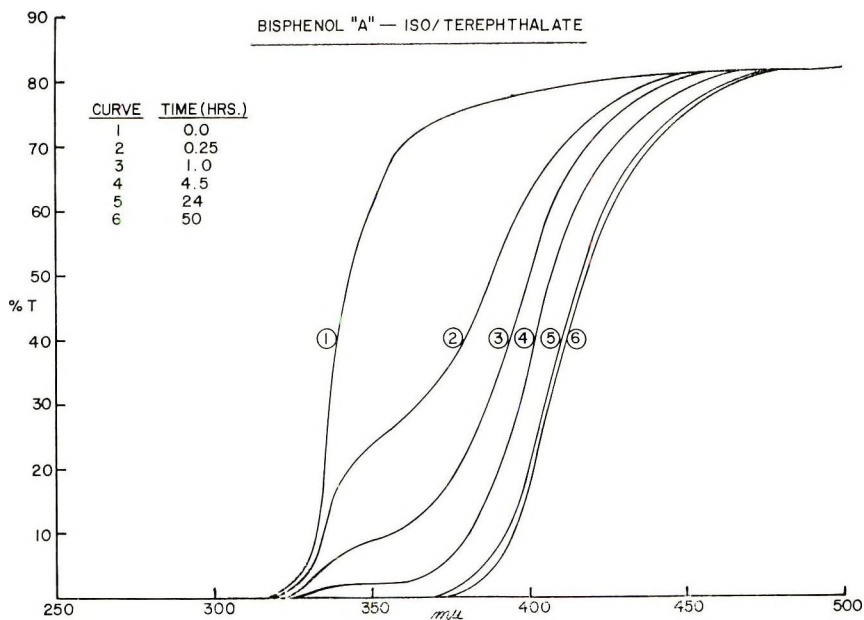


Fig. 4. Shift of ultraviolet absorption spectrum by polymer 17 film during 50 hr of ultraviolet irradiation by 450-W Hanovia lamp (film thickness, 0.4 mil).

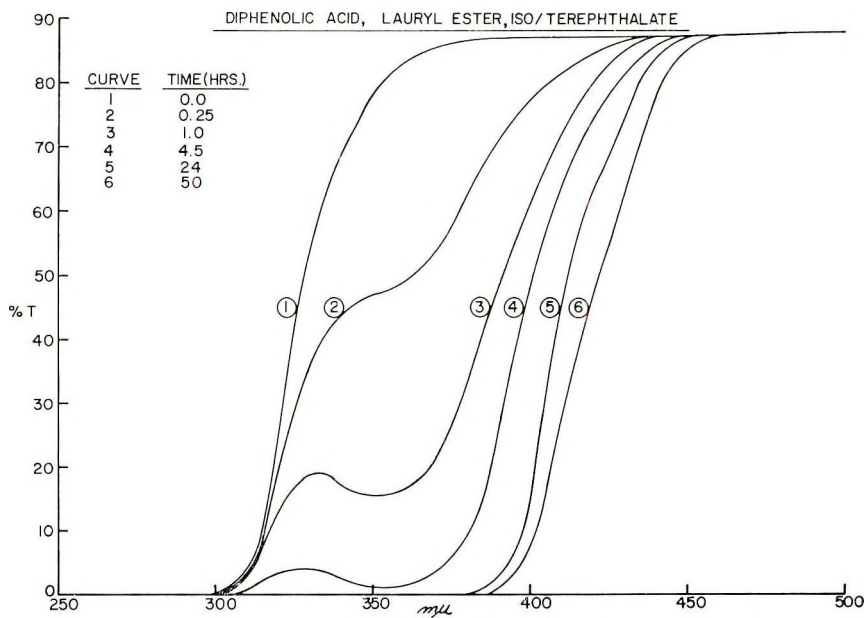


Fig. 5. Broadening of ultraviolet absorption spectrum by polymer 41 film during 50 hr of ultraviolet irradiation by 450-W Hanovia lamp (film thickness, 0.4 mil).

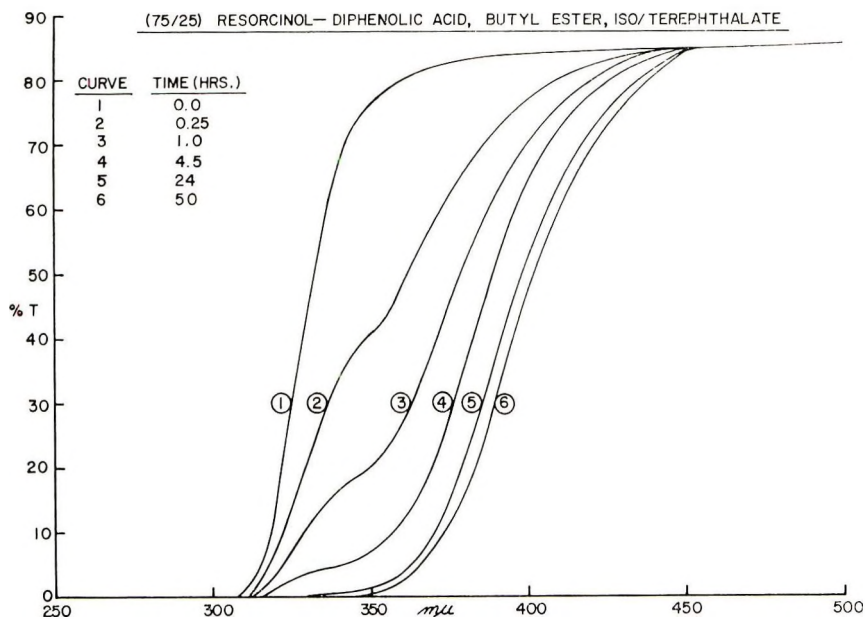


Fig. 6. Broadening of ultraviolet absorption spectrum by polymer 21 film during 50 hr of ultraviolet irradiation by 450-W Hanovia lamp (film thickness, 0.4 mil).

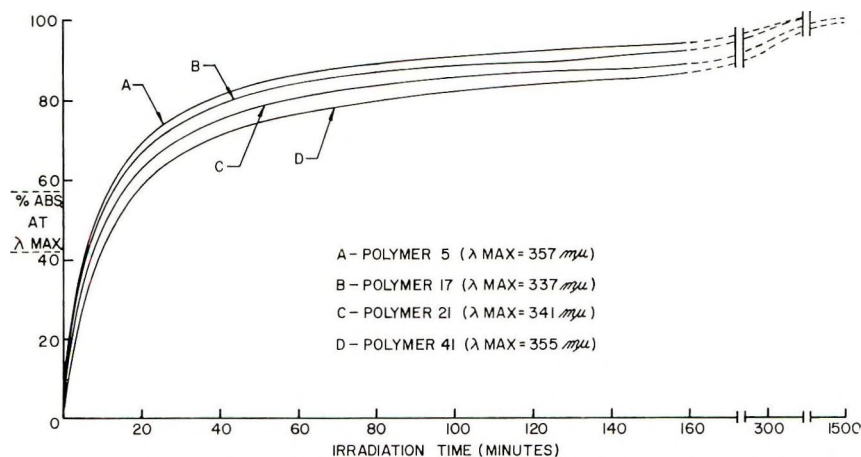


Fig. 7. Rearrangement rates of polyesters 5, 17, 21, and 41 during ultraviolet irradiation by 450-W Hanovia lamp (film thickness, 0.4 mil).

essentially is the same, it is shifted about 25  $\mu$  towards the lower wave lengths. Consequently only 15% absorption occurs at 410  $\mu$ , and a relatively colorless appearance thus is obtained with rearranged polymer 17. Whether a difference in the thickness of the rearranged skins also exists and whether such a difference is another variable influencing the degree of yellowing have not been determined.

To integrate the photochemical rearrangement mechanism with a better balance of other surface coating properties, modified polyester structures based on polymers 5 and 17 were examined. For correspondingly related polyesters 41 and 21 (Table II), the ultraviolet spectra of Figures 5 and 6, analogous to Figures 3 and 4, respectively, were obtained.

The strong similarity in the ultraviolet absorption spectra and in the rearrangement rates of Figure 3 compared to 5 and of Figure 4 compared to 6 indicates that the structurally modified polyesters show essentially the same photochemical rearrangement performance as their parent polymers.

A more direct comparison of the four rearrangement rates of Figures 3–6 is shown in Figure 7. The curves resulted from plotting the increasing amount of absorption at each newly formed  $\lambda_{\max}$  in the ultraviolet range as a function of irradiation time.

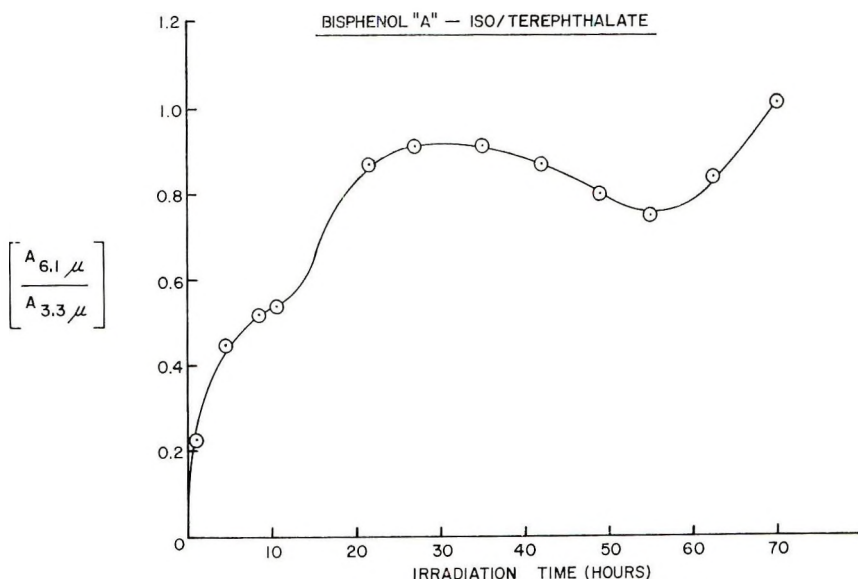
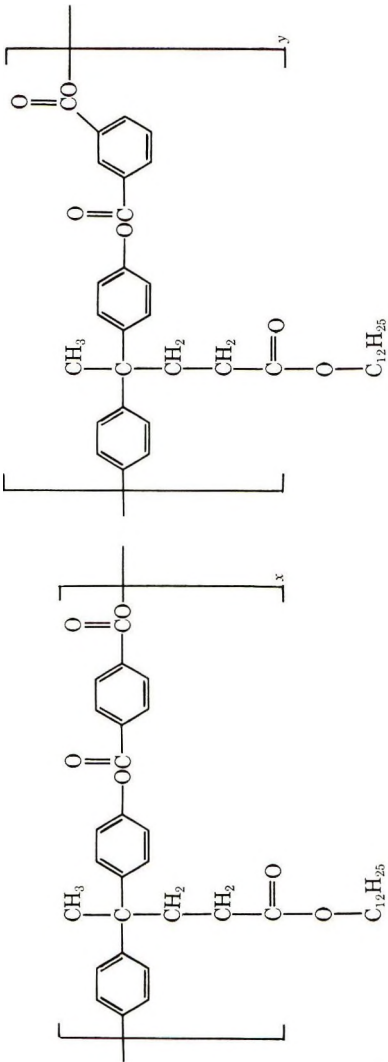
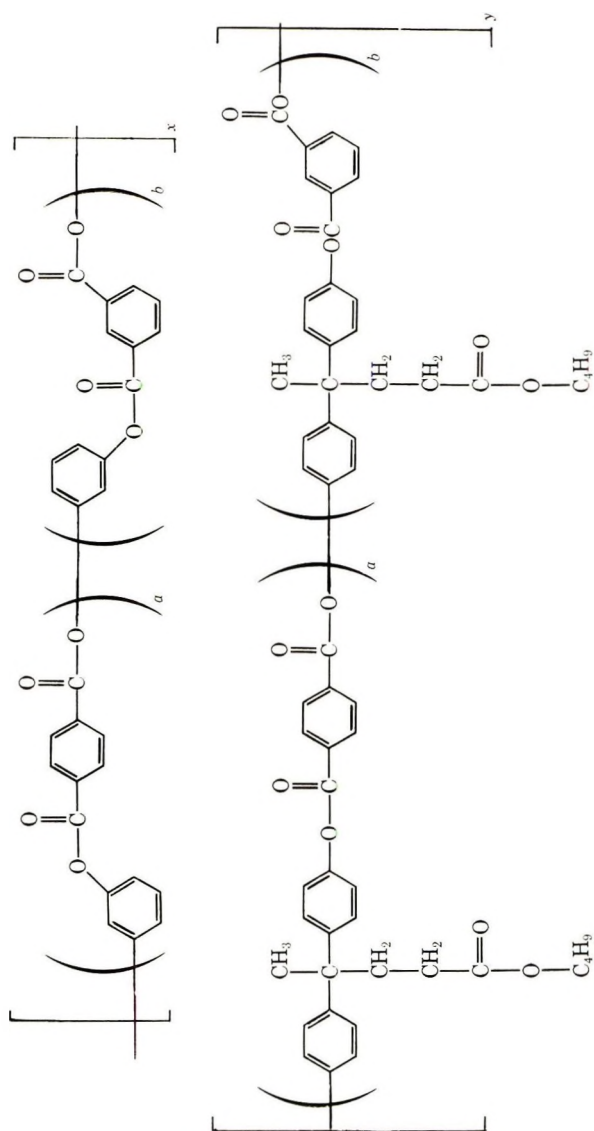


Fig. 8. Rearrangement rate of polyester 5 during ultraviolet irradiation by 450-W Hanovia lamp (film thickness, 0.46 mil).

In Figure 7, any early variations in absorption values for the rearranging polyesters (5 and 41) are essentially cancelled after the curves achieve 100% absorption in their plateau region. Unfortunately, once maximum absorption has been attained, ultraviolet measurements also become useless for detecting further increases in the thickness of rearranged film. However, this limitation can be overcome by plotting changes in the appropriate infrared absorbance ratios as a function of time. This alternative technique then permits an investigation of longer irradiation times than is indicated in Figure 7. Thus, in Figure 8 the absorbance ratio of the *o*-hydroxybenzophenone carbonyl band ( $6.1 \mu$ ) to the C–H band ( $3.3 \mu$ ) is plotted as a function of ultraviolet irradiation time. It should be noted at



Polyester 41 (x:y = 1:1)

Polyester 21 ( $x:y = 3:1$ ) ( $a:b = 1:1$ )



this point that C-H absorbance is assumed for this purpose to remain constant during irradiation, even though a slight loss in peak intensity theoretically can be expected by the conversion of some *ortho* C-H hydrogen atoms to phenolic OH groups. However, since the amount of rearrangement in the total film is relatively small, this appears to be a useful assumption.

In both Figures 7 and 8, the rate curves of polymer 5 show a similar pattern of increasing rearrangement during the initial irradiation stage. Beyond 12 hr of irradiation, however, the curve of Figure 8 reveals a surprising increased rate for ketone absorbance to a maximum level, followed by a significant decrease at 35 hr to a lower level. At 55 hr, the absorbance ratio increases again to a still higher level than originally. This loss-and-gain pattern thus far has been typical of all the polyesters found to undergo the photochemical Fries rearrangement. Consistent with the mechanism proposed in the literature for related monomeric systems, the loss of ketone absorbance is believed to correlate with eventual ultraviolet degradation of the uppermost layers of *o*-hydroxybenzophenone polymer, via both chain cleavage and carbon monoxide evolution.<sup>21-24</sup> Interestingly, such a mechanism logically predicts an initial decrease in the *o*-hydroxybenzophenone layer thickness. If this occurs, then subsequent ultraviolet irradiation should penetrate the now thinner skin to reach still unrearranged polyester; and should produce compensating rearrangement by the newly irradiated polyester layers. Such a distinct stage of rearrangement could explain the new carbonyl increase observed in Figure 8, although it does not account for the even higher values obtained compared to those before degradation. Nevertheless, *the elements of a "healing" mechanism appear to be inherent in this type of polymeric system, with the original polyester film functioning as a reservoir to maintain an essentially constant poly(o-hydroxybenzophenone) skin thickness.* The life of such a coating then should depend directly on the rate of degradation of the "skin" plus the reserve thickness of the polyester available.

If degradation actually does occur at the irradiated film surface, a decrease in the molecular weight at the surface should result and consequently might be detectable by changes in solution viscosity. Significantly, these polymers have displayed no insolubilization under the conditions of irradiation employed. A major complication in this hypothesis, however, was uncertainty about whether the degraded skin constitutes a sufficiently large portion of the total film to influence the final viscosity. Table V compares the inherent viscosities of some representative polyester films, unirradiated and also after 50 hr of irradiation.

Unfortunately, the data of Table V are inconclusive. The minute decreases in viscosity observed after irradiation could result as well from the formation of newly rearranged polymer as from degradation of the latter. Interestingly, of all the Table V polyesters, only 41 shows a significantly different pattern of solubility behavior during irradiation. Unlike the others, it crosslinks. A comparison with homologous structures 34 and 38,

TABLE V  
Viscosity of Polyester Films after 50 Hr of Ultraviolet Irradiation<sup>a</sup>

Polyester no. (Table II)	Inherent viscosity (30°C), dl/g		$\Delta$ inherent viscosity
	Unirradiated	Irradiated	
5	0.92	0.88	-0.04
17	0.49	0.44	-0.05
21	0.46	0.44	-0.02
34	0.45	0.44	-0.01
38	0.48	0.47	-0.01
41	0.89	Gel	—

<sup>a</sup> With 450-W Hanovia lamp; film thickness 0.4 mil.

which differ from 41 only by the much shorter lengths of their aliphatic side chains, suggests that crosslinking in 41 probably is caused by the longer lauryl chains, possibly by free radical mechanisms analogous to those in polyethylene.

One major question of interest in this work concerns the thickness of the rearranged skin. What is the maximum thickness achievable? For determining this, such approaches as chelation of the hydroxy ketone structure or oxidation of the phenolic hydroxyl group on the film itself were unsuccessful. However, reflectance infrared spectrophotometry proved to be a useful technique for this purpose. By duplicating the procedures used to obtain Figures 1 and 2, a series of polymer 5 films of increasing thickness were irradiated on one side with strong ultraviolet light for 60 hr. Then ATR spectra of the bottom (unirradiated) surfaces were obtained. As expected, these showed a maximum of rearrangement for the thinnest film; and no rearrangement for a sufficiently thick film. Figure 9 shows the change in absorbance ratio of the [ketone (6.15  $\mu$ ) peak/aromatic (6.25  $\mu$ ) peak] versus film thickness, compared to the absorbance ratio obtained from a transmission spectrum of an essentially totally rearranged film. The latter represents the maximum achievable by the experimental approach used.

As indicated in Figure 9, the extrapolated maximum thickness of polymer 5 "skin" under these irradiation conditions appears to be 0.46 mil. The effects of a weaker source of irradiation, even of sunlight, or of another polyester structure on the skin thickness have not been determined. Of greater significance, however, is the fact that even rearranged polyester films less than 0.1 mil thick furnish complete protection to ultraviolet-sensitive substrates. The protective aspect will be presented in more detail in the next section.

With the aromatic polyesters examined in this work, the only structural requirement to produce the photochemical Fries rearrangement under ultraviolet irradiation has been the presence of at least one unsubstituted position on the phenol rings *ortho* to the ester groups. Thus, of all the polyphenyl esters investigated here, only two failed to rearrange under the irradiation conditions used in this work. These were derivatives of poly-

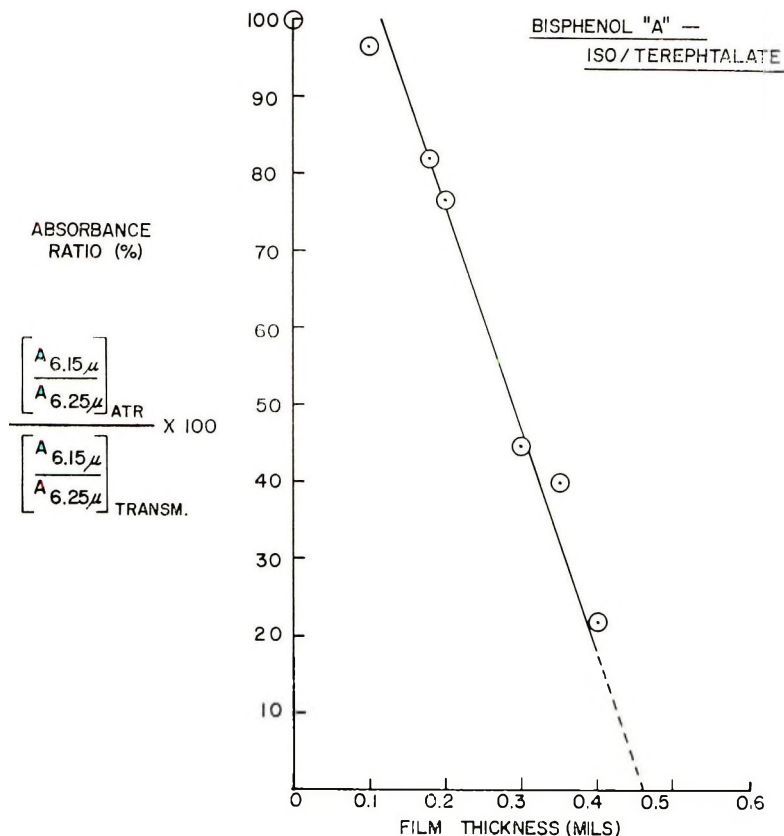


Fig. 9. Influence of film thickness on infrared absorbance ratio taken from reflectance spectrum of bottom (unirradiated) surface of polyester 5 after 60 hr of ultraviolet irradiation by 450-W Hanovia lamp. Identical absorbance ratio taken from transmission infrared spectrum on rearranged 0.1-mil film represents 100%.

ester 5 completely substituted in the phenol ring *ortho* positions either by methyl groups (polyester 57, Table II) or by chloro groups (polyester 58, Table II). The lack of ketone formation ( $6.2\mu$ ) and hence of rearrangement by these substituted polyesters following irradiation is illustrated in Figure 10.

Even after 70 hours of such ultraviolet irradiation, the tetramethyl polyester still permitted 97% transmission in the 300–400  $m\mu$  region and the tetrachloro polyester, 94.5% transmission. In contrast, the 2,2'-dimethyl polyester (polyester 56, Table II), with one unsubstituted *ortho* position available on each phenol ring, does undergo the rearrangement readily, as indicated in Figure 11.

Predictably, this polymer after comparable ultraviolet irradiation permitted only about 60% transmission at 350  $m\mu$  because of the absorption band which formed during the rearrangement. Interestingly, in contrast to the unreactive behavior of the chlorinated polymer shown in Figure 10, Kobsa<sup>25</sup> has stated that the monomeric compound, 2,6-dichloro-4-*tert*-butylphenyl

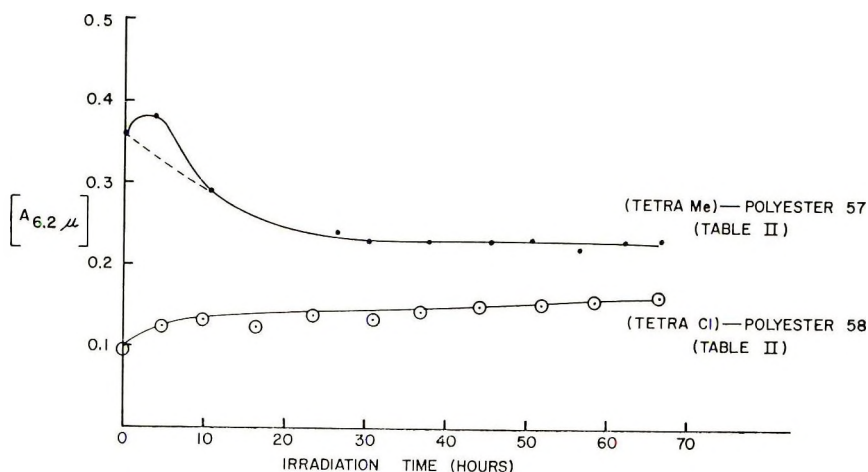


Fig. 10. Effect of ultraviolet irradiation by 450-W Hanovia lamp on films of polyester 5 substituted in all phenol ring *ortho* positions.

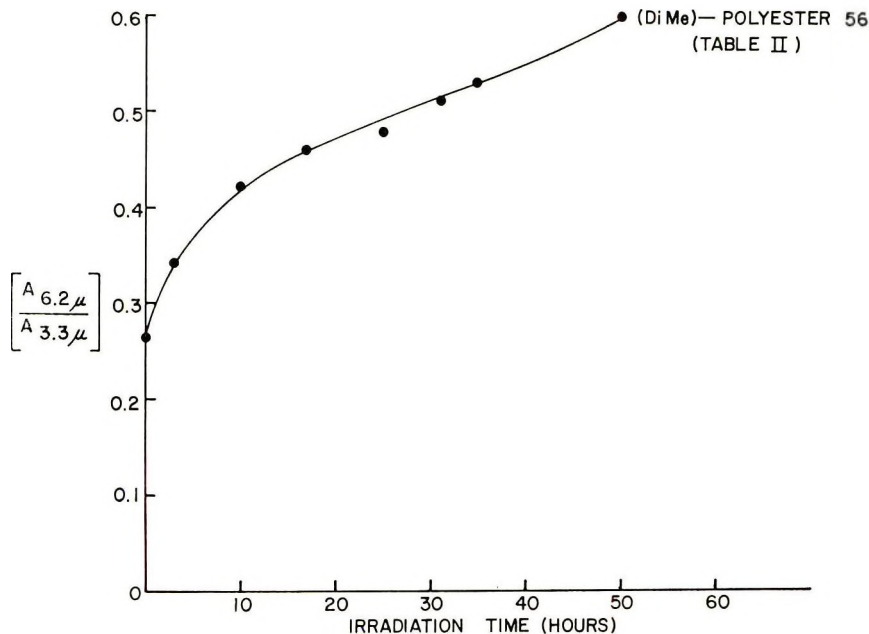


Fig. 11. Effect of ultraviolet irradiation by 450-W Hanovia lamp on film of polyester 5 substituted on one-half of available phenol ring *ortho* positions by methyl groups.

benzoate, does undergo the photochemical Fries rearrangement accompanied by the expulsion of one of the two chlorine atoms.

Some evidence also was obtained clarifying the stability of the *o*-hydroxy-benzophenone polymer structure under ultraviolet irradiation. The earlier results of Figure 8 were examined in greater detail and are presented in Figure 12.

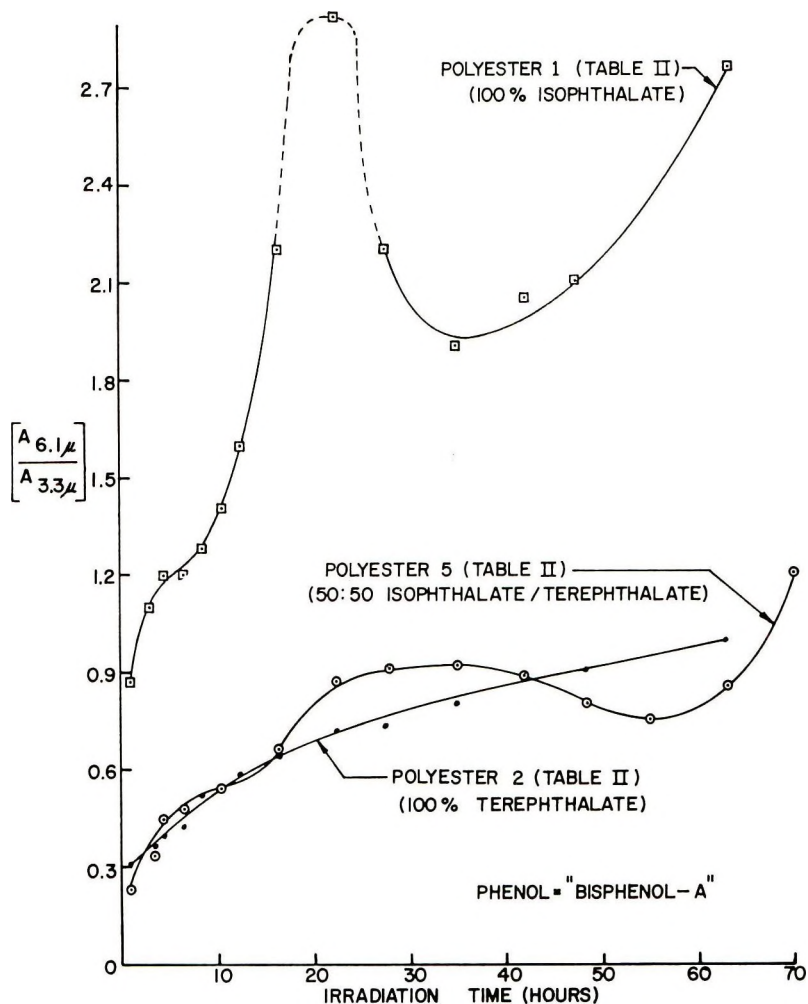


Fig. 12. Effect of ultraviolet irradiation by 450-W Hanovia lamp on films of polyester 5 copolymer and its parent polymers

Polyester 5, the 50:50 isophthalate/terephthalate copolymer of bisphenol-A, was compared with polyester 1, the 100% isophthalate polymer, and with polyester 2, the 100% terephthalate polymer. While the rearranged isophthalate polymer degrades relatively rapidly, the rearranged terephthalate polymer appears comparatively stable; and the 50:50 copolymer falls somewhere between their performances. Apparently, therefore, the ultraviolet stability of the *o*-hydroxybenzophenone group is greatly influenced by the positions of the carboxylic groups on the acid ring. Undoubtedly the choice and location of other substituents can exert similar effects on the degradation mechanism, which has been discussed earlier in connection with Figure 8.

Finally, although Coppinger and Bell<sup>26</sup> state that the monomeric phenyl esters studied by them did not undergo the photo Fries rearrangement when irradiated by wavelengths of light greater than 280 mμ, our observations indicate that polyester 5 undergoes significant rearrangement even with



wavelengths greater than 300  $m\mu$ . As a filter for this experiment, soft glass sheet with the transmission characteristics shown in Figure 13 was used.

A polyester 5 film protected by the glass filter and irradiated by a 100-W Hanovia lamp (from a distance of 6 in.) for 865 hr underwent rearrangement, as indicated by the appearance of carbonyl absorption at 6.2  $\mu$  and of *o*-hydroxybenzophenone absorption at 354  $m\mu$ . The amount of carbonyl produced in the film after 865 hr behind the filter was equivalent to that produced after 120 hr of the same radiation exposure without protection.

### Protective Coating Effectiveness

The effectiveness of such polymers for protecting ultraviolet-sensitive materials was screened by coating appropriate substrates with thin films (0.3–0.5 mils) of the polyesters and exposing the resulting samples to accelerated ultraviolet irradiation. As coatings, polyesters 5, 17, 21, 41 and other similar materials were used. The results are presented in Table VI.

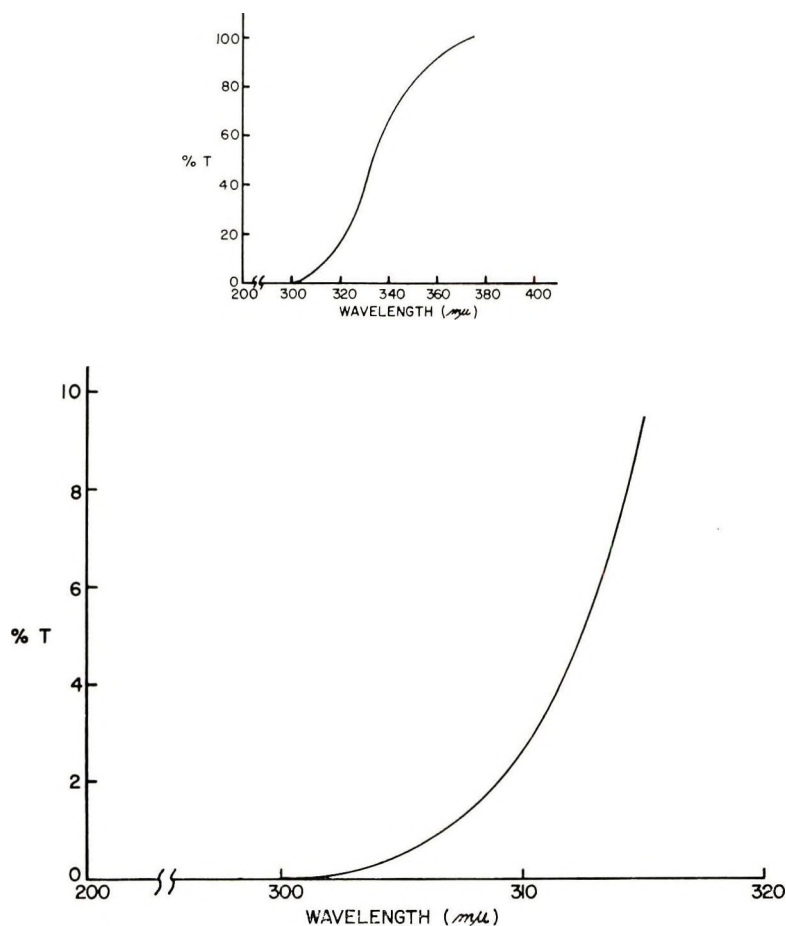


Fig. 13. Ultraviolet transmission spectrum of 96-mil thick soft glass filter. Photomultiplier tube =  $20\times$ .

TABLE VI  
Protection of Substrates Coated with Ultraviolet-Barrier Resins during Accelerated Irradiation by Various Ultraviolet Sources

Substrate	Type of Exposure	Time, hr	Unirradiated (initial)	Irradiated	
				Protected (coated) <sup>a</sup>	Unprotected (uncoated)
A. Excellent Protection					
Poly(vinyl chloride) Translucent, neutral color, rigid sheet	Weather-O-Meter	1120	"Pearl" color, slight gloss	Very slight yellowing where irregular in coating thickness; physical props. maintained	Complete blackening or dark brown; brittle
Translucent, neutral color, rigid sheet	450-W UV lamp	180	Same as above	No change	Sample turned a deep black-blue color
Plasticized sheet, transparent	Westinghouse Sun Lamp	2106	Polyester film laminated to PVC; some haze due to interfacial polymer mixing	Virtually unchanged; no visible yellowing; retained transparency	Yellow-tan color developed; with loss of plasticizer, frosty appearance of surface
Cellulose acetate butyrate	450-W UV lamp	232	Transparent sheet with 0% yellow	1.5% yellow measured; no visible changes	Definite yellow measured as 16%; slight frosting of surface
Cellulose nitrate	450-W UV lamp	300	Transparent sheet with 1.5% yellow initially	An increase of 4% in yellowing occurred; retained excellent transparency	A dark tan color developed, with loss in transparency at about 120 hr
Poly(vinyl alcohol)	450-W UV lamp	96	Colorless, transparent and flexible	No visible change	Very yellow, brittle
Nylon 66	450-W UV lamp	96	White, opaque and flexible	No visible yellowing, still flexible	Straw color developed with loss of flexibility
Polycarbonate of bisphenol-A	450-W UV lamp	96	Transparent, flexible	Retained transparency and flexibility	Deep yellow color formed with loss in transparency
Poly(ethylene terephthalate)	450-W UV lamp	96	Clear, tough and flexible	No visible changes; properties retained	Very brittle with loss of transparency; very slight color change

Poly(vinyl butyral)	450-W UV lamp	96	Transparent, colorless and flexible
Poly(vinyl acetate)	450-W UV lamp	96	Colorless and transparent
Poly(methyl methacrylate)	450-W UV lamp	96	Transparent, colorless and rigid
Polyacrylonitrile	450-W UV lamp	96	Opaque, white
Polyethylene	450-W UV lamp	96	Translucent, flexible
Polystyrene	450-W UV lamp	96	Transparent, colorless
Poly(vinylidene chloride-co-vinyl chloride) (Saran, Dow Chemical)	450-W UV lamp	96	Transparent, flexible and colorless
Polypropylene	450-W UV lamp	96	Opaque, white, rigid
Cellulose	450-W UV lamp	96	Opaque, in form of undyed fibers
Cellulose	450-W UV lamp	96	In the form of red colored fibers
"Kodacolor" Photographic Prints (Eastman Kodak)	80-W fluorescent lamp	250	Complete color spectrum
Copper	Weather-O-Meter	550	Glossy, red-orange
Brass	Weather-O-Meter	150	Bright and shiny
Muntz Metal	Weather-O-Meter	150	Bright and shiny

No change	Tan color present with loss of flexibility and some frosting of surface
No visible change	Yellow color with loss in flexibility
No visible change	Sl. yellow color; slight frosting of surface
No visible change or loss in properties	Brown color with loss in tensile strength
No change noticeable	Very brittle; many cracks throughout sample
No visible change	Very deep yellow; very brittle
No visible change	Dark brown in color and very brittle
No visible change	Sample disintegrated to a powder
No loss in color or physical properties	Brown color developed
No loss in physical properties; some bleaching of color noticeable	Color completely bleached away; brown color developed
Very slight fading noticeable	Complete bleaching of all colors to a red-pink coloration
No change	Formation of "rust" spots; severe staining with discoloration
No change	Darkening of color with staining
No change	Slight discoloration

TABLE VI (continued)

Substrate	Type of Exposure	Time, hr	Unirradiated (initial)	Irradiated	
				Protected (coated) <sup>a</sup>	Unprotected (uncoated)
B. Good Protection					
Copper	Weather-O-Meter	754	Bright and shiny	Slight discoloration or fading of color	Severe discoloration and staining
Brass	Weather-O-Meter	754	Bright and shiny	Very slight discoloration	Severe discoloration and staining
Muntz Metal	Weather-O-Meter	754	Bright and shiny	Very slight discoloration	Staining and much discoloration
"Kodacolor" Photographic Transparencies (Eastman Kodak Co.)	450-W UV lamp	48	Transparency with variety of colors	Slight fading of certain colors (tan, green, grey)	All colors faded
Polystyrene	Westinghouse Sun Lamp	1000	Clear, colorless	Slight yellowing	Very deep yellowing
Fluorescent Dyes, Paint (Red) <sup>b</sup>	450-W UV lamp	30	Brilliant red fluorescence (0.8 mil film)	Slight loss in fluorescence and darkening of red color	Fluorescence destroyed within 6 min; color darkened, then began to bleach
"Kodacolor" Photographic Prints (Eastman Kodak Co.)	450-W UV lamp	4.5	Complete color spectrum	Visual estimation is >90% retention of color intensity	All colors bleached to a light pinkish color
C. Fair Protection					
Fluorescent paints (red color) <sup>b</sup>	450-W UV lamp	50	Brilliant red fluorescence	Fluorescence destroyed; some darkening of red color	Fluorescence destroyed within 6 minutes; color darkened then bleached
Pine and cedar wood	Weather-O-Meter	150	Glossy, light colored	Darkening of wood in sections; some yellowing	Severe staining and initial yellowing followed by bleaching

<sup>a</sup> The substrates listed in the table were coated with a solution of the polyester at a thickness which would give a dry film thickness in the range of 0.3-0.5 mil.

<sup>b</sup> The fluorescent materials were coated with solutions of polyesters which would give a dry film thickness in the range of 0.8-1.0 mil.



As can be observed in Table VI, the degree of protection conferred by the coatings against ultraviolet irradiation alone is almost always very good-to-excellent. Similar protection performance also is demonstrated in Figure 14 on cellulose nitrate, a material notoriously sensitive to ultraviolet degradation.

However, Table VI also indicates that, in specific cases, these coatings

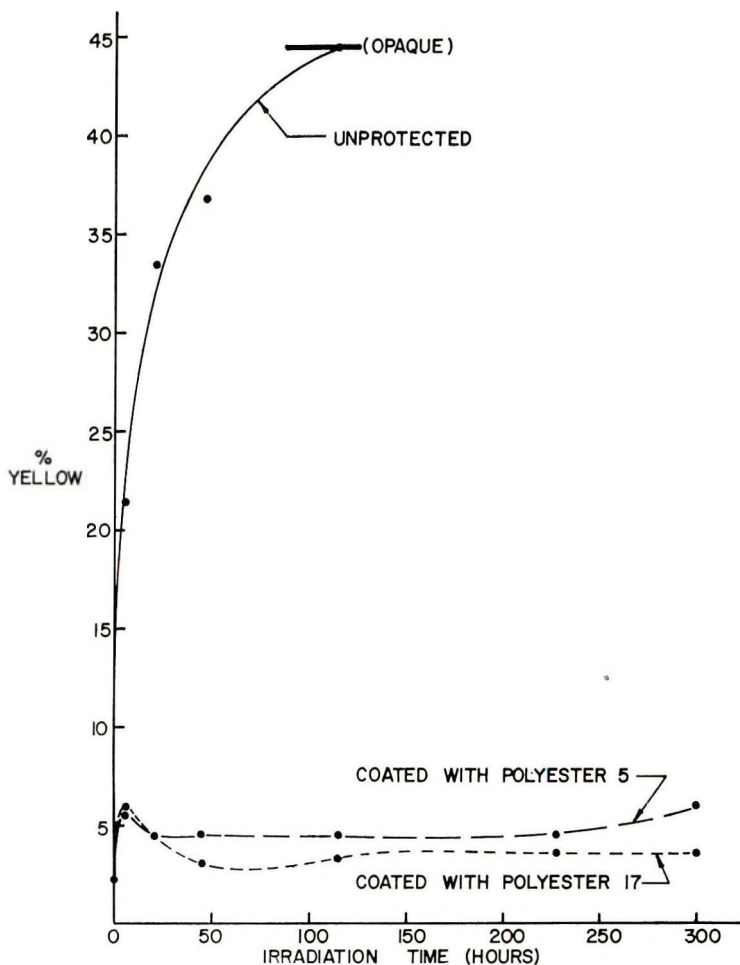


Fig. 14. Irradiation of protected vs. unprotected cellulose nitrate coated with polyesters 5 and 17 by 450-W Hanovia lamp (film thickness, 0.3–0.5 mil).

may perform less effectively when other weathering variables are introduced in addition to ultraviolet irradiation. Thus exposure of some coated substrates, such as metals and wood, to ultraviolet irradiation in the Weather-O-Meter (where moisture and heat are added factors) produced a decrease in the protection contributed by such coatings. Overall, however, the protection afforded by these coatings remains promising. Prior

to 1970, we know of no clear coatings which equal or surpass their performance. Patents describing these polymers have issued.<sup>27</sup>

Exterior weathering tests are in progress.

## CONCLUSIONS

Certain phenyl polyesters rearrange chemically under ultraviolet irradiation to produce a thin "skin" which is opaque to ultraviolet light but still visually transparent. Thin coatings of the clear rearranged polymers completely protect substrates ordinarily sensitive to ultraviolet light. As the skin ultimately degrades under extended ultraviolet irradiation, more of the now exposed underlying polyester layer apparently rearranges to compensate for the loss. Thus the clear coating functions both as a protective skin and a rearrangeable reservoir.

The help and contributions of M. D. Kellert, Dr. I. Serlin, E. Lavin, Dr. R. N. Crozier, T. B. O'Connor and R. V. DeShay in various phases of this work are gratefully acknowledged.

## References

1. D. A. Gordon, "Light Stabilizers", in *Encyclopedia of Basic Materials for Plastics*, H. R. Simonds and J. M. Church, Eds., Reinhold, New York, 1967.
2. *Chem. Week*, p. 83 (March 28, 1964).
3. R. G. Schmitt and R. C. Hirt, *J. Polym. Sci.*, **61**, 361 (1962).
4. A. Strobel and S. Catino, *Ind. Eng. Chem., Prod. Res. Dev.*, **1**, 241 (1962).
5. J. Fertig, A. I. Goldberg, and M. Skoultchi, *J. Appl. Polym. Sci.*, **9**, 903 (1965).
6. J. Fertig, A. I. Goldberg, and M. Skoultchi, *J. Appl. Polym. Sci.*, **10**, 663 (1966).
7. Z. Osawa, K. Matsui, and Y. Ogiwara, *J. Macromol. Sci.-Chem.*, **A1**, 581 (1967).
8. D. Belluš and P. Hrdlovič, *Chem. Rev.*, **67**, 599 (1967).
9. M. R. Sandner and D. J. Trecker, *J. Amer. Chem. Soc.*, **89**, 5725 (1967).
10. D. V. Rao and V. Lamberti, *J. Org. Chem.*, **32**, 2896 (1967).
11. J. S. Bradshaw, E. L. Loveridge, and L. White, *J. Org. Chem.*, **33**, 4127 (1968).
12. H. J. Hageman, *Tetrahedron*, **25**, 6015 (1969).
13. V. V. Korshak, S. V. Vinogradova, S. A. Siling, S. R. Rafikov, Z. Y. Fomina, and V. V. Rode, *J. Polym. Sci. A-1*, **7**, 157 (1969).
14. V. V. Rode and E. E. Said-Galiev, *Bull. Acad. Sci. USSR, Div. Chem. Sci.*, **1969**, 2149.
15. P. A. Mullen and N. Z. Searle, *J. Appl. Polym. Sci.*, **14**, 765 (1970).
16. W. M. Eareckson III, *J. Polym. Sci.*, **40**, 399 (1959).
17. P. W. Morgan, *J. Polym. Sci. A*, **2**, 437 (1964).
18. P. Small, in *Polymer Handbook*, J. Brandrup, and E. H. Immergut, Eds., Interscience, New York, 1966, Sect. 4, pp. 341-68.
19. M. Okawara, S. Tani, and E. Imoto, *Kogyo Kagaku Zasshi*, **68**, 223 (1965).
20. S. B. Maerov, *J. Polym. Sci. A*, **3**, 487 (1965).
21. R. C. Hirt, N. Z. Searle, and R. G. Schmitt, *SPE Trans.*, **1**, 21 (1961).
22. A. F. Strobel and S. C. Catino, *Ind. Eng. Chem., Prod. Res. Dev.*, **1**, 241 (1962).

23. V. V. Rode, A. S. Yarov, and S. R. Rafikov, *Vysokomol. Soedin.*, **6**, 2168 (1964).
24. S. R. Rafikov, S. V. Vinogradova, V. V. Korshak, and Z. Y. Fomina, *Vysokomol. Soedin.*, **A9**, 98 (1967).
25. H. Kobsa, *J. Org. Chem.*, **27**, 2293 (1962).
26. G. M. Coppinger and E. R. Bell, *J. Phys. Chem.*, **70**, 3479 (1966).
27. U.S. Pats. 3,444,129, May 13, 1969; 3,460,961, Aug. 12, 1969; 3,492,261, Jan. 27, 1970; 3,503,779, Mar. 31, 1970; and 3,506,470, April 14, 1970.

Received March 4, 1971

## Quantitative Treatment of the Dye Partition Method of Analysis of Surfactants and of Ionic Groups in High Polymers

B. M. MANDAL and S. R. PALIT, *Department of Physical Chemistry,  
Indian Association for the Cultivation of Science,  
Jadavpur, Calcutta-32, India*

### Synopsis

A quantitative treatment of the extraction of ionic dyes from aqueous solutions into organic solvents of low dielectric constant by surfactants or polymers with ionic groups having a charge opposite to that of the dye ion, is presented. The assumption is made that the extracted species are ion-paired in the organic phase. Based on this, a graphical extrapolation method is suggested for the quantitative estimation of ionic groups in polymers. Theoretically, the method should yield quantitative results irrespective of polymer chain length and character. This method of analysis does not require any calibration data.

### INTRODUCTION

The dye extraction method of analysis of surfactants as well as ionic groups in polymers at near micronormal concentration is widely practiced.<sup>1</sup> The principle of this method and its physico-chemical aspects have been discussed qualitatively by Mukerjee<sup>2</sup> for surfactants and by Palit<sup>3</sup> for polymers. Analysis of the surfactants is usually done with the help of calibration data obtained with known concentrations of the surfactant under test. For polymers, calibration data for every polymer of every chain length are difficult to obtain because such tailor made polymer samples with known amounts of ionic groups are not easily available. Palit<sup>4</sup> chose surfactants as reference for the analysis of polymer endgroups. In a recent paper<sup>5</sup> we have shown that the dye extraction depends on the chain length of the polymer as well as on the character of the solvent. Use of surfactants (chain length considerably lower than in most polymers) as reference for the analysis of polymer endgroups may lead to high results. The extent of this overestimation depends on the character of the solvent. A dipolar solvent reduces this overestimation greatly. It would be only fortuitous if a solvent which completely eliminates the chain length effect is found. In view of these complications the calibration data method does not yield highly quantitative results in the estimation of polymer endgroups. In the present paper a quantitative theoretical analysis of the dye partition

method is presented, and a procedure to obtain truly quantitative results is suggested. The present method will be referred to as the intercept method.

## THEORETICAL TREATMENT

### Anionic Surfactant

Let us consider the extraction of methylene blue from aqueous solution into an organic solvent by sodium lauryl sulfate. Methylene blue cation binds with lauryl sulfate in 1:1 stoichiometric proportion.<sup>2,6</sup> The extraction process may be represented by



where the subscripts o and w refer to the organic and aqueous phases, respectively. The assumption is made that in the solvent of low dielectric constant used in extraction, the dye and lauryl sulfate exist as an ion pair. The basis of this assumption is given later. The equilibrium will be represented by

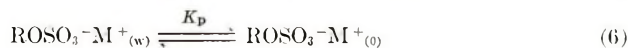
$$K_E = (\text{ROSO}_3^-\text{D}^+)_o / (\text{ROSO}_3^-)_w (\text{D}^+)_w \quad (2)$$

where the parentheses stand for activity.

Let  $C$  be the concentration of the lauryl sulfate used and  $X$  the concentration of extracted dye lauryl sulfate ( $\text{ROSO}_3^-\text{D}^+$ ) in the organic phase. Then,

$$C - X = [\text{ROSO}_3^-]_w + [\text{ROSO}_3^-\text{D}^+]_w + [\text{ROSO}_3^-\text{M}^+]_o + [\text{ROSO}_3^-\text{M}^+]_w \quad (3)$$

( $\text{M}^+$  may be any metal ion or  $\text{H}^+$  ion present in the system with which lauryl sulfate may form an ion pair in the aqueous or in the organic phase). Further let  $K_A$ ,  $K'_A$ , and  $K_p$  describe the following ion association and partition equilibria.



Then, using the constants  $K_A$ ,  $K'_A$ , and  $K_p$  one obtains from eq. (3), assuming activity coefficients for the ion paired species to be unity,

$$C - X = [\text{ROSO}_3^-]_w + K_A [\text{ROSO}_3^-]_w [\text{D}^+]_w f_{D^+} + K'_A (1 + K_p) [\text{ROSO}_3^-]_w [\text{M}^+]_w f_{M^+} \quad (7)$$

where  $f_{D^+}$ ,  $f_{D^+}$ , and  $f_{M^+}$  represent the activity coefficients of  $\text{ROSO}_3^-$ ,  $\text{D}^+$ , and  $\text{M}^+$ , respectively, in the aqueous phase.

Thus



$$[\text{ROSO}_3^-]_{\text{w}} = \frac{C - X}{1 + K_{\text{A}}[\text{D}^+]_{\text{w}}f_{\text{D}^+} + K'_{\text{A}}(1 + K_{\text{p}})f_{\text{M}^+}[\text{M}^+]_{\text{w}}} \quad (8)$$

Inclusion of eq. (8) in eq. (2) gives

$$K_{\text{E}} = \frac{X\{1 + K_{\text{A}}[\text{D}^+]_{\text{w}}f_{\text{D}^+} + K'_{\text{A}}(1 + K_{\text{p}})f_{\text{M}^+}[\text{M}^+]_{\text{w}}\}}{(C - X)[\text{D}^+]_{\text{w}}} \quad (9)$$

Rearrangement of eq. (9) gives

$$\frac{C}{X} = 1 + \frac{K_{\text{A}}}{K_{\text{E}}}f_{\pm(\text{RD})}^2 + \frac{1}{[\text{D}^+]_{\text{w}}} \left\{ \frac{1}{K_{\text{E}}} + \frac{K'_{\text{A}}(1 + K_{\text{p}})f_{\pm(\text{RM})}^2[\text{M}^+]_{\text{w}}}{K_{\text{E}}} \right\} \quad (10)$$

where  $f_{\pm(\text{RD})}$  and  $f_{\pm(\text{RM})}$  represent the mean ionic activity coefficients of the long-chain electrolytes  $\text{ROSO}_3\text{D}$  and  $\text{ROSO}_3\text{M}$ , respectively. For dilute aqueous solutions, the activity coefficients should approach unity. Equation (10) then reduces to

$$\frac{C}{X} = 1 + \frac{K_{\text{A}}}{K_{\text{E}}} + \frac{1}{[\text{D}^+]_{\text{w}}} \left\{ \frac{1}{K_{\text{E}}} + \frac{K'_{\text{A}}}{K_{\text{E}}} (1 + K_{\text{p}})[\text{M}^+]_{\text{w}} \right\} \quad (11)$$

Further,  $X$  may be represented as

$$X = \frac{\text{Absorbance } (A_0) \text{ of the organic layer due to the extracted dye}}{\epsilon_{\text{RD}}t} \quad (12)$$

where  $t$  is the thickness of the optical path and  $\epsilon_{\text{RD}}$  is the molar absorbancy index of the dye surfactant salt in the organic solvent. Inclusion of eq. (12) in eq. (11) gives

$$\frac{1}{A_0} = \frac{1}{\epsilon_{\text{RD}}Ct} + \frac{K_{\text{A}}}{K_{\text{E}}\epsilon_{\text{RD}}Ct} + \frac{1}{[\text{D}^+]_{\text{w}}} \left\{ \frac{1}{K_{\text{E}}\epsilon_{\text{RD}}Ct} + \frac{K'_{\text{A}}(1 + K_{\text{p}})[\text{M}^+]_{\text{w}}}{K_{\text{E}}\epsilon_{\text{RD}}Ct} \right\} \quad (13)$$

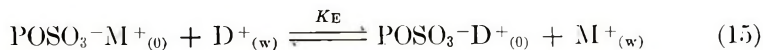
Thus from eq. (13) it is clear that at constant  $[\text{M}^+]_{\text{w}}$  a plot of the reciprocal of the organic phase absorbance versus the reciprocal of the equilibrium aqueous phase dye concentration should be linear for a given concentration of the surfactant, the dye concentration being varied. The intercept of such a plot is given by

$$\frac{1}{\epsilon_{\text{RD}}Ct} \left( 1 + \frac{K_{\text{A}}}{K_{\text{E}}} \right) = \frac{1}{\epsilon_{\text{RD}}Ct} \left\{ 1 + \frac{(\text{ROSO}_3^-\text{D}^+)_{\text{w}}}{(\text{ROSO}_3^-\text{D}^+)_{\text{o}}} \right\} \quad (14)$$

The quantity  $\epsilon_{\text{RD}}Ct$  corresponds to the organic phase absorbance when sodium lauryl sulfate is completely converted to dye lauryl sulfate and completely extracted into the organic phase.

### Polymer with Anionic Endgroups ( $\text{SO}_3^-$ , $\text{OSO}_3^-$ )

When a polymer insoluble in water but soluble in low dielectric constant organic solvents is used, the extraction process may be represented by



$\text{M}^{+}$  may be  $\text{H}^{+}$  or any alkali metal ion. In a given solvent  $K_E$  may vary with the chain length of the polymer and its polarity.<sup>5</sup> If  $C$  is the concentration of the polymer used and  $X$  the concentration of the extracted dye polymer ion pair we have

$$K_E = \frac{X[\text{M}^{+}]_w f_{\text{M}^{+}}}{(C - X)[\text{D}^{+}]_w f_{\text{D}^{+}}} \quad (16)$$

where  $f_{\text{M}^{+}}$  and  $f_{\text{D}^{+}}$  represent the activity coefficients of the subscript ions. Assumption of unit activity coefficients for dilute solutions yields, from eq. (16)

$$C/X = 1 + ([\text{M}^{+}]_w/K_E[\text{D}^{+}]_w) \quad (17)$$

Representing  $X$  as in eq. (12) we get from eq. (17)

$$\frac{1}{A_0} = \frac{1}{\epsilon_{\text{RD}}Ct} + \frac{[\text{M}^{+}]_w}{K_E\epsilon_{\text{RD}}Ct[\text{D}^{+}]_w} \quad (18)$$

$A_0$  refers to the absorbance of the organic phase following extraction and after correction for the blank.

From eq. (18) it is evident that at constant  $[\text{M}^{+}]$  a plot of the reciprocal of the organic phase absorbance ( $A_0$ ) versus reciprocal of the equilibrium aqueous phase  $[\text{D}^{+}]$  will be linear for a fixed concentration of the polymer, the dye concentration being varied. The reciprocal of intercept at  $1/A_0$  axis corresponds to the organic phase absorbance for the complete conversion of the polymer sulfate to the dye polymer ion pair and its complete extraction into the organic solvent. The intercept for a fixed concentration of the polymer should be independent of polymer polarity and chain length. The intercept will, however, depend on the nature of the solvent, since the absorbancy index of the dye polymer ion pair varies with the solvent. Thus, the major source of error in the use of surfactant as reference for the analysis of polymer endgroup could be overcome by way of a plot of  $1/A_0$  versus  $1/[\text{Dye}]$  for a given concentration of the polymer as indicated in equation (18). Equation (13) is more complex than is eq. (18). The intercept for the former contains an extra term, viz. the partition coefficient of the dye surfactant ion pair between water and the organic solvent. For a water-insoluble polymer this partition coefficient is obviously zero. This consideration reduces eq. (14) to the intercept for eq. (18).

Thus for the analysis of anionic endgroups ( $\text{SO}_3^-$ ,  $\text{OSO}_3^-$ , etc.) in polymers it is necessary to perform a few extraction experiments at fixed polymer and varying dye concentration. The absorbance of the organic layer is then measured and corrected for the blank. The concentration of the dye (methylene blue) in the aqueous layer is also determined spectrophotometrically. The reciprocals of these data are then plotted against each other. The intercept of the line at  $1/A_0$  is determined. The desired con-

centration of the ionic group will be obtained from the value of the intercept when  $\epsilon_{RD}$  is known [see eq. (18)].

The problem now remains how to determine the molar absorptancy index ( $\epsilon_{RD}$ ) of the dye polymer ion pair in the organic solvent. This value may be approximated by using that for the dye surfactant salt. For this, the methylene blue lauryl sulfate salt was prepared;<sup>6</sup> its molar absorptancy index in chloroform at 655 nm was found to be  $9.07 \times 10^4$  l./mole-cm.

### Cationic Surfactants (Long-Chain Ammonium or Quaternary Ammonium Salts)

Anionic dyes, such as bromophenol blue,<sup>2,7</sup> orange II,<sup>8</sup> or disulfine blue VN 150, are generally used for the estimation of cationic surfactants by the calibration data method. In this laboratory disulfine blue VN 150 in 0.01*N* HCl is generally used. A study with the latter dye reveals that for a given concentration of the amine the amount of dye extracted into chloroform from 0.01*N* HCl depends greatly on the chain length as well as the class of the amine.<sup>9</sup> This is expected in view of the fact that the equilibrium constant  $K_E$  for the dye extraction equilibrium should depend on the above two factors.

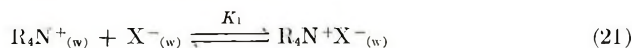


All but one of the R groups in eq. (19) may also be hydrogen atoms representing protonated amines, and  $D^{-}$  is the anionic dye.

The theoretical treatment yields eq. (20), if the activity coefficients are assumed to be unity for the dilute solutions:

$$\frac{1}{A_0} = \frac{1}{\epsilon_{RD}Ct} + \frac{K_2}{K_E\epsilon_{RD}Ct} + \frac{1}{[D^{-}]} \left\{ \frac{1}{K_E\epsilon_{RD}Ct} + \frac{K_1(1 + K_p)[X^{-}]}{K_E\epsilon_{RD}Ct} \right\} \quad (20)$$

where  $A_0$  is the absorbance of the organic phase after extraction;  $C$  is the concentration of surfactant originally used;  $t$  is the thickness of the optical path; and  $K_1$ ,  $K_2$ , and  $K_p$  are defined as follows:



$$K_p = (R_4N^{+}X^{-})_o / (R_4N^{+}X^{-})_w \quad (23)$$

Further,  $X^{-}$  represents an inorganic anion with which the surfactant cation forms an ion pair either in the organic or the aqueous phase. From eq. (20) it is clear that a plot of the reciprocal of the absorbance of the organic phase following extraction versus the reciprocal of the equilibrium aqueous phase dye concentration at a constant concentration of  $X^{-}$  should be linear for a given concentration of the surfactant, the dye concentration being varied. The intercept of this line at  $1/A_0$  axis is given by

$$\frac{1}{\epsilon_{RD}Ct} + \frac{K_2}{K_E\epsilon_{RD}Ct} = \frac{1}{\epsilon_{RD}Ct} \left\{ 1 + \frac{(R_4N^+D^-)_w}{(R_4N^+D^-)_0} \right\} \quad (24)$$

where  $\epsilon_{RD}$  is the molar absorptancy index of the dye surfactant salt RD. The intercept should depend on the amine class and chain length, since the partition coefficient  $(R_4N^+D^-)_w/(R_4N^+D^-)_0$  is dependent on these two factors. The slope of the plot will however depend on the nature of the counteranion  $X^-$  and is determined by the degree of preference the surfactant ions exhibit for the counteranions  $X^-$  and for the anionic dye for extraction into the organic phase. Both  $X^-$  and  $D^-$  compete with each other for extraction by  $R_4N^+$ . With the use of disulfine blue dye we have achieved the predicted results for extraction into chloroform. These will be published elsewhere.

### Polymeric Ammonium or Quaternary Ammonium Salts

For polymers the relevant expression for dye extraction is



where **P** represents the polymeric chain attached to nitrogen and the **R** may be alkyl groups or hydrogen atoms. All other notations have the same meaning as above. A treatment analogous to that above furnishes the equation

$$\frac{1}{A_0} = \frac{1}{\epsilon_{RD}Ct} + \frac{[X^-]_w}{\epsilon_{RD}CtK_E[D^-]_w} \quad (26)$$

Here **RD** stands for  $PR_3N^+D^-$ , and  $A_0$  is, as usual, the absorbance of the organic phase corrected for the blank. All other symbols have been previously defined. The intercept for the  $1/A_0$  versus  $1/[D^-]_w$  plot is given by  $1/\epsilon_{RD}Ct$ . The reciprocal of the intercept corresponds to the organic phase absorbance when the polymeric ammonium or quaternary ammonium salt is completely converted to the dye polymer ion pair and completely extracted into the organic solvent. The intercept for a given concentration of the polymeric amine should be independent of the amine class and chain length, since no assumption prejudicial to that effect was made for this treatment. The intercept expression for the polymer also follows from that of the surfactant [eq. (24)] when it is considered that the partition coefficient  $(R_4N^+D^-)_w/(R_4N^+D^-)_0$  is zero for a water insoluble polymer. The slope of the plot may, however, depend on the nature of the amine in as much as  $K_E$  depends on it.

For the estimation of polymeric ammonium or quaternary ammonium salts it is necessary to perform a few dye extraction experiments at fixed polymer and varying dye concentration. The counteranion concentration should also remain constant. This is achieved by performing the experiments at fixed acidity. Presence of a 0.01 or 0.001*N* mineral acid is necessary to avoid hydrolysis when amine or ammonium salt is to be estimated.



The reciprocal of the organic phase absorbance after blank correction is plotted against the reciprocal of the anionic dye concentration in the aqueous phase at equilibrium according to eq. (26). The desired amine concentration is then obtained from the intercept when the molar absorptancy index  $\epsilon_{RD}$  of the dye polymer ion pair is known.

The required value of this absorptancy index was obtained by following this intercept method and using a water-insoluble amine salt as the extractant. We used trilaurylammonium hydrochloride as the extractant and disulfine blue VN 150 as the dye. The experimental results for this system are given in Figure 1. The value of  $\epsilon_{RD}$  in chloroform at 630 nm determined from the intercept of the lines at  $1/A_0$  axis (Fig. 1) is  $1.28 \times 10^5$  l./mole-cm.

It should be noted here that disulfine blue is a pH indicator dye.  $D^-$  stands for the base form of this dye which has an absorption peak at 640 nm in aqueous solution; the corresponding acid form does not absorb at this wavelength. The molar absorptancy index of the base form at 640 nm is 96,220 l./mole-cm. Therefore, the data for the abscissa of Figure 1 are obtained from the measurement of the absorbance of the equilibrium aqueous phase at 640 nm. The applicability of eq. (26) also suggests that one disulfine blue ion requires one ion of the cationic extractant for extraction into the organic phase.

### Some Test of the Equations

A few tests of the equations derived in this paper are given. Figure 2 shows that the reciprocal of the organic phase absorbance versus the reciprocal of the methylene blue concentration at equilibrium in the aqueous phase is linear at fixed concentrations of sodium lauryl sulfate (NaLS). The intercepts are inversely proportional to NaLS concentration as required by eq. (14).

Figure 1 shows eq. (26) is applicable when, for example, trilaurylammonium hydrochloride and disulfine blue were used as the extractant and the dye, respectively. The effect of the nature, as well as the concentration, of the counter anion on the slope of the plot is consistent with eq. (26).  $K_E$  [eq. (25)] is obviously larger when the counteranion is sulfate than when it is chloride. The intercept is, as expected, independent of the nature of the acid present in the system. The lower slope in  $H_2SO_4$  acidified system (Fig. 1) suggests that  $H_2SO_4$  should be preferred when amine is to be estimated by this intercept method, since a lower slope minimizes the error in determining the intercept.

### General Comments

It should be noted that the equations derived in this paper are valid when the extractant ion binds with one dye ion. If a different stoichiometry is operative, necessary modifications should be made.



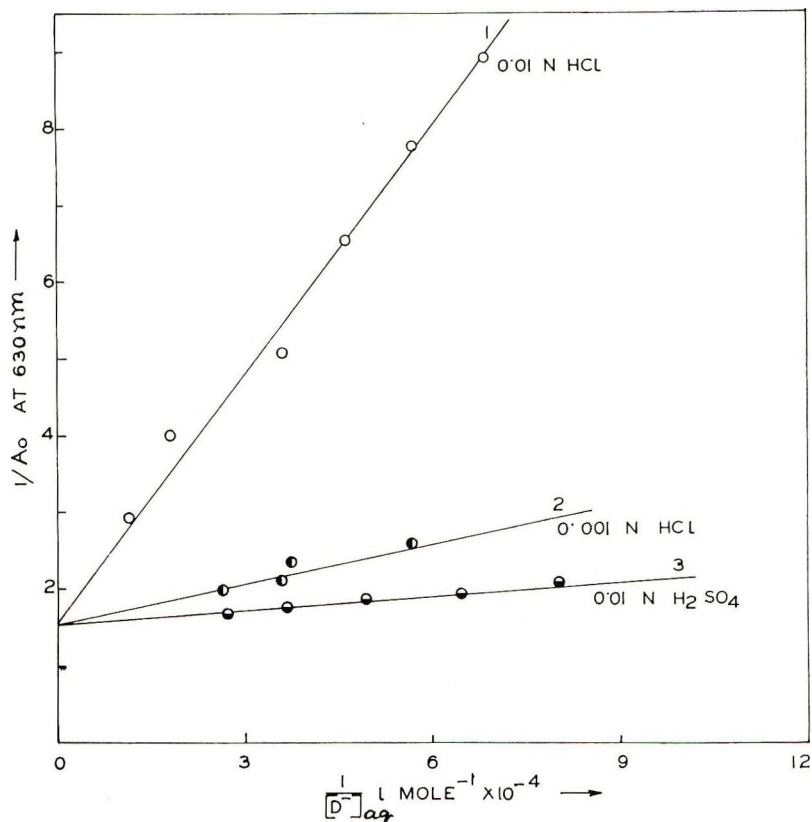


Fig. 1. Extraction of disulfine blue VN150 from various acid solutions into chloroform by triaurylammonium salts ( $1 \times 10^{-6}$  mole/l.).  $A_0$  values are for measurements in 5 mm cell.

Again, the theoretical treatment is based on the assumption that the extracted species exists as an ion pair. The solvent and the concentration of the extracted species determine their states of existence. For example, Diamond et al.<sup>10,11</sup> showed for triaurylammonium salts that they exist either as ion pairs or as still-higher ion aggregates (depending on concentration) in organic solvents of low dielectric constant. The highest concentration below which no association beyond ion pairing takes place depends upon the character of the solvent. Dielectric constant as well as specific chemical effects control such phenomena. For solvents such as chloroform, chlorobenzene, *o*-dichlorobenzene, and anisole the concentrations permitting aggregation of ion pairs are much larger than those usually employed ( $10^{-6}$  to  $10^{-5}$  molar) in the dye partition method of estimation. Benzene is intermediate in this regard. The proposed method should be applicable to a polymer regardless of its polarity and chain length as long

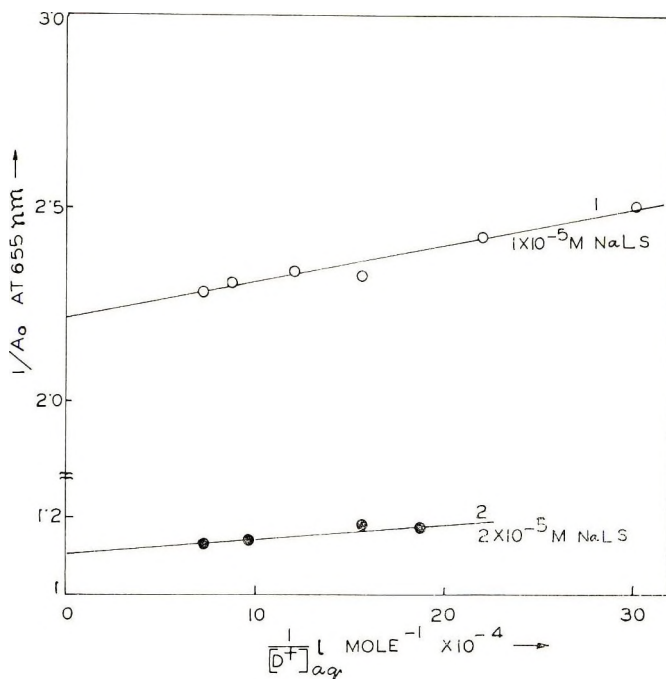


Fig. 2. Extraction of methylene blue from 0.01*N* HCl into chloroform by NaLS. NaLS concentrations indicated.  $A_0$  values are for measurements in 5 mm cells.

as the solvent used and the concentration of the polymer do not allow aggregation of the extracted dye polymer ion pair.

It should be noted that eqs. (13), (18), (20), and (26) require that the proposed plot of the reciprocal of the organic phase absorbance versus the reciprocal of the aqueous dye concentration for a given concentration of the extractant should be made at a fixed counterion (other than the dye ion) concentration of the extractant. Since the concentration of the extractant used is of the order of  $10^{-6}$ – $10^{-3}M$ , a  $10^{-3}M$  counterion concentration should be sufficient. Thus, the presence of  $10^{-2}N$ , preferably  $10^{-3}N$  acid would be adequate. The low acidity is preferable because in dilute solution the assumption of unit activity coefficients for the various species will be valid.

A further point is noteworthy. Some ionic dyes polymerize and exhibit metachromacy with increasing concentration. The proposed plots require that only the monomeric dye concentration be used. With metachromatic dyes, such as methylene blue, very dilute dye solutions should therefore be used.

The authors are grateful to Messers Rhône-Poulenc for a gift sample of triaurylamine and to Imperial Chemical Industries (London) for a gift sample of disulfine blue VN 150.

### References

1. S. R. Palit and B. M. Mandal, *J. Macromol. Sci.-Revs.*, **C2**, 225 (1968).
2. P. Mukerjee, *Anal. Chem.*, **28**, 870 (1956).
3. S. R. Palit, *Makromol. Chem.*, **36**, 89 (1959); *ibid.*, **38**, 96 (1960).
4. P. Ghosh, S. C. Chadha, A. R. Mukherjee, and S. R. Palit, *J. Polym. Sci. A*, **2**, 4433 (1964).
5. G. Roy, B. M. Mandal, and S. R. Palit, paper presented at the Symposium on Polymer Colloids, American Chemical Society Meeting, Chicago, Ill., September 13-18, 1970.
6. P. Mukerjee and K. J. Mysels, *J. Amer. Chem. Soc.*, **77**, 2937 (1955).
7. A. Mukherjee and P. Mukerjee, *J. Appl. Chem.*, **12**, 127 (1962).
8. A. V. Few and R. H. Ottewill, *Colloid Sci.*, **11**, 34 (1956).
9. S. Maiti and M. K. Saha, *Sci. Cult. (Calcutta)*, **32**, 249 (1966).
10. J. J. Bucher and R. M. Diamond, *J. Phys. Chem.*, **69**, 1565 (1965).
11. W. Müller and R. M. Diamond, *J. Phys. Chem.*, **70**, 3469 (1966).

Received April 7, 1971

Revised June 15, 1971

## Mechanism of Propagation and Degenerate Chain Branching in the Oxidation of Polypropylene and Polyethylene

N. V. ZOLOTOVA and E. T. DENISOV, *Institute of Chemical Physics, Moscow, USSR*

### Synopsis

Samples of polypropylene with adjacent and isolated hydroperoxide groups have been prepared. The rate constants of free-radical formation from solid hydroperoxides were measured by the inhibitor method. It was found that the free radicals yielded by adjacent hydroperoxide groups are formed more rapidly. The main reaction of free-radical formation in oxidized polypropylene is of the type:  $\text{ROOH} + \text{ROOH} \rightarrow \text{RO}^\cdot + \text{H}_2\text{O} + \text{RO}_2^\cdot$ . The average yield of free radicals from polypropylene hydroperoxide is 2-4%. Oxygen has no effect on the yield of free radicals. However, the pressure of oxygen  $P_{\text{O}_2}$  affects the rate of degenerate chain branching in polypropylene. The number of adjacent hydroperoxide groups and the rate of initiation increase with  $P_{\text{O}_2}$ . Consequently, a reaction of the type,  $\text{R}^\cdot + \text{RH} \rightarrow \text{RH} + \text{R}^\cdot$ , plays an important part in transport of free valence through solid polymer. This reaction is very fast in polyethylene, and no adjacent hydroperoxide groups are formed. The free radicals from polyethylene hydroperoxide are found to form by a reaction of the type:  $\text{ROOH} \rightarrow \text{RO}^\cdot + \text{HO}^\cdot$ .

### INTRODUCTION

Hydroperoxide groups formed by oxidation of polymers play an important part in the mechanism of oxidation. When decomposing to free radicals, these groups induce autoinitiation of chain oxidation. The decomposition of hydroperoxide groups of polypropylene (PPH) was studied by several investigators.<sup>1-7</sup> Two mechanisms of free radical formation were discussed.

It will be noted that conclusions concerning the mechanism of formation of free radicals from PPH in the solid phase were drawn from indirect experimental data (kinetics of oxygen consumption, disappearance of hydroperoxide groups). Reliable conclusions can also be made from direct experimental measurements of the rates of free-radical formation in solid polymer. The inhibitor can be used for this purpose. The present investigation is devoted to rate constants of free-radical formation from PPH and polyethylene hydroperoxide (PEH).

Oxygen pressure plays an important part in PP oxidation. While the rate of hydrocarbon oxidation does not depend upon  $P_{\text{O}_2}$ , the rate of autooxidation of PP increases with  $P_{\text{O}_2}$ .<sup>1,3,8</sup> It is suggested that the oxygen molecule enters the cage to react with one of the radicals and increase the yield of

free radicals from the cage.<sup>1</sup> No direct verification of this hypothesis has been made. The contribution of  $P_{O_2}$  to the mechanism of propagation and free-radical formation in the oxidation of solid PP and PE was investigated.

## EXPERIMENTAL

Commercial isotactic polypropylene (PP) with  $\bar{M}_v = 4.2 \times 10^5$  (measured viscometrically in decalin at 135°C) was purified by precipitation from its solution in xylene after adding ethanol at 120°C. Hydroperoxide of PP (PPH) was produced by oxidation of 2% PP solution in chlorobenzene or cumene (not actually a solution but PP in a swollen state) for 3–6 hr at 110°C with methyl ethyl ketone peroxide as initiator with intensive oxygen sparging. The yield of hydroperoxide groups was 0.065–0.65 mole/kg. Oxidation of PP in cumene yielded PPH<sub>i</sub> with isolated hydroperoxide groups. Oxidation of PP in chlorobenzene gave PPH<sub>a</sub> with many adjacent hydroperoxide groups. The samples of solid PP with dicumyl peroxide ROOR were prepared as follows.

A 1-g portion of PP was dissolved in chlorobenzene at 120°C, a solution of ROOR in chlorobenzene was added, and after agitation the solution was poured out on a glass. The PP film was 10–20  $\mu$  thick, [ROOR] was  $7 \times 10^{-2}$ – $23 \times 10^{-2}$  mole/l. Inhibitors were introduced in the same way.

The rate  $W_i$  of free-radical formation from PPH in a chlorobenzene solution (0.1–0.2%) has been measured by the inhibitor method. As it is often impossible to estimate  $k_i$  of hydroperoxide from the induction period the initial rate of inhibitor consumption  $W_{InH}$  was measured in the presence of PPH, and  $W_i$  was found to be  $W_i = fW_{InH}$  ( $f$  is the stoichiometric coefficient of inhibition). The inhibitor was introduced in a concentration ensuring termination of all chains, so that  $k(RO_2 \cdot + InH) [InH] \gg [k(RO_2 \cdot + RO_2 \cdot)W_i]^{1/2}$ , and actually  $W_i = fW_{InH}$ . The following inhibitors were used;  $\alpha$ -naphthol ( $f = 2$ ), phenyl- $\beta$ -naphthylamine ( $f = 4$ ),  $N,N$ -di- $\beta$ -naphthyl- $p$ -phenylenediamine ( $f = 2$ ). The latter appeared to react with hydroperoxide groups with a rate coefficient  $k' = 6.0 \times 10^7 \exp\{-15000/RT\}$  l./mole-sec. This was taken into account in calculating  $W_i:W_i = f(W_{InH} - k' [PPH][InH])$ . Analysis was made using the following methods.  $\alpha$ -Naphthol was transformed into a colored compound by diazotization and coupling with  $p$ -sulphophenyldiazoniumsulfate, the concentration of this compound was estimated spectrophotometrically at  $\lambda = 536$  nm ( $\epsilon = 2.1 \times 10^3$  l./mole-cm). Phenyl- $\beta$ -naphthylamine was analyzed spectrophotometrically at  $\lambda = 309$  nm ( $\epsilon = 1.6 \times 10^4$  l./mole-cm). In the presence of dinaphthyl- $p$ -phenylenediamine, the rate of formation of dinaphthyl- $p$ -phenylenequinonediimine was measured spectrophotometrically at  $\lambda = 485$  nm ( $\epsilon = 1.1 \times 10^4$  l./mole-cm). With a solid polymer, the inhibitor was extracted with chlorobenzene and then analyzed.

The rate of free-radical formation in solid PPH was evaluated from the initial rate of oxygen consumption  $W$ . In the absence of inhibitor  $W$



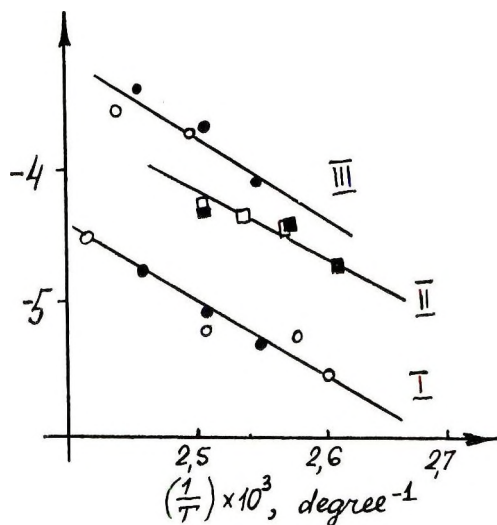


Fig. 1. Arrhenius plots of  $k_i$ : (I) for  $k_i(P_{il})$  and  $k_i(P_{is})$ ; (II) for  $k_i(P_{al})$  and  $k_i(P_{as})$ ; (III) for  $k_d(P_{il})$  and  $k_d(P_{is})$ ; (○) solid state and (●) liquid phase.

$\sim \sqrt{W_i}$ . The coefficient of proportionality between  $W$  and  $\sqrt{W_i}$  was measured when PP was oxidized in the presence of dicumyl peroxide ROOR. The rate of free-radical formation from ROOR in solid PP was measured by the inhibitor method. The rate constant of initiation by hydroperoxide groups of PP was calculated as

$$k_i(P_s) = (W_{PPH}^2/[PPH_s])(k_{i,ROOR}[ROOR]/W_{ROOR}^2)$$

where  $W_{PPH}$  and  $W_{ROOR}$  are the rates of  $O_2$  consumption in experiments with PPH and ROOR, respectively.

The consumption of  $O_2$  from air was measured manometrically. The  $k_i$  values obtained are given in Tables I and II and in Figure 1. As seen from Table II and Figure 1, the values of  $k_i(P_{il})$  (measured by the inhibitor method in a solution of chlorobenzene) and  $k_i(P_{is})$  (measured by oxygen consumption in the solid state) are almost just  $k_i(P_{al})$  and  $k_i(P_{as})$ . The rate coefficient of PEH decomposition of free radicals was measured by the inhibitor method in the solid as well as in the liquid phase. The rate constant of hydroperoxide group decomposition  $k_d$  was estimated by its disappearance in the absence of oxygen. Hydroperoxide groups were analyzed iodometrically.

## RESULTS AND DISCUSSION

### Formation of Free Radicals from Isolated and Adjacent Hydroperoxide Groups

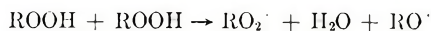
Hydroperoxides of hydrocarbons are known to decompose to free radicals by unimolecular and bimolecular reactions:<sup>10</sup>

TABLE I  
Rate Constants of Decomposition of Dicumyl Peroxide ROOR and PPH with Isolated (i) and Adjacent (a)  
Hydroperoxide Groups in the Solid (s) and Liquid (l) Phase

Temp, °C	$k_i[\text{ROOR}]_{is}$ $\text{sec}^{-1}$ (method of inhibitors)	$\frac{W_{O_2}}{\sqrt{[\text{ROOR}]_{is}}}$ $\frac{\text{mole}^{1/2}}{\text{kg}^{1/2}\text{-sec}}$	$\frac{W_{O_2}}{\sqrt{[\text{PPH}]_{is}}}$ $\frac{\text{mole}^{1/2}}{\text{kg}^{1/2}\text{-sec}}$	$\frac{W_{O_2}}{\sqrt{[\text{PPH}]_{as}}}$ $\frac{\text{mole}^{1/2}}{\text{kg}^{1/2}\text{-sec}}$	$k_i(P_{is})$ $\text{sec}^{-1}$ ( $O_2$ consumption)	$k_i(P_{il})$ $\text{sec}^{-1}$ (method of inhibitors)	$k_i(P_{as})$ $\text{sec}^{-1}$ ( $O_2$ consumption)	$k_i(P_{al})$ $\text{sec}^{-1}$ (method of inhibitors)
110	$3.5 \times 10^{-6}$	$6.3 \times 10^{-5}$	$5 \times 10^{-5}$	$1.4 \times 10^{-4}$	$2.2 \times 10^{-6}$	$1.6 \times 10^{-6}$	$1.7 \times 10^{-5}$	
115	$1.0 \times 10^{-5}$	$1.0 \times 10^{-4}$	$7.1 \times 10^{-5}$	$1.9 \times 10^{-4}$	$5.0 \times 10^{-6}$	$3.0 \times 10^{-6}$	$3.6 \times 10^{-6}$	$3.5 \times 10^{-5}$
120	$1.8 \times 10^{-5}$	$2.0 \times 10^{-4}$	$1.4 \times 10^{-4}$	$3.2 \times 10^{-4}$	$8.8 \times 10^{-6}$	$4.5 \times 10^{-6}$	$4.6 \times 10^{-6}$	
125	$3.2 \times 10^{-5}$	$3.0 \times 10^{-4}$	$1.3 \times 10^{-4}$	$4.0 \times 10^{-4}$	$6.0 \times 10^{-6}$	$7.3 \times 10^{-6}$	$5.7 \times 10^{-6}$	$4.2 \times 10^{-6}$
130	$7.6 \times 10^{-5}$	$3.5 \times 10^{-4}$	$1.8 \times 10^{-4}$	$5.6 \times 10^{-4}$	$2.0 \times 10^{-5}$	$1.1 \times 10^{-5}$	$2.0 \times 10^{-4}$	
140	$1.4 \times 10^{-4}$	$6.4 \times 10^{-4}$	$3.2 \times 10^{-4}$		$3.4 \times 10^{-5}$	$2.8 \times 10^{-5}$		

TABLE II  
 The Rate Constants

No.	$k$	Temp, °C	$k$ , sec <sup>-1</sup>	$k$ (125°C), sec <sup>-1</sup>
1	$k_i(P_{11})$	119-134	$2.5 \times 10^{12} \exp$ $\{-32000/RT\}$	$6.6 \times 10^{-6}$
2	$k_i(P_{18})$	115	$5.0 \times 10^{-6}$	$6.0 \times 10^{-6}$
3	$k_i(P_{a1})$	115	$3.5 \times 10^{-5}$	$4.2 \times 10^{-5}$
		125	$4.2 \times 10^{-5}$	$5.7 \times 10^{-5}$
4	$k_i(P_{as})$		$2.4 \times 10^6 \exp$ $\{-19000/RT\}$	
5	$k_a(P_{11})$	119-134	$3.8 \times 10^{10} \exp$ $\{-26000/RT\}$	$2.0 \times 10^{-4}$
6	$k_a(P_{is})$	135	$2.6 \times 10^{-4}$	
		125	$1.8 \times 10^{-4}$	$1.8 \times 10^{-4}$
7	$k_a(P_{a1})$	125	$6.0 \times 10^{-4}$	$6.0 \times 10^{-4}$
8	$k_i(E)$	78-130	$1.6 \times 10^{14} \exp$ $\{-35000/RT\}$	$1.0 \times 10^{-5}$
9	$k_a(E)$	90-130	$8.5 \times 10^{15}$ $\{-35000/RT\}$	$5.4 \times 10^{-4}$



The second reaction is energetically more advantageous than the first. Isolated as well as adjacent hydroperoxide groups are produced in PP oxidation. To clear up the role of isolated and adjacent OOH groups, two PPH samples were prepared.

PPH produced by oxidation of PP in chlorobenzene contains many adjacent hydroperoxide groups linked by hydrogen bonds, PPH<sub>a</sub>, as established by Chien.<sup>9</sup>

The PPH with isolated hydroperoxide groups PPH<sub>i</sub> was synthesized by co-oxidation of PP with cumene. Under these conditions peroxy radicals of cumene attack the C—H bonds of PP. The peroxy radical of PP attacks the cumene molecule more readily than the C—H bond of PP (the C—H bond of cumene is more reactive than that of PP); therefore the PPH formed contains preferentially isolated hydroperoxide groups. It is seen from Table II that the PPH<sub>i</sub> decay to free radicals is slower than that of PPH<sub>a</sub> [at 125°  $k_i(P_{as})$  is nearly ten times higher than  $k_i(P_{is})$ ], i.e., the adjacent hydroperoxide groups decompose more readily than the isolated ones. Thus, decay of adjacent hydroperoxide groups is the main reaction of degenerate chain branching in PP oxidation.

### Role of P<sub>O</sub><sub>2</sub> in Autoxidation of PP

Chain termination in initiated oxidation of solid polymers proceeds by reaction between two peroxide radicals, provided the polymer films are sufficiently thin. This follows from independence of the oxidation rate of P<sub>O</sub><sub>2</sub> (for example, see oxidation of PE<sup>11</sup>). On the contrary, autoxidation

of PP becomes faster with increasing  $P_{O_2}$ .<sup>1,3,8,12</sup> This was suggested to be connected with participation of  $O_2$  in the process of free radical exit of the cage.<sup>1</sup> If this is the case, the rate of formation of free radicals in the presence of oxygen must be higher than that in its absence. However rate of disappearance of the inhibitor of the reaction with free radicals is the same both in the presence and in the absence of  $O_2$  in the liquid and in the solid state (Fig. 2). Thus, oxygen does not participate in the formation of free radicals from hydroperoxide and their exit from the cage.

As was shown above, when two hydroperoxide groups are adjacent, they decay to free radicals more rapidly than isolated groups. In this connection, the following hypothesis about the mechanism of solid polymer oxidation can be proposed. Peroxy radicals formed in oxidation of PP attack the nearest C—H bond which may be either the  $\beta$  C—H bond of the same molecule or the C—H bond of another molecule. As a result the hydroperoxide group and alkyl radical become adjacent. The alkyl radical can react with oxygen or with the nearest C—H bond. In the first case two adjacent hydroperoxide groups arise. The reaction of alkyl radical with the C—H bond yields a single hydroperoxide group. In other words, the competition of two reactions plays an important part in oxidation of PP:

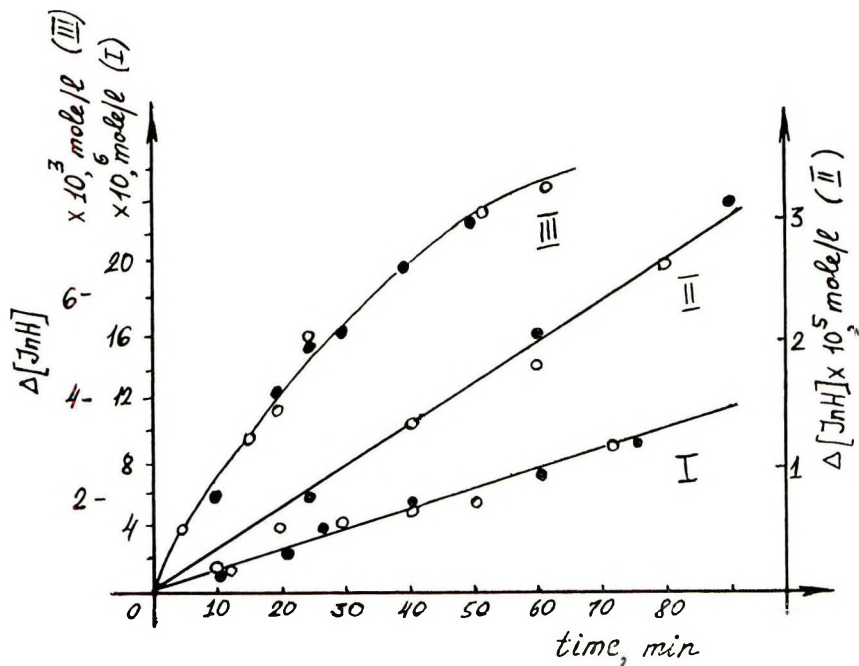
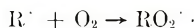
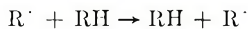


Fig. 2. Kinetics of inhibitor consumption in (○) the presence and (●) in the absence of oxygen in experiments with hydroperoxides: (I) PPH in a chlorobenzene solution,  $T = 120^\circ\text{C}$ , InH =  $\alpha$ -naphthol; (II) PEH in a chlorobenzene solution,  $T = 110^\circ\text{C}$ , InH =  $N,N'$ -di- $\beta$ -naphthyl- $p$ -phenylenediamine; (III) PPH in the solid state,  $T = 120^\circ\text{C}$ , InH- $\alpha$ -naphthol.

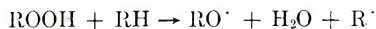
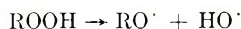


The first reaction can be very important in co-oxidation of hydrocarbons.<sup>13</sup> The ratio of adjacent to isolated hydroperoxide groups must depend upon  $P_{O_2}$ . The probability of formation of adjacent hydroperoxide groups, the rate of free-radical formation, and thus the rate of oxidation increase with  $P_{O_2}$ . If this hypothesis is reliable, the higher  $P_{O_2}$ , the greater must be the rate constant of free-radical formation from hydroperoxide groups. Therefore a dependence between  $k_i$  and  $P_{O_2}$  at which this PPH was produced must be observed. To verify this hypothesis, samples of PPH were produced by oxidation of solid PP at different  $P_{O_2}$ , and the rates of free-radical formation were measured by the inhibitor method in chlorobenzene solution. It was found that  $k_i$  increased with  $P_{O_2}$  at which PP was oxidized (Fig. 3). Therefore the role of  $P_{O_2}$  in the oxidation of solid PP consists in formation of adjacent hydroperoxide groups. The ratio  $[ROOH]_{\text{adjac}}/[ROOH]_{\text{isol}}$  is higher and the oxidation is faster with higher  $P_{O_2}$ .

The  $k_i$  value for decomposition of PEH to free radicals is the same for PEH produced by oxidation of PE in chlorobenzene, by oxidation of PE in cumene, by oxidation of solid PE at 1 atm  $O_2$  and at 10 atm  $O_2$ . Consequently, the oxidation of PE yields isolated hydroperoxide groups.

### Formation of Free Radicals from Isolated Hydroperoxide Groups

The isolated hydroperoxide groups can decay to radicals by the reactions:<sup>10</sup>



When free radicals are formed by the first reaction,  $k_i(P_{is})$  and  $k_i(E_S)$  can be

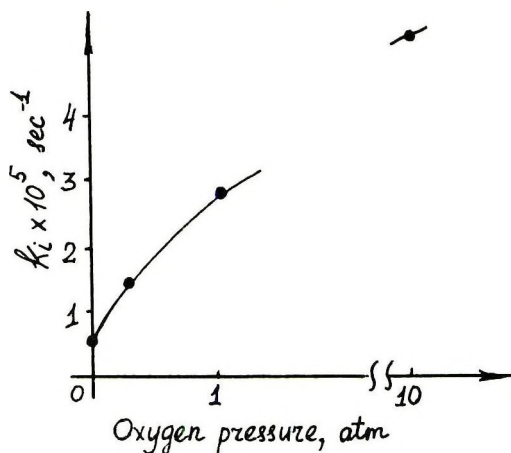


Fig. 3. Dependence of  $k_i$  (measured by inhibitor method in chlorobenzene solution at 120°C) on  $P_{O_2}$  at which PP was oxidized in solid state at 120°C. The point at  $P_{O_2} = 0$  corresponds to PPH, produced by oxidation of PP in cumene solution.



TABLE III  
Rate Constants of Hydroperoxide Decomposition

No.	Constants	Temp, °C	$k_d$ , sec <sup>-1</sup>	$E$ , kcal/mole	$k_d$ (at 130°C), sec <sup>-1</sup>	Reference
1	$k_d(P)$	90-120	$1.0 \times 10^{13} \exp \left\{ -\frac{27700}{RT} \right\}$	27.7	$2.4 \times 10^{-3}$	3
2	$k_d(P)$	130	$8.4 \times 10^{-4}$	—	$8.4 \times 10^{-4}$	1
3	$k_d(P)$	130	$7.3 \times 10^{-4}$	27.8	$7.3 \times 10^{-4}$	1
4	$k_d(P)$	130	$7.0 \times 10^{-4}$	$25 \pm 2$	$7.0 \times 10^{-4}$	2
5	$k_d(P)$	110-140	$4 \times 10^8 \exp \left\{ -\frac{23000}{RT} \right\}$	23	$1.0 \times 10^{-3}$	4
6	$k_d(E)$	100-120		25	$1.7 \times 10^{-4}$ (120°C)	4
7	$k_d(P_{11}) = k_d(P_{1a})$	119-134	$3.8 \times 10^{10} \exp \left\{ -\frac{26000}{RT} \right\}$	26	$3.4 \times 10^{-4}$	Present
8	$k_d(P_{a1})$	125	$6.0 \times 10^{-4}$		$6.0 \times 10^{-4}$ (125°C)	paper
9	$k_d(E)$	90-130	$8.5 \times 10^{15} \exp \left\{ -\frac{35000}{RT} \right\}$	35	$8.5 \times 10^{-4}$	"

close. When the second reaction is predominant as suggested by Pudov and Neiman,<sup>2</sup>  $k_i(P_{is}) \gg k_i(E_s)$ , the C—H bond in PP is weaker than that in PE. Experimental data are in favor of the first mechanism, as  $k_i(P_{is}) \approx k_i(E_s)$ , and contradict the second.

The close  $k_i$  values for the polymer OOH group and for *tert*-butyl hydroperoxide ( $k_i = 3.6 \times 10^{12} \exp\{-33000/RT\}$ ,  $\text{sec}^{-1}$  at  $125^\circ\text{C}$ ,  $k_i = 3 \times 10^{-6}$  as measured by the inhibitor method in chlorobenzene<sup>14</sup>) are consistent with the first reaction. Activation energies for  $k_i(P_{is})$  and  $k_i(E_s)$  are very close to those of the O—O bonds in hydroperoxides.

It is interesting to note that  $k_i(P_{is})$  and  $k_i(P_{il})$  are close; consequently  $k_i$  does not depend on the polymer phase. This may be simply explained by the high activity of the hydroxyl formed. Hydroxyl reacts with C—H bonds of organic compounds with  $k \approx 10^9$  l./mole-sec. Therefore the exit of free valence from the cage is very fast and does not depend on viscosity.

### Decomposition of Hydroperoxide Groups

The decay of OOH groups in polymer in the absence of  $\text{O}_2$  is considerably faster than the formation of free radicals coming out of the cage (Table II). The rate constants  $k_d$ , estimated by various authors are fairly close (Table III). The ratio  $k_i/2k_d$  at  $125^\circ\text{C}$  is  $1.8 \times 10^{-2}$  for PPH<sub>i</sub>,  $3.5 \times 10^{-2}$  for PPH<sub>a</sub>,  $9 \times 10^{-3}$  for PEH. These values differ from those reported by Chien et al.,<sup>4</sup> however not for the solid state. Inhibitors have no appreciable effect on  $k_d$ .<sup>4</sup> The above facts may be explained in the following way.

When the hydroperoxide group decomposes to  $\text{RO}^\cdot$  and  $\text{HO}^\cdot$  radicals, the latter diffuses or reacts very readily with the C—H bond, and the probability of the free valence outcome from the cage is very high. When two adjacent peroxide groups decompose to form  $\text{RO}^\cdot$  and  $\text{RO}_2^\cdot$  which cannot recombine with formation of a stable molecule, the probability of free valence outcome from the cage will be expected to be higher. The reaction of hydroperoxide group with the C—H bond can be assumed to be the main reaction of decomposition of hydroperoxide groups without initiation of chains. The latter is accounted for by fast recombination of the macroradicals  $\text{RO}^\cdot$  and  $\text{R}^\cdot$ .

### References

1. V. S. Pudov, B. A. Gromov, E. G. Sklyarova, and M. B. Neiman, *Neftekhimika*, **3**, 743 (1963).
2. V. S. Pudov and M. B. Neiman, *Neftekhimika*, **2**, 918 (1962).
3. V. V. Dudorov, Thesis Cand. Sci., Gorkii State University, 1964.
4. J. C. W. Chien, E. J. Vandenberg, and H. Jabloner, *J. Polym. Sci. A-1*, **6**, 25, 381, 393 (1968).
5. M. B. Neiman, *Usp. Khim.*, **33**, 28 (1964).
6. V. S. Pudov and M. B. Neiman, *Starenije i Stabilizatsiya Polimerov*, Nauka, Moscow, 1966, p. 5.
7. V. S. Pudov and A. L. Buchachenko, *Usp. Khim.*, **39**, 130 (1970).

8. M. Yukio and E. Hirofumi, *Kobunshi Kagaku*, **21**, 441 (1964).
9. J. C. W. Chien, E. J. Vandenberg, and H. Jabloner, *J. Polym. Sci. A-1*, **6**, 375 (1968).
10. N. M. Emanuel, E. T. Denisov, and Z. K. Maizus, *Liquid-Phase Oxidation of Hydrocarbons*, Plenum Press New York, 1967.
11. Yu. V. Shilov and E. T. Denisov, *Vysokomol. soedin.*, **9**, 1812 (1969).
12. C. R. Boss and J. C. W. Chien, *J. Polym. Sci. A-1*, **6**, 1543 (1966).
13. V. S. Rafikova, I. P. Skibida, Z. K. Maizus, and N. M. Emanuel, *Dokl. Akad. Nauk SSSR*, **182**, 357 (1968).
14. E. T. Denisov, *Dokl. Akad. Nauk SSSR*, **146**, 394 (1968)

Received November 16, 1970

Revised June 15, 1971

## Low-Temperature Polyesterification in the Presence of Tertiary Amines

S. V. VINOGRADOVA, V. A. VASNYEV, T. I. MITAISHVILI,  
AND A. V. VASIL'YEV, *Institute of Organo-Element Compounds,  
Moscow, U.S.S.R.*

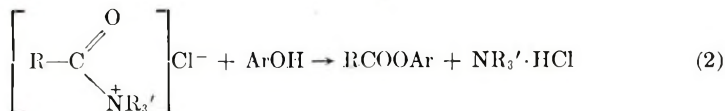
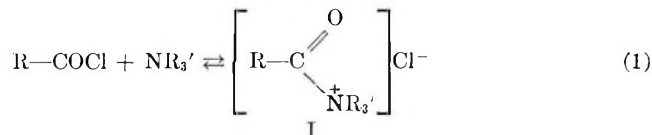
### Synopsis

Several variations of catalysis (nucleophilic and general basic) responsible for the low-temperature polyesterification in solution have been investigated. The type of catalysis which predominates depends on the chemical structure of the initial reagents and the reaction conditions. Increasing basicity of the tertiary amine and increasing acidity of the bisphenol promote the general base catalysis.

### Results and Discussion

Polycondensation of dicarboxylic acid chlorides with diols in the presence of tertiary amines offers a means of obtaining polyesters at low temperatures. Formally it could be suggested that tertiary amine would act as a hydrogen chloride acceptor in this reaction, shifting the equilibrium so as to form ester bonds. However, it was shown that even in the case when hydrogen chloride is under pressure in the system, the equilibrium constant of the reaction of phenyl benzoate with HCl in ditolylmethane at 40°C is as low as  $2.35 \times 10^{-4}$ , which can be only an indication of practical irreversibility of the polycondensation of dicarboxylic acid chlorides with bisphenols. Thus, one must assume that the behavior of tertiary amines in a low-temperature polycondensation would be determined by their capability to catalyze this reaction.

At present, the following scheme [eqs. (1) and (2)] of nucleophilic catalysts is proposed for similar acylation reactions.<sup>2</sup>



A number of factors support this scheme. (1) Substitution of the chlo-

rine atom ( $\sigma_1 = 0.47$ ) for a more electron-accepting group  $-\text{NR}_3'$ , ( $\sigma_1 = 0.92$ ) should appreciably increase electrophilic reactivity of the carbon atom at the carbonyl group of the acid chloride reactant and thereby considerably decrease the energy barrier for its bimolecular interaction with nucleophilic phenol reactant. (2) It is known that the interaction of tertiary amines with carboxylic acid chlorides yields *N*-acylammonium compounds similar to I which act as strong acylating agents for hydroxylic groups.<sup>3,4</sup> (3) Infrared spectra and NMR data show that under low-temperature polycondensation conditions the ability of tertiary amines to form complexes with terephthaloyl chloride is related to their ability to catalyze polycondensation of the acid chloride with phenolphthalein.<sup>5</sup>

However, some data obtained may not be explained from the viewpoint of nucleophilic catalysis. Under given conditions, the molecular weight of polyarylate increased with bisphenol acidity (Fig. 1). For the series of bisphenols investigated, there is the following dependence of the coefficient of polymerization  $\bar{n}_w$  on  $\text{p}K_{a1}$ , the first acidity constant of bisphenol determined by potentiometric titration in dimethyl sulfoxide at 25°C:

$$\bar{n}_w = 1560 - 116\text{p}K_{a1} \quad (3)$$

Nevertheless, it should be noted that eq. (3) was derived for a rather narrow  $\text{p}K_{a1}$  range (12.5–13.2), and the validity of this equation for other cases remains to be solved. The common tendency found shows yet that the increasing acidity of bisphenol produces more favorable conditions for low temperature polycondensation. Some other data point to the very same fact. For instance, when using weakly acidic aliphatic diols under conditions given in Figure 1, only fairly low molecular weight polyesters may be prepared ( $\bar{n}_w < 15$ ). Copolycondensation of terephthaloyl chloride, phenolphthalein, and ethylene glycol in the molar ratio 1:1:1 in the presence of triethylamine yields practically homogeneous polyester of phenolphthalein. All these results may hardly be accounted for by the scheme of nucleophilic catalysis [eqs. (1) and (2)], when tertiary amine leads only to increasing electrophilic reactivity of the acid chloride component. According to this scheme, increasing acidity of diol (and, consequently, its decreasing basicity) should create less favorable conditions for low-temperature polyesterification, and that would be inconsistent with our data.

These results enable one to suggest that under low-temperature polyacylation a general basic catalysis would be possible:



According to the scheme of the general basic catalysis [eqs. (4)–(6)], increased acidity of the phenol component causes more favorable conditions for the acylation reaction, which explains well the results mentioned above



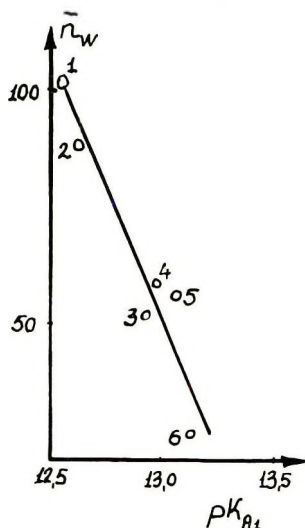
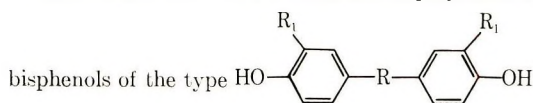


Fig. 1. Dependence of the coefficient of polymerization of polyarylates ( $\bar{n}_w$ ) on  $pK_{a1}$  of



where  $R_1$  and  $R$  may be: (1) Cl,  $\text{CH}_3\text{CCH}_3$ ; (2) H,

(3) H,

The polyarylates were obtained by method A.

(Fig. 1). Indeed, increasing acidity of the hydroxyl-containing reagent should promote the formation of its associates with tertiary amines, which is in particular confirmed by the PMR data. Thus, we found that a chemical shift of the proton of the phenol hydroxyl (concentration is 0.52 mole/l.) in the presence of an equimolar amount of triethylamine in dichloroethane would adequately be correlated to the  $pK_a$  of phenol:

$$\delta = (21.93 - 1.30 pK_a) \pm 0.40$$

$$r = 0.95 \quad (7)$$

where  $\delta$  is the chemical shift in ppm at  $34^\circ\text{C}$ ; the operating frequency is 60 Mcps on the R-12 Perkin-Elmer spectrometer;  $pK_a$  is the acidity constant of phenol measured in water at  $20^\circ\text{C}$ . It should be noted that the results given above for low-temperature polyesterification are obtained in the presence of a strong base such as triethylamine ( $pK_a = 10.87$ ). It is rather probable that the use of weaker bases, for instance, pyridine ( $pK_a = 5.23$ ) would give rise to opposite tendencies. The re-

results obtained with model reactions for competitive acylation indirectly confirm this assumption. It was found that, on reacting benzoyl chloride (0.4 mole/l.) with phenol and methanol in dichloroethane the product composition depends on the nature of tertiary amine. For instance, in the presence of equimolar amounts of triethylamine the ratio of conversion of benzoyl chloride to phenyl benzoate and to methyl benzoate equals 3.5, and in the presence of pyridine 0.18. This indicates that in with triethylamine phenol is more reactive, which agrees with the general basic catalysis, while with pyridine methanol is more reactive, which may better be explained by the nucleophilic catalysis. The results obtained with diethylaniline ( $pK_a = 6.56$ ) indicate that nucleophilic catalysis is also more probable in the presence of weakly basic tertiary amines. Really, as shown by PMR data, this tertiary amine does not form hydrogen bonds with phenol, but, nevertheless, diethylaniline assures the occurrence of the acylation reaction.<sup>7</sup>

The above data permit the suggestion that during low-temperature polyesterification in the presence of tertiary amines two catalytic pathways are possible: nucleophilic and general basic. One or the other may predominate, depending on the chemical structure of initial reagents, tertiary amines and reaction conditions. From this point of view, the results of polycondensation of terephthaloyl chloride and bis(4-oxy-3-chlorophenyl)-2,2-propane in dichloroethane solution in the presence of triethylamine may probably be of interest. The curve for reduce viscosity of this polyarylate proved to have two maxima depending on temperature (Fig. 2). It is likely that the double catalytic action of tertiary amine in this process would be responsible for this fact.

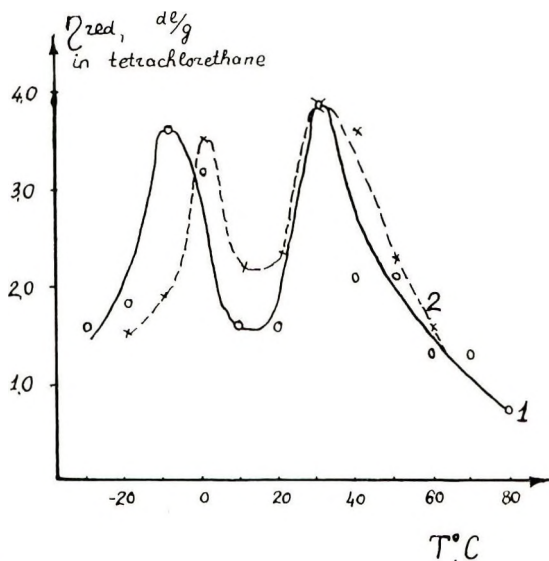


Fig. 2. Temperature dependence of the reduced viscosity of polyarylate of bis(4-oxy-3-chlorophenyl)-2,2-propane obtained by (1) method A; (2) method B.

We believe that the investigation of the kinetics of low-temperature polyesterification will give more detailed insight into several variations of catalysis initiated by tertiary amines in this process.

### Experimental

Initial condensing compounds were purified by the methods described, and their constants corresponded to literature data.<sup>8</sup> Triethylamine and pyridine were treated with benzoyl chloride.<sup>9</sup> The competitive acylation reaction was carried out in a thermostatted cell ( $\pm 0.1^\circ\text{C}$ ) by adding benzoyl chloride to phenol, methanol, and tertiary amine solution in dichloroethane. Molar ratio of the initial reagents was 1:1:1:1, respectively. Low-temperature polycondensation was performed by two methods.<sup>9</sup> In method A, terephthalic acid chloride was added to bisphenol and triethylamine solution in dichloroethane, molar ratio being 1:1:2, respectively. The initial concentration of bisphenol was 0.2 mole/l.; reaction time, 1 hr. In method B, triethylamine was added to the solution of bisphenol and terephthalic acid chloride. The reduced viscosity of a 0.5% solution of polyarylates was measured in tetrachloroethane at  $25^\circ\text{C}$ .

### References

1. R. S. Velichkova, V. V. Korshak, S. V. Vinogradova, V. A. Vasnyev, N. S. Enikolopyan, *Dokl. Akad. Nauk SSSR*, **174**, 1091 (1967).
2. M. L. Bender, *Mechanism of Catalysis of Nucleophilic Reactions of Carboxylic Acid Derivatives*, Izdatelstvo Mir, Moscow, 1964.
3. H. Adkins and O. E. Thompson, *J. Amer. Chem. Soc.*, **71**, 2242 (1949).
4. F. Klages and E. Zange, *Ann.*, **607**, 35 (1957).
5. V. V. Korshak, S. V. Vinogradova, V. A. Vasnyev, and T. I. Mitaishvili, *Vysokomol. Soedin.*, **10A**, 2182 (1968).
6. A. Albert and E. Serjeant, *Ionization Constants of Acid and Bases*, Izdatelstvo Khimiya, Moscow-Leningrad, 1964, p. 126.
7. S. V. Vinogradova, V. A. Vasnyev, E. I. Fedin, V. V. Korshak, *Izv. Akad. Nauk SSSR, Ser. Khim.*, **1967**, 1620.
8. S. V. Vinogradova, V. A. Vasnyev, and V. V. Korshak, *Vysokomol. Soedin.*, **9B**, 522 (1967).
9. S. V. Vinogradova, V. A. Vasnyev, V. V. Korshak, and T. I. Mitaishvili, *Vysokomol. Soedin.*, **11A**, 73 (1969).

Received September 30, 1970

Revised June 30, 1971

## Rotational Mobility of Nitroxyl Radicals in Polyesters

SUSAN C. GROSS, *Research Laboratories, Eastman Kodak Company  
Rochester, New York 14650*

### Synopsis

Rotational mobility of nitroxyl radicals in polyester films was investigated at temperatures from  $-180$  to  $+240^{\circ}\text{C}$  by ESR spin-probe techniques. Evidence obtained indicated that mobility of radicals was related to polymer structure and reflected increased volume made available to the probe molecule by the polymer matrix. A single correlation time, which followed the form  $\tau_c = \tau_0 \exp\{E_a/RT\}$ , was calculated for the temperature range of rapid reorientation ( $\sim 10^9$  Hz) of nitroxyl radicals.  $E_a$  ranged from 5 to 25 kcal/mole for various systems. Uniaxially oriented semicrystalline polymer matrix restricted radical mobility to a greater extent than a semicrystalline biaxially oriented sample. Effective local viscosity encountered by a nitroxyl radical in several polymers was calculated as 9–13 poise.

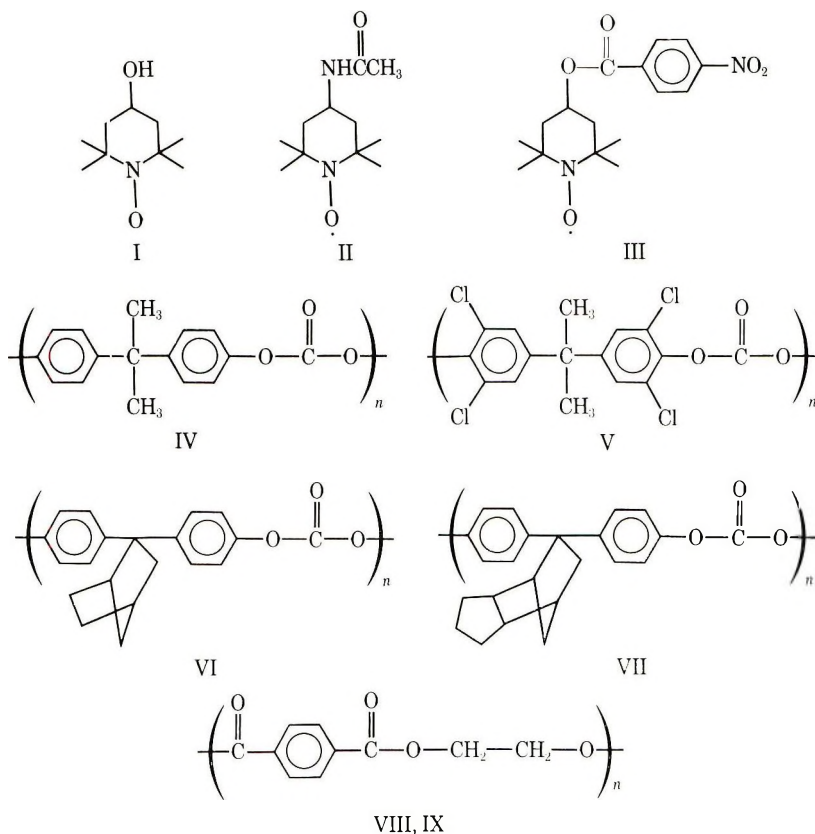
### INTRODUCTION

The behavior of small additive molecules in polymers in the glassy state was investigated by use of ESR spin-probe techniques similar to those of Stryukov et al.<sup>1,2</sup> Since detection and evaluation of polymer motions reflected in the ESR spectrum of the nitroxide radicals may aid in correlating polymer structure with observed mechanical properties, it was of interest to study the rotational mobility of several nitroxyl radicals in amorphous polyester films typically prepared by solvent casting and one example of a nitroxide in biaxially and uniaxially oriented samples of semicrystalline polymer.

### EXPERIMENTAL

#### Materials

For this purpose, nitroxyl radicals 4-hydroxy-2,2,6,6-tetramethylpiperidine-1-oxyl (I); 4-acetamido-2,2,6,6-tetramethylpiperidine-1-oxyl (II); and 2,2,6,6-tetramethyl-4-(*p*-nitrobenzoyloxy)piperidine-1-oxyl (III) were incorporated into the polyesters, poly [(4,4'-isopropylidene-1,1'-diphenylene) carbonate] (IV); poly [(4,4'-isopropylidene-2,2',6,6'-tetrachloro-1,1'-diphenylene) carbonate] (V); poly [(4,4'-(1,1'-diphenylene) carbonate] (VI); poly [(4,4'-hexahydro-4,7-methanoindan-5-ylidene-1,1'-diphenylene) carbonate] (VII); uniaxially orientated poly(ethylene terephthalate) (VIII); and biaxially orientated poly(ethylene terephthalate) (IX).



### Sample Preparation

Nitroxides I–III were incorporated into purified polyesters IV–VII by dissolving 100 ppm (w/w) nitroxide/polymer in dichloromethane. Films were cast from these solutions. Semicrystalline films of polymer VIII and IX were soaked in dichloromethane solutions of nitroxide at 25°C to allow diffusion of the nitroxide into the film. Treated films were washed with hexane for 24 hr prior to use to ensure removal of adsorbed material. All films were dried in a vacuum oven to constant weight and checked for absence of solvent.

Glass transition temperatures ( $T_g$ ) were determined at 10°C/min under  $N_2$  by using a DuPont 900 differential scanning calorimeter (DSC). Films with and without added nitroxide were measured. No change in  $T_g$  was detected due to the additive. At this rate of heating, additional crystallization of samples VIII and IX was noted at 107 and 128°C, respectively. Temperature for onset of this crystallization as detected by DSC varied inversely with initial crystallinity of the sample and reached a maximum of 144°C when an initially amorphous sample was used.

The x-ray diffraction data showed that the cast films of polymers IV–VII



remained amorphous. Samples of VIII and IX containing nitroxides were each 50–60% crystalline with similar-sized crystallites.

### ESR Measurements

ESR spectra were recorded by using portions of tested films sealed (in air) in 3 mm OD quartz tubes. A Varian E-4 EPR spectrometer was used. Microwave power was limited to 1 mW to prevent signal saturation. A Varian variable temperature accessory, calibrated with an iron-constantan thermocouple, was used to heat or cool the samples.

## DISCUSSION OF RESULTS

### ESR Theory

The line shape of the ESR spectrum of a radical is related to its rotational motion; therefore, effects of temperature and polymer matrix which alter the spectrum of the nitroxyl radical<sup>3</sup> may be used to study its mobility in a polymeric environment. A single correlation time  $\tau_c$  may be used to describe the probability of reorientation per unit time (seconds). This correlation time was calculated according to treatments in the literature<sup>4–6</sup> relating the observed line width to rate of nitroxide motion via the spin-spin relaxation parameter  $T_2$ . This method is limited to “rapid” motion of the nitroxide radical such that  $\tau_c$  is between  $10^{-9}$  and  $10^{-10}$  sec.

In the region of “rapid” motion, the relationship between measured hyperfine splitting (hfs) and  $g$ -tensor parameters and line width are expressed in eq. (1),

$$\frac{T_2(0)}{T_2(\bar{M})} = 1 - (4\tau_c/15)b \Delta\gamma B_0 T_2(0)M + (\tau_c b^2/8) T_2(0)M^2 \quad (1)$$

where  $1/T_2 = \pi\sqrt{3} \Delta\nu$ ,  $\Delta\nu$  is the peak-to-peak line width of the Lorentzian derivative curve of the experimental spectra,  $b = 4\pi/3(A - B) =$  contribution of anisotropic hfs constants ( $A \cong 87\text{Mc}$ ,  $B = C \cong 14\text{Mc}$ ),  $\Delta\gamma = (-|\beta|/\hbar)[g_{zz} - 1/2(g_{xx} + g_{yy})] \cong 4 \times 10^4$  (for values determined on nitroxide single crystals),<sup>7</sup> and  $B_0 =$  external magnetic field ( $\sim 3400$  gauss). Rearrangement<sup>7,8</sup> of eq. (1) offers two ways to calculate  $\tau_c$  from experimental ESR curves on including [eq. (2)] and excluding [eq. (3)] the anisotropic  $g$ -tensor parameter  $\Delta\gamma$ .

$$\tau_c = -0.65 \times 10^{-9} W_0 [(h_0/h_1)^{1/2} - (h_0/h_{-1})^{1/2}] \quad (2)$$

$$\tau_c = 0.65 \times 10^{-9} W_0 [(h_0/h_1)^{1/2} + (h_0/h_{-1})^{1/2} - 2] \quad (3)$$

where  $W_0$  is line width of the center ( $M = 0$ ) line in gauss and  $h_1$ ,  $h_0$  and  $h_{-1}$  are the line heights of the first derivative spectrum of the low, center, and high field lines, respectively.

### Experimental Results

Spectra for nitroxides in several polymers were obtained at temperatures from  $-180$  to  $+240^{\circ}\text{C}$ . The temperature at which a particular line shape is observed will be different for the various nitroxide-polymer samples since the line shape depends on the mobility of the nitroxide in the host polymer. Spectra of nitroxide II in polymer V (Fig. 1) are representative of those obtained for other samples. Regions of "strongly hindered" (a), "intermediate" (b,c), and "rapid" (d) rotational motion are illustrated.

The separation between extrema of the high and low field lines of spectra due to "strongly hindered" nitroxides was  $\sim 66$  gauss, equivalent to the theoretical value of  $2A_{zz}$ , where  $A_{zz}$  is the anisotropic hfs contribution of the nitroxide axis parallel to the external magnetic field.

"Intermediate" spectra illustrate both the gradual decrease of the extrema separation (see arrows) and appearance of a narrower spectrum which occurs as the temperature increases and indicates that some nitroxyl radicals experience a different rate of tumbling than others in the polymeric environment. When a radical is mixed into a polymer to simulate non-bonded additives, the number of regions with sufficient volume to permit rapid tumbling of the probe molecule cannot be specified. No dependence of nitroxyl radical mobility on molecular weight of the polymers was noted. However, moles of polymer chain end sites calculated from osmotic pressure average molecular weight exceeded moles of added nitroxyl radicals by a factor of 10 in the samples used.

Spectrum 1 d is characteristic of "rapid" nitroxide rotation, where conditions to describe rate of nitroxide rotation in terms of  $\tau_c$  are met. In the

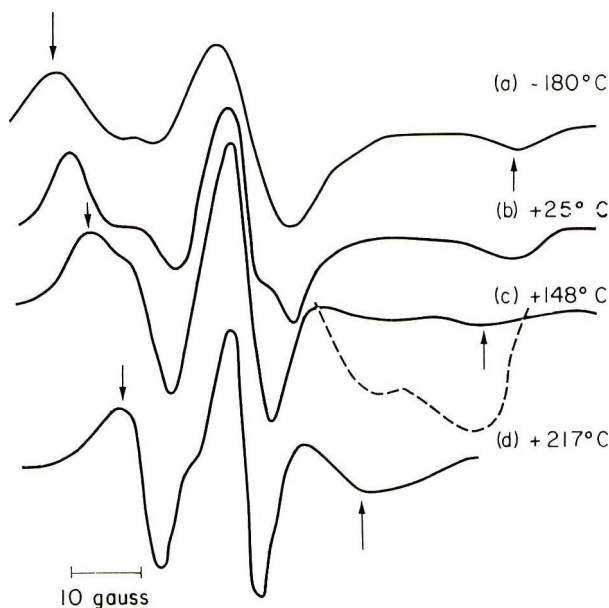


Fig. 1. ESR spectra of nitroxide II in polymer V.

region of rapid nitroxide rotation,  $\tau_c$  was calculated by using both eqs. (2) and (3). As previously reported,<sup>1,8</sup> a somewhat shorter rotational correlation time is calculated from eq. (3) than from eq. (2). Values of  $\tau_c$  for nitroxide I in polymer V at 140°C were  $5.6 \times 10^{-9}$  sec [eq. (3)] and  $2.6 \times 10^{-9}$  sec [eq. (2)]. Subsequent discussion will refer to values calculated from eq. (3).

Apparent activation energy for rotational mobility of the nitroxides in various polymer matrices was estimated from the slope of the line obtained when rotational frequency, expressed as  $\ln(1/\tau_c)$ , was plotted vs temperature ( $10^3/T^\circ\text{K}$ ). Values are collected in Table I.

TABLE I  
Apparent Rotational Activation Energy of Nitroxides in Polyester Films

Polymer	$T_g$ , °C	$E_{ax}$ , kcal/mole			
		Nitroxide I		Nitroxide II	
		$<T_g$	$>T_g$	$<T_g$	$>T_g$
IV	148	2.4	11.0	a	26.0
V	215	2.4	b	7.0	20.0
VI	235	1.6	b	8	b
VII	254	1.9	b	8.0	b
VIII	84			a	8.75
IX	84			a	19.2

<sup>a</sup> No "rapid" motion  $<T_g$ .

<sup>b</sup> Insufficient data points.

Experimental conditions were so chosen that the velocity condition,  $\tau_c \leq 10^{-9}$  sec, was met below the  $T_g$  of the host polymer in several cases. This is in contrast to previously reported<sup>1,9,10</sup> work on nitroxides in addition polymers where measurements were made well above the polymer's  $T_g$ . It was found that the temperature dependence of  $\tau_c$  was Arrhenius in nature [ $\tau_c = \tau_0 \exp \{E_a/RT\}$ ] when  $\tau_c$  was calculated from data obtained solely above or below the polymer  $T_g$ .

When  $\tau_c$  was obtained over a temperature range extending both above and below the  $T_g$  of a nitroxide-polymer combination, temperature dependence was then described by two straight lines of different slopes. The slope change occurred over a temperature range corresponding to the glass transition region of the host polymer. An example of this is shown in Figure 2.

Calculation of  $\tau_c$  for nitroxide II in either semicrystalline sample (VIII or IX) was not possible until the temperature exceeded both the  $T_g$  (84°C, 10°/min) and the onset of additional crystallization noted by DSC. Nitroxide I in polymer VIII attained "rapid" mobility by 100°C. Some increased mobility of probes I and II was noted at ~85°C by appearance of an "intermediate" spectrum similar to that obtained in Figure 1c. Hindered rotation of probe II may be due to its size, not crystallization of VIII or

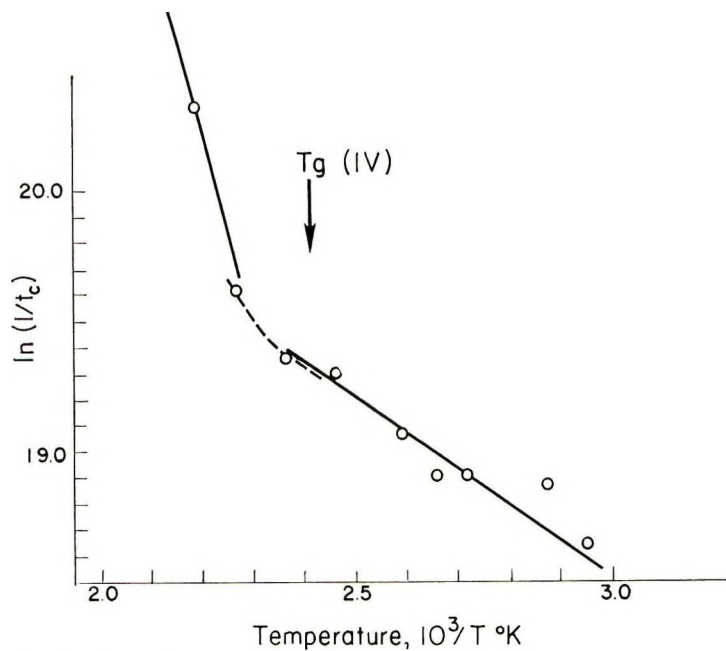


Fig. 2. Temperature dependence of rotational frequency of nitroxide I in polymer IV.

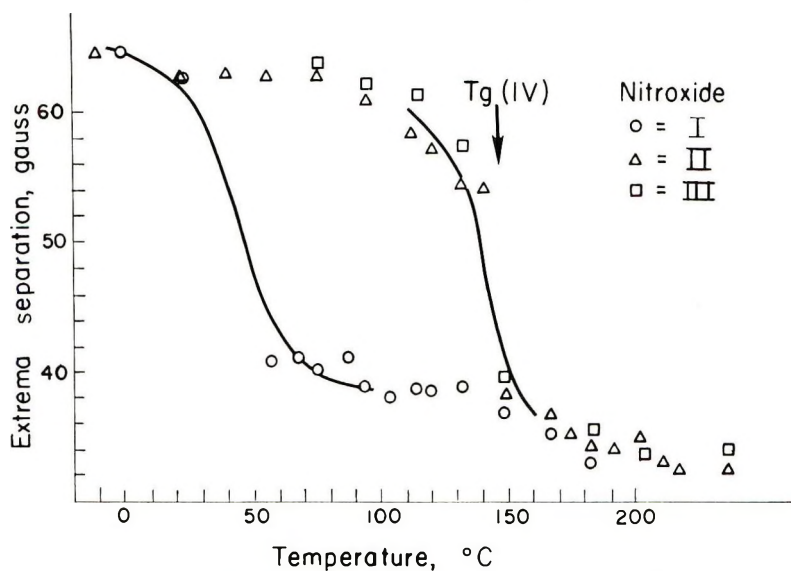


Fig. 3. Extrema separation of nitroxides in polymer IV.

IX, as it did not achieve rapid mobility below 140°C in samples of the amorphous polymers. An effect on apparent activation energy of nitroxide II was noted when uniaxially (VIII) and biaxially (IX) oriented samples of poly(ethylene terephthalate) were compared.

At temperatures where the nitroxides were rotating at a rate less than  $10^9$  Hz, the influence of anisotropic hyperfine structure and  $g$ -tensors prevents analysis by the equations discussed. Data from these strongly hindered and intermediate regions were treated by plotting the extrema separation (gauss) of the spectra representing  $2A_{zz}$  hfs versus the temperature ( $^{\circ}\text{C}$ ) at which the spectra were recorded. Plots of this type show onset of rapid nitroxide tumbling in the polymer matrix which averages the anisotropic components to produce a spectrum varying only in line width. This event is marked by a sharp decrease of extrema separation and occurred below the  $T_g$  of most amorphous samples studied. When the  $T_g$  was approached, extrema separations further decreased from  $\sim 40$  to 33 gauss, the limiting value of isotropic hfs for these nitroxides in room-temperature hydrocarbon solutions. Table II lists the temperature at which the extrema separation was 50 gauss ( $1/\tau_c \sim 10^9$  Hz) and the temperature range of a 60–40 gauss decrease of hfs for the samples studied. Figures 3 and 4 illustrate plots of this type.

It has been proposed<sup>1</sup> that values of  $\tau_c$  determined by ESR measurements of radical mobility can be used to estimate the microscopic viscosity encountered by a nonbonded nitroxide in a host polymer.

Local viscosities of 9–13 poise were calculated for nitroxide I in polymers IV, V, VI, and VII by using the Stokes-Einstein formula in eq. (4)

$$\eta_{\text{rot}}^{\text{M}} = (3kT/4\pi a^3)\tau_c \quad (4)$$

where  $a = 4 \text{ \AA}$  is the radius of I,  $\tau_c$  = values calculated for above samples by ESR measurements at  $T = 382^{\circ}\text{K}$  and  $T = (T_g - 353)^{\circ}\text{K}$ . Although

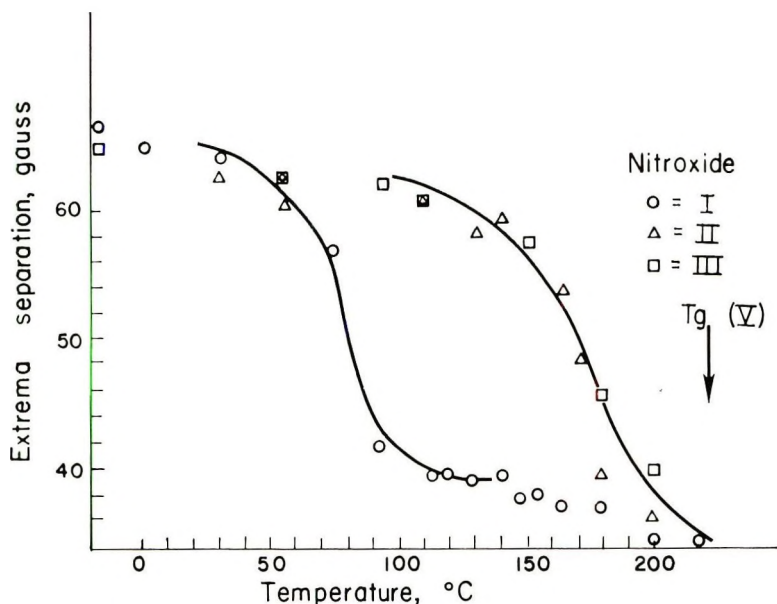


Fig. 4. Extrema separation of nitroxides in polymer V.



TABLE II  
Temperature Range and Midpoint for Onset of Rapid Nitroxide Motion

Polymer	Onset of rapid motion, °C		
	Nitroxide I	Nitroxide II	Nitroxide III
IV	46(40–56)	140(120–148)	138(100–144)
V	80(64–100)	174(130–204)	172(140–180)
VI	50(40–56)	170(140–180)	
VII	44(40–56)	170(130–200)	
VIII	96(75–100)	140(110–150)	
IX		140(130–156)	

the absolute value of  $\eta_{\text{rot}}^{\text{M}}$  depends on assumption of a spherical radical undergoing Brownian motion in the polymeric medium, the effective microscopic viscosity encountered by the radical was several orders of magnitude less than the macroscopic viscosity of a polymer below or near the glass transition region.

## CONCLUSION

It was concluded from these investigations that the effect of localized polymer motions occurring below  $T_g$ , as well as those motions at higher temperatures, was reflected in nitroxyl radical spectra. Onset of rapid rotational mobility of the nitroxyl radicals in a series of polycarbonates seemed to be hindered by bulky chloro-substituents *ortho* to the carbonate linkage of polymer V when compared with polymers IV, VI, or VII, although VI and VII had a higher  $T_g$  than V owing to bulky substituents located on the pivotal carbon atom.

The order of magnitude ( $\sim 3$  kcal/mole) of the apparent energy barrier to reorientation of nitroxide I in the glassy region of the polycarbonates is similar to that required for bending and stretching of polyester chain units observed by infrared spectroscopy. A higher value ( $\sim 8$  kcal/mole) was calculated for the larger nitroxide II.

It must be remembered that the nitroxides in this study represent non-bonded additives; therefore, motion of a specific polymeric moiety cannot be identified as solely responsible for permitting the observed increase in additive mobility. The observed changes in temperature dependence of  $\tau_c$  near the  $T_g$  of a host polymer is in accord with properties of the glass transition region.

## References

1. V. B. Stryukov and Ė. G. Rozantsev, *Vyskomol. Soedin.*, **A10**, 626 (1968).
2. V. B. Stryukov, Yu. S. Karimov, and Ė. G. Rozantsev, *Vyskomol. Soedin.*, **B7**, 493 (1967).
3. O. H. Griffith and A. S. Waggoner, *Accts. Chem. Res.*, **2**, 17 (1969).
4. D. Kivelson, *J. Chem. Phys.*, **33**, 1094 (1960).

5. H. M. McConnell, *J. Chem. Phys.*, **25**, 709 (1956).
6. J. H. Freed and G. K. Fraenkel, *J. Chem. Phys.*, **39**, 326 (1963).
7. O. H. Griffith, D. W. Correll, and H. M. McConnell, *J. Chem. Phys.*, **43**, 2909 (1965).
8. T. J. Stone, T. Buckman, P. L. Nordio, and H. M. McConnell, *Proc. Nat. Acad. Sci. U. S.*, **54**, 1010 (1965).
9. G. P. Rabold, *J. Polym. Sci. A-1*, **7**, 1203 (1969).
10. R. Lenk and A. Rousseau, *Magnetic Resonance and Radio Frequency Spectroscopy* (Proceedings of the XVth Colloque AMPERE, Grenoble, September 1968), P. Averbuch, Ed., North-Holland, Amsterdam, 1969, p. 285.

Received June 28, 1971

Revised August 12, 1971

## **Polymers Containing Anthraquinone Units: Polymers from 1,5-Diaminoanthraquinone and Aralkyldiketones**

ROY M. MORTIER, P. K. DUTT, J. HOEFNAGELS, and  
C. S. MARVEL, *Department of Chemistry, The University of Arizona,  
Tucson, Arizona 85721*

### **Synopsis**

Schiff's-base polymers have been formed by the condensation of 1,5-diaminoanthraquinone with 1,4- and 1,3-diacetylbenzene and 2,6-diacetylpyridine. These polymers were soluble in methanesulfonic and concentrated sulfuric acids (1,4-diacetylbenzene polymer) or *N,N*-dimethylacetamide. The polymer formed from 1,4-diacetylbenzene was ring-closed in polyphosphoric acid to yield a thermally stable polymer soluble in concentrated sulfuric acid which lost only 10% of its weight at 900°C in a TGA test.

### **INTRODUCTION**

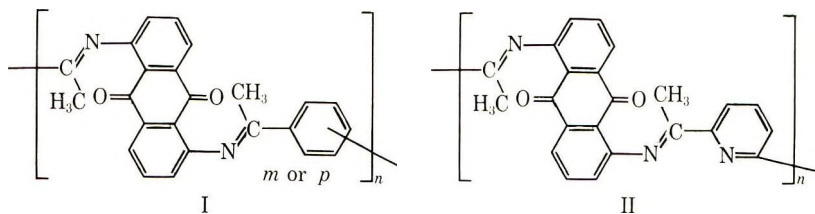
There are now available many polymeric materials having a high degree of thermal stability. These polymers tend to be of the ladder or partial-ladder type containing polyaromatic heterocyclic units.<sup>1</sup> As a consequence of their chemical structure the polymers are usually soluble only in solvents such as methanesulfonic, concentrated sulfuric and polyphosphoric acids. Thus it is hoped that the introduction of anthraquinone units into the polymer will permit solubilization of the polymer by reduction of the quinone groups.<sup>2</sup>

The reducing agent may be an alkaline solution of sodium hydrosulfite by which means the polymer can be wet-spun into fibers which on treatment with acid and air will revert to the original anthraquinone structure. This technique has been shown to be viable by Marvel and co-workers.<sup>3,4</sup>

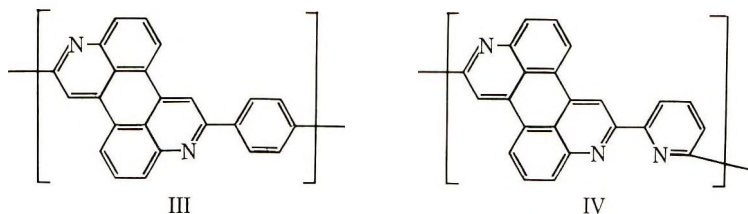
This paper describes the synthesis of partial-ladder polymers and model compounds built on anthraquinone units.

### **RESULTS AND DISCUSSION**

Polymerization reactions have been attempted using 1,5-diaminoanthraquinone with 1,3- and 1,4-diacetylbenzene and 2,6-diacetylpyridine in order to form the Schiff's-base polymer I and II.



These polymers were then "ring-closed" by treatment with polyphosphoric acid to give poly(benzo[1,2,3-*de*:4,5,6-*d'**e'*]diquinoline-2,8-diyl-*p*-phenylene) (III) and poly(benzo[1,2,3-*de*:4,5,6-*d'**e'*]diquinoline-2,8-diyl-2,6-pyridine) (IV).



### Model Reactions

The Schiff's-base condensation product of 1,5-diaminoanthraquinone and acetophenone (V) has been prepared in refluxing nitrobenzene using acetic acid as catalyst. The product was isolated and on treatment with polyphosphoric acid eliminated water to give a closed structure (VI). When an excess of acetophenone and anhydrous zinc chloride as the catalyst were used the closed structure (VI) was obtained directly.

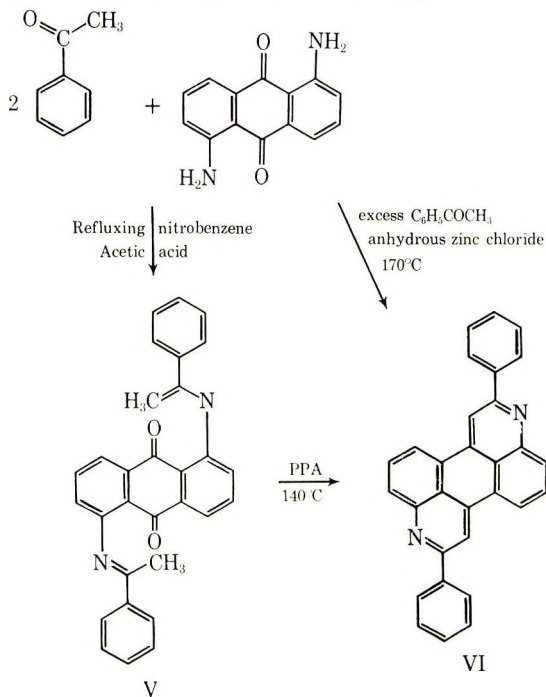


TABLE I  
Polycondensation Reactions of 1,5-Diaminoanthraquinone

Expt.	Comonomer <sup>a</sup>	Solvent <sup>b</sup>	Temperature, °C	Catalyst <sup>c</sup>	Time, hr	Solvents for Product <sup>b</sup>	Remarks
1	1,4-DAB	C <sub>6</sub> H <sub>5</sub> NO <sub>2</sub>	180	ZnCl <sub>2</sub>	6	—	Insoluble product
2	1,4-DAB	C <sub>6</sub> H <sub>5</sub> NO <sub>2</sub>	170	None	40	—	No reaction
3-7	1,4-DAB	C <sub>6</sub> H <sub>5</sub> NO <sub>2</sub>	140-170	ZnCl <sub>2</sub>	4-20	Acetone DMAc	Partially condensed products, 0.05 ≤ $\eta_{inh}$ ≤ 0.12 dl/g
8	1,3-DAB or 2,6-DAP	DMAc	170	HOAc	48	—	No reaction
9	1,4-DAB	C <sub>6</sub> H <sub>5</sub> NO <sub>2</sub>	160	HOAc/Ac <sub>2</sub> O	24	—	93% yield of 1,5-diacetamido anthraquinone
11	1,4-DAB	C <sub>6</sub> H <sub>5</sub> NO <sub>2</sub>	160	CCl <sub>3</sub> CO <sub>2</sub> H	22	—	No reaction
12	1,4-DAB	DMAc	170	CF <sub>3</sub> CO <sub>2</sub> H	90	DMAc	Unknown product
13	Self-condensation of 1,4-DAB	C <sub>6</sub> H <sub>5</sub> NO <sub>2</sub>	160	ZnCl <sub>2</sub>	22	—	Quantitative recovery of monomers
14	Self condensation of 1,5-DAAQ	C <sub>6</sub> H <sub>5</sub> NO <sub>2</sub>	170	ZnCl <sub>2</sub>	23	—	
15	1,4-DAB	Melt	240	None	1/2	Conc. H <sub>2</sub> SO <sub>4</sub> MeSO <sub>3</sub> H	Polymer; $\eta_{inh}$ = 0.46 dl/g
16	1,4-DAB	Melt	200	None	7	Conc. H <sub>2</sub> SO <sub>4</sub> MeSO <sub>3</sub> H	Polymer; $\eta_{inh}$ = 0.21 dl/g
17	1,4-DAB	Melt	170	None	20	Conc. H <sub>2</sub> SO <sub>4</sub> DMAc (partially)	Polymer; $\eta_{inh}$ = 0.28 dl/g
18	1,3-DAB	Melt	240	None	1	—	No reaction; comonomers sublimed
19	2,6-DAP	Scaled tube	250	None	1	DMAc	Polycondensation took place
20	1,3-DAB						
21	2,6-DAP						

<sup>a</sup> Comonomers: diacetylbenzene (DAB), diacetylpyridine (DAP), diaminoanthraquinone (DAAQ).

<sup>b</sup> Solvents: N,N'-dimethylacetamide (DMAc).

<sup>c</sup> Catalysts: glacial acetic acid (HOAc), acetic anhydride (Ac<sub>2</sub>O).



### Polycondensations

Polycondensations were carried out in solution, in the melt and in sealed tubes. Initially 1,4-diacetylbenzene was the comonomer used with 1,5-diaminoanthraquinone. 1,3-Diacetylbenzene and 2,6-diacetylpyridine were later introduced in order to try to improve the solubility of the polymers. The reactions are summarized in Table I.

Reactions in solution using 1,4-diacetylbenzene and 1,5-diaminoanthraquinone yielded, at best, partially condensed structures of low molecular weight. Elemental analyses and infrared spectra indicated that these products contained N-H groups. The inherent viscosities, measured in dimethylacetamide at 30°C were in the range 0.05–0.12 dl/g. Replacement of zinc chloride by acetic acid or trichloroacetic acid as catalyst did not yield any polymeric products. Use of an acetic acid–acetic anhydride mixture as catalyst gave a 93% yield of 1,5-diacetamido-anthraquinone.

As the reaction was catalyzed by acids, noted in the synthesis of the model compounds (V and VI), a stronger acid than those previously used was employed. However, the use of trifluoroacetic acid as catalyst and dimethylacetamide as solvent gave rather ambiguous results. The infrared spectrum did not show the sharp doublet at 3305 and 3410  $\text{cm}^{-1}$  (N-H) which is characteristic of 1,5-diaminoanthraquinone nor the diketone carbonyl peak at 1650  $\text{cm}^{-1}$ . The inherent viscosity of the product was <0.02 dl/g, and the microanalysis did not assist in elucidating the structure of the product.

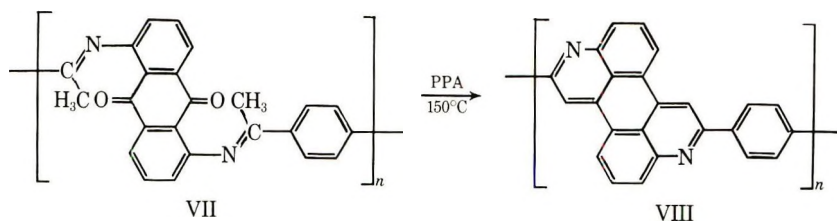
It should be noted that all reactions in solution (and in the melt) were carried out in a nitrogen atmosphere.

Melt polycondensations, carried out at atmospheric pressure under nitrogen, were complicated by the ease of sublimation of the diacetyl monomers. Polymers were obtained from 1,5-diaminoanthraquinone and 1,4-diacetylbenzene (Table I, expts. 15–17), even though some of the latter was lost by sublimation. The polymers were soluble in methane-sulfonic and concentrated sulfuric acids, and microanalysis and infrared data indicated the formation of an open (Schiff's base) structure (VII).

Use of either 1,3-diacetylbenzene or 2,6-diacetylpyridine did not yield any polymeric products presumably because, as these monomers are more volatile than 1,4-diacetylbenzene, the rate of sublimation was too great. However, when reactions with 1,3-diacetylbenzene or 2,6-diacetylpyridine were done in sealed tubes (Table I, expts. 20 and 21), polycondensation took place, giving products which were soluble in dimethylacetamide. The elemental analyses indicated the formation of the Schiff's-base polymer.

### Ring Closing

The Schiff's base polymers were treated with polyphosphoric acid at 150°C in order to form ring-closed structure (VIII).



The experiments are summarized in Table II.

TABLE II  
Treatment of Schiff's Base Polymers with Polyphosphoric Acid

Expt.	Polymer from (Table I)	Solvent <sup>a</sup>	Temperature, °C	Time, hr	Solvents for product	Remarks
1	expt. 15	PPA	150	5 hr	Conc. H <sub>2</sub> SO <sub>4</sub> , MeSO <sub>3</sub> H	$\eta_{inh} = 0.56$ dl/g
2	expt. 16	PPA	160	6 hr	Conc. H <sub>2</sub> SO <sub>4</sub> (partially)	Product appeared to be crosslinked
3	expt. 21	PPA	150	5 hr	MeSO <sub>3</sub> H	Unsatisfactory analysis for closed structure

<sup>a</sup> Solvent: polyphosphoric acid (PPA).

A successful ring-closing experiment (Table II, expt. 1) was carried out on the Schiff's-base polymer formed from 1,4-diacetylbenzene and 1,5-diaminoanthraquinone (Table I, expt. 15). The final product was soluble only in methanesulfonic and concentrated sulfuric acids. It had an inherent viscosity of 0.56 dl/g (0.5% in sulfuric acid at 30°C). Thermogravimetric analysis in nitrogen at a heating rate of 3°C/min (Fig. 1) showed the polymer to be stable up to 900°C (10% weight loss at this temperature). The initial decomposition temperature in air at the same heating rate was 440°C.

Treatment of the polymer formed from 2,6-diacetylpyridine and 1,5-diaminoanthraquinone (Table I, expt. 21) with polyphosphoric acid gave a product soluble only in methanesulfonic acid (Table II, expt. 3). The elemental analysis and infrared spectrum of the product were unsatisfactory for the ring-closed polymer.

## EXPERIMENTAL

### Monomers

**1,5-Diaminoanthraquinone.** Technical grade material was acetylated followed by hydrolysis and recrystallization from nitrobenzene. The material was partially freed from solvent by pumping under vacuum and

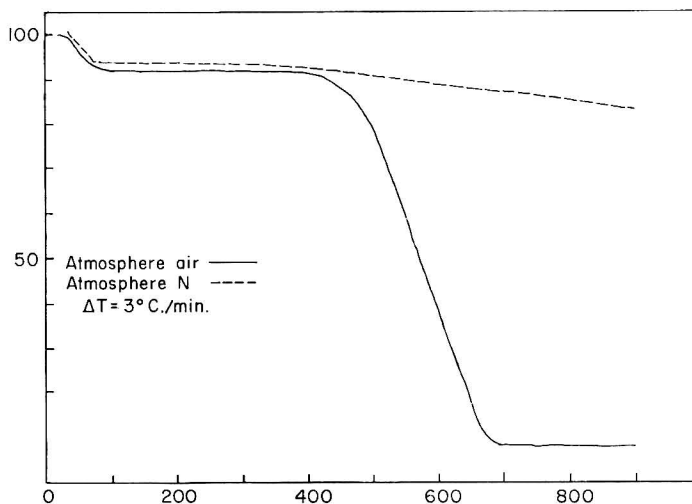


Fig. 1. TGA curve for partial ladder polymer from 1,4-diacetylbenzene and 1,5-diaminoanthraquinone

finally purified by Soxhlet extraction with ethanol for 48 hr. The material had mp 319–320°C (corr).

ANAL. Calcd for  $C_{14}H_{10}N_2O_2$ : C, 70.58%; H, 4.20%; N, 11.77%. Found: C, 70.82%; H, 4.14%; N, 11.96%.

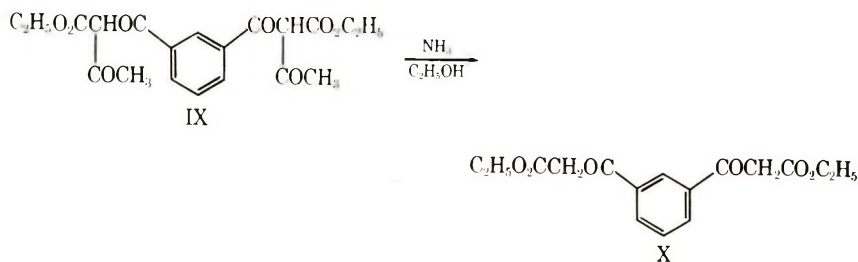
**1,4-Diacetylbenzene.** Commercial material was crystallized twice from ethanol and was further purified by sublimation at 0.25 mm Hg pressure and a temperature of 90°C. The material had mp 114–114.5°C (corr).

ANAL. Calcd for  $C_{10}H_{10}O_2$ : C, 74.08%; H, 6.17%. Found: C, 73.80%; H, 6.31%.

**2,6-Diacetylpyridine.** Commercial material was recrystallized from ether and sublimed. The purified material had mp 78°C.

**1,3-Diacetylbenzene.** This material was prepared from isophthaloyl chloride<sup>5</sup> by the method of Ruggli and Gassenmeier.<sup>6</sup>

A mixture of isophthalic acid (40 g), phosphorus pentachloride (200 g), and phosphorus oxychloride (130 g) was heated for 6 hr on a water bath. The phosphorus oxychloride was removed by distillation, and pure isophthaloyl chloride was obtained by vacuum distillation. The yield was theoretical and the material had bp 146°C (15 cm Hg).<sup>5</sup> Freshly prepared sodium ethylacetoacetate (60 g, prepared from sodium and ethyl acetoacetate in dry ether) was suspended in dry benzene (200 ml), and isophthaloyl chloride (40 g) in benzene (160 ml) was added dropwise to the stirred suspension. After heating for 4 hr on a water bath, the reaction mixture was filtered and the filtrate evaporated to dryness. The residue was vacuum-distilled to give product IX, bp 150–158°C (15 mm Hg).



A solution of IX in 10% alcoholic ammonia (225 ml) was stirred at 60°C on a water bath for 1 hr. The reaction mixture was cooled, poured into water, acidified with 5% hydrochloric acid, and the resultant solution extracted with ether. The ether layer was washed with water, dried with anhydrous magnesium sulfate and, after filtering, evaporated to dryness to give product X as the residue. This material (15 g) was heated for 4 hr in 60 ml of 15% sulfuric acid on a water bath. The reaction mixture was cooled, extracted with ether, and the ether extract treated with sodium bicarbonate, washed with water, and dried with calcium chloride. After filtration, the ether was removed by distillation and the residue was distilled at 15 mm Hg pressure to give 1,3-diacetylbenzene. The material had by 150–155°C/15 mm Hg; mp 31–32°C.

### Model Compounds (V and VI)

**Reaction Catalyzed by Acetic Acid.** 1,5-Diaminoanthraquinone (0.238 g) was mixed with acetophenone (3 ml) and nitrobenzene (25 ml) containing glacial acetic acid (2 ml) and the mixture refluxed for 16 hr. The product was filtered off, dried, and extracted with ethanol, giving a 95% yield of V which was soluble in dimethylacetamide.

ANAL. Calcd. for  $C_{30}H_{22}N_2O_2$ : C, 81.5%; H, 5.0%; N, 6.3%. Found: C, 81.8%; H, 5.2%; N, 6.5%.

The above product was treated with polyphosphoric acid (10 g) at 140°C for 2 hr. The cooled reaction mixture was precipitated into water, filtered and the product extracted with water to render it acid free. The product VI was insoluble in dimethylacetamide but soluble in concentrated sulfuric acid.

ANAL. Calcd for  $C_{30}H_{18}N_2$ : C, 88.6%; H, 4.4%; N, 6.9%. Found: C, 87.8%; H, 4.6%; N, 7.0%.

**Reaction Catalyzed by Zinc Chloride.** A mixture of 1,5-diaminoanthraquinone (0.238 g) and anhydrous zinc chloride (0.10 g) in an excess of acetophenone was heated at 170°C under nitrogen for 3½ hr. The reaction mixture was cooled, and the precipitated product separated, extracted with ethanol, and dried.

ANAL. Calcd for  $C_{30}H_{18}N_2$ : C, 88.6%; H, 4.4%; N, 6.9%. (Product VI) Found: C, 87.3%; H, 4.5%; N, 7.1%.

### Polycondensations in Solution

**Polymer from 1,4-Diacetylbenzene and 1,5-Diaminoanthraquinone (Table I, Expt. 7).** Equimolar quantities of 1,5-diaminoanthraquinone (0.955 g, 0.004 mole) and 1,4-diacetylbenzene (0.650 g, 0.004 mole) were added to a 100 ml three-necked flask fitted with a nitrogen inlet, sealed stirrer, and air condenser. Nitrobenzene (40 ml) and anhydrous zinc chloride (0.55 g, 0.004 mole) were added and the mixture heated at 160–170°C for 4 hr and then 140–150°C for 16 hr.

After cooling, the reaction mixture was added to ethanol (200 ml) and the resultant mixture filtered. The precipitate was collected, washed with water, and dried under vacuum (0.35 g, 25% yield). The product was a red-brown powder soluble in dimethylacetamide with  $\eta_{inh} = 0.12$  dl/g (0.5% solution at 30°C). The material softened at 285°C but did not melt. The infrared spectrum showed a broad doublet at 3305 and 3410  $\text{cm}^{-1}$  (N-H), although the intensity was much reduced compared with the doublet found in the spectrum of 1,5-diaminoanthraquinone.

ANAL. Calcd for  $\text{C}_{24}\text{H}_{16}\text{N}_2\text{O}_2$  (polymer): C, 79.1%; H, 4.4%; N, 7.7%. Found: C, 74.54%; H, 4.36%; N, 8.48%.

**1,4-Diacetylbenzene, Acetic Acid-Catalyzed (Table I, Expt. 10).** A mixture of 1,5-diaminoanthraquinone (2.38 g, 0.01 mole), 1,4-diacetylbenzene (1.62 g, 0.01 mole), glacial acetic acid (1.0 ml), acetic anhydride (4.0 ml), and nitrobenzene (50 ml) were heated at 160°C for 24 hr under nitrogen in a 100 ml three-necked flask.

After cooling, the reaction mixture was poured into petroleum ether (40/60; 300 ml) to yield a brown precipitate. The precipitate was filtered off and dried under vacuum (3.0 g). The analysis, melting point, and infrared spectrum showed the product to be 1,5-diacetamidoanthraquinone (93% yield). The mp was 316°C with decomposition.

ANAL. Calcd for  $\text{C}_{18}\text{H}_{14}\text{N}_2\text{O}_4$ : C, 67.2%; H, 4.3%; N, 8.7%. Found: C, 67.3%; H, 4.4%; N, 8.6%.

**Self-Condensation of Monomers (Table I, Expts. 13 and 14).** 1,5-Diaminoanthraquinone (1.0 g, 0.0042 mole) and zinc chloride (0.75 g, 0.0055 m) were added to a 100-ml three-necked flask fitted with a nitrogen inlet, sealed stirrer and air condenser. Nitrobenzene (50 ml) was added and the mixture heated at 170°C for 23 hr under a slow stream of nitrogen. After cooling, the reaction mixture was added to petroleum ether (40/60; 500 ml). Water (100 ml) was added and the mixture stirred for 12 hr.

The insoluble material was filtered off and air-dried overnight. It had mp 320°C, and its infrared spectrum was identical with that of 1,5-diaminoanthraquinone. The yield was quantitative.

ANAL. Calcd for  $\text{C}_{15}\text{H}_{10}\text{N}_2\text{O}_2$ : C, 70.6%; H, 4.2%; N, 11.8%. Found: C, 69.8%; H, 4.2%; N, 11.6%.

1,4-Diacetylbenzene was treated similarly. The reaction mixture was allowed to cool and then added to a large excess of petroleum ether. A



white precipitate of 1,4-diacetylbenzene was formed, and the monomer (infrared, mp 114°C) was recovered quantitatively.

### Melt Polycondensations

**Polymer from 1,4-Diacetylbenzene and 1,5-Diaminoanthraquinone (Table 1, Expt. 15).** The Schiff's base polymer (VII) was prepared by the melt condensation of 1,4-diacetylbenzene (0.324 g, 0.002 mole) and 1,5-diaminoanthraquinone (0.476 g, 0.002 mole). The reactants were ground together, and the intimate mixture was placed in a polymerization tube of the type described by Foster and Marvel.<sup>7</sup> The system was purged with nitrogen and quickly placed in a metal bath at 240°C, this temperature being maintained for 1/2 hr. Sublimation of both monomers was observed. The product was cooled under nitrogen, crushed, and extracted with ethanol and dimethylacetamide. The yield of polymer was 89% and it had an inherent viscosity in concentrated sulfuric acid at 30°C of 0.46 (0.48% solution).

ANAL. Calcd for  $C_{24}H_{16}N_2O_2$ : C, 79.1%; H, 4.4%; N, 7.7%. Found: C, 78.8%; H, 4.2%; N, 7.5%.

When this reaction was repeated at a lower temperature (Table I, expt. 16), the reaction was stopped intermittently in order to collect the sublimate and regrind the reactants. The product from this reaction, a black brittle material was obtained in 89% yield. The material was partially soluble in methanesulfonic and concentrated sulfuric acids (72%). The inherent viscosity of the product was 0.21 dl/g. The infrared spectrum showed the absence of both the sharp  $NH_2$  doublet at 3305 and 3410  $cm^{-1}$  characteristic of 1,5-diaminoanthraquinone and the broad diacetylbenzene carbonyl peak at 1650  $cm^{-1}$ . The product did not soften below 500°C, but there was a small amount of white sublimate at 300°C.

ANAL. Calcd for polymer (open): C, 79.1%; H, 4.4%; N, 7.7%. Calcd for polymer (closed): C, 87.8%; H, 3.7%; N, 8.5%. Found: C, 81.4%; H, 4.0%; N, 8.5%.

### Polycondensations in Sealed Tubes

**1,3-Diacetylbenzene and 2,6-Diacetylpyridine (Table 1, Expts. 20 and 21).** 1,5-diaminoanthraquinone (0.002 mole) was ground together with 1,3-diacetylbenzene (0.002 mole) and 2,6-diacetylpyridine (0.002 mole). The intimate mixtures were introduced into medium-walled pyrex tubes which were flushed with nitrogen. After sealing, the tubes were placed in a metal bath and heated for 1 hr at 250°C. After cooling, the products were removed from the tubes, crushed extracted with ethanol and dried under vacuum at 70°C.

ANAL. Calcd for  $C_{24}H_{16}N_2O_2$ : C, 79.1%; H, 4.4%; N, 7.7%. Found: C, 75.4%; H, 4.11%; N, 8.41%.

ANAL. Calcd for  $C_{23}H_{15}O_2N_3$ : C, 75.6%; H, 4.1%; N, 11.5%. Found: C, 76.6%; H, 4.0%; N, 11.3%; residue, 1.2%.

### Ring Closures

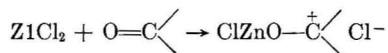
**Polymer from 1,4-Diacetylbenzene (Table II, Expt. 1).** The Schiff's-base polymer (VII; Table I, expt. 15) (0.50 g) was mixed with polyphosphoric acid (10 g) in a 100-ml three-necked flask fitted with a mechanical stirrer and nitrogen inlet. The mixture was heated at 150°C for 5 hr with stirring. After cooling, the reaction mixture was added to water and the precipitated polymer filtered off, extracted with water and alcohol and finally dried under vacuum at 60°C. The inherent viscosity of the polymer in concentrated sulfuric acid at 30°C was 0.56 dl/g (0.50% solution). A thermogravimetric analysis under nitrogen at a heating rate of 3°C/min showed only 10% weight loss at 900°C. The initial decomposition temperature in air at the same heating rate was 440°C (Fig. 1).

ANAL. Calcd for  $C_{24}H_{12}N_2$ : C, 87.8%; H, 3.7%; N, 8.5%. Found: C, 86.4%; H, 3.6%; N, 8.4%; Residue, 0.9%.

### SUMMARY

Aralkyldiketones have been polymerized with 1,5-diaminoanthraquinone by various means to form Schiff's-base polymers. These polymers have been treated with polyphosphoric acid in attempts to produce totally ring-closed polymers having a partial-ladder type structure. Melt polymerizations have been successful for 1,4-diacetylbenzene but when 2,6-diacetylpyridine or 1,3-diacetylbenzene were used no polymers were formed due to sublimation of these monomers. They were polymerized with 1,5-diaminoanthraquinone when the reactions were done in sealed tubes.

Only low molecular weight polymers ( $\eta_{inh} \leq 0.12$  dl/g) were formed when the reactions were carried out in solution. The use of zinc chloride as catalyst may have limited the growth of the polymer as it is known that it can complex with ketones:<sup>8</sup>



Also, it is possible that, due to the long reaction times and high temperatures required to effect polycondensation, a solvent decomposition product or the solvent itself may have caused side reactions to take place. It should be noted that self-condensation of the comonomers did not appear to interfere in the polycondensations (Table I, expts. 13 and 14).

We are indebted to Dr. Kurt L. Loening, Chemical Abstracts Service, for the name of our polymers. We are indebted to Dr. G. F. L. Ehlers, Air Force Materials Laboratory, Wright-Patterson Air Force Base, for the thermogravimetric curves.

This work was supported by the Air Force Materials Laboratory, Air Force Systems Command, Wright-Patterson Air Force Base, Ohio.

### References

1. A. H. Frazer, *High Temperature Resistant Polymers*, Interscience, New York, pp. 138-210.
2. E. Grandmougin, *Chem. Ber.*, **39**, 3563 (1906).
3. W. Bracke and C. S. Marvel, *J. Polym. Sci. A-1*, **8**, 3177 (1970).
4. J. Szita, L. H. Brannigan, and C. S. Marvel, *J. Polym. Sci. A-1*, **9**, 691 (1971).
5. J. Schreder, *Chem. Ber.*, **7**, 708 (1874).
6. P. Ruggli and E. Gassenmeier, *Helv. Chim. Acta*, **22**, 496 (1939).
7. R. T. Foster and C. S. Marvel, *J. Polym. Sci. A1*, **3**, 417 (1967).
8. P. K. Dutt and S. R. Palit, *J. Polym. Sci. B.*, **3**, 801 (1965).

Received July 22, 1971

## Side-Chain Crystallinity. II. Heats of Fusion and Melting Transitions on Selected Copolymers Incorporating *n*-Octadecyl Acrylate or Vinyl Stearate

EDMUND F. JORDAN JR., BOHDAN ARTYMYSHYN, ANTHONY SPECA, and A. N. WRIGLEY, *Eastern Regional Research Laboratory, Eastern Marketing and Nutrition Research Division, Agricultural Research Service, U. S. Department of Agriculture, Philadelphia, Pennsylvania 19118*

### Synopsis

The heats of fusion and the melting transitions of the crystallinity present in the side chains were determined for selected copolymers incorporating *n*-octadecyl acrylate or vinyl stearate. A major purpose of this investigation was to ascertain the effect of interrupting the long ordered 18-carbon side chains by randomly interspersed amorphous side chains of various lengths. For this purpose the lower acrylate homologs ( $C_1$  through  $C_8$  and including oleyl,  $C_{18}$ ) were copolymerized over the composition range with *n*-octadecyl acrylate. It was found that simple dilution of the crystalline component (from comonomer b) by the amorphous component (from comonomer a) governed the decline in the heats of fusion and the fraction of crystallinity present. High crystallization rates were encountered because equilibrium crystallinity was nearly achieved for most of the copolymers. Melting point depression was less than theory in copolymers having short amorphous comonomer side chain lengths, but approached the theoretical depression as these side chains became very long. Thus the outer methylene sequences (the crystalline sequences) of the fatty co-units could bridge the smaller amorphous a units, giving rise to larger crystal sizes than theory specified. Main-chain stiffness, when present in the melt, had a small effect on the distribution of crystallite sizes but exhibited a much larger influence in preventing the attainment of equilibrium crystallinity, especially at high amorphous comonomer compositions. However, crystallinity was still high compared with that of copolymers described in the literature crystallizing through their main-chain units. When long blocks of crystalline segments were present (as in compositionally heterogeneous vinyl stearate copolymers), melting point depression was small and followed the theoretical probability sequence function.

### INTRODUCTION

Much interest has centered<sup>1a,2</sup> on the crystallization phenomenon in copolymers in which one co-unit of the main chain is capable of crystallizing. The Flory theory of the equilibrium crystallization of polymers<sup>3</sup> required that sequence length distribution, and not the chemical nature of the amorphous component, determined the melting point depression. A very broad distribution of crystal sizes and lowered crystallinities were

postulated to be present in copolymers. Consequently, melting was predicted to occur over a wide temperature range. Theory<sup>4</sup> further required that equilibrium crystallization could only be attained in the limit of infinite time. The extent of realizable crystallinity would reside somewhere between this unattainable limit, and the equally unattainable limit of zero time imposed by cold crystallization.<sup>4</sup> In copolymers the development of crystallinity would be expected to be much slower than in homopolymers, and its extent greatly reduced by the presence of noncrystallizable units.

Many experimental studies<sup>1a,2</sup> have been directed toward confirming these predictions. Copolymers of polyethylene have received the most attention.<sup>1a,5-12</sup> While the data supported most of the features of Flory's theory, melting point depressions and decline in crystallinity were greater than predicted. Both deviations are attributable to failure to approach a sufficiently high state of equilibrium crystallization.<sup>4</sup>

Crystallinity in polyesters and polyamides and in copolymers formed from a single monomer by varying the syndiotactic and isotactic placements, has been reviewed.<sup>1a</sup> The sterically-ordered copolymers usually exhibited low crystallinities with only one stereoisomer crystallizing. In contrast, each component of the polyesters and polyamides could generally crystallize, leading to crystallinity over all compositions.<sup>1a,13</sup> The latter systems often exhibited isomorphism. Again, the broad features of the theory<sup>3</sup> were experimentally supported, but the anomalies already discussed tended to appear.<sup>4</sup>

All of these investigations have considered only copolymer systems in which the crystallizing component is part of the main chain. The special case of crystallization involving units having side chains has received relatively little attention. Some qualitative studies have been made, however. Melting points, obtained by refractometry, for copolymers of vinyl stearate and vinyl acetate, decreased progressively with increase in vinyl acetate,<sup>14</sup> while those for copolymers of poly-*N*-*n*-octadecylacrylamide with acrylonitrile<sup>15</sup> or vinylidene chloride,<sup>16</sup> by differential scanning calorimetry, showed little depression. Main-chain crystallinity of vinylidene chloride segments was apparent over a limited composition range in the last system<sup>16</sup> as was that of the vinyl alcohol units in copolymers with vinyl stearate.<sup>17</sup> Copolymers of *n*-octadecyl and *n*-tetradecyl methacrylate showed isomorphic replacement.<sup>18</sup> The melting points of the side chains in copolymers of *n*-octadecyl and methyl methacrylate were diffuse, but were little depressed by the short methyl branches.<sup>18</sup>

The general aim of this investigation was to study quantitatively the decline in side-chain crystallization and the depression of melting point for a variety of copolymer systems. The thermodynamic data were obtained by differential scanning calorimetry. In the first paper of this series<sup>19</sup> the thermodynamic properties of homopolymers of the higher poly-(*n*-alkyl acrylates), poly-*N*-*n*-alkylacrylamides, and poly(vinyl esters) were studied. It was shown that only the outer methylene units in the side chains form a crystal lattice in these systems. The critical side-chain



length required to maintain a stable nucleus varied among these homologous series. For the poly(*n*-alkyl acrylates) it was above 9.2 carbon atoms.

Three different lines of investigation of the side-chain crystallinity in copolymers were pursued. The first, constituting a major purpose of this work, was to test the effect of interrupting the long, ordered 18-carbon side chains in poly(*n*-octadecyl acrylate) by randomly interspersed amorphous side chains of various lengths. For this purpose each of the lower *n*-alkyl acrylates ( $C_1$  through  $C_8$ ) was selected for copolymerization with *n*-octadecyl acrylate over the complete range of composition. With this selection complete randomness in sequence lengths<sup>20</sup> would be assured. Because of its amorphous nature<sup>16</sup> and similar reactivity ratios<sup>21</sup> oleyl acrylate was also chosen as an example in this series. All of these copolymers would be expected to have low glass transition temperatures. The second line of investigation inquired into the effect of using stiff amorphous comonomers having high glass transition temperatures and small side groups on the decrease in crystallinity and melting point with decrease in *n*-octadecyl acrylate. Finally, the third line of investigation took up the case of non-random copolymers in which blocks of crystalline side chains would be present. In the paper immediately following this,<sup>22</sup> the influence of developing crystallinity on the glass transition temperatures of these copolymers will be presented.

## EXPERIMENTAL

### Lower *n*-Alkyl Acrylates, Methyl Methacrylate, and Acrylonitrile

All were the purest monomers from commercial sources. The acrylates were treated with aqueous alkali to remove the inhibitor and dried; methyl methacrylate and acrylonitrile were distilled immediately before use.

### Higher Fatty Comonomers

The preparation and purification of *n*-octadecyl acrylate has been described.<sup>19</sup> Oleyl acrylate was prepared and purified by the procedure used for *n*-dodecyl and *n*-tetradecyl acrylate,<sup>19</sup> except that a single acetone crystallization (3 ml/g) was employed at  $-60^{\circ}\text{C}$  as the final purification step. The yield was 52%, and the ester was 99.4% octadecenyl acrylate by gas-liquid chromatography but contained about 20% elaidyl acrylate by infrared analysis.

ANAL. Calcd: C, 78.20%; H, 11.88%. Found: C, 78.40; H, 11.66%.

Vinyl stearate<sup>23</sup> was obtained from the White Chemical Company. It was purified by four crystallizations from acetone (10 ml/g) at  $-20^{\circ}\text{C}$ . The yield was 59% and the purity was 98.8% by gas liquid chromatography.

### Polymerization Procedure

All polymerizations were conducted in sealed vessels, under nitrogen, in benzene solution (4 mole benzene/mole of total monomer), for 48 hr at

60°C, using 0.2 mole-% bis-azo isobutyronitrile as the initiator. Exceptions were *n*-octadecyl acrylate copolymers with, respectively, methyl methacrylate and oleyl acrylate, where the benzene monomer ratio was 1, and with *n*-butyl acrylate and acrylonitrile, where the ratio was 3. Vinyl stearate-methyl methacrylate copolymers were made at 60°C for 72 hr using a solvent to comonomer mole ratio of unity. Most yields were between 85 to 95%. Some low yields were encountered in the mid-composition range of the vinyl stearate-methyl methacrylate copolymers (39–70%). The copolymers were purified by extraction with hot methanol (or petroleum ether, when soluble in methanol) till free of all monomers. They were then dried in thin layers. Copolymer compositions, determined from elementary analyses, agreed with feed compositions within experimental error. Consequently, to reduce experimental scatter, the thermodynamic data were correlated with feed compositions. Exceptions were the vinyl stearate copolymers, where copolymer compositions derived from elemental analysis were used.

### Calorimetric Procedures

The procedures of Jordan et al.<sup>19</sup> were followed exactly. Hard, brittle samples and hard, waxy samples were ground to powders or small granules and weighed on a Cahn balance in regular sample cups; soft sticky polymers were weighed (Cahn balance) into the crimped solvent cups provided with the instrument. Minimum sample weights (usually 1–2 mg) were used for melting point. The ends of the fusion curves were taken as the temperature of melting. As will be seen from the text, this interpretation was the only feasible one. This interpretation is justified by the principle<sup>1a,5</sup> that the final disappearance of crystallinity, under equilibrium conditions, is the thermodynamic melting point. In this work, where equilibrium was only approached, the melting points are necessarily approximate. Melting points of the side-chain crystallites of homopolymers by differential scanning calorimetry do seem to be close to equilibrium values, however.<sup>19</sup> Maximum sample weights (14–25 mg) were employed for the fusion endotherms. Methanol or other liquid treatments were not used in this series to increase the extent of crystallization because of the varied solubilities of these copolymers. A computer (IBM 1130) was used for all calculations.

### Molecular Weight Measurements

The osmometric procedure was described.<sup>15</sup> The solvent was toluene.

## RESULTS AND DISCUSSION

### Thermodynamic Quantities and Molecular Weight Measurements

The heats of fusion, melting transitions, and molecular weight measurements for all of the copolymer systems studied in this investigation are listed in Table I. In this paper designation b will refer to crystalline units derived from *n*-octadecyl acrylate or vinyl stearate in the chain, while

TABLE I  
Composition, Degrees of Polymerization, Heats of Fusion, and  
Melting Points for the Copolymers

Experi- ment number	Fatty ester in copolymer <sup>a</sup>		DP <sub>n</sub>	Crystallinity properties			
	Mole fraction	Weight fraction		$\Delta H_f$ , cal/g	$x_c^b$	$x_c/x_{cmax}^c$	$T_m$ , °C
MONOMER		<i>n</i> -Octadecyl acrylate and methyl acrylate					
1	0.050	0.166	1596	0.564	0.01	0.159	17.0
2	0.075	0.234	1660	1.17	0.03	0.234	27.0
3	0.100	0.295	1704	2.62	0.05	0.416	33.0
4	0.125	0.350	1886	7.25	0.13	0.971	42.0
5	0.150	0.399	1394	7.31	0.13	0.859	39.0
6	0.200	0.485	1226	8.77	0.16	0.847	42.0
7	0.300	0.618	1113	12.50	0.22	0.948	52.0
8	0.400	0.715	950.6	15.39	0.27	1.01	47.0
9	0.500	0.790	962.9	17.42	0.31	1.03	48.0
10	0.600	0.850	862.7	17.49	0.31	0.964	51.0
11	0.700	0.898	792.5	18.94	0.34	0.988	52.0
12	1.000	1.000	852.9	21.34	0.38	1.00	56.0
		<i>n</i> -Octadecyl acrylate and ethyl acrylate					
13	0	0	1221	0	0	0	—
14	0.050	0.146	1321	1.96	0.03	0.629	17.0
15	0.100	0.265	1845	4.75	0.08	0.840	30.0
16	0.125	0.317	1278	6.07	0.11	0.897	28.0
17	0.150	0.364	1020	6.55	0.12	0.843	34.0
18	0.200	0.448	863.5	8.93	0.16	0.934	39.0
19	0.300	0.582	680.2	11.50	0.21	0.926	43.0
20	0.400	0.684	688.3	14.70	0.26	1.01	45.0
21	0.500	0.764	628.8	16.22	0.29	0.995	46.0
22	0.600	0.829	583.9	17.42	0.31	0.985	47.0
23	0.750	0.907	594.2	19.11	0.34	0.987	51.0
MONOMER		<i>n</i> -Octadecyl acrylate and <i>n</i> -butyl acrylate					
24	0	0	1938	0	0	0	—
25	0.050	0.118	1591	1.63	0.03	0.647	-12.0
26	0.075	0.170	1452	1.28	0.02	0.353	1.0
27	0.100	0.219	1497	3.37	0.06	0.721	10.0
28	0.125	0.266	1407	4.09	0.07	0.721	16.0
29	0.150	0.309	1202	5.68	0.10	0.861	22.0
30	0.200	0.387	1425	6.97	0.12	0.844	28.0
31	0.300	0.519	1543	9.54	0.17	0.861	35.0
32	0.400	0.628	1357	12.70	0.23	0.948	42.0
33	0.500	0.719	—	14.37	0.26	0.937	44.5
34	0.750	0.883	916.7	18.40	0.33	0.977	50.0
		<i>n</i> -Octadecyl acrylate and <i>n</i> -octyl acrylate					
35	0	0	826.5	0	0	0	—
36	0.050	0.085	776.3	0.73	0.01	0.402	-13.0
37	0.075	0.125	790.0	1.26	0.02	0.472	-6.0
38	0.100	0.164	768.0	2.24	0.04	0.640	0
39	0.125	0.201	758.2	3.09	0.06	0.720	6.0
40	0.150	0.237	734.0	3.17	0.06	0.627	9.0
41	0.200	0.306	684.8	5.32	0.09	0.815	15.0
42	0.300	0.430	631.3	8.44	0.15	0.920	26.0
43	0.400	0.540	589.1	10.80	0.19	0.937	33.0
44	0.500	0.638	575.5	11.61	0.21	0.853	40.0
45	0.750	0.841	457.1	15.04	0.27	0.838	47.0

(continued)

TABLE I (continued)

Experiment number	Fatty ester in copolymer <sup>a</sup>		DP <sub>n</sub>	Crystallinity properties			
	Mole fraction	Weight fraction		$\Delta H_f$ , cal/g	$x_c^b$	$x_c/x_{cmax}^c$	$T_m$ , °C
<i>n</i> -Octadecyl acrylate and 2-ethylhexyl acrylate							
46	0	0	385.8	0	0	0	—
47	0.050	0.085	380.6	0.52	0.01	0.287	-13.0
48	0.075	0.125	382.0	1.17	0.02	0.439	-5.0
49	0.100	0.164	378.2	1.72	0.03	0.492	-9.0
50	0.125	0.201	393.0	2.07	0.04	0.483	-1.0
51	0.150	0.237	371.6	2.70	0.05	0.534	10.0
52	0.200	0.306	352.3	4.79	0.09	0.734	16.0
53	0.300	0.430	379.1	7.95	0.14	0.866	27.0
54	0.400	0.540	387.7	10.13	0.18	0.879	32.0
55	0.500	0.638	400.9	11.51	0.21	0.845	38.0
56	0.600	0.725	406.1	12.68	0.23	0.820	41.0
57	0.750	0.841	425.6	15.09	0.27	0.841	47.0
<i>n</i> -Octadecyl acrylate and <i>n</i> -dodecyl acrylate							
58	0	0	930.6	8.75	0.16	1.00	12.0
59	0.050	0.067	677.1	8.40	0.15	0.876	13.0
60	0.075	0.099	614.1	8.71	0.16	0.872	20.0
61	0.100	0.131	602.9	8.90	0.16	0.839	17.0
62	0.125	0.162	815.9	9.11	0.17	0.845	22.0
63	0.150	0.193	762.9	9.56	0.17	0.856	21.0
64	0.200	0.253	665.6	10.30	0.19	0.863	24.0
65	0.300	0.367	553.8	11.10	0.20	0.851	27.0
66	0.400	0.474	561.2	11.54	0.21	0.785	32.0
67	0.500	0.574	520.8	12.52	0.22	0.784	36.0
68	0.600	0.670	475.8	13.27	0.24	0.772	40.0
69	0.750	0.802	352.9	16.94	0.33	0.980	47.0
MONOMER	<i>n</i> -Octadecyl acrylate and oleyl acrylate <sup>d</sup>						
70	0.075	0.076	—	0	0	0	-8.0
71	0.100	0.101	—	0.90	0.02	0.418	-3.0
72	0.125	0.126	—	1.50	0.03	0.558	-1.0
73	0.150	0.151	—	1.47	0.03	0.456	3.0
74	0.200	0.201	—	2.42	0.04	0.564	12.0
75	0.300	0.301	—	5.15	0.09	0.802	22.0
76	0.400	0.402	—	7.14	0.13	0.832	30.0
77	0.500	0.502	101.2	8.44	0.15	0.788	37.0
78	0.600	0.602	81.1	10.84	0.19	0.844	40.0
79	0.750	0.751	88.3	12.62	0.23	0.748	46.0
<i>n</i> -Octadecyl acrylate and methyl methacrylate							
80	0	0	1452	0	0	0	—
81	0.050	0.146	1189	0	0	0	—
82	0.075	0.208	1012	0	0	0	—
83	0.100	0.265	1014	0.504	0.01	0.089	44.0
84	0.125	0.317	1067	0.721	0.01	0.107	46.0
85	0.150	0.364	1053	1.43	0.03	0.134	47.0
86	0.200	0.448	1027	2.28	0.04	0.239	49.0
87	0.300	0.582	1008	4.63	0.08	0.373	52.0
88	0.400	0.683	1148	7.15	0.13	0.491	52.0
89	0.500	0.764	1200	9.59	0.17	0.588	53.0
90	0.600	0.829	1054	15.09	0.27	0.853	54.0
91	0.750	0.907	—	17.45	0.31	0.902	56.0

TABLE I (continued)

Experiment number	Fatty ester in copolymer <sup>a</sup>		DP <sub>n</sub>	Crystallinity properties			
	Mole fraction	Weight fraction		$\Delta H_f$ , cal/g	$x_c^b$	$x_c/x_{cmax}^c$	$T_m$ , °C
<i>n</i> -Octadecyl acrylate and acrylonitrile							
92	0	0	346.2 <sup>e</sup>	0	0	0	—
93	0.050	0.244	342.9 <sup>e</sup>	0	0	0	—
94	0.075	0.331	343.2 <sup>e</sup>	0	0	0	—
95	0.100	0.405	331.6 <sup>e</sup>	—	0	0	35.0
96	0.125	0.466	310.9 <sup>e</sup>	1.71	0.03	0.172	37.0
97	0.150	0.519	331.6 <sup>f</sup>	2.75	0.05	0.248	39.0
98	0.200	0.604	491.4 <sup>f</sup>	4.40	0.08	0.341	45.0
99	0.300	0.724	520.4 <sup>f</sup>	6.40	0.11	0.414	56.0
100	0.400	0.790	593.3	9.88	0.18	0.586	56.0
101	0.500	0.860	558.3	11.73	0.21	0.639	55.5
102	0.600	0.903	554.8	15.43	0.28	0.801	57.0
103	0.750	0.941	640.1	20.11	0.36	1.00	57.0
Vinyl stearate and methyl methacrylates <sup>g</sup>							
104	0.024	0.070	1257	0	0	0	—
105	0.036	0.104	1112	0.62	0.01	0.303	56.0
106	0.046	0.129	1020	0.43	0.01	0.167	58.0
107	0.076	0.203	958.8	1.17	0.02	0.291	57.0
108	0.158	0.368	906.5	3.18	0.06	0.436	58.0
109	0.183	0.410	728.1	6.39	0.11	0.786	58.0
110	0.197	0.433	613.5	6.13	0.11	0.714	58.0
111	0.377	0.622	449.8	11.30	0.20	0.917	59.0
112	0.414	0.687	411.8	9.34	0.16	0.686	58.0
113	0.375	0.650	275.3	9.13	0.16	0.709	57.0
114	0.744	0.900	265.6	16.56	0.29	0.928	57.0
115	0.902	0.966	254.6	17.93	0.32	0.937	56.0
116	0.950	0.983	230.0	19.95	0.35	1.02	57.0
117	1.00	1.00	157.5	19.82	0.38	1.00	58.0
Vinyl stearate and 2-ethylhexyl acrylates <sup>g</sup>							
118	0.043	0.070	403.5	0	0	0	—
119	0.054	0.088	416.0	0	0	0	—
120	0.076	0.121	476.4	0	0	0	—
121	0.062	0.099	491.9	0	0	0	—
122	0.130	0.201	487.2	0	0	0	—
123	0.116	0.181	637.2	0.464	0.01	0.129	47.0
124	0.213	0.314	617.6	0.937	0.02	0.151	55.0
125	0.282	0.398	449.6	3.30	0.06	0.418	58.0
126	0.333	0.457	405.4	5.56	0.10	0.614	58.0
127	0.523	0.649	276.1	9.24	0.16	0.718	57.0
128	0.730	0.820	245.9	13.41	0.24	0.825	56.0

<sup>a</sup> Feed composition; found compositions by elemental analysis agreed within experimental error.

<sup>b</sup> Equation (8).

<sup>c</sup> Equation (7).

<sup>d</sup> Partially crosslinked. Sol fraction was about 10% in experiments 77–79.

<sup>e</sup> Dimethylformamide used.

<sup>f</sup> Dimethylformamide–toluene (50/50) used.

<sup>g</sup> Copolymer compositions are from elemental analysis.



other co-units will receive the designation a. All of these except *n*-dodecyl acrylate were amorphous. The degrees of polymerization  $DP_n$  were calculated from osmometric molecular weights by using a weighted average of the molecular weights for the two comonomers. Degrees of polymerization generally fell with increasing b component. This probably reflects transfer to monomer.<sup>24</sup> Notable exceptions were the copolymers of *n*-octadecyl acrylate and acrylonitrile, where the trend was reversed. No ready explanation is offered for this phenomenon except that it seems to occur in precipitation copolymerization<sup>15</sup> incorporating acrylonitrile. Not surprisingly,<sup>24</sup> the decline in molecular weights with increasing oleyl acrylate is marked.

The first five and the seventh system in Table I provide data relevant to the first line of investigation called for in the introduction. These are the all-acrylate copolymers having amorphous side chains of various lengths and low glass transition temperatures. They will be referred to as series 1 in the discussion below. The next two systems in Table I have high glass transition temperatures and thus satisfy the second aim of the introduction. These will be called series 2. The last two are nonrandom copolymers, as in the third specification, and will be labeled series 3.

Melting points and the heats of fusion for all of the systems (Series 1, 2, 3, Table I) declined in a regular fashion from the values for the respective crystalline homopolymers (expts. 12 and 117) as the content of b units decreased. The melting point depression will be treated in detail below. From thermodynamic data on homopolymers,<sup>19</sup> the heats of fusion were

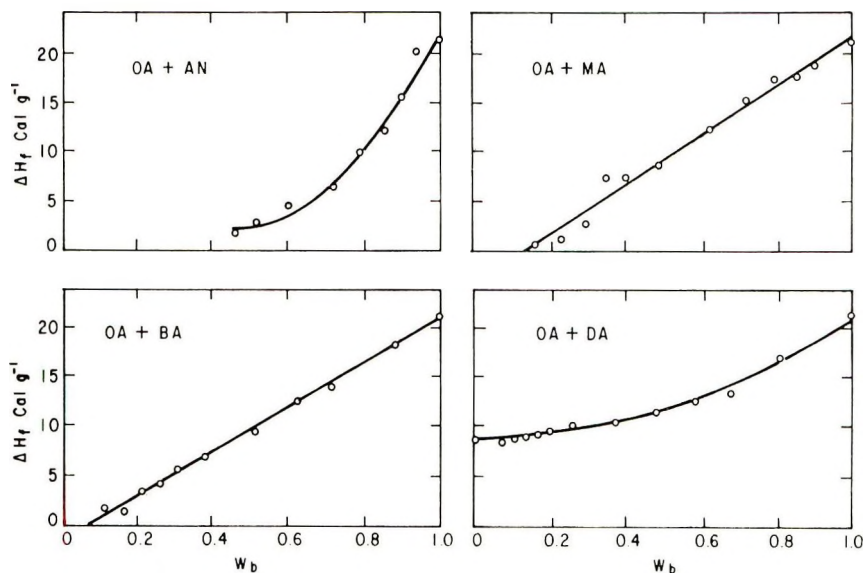


Fig. 1. Heats of fusion vs. the weight fraction  $w_b$  of *n*-octadecyl acrylate for several typical copolymer systems. Designations are: OA, *n*-octadecyl acrylate; AN, acrylonitrile; MA, methyl acrylate; BA, *n*-butyl acrylate; DA, *n*-dodecyl acrylate.

found to be proportional to the crystallinity present. This proportionality would be expected to be followed by the copolymers. The slope for the decline of the heat of fusion with decreasing  $w_b$  was relatively small for the copolymers made using the amorphous *n*-alkyl acrylate homologs (series 1, expts. 1–57 and 70–79). This is illustrated in Figure 1 for the *n*-octadecyl acrylate–methyl acrylate system (OA + MA) and for the *n*-octadecyl acrylate–butyl acrylate system (OA + BA). In all of these entirely acrylate systems the glass temperatures of the copolymers at low *n*-octadecyl acrylate content were low (all were below  $-10^\circ\text{C}$ ), indicating that chain mobility of the molten copolymers was high.<sup>25</sup> Thus the low glass temperatures permitted rapid crystallization<sup>1b</sup> at the low supercooling employed. In contrast, copolymers with relatively high values of  $T_g$ , approximately  $26^\circ\text{C}$ , (series 2, Table I), showed larger decreases in  $\Delta H_f$  with decreasing  $w_b$  and equally large decreases in crystallinity. The slopes of the  $\Delta H_f$ –composition curves at high  $w_b$  were therefore considerably greater. Examples are copolymers of *n*-octadecyl acrylate with methyl methacrylate (expts. 80–91) and acrylonitrile (expts. 92–103), respectively. This is also illustrated in Figure 1 for the *n*-octadecyl acrylate–acrylonitrile system (OA + AN). Changes in the programmed rate of cooling and heating had little effect on the areas under the fusion curves or on the melting temperature. Thus the fusion phenomena for these samples were comparatively insensitive to details of their thermal history. Consequently the development of metastable crystallites requiring rapid heating rates for their preservation<sup>26–28</sup> and the complications of multiple peaks arising from different cooling rates<sup>29</sup> were absent in this work.

The heats of fusion for copolymers of *n*-octadecyl and *n*-dodecyl acrylate (expts. 58–69), where each component is crystalline,<sup>19</sup> fell between the values for the respective homopolymers. This can be seen (OA + DA) in Figure 1. Their melting transitions have already been shown<sup>19</sup> to be linear with composition. Consequently the crystallinity here is a good example of solid solution formation involving the methylene groups in the side chains.<sup>18,19</sup> They resemble certain polyamide systems in retaining crystallinity over all composition ranges<sup>1a</sup> and in exhibiting isomorphism.<sup>1a,18</sup>

As overall crystallinity declined with dilution by *a* units, the melting peaks traced by differential scanning calorimetry became increasingly broad for all of the copolymers in Table I. Such broadening of melting peaks has provided qualitative indication of broadening distribution of crystal sizes in representative cases.<sup>30,31</sup> Typical curves found for all of the copolymer systems in Table I are shown in Figure 2. The scanning curves increased in breadth from the lowest number to the highest as  $w_b$  declined for all of the copolymers. The melting range increased from about  $22^\circ\text{C}$  for curve 1 to about  $45^\circ\text{C}$  for curve 4, but was very wide ( $50$ – $70^\circ\text{C}$ ) for curves 3 and 4 of the higher amorphous acrylate systems. In the all-acrylate systems (series 1), an increase in amorphous side-chain length of

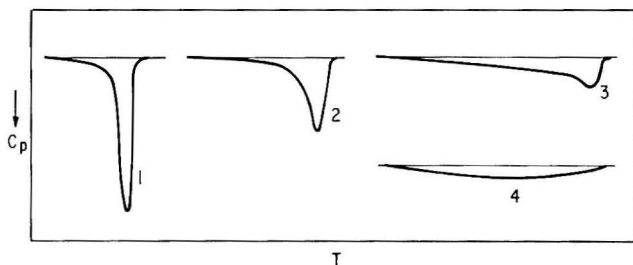


Fig. 2. Typical fusion endotherms for the copolymers by differential scanning calorimetry. *n*-Octadecyl acrylate-ethyl acrylate copolymers, selected as representative and listed in Table I, gave endotherm traces as follows: (1) experiment 23; (2) experiment 20; (3), experiment 18; (4) experiment 14.

the a component produced a broader crystallite distribution at higher values of  $w_b$ . With copolymers having a high  $T_g$  (series 2), broadening also was found even at a high proportion of fatty comonomer. This probably occurred because the segmental restraints imposed on the main chain prevented much perfection of the phase in finite times.<sup>4</sup> A similar situation has already been encountered in the bulk annealing of the poly-*N*-*n*-alkylacrylamide homopolymers,<sup>19</sup> whose  $T_g$  was relatively high. It can be readily seen from these curves why the ends of the fusion curves were designated as the melting points in Table I.

Values of the heats of fusion  $\Delta H_f$  for the pertinent data in Table I, versus the weight fraction,  $w_b$ , of the b comonomer (selectively illustrated in Fig. 1) were curve fitted using the computer. The relationship was

$$\Delta H_f = \Delta H_{f0'} + k_1 w_b + k_2 (w_b)^2 \quad (1)$$

where  $\Delta H_{f0'}$  is the intercept and  $k_1$  and  $k_2$  are the constants of the parabolic curve. The computed constants are given in Table II. Equation (1) was linear ( $k_2 = 0$ ) for the entirely *n*-alkyl acrylate copolymers (series 1), containing noncrystallizing a co-units (first five and the seventh system in Table II). Values of  $k_1$  were close to the limiting value of 21.3 cal/g (with  $\Delta H_{f0'}$  the origin) required for equilibrium crystallization<sup>4</sup> for the last three systems; the first three approached that value less closely. The constants for the other systems have no obvious physical meaning other than to permit computation of smoothed data.

The marked retention of crystallinity as the mole fraction  $m_b$  or the weight fraction  $w_b$  of *n*-octadecyl acrylate (or vinyl stearate) decreased in all of the copolymers in Table I stood in striking contrast to the rapid reduction in crystallinity usually found for copolymers of polyethylene<sup>1a,5-12</sup> and for other copolymers.<sup>1a</sup> With ethylene copolymers values of  $k_1$  [eq. (1)] three to six times those in Table II are frequently encountered<sup>9,32,33</sup> with different foreign inclusions in the chain. In fact, the extent of crystallinity of the copolymers of the present study lies close to the equilibrium limit,<sup>4</sup> especially for series 1 copolymers (Fig. 1). The data permit

TABLE II  
Curve Fitting Parameters for the Various Equations

System <sup>a</sup>	Equation (1)			Equation (10)		
	$\Delta H_{f0}'$	$k_1$	$k_2$	Intercept $\times 10^4$	$R/\Delta H_{f0} \times 10^4$	$\Delta H_{f0}$ , cal/mole
OA + MA	-3.58	25.5		0.065 <sup>b</sup>	-1.019	19,500
OA + EA	-1.35	22.8		0.087	-1.251	15,890
OA + BA	-1.81	22.9		-0.283 <sup>b</sup>	-2.144	9,269
OA + OCA	-1.32	21.4		-0.092	-2.764	7,190
OA + EHA	-1.86	21.5		-0.071 <sup>b</sup>	-2.662	7,465
OA + DA	8.79	0.029	12.2			
OA + OLA	-1.65	21.4		0.111	-2.917	6,812
OA + MMA	9.24	-37.7	51.0	-0.00012	-0.5044	39,400
OA + AN	16.6	-62.8	68.3	-0.181	-1.020	19,480
VS + MMA	-0.830	10.0	10.4	0.0864	0.00911	—
VS + EHA	-1.87	8.07	13.5	-0.250	-0.4556	43,620

<sup>a</sup> Arranged as in Table I.

<sup>b</sup> One or two data points were out of line; these were not included.

an estimation of the extent that experimental crystallinity approaches this limit.

Under equilibrium conditions<sup>4</sup> the crystallinity  $x_{c\max}$  for each mole of crystalline b units is

$$x_{c\max} = m_b = (m_b/w_b)[W_b/(W_b + W_a)] \quad (2)$$

where  $W_b$  is the weight of all b units and  $W_a$  is the weight of the a units. In like manner  $m_b$  and  $w_b$  are the respective mole and weight fractions of b units. When each crystallizing b unit is only partially crystalline, that is, crystalline in a portion only of its side chain,<sup>19</sup> then eq. (2) becomes

$$x_{c\max} = x_{c0}m_b = x_{c0}(m_b/w_b)[W_b/(W_b + W_a)] \quad (3)$$

where  $x_{c0}$  is the fraction crystallinity of the b homopolymer unit.<sup>19</sup> Molecular weights of the a and b units are often dissimilar, as in the present systems. It is conceivable that, in special cases, when the molecular weight of b units exceeds that of a units, the crystallinity in a copolymer system would correspond to simple dilution of the b by a units, thus

$$x_{c\max} = x_{c0}w_b \quad (4)$$

In such cases, however, each crystallizing unit would be required to contribute a multiplicity of segments to the crystalline phase, except in the trivial case where  $m_b = w_b$ . Under these circumstances, then

$$x_{c\max} = C_1m_b - C_2(m_b)^2 + \dots \quad (5)$$

Also under these circumstances, the maximum heat of fusion (in cal/g) would likewise correspond to simple dilution; thus

$$\Delta H_{f\max} = w_b\Delta H_{f0} \quad (6)$$

because  $x_{c0}$  is proportional to  $\Delta H_{f0}$ , the heat of fusion of the crystalline homopolymer.<sup>19</sup> The ratio of the experimental crystallinity of a crystallizable unit to the maximum attainable by the unit, on a weight basis would then be

$$x_c/x_{c\max} = \Delta H_f/\Delta H_{f\max} \quad (7)$$

where  $x_c$  is the experimental crystallinity and  $\Delta H_f$  is the observed heat of fusion. The ratio is a measure of the extent of attainment of equilibrium crystallization.<sup>34</sup>

These requirements are met by the copolymers of this investigation. Figure 1 shows that the decline in the heat of fusion is governed largely by dilution by a units, especially in series 1 copolymers. Because the molecular weight for b units is greater than for a units, each crystalline unit must contribute a block of side-chain methylene groups to the crystal lattice.<sup>19</sup> In turn, sequences of side chains are segmentalized by the interruption of a units. The extent of interruption should be determined, then, by both the frequency of occurrence of a units and by their lengths. Short a unit lengths, extending from an amorphous, and, hence, somewhat conformationally free, main chain could permit b side-chain crystal lattices to bridge the a units. Experimental crystallite sizes and perfection would then be higher and melting point depression less than required by theory.<sup>3</sup> Rates of crystallization would be increased because of the conformational freedom conferred by the amorphous main chain. Higher rates would also result from crystal growth intramolecularly initiated in local volume elements, which can proceed without the segmental sorting of main chains characteristic of ordinary crystallizing copolymers.<sup>3,4</sup> Consequently, equilibrium conditions could be approached in finite times at high b unit concentrations. The formation of stable nuclei would be prevented at low  $w_b$  so that  $x_c/x_{c\max}$  would rapidly decline. The extent to which these predictions are fulfilled by the available data will constitute the main emphasis of the balance of this paper.

With these requirements met, the experimental crystallinity  $x_c$  becomes

$$x_c = (x_c/x_{c\max})(w_b x_{c0}) \quad (8)$$

Values of the extent of equilibrium crystallinity  $x_c/x_{c\max}$  and the experimental crystallinity  $x_c$  are listed in Table I. As a generalization, the ratios are much higher than would be found for ordinary crystalline copolymers.<sup>9,32,33</sup> The ratios follow the trends previously discussed for the heats of fusion. A small decline in the ratio with decrease in  $w_b$  can be observed for the entirely acrylate copolymers, whose glass transitions are low. A more rapid decline was found in the ratio for the copolymers of higher  $T_g$  (series 2), where chain stiffness in the melt was prevalent. Even in stiff chains, conformational adjustments can apparently occur in short enough times to produce greater crystallinity than is found in copolymers crystallizing through main-chain units. Moreover, the degree to which  $x_c/x_{c\max}$  approaches unity with increasing  $w_b$  is restricted more by main-chain



stiffness than by interference by sequences of a units. For example, at  $w_b = 0.30$ ,  $x_c/x_{cmax}$  for *n*-octadecyl acrylate-oleyl acrylate (expt. 75) is 0.80 and for the *n*-octadecyl acrylate-methyl methacrylate (expt. 84) copolymer the ratio is only 0.11. On a mole base, the ratios are closer, being 0.80 and 0.37 respectively, but still remain higher for the system of lower glass transition. It may be concluded that the ability of each crystallizing co-unit to contribute several units to a side-chain lattice facilitates attainment of equilibrium, but that main-chain stiffness opposes its attainment.

In copolymers of *n*-octadecyl acrylate with *n*-dodecyl acrylate (expts. 58 and 59), the ratio  $x_c/x_{cmax}$ , viewed as a function of  $w_b$ , decreased from unity and went through a shallow minimum. This suggests that some disordered regions were present in this isomorphous system.

Blocks of sequences of vinyl stearate units would be expected in the two sets of vinyl stearate copolymers (series 3, Table I). This would result from the compositional heterogeneity imposed by the divergent copolymerization parameters for the comonomer pairs. In spite of the block character of these systems, the slope of the curve  $x_c/x_{cmax}$  against  $w_b$  for vinyl stearate copolymerized with methyl methacrylate was similar to that of *n*-octadecyl acrylate with the same comonomer. An averaging of the contributions from the crystalline and amorphous blocks seemed to produce these results. The rapid decline of  $x_c/x_{cmax}$  with decreasing  $w_b$  for the 2-ethylhexyl acrylate copolymers with vinyl stearate suggests that in this case the influence of the amorphous blocks predominates.

### Melting Point Depression

The equation for the melting point depression of copolymers in which only one component crystallizes is given by the general theory of Flory<sup>3</sup>

$$(1/T_m) - (1/T_{m0}) = (-R/\Delta H_{f0}) \ln p \quad (9)$$

where  $T_m$  and  $T_{m0}$  are the equilibrium melting points of, respectively, the copolymers and the homopolymer and  $p$  is the probability that a crystallizable b unit will be succeeded by another b unit. The heat of fusion  $\Delta H_{f0}$  is the value for the entirely crystalline phase of the b comonomer and should equal the quantity obtained from the homopolymer by using a diluent.<sup>1c</sup> That it rarely does so is attributed to the experimental impossibility of detecting the melting of the extremely small fraction of large crystallites actually present in copolymers.<sup>1a,c,3,4</sup> For a random copolymer,  $p$  becomes indistinguishable with the mole fraction of b units, designated  $m_b$ . Thus,

$$(1/T_m) - (1/T_{m0}) = (-R/\Delta H_{f0}) \ln m_b \quad (10)$$

Consequently, plots of  $(1/T_m) - (1/T_{m0})$  versus  $\ln m_b$  should yield  $\Delta H_f$  from the slope.

The melting points, listed in Table I, were inserted into eq. (10) and treated by regression analysis by using the computer. The appropriate

constants are given in Table II. Values of  $\Delta H_{f0}$  are also listed in column 7 of this table. The apparent heat of fusion,  $\Delta H_{f0}$ , for the copolymers containing *n*-octadecyl acrylate decreases as the side-chain length  $n_a$  of the amorphous a co-unit becomes greater (series 1 and 2). It appears to reach a limiting value when  $n_a$  is 18 carbon atoms. This is close to the value of  $\Delta H_{f0}$  for poly(*n*-octadecyl acrylate),<sup>19</sup> which was 6925 cal/mole. Values of the slope,  $(R/\Delta H_{f0})$  in eq. (10) (Table II) indicate that the rate of melting point depression decreases as the length of the a unit decreases.  $R/\Delta H_{f0}$  approaches a constant value as  $n_a$  becomes very great. It would seem, at least across short ranges of  $n_a$ , that

$$R/\Delta H_{f0} = (R/\Delta H_{f0})_0 + \delta(\ln n_a) \quad (11)$$

The appropriate constants (Table II) are plotted against  $\ln n_a$  in Figure 3. The parameters are given in the figure. Substituting eq. (11) into eq. (10) and rearranging yields

$$T_m = 1/\{[(R/\Delta H_{f0}) + \delta(\ln n_a)] - \ln m_b\} + (1/T_{m0}) \quad (12)$$

Melting points calculated by using eq. (12) are compared with found values in Table III. Thus, melting points of random copolymers having co-units composed of crystallizing 18-carbon side chains and  $n_a$  of any magnitude between 1 and at least 20 can be calculated by eq. (12) by employing only the constants of Figure 3.

It may be concluded that sequence distribution produces a melting-point depression of theoretical magnitude, as in eq. (10), only when the length of the amorphous a units equals or exceeds the length of the crystallizing side chains. Then, and only then, do the crystallite lengths fully correspond to sequence distances as required.<sup>3</sup> In contrast to copolymers crystallizing through the main chain, the amorphous main chains and immediately adjacent side-chain methylene groups<sup>19</sup> of the present copoly-

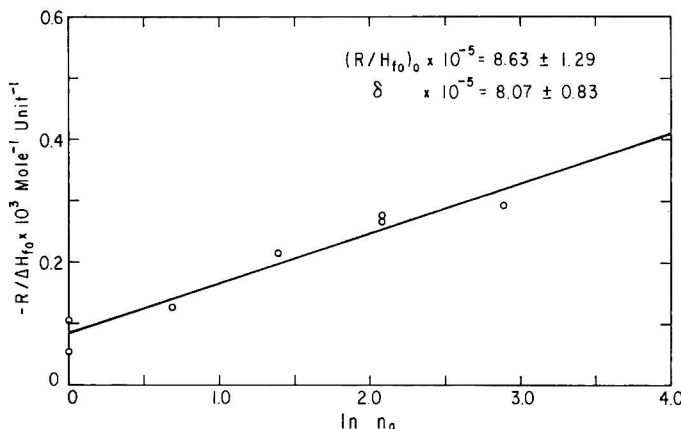


Fig. 3. Relationship between the quantity  $R/\Delta H_{f0}$  and the number of methylene groups in the side chain of amorphous comonomer a.

TABLE III  
Comparison of Melting Points Calculated by Equation (12) with Experimental Values

Mole fraction <sup>a</sup>	Melting point, °K							
	OA + MA		OA + BA		OA + OCA		OA + OLA	
	Calcd	Found	Calcd	Found	Calcd	Found	Calcd	Found
0.050	304	290	276	261	264	260		
0.075	307	300	282	274	271	267	259	265
0.100	310	306	287	283	277	273	266	270
0.15	313	312	294	295	285	282	275	276
0.20	316	315	299	301	291	288	282	285
0.30	319	325	306	308	300	299	293	295
0.40	322	320	311	315	307	306	301	303
0.50	324	321	316	318	312	313	308	310
0.60	325	324					313	313
0.75	327 <sup>b</sup>	325 <sup>b</sup>	324	323	322	320	320	319
1.00	330	330	330	330	330	330	330	330

<sup>a</sup> Feed composition.

<sup>b</sup> Mole fraction of fatty ester was 0.70.

mers enjoy greater freedom; the localized availability of crystallizable outer-chain methylene groups then results in crystallization at rates high enough to approach equilibrium values. Consequently, when *a* units reach a critical length of about 18 carbon atoms, the calculated  $\Delta H_{f0}$  approaches the value found for homopolymers.<sup>1c,3,4</sup> Main-chain stiffness in the melt (as in series 2 copolymers) makes little contribution to  $T_m$  depression but does affect rates of crystallization at high *a*-unit content. Thus, the experimental observations obey the requirements specified earlier in this paper for copolymers crystallizing through side chains.

Melting points of vinyl stearate copolymers (series 3, Table I) show little depression, as would be expected.<sup>1a,3</sup> Here the exceptionally long blocks of vinyl stearate units are retained and the data consequently would follow eq. (9).

As has been discussed, when short *a* units occur in these systems (Table I), they are largely bridged by developing side-chain crystallinity. As *a* units increase in length, their effect on reducing the crystallite size of the most perfect crystal increases. Consequently, it is possible to calculate a mole fraction of *b* units based on the crystallite size at equilibrium melting. Because melting point depression increases as crystal size decreases, use can be made of eq. (10) to calculate  $m_b$ , but using  $\Delta H_{f0} = 6925$  cal/mole, which is the value of  $\Delta H_{f0}$  for poly(*n*-octadecyl acrylate). If these values of  $m_b$ , designated  $m_{bc}$ , fall on theoretical plots for  $\Delta H_{fmax}$  [eq. (6)] of  $x_{cmax}$  [eq. (4)], the condition of equilibrium crystallinity required by eq. (3) will be met. Data are shown in Figure 4 where  $x_{cmax}$  is plotted as a function of  $m_{bc}$  for the systems whose melting points are listed in Table III. For the calculation of  $m_{bc}$  the calculated melting points of Table III were used. An exception was the methyl acrylate system where found values were

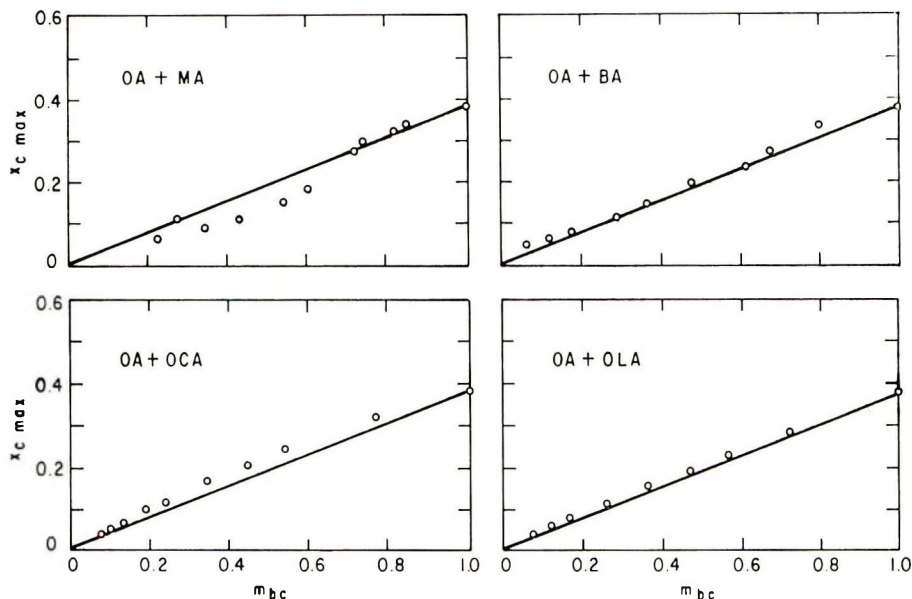


Fig. 4. Plots of  $x_{c \max}$  vs. the mole fraction of crystalline co-unit b: (O) calculated by using eq. (10) (—) theoretical:  $x_{c \max}$  at  $m_{bc} = 1$  is  $x_{c0}$ .<sup>19</sup>

employed. As can be seen, the conditions of eq. (3) are generally met. The apparent differences found in this work for copolymers crystallizing through their side chains, compared with other types of crystallizing copolymers,<sup>1a,4,5-13</sup> appear to have a simple coherent explanation.

### SUMMARY AND CONCLUSIONS

The thermodynamics of the crystallinity present in the side chains of selected copolymers has been treated experimentally. Consideration was given to the development of crystallinity in the side chains of b co-units interrupted by randomly dispersed a units of varied lengths. It was concluded that (1) reduction in crystal size was proportional to the amorphous side-chain length; (2) rates of crystallization were high so that equilibrium crystallization was approached at high b-unit concentrations; (3) chain stiffness in the melt had some broadening effect on crystal-size distribution but made a much larger contribution to retarding the attainment of equilibrium; (4) the presence of long blocks of b co-units, as in the heterogenous vinyl stearate copolymers, depressed melting points only slightly, following the accepted theoretical probability sequence function; (5) crystallinity development seemed dependent on stable crystal nuclei forming largely intramolecularly in small volume elements and growing because of the unrestrained cooperative movements of amorphous main-chain and side-chain units.

The authors wish to thank Dr. C. L. Ogg, Miss Oksana Panasiuk, Mrs. Marta T. Lukaszewycz, and Mrs. Annette S. Kravitz for the elementary analysis of the monomers and copolymers. They are also grateful to Mrs. Ruth D. Zabarsky for the operation of the computer.

Reference to a commercial product does not constitute recommendation by the U. S. Department of Agriculture over any other similar products not mentioned.

### References

1. L. Mandelkern, *Crystallization of Polymers*, McGraw-Hill, New York, 1964, (a) pp. 74-116; (b) pp. 215-290; (c) pp. 38-71.
2. L. Mandelkern, *Rubber Chem. Technol.*, **32**, 1392 (1959).
3. P. J. Flory, *Trans. Faraday Soc.*, **51**, 848 (1955).
4. B. Wunderlich, *J. Chem. Phys.*, **29**, 1395 (1958).
5. C. H. Baker and L. Mandelkern, *Polymer*, **7**, 7 (1966).
6. T. Arakawa and B. Wunderlich, *J. Polym. Sci. A-2*, **4**, 53 (1966).
7. R. G. Griskey and G. N. Foster, *J. Polym. Sci. A-1*, **8**, 1623 (1970).
8. D. Bodily and B. Wunderlich, *J. Polym. Sci. A-2*, **4**, 25 (1966).
9. P. M. Kamath and R. W. Wakefield, *J. Appl. Polym. Sci.*, **9**, 3153 (1965).
10. A. Barlow and R. C. Campbell, *J. Appl. Polym. Sci.*, **11**, 2001 (1967).
11. E. P. Otocka, T. K. Kwei, and R. Solovey, *Makromol. Chem.*, **129**, 144 (1969).
12. R. L. Alexander, H. D. Ansporn, F. E. Brown, B. H. Clambitt, and R. H. Hughes, *Polymer Eng. Sci.*, **6**, 5 (1966).
13. M. H. Theil and L. Mandelkern, *J. Polym. Sci. A-2*, **8**, 957 (1970).
14. W. S. Port, E. F. Jordan, Jr., J. E. Hansen, and D. Swern, *J. Polym. Sci.*, **9**, 493 (1952).
15. E. F. Jordan, Jr., G. R. Riser, W. E. Parker, and A. N. Wrigley, *J. Polym. Sci. A-2*, **4**, 975 (1966).
16. E. F. Jordan, Jr., G. R. Riser, B. Artymyshyn, W. E. Parker, J. W. Pensabene, and A. N. Wrigley, *J. Appl. Polym. Sci.*, **13**, 1777 (1969).
17. E. F. Jordan, Jr., W. E. Palm, D. Swern, L. P. Witnauer, and W. S. Port, *J. Polym. Sci.*, **32**, 33 (1958).
18. S. A. Greenberg and T. Alfrey, *J. Amer. Chem. Soc.*, **76**, 6280 (1954).
19. E. F. Jordan, Jr., D. W. Feldeison, and A. N. Wrigley, *J. Polym. Sci. A-1*, **9**, 1835 (1971).
20. E. F. Jordan, Jr., K. M. Doughty, and W. S. Port, *J. Appl. Polym. Sci.*, **4**, 203 (1960).
21. E. F. Jordan, Jr., R. Bennett, A. C. Shuman, and A. N. Wrigley, *J. Polym. Sci. A-1*, **8**, 3113 (1970).
22. E. F. Jordan, Jr., *J. Polym. Sci. A-1*, **9**, 3367 (1971).
23. D. Swern and E. F. Jordan, Jr., *J. Amer. Chem. Soc.*, **70**, 2334 (1948).
24. E. F. Jordan, Jr., B. Artymyshyn, and A. N. Wrigley, *J. Polym. Sci. A-1*, **7**, 2605 (1969).
25. L. E. Nielsen, *Mechanical Properties of Polymers*, Reinhold, New York, 1962, pp. 11-15.
26. B. Wunderlich, P. Sullivan, T. Arakawa, A. B. Dieyan, and J. F. Flood, *J. Polym. Sci. A*, **1**, 3581 (1963).
27. B. Wunderlich, *Polymer*, **5**, 125 (1964).
28. B. Wunderlich, *Polymer*, **5**, 611 (1964).
29. A. P. Gray and K. Casey, *J. Polym. Sci.*, **2**, 381 (1964).
30. B. Ke, *J. Polym. Sci.*, **42**, 15 (1960).
31. B. Wunderlich and W. H. Kashdan, *J. Polym. Sci.*, **50**, 71 (1961).
32. B. Wunderlich and D. Poland, *J. Polym. Sci. A*, **1**, 357 (1963).
33. M. J. Richardson, P. J. Flory and J. B. Jackson, *Polymer*, **4**, 221 (1963).
34. R. L. Miller, in *Encyclopedia of Polymer Science and Technology*, H. F. Mark, N. G. Gaylord, and N. Bikales, Eds., Interscience, New York, 1966, Vol. 4, p. 449.

Received June 8, 1971

Revised June 29, 1971



## Side-Chain Crystallinity. III. Influence of Side-Chain Crystallinity on the Glass Transition Temperatures of Selected Copolymers Incorporating *n*-Octadecyl Acrylate or Vinyl Stearate

EDMUND F. JORDAN, JR., *Eastern Regional Research Laboratory, Eastern Marketing and Nutrition Research Division, Agricultural Research Service, U. S. Department of Agriculture, Philadelphia, Pennsylvania 19118*

### Synopsis

The influence of side-chain crystallinity on the glass transition temperatures of selected copolymers was investigated. The copolymers were selected, in part, from those whose crystallinity was treated in the preceding paper. These included the lower amorphous acrylate esters, such as methyl, ethyl, *n*-butyl, and 2-ethylhexyl acrylates, together with methyl methacrylate and acrylonitrile, each copolymerized with *n*-octadecyl acrylate over the range of composition. The decline in the glass transition temperature was linear with increasing weight fraction of *n*-octadecyl acrylate for all systems in the composition range where the copolymers were essentially amorphous. The extrapolated  $T_g$  for the amorphous state of poly(*n*-octadecyl acrylate), and for amorphous poly(oleyl acrylate), was close to  $-111^\circ\text{C}$ . This coincided with a value previously obtained by an extrapolation of data on homologs. Beyond a critical fraction of octadecyl acrylate (0.3 to 0.5), developing side-chain crystallinity in *n*-octadecyl acrylate raised the glass temperature steadily for all systems, up to a value of  $17^\circ\text{C}$ , obtained for the crystalline homopolymer. Crystallinity did not develop in stiff copolymers until  $T_g$  was about  $30^\circ\text{C}$  below the melting point of the most perfect crystals. In compositionally heterogeneous copolymers incorporating vinyl stearate, blocks of crystalline units appeared to be dispersed in a glassy matrix of amorphous co-units. An empirical equation was derived which fitted the experimental data for random copolymers, over all composition ranges, with fair accuracy.

### INTRODUCTION

The influence of crystallinity on the glass transition temperature of polymers is not readily predictable.<sup>1,2</sup> It might be reasonable to expect that the glass transition would always rise as crystallinity increased. In analogy with covalent crosslinking,<sup>3</sup> crystallites are thought, by tying certain chains together, to restrict their segmental motion, thus raising  $T_g$ . Indeed, for many crystalline homopolymers the glass transition was raised.<sup>1,2,4-8</sup> Some, however, showed no change,<sup>9,10</sup> and one system even showed a decrease<sup>11,12</sup> in  $T_g$ . These conflicting observations have not received a uni-

fied explanation, although the behavior of individual systems was rationalized in some of the reports.

The crystallinity present in all of these polymers involved an ordering of main-chain units. No known studies have been made relating a shift of the glass transition in copolymers to crystallinity occurring in side chains. The disrupting influence of side-chain crystallites on the viscoelastic properties of the higher methyl methacrylates has long been known.<sup>13,14</sup> Some limited observations indicated that developing side-chain crystallinity induced a strongly adverse effect on the mechanical properties of copolymers,<sup>15,16</sup> without, however, affecting the monotonic decline of their flex temperatures.

In this study the change of the glass temperature with composition was followed for most of the copolymers whose heats of fusion and melting points were determined in the previous paper.<sup>17</sup> Included in the present study were copolymers of *n*-octadecyl acrylate with the lower amorphous acrylate homologs, such as methyl (MA), ethyl (EA), *n*-butyl (BA), 2-ethyl hexyl (EHA) and with stiff comonomers, such as methyl methacrylate (MMA) and acrylonitrile (AN), over the range of composition. Also included were copolymers of vinyl stearate (VS) and oleyl acrylate (OLA) with methyl methacrylate. It was expected that a comprehensive picture of the influence of side-chain crystallinity on  $T_g$  would result from the large amount of experimental data collected here. A major consideration centered on detecting any shift in  $T_g$  with increasing side-chain crystallinity, conferred by increasing weight fraction of either *n*-octadecyl acrylate or vinyl stearate. Differential scanning calorimetry was used to measure the glass transition temperatures. The conventions and designations of the preceding paper<sup>17</sup> were followed here. A subsequent paper will demonstrate the effect on some mechanical properties of the interrelation of side-chain crystallinity and the glass transition.

## EXPERIMENTAL

The preparation, purification, and analysis of the various monomers and copolymers were fully described in the preceding paper.<sup>17</sup> The operation of the differential scanning calorimeter was the same, except that scanning speeds of 40°C/minute (through three separate scans), 20 and 10°C/min (through one scan each) were employed for each sample. Scanning ranges were from -90°C to 20°C above the melting transition. Largest sample weights (14 to 25 mg.) were used for maximum sensitivity. All computations were performed with an IBM 1130 computer by procedures previously described.<sup>16</sup>

## RESULTS AND DISCUSSION

### Glass Transition Temperatures

Most of the copolymer systems investigated and their glass transition temperatures are listed in Table I. In addition, copolymer composition,

TABLE I  
 Glass Transition Temperatures Found for the Copolymers

Fatty ester in copolymer, mole fraction <sup>a</sup>	Glass transition temperature, °C <sup>b</sup>						
	OA + MA	OA + EA	OA + BA	OA + EHA	OA + MMA	OA + AN	VS + MMA <sup>c</sup>
0	6 <sup>d</sup>	-23.0	-55.0	-77.0	101.6	92.0	101.6
0.050	-10.3	-29.7	-62.0	-78.7	77.0	52.0	109.0
0.075	-20.7	—	-66.0	-80.0	57.8	34.3	89.0
0.100	-31.7	-43.0	-66.4	-80.0	38.0	11.0	88.0
0.125	-39.2	-53.0	-73.0	-82.0	39.0	4.0	86.0
0.150	-48.3	-48.4	-55.0	-83.0	26.0	-13.0	82.0
0.200	-49.3	-55.0	-49.0	-83.0	17.0	-25.0	79.0
0.300	-54.0	-33.0	-48.0	-43.0	22.0	-23.0	77.0
0.400	3.7	-18.0	-33.0	-38.0	20.7	-19.0	—
0.500	10.7	1.0	5.0	-17.0	20.7	-13.0	72.0
0.600	21.0	9.0	—	-13.0	17.0	-2.0	—
0.750	17.0 <sup>e</sup>	6.0	14.0	-13.4	21.0	7.0	75.0
1.00	17.0	17.0	17.0	17.0	17.0	17.0	—

<sup>a</sup> Feed composition; compositions found by elemental analysis agreed within experimental error. For the corresponding weight fractions, see Table I of the previous paper.

<sup>b</sup> Designations are: OA, n-octadecyl acrylate; MA, methyl acrylate; EA, ethyl acrylate; BA, n-butyl acrylate; EHA, 2-ethyl hexyl acrylate; MMA, methyl methacrylate; AN, acrylonitrile; VS, vinyl stearate.

<sup>c</sup> Mole fractions, of vinyl stearate, calculated from elemental analysis, were 0, 0.024, 0.036, 0.046, 0.076, 0.183, 0.197, 0.377, 0.414, 0.375, 0.744, 0.902.

<sup>d</sup> Data from Brandrup and Immergut.<sup>25</sup>

<sup>e</sup> Mole fraction was 0.70.

degree of polymerization and glass transition temperature are listed in Table II for copolymers of oleyl acrylate and methyl methacrylate. *n*-Octadecyl acrylate and vinyl stearate are the crystallizing co-units. Most of the glass transition data that follow are correlated with weight fraction; weight fractions for all of the copolymers, except those in Table II, are listed in Table I of the preceding paper<sup>17</sup> and correspond to the mole fractions listed in Table I of this paper. For convenience, the order in both tables is the same.

The onset temperature was taken in this work to be the glass transition temperature,  $T_g$ . This interpretation of  $T_g$  is shown as curve 1 in Figure 1B. The choice is somewhat controversial, however. The generally accepted methods of obtaining  $T_g$  from DSC traces<sup>18-21</sup> involve extrapolation of the inflection point, or endotherm maximum,<sup>22</sup> of the heat capacity curves for successive finite scanning speeds to zero rate. This method, which recognizes the rate dependency of the transition,<sup>23</sup> is supported on theoretical grounds.<sup>19,20</sup> However, the alternate method of using the onset temperature apparently gives values independent of scanning speed,<sup>24</sup> which are close to accepted literature values. In the present work, values of  $T_g$  within about 1-4°C of literature values,<sup>25a</sup> usually obtained by other

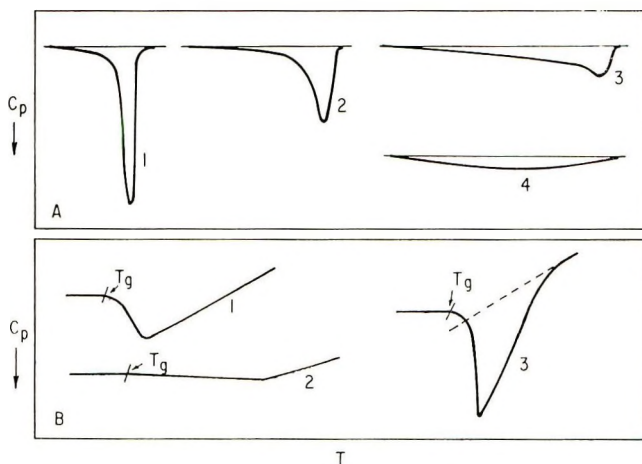


Fig 1. Typical scanning curves for the copolymers. (A) Fusion endotherms of *n*-octadecyl acrylate-ethyl acrylate copolymers, selected as representative with various mole fractions of *n*-octadecyl acrylate, as listed in Table I: (1) 0.75; (2) 0.40; (3) 0.20; curve (4) 0.05. (B) Glass transition curves of systems selected as representative from Table I: (1) ethyl acrylate copolymer system, mole fraction *n*-octadecyl acrylate 0.05; (2) methyl methacrylate copolymer system, mole fraction of *n*-octadecyl acrylate, 0.075; (3) methyl methacrylate copolymer system, mole fraction of *n*-octadecyl acrylate, 0.40.

methods, were obtained by this procedure for polyacrylonitrile, poly(methyl methacrylate), poly(vinyl chloride), poly(ethyl acrylate), and (*n*-butyl acrylate). Glass transitions were obtained at two and sometimes three different scanning speeds and averaged. It would appear that errors inherent in the use of the onset temperature at varied scanning speeds just

TABLE II  
Glass Transition Temperatures, and Degree of Polymerization  
of Oleyl Acrylate-Methyl Methacrylate Copolymers

Experiment number	Oleyl acrylate in copolymer		DP <sub>n</sub> <sup>a</sup>	T <sub>g</sub> , °C
	Mole fraction	Weight fraction		
1	0.050	0.145	1631	73.6
2	0.075	0.207	1663	61.3
3	0.100	0.264	1448	50.3
4	0.125	0.315	1016	21.7
5	0.150	0.362	872.8	26.0
6	0.200	0.448	787.7	5.0
7	0.300	0.580	383.9	-14.3
8	0.400	0.682	267.1	-42.3
9	0.500	0.763	193.1	-49.0
10	0.600	0.829	152.6	-57.0
11	0.750	0.906	128.9	-45.0

<sup>a</sup> Calculated from osmometric molecular weights by using a weighted average of the molecular weights of the two comonomers. Copolymers were partially crosslinked. The soluble fraction decreased from 94% to 6% from experiments 1 to 11.



manage to compensate for rate effects. In any event, in this work, the onset temperature was the only reproducible temperature. Some scans on amorphous copolymers were obtained indicating very small heat capacity differences between the liquid and glassy states, respectively (curve 2, Figure 1B). In many the inflection point was completely masked by the presence of crystallinity (curve 3, Figure 1B). In the latter cases, the onset of melting (intersection of the dashed line) and the temperature interpreted to be  $T_g$  nearly coincided. The trends of the data in passing from the completely amorphous copolymers to the crystalline systems supported the interpretation of  $T_g$ . This convergence seems to be a unique characteristic of these systems.

### Relation of $T_g$ to Copolymer Composition in the Amorphous Region

The copolymers retained their amorphous character between the limits of 0 and 0.5 maximum for the long side-chain comonomer. This is the region considered in the discussion that follows.

Many theoretical expressions have been derived for the glass transitions of amorphous copolymers<sup>26</sup> as a function of composition. Most of these are extensions of treatments obtained from kinetic and thermodynamic theories relating to the vitreous transition in solids.<sup>1</sup> An expression which is empirical but seems to apply to many systems measured is<sup>27</sup>

$$T_g = T_{ga}w_a + T_{gb}w_b + Kw_aw_b \quad (1)$$

Here  $T_{ga}$  and  $T_{gb}$  are the glass transitions of the respective homopolymers,  $w_a$  and  $w_b$  are their weight fractions, and  $K$  is an empirical constant. In the special case where  $K = 0$ , eq. (1) becomes

$$T_g = T_{ga}w_a + T_{gb}w_b \quad (2)$$

Because  $T_g$  is linear here with respect to composition

$$T_g = T_{ga} - kw_b \quad (3)$$

where  $k$  is the slope [ $T_{gb} < T_{ga}$ ;  $k = (T_{ga} - T_{gb})$ ] and  $T_{ga}$  the intercept of plots of experimental  $T_g$  against weight fraction of the b comonomer. The glass transition-composition data for all of the copolymer systems in Table I and II, through the composition region where the copolymers are amorphous, followed eq. (3). The parameters for the various copolymer systems are listed in Table III. The magnitude of  $k$  steadily decreased as  $T_{ga}$  decreased. These data illustrate the monotonic decline in  $T_g$  expected with composition<sup>1, 15, 16</sup> with no attending complications of curve maxima or minima.<sup>28, 29</sup>

Typical data are shown in Figure 2 for copolymers of *n*-octadecyl acrylate or oleyl acrylate with methyl methacrylate. The data for the *n*-octadecyl system, shown as the solid line, at the left side of the plot, up to a weight fraction of 0.365, represent the decline in  $T_g$  in the absence of appreciable crystallinity. Above this weight fraction the  $T_g$ -composition curve is



TABLE III  
Curve Fitting Parameters for Various Equations

System	Equation (3)*		Equations (9) and (10)		
	$T_{ga}$	$k$	$(x_c/x_{c\max})_0$	$\alpha$	$\beta$
OA + MA	280.1	126.0			
OA + EA	250.9	77.59			
OA + BA	218.3	63.10			
OA + EHA	195.9	21.66			
OA + MMA	375.8	213.4			
OLA + MMA	374.5	210.0			
OA + AN	368.8	200.6			
VS + MMA	369.9	30.86			
Set 1			0.3250	1.639	-1.023
Set 2			0.1030	-0.3567	1.290

\* From Table I the glass transition temperatures correlated corresponded to these mole fractions of the  $C_{18}$  component: MA, 0.050 to 0.20; EA, 0 to 0.20; BA, 0 to 0.125; EHA, 0 to 0.20; MMA, 0 to 0.150; AN, 0 to 0.20; VS + MMA, all mole fractions.

affected by developing crystallinity. In contrast,  $T_g$  for the entirely amorphous oleyl acrylate-methyl methacrylate copolymers, shown as the line, declined linearly to a weight fraction of about 0.73. Appreciable crosslinking through the oleyl side chain is thought to distort the curve beyond this point.<sup>3</sup> Poly(oleyl acrylate), like poly-*N*-oleylaerylamide,<sup>16</sup> is entirely amorphous, as revealed by differential scanning calorimetry. Both amorphous curves extrapolate to values for the respective homopolymers near 162°K ( $-111^\circ\text{C}$ ). This is the value marked with a star in the figure. A  $T_g$  of 162°K was the value assigned as the glass transition of a variety of structurally varied homopolymers having 18 carbon linear side chains when in their amorphous state.<sup>15</sup> It had been obtained by extrapolating the glass transition temperature of several systems of amorphous

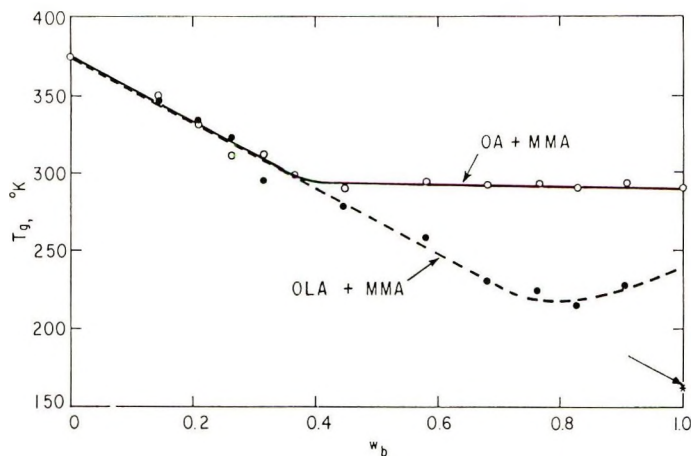


Fig. 2. Plot of glass transition temperature vs. weight fraction of fatty ester for copolymers of, respectively, *n*-octadecyl acrylate or oleyl acrylate with methyl methacrylate.

lower homologs to a side-chain length of 18 carbon atoms by using the relation<sup>15</sup>

$$T_g = T_{g0} - \beta(\ln \alpha) \quad (4)$$

where  $\alpha$  is the number of flexible bonds in the unit,  $\beta$  is the rate of change of  $T_g$  with  $\ln \alpha$ , and  $T_{g0}$  is a constant characteristic of a homologous series. Thus these data on copolymers, in particular the data on the amorphous oleyl system, confirm the reported  $T_g$  for the amorphous state of poly(*n*-octadecyl acrylate) and for poly(oleyl acrylate). Further confirmation is found in the amorphous regions of the  $T_g$ -composition curves for several other systems. These are shown as the linear portions of the curves in Figure 3. Again all of the data follow eq. (3), and extrapolation leads to  $T_{gb}$ , near 162°K (−111°C).

In this connection the glass temperature of polymethylene deserves consideration. It now appears that the true glass transition for linear polyethylene is −130°C (143°K).<sup>9,30</sup> This coincides with the  $\gamma$  transition<sup>2</sup> for the hydrocarbon. This value is very close to a temperature of −135°C found<sup>31</sup> by extrapolation of the  $T_g$  of a series of poly(alkylene oxide)s, of varying methylene length,  $-(CH_2)_nO-$  to the limit of polymethylene by using the method of Grieverson.<sup>32</sup> The value of  $T_g$  at  $n = 18$  is about −125°C by this method. Thus the glass transition temperatures for poly(oleyl acrylate), and for the amorphous state of poly(*n*-octadecyl acrylate) and probably of other flexible linear 18-carbon homopolymers such as poly(vinyl stearate), poly(*n*-octadecyl vinyl ether), and poly(*n*-octadecyl methacrylate),<sup>33</sup> lie close to −111°C. At very long extensions of the side chains the glass transition for amorphous polymethylene (−130°C) would be approached for all systems.

### Relation of $T_g$ to Composition in the Crystalline Region

The solid or dashed lines extending to the right on the curves in Figures 2 and 3 continue the experimental values of the glass transition-composition curve (Tables I and II). It is obvious that the regular decline of  $T_g$  beyond a weight fraction of *n*-octadecyl acrylate of about 0.4 is reversed by developing crystallinity. In Figure 3, as the temperature rises for such a composition, the lower part of the dotted line marks the onset of crystallite melting; the upper part of the line is where the last trace of crystallinity disappears. The latter was taken as  $T_m$  in the preceding paper. In the numbered regions, scanning curves had the appearance of the corresponding curves of insert A, Figure 1. The spread of the curves is taken as an indication of the distribution of crystallite sizes<sup>34</sup> found as composition changed. Temperature intervals were from 22 to about 45°C. The position of each number in Figure 3 marks the approximate beginning of the melting range indicated. Of course, the regions to the left of the dotted area are the completely amorphous regions discussed above.

The curves show (Fig. 3) that main-chain stiffness has an appreciable effect on the development of crystallinity in the copolymers. In the

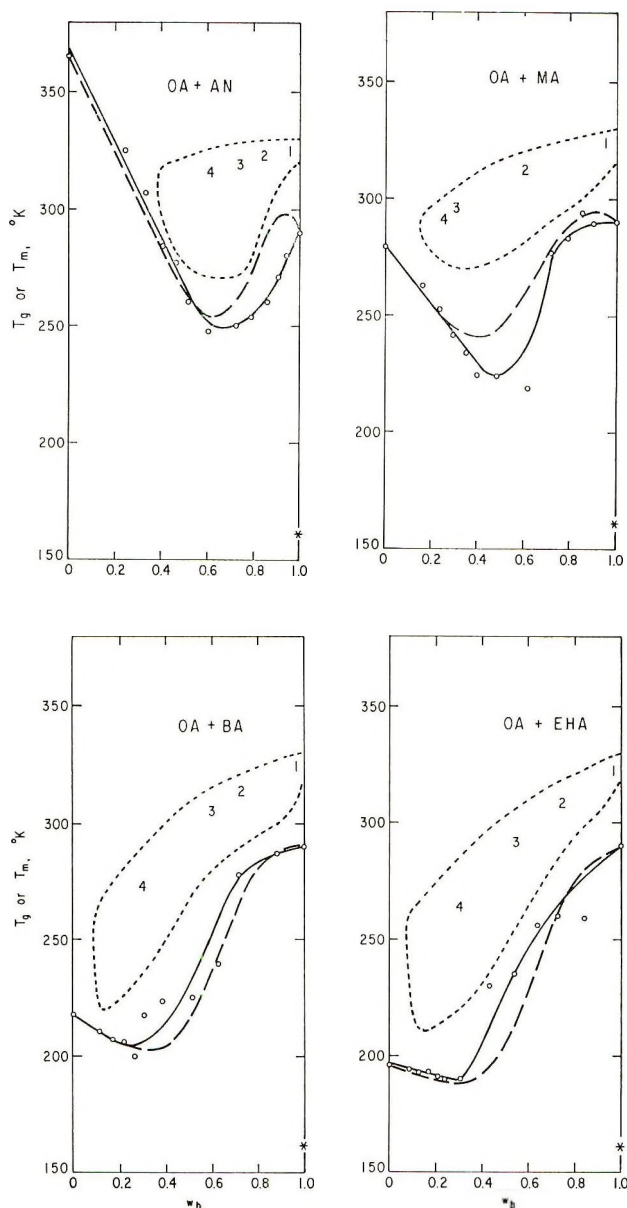


Fig. 3. Effect of side-chain crystallinity on the glass transition temperatures of copolymers of *n*-octadecyl acrylate with various comonomers: (—) experimental data for  $T_g$ ; (---)  $T_g$  calculated by using eq. (8); (···) crystallinity range. Abscissa, weight fraction *n*-octadecyl acrylate.

*n*-octadecyl acrylate-acrylonitrile (OA + AN) system, measurable crystallinity, as indicated by the dotted line, was not present till the glass transition temperatures had been reduced to about 290°K (17°C). This occurred at a weight fraction of about 0.4 *n*-octadecyl acrylate. Somewhat

similar results were found for the *n*-octadecyl acrylate-methyl methacrylate copolymers (Table I). In contrast, as  $T_g$  progressively decreased with change to more flexible comonomers (MA, BA, EHA), crystallinity first appeared at smaller weight fractions of the long-chain ester. In the latter systems equilibrium crystallinity was approached over a much wider composition range than was found in the former. This phenomenon has been discussed in the preceding paper.<sup>17</sup> It may be concluded that before appreciable crystal formation began in these copolymers, glass transitions were reduced some 20 to 30°C below the equilibrium melting point. The composition range at which this occurs will be determined by the difference between  $T_{gb}$  and  $T_{ga}$  for the respective homopolymers, that is, by the magnitude of  $k$  in Table III. At a composition somewhat higher in component b, characteristic of each system,  $T_g$  begins to rise. It is possible that this rise corresponds to the region where crystal impingement becomes important.<sup>2</sup>

While the amorphous region has been adequately described by eq. (3), it might be helpful to develop a relation governing the extent of change of  $T_g$  with composition that will include the region where side-chain crystallinity developed. The simplest expression to be considered is an additive one, such that

$$T_g = w_a T_{ga} + w_b' T_{gb} + w_c' T_{gc} \quad (5)$$

In this expression  $T_{ga}$  is the glass transition temperature of amorphous homopolymer a,  $T_{gb}$  is that of the hypothetical amorphous state of crystalline homopolymer b, and  $T_{gc}$  its observed glass transition (Fig. 3). For poly(*n*-octadecyl acrylate)  $T_{gc}$  was 290°K (17°C). In eq. (5)  $w_a$  is the weight fraction of homopolymer a and  $w_b = w_b' + w_c'$ . The weight fraction of crystallizable comonomer is  $w_b$ , and  $w_b'$  and  $w_c'$  are the portions of  $w_b$  that are amorphous and crystalline, respectively. These quantities may be computed as

$$w_b' = (1 - x_c/x_{c \max})w_b \quad (6)$$

$$w_c' = (x_c/x_{c \max})w_b \quad (7)$$

The ratio  $x_c/x_{c \max}$  relates experimental crystallinity for the copolymer,  $x_c$ , to the maximum crystallinity possible at equilibrium. These ratios were discussed in the preceding paper<sup>17</sup> and are found there in Table I.

Equation (5), however, did not fit the experimental data. Apparently at low  $w_b$  the contribution of crystallinity to rendering the main chain rigid is reduced, and the amorphous contributions predominate, so that the proposed partition is not adequate. Similarly, at high  $w_b$  the effect of crystalline impingements would intensify. Consequently eq. (5) can be modified by introducing a parameter as an exponent which will be sensitive to the initially small and later intense influence of developing crystallinity with increasing *n*-octadecyl acrylate. If the exponent is assumed to be linear with composition of *n*-octadecyl acrylate, eq. (5) becomes

$$T_g = w_a T_{ga} + [w_b' + (w_c' - w_c'^{C+k_s w_b})] T_{gb} + (w_c'^{C+k_s w_b}) T_{gc} \quad (8)$$



with

$$w_c' = [(x_c/x_{c \max})_0 + \alpha w_b + \beta w_b^2]w_b \quad (9)$$

and

$$w_b' = 1 - w_c' \quad (10)$$

By an iterative procedure,  $C$  and  $k_s$  were assigned the values of 4.0 and  $-4.0$ . To obtain  $w_c'$  and  $w_b'$  through eqs. (9) and (10), values of  $x_c/x_{c \max}$  were correlated against  $w_b$  (Table I in the preceding paper), the curve fitting being carried through a fifth degree polynomial and analyzed for significance by an  $F$  test in the computer. The significant constants are shown in Table III. Two sets of constants were required. Parameters for systems of high main-chain mobility (the entirely  $n$ -alkyl acrylate copolymers) are listed in set 1. When main chains were stiff (methyl methacrylate, acrylonitrile), the constants of set 2 applied.

Glass transition temperatures calculated by using eq. (8) are shown in Figure 3 as the dashed lines. The empirical equation appears to describe the main features of the experimental data fairly well. It is versatile enough (providing the correct constants of Table III are employed) to apply to the usual range of  $T_g$  (100 to  $-80^\circ\text{C}$ ) encountered in copolymers. Consequently the changing glass-transition temperature, introduced by side-chain crystallinity, appears to be adequately described by this simple relationship.

When copolymer compositions are highly heterogeneous, both the crystalline and amorphous co-units polymerize in blocks and usually aggregate into separate domains. Consequently, developing side-chain crystallinity should little influence the apparent glass transition. This was found for

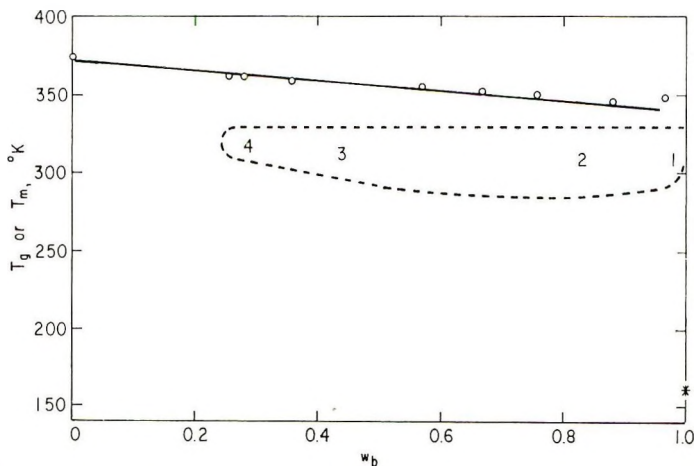


Fig. 4. Effect of side-chain crystallinity on the glass transition temperature of copolymers of vinyl stearate and methyl methacrylate: (—) glass transition temperature; (---) melting transition temperature. Abscissa, weight fraction vinyl stearate.



copolymers of vinyl stearate and methyl methacrylate (Table I), in which compositional heterogeneity is marked.<sup>25b</sup> Data are shown in Figure 4. Apparently, domains rich in methyl methacrylate suffered little decrease in  $T_g$  with increase in the overall weight fraction of vinyl stearate. Consequently the value of  $k$  in Table III was low. The value of  $T_{gb}$  for amorphous poly(vinyl stearate), shown as the star in the figure, was never approached. This contrasts with the curves in Figure 2 for random copolymers. On the other hand, chains rich in vinyl stearate, crystallizing in the region marked by the dotted line, showed little melting point depression. This behavior is different from that found for random copolymers in Figure 3. The plots in Figure 4, consequently, reflect the aggregation of the crystalline and amorphous domains. The limit of this behavior would be incompatible mixtures of the two homopolymers.

### SUMMARY AND CONCLUSIONS

The effect of crystallinity developing in side chains on the glass transition temperature of selected copolymers was investigated. The decline in the glass transition for all of these copolymer systems was linear with respect to  $n$ -octadecyl acrylate in the composition range where the copolymers were essentially amorphous. The extrapolated  $T_g$  of poly( $n$ -octadecyl acrylate) in the amorphous state, as well as for amorphous poly(oleyl acrylate), was close to  $-111^\circ\text{C}$ . This coincided with the value previously obtained by an extrapolation of data on series of homologs. Beyond a critical composition, developing side-chain crystallinity raised the glass temperature steadily, up to a value of  $17^\circ\text{C}$ , obtained for the crystalline homopolymer. Crystallinity did not develop in any random system until the glass transition temperature had been reduced to about  $30^\circ\text{C}$  below the melting point of the most perfect crystals. Compositionally heterogeneous copolymers acted as if chains containing blocks of crystalline units were dispersed in a glassy matrix of largely amorphous co-units. An empirical equation was derived which fitted the experimental data for random copolymers over the composition range with fair accuracy.

The author thanks Mrs. Ruth D. Zabarsky for the operation of the computer.

### References

1. M. Shen and A. Eisenberg, *Rubber Chem. & Technol.*, **43**, 95 (1970); *ibid.*, **43**, 163 (1970).
2. L. E. Neilson, *Mechanical Properties of Polymers*, Reinhold, New York, 1962, pp. 180-189.
3. L. E. Neilson, *J. Macromol. Sci. C*, **3**, 69 (1969).
4. S. Newman and W. P. Cox, *J. Polym. Sci.*, **46**, 29 (1960).
5. B. E. Read, *Polymer*, **3**, 529 (1962).
6. T. M. Connor, B. E. Read, and G. Williams, *J. Appl. Chem.*, **14**, 74 (1964).
7. J. A. Faucher, J. V. Koleske, J. R. Santee, J. S. Stratta, and C. W. Wilson, III, *J. Appl. Phys.*, **37**, 3962 (1966).
8. D. W. Woods, *Nature*, **174**, 753 (1954).

9. F. C. Stehling and L. Mandelkern, *J. Polym. Sci. B*, **7**, 255 (1969).
10. J. D. Hoffman and J. J. Weeks, *J. Nat. Bur. Stand.*, **60**, 465 (1958).
11. J. H. Griffith and B. G. Ranby, *J. Polym. Sci.*, **44**, 369 (1960).
12. B. G. Ranby, K. S. Chan, and H. Brumberger, *J. Polym. Sci.*, **58**, 545 (1962).
13. S. F. Kurath, T. P. Yin, J. W. Berg, and J. D. Ferry, *J. Colloid Sci.*, **14**, 147 (1959).
14. P. R. Saunders and J. D. Ferry, *J. Colloid Sci.*, **14**, 239 (1959).
15. E. F. Jordan, Jr., G. R. Riser, W. E. Parker, and A. N. Wrigley, *J. Polym. Sci. A-2*, **4**, 975 (1966).
16. E. F. Jordan, Jr., G. R. Riser, B. Artymyshyn, W. E. Parker, J. W. Pensabene, and A. N. Wrigley, *J. Appl. Polym. Sci.*, **13**, 1777 (1969).
17. E. F. Jordan, Jr., B. Artymyshyn, A. Specia, and A. N. Wrigley, *J. Polym. Sci. A-1*, **9**, 3349 (1971).
18. J. M. Barton, *Polymer*, **10**, 151 (1968).
19. S. Strella, *J. Appl. Polym. Sci.*, **7**, 569 (1963).
20. S. Strella and P. F. Erhardt, *J. Appl. Polym. Sci.*, **13**, 1373 (1969).
21. G. L. Taylor and S. Davison, *J. Polym. Sci. B*, **6**, 699 (1968).
22. A. Lambert, *Polymer*, **10**, 319 (1969).
23. S. M. Ellerstein, in *Thermoanalysis of Fibers and Fiber-Forming Polymers* (*Appl. Polym. Symp.*, **2**), R. F. Schwenker, Ed., Interscience, New York, 1966, p. 111.
24. H. G. Elias and O. Etter, *J. Macromol. Sci. A-1*, 943 (1967).
25. J. Brandrup and E. H. Immergut, *Polymer Handbook*, Wiley, New York 1966, (a) III, pp. 61-72; (b) II, 352-362.
26. L. A. Wood, *J. Polym. Sci.*, **28**, 319 (1958).
27. M. C. Shen and A. V. Tobolsky, in *Plasticization and Plasticizer Processes*, R. F. Gould, Ed., American Chemical Society, 1965, pp. 27-34.
28. K. H. Illers, *Kolloid Z.*, **190**, 16 (1963).
29. K. H. Illers, *Ber. Bunsenges. Physik. Chem.*, **70**, 353 (1966); *Chem. Abstr.*, **64**, 17732a (1966).
30. F. C. Stehling and L. Mandelkern, *Macromolecules*, **3**, 242 (1970).
31. J. A. Faucher and J. V. Koleski, *Polymer*, **9**, 44 (1968).
32. B. M. Grievson, *Polymer*, **1**, 499 (1960).
33. S. S. Rogers and L. Mandelkern, *J. Phys. Chem.*, **61**, 985 (1957).
34. B. Ke, *J. Polym. Sci.*, **42**, 15 (1960).

Received June 8, 1971

Revised June 29, 1971

## Analysis of Polymerization Rates in Radical Polymerization with Primary Radical Termination of Some Methacrylates

KATSUKIYO, ITO, *Government Industrial Research Institute, Nagoya,  
Kita-Ku, Nagoya, Japan*

### Synopsis

Polymerization rates in polymerizations with primary radical termination of ethyl methacrylate,  $\beta$ -phenylethyl methacrylate,  $\beta$ -methoxyethyl methacrylate, and phenyl methacrylate initiated by 2,2'-azobis-(2,4-dimethylvaleronitrile) at 60°C were analyzed by using a simple linear equation. The values obtained of  $k_{ti}/k_i k_p$  (where  $k_{ti}$  is the primary radical termination rate constant,  $k_i$  is the rate constant of addition on to monomer of primary radical, and  $k_p$  is the propagation rate constant) on these analyses are discussed on the theoretical base.

### INTRODUCTION

In the previous paper,<sup>1</sup> in order to analyze polymerization rate  $R_p$  in the polymerization with primary radical termination, the following inequality was derived.

$$A \left( 1 - \frac{B[C]^{1/2}}{[M]} + \frac{2B^2[C]}{[M]^2} - \dots \right) \geq \frac{R_p}{[M][C]^{1/2}}$$

$$\geq A \left( 1 - \frac{B[C]^{1/2}}{[M]} + \frac{2B^2[C]}{[M]^2} - \dots \right) \quad (1)$$

$$A = (2fk_d k_t)^{1/2} k_p$$

$$B = (2fk_d/k_t)^{1/2} k_{ti}/k_i$$

Here,  $[C]$  and  $[M]$  are, respectively, the concentrations of initiator and monomer,  $f$  is the initiator efficiency, and  $k_d$ ,  $k_p$ ,  $k_i$ ,  $k_t$ , and  $k_{ti}$  are the rate constants of the decomposition of initiator, propagation, addition onto monomer of primary radical, chain termination, and primary radical termination, respectively.

When  $B[C]^{1/2}/[M] \ll 1$ , inequality (1) becomes a simple linear equation:<sup>2</sup>

$$\frac{R_p}{[M][C]^{1/2}} = A \left( 1 - \frac{A k_{ti} [C]^{1/2}}{k_i k_p [M]} \right) \quad (2)$$

By using this equation, the values of  $k_{ti}/k_i k_p$  in various polymerization systems have been calculated.<sup>2,3</sup>

In this paper, polymerization rates in polymerizations of ethyl methacrylate (EMA),  $\beta$ -phenyl methacrylate (PEMA),  $\beta$ -methoxyethyl methacrylate (MEMA), and phenyl methacrylate (PMA) initiated by 2,2'-azobis(2,4-dimethyl valeronitrile) (ABVN) are analyzed by using eq. (2).

## EXPERIMENTAL

### Material

PEMA and MEMA were prepared by ester exchange between appropriate alcohols and a 4*M* excess of methyl methacrylate (MMA) in the presence of small amount of *p*-toluenesulfonic acid as a catalyst. PMA was prepared by the reaction methacryl chloride and sodium phenoxide.

The above monomers and commercial EMA were washed three times with 5% sodium hydroxide and twice with water, respectively. Each monomer was dried over with sodium sulfate and fractionally distilled under reduced pressure. The middle cut of monomer (EMA, bp 55°C/55 mm Hg; PEMA, 109°C/4 mm; MEMA, 60°C/9 mm; PMA, 82°C/5 mm) was retained and stored in the dark at -25°C until used.

Pure ABVN was supplied by Wako Pure Chemical Industries. ABVN was also stored at -25°C until used.

All solvents used were reagent grade.

### Procedure

Measurement of polymerization rate was carried out by using the same dilatometer as used in the preceding work.<sup>3</sup> The initiator ( $[C] \leq 0.025$  mole/l.), monomer, and dimethyl carbitol (DC) as solvent (monomer:DC = 1:3 by volume) in the dilatometer was degassed by successive freeze-thaw cycles and then sealed under a vacuum of about  $10^{-4}$  mm Hg. The dilatometer was maintained at  $60 \pm 0.02^\circ\text{C}$ . The value of  $k_d$  at 60.0°C is calculated to be  $5.45 \times 10^{-4}$  l/sec.<sup>5</sup>

Total shrinkage for each polymerization was calculated by using the densities for monomer and polymer shown in Table I.

## RESULTS AND DISCUSSION

Relationship between  $R_p/[M][C]^{1/2}$  and  $[C]^{1/2}/[M]$  in the polymerization of EMA, PEMA, MEMA, or PMA is given in Figure 1. The range of  $[C]^{1/2}/[M]$  of eq. (2) available [EMA,  $\leq 0.06$  (l./mole)<sup>1/2</sup>; PEMA,  $\leq 0.09$

TABLE I  
Densities for Monomer and Polymer at 60°C

	EMA	MEMA	PEMA	PMA
$d_{\text{monomer}}$ , g/cc	0.8751	0.9560	0.9902	1.0240
$d_{\text{polymer}}$ , g/cc	1.1080	1.1448	1.1697	1.1933

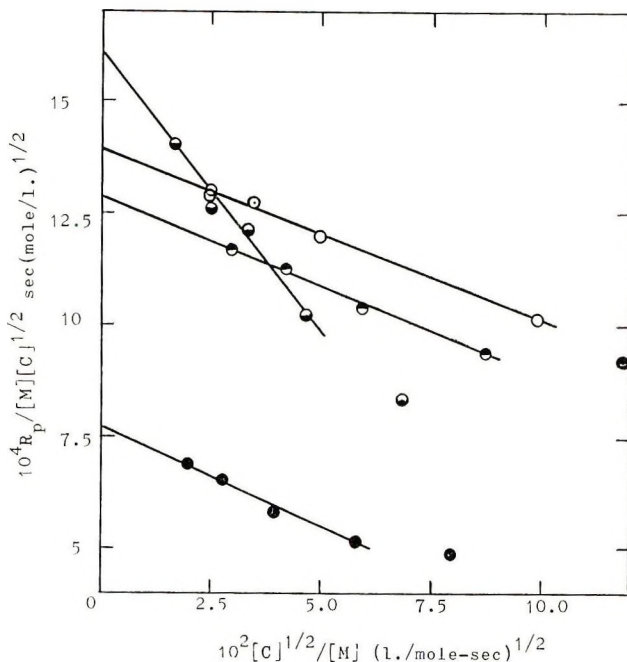


Fig. 1. Relationships between  $R_p/[M][C]^{1/2}$  and  $[C]^{1/2}/[M]$  in the polymerizations of (●) EMA, (◐) MEMA, (◑) PEEMA, and (○) PMA initiated by ABVN at 60.0°C.

$(\text{l./mole})^{1/2}$ ; PMA,  $\leq 0.10 (\text{l./mole})^{1/2}$ ] increases with increasing  $A$  [for EMA,  $A = 7.73 \times 10^{-4}$ ; for PEEMA,  $A = 12.8 \times 10^{-4}$ ; for PMA,  $A = 13.90 \times 10^{-4} \text{ sec}(\text{mole/l.})^{1/2}$ ]. However, in the polymerization of MEMA, in spite of the large value of  $A = 16.1 \times 10^{-4} \text{ sec}(\text{mole/l.})^{1/2}$  the range of  $[C]^{1/2}/[M]$  of eq. (2) is quite small,  $[C]^{1/2}/[M] \leq 0.05 (\text{l./mole})^{1/2}$  because  $AB$  is very large. These results show that eq. (2) may be available in the range of  $0 \leq B[C]^{1/2}/[M] \leq 1/3$ .

The values of  $k_{ti}/k_i k_p$  are calculated from the above linear relations on the basis of eq. (2) and collected in Table II. If the value of  $f$  in this case is identical with the value of  $f$  for 2,2'-azobis(2,4-dimethyl butyronitrile),  $f$  may be 0.51.<sup>4</sup> Thus, we obtain  $(2fk_d) = 5.57 \times 10^{-5}/\text{sec}$ .<sup>3</sup> On the basis of this value, the values of  $k_i/k_p^2$  were calculated from the value of  $A$  and are collected in Table II.

TABLE II  
Values of  $k_i/k_p^2$  and  $k_{ti}/k_i k_p$  at 60°C

	MMA	EMA	MEMA	PEMA	PMA
$k_i/k_p^2$ , mole-l./sec	144 <sup>a</sup>	93.0	21.4	33.7	54.0
$10^{-3}k_{ti}/k_i k_p$ , mole l./sec	7.33 <sup>a</sup>	11.5	4.82	2.38	1.96
$(k_{ti}/k_i)(k_p/k_i)$	50.9	124	225	70.6	27.1

<sup>a</sup> Values obtained in the previous paper.<sup>3</sup>



If the value of  $k_t$  may be approximated to the value of  $k_p$ , the primary radical termination rate constant may be one hundred times the chain termination rate constant (Table II). Unfortunately, the values of  $k_t$  and  $k_p$  are unknown, and this approximation may be only qualitative.

The author wishes to thank Wako Pure Chemical Industries for supplying ABVN.

### References

1. K. Ito and T. Matsuda, *J. Appl. Polym. Sci.*, **14**, 311 (1970).
2. K. Ito and T. Matsuda, *Bull. Chem. Soc. Japan*, **42**, 1758 (1969).
3. K. Ito, *J. Polym. Sci.*, in press.
4. G. S. Hammond, J. N. Sen, and C. R. Boozer, *J. Amer. Chem. Soc.*, **77**, 3244 (1955).

Received April 11, 1971

## Temperature Effects in $\gamma$ -Initiated Polymerization of Styrene. II.

S. P. SOOD, *Department of Chemistry, University of Hawaii, Hilo Campus, Hawaii* and J. W. HODGINS, *Department of Chemical Engineering, McMaster University, Hamilton, Ontario, Canada*

### Synopsis

Experimental data are presented for the  $\gamma$ -initiated polymerization of commercial styrene at a series of temperatures above ambient. Examination of the early stages of polymerization (up to 10% conversion) has led to the following conclusions. For this system, there exists a critical temperature (109°C) above which the rate of polymerization is independent of dose rate, over a wide range of  $\gamma$ -intensities. This dose rate independence is ascribed to a "limiting rate of initiation," characteristic of the intensity range. A consequence of this is that at a given temperature above the critical temperature the degree of polymerization is also dose rate-independent. The above phenomena can be expected in any vinyl monomer where the monomer is fairly active and produces relatively stable radicals. Experimental procedure is described, and kinetic analysis presented to substantiate the conclusions.

### Introduction

Radiation-induced polymerization of vinyl monomers has been extensively investigated during the past several decades. At low conversions and at normal temperatures the polymerization reaction is initiated by free radicals and the kinetic data can be well explained in terms of conventional free radical mechanisms. Chapiro<sup>1</sup> has reviewed the developments in this field covering the period up to 1962.

Recent developments reported by Chen and Stamm,<sup>2</sup> Okamura et al.,<sup>3</sup> and Johnson et al.<sup>4</sup> have stimulated renewed interest in this field. Chen and Stamm reported evidence for the existence of ionic and free-radical mechanisms in the polymerization of styrene at low temperatures, while other workers<sup>3,4</sup> reported that the radiation-induced polymerization of extremely "dry" liquid styrene proceeds via an ionic mechanism. Considerably faster rates of polymerization and high  $G_{\text{styrene}}$  values were obtained in the ionic polymerization as compared to free radical reaction.\*

In the present investigation a comprehensive study of the polymerization of liquid styrene was carried out at relatively higher temperatures and several dose rates. In all cases the reactions were studied up to 100% conversion with the objective of developing kinetic models for the polymerization of styrene at high conversions. These results will be reported later.

\*  $G_{\text{styrene}}$  is the number of monomer units reacted per 100 eV absorbed.

In this study, by using  $\gamma$  initiation, unusual and unexpected temperature effects on the rates and the degrees of polymerization of styrene have been observed and reported in part earlier.<sup>5</sup> A tentative explanation for the temperature phenomenon is presented on the basis of kinetic analysis of data for conversions up to about 10%.

### Experimental Procedures

Commercial styrene (supplied by Polymer Corporation of Canada) was chosen as the reactant, since the applicability of this work to industrial practice was considered of importance. The monomer analysis was as follows: styrene, 99.630 wt-%; ethylbenzene 0.032%; isopropylbenzene, 0.123%; *n*-propylbenzene, 0.090%; *sec*-butylbenzene, 0.039%;  $\alpha$ -methylstyrene, 0.037%; sulfur, 0.0004%; chlorides, 0.0001%; benzaldehyde, 0.0033%; peroxide ( $\text{H}_2\text{O}_2$ ), 0.0012%; polymer, 0.0016%; water, saturated (500 ppm).

The reaction vials were made from 18-mm diameter Pyrex tubing and cleaned with an oxidizing mixture (50:50) of boiling concentrated sulfuric and nitric acids. The vials were then rinsed five times with tap water; three times with distilled water; three times with reagent grade acetone and dried overnight at 110–120°C.

The samples for irradiation were prepared by delivering 10 cc of styrene into the reaction vials and the dissolved air removed from the monomer in a cycle of freezing, pumping, and thawing, repeated twice before sealing under vacuum at about  $10^{-5}$  mm Hg pressure.

Conversions were determined by standard gravimetric procedure using about tenfold volume of methanol for precipitation of dioxane solutions of polymer-monomer mixtures. For very high conversions, the residual monomer was determined by ultraviolet spectrophotometry.<sup>6</sup>

Irradiation of samples was carried out in an air oven by use of a  $^{60}\text{Co}$  source (nominally 5000 Ci) described elsewhere.<sup>7</sup> The samples were positioned in a uniform field of radiation intensity and dosimetric calibration at sample positions was accomplished by Fricke dosimetry<sup>8</sup> by using vials of approximately the same dimensions and geometry as the reaction vials.

The design of our irradiator has some useful and versatile features. The air oven is shown in Figure 1 with a concentric arrangement of aluminum cylinders fabricated to uniform diameters and fixed in position on a stand. The sample vials were attached to these cylinders by a ring-and-clip arrangement so that all the samples fixed to any one cylindrical sample holder were at a uniform distance from the axis of the source and in a field of uniform radiation intensity. It was necessary to use two additional stainless steel cylinders (inner two cylinders) in proximity to the  $^{60}\text{Co}$  source to prevent breakage of the sample vials while removing or positioning the source for irradiation. With this arrangement it was possible to investigate three different dose rates at one time. Four or five different dose rates may be investigated simultaneously by adding additional cylindrical sample

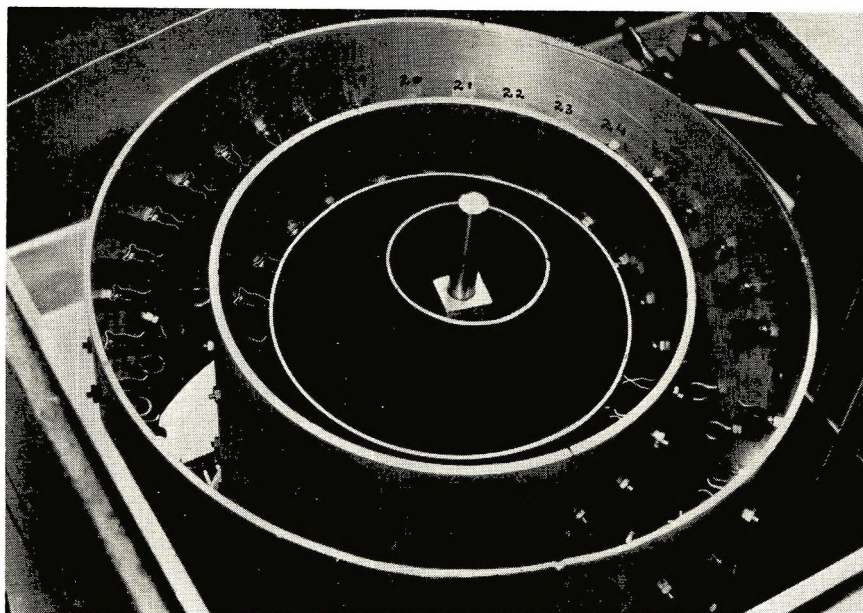


Fig. 1. Irradiation apparatus.

holders. Up to 66 samples may be irradiated simultaneously. The irradiation chamber was heated by blowing air over a series of heaters.

### Results and Discussion

At the outset, in this study polymerization of styrene was investigated up to 100% conversions at 50, 74, and 89°C at dose rates of 178, 58, and 24 rad/sec for each temperature. In addition, conversions to about 10% were also investigated at 99 and 109°C for the same dose rates. For this monomer all conversion curves are sigmoid in character and complete conversion of monomer to polymer was achieved over the entire range of the experimental conditions investigated. Typical conversion curves are shown in Figures 2-4.

This paper offers a kinetic analysis of the linear portion of these sigmoid curves (to 10% conversion); relevant data are listed in Table I. Further study is in progress on the kinetic processes represented in the upper portion of the curve.

In Figure 5 are presented the plots of rates of polymerization against dose rate for the various temperatures investigated in this study. The temperature dependence of the rate and the degree of polymerization on the dose rate is rather unexpected. Chapiro<sup>1</sup> has developed a simple kinetic expression for low conversion, as follows:

$$R_p = (k_p/k_t^{1/2})(\phi_m[M]I)^n[M] \quad (1)$$



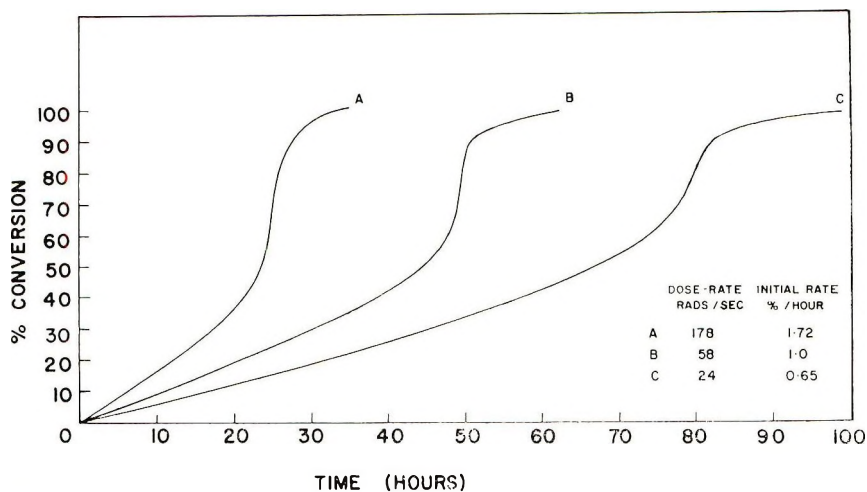


Fig. 2.  $\gamma$ -Ray-induced polymerization of bulk styrene. Plot of percent conversion against reaction time at various dose rates. Temperature  $50^{\circ}\text{C}$ .

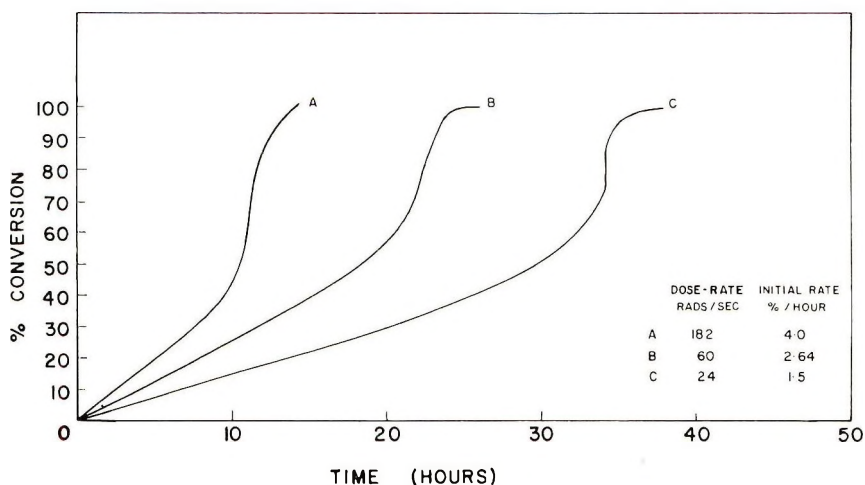


Fig. 3.  $\gamma$ -Ray-induced polymerization of bulk styrene. Plot of per cent conversion against reaction time at various dose rates. Temperature  $74^{\circ}\text{C}$ .

where  $R_p$  is the rate of polymerization,  $k_p$  and  $k_t$  are the propagation and termination rate constants, respectively,  $\phi_m[M]$  is the rate of production of free radicals per unit radiation dose,  $I$  is the dose rate, and  $[M]$  the monomer concentration.

Many workers have found that  $n$ , the exponent of the dose rate, is 0.5 for low conversions; our experiments at  $50^{\circ}\text{C}$  and  $74^{\circ}\text{C}$  confirm this observation.

However, above  $74^{\circ}\text{C}$ , the value of  $n$  decreases linearly with rising tem-



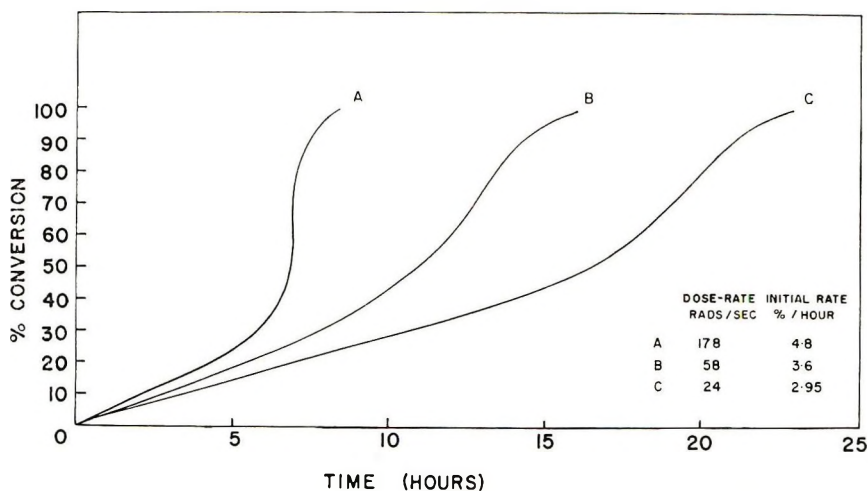


Fig. 4.  $\gamma$ -Ray-induced polymerization of bulk styrene. Plot of per cent conversion against reaction time at various dose rates. Temperature 59°C.

perature, until above about 109°C under the radiation conditions specified, the rate of conversion becomes independent of dose rate.

A similar trend of the temperature dependence is also observed for the average degree of polymerization  $\bar{P}_n$ . In Figure 6 are given the plots of  $\bar{P}_n$  against dose rate; the results are tabulated in Table II.

From the steady-state free-radical polymerization kinetics the following relationship can be derived,<sup>12</sup> assuming chain-transfer to the monomer and termination by recombination:

$$1/\bar{P}_n = (k_t R / 2k_p^2 [M]^2) + (k_{trm} / k_p) \quad (2)$$

where  $\bar{P}_n$  is the average degree of polymerization and  $k_{trm}$  is the rate constant for the chain transfer to the monomer. Other constants are defined earlier.

In Figures 7 and 8, the reciprocal of the number-average degree of polymerization  $\bar{P}_n$  is plotted against the overall rate of polymerization for the various temperatures investigated in this study. The number-average molecular weight ( $\bar{M}_n$ ) was determined by membrane osmometry.

The intercept of each of these plots is zero indicating that chain transfer to the monomer is negligible, which is in agreement with literature. From the slope,  $k_t/k_p^2$  ratios were obtained, where slope =  $k_t/2k_p^2[M]^2$ ; the values are listed in Table I.

The values of  $k_p^2/k_t$  are plotted against  $1/T$  in Figure 9 to obtain the temperature dependence of  $k_p^2/k_t$  ratios. For comparison purposes, data of Huang et al.,<sup>13</sup> Tobolsky and Offenbach,<sup>14</sup> and Matheson et al.<sup>15</sup> are also plotted along with the present data which are in excellent agreement with

TABLE I  
Summary of Experimental Results for the  $\gamma$ -Initiated Polymerization of Liquid Styrene

Temperature, °C	Dose rate, rad/sec	Conversion, %/hr <sup>a</sup>	$R_p \times 10^5$ , mole/l.-sec	Corrected $R_p \times 10^5$ , mole/l.-sec <sup>b</sup>	$\bar{M}_n$ (osmometry)	$\bar{P}_n$	$k_t/2k_p^2$
50 ± 0.2	178	1.72	4.22	4.22	60,400	580	2690
	58	1.0	2.45	2.45	119,800	1140	
	24	0.65	1.59	1.59	214,500	2060	
74 ± 0.2	182	4.0	9.17	9.17 (8.72)	143,000	1375	542
	60	2.5	5.73	5.69 (5.28)	221,000	2120	
	24	1.5	3.44	3.37	344,000	3300	
89 ± 0.2	178	4.8	10.83	10.62	211,500	2025	284
	58	3.6	8.12	7.74	361,000	3460	
	24	2.95	6.65	6.50	400,000	3830	
99 ± 0.5 <sup>c</sup>	170	6.0	13.39	12.64 (12.68)	205,000	1960	220
	54	5.1	11.39	10.50 (10.94)	296,000	2830	
	21	4.8	10.72	9.73	302,000	2900	
109 ± 1 <sup>c</sup>	178	8.40	18.55	16.32	—	—	—
	58	8.20	18.11	15.81	—	—	—
	24	8.15	18.0	15.79	—	—	—

<sup>a</sup> Thermal rates of polymerization from Boundy-Boyer<sup>11</sup> are 0.025, 0.3, 0.95, 2.0, and 4.0% per hour at 50, 74, 89, 99, and 109°C, respectively.

<sup>b</sup> Rates in parentheses normalized to dose rates of 0.64, 0.21, and 0.09 Mrad/hr. These values were taken from the plots of polymerization rates vs. dose rates.

<sup>c</sup> Correction for thermal component<sup>9,10</sup>  $R_{\text{rad}} = (R_{\text{total}}^2 - R_{\text{thermal}}^2)^{1/2}$ .

TABLE II  
Dose Rate Exponent as a Function of Polymerization Rate and Degree of Polymerization

$T, ^\circ\text{C}$	$n$ (for $R_p \propto I^n$ )	$n$ (for $\bar{P}_n \propto I^n$ )
50	0.50	-0.62
74	0.48	-0.43
89	0.27	-0.33
99	0.13	-0.20
109	0.005	—

those of other workers. The resulting Arrhenius type relationship is expressed as:

$$k_p^2/k_t = 2.85 \times 10^4 e^{-12,027/RT}$$

Energies of activation  $\epsilon_a$  for the polymerization reactions were calculated for the three dose rates employed, and the values are listed in Table III. It will be noted that in the temperature range 19–74°C our data agree well with those in the literature.

From the data plotted in Figure 10, however, activation energies are higher in the range 74–109°C. This could be the result of a parallel initiation reaction which becomes significant above 74°C. The data points labeled I, II, and III are considered experimentally valid. Further data are now being assembled for the temperature range 74–100°C.

In order to understand the nature of parallel initiation and to elucidate the meaning of the data points labeled I, II, and III in Figure 10, the rates

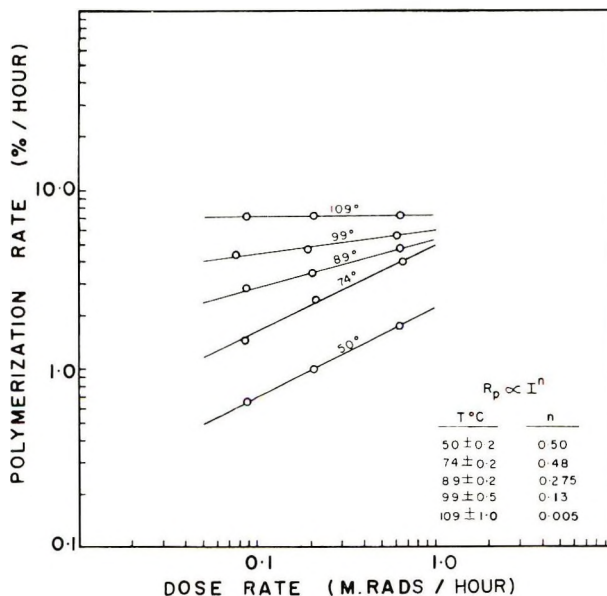


Fig. 5. Influence of temperature on the rate of  $\gamma$ -initiated polymerization of styrene.

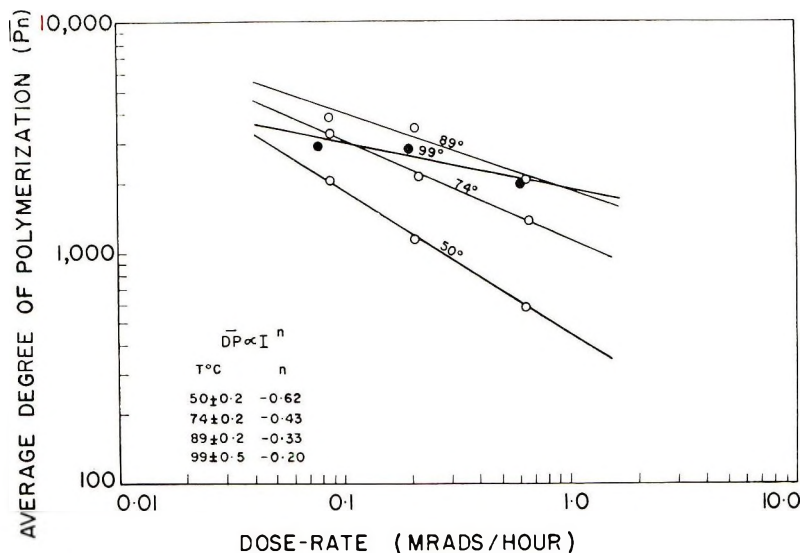


Fig. 6. Influence of temperature on the average degree of polymerization in the  $\gamma$ -initiated polymerization of styrene.

of initiation  $R_i$  are plotted against  $1/T$  in Figure 11. The rates of initiation were calculated by using the following expression:

$$R_{i(\gamma)} = R_{i(\text{total})} - R_{i(\text{thermal})} \quad (3)$$

where

$$R_{i(\text{total})} = R_p^2 / (k_p^2 [M]^2 / k_t) \quad (4)$$

and

$$R_{i(\text{thermal})} = 2k_i [M]^2 \quad (5)$$

In these expressions  $R_p$  is the observed rate of polymerization in mole/l.-sec;  $k_t$  and  $k_p$  are the termination and propagation rate constants, respectively;  $k_i$  is the initiation rate constant, and  $[M]$  is the molar concentration of monomer. The values for  $k_i$  were obtained from the Roche and Price<sup>11</sup> expression:

$$k_i = 1.885 \times 10^6 e^{-13,900/T} \quad (6)$$

TABLE III  
Activation Energy  $\epsilon_a$  of Polymerization Reaction

Dose rate, <i>Mrad/hr</i>	$\epsilon_a$ , kcal/mole		Huang et al. <sup>13</sup>
	This work		
0.64	6.2		6.1
0.21	9.7(74–109°C)	6.0(19–74°C)	6.1
0.09	12.7(74–109°C)	6.2(19–74°C)	6.1

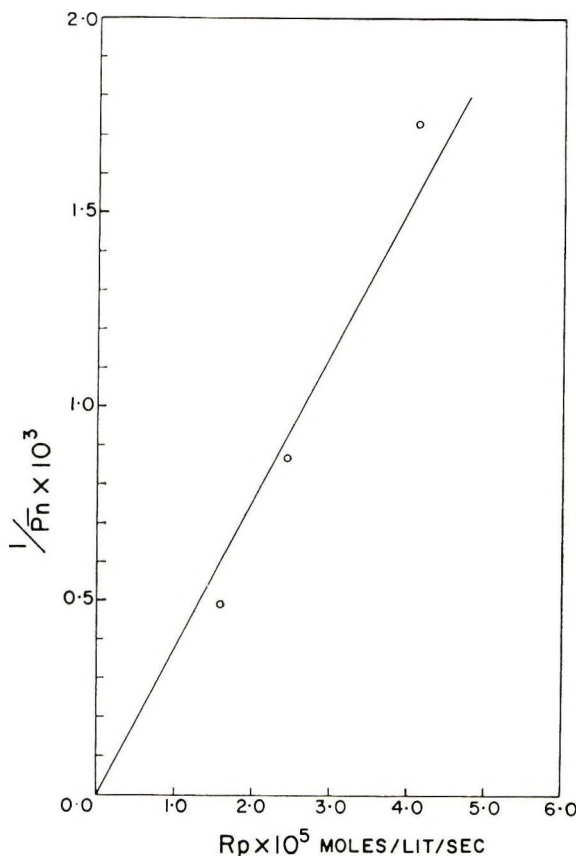


Fig. 7. Plot of the reciprocal of the number-average degree of polymerization vs. the rate of the  $\gamma$ -ray-initiated polymerization of styrene. Temperature 50°C.

This expression for  $R_{t(\gamma)}$  takes account of the thermal contribution to the overall rate of polymerization which becomes increasingly significant above 74°C.

This plot reveals some interesting features related to the observed phenomena and the following tentative conclusions may be drawn.

(1) For the temperature range 50–74°C, the slopes labeled A, pertain to the region where  $R_p \propto I^{1/2}$ , and the observed increase in the rate of initiation ( $R_i$ ) is due to an increased ability of the primary free radicals to initiate growing chains. This is the normal temperature effect and is observed for all dose rates investigated in this study. Furthermore the regularity of the data justifies confidence that the data points labeled I, II, and III in Figure 10 are valid.

(2) In the case of 0.64 Mrad/hr dose rate, the rate of initiation  $R_i$  exhibits a maximum at 74°C and the  $R_i$  decreases between that temperature and about 92°C (region labeled C), possibly due to the recombination of



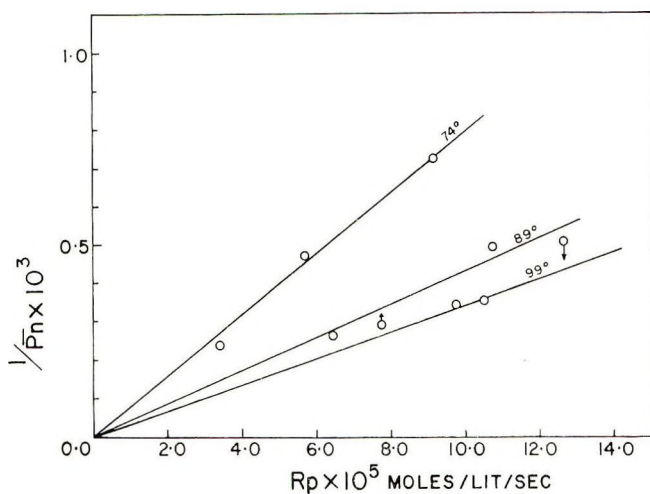


Fig. 8. Plot of the reciprocal of the number-average degree of polymerization vs. the rate of the  $\gamma$ -ray-initiated polymerization of styrene.

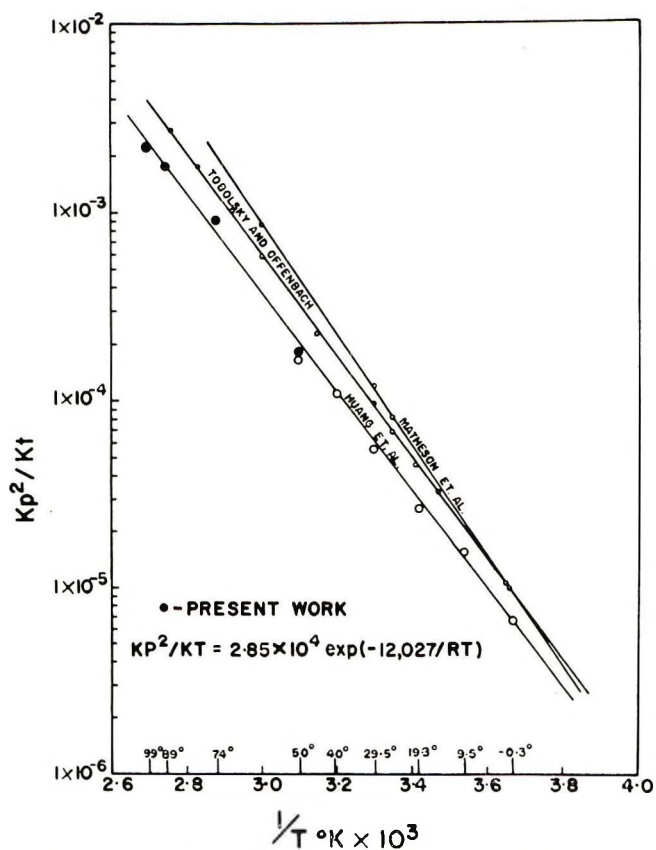


Fig. 9. Radiation-induced polymerization of styrene. Plot  $k_p^2/k_t$  vs.  $1/T$ .

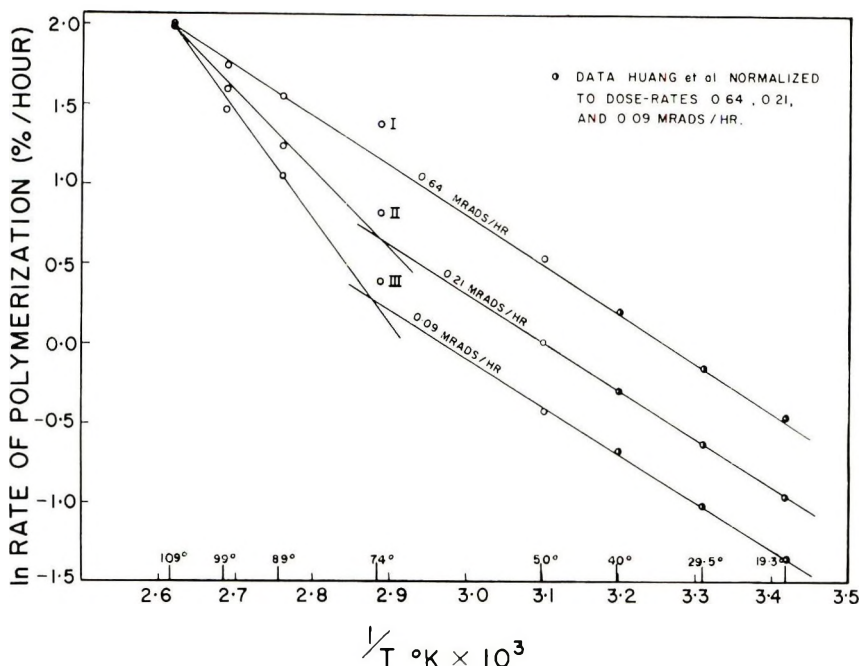


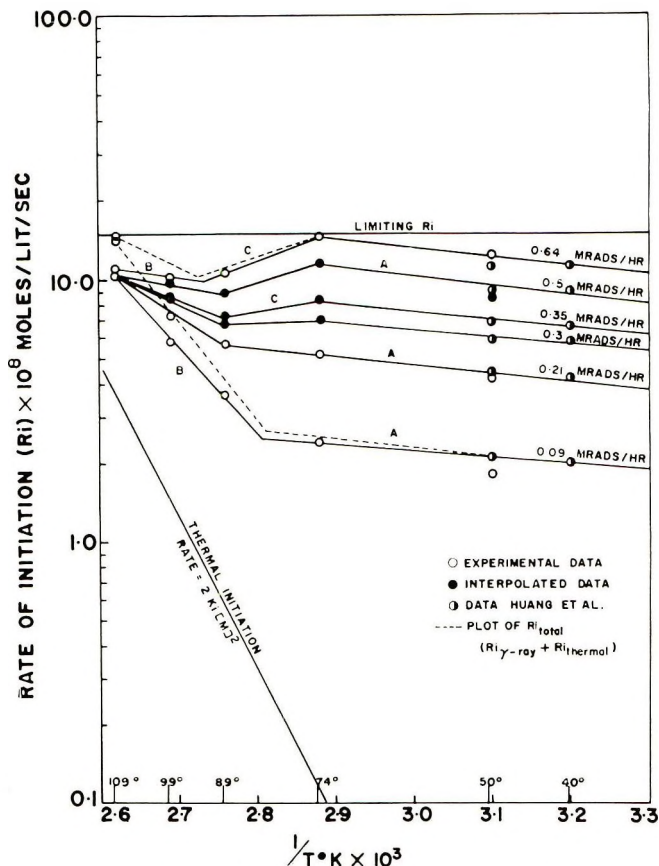
Fig. 10. Overall activation energy for radiation-induced polymerization of styrene. Plot of polymerization rate vs.  $1/T$ .

primary free radicals; again  $R_i$  increases slightly over the temperature range of 90–109°C.

If the observed maximum  $R_i$  at 74°C for this dose rate is caused by the primary free radical recombination reaction assuming greater importance at higher temperatures, then for this range of radiation intensity, the total rate of initiation

$$R_{i(\text{total})} = R_p^2 k_t / k_p^2 [M]^2$$

should not exceed the  $R_{i(\gamma)}$  observed at 74°C for the 0.64 Mrad/hr dose rate. In order to validate this assumption,  $R_{i(\text{total})}$  for the dose rates of 0.64 and 0.09 Mrad/hr is also plotted in this figure. Indeed the  $R_{i(\text{total})}$  does not exceed the  $R_{i(\gamma)}$  value at 74°C indicating that within the polymerizing system there is a certain "critical primary free radical population." Up to this population the radicals initiate growing chains, but any subsequent increase in the free radical population (caused thermally or by a second  $\gamma$ -ray initiation) has no additional initiation effect. In order to check the nature of the slopes labeled A, B, and C for the 0.64 Mrad/hr dose rate plot, interpolated data for the dose rates of 0.5, 0.35, and 0.30 Mrad/hr are also plotted for comparison purposes. In all cases, similar breaks in the Arrhenius plot are also observed. However, as we approach lower dose rates the C portion of the plot for 0.64 Mrad/hr dose rate disappears, indicating

Fig. 11. Plot of rate of initiation vs.  $1/T$ .

that a primary free-radical recombination reaction is not occurring to any appreciable extent at these intensities of radiation.

(3) For the dose rates of 0.21 and 0.09 Mrad/hr, breaks in the Arrhenius plots are observed at temperatures of about 85 and 92°C, respectively, indicating the probable existence of a parallel initiation. However, from the shape of the slopes in the region labeled B, it appears that such breaks exist in all these plots although these slopes are continually decreasing with increasing dose rate. The fact that slopes B converge for all the dose rates investigated, leads to the conclusion that there are two competing reactions:



Reaction (7a) would predominate at high temperatures, under the radiation conditions of the experiments described.

Olaj<sup>16</sup> and Pryor et al.<sup>17</sup> have observed that primary free radicals from one source (e.g., thermal) interfere with radicals generated from another source

(e.g., initiator). However, in the present work, a more complicated system is being considered. In addition to the  $\gamma$ -ray and thermal initiations accompanied by primary free-radical recombination reactions, the possibility of the existence of parallel  $\gamma$ -initiations and an uncorrected thermal component is being considered.

In order to establish the nature of parallel initiation, the initiation rate constants  $k_i$  and the energies of initiation  $E_i$  were determined on assuming  $E_{i(\gamma)} = 0$ , while for thermal polymerization  $E_i \neq 0$ .

Assuming that the rates of initiation  $R_i$  due to the parallel initiation reactions are additive, then the total  $\gamma$ -initiation rate becomes:

$$R_{i(\text{total } \gamma)} = R_{i(\text{total})} - R_{i(\text{thermal})} = R_i(1) + R_i(2)$$

where  $R_i(1) = \phi m_1[M]I$  and  $R_i(2)$  is due to the unknown parallel initiation;  $\phi m_1[M]$  is the rate of production of free radicals  $m_1$  in the monomer, expressed in moles per litre per unit radiation dose. For the purpose of uniformity  $\phi m_1$  is redefined as  $k_i(1)$ , the initiation rate constant. Considering various possibilities for the parallel initiation,  $R_i(2)$  may be expressed as follows:

$$R_i(2) = \phi m_2[M] I \quad (8)$$

$$R_i(2) = k_i(2)[M]I$$

or

$$R_i(2) = \phi m_2[M]/I \quad (9)$$

$$R_i(2) = k_i(2)'[M]/I$$

or

$$R_i(2) = 2k_i(2)''[M]^2 \quad (10)$$

where eqs. (8) and (9) describe parallel initiations due to  $\gamma$ -rays and eq. (10) is possibly uncorrected thermal component as the rates of thermal polymerization in the temperature range 74–109°C become significant.  $R_i(2)$  was evaluated by extrapolation of the 40–70°C portion of the curves in Figure 11, on the basis that  $R_i(2) = R_i(\text{experimental}) - R_i$  (by extrapolation). This extrapolation is justifiable by the assumption that the rate of  $\gamma$ -initiation is independent of temperature. The initiation rate constants were evaluated and are listed in Table IV.

The Arrhenius plots of  $k_i(2)$ ,  $k_i(2)'$ , and  $k_i(2)''$  are linear and the  $E_i$  values obtained from the slopes of these plots are of the same order of magnitude as the thermal polymerization of styrene ( $E_t \sim 14,000$  cal). The temperature dependence of  $k_i(2)''$  for the  $R_i$  data uncorrected for thermal component is:

$$k_i(2)'' = 6.92 \times 10^7 e^{-14,850/T} \quad (11)$$

TABLE IV  
Initiation Rates as a Function of Temperature and Dose Rate

Temp, °C	Dose rate, Mrad/hr	$R_i \times$ $10^8$ , mole/l.- sec <sup>a</sup>	$k_i(1) \times$ $10^{11}$ , l./mole- sec	$R_i(2) \times$ $10^8$ , mole/l.- sec <sup>a</sup>	$k_i(2) \times$ $10^{11}$ , l./mole- sec	$k_i(2)' \times$ $10^8$ , l./mole- sec	$k_i(2)'' \times$ $10^{10}$ , l./mole- sec <sup>a</sup>
50	0.64	12.5	8.3				
	0.21	4.2	8.6	—	—	—	—
	0.09	1.8	8.8				
74	0.64	14.4	11.0				
	0.21	5.2	10.8	—	—	—	—
	0.09	2.4	12.1				
89	0.09	3.64	—	1.08	5.5	3.2	0.82
		(4.17)		(1.44)			(1.1)
99	0.09	5.81	—	3.13	16.3	9.3	2.41
		(7.27)		(4.5)			(3.48)
109	0.09	10.15	—	7.25	38.1	21.9	5.74
		(13.08)		(10.99)			(8.7)

<sup>a</sup> Values in parentheses are for  $R_i$  uncorrected for the thermal component.

which compares with the Roche and Price<sup>11</sup> expression for thermal polymerization of styrene.

$$k_i = 1.885 \times 10^6 e^{-13,900/T} \quad (6)$$

A reasonable conclusion is that the parallel initiation reaction is not due to  $\gamma$  initiation but corresponds to the thermal process. However, it may be remarked that the initiation rate constants  $k_i(2)''$  obtained in this study are higher than those of Roche and Price.

Thus, in the absence of primary free radical recombination,  $R_p$  in this study may be accounted for by the expression:

$$R_{p(\text{total})} = R_{p(\gamma)} + R_{p(\text{thermal})} \\ = k_p/k_t^{1/2} \{ k_i(1) [M] I \}^{1/2} [M] + k_p/k_t^{1/2} (2k_i)^{1/2} [M]^2 \quad (12)$$

$R_p$  can be calculated using the values of the rate constants derived in this study, i.e.,  $k_i(1)$ ,  $k_i(2)$ , and  $k_p/k_t^{1/2}$ . In all cases the calculated value is higher than the experimentally determined value. Using the initiation rate constant ( $k_i$ ) obtained for the thermal component from the Roche and Price data, the calculated overall rates of polymerization are lower than those observed. Thus, the thermal component is not fully accounted for.

In this discussion, it has been shown that there are two parallel initiation reactions taking place (one  $\gamma$ -ray and the other thermal) and at these high radiation intensities and elevated temperatures the situation is complicated due to the primary free-radical recombination reaction assuming relatively greater importance.

For the kinetic analysis of these results, we employ the kinetic scheme of Chapiro<sup>1</sup> (Table V).



TABLE V

Reaction	Rate
(a) Initiation (formation of primary free radicals)	
$A \xrightarrow{\sim} 2R^{\cdot}$	$R_i = \phi_A I [M]$
(b) Recombination of primary radicals	
$R^{\cdot} + R^{\cdot} \rightarrow R_2$	$k_{00} [R^{\cdot}]^2$
(c) Addition onto the monomer	
$R^{\cdot} + M \rightarrow RM^{\cdot}$	$k_{p0} [R^{\cdot}] [M]$
(d) Propagation	
$RM_n^{\cdot} + M \rightarrow RM_{n+1}^{\cdot}$	$k_p [RM_n^{\cdot}] [M]$
(e) Mutual termination	
$RM_n^{\cdot} + RM_m^{\cdot} \rightarrow P_{n+m} \text{ (or } P_n + P_m)$	$k_t [RM^{\cdot}]^2$
(f) Termination by primary free radicals	
$RM_n^{\cdot} + R^{\cdot} \rightarrow P_n$	$k_{t0} [RM^{\cdot}] [R^{\cdot}]$

In Table V, A is any molecule present in the reacting mixture (monomer, solvent etc.);  $R^{\cdot}$  is a primary radical; M the monomer;  $RM_n^{\cdot}$  a growing polymer chain, and  $P_n$  a "dead" polymer.

In this kinetic scheme, the rate constants  $k_{00}$ ,  $k_t$ , and  $k_{t0}$  pertain to the mutual interaction of two free radicals. Such reactions proceed very rapidly and require only low energy of activation, if any. The absolute values of such rate constants are of the order of  $10^6$  to  $10^9$  l./mole-sec. Owing to the relative size of the various free radicals involved, it can be assumed that the rate constants will lie in the following order:

$$k_{00} > k_{t0} > k_t$$

The addition reactions of a free radical to a vinyl monomer double bond (with rate constants  $k_{p0}$  and  $k_p$ ) require energies of activation of the order of 5–8 kcal/mole, with absolute values for these constants of the order of  $10^{-10}$  l./mole-sec at room temperature.

In the present investigation, the experimental data indicate that for temperatures of 50 and 74°C, the stationary concentrations of the primary free radicals ( $R^{\cdot}$ ) and of the growing chains ( $RM^{\cdot}$ ) are fairly low and thus  $R_i \ll k_{p0}^2 [M]^2 / 4 k_{00}$  and  $k_{t0} [RM^{\cdot}] \ll k_{p0} [M]$ . The overall rate is given by the expression:

$$R_p = k_p / k_t^{1/2} (R_i)^{1/2} [M] \quad (13)$$

At these temperatures, reactions (b) and (f) do not occur to any appreciable extent and the exponent of the dose rate in this expression was found experimentally to be one-half.

For temperatures of 89, 99, and 109°C, the dose rate exponent gradually decreases from its value of 0.5 to zero indicating that the rate expression (13) does not apply at these temperatures. It has been reported in the literature<sup>1</sup> that at high intensities of radiation, where  $R_i$  is sufficiently great, the rate of polymerization becomes independent of the rate of initiation. Under these conditions, reaction (b) in the kinetic scheme is no longer negligible compared to reaction (c) and the rate of polymerization is not proportional to the square root of the rate of initiation ( $R_i$ ).

In the present investigation a situation analogous to the high intensities of radiation arises as more and more primary free radicals are being generated thermally in addition to the free radicals formed by gamma rays. Thus, due to the predominance of reaction (b) both the observed rates of initiation  $R_i$  and the rate of polymerization  $R_p$  decrease. This effect is dramatically noticeable in Figure 11 in the case of 0.64 Mrad/hr dose rate.

The foregoing kinetic scheme yields the following rate expression:

$$R_p = \frac{k_{p0}k_p}{(2k_{00})^{1/2}k_i^{1/2}} [M]^2 \left\{ \left( 1 + \frac{4k_{00}R_i}{k_{p0}^2[M]^2} \right)^{1/2} - 1 \right\} \quad (14)$$

As the absolute values of the rate constants  $k_{p0}$  and  $k_{i0}$  are not known, and no experimental determination of  $R_i$  has been made in this study, it is not possible to apply rate expression (14) above to the present study without making certain assumptions. It is assumed that the overall rate of polymerization is given by the expression:

$$R_p = k_p/k_i^{1/2} \{ k_i(1) [M] I \}^{1/2} [M] + k_p/k_i^{1/2} (2k_i)^{1/2} [M]^2 \quad (15)$$

and the observed deviations from the rate expressed in eq. (15) above arise due to the competing reactions (b) and (c) in the kinetic scheme. On the basis of expression (15), theoretical rates of polymerization and the rates of initiation, where

$$R_i = R_p^2 / (k_p^2 [M]^2 / k_i) \quad (16)$$

are calculated for the dose rates of 0.64, 0.21, and 0.09 Mrad/hr and the calculated values listed in Table VI.

Thus, by employing the calculated rates of initiation  $R_i$  listed in Table VI,  $k_{p0}/k_{00}$  ratios can be evaluated.

The expression (14) can be further simplified if:

$$k_{p0}/k_{00}^{1/2} = \alpha \quad (17)$$

$$a = k_p [M]^2 / k_i^{1/2} \sqrt{2} \quad (18)$$

$$b = 4/[M]^2 \quad (19)$$

then

$$R_p = \alpha a \left[ \left( 1 + \frac{bR_i}{\alpha^2} \right)^{1/2} - 1 \right]^{1/2} \quad (20)$$

TABLE VI  
 Theoretical Values of Rates of Polymerization and Initiation

Temperature °C	Dose rate, Mrad/hr	$R_p \times 10^5$ , mole/l.-sec		$R_{p(\text{total})} \times 10^5$	$R_i \times 10^8$ , mole/l.-sec
		$\gamma$ -Rays	Thermal		
50	0.64	4.22	—	4.22	12.5
	0.21	2.45	—	2.45	4.2
	0.09	1.59	—	1.59	1.8
74	0.64	8.05	1.22	9.27	16.4
	0.21	4.6	1.22	5.82	6.46
	0.09	2.96	1.22	4.18	3.33
89	0.64	11.4	3.9	15.3	22.1
	0.21	6.51	3.9	10.41	10.3
	0.09	4.2	3.9	8.1	6.18
99	0.64	13.85	8.6	22.45	32.0
	0.21	7.91	8.6	16.51	17.3
	0.09	5.1	8.6	13.7	11.9
109	0.64	16.8	15.9	32.7	45.7
	0.21	9.6	15.9	25.5	27.8
	0.09	6.2	15.9	22.1	20.9

and

$$\alpha^2 = R_p^4 / (a^4 b R_i - 2a^2 R_p^2) \quad (21)$$

$$R_i = (R_p^4 / \alpha^2 a^4 b) + (2R_p^2 / a^2 b) \quad (22)$$

Using calculated  $R_i$  values from Table VI and expression (21),  $k_{p0^2}/k_{00}$  ratios are calculated and the rates of initiation  $R_i$  are calculated with the help of expression (22) using experimental values of the rates of polymerization. These values are listed in Table VII.

From Table VII it is noticeable that there is excellent agreement between the rates of initiation  $R_i$  calculated from two different expressions, indicat-

 TABLE VII  
 Initiation Rates Calculated from Experimental Polymerization Rates

Temperature, °C	Dose rate, Mrad/hr	$(k_{p0^2}/k_{00}) \times 10^7$	$R_i \times 10^8$ , mole/l.-sec	
			From eq. (21)	From eq. (16)
109	0.64	9.53	14.63	14.7
	0.21	5.54	13.97	14.0
	0.09	3.73	13.82	13.85
99	0.64	5.01	11.70	11.74
	0.21	3.14	8.67	8.69
	0.09	2.19	7.26	7.27
89	0.64	16.6	11.61	11.06
	0.21	1.76	6.25	6.22
	0.09	—	—	—

ing that the contribution from the first term ( $R_p^4/\alpha^2 a^4 b$ ) in expression (22) is negligible.

From the data obtained in the present study, it is not possible to determine the individual rate constants  $k_{p0}$  and  $k_{00}$  but the  $k_{p0}^2/k_{00}$  ratios listed in Table VII indicate that  $k_{00} \gg k_{p0}$ , and recombination of the primary free radicals is the route by which the surplus free radicals are used up in the temperature range 74–109°C. The  $k_{p0}^2/k_{00}$  ratios ( $1.76 \times 10^{-7}$  to  $16.6 \times 10^{-7}$ ) are consistent with reasonable values for  $k_{p0}$  and  $k_{00}$  individually.

### Degree of Polymerization

In order to rationalize the observed rates of polymerization we have employed a simplified kinetic scheme for the temperature range 50–74°C, while the addition of reactions (b), (c), and (f) to the simplified kinetic scheme was necessary to treat the experimental data for the temperature range 74–109°C.

Thus, for the higher temperature range 74–109°C, if termination occurs by disproportionation, the number-average degree of polymerization  $\bar{P}_n$  is given by the expression:

$$\bar{P}_n = R_p/k_{p0}[R^\cdot][M] \quad (23)$$

and substitution for  $[R^\cdot]$  gives:

$$\bar{P}_n = \frac{(2 k_{00})^{1/2} k_p}{k_{p0} k_t^{1/2}} \left\{ \left( 1 + \frac{4 k_{00} R_i}{k_{p0}^2 [M]^2} \right)^{1/2} - 1 \right\}^{-1/2} \quad (24)$$

In cases where termination is by combination,  $\bar{P}_n$  is twice as great.

By using the calculated values of  $k_{p0}/k_{00}^{1/2}$  and the  $R_i$  listed in Table VII, the number-average degree of polymerization  $\bar{P}_n$  was calculated; the values are listed in Table VIIIA. Table VIIIB gives values calculated on the basis of the simplified kinetics scheme.

TABLE VIIIA  
Degree of Polymerization as a Function of Temperature and Dose Rate

Temp, °C	Dose rate, Mrads/hr	$R_i \times 10^8$ , mole/l.-sec	$(k_{p0}^2/k_{00})$ $\times 10^7$	$\bar{P}_n$ (cal- culated)	$\bar{P}_n$ (experi- mental)
109	0.64	14.70	9.53	1263	—
	0.21	14.01	5.54	1292	—
	0.09	13.85	3.73	1298	—
99	0.64	11.74	5.01	1163	1960
	0.21	8.69	3.14	1351	2830
	0.09	7.27	2.19	1477	2900
89	0.64	11.06	16.60	953	2025
	0.21	6.22	1.76	1292	3460*

TABLE VIIIB

Temp, °C	Dose rate, Mrad/hr	$R_i \times 10^4$ , mole/l.-sec	$R_p \times 10^5$ , mole/l.-sec	$\bar{P}_n = R_p/R_i$	$\bar{P}_n$ (experi- mental)
89	0.09	4.17	6.63	1590	3830*
74	0.64	14.48	8.70	600	1375
	0.21	5.30	5.26	995	2120
	0.09	2.50	3.61	1445	3300*
50	0.64	12.50	4.22	338	580
	0.21	4.20	2.45	584	1140
	0.09	1.80	1.59	984	2060

\* The values of  $\bar{P}_n$  in Table VIII identified by an asterisk are suspect, due to questionable osmometric data.

Our conclusion is that termination occurs probably exclusively by combination, since in all cases the experimental values of  $\bar{P}_n$  would be twice as large as those calculated, if one were to assume termination by disproportionation. This same fact eliminates the possibility of termination of the growing chains by primary radicals (e.g.,  $RM_n\cdot + R\cdot \rightarrow$  dead polymer). This latter reaction is, therefore, of little significance compared with reaction (b) in the kinetic scheme, Table V (mutual recombination).

### Summary and Conclusions

In the range 50–74°C, the rate of polymerization and degree of polymerization  $D_p$  bear a square root relationship to the intensity of radiation, namely  $R_p \propto I^{1/2}$  and  $D_p \propto I^{-1/2}$ . Above 74°C, the dose rate exponent decreases as a linear function of temperature, becoming zero at about 109°C. This deviation from the classic square root relationship occurs because of a change in the relative significance of reaction (b) and (c) in the kinetic scheme (Table V). At higher dose rates, mutual recombination of primary free radicals assumes major significance. For this reason, at lower dose rates the thermal component of the polymerization reaction is quite apparent and becomes less obvious when Arrhenius plots are made for the higher dose rate experiments.

In the dose rate range of 0.09–0.64 Mrad/hr, the competition between reactions (b) and (c) is such that  $R_p$  and  $D_p$  remain constant for the whole range of dose rate. It is probable that the dose-rate independence of  $R_p$  and  $D_p$  observed above 109°C will hold for a range of radiation intensity as high as twentyfold. The temperature at which this situation obtains is a function of the range of intensity.

This dose-rate independence has been ascribed to a "limiting" rate of initiation  $R_i$ , which is characteristic of the intensity range. Assuming stationary state kinetics for low conversions, the rate of reaction is:

$$R_p = -dM/dt = k_p[M][RM\cdot] \quad (25)$$



On the basis of the limiting rate of initiation, over the intensity range described,  $[RM^\cdot]$  will be a constant. At 109°C, the rate expression (25) will be

$$R_{p(\text{thermal} + \gamma)} = k_p[M] \times \text{constant} \quad (26)$$

$k_t$  was evaluated in the relationship of Matheson et al.,<sup>15</sup> and substituted in the expression

$$[RM^\cdot] = (R_i/k_t)^{1/2} \quad (27)$$

to give a value of  $5.1 \times 10^{-8}$  mole/l. as the limiting concentration  $[RM^\cdot]$ . Therefore, the total rate of polymerization (for  $\gamma$  initiation and thermal initiation) above 109°C is

$$R_{p(\text{total})} = k_p[M] (5.1 \times 10^{-8}) + (k_p/k_t^{1/2})(2k_i)^{1/2}[M]^2 \quad (28)$$

A consequence of eq. (28) is that the dose rate exponent of  $R_p$  and  $D_p$  can be expected to be zero.

This dose rate independence can be expected in polymerizations where the vinyl monomer is fairly reactive, but its radical is relatively stable. In other cases, this dose rate independence may be achieved by a combination of chemical catalysis and a specific range of gamma intensity.

Work currently in progress suggests that the temperatures quoted in this paper are capable of refinement by the use of smaller reaction vials. Therefore, while the temperatures quoted bear valid relative relationships, the absolute values may be slightly low.

The authors are pleased to have the opportunity to acknowledge the generous financial support of the National Research Council of Canada. Much of the viscometry and osmometry was performed by Mr. J. Cheesman and Mr. H. Cheng, whose assistance is gratefully acknowledged.

## References

1. A. Chapiro, *Radiation Chemistry of Polymeric Systems*, Wiley, New York, 1962.
2. C. S. H. Chen and R. F. Stamm, *J. Polym. Sci.*, **58**, 369 (1962).
3. S. Okamura, K. Ueno, and K. Hayashi, *J. Polym. Sci. B*, **3**, 363 (1965).
4. R. C. Potter, C. L. Johnson, D. J. Metz, and R. H. Bretton, *J. Polym. Sci. A-1*, **4**, 419 (1966).
5. S. P. Sood and J. W. Hodgins, *J. Polym. Sci. B*, **8**, 529 (1970).
6. J. E. Newell, *J. Anal. Chem.*, **23**, No. 3, 445 (March 1951).
7. J. W. Hodgins, G. N. Werezak, and S. L. Ross, *Can. J. Chem. Eng.*, **43**, 117 (1964).
8. A. J. Swallow, *Radiation Chemistry of Organic Compounds*, Pergamon Press, New York-London, 1960.
9. W. A. Noyes and P. A. Leighton, *The Photochemistry of Gases*, Reinhold, New York, 1941, p. 119.
10. R. W. Lenz, *Organic Chemistry of Synthetic High Polymers*, Interscience, New York, 1968, p. 316.

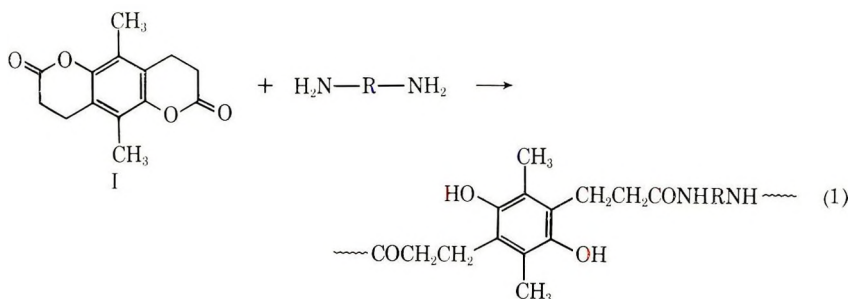
11. R. H. Boundy and R. F. Boyer, *Styrene—Its Polymers, Copolymers, and Derivatives*, Reinhold, New York, 1952, p. 216.
12. C. H. Bamford, W. G. Barb, A. D. Jenkins, and P. F. Onyon, *The Kinetics of Vinyl Polymerization by Radical Mechanisms*, Butterworths, London, 1958.
13. R. Y. M. Huang, J. F. Westlake, and S. C. Sharma, *J. Polym. Sci. A-1*, **7**, 1729 (1969).
14. A. V. Tobolsky and J. Offenbach, *J. Polym. Sci.*, **16**, 311 (1955).
15. M. S. Matheson, E. E. Auer, E. B. Bevilacqua, and E. J. Hart, *J. Amer. Chem. Soc.*, **73**, 1700 (1951).
16. O. F. Olej, *Monatsh. Chem.*, **97**, 1437 (1966).
17. W. A. Pryor and J. H. Coco, *Macromolecules*, **3**, No. 5, 500 (1970).

Received February 1, 1971

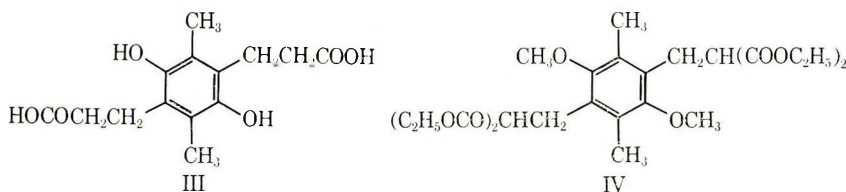
## NOTES

*Preparation and Ring-Opening Polymerization of  
2,5-Dimethylhydroquinone-bis- $\delta$ -lactone*

Iwakura et al.<sup>1</sup> first reported the polyaddition of bislactone with diamine to form linear polyamide. Nakabayashi and Cassidy<sup>2</sup> prepared redox polymers from bislactone of hydroquinone-biscarboxylic acid and diamine. We have tried to synthesize 2,5-dimethylhydroquinone-bis- $\delta$ -lactone (I) and its related polymers (II) by the ring-opening reaction of I with diamine. This paper reports some results with our experiments.



The monomer (I), 5,10-dimethyl-3H,4H,8H,9H-benzo[1,2-b: 4,5-b']dipyran-2,7-dione, the bislactone of 2,5-dimethylhydroquinone-3,6-bis(ethyl-2'-carboxylic acid) (III), was prepared in one step from the malonic ester (IV), 1,4-dimethoxy-2,6-dimethyl-3,6-bis(2',2'-dicarbethoxyethyl)benzene, by heating IV in hydrobromic acid at 140–160°C for several hours.



The infrared spectrum (KBr disk) of the purified product showed a characteristic lactone carboxyl band at  $1755\text{ cm}^{-1}$  and no hydroxyl and carboxylic acid bands. The NMR spectrum in  $\text{CDCl}_3$  gave signals at  $\delta = 2.23$  (s, 6H,  $\text{CH}_3$ ) and  $2.85$  (qu, 8H,  $\text{CH}_2$ ). The mass spectrum (calcd MW = 246.25) showed peaks at  $m/e = 246$  (relative intensity: 23), 218 (9), 204 (18), 190 (70), 176 (28), 162 (100) and 134 (42). These spectral data and elementary analysis support the formation of the bislactone (I).

As a model reaction, the bislactone (I) was treated with *n*-butylamine in dimethylacetamide (DMAc) at room temperature. The infrared spectrum of the product (V) showed bands at  $3300\text{ cm}^{-1}$  assignable to NH and OH, at  $1555\text{ cm}^{-1}$  to NH, and  $1635\text{ cm}^{-1}$  to amide carbonyl.

TABLE I  
Characteristic Data of Polymers

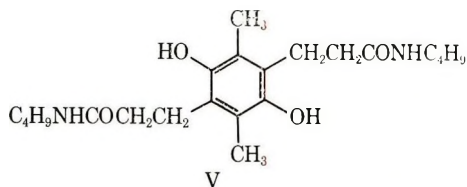
No.	Diamine	Form <sup>a</sup>	$\eta_{sp}/c$		Ultraviolet <sup>c</sup>		Infrared, $\text{cm}^{-1}$		Softening temp, °C
			dl/g	Solvent <sup>b</sup>	$\lambda_{\text{max}}$ m $\mu$	$\epsilon \times 10^{-3}$	OH/NH	Amide	
1	Tetramethylene	Ox	0.09	Formic acid	270	15.0	3300	1640, 1550	220-230
2	Hexamethylene	Ox Red	0.18	"	268	14.9	3300	1640, 1550	230-235
3	Decamethylene	Ox Red	0.19	HMPA	294 <sup>d</sup>		3310 3310	1640, 1560 1640, 1560	220-230
4	<i>m</i> -Xylylene	Ox Red	0.11	DMAC	290	6.5	3300 3300	1640, 1550 1645, 1560	210-220
5	Piperazine	Ox Red	0.08	DMSO			3430	1620	285-290
6	<i>n</i> -Butyl (model compound)	Ox Red			271 290	20.9 4.2	3300 3300	1635, 1551 1640, 1561	177-178

<sup>a</sup>Ox: oxidized form of redox polyamide or model compound. Red: reduced form.

<sup>b</sup> $\eta_{sp}/c$  at 25°C, concentration = 0.50 g/100 ml in HMPA (hexamethylphosphoramide), DMAC (*N,N*-dimethylacetamide), or DMSO (dimethyl sulfoxide).

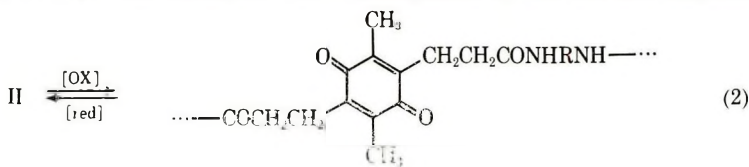
<sup>c</sup>Ultraviolet spectra taken in formic acid except as noted.

<sup>d</sup>In HMPA.



The bislactone (I) was polymerized under nitrogen atmosphere at 50–70°C in DMAc with diamines including hexamethylenediamine, *m*-xylylenediamine, and piperazine. Polymers (II) were obtained in the form of white to light brown flakes in good yield. The polymers were soluble in DMAc, dimethyl sulfoxide (DMSO), formic acid (FA), or hexamethylphosphoramide (HMPA), but insoluble in the usual organic solvents. Viscosities of the polymers were  $\eta_{sp}/c = 0.08$ – $0.19$  dl/g at 25°C.

Although the ring-opening reaction of bislactone with diamine should yield the reduced forms (II) according to eq. (1) the ultraviolet-spectral study revealed that the polymers so obtained were of the oxidized forms (VI). This can be explained by assuming that the reduced forms (II) had been oxidized to VI on contact with air during working-up of (II). The assumption would be supported by the fact that alkyl-sub-



stituted hydroquinones have lower redox potentials than hydroquinone itself and that they are, therefore, inclined to be oxidized more easily. The reduction of VI could be carried out by shaking it with a saturated aqueous solution of sodium hydrosulfite. The reduced forms (II) were oxidized by adding stoichiometric amts. of ceric ammonium nitrate in DMAc. The infrared spectra of the oxidized polymers showed quinone carbonyl band at  $1650\text{ cm}^{-1}$ . Characteristic data of the polymers are summarized in Table I.

Since no suitable solvent could be found, our attempts to determine redox potentials by titration<sup>3</sup> were unfortunately in vain. The replacement of hydrogens of hydroquinone ring with methyl seems to have been ineffective toward the improvement of solubility of the polymers.

## EXPERIMENTAL

### Bislactone (I), 5,10-Dimethyl-3H,4H,8H,9H-benzo[1,2-b: 4,5-b']dipyran-2,7-dione

A mixture of 15.3 g (0.030 mole) of the malonic ester (IV) and 200 ml of 48% hydrobromic acid was placed in a 1-liter round-bottomed flask and heated with stirring. Up to a bath temperature of 120°C, ethyl bromide distilled. Then, the temperature was raised to 140°C until foaming ceased. After the temperature had been raised to 160°C, the reaction mixture was refluxed for 3 hr. The raw product crystallized from the solution upon cooling. It was filtered, washed with water, and dried. Recrystallization from acetonitrile gave white needles, mp 259–261°C, in a yield of 5.4 g (73%).

ANAL. Calcd for  $C_{14}H_{14}O_4$ : C, 68.28%; H, 5.73%. Found: C, 68.22%; H, 5.78%.

### Malonic ester (IV), 1,4-Dimethoxy-2,5-dimethyl-3,6-bis(2',2'-dicarboethoxyethyl)benzene

In a sodium alcoholate solution, prepared from 3.2 g (0.14 g-atom) metallic sodium and 300 ml absolute ethyl alcohol were added 22.4 g (0.14 mole) of ethyl malonate



within 30–45 min with stirring. After 15 min, 15 g (0.057 mole) of 1,4-bis(chloromethyl)-2,5-dimethoxy-3,6-dimethylbenzene<sup>4</sup> was added in one portion. The mixture was refluxed for 3 hr. After the solvent was removed *in vacuo*, the residue was poured into 1 liter ice water. The crude product was filtered, washed with water, dried, and recrystallized from ethyl alcohol. White needles, mp 58–59°C, were obtained in a yield of 22.7 g (78%).

ANAL. Calcd for  $C_{26}H_{38}O_{10}$ : C, 68.54%; H, 8.63%. Found: C, 68.35%; H, 8.62%.

The NMR spectrum in  $CDCl_3$  showed signals at  $\delta$ : 1.19 (*tr*), 2.22 (*s*), 3.23 (*d*), 3.64 (*s*), 3.78 (*tr*), and 4.14 (*qu*).

#### Model Compound (V), 2,5-Dimethylhydroquinone-3,6-bis(ethyl-2'-*n*-butylamide)

In 10 ml of DMAc were dissolved 0.49 g (0.2 mmole) of the bislactone (I) and 0.29 g (0.4 mmole) of *n*-butylamine. The mixture was stirred for 2 hr at room temperature under a slight stream of nitrogen. After evaporation of the solvent *in vacuo* at 60–70°C, the residue was recrystallized from acetonitrile. Light yellow needles melted at 172°C and weighed 0.63 g (81%).

ANAL. Calcd for  $C_{22}H_{36}N_2O_4$ : C, 67.66%; H, 9.29%; N, 7.18%. Found: C, 67.77%; H, 9.34%; N, 7.09%.

#### General Polymerization Procedure

Exactly 0.426 g (0.173 mmole) of the bislactone (I) and 0.201 g (0.173 mmole) of hexamethylenediamine were mixed with 20 ml DMAc. Under a slight stream of nitrogen, the mixture was heated to 70–80°C with stirring for 4 hr. After DMAc was removed *in vacuo*, the viscous solution was poured into 20 ml of water, whereupon the polyamide precipitated as white to slightly brown flakes. The polymer was twice reprecipitated from DMAc-methanol to give 0.44 g (70%).

#### Measurement

Viscosities were measured with an Ostwald-type viscometer. Infrared data were obtained with a Perkin-Elmer Model 421 spectrometer; NMR data were obtained with a Varian Associates Model A-60 spectrometer (the letters within the parentheses having the meanings: *s*, singlet; *d*, doublet; *tr*, triplet; *qu*, quadruplet; and *m*, multiplet). The mass spectrum was obtained with a Hitachi Perkin-Elmer Model RMU-6 spectrograph (temperature, 200°C; ion current,  $7 \times 10^{-12}$  A; multiplier voltage, 1.5).

We thank Dr. Akira Terahara, Yale University, for the measurement and interpretation of the spectral data. One of us (S.I.) is indebted to The United States Public Health Service for postdoctoral support at Yale University. We would like to express our appreciation to Professor H. G. Cassidy for initially suggesting work in this area and for his encouragement throughout the work.

#### References

1. Y. Iwakura, K. Hayashi, M. Shimizu, and T. Watanabe, *Makromol. Chem.*, **95**, 228 (1966).
2. N. Nakabayashi and H. G. Cassidy, *J. Polym. Sci. A-1*, **7**, 1275 (1969).

3. H. G. Cassidy and K. A. Kun, *Oxidation-Reduction Polymers*, Interscience, New York, 1965, pp. 107 ff.
4. H. G. Cassidy and K. A. Kun, in *Encyclopedia of Polymer Technology*, Vol. 5, Wiley, New York, 1966, pp. 693 ff.
5. L. I. Smith and J. Nicols, *J. Amer. Chem. Soc.* **65**, 1744 (1943).

SUSUMU IWABUCHI\*  
MITSURU UEDA  
KUNIHARU KOJIMA

Department of Applied Chemistry  
Faculty of Engineering  
Chiba University  
Yayoi-cho, Chiba, Japan

Received July 18, 1971

Revised August 12, 1971

\*To whom correspondence should be addressed.

### Poly- $\alpha$ -acetoxy-4-vinylpyridine

Haas et al.<sup>1</sup> synthesized  $\alpha$ -acetoxy-4-vinylpyridine from 4-vinylpyridine via several steps and polymerized it by use of azobisisobutyronitrile (AIBN). In their report,<sup>1</sup> the main discussion focused on the synthesis of the monomer; the physical properties of the polymer were not described in detail except for the disappearance of the  $\text{C}=\text{C}$ -stretching vibration ( $1650\text{ cm}^{-1}$ ) in the infrared spectrum in the polymer.

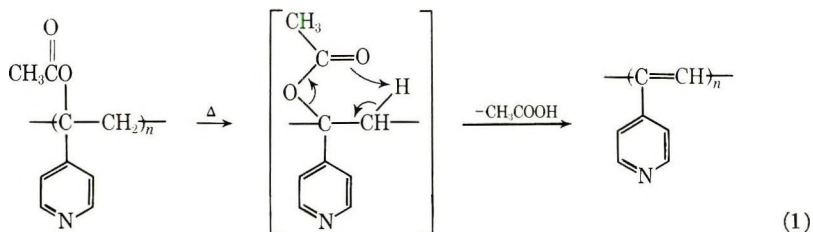
The present authors polymerized  $\alpha$ -acetoxy-4-vinylpyridine with  $\gamma$ -rays and obtained additional physical data, including data on pyrolysis. The monomer,  $\alpha$ -acetoxy-4-vinylpyridine, was synthesized by a modification of the method of Aaron et al.<sup>2</sup> and Haas et al.<sup>1</sup> from (4-pyridyl)-1,2-ethanediol and acetic anhydride. Regarding the synthesis of (4-pyridyl)-1,2-ethanediol from 4-vinylpyridine, the present authors found a more favorable way avoiding the formation of the by-product isonicotinic acid.  $\alpha$ -Acetoxy-4-vinylpyridine was also obtained by a more preferable method avoiding the formation of the by-product 4-acetylpyridine. Details of the monomer synthesis will be presented elsewhere.

Poly- $\alpha$ -acetoxy-4-vinylpyridine which was obtained by  $\gamma$ -ray polymerization has a slightly paler brown color than the polymer obtained by the AIBN method. The polymer is soluble in methanol and chloroform, partly soluble in benzene, insoluble in diethyl ether and petroleum ether, and favorably reprecipitated with chloroform and either diethyl ether or petroleum ether.

Differential scanning calorimetry (DSC) showed that the onset of decomposition of the polymer was at  $214^\circ\text{C}$ . The infrared absorption spectrum was not significantly different from that of the polymer obtained by the AIBN method.<sup>1</sup>

The x-ray diffraction pattern is given in Figure 1, which seems to indicate relatively lower crystallinity. Although the NMR spectrum was not sharp (60 Mcps,  $\text{CDCl}_3$  as a solvent), we observed  $\text{CH}_3$ - in the acetyl group at  $2.28\delta$ ,  $-\text{CH}_2-$  in the backbone chain at  $1.21\delta$ , and the protons in the pyridyl ring approximately at  $7.00\delta$  and  $8.50\delta$ .

We performed a pyrolysis of the polymer using a thermogravimetric analyser (TGA). Deacetylation is thought to proceed according to the molecular reaction via the scheme (1).



From the TGA curve, we calculated the activation energy of the deacetylation using a van Krevelen plot<sup>3</sup> (Fig. 2). The activation energy was  $17.5\text{ kcal/mole}$  and a first-order reaction was obtained. This relatively lower activation energy may result from the gain of the conjugation energy by the formation of repeating double bonds. The formed polyene derivative was a lustrous black powder, and no carbonyl absorption was observed in its infrared absorption spectrum.

### EXPERIMENTAL

#### $\alpha$ -Acetoxy-4-vinylpyridine

Haas et al.<sup>1</sup> obtained (4-pyridyl)-1,2-ethanediol from 4-vinylpyridine, potassium permanganate, and water at  $0\text{--}5^\circ\text{C}$ . We added magnesium sulfate to the above reagent

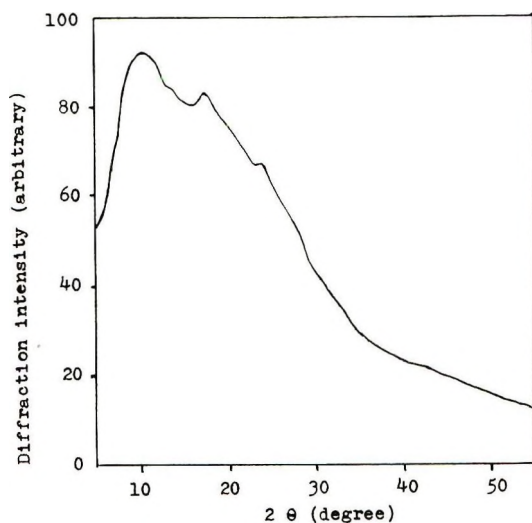


Fig. 1. The x-ray diffraction pattern of poly- $\alpha$ -acetoxy-4-vinylpyridine.

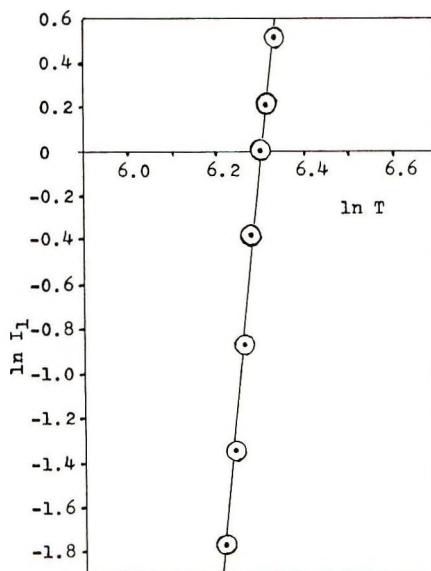


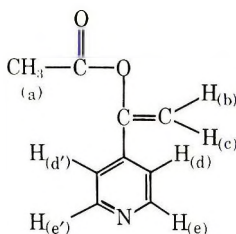
Fig. 2. van Krevelen plot for the TGA curve of poly- $\alpha$ -acetoxy-4-vinylpyridine.

combination to avoid the formation of isonicotinic acid. Magnesium sulfate takes an important role by consuming potassium hydroxide formed from potassium permanganate in the Haas's process. The molar ratio of the reagents, 4-vinylpyridine:KMnO<sub>4</sub>:MgSO<sub>4</sub>:H<sub>2</sub>O, is 3:2:1:4 (usually excess water is used). The reaction temperature was 2–5°C and the reaction time was about 30 min. The yield of (4-pyridyl)-1,2-ethanediol was 84% or quantitative. In the process of acetylation of (4-pyridyl)-1,2-ethanediol with acetic anhydride,<sup>1</sup> the main by-product is 4-acetylpyridine which seemed to be produced by the reaction with the contaminated water in the (4-pyridyl)-1,2-ethanediol. A dehydration procedure is required to obtain a higher yield of  $\alpha$ -acetoxy-4-vinylpyridine. The present authors dissolved (4-pyridyl)-1,2-ethanediol in ethanol, and added benzene

to the ethanolic solution to remove water azeotropically. Repeating the azeotropic removal of water increased the yield. The yield of the polymerization grade product was approximately 50% from (4-pyridyl)-1,2-ethanediol; bp 80°C/0.58 mm Hg.

ANAL. Calcd for  $C_9H_9O_2N$ : C, 66.2%; H, 5.6%; N, 8.6%. Found: C, 66.3%; H, 5.6%; N, 8.4%.

The infrared spectrum was exactly the same as the one reported by Haas et al.,<sup>1</sup> showing  $C=C$  at  $1650\text{ cm}^{-1}$ . NMR (60 Mcps, TMS reference, in  $CDCl_3$  at room temperature):  $H_{(a)}$ , 2.25  $\delta$ ;  $H_{(b)}$ , 5.28  $\delta$ ;  $H_{(c)}$ , 5.80  $\delta$ ;  $H_{(d)} = H_{(d')}$ , 7.42  $\delta$ ;  $H_{(e)} = H_{(e')}$ , 8.70  $\delta$ .  $|J_{(b)(c)}|$  is 2.5 cps which indicates that there are geminal protons, and that the acetoxy group is on the  $\alpha$ -carbon.



### Polymerization

$\alpha$ -Acetoxy-4-vinylpyridine was degassed four times with the aid of liquid nitrogen under vacuum and was sealed off under vacuum in a tube. The polymerization was carried out at room temperature with  $\gamma$ -rays of the dose rate of  $2.1 \times 10^5$  R/hr for 62.5 hr. Then tube was opened, and the contents were poured into diethyl ether. The precipitated polymer was separated by centrifugation (3500 rpm). The crude polymer was reprecipitated several times from chloroform/diethyl ether; yield, approximately 3%; mp 214°C (dec);  $\eta_{sp}/c = 0.093$  ( $c = 1$ , 35°C in  $CHCl_3$ ).

### Measurements

The DSC was carried out using a Perkin-Elmer Model 1B and the temperature was raised at the rate of 16°C/min. The thermogravimetric analysis (TGA) was carried out with a Rigakudenki thermoflux analyser, type 8021. The temperature was raised at the rate of 5°C/min. The x-ray measurement was done with a Rigakudenki diffractometer (CuK $\alpha$ , 30 kV, 15 mA).

### References

1. H. C. Haas, H. S. Kolesinski, and N. W. Schuler, *J. Polym. Sci. B*, **3**, 879 (1965).
2. H. S. Aaron, O. O. Owens, P. D. Rosenstock, S. Leonard, S. Elkin, and J. I. Miller, *J. Org. Chem.*, **30**, 1331 (1965).
3. D. W. van Krevelen, C. van Heerden, and F. Huntjens, *Fuel*, **30**, 253 (1951).

TOSHIYUKI FURUYAMA  
KOICHI MORI  
RYOICHI WAKASA

Technical Research Laboratory  
Asahi Chemical Ind. Co. Ltd.  
Nakadai, Itabashi-ku, Tokyo 174  
Japan

Received July 27, 1971  
Revised August 25, 1971



*Contents (continued)*

EDMUND F. JORDAN, JR., BOHDAN ARTYMYSHYN, ANTHONY SPECA, and A. N. WRIGLEY: Side-Chain Crystallinity. II. Heats of Fusion and Melting Transitions on Selected Copolymers Incorporating <i>n</i> -Octadecyl Acrylate or Vinyl Stearate. . . . .	3349
EDMUND F. JORDAN, JR.: Side-Chain Crystallinity. III. Influence of Side-Chain Crystallinity on the Glass Transition Temperatures of Selected Copolymers Incorporating <i>n</i> -Octadecyl Acrylate or Vinyl Stearate. . . . .	3367
KATSUKIYO ITO: Analysis of Polymerization Rates in Radical Polymerization with Primary Radical Termination of Some Methacrylates. . . . .	3379
S. P. SOOD and J. W. HODGINS: Temperature Effects in $\gamma$ -Initiated Polymerization of Styrene. II. . . . .	3383
NOTES	
SUSUMU IWABUCHI, MITSURU UEDA, and KUNIHARU KOJIMA: Preparation and Ring-Opening Polymerization of 2,5-Dimethylhydroquinone-bis- $\delta$ -lactone. . . .	3405
TOSHIYUKI FURUYAMA, KOICHI MORI, and RYOICHI WAKASA: Poly- $\alpha$ -acetoxy-4-vinylpyridine . . . . .	3411

The *Journal of Polymer Science* publishes results of fundamental research in all areas of high polymer chemistry and physics. The *Journal* is selective in accepting contributions on the basis of merit and originality. It is not intended as a repository for unevaluated data. Preference is given to contributions that offer new or more comprehensive concepts, interpretations, experimental approaches, and results. Part A-1 *Polymer Chemistry* is devoted to studies in general polymer chemistry and physical organic chemistry. Contributions in physics and physical chemistry appear in Part A-2 *Polymer Physics*. Contributions may be submitted as full-length papers or as "Notes." Notes are ordinarily to be considered as complete publications of limited scope.

Three copies of every manuscript are required. They may be submitted directly to the editor: For Part A-1, to C. G. Overberger, Department of Chemistry, University of Michigan, Ann Arbor, Michigan 48104; and for Part A-2, to T. G. Fox, Mellon Institute, Pittsburgh, Pennsylvania 15213. Three copies of a short but comprehensive synopsis are required with every paper; no synopsis is needed for notes. Books for review may also be sent to the appropriate editor. Alternatively, manuscripts may be submitted through the Editorial Office, c/o H. Mark, Polytechnic Institute of Brooklyn, 333 Jay Street, Brooklyn, New York 11201. All other correspondence is to be addressed to Periodicals Division, Interscience Publishers, a Division of John Wiley & Sons, Inc., 605 Third Avenue, New York, New York 10016.

Detailed instructions in preparation of manuscripts are given frequently in Parts A-1 and A-2 and may also be obtained from the publisher.

# Two Professional Journals from Wiley-Interscience

## JOURNAL OF APPLIED POLYMER SCIENCE

Board of Editors: H. Mark, W. Cooper, M. Morton, B. Ranby, P. Weiss

A necessary complement to the *Journal of Polymer Science*, the *Journal of Applied Polymer Science* is a convenient, comprehensive source of information on polymer research. Articles concentrate on systems, compounds, and products of technological significance in the field. Major areas treated include the analysis of polymers, including instrumental methods; testing of plastics, elastomers, films, and fibers; adhesion and adhesives; emulsions and latex; mechanical properties; ion-exchange; diffusion and permeability; aging of polymers; extrusion and molding; and reinforcement and vulcanization. The journal's Symposia volumes contain proceedings of important borderline fields.

A Selection of Forthcoming Articles to  
be published in the  
*Journal of Applied Polymer Science*—

- *Crack Initiation in PVC for Subsequent Linear Elastic Fracture Mechanics Analysis*—P. G. Faulkner and J. R. Atkinson
- *Crease Recovery and Cuprammonium Solubility of Some Cross-Linked Cotton Fibers*—Frank S. H. Head
- *Non-Newtonian Flow and the Steady State Shear Compliance*—W. M. Prest, Jr., Roger S. Porter, and J. M. O'Reilly
- *Oligomer of O-Xylene as a Heat Stabilizer for Isotactic Polypropylene*—John Boor, Jr.
- *The Relation between Melt Flow Properties and Molecular Weight of Polyethylene*—Shigeru Saeda, Junji Yotsuyanagi, and Kinya Yamaguchi
- *Characterization of Ethylene Propylene Rubber and Ethylene Propylene Diene Rubber Networks*—A. M. Hassan and L. N. Ray, Jr.

Volume XV-Monthly, plus Symposia  
Subscription Price: \$150.00  
Foreign Postage: \$6.00  
Back Volume prices on request

The journal is also available in a microfilm edition. Volume 1 (1959) through Volume XIII (1969) is available for \$320.00. (This price applies only to subscribers to the journal. Prices for non-subscribers available on request.) Prices for individual volumes are available on request.

## BIOPOLYMERS

An International Journal of Research  
on Biological Macromolecules

Editor: Murray Goodman, *Polytechnic Institute of Brooklyn*

Editorial Board: Elkan Blout, *Harvard Medical School*; D. F. Bradley, *Polytechnic Institute of Brooklyn*; Ephraim Katchalski, *The Weizmann Institute of Science, Rehovot, Israel*; Arthur Peacocke, *St. Peter's College, Oxford, England*; I. Tinoco, Jr., *University of California, Berkeley*

*Biopolymers* includes original research papers on biological macromolecules, related synthetic macromolecules, as well as relevant model compounds. The studies of such macromolecules involve their physical chemistry, organic chemistry, and biophysics. Covered in these three broad fields are synthesis, including biosynthesis, structure, chemical modification and reactions, catalytic function (in molecular terms) and other reaction mechanisms, macromolecular interactions, and organization. Three main types of articles are published in *Biopolymers*: manuscripts based on original research, short communications containing significant and novel results, and perspectives in biopolymer research. In the latter type of article, contributors present pertinent historical background, discuss and correlate current views, and suggest possible lines of development in future work.

A Selection of Forthcoming Articles  
to be published in *Biopolymers*—

- *A Model of the Orientation Symmetry of Water Molecules in the Biopolymers (by NMR Spectra)*—A. A. Khanagov
- *Optical Rotatory Dispersion of Mucopolysaccharides. III. Ultraviolet Circular Dichroism and Conformational Specificity in Amide Groups*—Audrey L. Stone
- *A Comparison of Helix Stabilities of Poly-L-Lysine, Poly-L-Ornithine and Poly-L-Diaminobutyric Acid*—M. J. Grouke and Julian H. Gibbs
- *Simple Methods for the Orientation of DNA Molecules in Films Suitable for Optical Studies*—T. Kurucsev and J. R. Zdziewicz
- *Optical Rotatory Dispersion of Polypeptides in the Near Infrared Region*—Yu. N. Chirgadze, S. Yu. Venyaminov, and V. M. Lobachev
- *Molecular Beams of Macroions. III. Zein and Polyvinylpyrrolidone*—G. A. Clegg and M. Dole

Volume X-Monthly  
Subscription Price: \$70.00  
Foreign Postage: \$4.00  
Back volume prices on request

## WILEY-INTERSCIENCE

a division of JOHN WILEY & SONS, Inc.

605 Third Avenue, New York, N.Y. 10016

In Canada: 22 Worcester Road, Rexdale, Ontario